

# UC Riverside

## UC Riverside Electronic Theses and Dissertations

### Title

Intramolecular Carbene Insertion Into Strained Cyclopropyl C–C Bonds and Synergistic Brønsted/Lewis Acid Catalyzed Friedel–Crafts Alkylations of Unactivated Tertiary and Secondary Alcohols

### Permalink

<https://escholarship.org/uc/item/79q211zs>

### Author

Pan, Aaron

### Publication Date

2024

Peer reviewed|Thesis/dissertation

UNIVERSITY OF CALIFORNIA  
RIVERSIDE

Intramolecular Carbene Insertion into Strained Cyclopropyl C–C Bonds and Synergistic  
Brønsted/Lewis Acid Catalyzed Friedel–Crafts Alkylations of Unactivated Tertiary and  
Secondary Alcohols

A Dissertation submitted in partial satisfaction  
of the requirements for the degree of

Doctor of Philosophy

in

Chemistry

by

Aaron Pan

June 2024

Dissertation Committee:  
Dr. Kevin G. M. Kou, Chairperson  
Dr. Richard J. Hooley  
Dr. Michael C. Pirrung

Copyright by  
Aaron Pan  
2024

The Dissertation of Aaron Pan is approved:

---

---

---

Committee Chairperson

University of California, Riverside

## ABSTRACT OF THE DISSERTATION

Intramolecular Carbene Insertion into Strained Cyclopropyl C–C Bonds and Synergistic Brønsted/Lewis Acid Catalyzed Friedel–Crafts Alkylations of Unactivated Tertiary and Secondary Alcohols

by

Aaron Pan

Doctor of Philosophy, Graduate Program in Chemistry  
University of California, Riverside, June 2024  
Dr. Kevin G. M. Kou, Chairperson

Despite the plethora of synthetic and catalysis methodologies developed for the direct activation of carbon–carbon (C–C) bonds, its direct insertion by carbene or carbenoid intermediates is unprecedented. This is intriguing, provided the versatility of carbene and carbenoid intermediates in inserting into strong C–H, O–H, N–H, Si–H, and B–H bonds. The approach detailed in this chapter entails targeting metal carbenoid insertion into strained C–C bonds. Synthesis routes to generate substrates for metal-carbene-mediated C–C insertions were developed. Initial studies with the diazo compounds synthesized thus far have led to cyclization and C–H insertion products, suggesting a high barrier to C–C insertion, despite attempts to disfavor C–H insertion.

Dual Brønsted/Lewis acid catalysis involving environmentally benign, readily accessible protic acid and iron promotes site-selective *tert*-butylation of electron-rich arenes using di-*tert*-butylperoxide. This transformation inspired the development of a

synergistic Brønsted/Lewis acid catalyzed aromatic alkylation that fills a gap in the Friedel–Crafts reaction literature by employing unactivated tertiary alcohols as alkylating agents, leading to new quaternary carbon centers. Corroborated by DFT calculations, the Lewis acid serves a role in enhancing the acidity of the Brønsted acid. The use of non-allylic, non-benzylic, and non-propargylic tertiary alcohols in Friedel–Crafts reactions would give rise to synthetically-important all-carbon quaternary carbons; however, such substrates are poorly reactive and underexplored in this area.

The intermolecular Friedel–Crafts alkylation represents a straightforward approach to synthesizing C(sp<sup>2</sup>)–C(sp<sup>3</sup>) bonds. When readily accessible alcohols are utilized directly as the alkylating agents, the sole byproduct generated is water. Traditional Friedel–Crafts alkylation reactions are typically limited to alkyl (pseudo)halides and activated alcohols that form stabilized carbocations. However, by using inexpensive and abundant ZnCl<sub>2</sub> and camphorsulfonic acid (CSA) as catalysts, we developed a site-selective Friedel–Crafts alkylation of phenolic derivatives with unactivated secondary alcohols. This catalytic process favors *ortho*-selectivity, even in the absence of steric influence. Mechanistic studies served to elucidate the origin of site-selectivity, favoring an S<sub>N</sub>1 pathway in which zinc and CSA function to scaffold both the phenolic and alcohol reactants for *ortho*-functionalization. This work highlights the efficacy of simple catalysts for achieving C(sp<sup>2</sup>)–C(sp<sup>3</sup>) bond synthesis, departing from conventional transition-metal-catalyzed cross-coupling methods.

## Table of Contents

1.1.1 Introduction – Carbenes and metal-carbene types .....	1
1.1.2 Carbene-mediated X–H, alkene, and alkyne bond activation reactions .....	4
1.2.1 Strategy for direct C–C bond activation .....	23
1.2.2 Synthesis of <i>gem</i> -dimethyl diazo compound <b>1.27</b> .....	25
1.2.3 Syntheses of 2'-cyclopropylbenzoyl diazo compounds <b>1.28–1.32</b> .....	33
1.2.4 Syntheses of quaternary-substituted cyclopropyl diazo compounds <b>1.75–1.78</b> .....	38
1.3 Conclusion .....	44
1.4 References .....	45
1.5 Experimental .....	50
1.5.1 General information .....	50
1.5.2 Experimental Procedures and Characterization Data .....	53
1.5.3 References .....	97
2.1 Introduction: Friedel–Crafts alkylation .....	98
2.1.1 Traditional Friedel-Crafts alkylation reactions .....	99
2.1.2 Other C(sp <sup>2</sup> )–C(sp <sup>3</sup> ) bond forming reactions .....	103
2.1.3 Tertiary alcohols in Friedel–Crafts alkylation reactions .....	105
2.2 Alkylations with DTBP .....	116
2.2.1 DTBP mechanistic and kinetic studies .....	119
2.3 Alkylations with <i>tert</i> -alkanols .....	124
2.3.1 Mechanistic studies through <i>tert</i> -butanol kinetic studies .....	132
2.3.2 Mechanistic studies through computational studies .....	137
2.4 Conclusion .....	141

2.5 References.....	142
2.6 Experimental.....	147
2.6.1 General Information.....	147
2.6.2 Dual Brønsted/Lewis acid-Catalyzed Friedel–Crafts <i>tert</i> -Alkylation.....	148
2.6.3 References.....	166
3.1.1 Friedel–Crafts alkylations with secondary benzyl/acyl alcohols or silyl ethers....	168
3.1.2 Friedel–Crafts alkylations with activated secondary alcohols.....	170
3.1.3 Friedel–Crafts alkylations with unactivated secondary alcohols.....	174
3.2.1 Development and optimization studies for the coupling of 3- <i>tert</i> -butylphenol and cyclohexanol.....	176
3.2.2 Substrate scope.....	179
3.2.3 Mechanistic studies to probe the origin of site-selectivity.....	183
3.3 Conclusion.....	192
3.4 References.....	193
3.5 Experimental.....	194
3.5.1 General Information.....	194
3.5.2 Experimental Procedures: Preparation of Secondary Alcohols.....	195
3.5.3 Reactions of Unactivated Secondary Alcohols.....	198
3.5.4 Mechanistic Studies.....	224
4.1 Appendix: NMR Spectra.....	227



## List of Figures

<b>Figure 1.1.</b> Carbene in its singlet and triplet state.....	1
<b>Figure 1.2.</b> Fischer- and Schrock-type carbenes.....	2
<b>Figure 1.3.</b> Common carbene precursors.....	3
<b>Figure 1.4.</b> Carbene formation from sulfonyl hydrazones.....	3
<b>Figure 1.5.</b> Reactions of metal-carbenes with various X–Y bonds.....	4
<b>Figure 1.6.</b> Intramolecular C–H activation/cyclization to exclusively form cyclopentenones.....	5
<b>Figure 1.7.</b> Select examples of metal-carbene mediated Si–H bond insertion.....	6
<b>Figure 1.8.</b> Select examples of metal-carbene mediated N–H bond insertion.....	8
<b>Figure 1.9.</b> Examples of N–H and S–H bond insertions.....	9
<b>Figure 1.10.</b> C=C bond insertions of styrene motifs to cyclopropanate.....	9
<b>Figure 1.11.</b> C=O bond insertion to form epoxides over C=C bond insertion.....	9
<b>Figure 1.12.</b> Competing C≡C bond insertion versus intramolecular 1,2-hydride shift..	10
<b>Figure 1.13.</b> Diazo-pyrrolidones partaking in an improved Büchner-Curtius-Schlotterbeck reaction.....	11
<b>Figure 1.14.</b> Arndt-Eistert synthesis for a formal C–C bond insertion of carboxylic acids.....	12
<b>Figure 1.15.</b> Importance of adding the ynolate intermediate to acidic ethanol.....	13
<b>Figure 1.16.</b> General Roskamp reaction to achieve C–H bond insertion.....	14
<b>Figure 1.17.</b> Chiral ligand-scandium catalyzed C–H bond insertion with $\alpha$ -alkyl- $\alpha$ -diazo esters.....	14
<b>Figure 1.18.</b> Enantioselective yttrium-catalyzed formal C–C bond insertion.....	15
<b>Figure 1.19.</b> Oxazaborolidinium-catalyzed formal C–C bond insertion over C–H bond insertion.....	16

<b>Figure 1.20.</b> Normal C–C bonds are inert. Adding strain to the C–C bond can help with oxidative addition.....	16
<b>Figure 1.21.</b> Total synthesis of two natural products through a key C–C bond insertion step.....	17
<b>Figure 1.22.</b> Formal alkyne insertion between a C–C bond via $\beta$ -carbon elimination/C–C activation.....	18
<b>Figure 1.23.</b> Synthesis of oxoindoles via $\beta$ -carbon elimination/C–C activation. ....	19
<b>Figure 1.24.</b> Formal C–C bond homologation of benzocyclobutanols.....	21
<b>Figure 1.25.</b> C–C bond insertion of acyclic 1,3-diketones.....	22
<b>Figure 1.26.</b> Formal C–C bond insertion of a C(sp <sup>2</sup> )-hybridized carbon.....	23
<b>Figure 1.27.</b> Suzuki cross-coupling.....	24
<b>Figure 1.28.</b> Side reaction with unprotected alcohol. ....	24
<b>Figure 1.29.</b> Target diazo substrates. ....	24
<b>Figure 1.30.</b> Synthesis progress of cyclopropyl ester <b>1.42</b> and <b>1.43</b> .....	26
<b>Figure 1.31.</b> Unsuccessful ring opening attempts with benzene to produce ester <b>1.38</b> . Switching to DMF was significant in successful ring opening to carboxylic acid <b>1.39</b> ...	27
<b>Figure 1.32.</b> Conditions to esterify carboxylic acid <b>1.39</b> to ester <b>1.41</b> . ....	28
<b>Figure 1.33.</b> Side reaction in the Suzuki cross-coupling.....	29
<b>Figure 1.34.</b> Alternate synthesis route involving previously developed Fe-catalysis.....	31
<b>Figure 1.35.</b> Coumarin <b>1.54</b> from iron-catalyzed coupling reaction.....	31
<b>Figure 1.36.</b> Unsuccessful attempt utilizing malonate to access diazo <b>1.55</b> .....	32
<b>Figure 1.37.</b> Shorter synthesis attempt to achieve target diazo compound <b>1.27</b> .....	33
<b>Figure 1.38.</b> Synthesis route to diazoacetyl <b>1.28</b> . ....	34
<b>Figure 1.39.</b> Initial attempts diazo-phenylacetophenone <b>1.29</b> . ....	34
<b>Figure 1.40.</b> Tentative successful route to diazo-phenylacetophenone <b>1.29</b> . ....	35
<b>Figure 1.41.</b> Synthesis route to ketoester-diazo <b>1.30</b> . ....	36

<b>Figure 1.42.</b> Synthesis route to thio-diazo <b>1.31</b> .	37
<b>Figure 1.43.</b> Observed C–H insertion of metal-carbenoids to spiro-cyclopropyl <b>1.74</b> and no desired C–C insertion to cyclobutyl <b>1.47</b> .	37
<b>Figure 1.44.</b> Re-strategized substrate designs and proposed retrosyntheses.	38
<b>Figure 1.45.</b> Synthesis route concluded to lactone <b>1.87</b> instead of methoxyketoester diazo <b>1.86</b> .	39
<b>Figure 1.46.</b> Synthesis route to methoxy-phenyl diazo <b>1.76</b> . Complex mixtures with metal-carbene reactivity.	40
<b>Figure 1.47.</b> Synthesis to ketoester diazo <b>1.75</b> . Major identifiable products involved in the metal-carbene reactions were Stevens rearrangement-type products.	41
<b>Figure 1.48.</b> Metal-carbene reactions with benzoyl diazo <b>1.99</b> also observed Stevens rearrangement-type reactivity.	42
<b>Figure 1.49.</b> Synthesis route to carboxylic acid cyclopropane <b>1.104</b> .	42
<b>Figure 1.50.</b> Alternative synthesis of carboxylic acid-cyclopropane <b>1.104</b> . Unsuccessful attempt to access diazo <b>1.109</b> from carboxylic acid <b>1.104</b> in one step.	43
<b>Figure 1.51.</b> Synthesis route to diazo <b>1.78</b> . Metal-carbene-mediated reactions failed to result in the desired C–C bond insertion of the cyclopropyl ring.	44
<b>Figure 2.1.</b> Friedel–Crafts alkylation with alkyl fluorides and catalytic borane monohydrate to initiate the reaction.	99
<b>Figure 2.2.</b> Friedel–Crafts reaction catalyzed by a molybdenum/chloranil complex.	101
<b>Figure 2.3.</b> A Friedel–Crafts alkylation utilizing a unique carborane as the Lewis acid.	102
<b>Figure 2.4.</b> Friedel–Crafts reaction with a protected aniline.	103
<b>Figure 2.5.</b> $\beta$ -Hydride elimination when a transition metal is on an alkyl group.	104
<b>Figure 2.6.</b> Nickel-catalyzed Kumada–Corriu–Tamao-type reaction for <i>tert</i> -butylation.	104
<b>Figure 2.7.</b> A Minisci reaction alkylates electron-deficient aromatic rings.	105
<b>Figure 2.8.</b> Tertiary benzylic alcohols undergoing intramolecular alkylation to form fluorenes.	106

<b>Figure 2.9.</b> Intramolecular cyclization of activated and unactivated tertiary alcohols. .	106
<b>Figure 2.10.</b> Calcium-catalyzed alkylation of electron-rich arenes via activated tertiary alcohols. ....	107
<b>Figure 2.11.</b> Tandem Friedel–Crafts alkylation/lactonization to form benzofuranones.	108
<b>Figure 2.12.</b> Tertiary allylic alcohols in Friedel–Crafts alkylation resulting in allylic shift products.....	109
<b>Figure 2.13.</b> Possible hydrogen bonding versus electron repulsion when alcohol binds to boronic acid.....	109
<b>Figure 2.14.</b> Unprotected indoles and other arenes partaking in iron-catalyzed Friedel–Crafts alkylation.....	110
<b>Figure 2.15.</b> Intramolecular alkylation of unactivated tertiary alcohol resulted in stereoinverted products. ....	111
<b>Figure 2.16.</b> Heterocyclic tertiary benzylic alcohols partaking in a Friedel–Crafts alkylation reaction.....	112
<b>Figure 2.17.</b> Coupling of hydroxy-oxindoles to electron-rich arenes under microwave conditions.....	113
<b>Figure 2.18.</b> Transition-metal free coupling of aryl boronic acids to tertiary propargylic alcohols. ....	114
<b>Figure 2.19.</b> Elimination side reactivity observed and favored under certain conditions. ....	114
<b>Figure 2.20.</b> Conditions for exclusive <i>para</i> - or <i>ortho</i> -alkylation.....	115
<b>Figure 2.21.</b> Example of utilizing DTBP to <i>tert</i> -butoxylate a copper complex in a patent. ....	115
<b>Figure 2.22.</b> Conditions for kinetic analysis. <i>Combined efforts with L. Gottemann</i> .....	121
<b>Figure 2.23.</b> Initial rates when varying [phenolic <b>2.5</b> ]. ....	121
<b>Figure 2.24.</b> Initial rates when varying [peroxide <b>2.6</b> ]. ....	121
<b>Figure 2.25.</b> Initial rates when varying [FeCl <sub>3</sub> ]. ....	121
<b>Figure 2.26.</b> Initial rates when varying [TFA]. ....	122

<b>Figure 2.27.</b> Plots of initial rates with respect to: .....	123
<b>Figure 2.28.</b> Plots of the normalized time scale method for determining catalyst order: blue circle = 6.2 mM FeCl <sub>3</sub> , red triangle = 9.4 mM FeCl <sub>3</sub> , grey square = 13 mM FeCl <sub>3</sub> . .....	124
<b>Figure 2.29.</b> Rates of induction period and exponential phase when varying [phenolic 2.5]. .....	133
<b>Figure 2.30.</b> Rates of induction period and exponential phase when varying [alcohol 2.37]. .....	133
<b>Figure 2.31.</b> Rates of induction period and exponential phase when varying [FeCl <sub>3</sub> ]. .	133
<b>Figure 2.32.</b> Rates of induction period and exponential phase when varying [HCl]. ....	134
<b>Figure 2.33.</b> <i>tert</i> -Alkylation of natural products. ....	135
<b>Figure 2.34.</b> (a) Fate of the alcohol. (b) Probing for a radical vs. polar pathway. ....	136
<b>Figure 2.35.</b> Free energy profile computed using DFT calculations for the course of ionization of <i>t</i> -BuOH (2.37) in the presence of the FeCl <sub>3</sub> /HCl acid pair and FeCl <sub>3</sub> . ....	139
<b>Figure 3.1.</b> Friedel–Crafts alkylation of acyl benzyl ethers to nucleophilic arenes. ....	168
<b>Figure 3.2.</b> Benzylic acetates and secondary alcohols for Friedel–Crafts reactions. ....	169
<b>Figure 3.3.</b> Friedel–Crafts alkylation with benzyl silyl ethers. ....	170
<b>Figure 3.4.</b> Tetrafluorophenylboronic acid-catalyzed Friedel–Crafts alkylation with secondary benzylic alcohols. ....	171
<b>Figure 3.5.</b> A green Friedel–Crafts alkylation method utilizing water as a green solvent. .....	172
<b>Figure 3.6.</b> Cyclopropyl-containing secondary alcohols quickly reacting in a Friedel– Crafts alkylation. ....	173
<b>Figure 3.7.</b> Substrate scope of rhenium-catalyzed Friedel–Crafts intramolecular cyclization. ....	174
<b>Figure 3.8.</b> Scope of acid-sensitive functional groups in the presence of rhenium catalyst versus TfOH. ....	174
<b>Figure 3.9.</b> Unactivated cycloalkyl alcohols undergoing iron-catalyzed Friedel–Crafts alkylations. ....	175

<b>Figure 3.10.</b> Intramolecular Friedel–Crafts alkylations with unactivated secondary alcohols. ....	176
<b>Figure 3.11.</b> Application to late-stage derivatization:.....	183
<b>Figure 3.12.</b> Mechanistic studies: .....	184
<b>Figure 3.13.</b> Reaction progress monitoring of: .....	185
<b>Figure 3.14.</b> Mechanistic studies: .....	186
<b>Figure 3.16.</b> Initial rates under standard conditions.....	187
<b>Figure 3.17.</b> Initial rates varying [phenolic <b>3.6</b> ]. .....	187
<b>Figure 3.18.</b> Initial rates varying [alcohol <b>3.42</b> ]. .....	188
<b>Figure 3.19.</b> Initial rates varying [ZnCl <sub>2</sub> ]......	188
<b>Figure 3.20.</b> Initial rates varying [( <i>R</i> )-CSA•H <sub>2</sub> O]. .....	189
<b>Figure 3.15.</b> Plots of initial rates with respect to: .....	189
<b>Figure 4.1.</b> <sup>1</sup> H NMR spectrum of <b>1.34</b> (400 MHz, 295 K, CDCl <sub>3</sub> ). .....	227
<b>Figure 4.2.</b> <sup>1</sup> H NMR spectrum of <b>1.37</b> (400 MHz, 295 K, CDCl <sub>3</sub> ). .....	228
<b>Figure 4.3.</b> <sup>1</sup> H NMR spectrum of <b>1.39</b> (400 MHz, 295 K, CDCl <sub>3</sub> ). .....	228
<b>Figure 4.4.</b> <sup>13</sup> C NMR spectrum of <b>1.39</b> (101 MHz, 295 K, CDCl <sub>3</sub> ). .....	229
<b>Figure 4.5.</b> <sup>1</sup> H NMR spectrum of <b>1.41</b> (400 MHz, 295 K, CDCl <sub>3</sub> ). .....	229
<b>Figure 4.6.</b> <sup>13</sup> C NMR spectrum of <b>1.41</b> (101 MHz, 295 K, CDCl <sub>3</sub> ). .....	230
<b>Figure 4.7.</b> <sup>1</sup> H NMR spectrum of <b>1.43</b> (600 MHz, 298 K, CDCl <sub>3</sub> ). .....	230
<b>Figure 4.8.</b> <sup>13</sup> C NMR spectrum of <b>1.43</b> (151 MHz, 298 K, CDCl <sub>3</sub> ). .....	231
<b>Figure 4.9.</b> <sup>1</sup> H NMR spectrum of <b>1.44</b> (400 MHz, 295 K, CDCl <sub>3</sub> ). .....	231
<b>Figure 4.10.</b> <sup>13</sup> C NMR spectrum of <b>1.44</b> (126 MHz, 298 K, CDCl <sub>3</sub> ). .....	232
<b>Figure 4.11.</b> <sup>1</sup> H NMR spectrum of <b>1.54</b> (500 MHz, 298 K, CDCl <sub>3</sub> ). .....	232
<b>Figure 4.12.</b> <sup>13</sup> C NMR spectrum of <b>1.54</b> (126 MHz, 298 K, CDCl <sub>3</sub> ). .....	233

<b>Figure 4.13.</b> $^1\text{H}$ NMR spectrum of <b>1.59</b> (400 MHz, 295 K, $\text{CDCl}_3$ ). .....	233
<b>Figure 4.14.</b> $^{13}\text{C}$ NMR spectrum of <b>1.59</b> (151 MHz, 298 K, $\text{CDCl}_3$ ). .....	234
<b>Figure 4.15.</b> $^{19}\text{F}$ NMR spectrum of <b>1.59</b> (564 MHz, 298 K, $\text{CDCl}_3$ ). .....	234
<b>Figure 4.16.</b> $^1\text{H}$ NMR spectrum of <b>1.28</b> (500 MHz, 298 K, $\text{CDCl}_3$ ). .....	235
<b>Figure 4.17.</b> $^{13}\text{C}$ NMR spectrum of <b>1.28</b> (151 MHz, 298 K, $\text{CDCl}_3$ ). .....	235
<b>Figure 4.18.</b> $^1\text{H}$ NMR spectrum of <b>1.66</b> (500 MHz, 298 K, $\text{CDCl}_3$ ). .....	236
<b>Figure 4.19.</b> $^1\text{H}$ NMR spectrum of <b>1.67</b> (500 MHz, 298 K, $\text{CDCl}_3$ ). .....	236
<b>Figure 4.20.</b> $^{13}\text{C}$ NMR spectrum of <b>1.67</b> (126 MHz, 298 K, $\text{CDCl}_3$ ). .....	237
<b>Figure 4.21.</b> $^1\text{H}$ NMR spectrum of <b>1.69</b> (500 MHz, 298 K, $\text{CDCl}_3$ ). .....	237
<b>Figure 4.22.</b> $^{13}\text{C}$ NMR spectrum of <b>1.69</b> (126 MHz, 298 K, $\text{CDCl}_3$ ). .....	238
<b>Figure 4.23.</b> $^1\text{H}$ NMR spectrum of <b>1.70</b> (500 MHz, 298 K, $\text{CDCl}_3$ ). .....	238
<b>Figure 4.24.</b> $^1\text{H}$ NMR spectrum of <b>1.30</b> (500 MHz, 298 K, $\text{CDCl}_3$ ). .....	239
<b>Figure 4.25.</b> $^{13}\text{C}$ NMR spectrum of <b>1.30</b> (126 MHz, 298 K, $\text{CDCl}_3$ ). .....	239
<b>Figure 4.26.</b> $^1\text{H}$ NMR spectrum of <b>1.74</b> (500 MHz, 298 K, $\text{CDCl}_3$ ). .....	240
<b>Figure 4.27.</b> $^{13}\text{C}$ NMR spectrum of <b>1.74</b> (126 MHz, 298 K, $\text{CDCl}_3$ ). .....	240
<b>Figure 4.28.</b> $^1\text{H}$ NMR spectrum of <b>1.79</b> (500 MHz, 298 K, $\text{CDCl}_3$ ). .....	241
<b>Figure 4.29.</b> $^1\text{H}$ NMR spectrum of <b>1.82</b> (500 MHz, 298 K, $\text{CDCl}_3$ ). .....	241
<b>Figure 4.30.</b> $^1\text{H}$ NMR spectrum of <b>1.83</b> (600 MHz, 298 K, $\text{CDCl}_3$ ). .....	242
<b>Figure 4.31.</b> $^1\text{H}$ NMR spectrum of <b>1.84</b> (500 MHz, 298 K, $\text{CDCl}_3$ ). .....	242
<b>Figure 4.32.</b> $^{13}\text{C}$ NMR spectrum of <b>1.84</b> (151 MHz, 298 K, $\text{CDCl}_3$ ). .....	243
<b>Figure 4.33.</b> $^1\text{H}$ NMR spectrum of <b>1.85</b> (500 MHz, 298 K, $\text{CDCl}_3$ ). .....	243
<b>Figure 4.34.</b> $^{13}\text{C}$ NMR spectrum of <b>1.85</b> (151 MHz, 298 K, $\text{CDCl}_3$ ). .....	244
<b>Figure 4.35.</b> $^1\text{H}$ NMR spectrum of <b>1.87</b> (600 MHz, 298 K, $\text{CDCl}_3$ ). .....	244
<b>Figure 4.36.</b> $^{13}\text{C}$ NMR spectrum of <b>1.87</b> (151 MHz, 298 K, $\text{CDCl}_3$ ). .....	245

<b>Figure 4.37.</b> $^1\text{H}$ NMR spectrum of <b>1.89</b> (600 MHz, 298 K, $\text{CDCl}_3$ ). .....	245
<b>Figure 4.38.</b> $^{13}\text{C}$ NMR spectrum of <b>1.89</b> (151 MHz, 298 K, $\text{CDCl}_3$ ). .....	246
<b>Figure 4.39.</b> $^1\text{H}$ NMR spectrum of <b>1.88</b> (600 MHz, 298 K, $\text{CDCl}_3$ ). .....	246
<b>Figure 4.40.</b> $^{13}\text{C}$ NMR spectrum of <b>1.88</b> (151 MHz, 298 K, $\text{CDCl}_3$ ). .....	247
<b>Figure 4.41.</b> $^1\text{H}$ NMR spectrum of <b>1.90</b> (600 MHz, 298 K, $\text{CDCl}_3$ ). .....	247
<b>Figure 4.42.</b> $^{13}\text{C}$ NMR spectrum of <b>1.90</b> (151 MHz, 298 K, $\text{CDCl}_3$ ). .....	248
<b>Figure 4.43.</b> $^1\text{H}$ NMR spectrum of <b>1.91</b> (400 MHz, 295 K, $\text{CDCl}_3$ ). .....	248
<b>Figure 4.44.</b> $^{13}\text{C}$ NMR spectrum of <b>1.91</b> (101 MHz, 295 K, $\text{CDCl}_3$ ). .....	249
<b>Figure 4.45.</b> $^1\text{H}$ NMR spectrum of <b>1.76</b> (600 MHz, 298 K, $\text{CDCl}_3$ ). .....	249
<b>Figure 4.46.</b> $^1\text{H}$ NMR spectrum of <b>1.76</b> (151 MHz, 298 K, $\text{CDCl}_3$ ). .....	250
<b>Figure 4.47.</b> $^1\text{H}$ NMR spectrum of <b>1.93</b> (600 MHz, 298 K, $\text{CDCl}_3$ ). .....	250
<b>Figure 4.48.</b> $^{13}\text{C}$ NMR spectrum of <b>1.93</b> (151 MHz, 298 K, $\text{CDCl}_3$ ). .....	251
<b>Figure 4.49.</b> $^1\text{H}$ NMR spectrum of <b>1.94</b> (600 MHz, 298 K, $\text{CDCl}_3$ ). .....	251
<b>Figure 4.50.</b> $^{13}\text{C}$ NMR spectrum of <b>1.94</b> (151 MHz, 298 K, $\text{CDCl}_3$ ). .....	252
<b>Figure 4.51.</b> $^1\text{H}$ NMR spectrum of <b>1.95</b> (500 MHz, 298 K, $\text{CDCl}_3$ ). .....	252
<b>Figure 4.52.</b> $^{13}\text{C}$ NMR spectrum of <b>1.95</b> (151 MHz, 298 K, $\text{CDCl}_3$ ). .....	253
<b>Figure 4.53.</b> $^1\text{H}$ NMR spectrum of <b>1.75</b> (500 MHz, 298 K, $\text{CDCl}_3$ ). .....	253
<b>Figure 4.54.</b> $^{13}\text{C}$ NMR spectrum of <b>1.75</b> (151 MHz, 298 K, $\text{CDCl}_3$ ). .....	254
<b>Figure 4.55.</b> $^1\text{H}$ NMR spectrum of <b>1.96</b> (500 MHz, 298 K, $\text{CDCl}_3$ ). .....	254
<b>Figure 4.56.</b> $^{13}\text{C}$ NMR spectrum of <b>1.96</b> (151 MHz, 298 K, $\text{CDCl}_3$ ). .....	255
<b>Figure 4.57.</b> $^1\text{H}$ NMR spectrum of <b>1.97</b> (600 MHz, 298 K, $\text{CDCl}_3$ ). .....	255
<b>Figure 4.58.</b> $^{13}\text{C}$ NMR spectrum of <b>1.97</b> (151 MHz, 298 K, $\text{CDCl}_3$ ). .....	256
<b>Figure 4.59.</b> $^1\text{H}$ NMR spectrum of <b>1.98</b> (500 MHz, 298 K, $\text{CDCl}_3$ ). .....	256
<b>Figure 4.60.</b> $^{13}\text{C}$ NMR spectrum of <b>1.98</b> (151 MHz, 298 K, $\text{CDCl}_3$ ). .....	257



<b>Figure 4.61.</b> $^1\text{H}$ NMR spectrum of <b>1.100</b> (500 MHz, 298 K, $\text{CDCl}_3$ ). .....	257
<b>Figure 4.62.</b> $^{13}\text{C}$ NMR spectrum of <b>1.100</b> (151 MHz, 298 K, $\text{CDCl}_3$ ). .....	258
<b>Figure 4.63.</b> $^1\text{H}$ NMR spectrum of <b>1.99</b> (500 MHz, 298 K, $\text{CDCl}_3$ ). .....	258
<b>Figure 4.64.</b> $^{13}\text{C}$ NMR spectrum of <b>1.99</b> (151 MHz, 298 K, $\text{CDCl}_3$ ). .....	259
<b>Figure 4.65.</b> $^1\text{H}$ NMR spectrum of <b>1.101</b> (500 MHz, 298 K, $\text{CDCl}_3$ ). .....	259
<b>Figure 4.66.</b> $^{13}\text{C}$ NMR spectrum of <b>1.101</b> (151 MHz, 298 K, $\text{CDCl}_3$ ). .....	260
<b>Figure 4.67.</b> $^1\text{H}$ NMR spectrum of <b>1.102</b> (500 MHz, 298 K, $\text{CDCl}_3$ ). .....	260
<b>Figure 4.68.</b> $^1\text{H}$ NMR spectrum of <b>1.103</b> (500 MHz, 298 K, $\text{CDCl}_3$ ). .....	261
<b>Figure 4.69.</b> $^{13}\text{C}$ NMR spectrum of <b>1.103</b> (151 MHz, 298 K, $\text{CDCl}_3$ ). .....	261
<b>Figure 6.70.</b> $^1\text{H}$ NMR spectrum of <b>1.107</b> (500 MHz, 298 K, $\text{CDCl}_3$ ). .....	262
<b>Figure 4.71.</b> $^{13}\text{C}$ NMR spectrum of <b>1.107</b> (151 MHz, 298 K, $\text{CDCl}_3$ ). .....	262
<b>Figure 4.72.</b> $^1\text{H}$ NMR spectrum of <b>1.108</b> (600 MHz, 298 K, $\text{CDCl}_3$ ). .....	263
<b>Figure 4.73.</b> $^{13}\text{C}$ NMR spectrum of <b>1.108</b> (151 MHz, 298 K, $\text{CDCl}_3$ ). .....	263
<b>Figure 4.74.</b> $^1\text{H}$ NMR spectrum of <b>1.104</b> (600 MHz, 298 K, $\text{CDCl}_3$ ). .....	264
<b>Figure 4.75.</b> $^{13}\text{C}$ NMR spectrum of <b>1.104</b> (151 MHz, 298 K, $\text{CDCl}_3$ ). .....	264
<b>Figure 4.76.</b> $^1\text{H}$ NMR spectrum of <b>1.110</b> (600 MHz, 298 K, $\text{CDCl}_3$ ). .....	265
<b>Figure 4.77.</b> $^1\text{H}$ NMR spectrum of <b>1.111</b> (600 MHz, 298 K, $\text{CDCl}_3$ ). .....	265
<b>Figure 4.78.</b> $^{13}\text{C}$ NMR spectrum of <b>1.111</b> (151 MHz, 298 K, $\text{CDCl}_3$ ). .....	266
<b>Figure 4.79.</b> $^1\text{H}$ NMR spectrum of <b>1.112</b> (500 MHz, 298 K, $\text{CDCl}_3$ ). .....	266
<b>Figure 4.80.</b> $^{13}\text{C}$ NMR spectrum of <b>1.112</b> (126 MHz, 298 K, $\text{CDCl}_3$ ). .....	267
<b>Figure 4.81.</b> $^1\text{H}$ NMR spectrum of <b>1.113</b> (600 MHz, 298 K, $\text{CDCl}_3$ ). .....	267
<b>Figure 4.82.</b> $^{13}\text{C}$ NMR spectrum of <b>1.113</b> (101 MHz, 295 K, $\text{CDCl}_3$ ). .....	268
<b>Figure 4.83.</b> $^1\text{H}$ NMR spectrum of <i>p</i> <b>ABSA</b> (600 MHz, 298 K, $\text{CDCl}_3$ ). .....	268
<b>Figure 4.84.</b> $^1\text{H}$ NMR spectrum of <b>1.114</b> or <b>1.115</b> (600 MHz, 298 K, $\text{CDCl}_3$ ). .....	269

<b>Figure 4.85.</b> $^{13}\text{C}$ NMR spectrum of <b>1.114</b> or <b>1.115</b> (101 MHz, 295 K, $\text{CDCl}_3$ ).....	269
<b>Figure 4.86.</b> $^1\text{H}$ NMR spectrum of <b>2.7</b> (500 MHz, 298 K, $\text{CDCl}_3$ ). .....	270
<b>Figure 4.87.</b> $^1\text{H}$ NMR spectrum of <b>2.8</b> (600 MHz, 298 K, $\text{CDCl}_3$ ). .....	270
<b>Figure 4.88.</b> $^{13}\text{C}$ NMR spectrum of <b>2.8</b> (151 MHz, 298 K, $\text{CDCl}_3$ ). .....	271
<b>Figure 4.89.</b> $^1\text{H}$ NMR spectrum of <b>2.9</b> (500 MHz, 298 K, $\text{CDCl}_3$ ). .....	271
<b>Figure 4.90.</b> $^{19}\text{F}$ NMR spectrum of <b>2.9</b> (564 MHz, 298 K, $\text{CDCl}_3$ ).....	272
<b>Figure 4.91.</b> $^1\text{H}$ NMR spectrum of <b>2.10</b> (500 MHz, 298 K, $\text{CDCl}_3$ ). .....	272
<b>Figure 4.92.</b> $^{13}\text{C}$ NMR spectrum of <b>2.10</b> (126 MHz, 298 K, $\text{CDCl}_3$ ). .....	273
<b>Figure 4.93.</b> $^1\text{H}$ NMR spectrum of <b>2.11</b> (600 MHz, 298 K, $\text{CDCl}_3$ ). .....	273
<b>Figure 4.94.</b> $^{13}\text{C}$ NMR spectrum of <b>2.11</b> (151 MHz, 298 K, $\text{CDCl}_3$ ). .....	274
<b>Figure 4.95.</b> $^1\text{H}$ NMR spectrum of <b>2.12</b> (500 MHz, 298 K, $\text{CDCl}_3$ ). .....	274
<b>Figure 4.96.</b> $^{13}\text{C}$ NMR spectrum of <b>2.12</b> (126 MHz, 298 K, $\text{CDCl}_3$ ). .....	275
<b>Figure 4.97.</b> $^1\text{H}$ NMR spectrum of <b>2.13</b> (500 MHz, 298 K, $\text{CDCl}_3$ ). .....	275
<b>Figure 4.98.</b> $^{13}\text{C}$ NMR spectrum of <b>2.13</b> (151 MHz, 298 K, $\text{CDCl}_3$ ). .....	276
<b>Figure 4.99.</b> $^1\text{H}$ NMR spectrum of <b>2.14</b> (400 MHz, 295 K, $\text{CDCl}_3$ ). .....	276
<b>Figure 4.100.</b> $^{13}\text{C}$ NMR spectrum of <b>2.14</b> (101 MHz, 295 K, $\text{CDCl}_3$ ). .....	277
<b>Figure 4.101.</b> $^1\text{H}$ NMR spectrum of <b>2.15</b> (500 MHz, 298 K, $\text{CDCl}_3$ ). .....	277
<b>Figure 4.102.</b> $^{13}\text{C}$ NMR spectrum of <b>2.15</b> (126 MHz, 298 K, $\text{CDCl}_3$ ). .....	278
<b>Figure 4.103.</b> $^{19}\text{F}$ NMR spectrum of <b>2.15</b> (376 MHz, 295 K, $\text{CDCl}_3$ ).....	278
<b>Figure 4.104.</b> $^1\text{H}$ NMR spectrum of <b>2.16</b> (500 MHz, 298 K, $\text{CDCl}_3$ ). .....	279
<b>Figure 4.105.</b> $^{13}\text{C}$ NMR spectrum of <b>2.16</b> (126 MHz, 298 K, $\text{CDCl}_3$ ). .....	279
<b>Figure 4.106.</b> $^1\text{H}$ NMR spectrum of <b>2.17</b> (600 MHz, 298 K, $\text{CDCl}_3$ ). .....	280
<b>Figure 4.107.</b> $^{19}\text{F}$ NMR spectrum of <b>2.17</b> (564 MHz, 298 K, $\text{CDCl}_3$ ).....	280
<b>Figure 4.108.</b> $^1\text{H}$ NMR spectrum of <b>2.40</b> (500 MHz, 298 K, $\text{CDCl}_3$ ). .....	281

<b>Figure 4.109.</b> $^{13}\text{C}$ NMR spectrum of <b>2.40</b> (126 MHz, 298 K, $\text{CDCl}_3$ ). .....	281
<b>Figure 4.110.</b> $^1\text{H}$ NMR spectrum of <b>2.41</b> (400 MHz, 295 K, $\text{CDCl}_3$ ). .....	282
<b>Figure 4.111.</b> $^{13}\text{C}$ NMR spectrum of <b>2.41</b> (101 MHz, 295 K, $\text{CDCl}_3$ ). .....	282
<b>Figure 4.112.</b> $^1\text{H}$ NMR spectrum of <b>2.42</b> (500 MHz, 298 K, $\text{CDCl}_3$ ). .....	283
<b>Figure 4.113.</b> $^{13}\text{C}$ NMR spectrum of <b>2.42</b> (126 MHz, 298 K, $\text{CDCl}_3$ ). .....	283
<b>Figure 4.114.</b> $^1\text{H}$ NMR spectrum of <b>2.92</b> (600 MHz, 298 K, $\text{CDCl}_3$ ). .....	284
<b>Figure 4.115.</b> $^{13}\text{C}$ NMR spectrum of <b>2.92</b> (151 MHz, 298 K, $\text{CDCl}_3$ ). .....	284
<b>Figure 4.116.</b> $^1\text{H}$ NMR spectrum of <b>2.43</b> (400 MHz, 295 K, $\text{CDCl}_3$ ). .....	285
<b>Figure 4.117.</b> $^{13}\text{C}$ NMR spectrum of <b>2.43</b> (101 MHz, 295 K, $\text{CDCl}_3$ ). .....	285
<b>Figure 4.118.</b> $^1\text{H}$ NMR spectrum of <b>2.45</b> (500 MHz, 298 K, $\text{CDCl}_3$ ). .....	286
<b>Figure 4.119.</b> $^{13}\text{C}$ NMR spectrum of <b>2.45</b> (126 MHz, 298 K, $\text{CDCl}_3$ ). .....	286
<b>Figure 4.120.</b> $^1\text{H}$ NMR spectrum of <b>2.46</b> (500 MHz, 298 K, $\text{CDCl}_3$ ). .....	287
<b>Figure 4.121.</b> $^{13}\text{C}$ NMR spectrum of <b>2.46</b> (151 MHz, 298 K, $\text{CDCl}_3$ ). .....	287
<b>Figure 4.122.</b> $^1\text{H}$ NMR spectrum of <b>2.47</b> (600 MHz, 298 K, $\text{CDCl}_3$ ). .....	288
<b>Figure 4.123.</b> $^{13}\text{C}$ NMR spectrum of <b>2.47</b> (151 MHz, 298 K, $\text{CDCl}_3$ ). .....	288
<b>Figure 4.124.</b> $^1\text{H}$ NMR spectrum of <b>2.94</b> (600 MHz, 298 K, $\text{CDCl}_3$ ). .....	289
<b>Figure 4.125.</b> $^{13}\text{C}$ NMR spectrum of <b>2.94</b> (151 MHz, 298 K, $\text{CDCl}_3$ ). .....	289
<b>Figure 4.126.</b> $^1\text{H}$ NMR spectrum of <b>2.48</b> (500 MHz, 298 K, $\text{CDCl}_3$ ). .....	290
<b>Figure 4.127.</b> $^{13}\text{C}$ NMR spectrum of <b>2.48</b> (126 MHz, 298 K, $\text{CDCl}_3$ ). .....	290
<b>Figure 4.128.</b> $^1\text{H}$ NMR spectrum of <b>2.49</b> (600 MHz, 298 K, $\text{CDCl}_3$ ). .....	291
<b>Figure 4.129.</b> $^{13}\text{C}$ NMR spectrum of <b>2.49</b> (151 MHz, 298 K, $\text{CDCl}_3$ ). .....	291
<b>Figure 4.130.</b> $^1\text{H}$ NMR spectrum of <b>2.39</b> (600 MHz, 298 K, $\text{CDCl}_3$ ). .....	292
<b>Figure 4.131.</b> $^{13}\text{C}$ NMR spectrum of <b>2.39</b> (151 MHz, 298 K, $\text{CDCl}_3$ ). .....	292
<b>Figure 4.132.</b> $^1\text{H}$ NMR spectrum of <b>2.50</b> (600 MHz, 298 K, $\text{CDCl}_3$ ). .....	293

<b>Figure 4.133.</b> $^{13}\text{C}$ NMR spectrum of <b>2.50</b> (151 MHz, 298 K, $\text{CDCl}_3$ ). .....	293
<b>Figure 4.134.</b> $^1\text{H}$ NMR spectrum of <b>2.51</b> (400 MHz, 295 K, $\text{CDCl}_3$ ). .....	294
<b>Figure 4.135.</b> $^{13}\text{C}$ NMR spectrum of <b>2.51</b> (101 MHz, 295 K, $\text{CDCl}_3$ ). .....	294
<b>Figure 4.136.</b> HSQC NMR spectrum of <b>2.51</b> ( $^1\text{H}$ NMR 400 MHz, $^{13}\text{C}$ NMR 101 MHz, 295 K, $\text{CDCl}_3$ ). .....	295
<b>Figure 4.137.</b> HMBC NMR spectrum of <b>2.51</b> ( $^1\text{H}$ NMR 400 MHz, $^{13}\text{C}$ NMR 101 MHz, 295 K, $\text{CDCl}_3$ ). .....	295
<b>Figure 4.138.</b> $^1\text{H}$ NMR spectrum of <b>2.52</b> (600 MHz, 298 K, $\text{CDCl}_3$ ). .....	296
<b>Figure 4.139.</b> $^{13}\text{C}$ NMR spectrum of <b>2.52</b> (151 MHz, 298 K, $\text{CDCl}_3$ ). .....	296
<b>Figure 4.140.</b> $^1\text{H}$ NMR spectrum of <b>2.98</b> (600 MHz, 298 K, $\text{CDCl}_3$ ). .....	297
<b>Figure 4.141.</b> $^{13}\text{C}$ NMR spectrum of <b>2.98</b> (151 MHz, 298 K, $\text{CDCl}_3$ ). .....	297
<b>Figure 4.142.</b> $^1\text{H}$ NMR spectrum of <b>2.53</b> (500 MHz, 298 K, $\text{CDCl}_3$ ). .....	298
<b>Figure 4.143.</b> $^{13}\text{C}$ NMR spectrum of <b>2.53</b> (126 MHz, 298 K, $\text{CDCl}_3$ ). .....	298
<b>Figure 4.144.</b> $^{19}\text{F}$ NMR spectrum of <b>2.53</b> (564 MHz, 298 K, $\text{CDCl}_3$ ). .....	299
<b>Figure 4.145.</b> $^1\text{H}$ NMR spectrum of <b>2.96</b> (500 MHz, 298 K, $\text{CDCl}_3$ ). .....	299
<b>Figure 4.146.</b> $^{13}\text{C}$ NMR spectrum of <b>2.96</b> (126 MHz, 298 K, $\text{CDCl}_3$ ). .....	300
<b>Figure 4.147.</b> $^{19}\text{F}$ NMR spectrum of <b>2.96</b> (376 MHz, 295 K, $\text{CDCl}_3$ ). .....	300
<b>Figure 4.148.</b> $^1\text{H}$ NMR spectrum of <b>2.89</b> (500 MHz, 298 K, $\text{CDCl}_3$ ). .....	301
<b>Figure 4.149.</b> $^1\text{H}$ NMR spectrum of <b>2.89</b> (126 MHz, 298 K, $\text{CDCl}_3$ ). .....	301
<b>Figure 4.150.</b> $^1\text{H}$ NMR spectrum of <b>3.7</b> (600 MHz, 298 K, $\text{CDCl}_3$ ). .....	302
<b>Figure 4.151.</b> $^1\text{H}$ NMR spectrum of <b>3.11</b> (500 MHz, 298 K, $\text{CDCl}_3$ ). .....	302
<b>Figure 4.152.</b> $^1\text{H}$ NMR spectrum of <b>2.57</b> (500 MHz, 298 K, $\text{CDCl}_3$ ). .....	303
<b>Figure 4.153.</b> $^1\text{H}$ NMR spectrum of <b>3.61</b> (400 MHz, 295 K, $d_8$ -THF). .....	303
<b>Figure 4.154.</b> $^1\text{H}$ NMR spectrum of <b>3.60</b> (500 MHz, 298 K, $\text{CDCl}_3$ ). .....	304
<b>Figure 4.155.</b> $^1\text{H}$ NMR spectrum of <b>3.8</b> (500 MHz, 298 K, $\text{CDCl}_3$ ). .....	304

<b>Figure 4.156.</b> $^{13}\text{C}$ NMR spectrum of <b>3.8</b> (151 MHz, 298 K, $\text{CDCl}_3$ ). .....	305
<b>Figure 4.157.</b> $^1\text{H}$ NMR spectrum of <b>3.10</b> (500 MHz, 298 K, $\text{CDCl}_3$ ). .....	305
<b>Figure 4.158.</b> $^{13}\text{C}$ NMR spectrum of <b>3.10</b> (101 MHz, 295 K, $\text{CDCl}_3$ ). .....	306
<b>Figure 4.159.</b> $^1\text{H}$ NMR spectrum of <b>3.12</b> (600 MHz, 298 K, $\text{CDCl}_3$ ). .....	306
<b>Figure 4.160.</b> $^{13}\text{C}$ NMR spectrum of <b>3.12</b> (151 MHz, 298 K, $\text{CDCl}_3$ ). .....	307
<b>Figure 4.161.</b> $^1\text{H}$ NMR spectrum of <b>3.13</b> (500 MHz, 298 K, $\text{CDCl}_3$ ). .....	307
<b>Figure 4.162.</b> $^{13}\text{C}$ NMR spectrum of <b>3.13</b> (151 MHz, 298 K, $\text{CDCl}_3$ ). .....	308
<b>Figure 4.163.</b> $^1\text{H}$ NMR spectrum of <b>3.14</b> (600 MHz, 298 K, $\text{CDCl}_3$ ). .....	308
<b>Figure 4.164.</b> $^{13}\text{C}$ NMR spectrum of <b>3.14</b> (101 MHz, 295 K, $\text{CDCl}_3$ ). .....	309
<b>Figure 4.165.</b> $^1\text{H}$ NMR spectrum of <b>3.15</b> (600 MHz, 298 K, $\text{CDCl}_3$ ). .....	309
<b>Figure 4.166.</b> $^{13}\text{C}$ NMR spectrum of <b>3.15</b> (101 MHz, 295 K, $\text{CDCl}_3$ ). .....	310
<b>Figure 4.167.</b> $^1\text{H}$ NMR spectrum of <b>3.17</b> (400 MHz, 295 K, $\text{CDCl}_3$ ). .....	310
<b>Figure 4.168.</b> $^{13}\text{C}$ NMR spectrum of <b>3.17</b> (151 MHz, 298 K, $\text{CDCl}_3$ ). .....	311
<b>Figure 4.169.</b> $^1\text{H}$ NMR spectrum of <b>3.18</b> (500 MHz, 295 K, $\text{CDCl}_3$ ). .....	311
<b>Figure 4.170.</b> $^{13}\text{C}$ NMR spectrum of <b>3.18</b> (151 MHz, 298 K, $\text{CDCl}_3$ ). .....	312
<b>Figure 4.171.</b> $^1\text{H}$ NMR spectrum of <b>3.19</b> + <b>3.66</b> (500 MHz, 295 K, $\text{CDCl}_3$ ). .....	312
<b>Figure 4.172.</b> $^{13}\text{C}$ NMR spectrum of <b>3.19</b> (101 MHz, 295 K, $\text{CDCl}_3$ ). .....	313
<b>Figure 4.173.</b> $^1\text{H}$ NMR spectrum of <b>3.20</b> (600 MHz, 295 K, $\text{CDCl}_3$ ). .....	313
<b>Figure 4.174.</b> $^{13}\text{C}$ NMR spectrum of <b>3.20</b> (101 MHz, 295 K, $\text{CDCl}_3$ ). .....	314
<b>Figure 4.175.</b> $^1\text{H}$ NMR spectrum of <b>3.21</b> (500 MHz, 298 K, $\text{CDCl}_3$ ). .....	314
<b>Figure 4.176.</b> $^{13}\text{C}$ NMR spectrum of <b>3.21</b> (101 MHz, 295 K, $\text{CDCl}_3$ ). .....	315
<b>Figure 4.177.</b> $^1\text{H}$ NMR spectrum of <b>3.22</b> (600 MHz, 298 K, $\text{CDCl}_3$ ). .....	315
<b>Figure 4.178.</b> $^{13}\text{C}$ NMR spectrum of <b>3.22</b> (101 MHz, 295 K, $\text{CDCl}_3$ ). .....	316
<b>Figure 4.179.</b> $^1\text{H}$ NMR spectrum of <b>3.67</b> + <b>3.68</b> (600 MHz, 298 K, $\text{CDCl}_3$ ). .....	316

<b>Figure 4.180.</b> $^{13}\text{C}$ NMR spectrum of <b>3.67</b> + <b>3.68</b> (151 MHz, 298 K, $\text{CDCl}_3$ ).....	317
<b>Figure 4.181.</b> $^1\text{H}$ NMR spectrum of <b>3.69</b> + <b>3.49</b> (600 MHz, 298 K, $\text{CDCl}_3$ ).....	317
<b>Figure 4.182.</b> $^1\text{H}$ NMR spectrum of the crude mixture of <b>3.63–3.65</b> (500 MHz, 298 K, $\text{CDCl}_3$ ). Assignments determined after purification.....	318
<b>Figure 4.183.</b> $^1\text{H}$ NMR spectrum of <b>3.23</b> + <b>3.70</b> (600 MHz, 298 K, $\text{CDCl}_3$ ).....	318
<b>Figure 4.184.</b> $^{13}\text{C}$ NMR spectrum of <b>3.23</b> + <b>3.70</b> (101 MHz, 295 K, $\text{CDCl}_3$ ).....	319
<b>Figure 4.185.</b> $^1\text{H}$ NMR spectrum of <b>3.71</b> (600 MHz, 298 K, $\text{CDCl}_3$ ).....	319
<b>Figure 4.186.</b> $^{13}\text{C}$ NMR spectrum of <b>3.71</b> (151 MHz, 298 K, $\text{CDCl}_3$ ).....	320
<b>Figure 4.187.</b> $^1\text{H}$ NMR spectrum of the crude mixture of <b>3.23</b> , <b>3.70</b> , <b>3.71</b> (400 MHz, 295 K, $\text{CDCl}_3$ ). Assignments determined after purification.....	320
<b>Figure 4.188.</b> $^1\text{H}$ NMR spectrum of <b>3.24</b> + <b>3.53</b> (500 MHz, 298 K, $\text{CDCl}_3$ ).....	321
<b>Figure 4.189.</b> $^{13}\text{C}$ NMR spectrum of <b>3.24</b> + <b>3.53</b> (151 MHz, 298 K, $\text{CDCl}_3$ ).....	321
<b>Figure 4.190.</b> $^1\text{H}$ NMR spectrum of <b>3.52</b> + impurity (500 MHz, 298 K, $\text{CDCl}_3$ ).....	322
<b>Figure 4.191.</b> $^1\text{H}$ NMR spectrum of crude mixture of <b>3.24</b> , <b>3.52</b> , <b>3.53</b> (500 MHz, 298 K, $\text{CDCl}_3$ ). Assignments determined after purification.....	322
<b>Figure 4.192.</b> $^1\text{H}$ NMR spectrum of <b>3.25</b> + <b>3.75</b> (400 MHz, 295 K, $\text{CDCl}_3$ ).....	323
<b>Figure 4.193.</b> $^{13}\text{C}$ NMR spectrum of <b>3.25</b> + <b>3.75</b> (126 MHz, 295 K, $\text{CDCl}_3$ ).....	323
<b>Figure 4.194.</b> $^1\text{H}$ NMR spectrum of the crude mixture of <b>3.25</b> , <b>3.75</b> (500 MHz, 298 K, $\text{CDCl}_3$ ). Assignments determined after purification.....	324
<b>Figure 4.195.</b> $^1\text{H}$ NMR spectrum of <b>3.26</b> + <b>3.78</b> (400 MHz, 295 K, $\text{CDCl}_3$ ).....	324
<b>Figure 4.196.</b> $^{13}\text{C}$ NMR spectrum of <b>3.26</b> + <b>3.78</b> (151 MHz, 298 K, $\text{CDCl}_3$ ).....	325
<b>Figure 4.197.</b> $^1\text{H}$ NMR spectrum of the crude mixture of <b>3.26</b> , <b>3.78</b> (500 MHz, 298 K, $\text{CDCl}_3$ ). Assignments determined after purification.....	325
<b>Figure 4.198.</b> $^1\text{H}$ NMR spectrum of <b>3.27</b> (500 MHz, 298 K, $\text{CDCl}_3$ ).....	326
<b>Figure 4.199.</b> $^{13}\text{C}$ NMR spectrum of <b>3.27</b> (151 MHz, 298 K, $\text{CDCl}_3$ ).....	326
<b>Figure 4.200.</b> $^1\text{H}$ NMR spectrum of <b>3.28</b> (500 MHz, 298 K, $\text{CDCl}_3$ ).....	327

<b>Figure 4.201.</b> $^{13}\text{C}$ NMR spectrum of <b>3.28</b> (151 MHz, 298 K, $\text{CDCl}_3$ ). .....	327
<b>Figure 4.202.</b> $^{19}\text{F}$ NMR spectrum of <b>3.28</b> (564 MHz, 298 K, $\text{CDCl}_3$ ). .....	328
<b>Figure 4.203.</b> $^1\text{H}$ NMR spectrum of <b>3.29</b> (500 MHz, 298 K, $\text{CDCl}_3$ ). .....	328
<b>Figure 4.204.</b> $^{13}\text{C}$ NMR spectrum of <b>3.29</b> (151 MHz, 298 K, $\text{CDCl}_3$ ). .....	329
<b>Figure 4.205.</b> $^1\text{H}$ NMR spectrum of <b>3.30</b> (600 MHz, 298 K, $\text{CDCl}_3$ ). .....	329
<b>Figure 4.206.</b> $^{13}\text{C}$ NMR spectrum of <b>3.30</b> (151 MHz, 298 K, $\text{CDCl}_3$ ). .....	330
<b>Figure 4.207.</b> $^1\text{H}$ NMR spectrum of <b>3.31</b> (500 MHz, 298 K, $\text{CDCl}_3$ ). .....	330
<b>Figure 4.208.</b> $^{13}\text{C}$ NMR spectrum of <b>3.31</b> (151 MHz, 298 K, $\text{CDCl}_3$ ). .....	331
<b>Figure 4.209.</b> $^1\text{H}$ NMR spectrum of <b>3.80</b> + thymol (600 MHz, 298 K, $\text{CDCl}_3$ ). .....	331
<b>Figure 4.210.</b> $^1\text{H}$ NMR spectrum of <b>3.32</b> (500 MHz, 298 K, $\text{CDCl}_3$ ). .....	332
<b>Figure 4.211.</b> $^{13}\text{C}$ NMR spectrum of <b>3.32</b> (151 MHz, 298 K, $\text{CDCl}_3$ ). .....	332
<b>Figure 4.212.</b> $^1\text{H}$ NMR spectrum of <b>3.33</b> (500 MHz, 298 K, $\text{CDCl}_3$ ). .....	333
<b>Figure 4.213.</b> $^{13}\text{C}$ NMR spectrum of <b>3.33</b> (151 MHz, 298 K, $\text{CDCl}_3$ ). .....	333
<b>Figure 4.214.</b> $^1\text{H}$ NMR spectrum of <b>3.43</b> (500 MHz, 298 K, $\text{CDCl}_3$ ). .....	334
<b>Figure 4.215.</b> $^{13}\text{C}$ NMR spectrum of <b>3.43</b> (151 MHz, 298 K, $\text{CDCl}_3$ ). .....	334
<b>Figure 4.216.</b> $^1\text{H}$ NMR spectrum of <b>3.44</b> (500 MHz, 298 K, $\text{CDCl}_3$ ). .....	335
<b>Figure 4.217.</b> $^{13}\text{C}$ NMR spectrum of <b>3.44</b> (151 MHz, 298 K, $\text{CDCl}_3$ ). .....	335
<b>Figure 4.218.</b> $^1\text{H}$ NMR spectrum of <b>3.45</b> (500 MHz, 298 K, $\text{CDCl}_3$ ). .....	336
<b>Figure 4.219.</b> $^1\text{H}$ NMR spectrum of <b>3.35</b> + <b>3.36</b> (400 MHz, 295 K, $\text{CDCl}_3$ ). .....	336
<b>Figure 4.220.</b> $^{13}\text{C}$ NMR spectrum of <b>3.35</b> + <b>3.36</b> (101 MHz, 295 K, $\text{CDCl}_3$ ). .....	337
<b>Figure 4.221.</b> $^1\text{H}$ NMR spectrum of <b>3.37</b> + <b>3.38</b> (600 MHz, 298 K, $\text{CDCl}_3$ ). .....	337
<b>Figure 4.222.</b> $^{13}\text{C}$ NMR spectrum of <b>3.37</b> + <b>3.38</b> (101 MHz, 295 K, $\text{CDCl}_3$ ). .....	338
<b>Figure 4.223.</b> $^1\text{H}$ NMR spectrum of <b>3.40</b> (600 MHz, 298 K, $\text{CDCl}_3$ ). .....	338
<b>Figure 4.224.</b> $^{13}\text{C}$ NMR spectrum of <b>3.40</b> (151 MHz, 298 K, $\text{CDCl}_3$ ). .....	339

<b>Figure 4.225.</b> $^1\text{H}$ NMR spectrum of <b>3.55</b> (500 MHz, 298 K, $\text{CDCl}_3$ ). .....	339
<b>Figure 4.226.</b> $^1\text{H}$ NMR spectrum of <b>3.46</b> + <b>3.47</b> (600 MHz, 298 K, $\text{CDCl}_3$ ). .....	340
<b>Figure 4.227.</b> $^{13}\text{C}$ NMR spectrum of <b>3.46</b> + <b>3.47</b> (101 MHz, 295 K, $\text{CDCl}_3$ ). .....	340
<b>Figure 4.228.</b> $^1\text{H}$ NMR spectrum of <b>3.48</b> (600 MHz, 298 K, $\text{CDCl}_3$ ). .....	341



## List of Tables

<b>Table 2.1.</b> Scope of <i>tert</i> -butylation of phenolic, aryl ether, and thiophene derivatives. 117	117
<b>Table 2.2.</b> Kinetic data for arene alkylation with di- <i>tert</i> -butylperoxide. .... 122	122
<b>Table 2.3.</b> Survey of conditions for direct Friedel–Crafts alkylation with phenolic <b>2.5</b> and alcohol <b>2.38</b> . .... 126	126
<b>Table 2.4.</b> Scope of dual Brønsted/Lewis acid catalyzed, C(sp <sup>2</sup> )–C(sp <sup>3</sup> ) coupling between phenolic and tertiary alcohol derivatives. <sup>a</sup> ..... 127	127
<b>Table 2.5.</b> Optimization conditions with 2-methylanisole ( <b>2.58</b> ). .... 129	129
<b>Table 2.6.</b> Scope of dual Brønsted/Lewis acid-catalyzed, C(sp <sup>2</sup> )–C(sp <sup>3</sup> ) coupling between arene and tertiary alcohol derivatives. <sup>a</sup> ..... 131	131
<b>Table 2.7.</b> Kinetic data for arene alkylation with <i>tert</i> -butanol. .... 132	132
<b>Table 2.8.</b> Free energy calculated from eqn (2.5) to estimate the increased Brønsted acid/Lewis acid pairs (HA/L) discussed in this study. .... 140	140
<b>Table 3.1.</b> Survey of conditions for direct Friedel–Crafts alkylation. .... 178	178
<b>Table 3.2.</b> Optimization of the reaction conditions. .... 179	179
<b>Table 3.3.</b> Scope of Friedel–Crafts alkylations with unactivated secondary alcohols. <sup>a</sup> . 181	181
<b>Table 3.4.</b> Racemic or enantioenrich alcohol <b>3.57</b> result in racemic product (±)- <b>3.15</b> .. 186	186
<b>Table 3.5.</b> Kinetic data for arene alkylation with adamant-2-ol. .... 190	190

## List of Schemes

<b>Scheme 1.1.</b> Generally accepted mechanisms of Rh-carbene or Rh-carbenoid formation.	4
<b>Scheme 1.2.</b> A concerted but asynchronous mechanism pathway, proposed by Nakamura and coworkers.	6
<b>Scheme 1.3.</b> General mechanism of nucleophilic X–H bond insertions.	6
<b>Scheme 1.4.</b> Mechanistic insights and possible intermediates in the O–H bond insertion.	7
<b>Scheme 1.5.</b> Proposed transition states for proton transfer catalysis.	8
<b>Scheme 1.6.</b> General mechanism of the Büchner-Curtius-Schlotterbeck reaction.	11
<b>Scheme 1.7.</b> Mechanism of the Kowalski ester homologation for formal C–C bond insertion.	13
<b>Scheme 1.8.</b> Proposed mechanism of oxidative addition into strained ring.	17
<b>Scheme 1.9.</b> Selective $\beta$ -carbon elimination of cyclobutanol-containing bicycles.	18
<b>Scheme 1.10.</b> Proposed mechanism of palladium-catalyzed Heck coupling/C–C bond activation.	20
<b>Scheme 1.11.</b> Proposed mechanism.	21
<b>Scheme 1.12.</b> Target transformation and proposed transition state.	23
<b>Scheme 1.13.</b> Proposed pathway to indanone <b>1.44</b> .	30
<b>Scheme 2.1.</b> Traditional Friedel-Crafts reaction and widely accepted mechanism.	98
<b>Scheme 2.2.</b> Proposed mechanism. Initiation with Lewis acid followed by autocatalysis with HF.	100
<b>Scheme 2.3.</b> Proposed mechanism of molybdenum/chloranil-catalyzed Friedel–Crafts alkylation.	101
<b>Scheme 2.4.</b> Proposed mechanism, with the possibility of forming HBr assisted by HFIP.	103
<b>Scheme 2.5.</b> Possible resonance-stabilization of benzylic tertiary carbocation.	110

<b>Scheme 2.6.</b> Proposed mechanism. Potential carbocation intermediate retaining stereochemistry. ....	111
<b>Scheme 2.7.</b> Proposed pathways for the decomposition of DTBP ( <b>2.6</b> ). (a) Fe(III) initiated pathway. (b) Fe(II) initiated pathway. ....	120
<b>Scheme 3.1.</b> Proposed mechanism. ....	191

## List of Abbreviations

ATR	attenuated total reflectance
BHT	butylated hydroxytoluene
Bn	benzyl
CAT	chiral amino-thiourea
cod	1,5-cyclooctadiene
CSA	camphorsulfonic acid
CyOH	cyclohexanol
DBU	1,8-diazabicyclo[5.4.0]undec-7-ene
DCE	dichloroethane
DCM	dichloromethane
DFT	density functional theory
dH <sub>2</sub> O	distilled water
DI	deionized
DIBAl-H	diisobutylaluminum hydride
DMF	<i>N,N</i> -dimethylformamide
DMSO	dimethylsulfoxide
DTBP	di- <i>tert</i> -butylperoxide
EAS	electrophilic aromatic substitution
EDA	ethyl diazoacetate
EI	electron ionization
ESI	electrospray ionization
EtOAc	ethyl acetate
FT-IR	fourier transform infrared spectroscopy
HFIP	1,1,1,3,3,3-hexafluoroisopropanol
HRMS	high-resolution mass spectrometry
IR	infrared
KHMDS	potassium bis(trimethylsilyl)amide
LDA	lithium diisopropylamide

LiTMP	lithium 2,2,6,6-tetramethylpiperidine
MHz	megahertz
NHC	nucleophilic heterocyclic carbene
NMR	nuclear magnetic resonance
OTf	trifluoromethanesulfonate
<i>p</i> -ABSA	4-acetamidobenzenesulfonyl azide
PCC	pyridinium chlorochromate
ppm	parts per million
SFC	supercritical fluid chromatography
TEMPO	(2,2,6,6-tetramethylpiperidin-1-yl)oxyl
TFA	trifluoroacetic acid
TfOH	trifluoromethanesulfonic acid
THF	tetrahydrofuran
TLC	thin layer chromatography
TMS	trimethylsilyl
Tp*Cu	copper hydrotris(3,5-dimethylpyrazolyl) borate
Ts	toluene sulfonyl

## Chapter 1 – Intramolecular Carbene Insertion into Strained Cyclopropyl C–C

### Bonds

#### 1.1.1 Introduction – Carbenes and metal-carbene types

Carbenes are neutral methylene motifs bearing a lone pair and a valence electron count of six: four electrons from the two bonds and an additional two electrons from the lone pair. In contrast to its triplet state, the singlet state is most common, resembling the trigonal planar geometry (**Figure 1.1**). Carbene motifs with unfilled valence shell tend to be very reactive and are generally unisolable, requiring synthesis *in situ*.

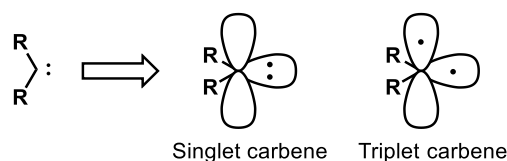


**Figure 1.1.** Carbene in its singlet and triplet state.

Within the last 4–5 decades, metal-carbenes (or carbenoids) have been developed and studied in depth. The reactivity of such metal-carbenes can be broken down into two main categories of carbenes: Fischer-type carbenes (electrophilic at the carbene site) and Schrock-type carbenes (nucleophilic at the carbene site). Fischer-type carbenes commonly involve electron-withdrawing groups as well as OR/NR<sub>2</sub> groups<sup>1</sup> attached to the carbene site, which enhance its electrophilic nature (**Figure 1.2**). Fischer-type carbenes tend to associate with late transition metals, such as rhodium, chromium, palladium, and iron. On the other hand, Schrock-type carbenes commonly involve electron-donating alkyl or aryl groups attached to the central carbene atom, which render it more electron-rich and

therefore increase its nucleophilicity. Most Schrock-type carbenes are associated with early transition metals, such as titanium, molybdenum, and tungsten. This chapter will delve into electrophilic Fischer-type carbenes, which is a major focus of this dissertation.

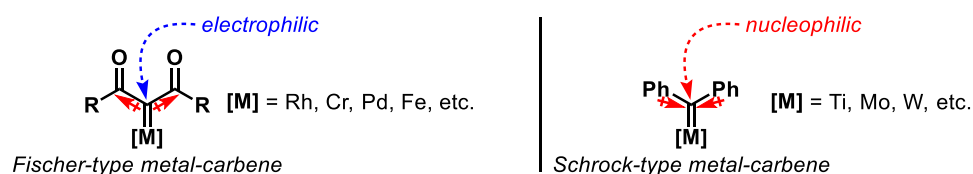


**Figure 1.2.** Fischer- and Schrock-type carbenes.

With a few exceptions, most metal-carbenes are too unstable to be isolable and therefore must be generated *in situ*. As such, precursors to generate metal-carbenes are utilized. The most common precursors to metal-carbenes are diazo and *N*-sulfonyl-type hydrazones due to their simple synthesis routes (**Figure 1.3**). Diazo compounds **1.1** can be accessed with diazo-transfer reagents, such as sulfonyl azides. It is worthy to mention the shock-sensitive and explosive nature of many azide (and diazo) reagents, and rigorous measures of care should be taken when handling such compounds.<sup>2</sup> Common *N*-sulfonyl-type hydrazones include *N*-tosyl and *N*-nosyl hydrazones **1.2**, which can be accessed by a condensation reaction of a ketone or aldehyde with the corresponding hydrazine. These hydrazones can be thought of as “masked” diazo compounds, where upon addition of a base, the proton on the nitrogen of the hydrazone motif is abstracted and the sulfonyl group departs to generate the diazo intermediate *in situ* (**Figure 1.4**). Exposure to photochemical or thermal conditions leads to N<sub>2(g)</sub> extrusion and direct formation of the requisite carbene.<sup>3</sup>

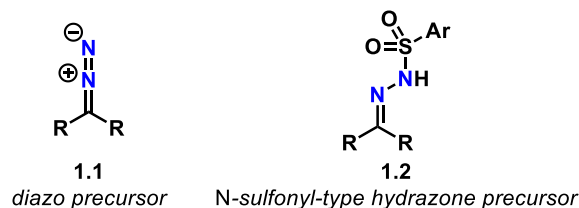


**Figure 1.3.** Common carbene precursors.

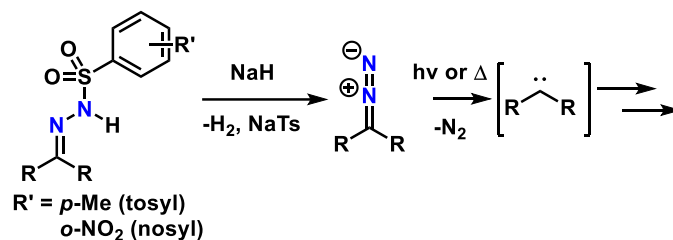
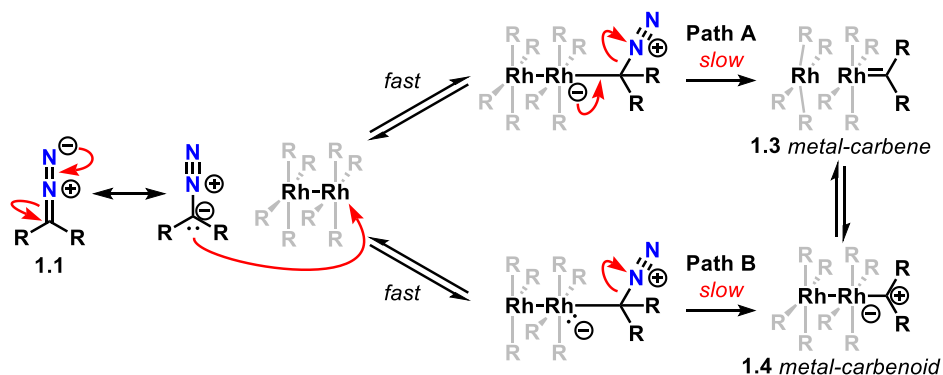


**Figure 1.4.** Carbene formation from sulfonyl hydrazones.

Alternatively, the metal-carbene can be formed when a late transition metal catalyst is added to these precursor compounds (**Scheme 1.1**). As a consequence of resonance contributions, the diazo compound (**1.1**) exhibits carbanionic character, which engages the metal. Formation of the metal-carbene **1.3** can occur through two generally accepted mechanisms: backbonding from the metal center can form the carbon-metal double bond (formally a “metal-carbene” **1.3**, path A) and extrude  $\text{N}_{2(\text{g})}$ , or  $\text{N}_{2(\text{g})}$  will leave to form a carbon-metal ylide (formally a “metal-carbenoid” **1.4**, path B). It has been observed experimentally by Pirrung and through calculations by Nakamura that the cleavage of the C–N bond is rate-determining in the formation of the rhodium-carbene or rhodium-carbenoid.<sup>4</sup> Although the carbon-rhodium double bond is commonly drawn and referred to as the metal-carbene species (**1.3**), the metal-carbenoid species (**1.4**) is the more correct representation due to the former having 20 electrons around rhodium. Due to their



instability, they often react extremely quickly, performing a wide variety of X–Y bond insertions (Y is most commonly H), as well as alkene and alkyne insertions.



**Scheme 1.1.** Generally accepted mechanisms of Rh-carbene or Rh-carbenoid formation.

### 1.1.2 Carbene-mediated X–H, alkene, and alkyne bond activation reactions

Activation of X–H bonds by carbene insertion to form new X–CR<sub>2</sub>–H bonds are common applications of metal-carbene reactivity (**Figure 1.5**). Many X–H bond insertion strategies have been studied and implemented, including but not limited to C–H, Si–H, O–H, N–H, and S–H bonds, as well as alkenes and alkynes.

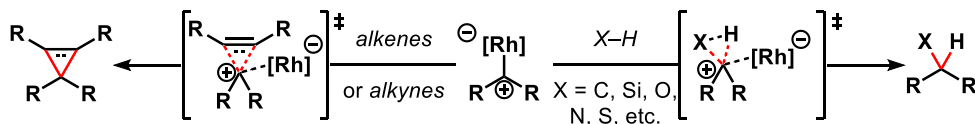


**Figure 1.5.** Reactions of metal-carbenes with various X–Y bonds.

In 1982, Taber and coworkers<sup>5</sup> studied the reactivity of intramolecular rhodium-catalyzed carbene C–H insertions in detail, where 5-membered rings were produced exclusively (**Figure 1.6**). As long as a C–H bond is present at the position in the carbon chain  $\delta$  from the carbene, the direct C–H bond activation pathway predominates regardless

of substitution, the presence of olefins, or the carbon chain length. These results suggest that formation of the five-membered ring predominates over cyclopropanation and cyclopropanation even in the presence of  $\pi$ -systems.

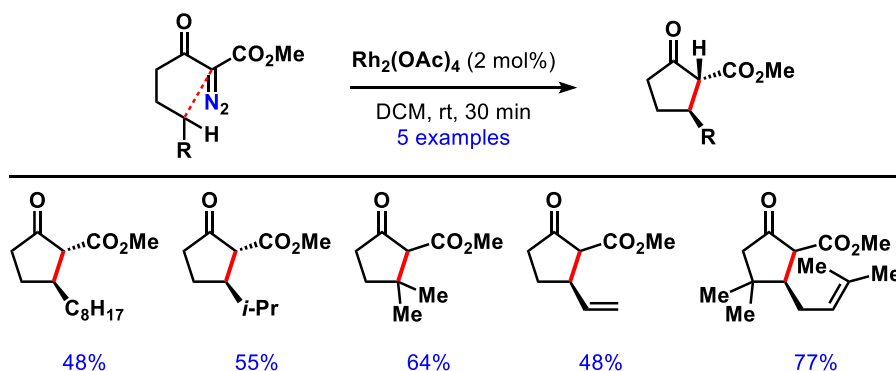
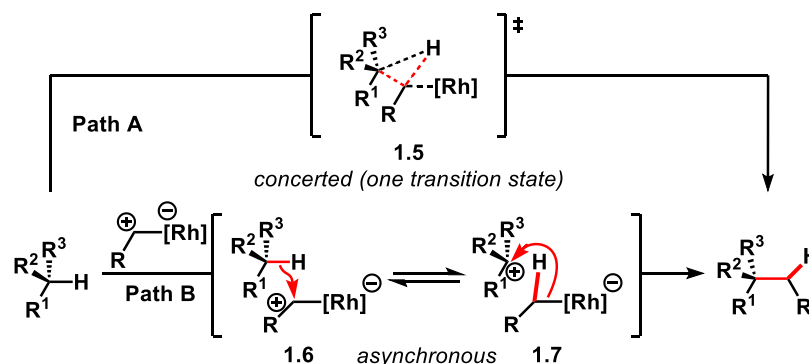


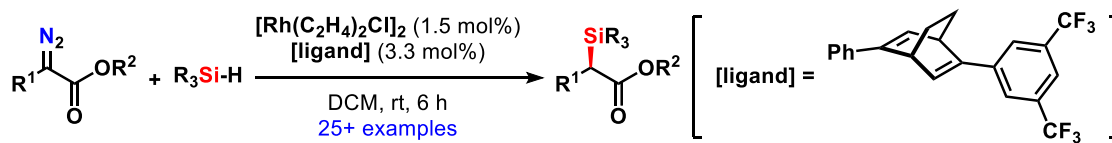
**Figure 1.6.** Intramolecular C–H activation/cyclization to exclusively form cyclopentenones.

The mechanism of C–H insertion is thought to be concerted, however Nakamura and coworkers<sup>4b</sup> reported the possibility of an asynchronous process (**Scheme 1.2**); although only one transition state is proposed (Path A, **1.5**), not all bonds forming and breaking are necessarily occurring at the same time (Path B, **1.6**  $\rightarrow$  **1.7**). Concerted but asynchronous mechanisms of other reactions have been previously reported.<sup>6</sup> A similar application to silanes is utilized, where the carbene is inserted between the Si–H bond (**Figure 1.7**).<sup>7</sup>

Insertion into O–H, N–H, and S–H bonds all occur through a more straightforward mechanism (**Scheme 1.3**), where the nucleophilic heteroatoms first attack the electrophilic carbene (**1.8**), followed by departure of the transition metal to form enolate or stabilized carbanion **1.9**, and a final proton transfer to arrive at product **1.10**.



**Scheme 1.2.** A concerted but asynchronous mechanism pathway, proposed by Nakamura and coworkers.



*select examples*

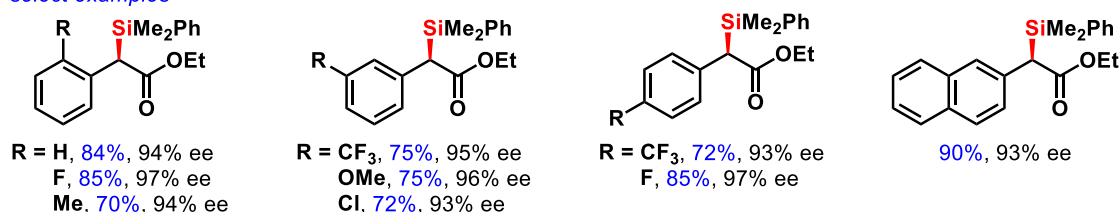
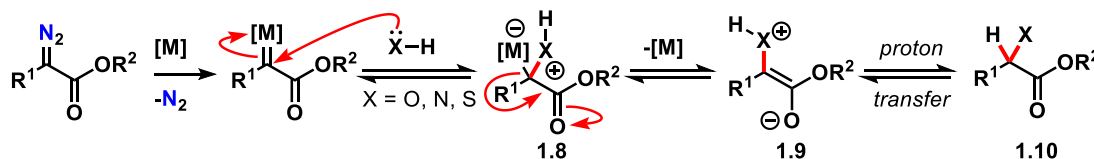


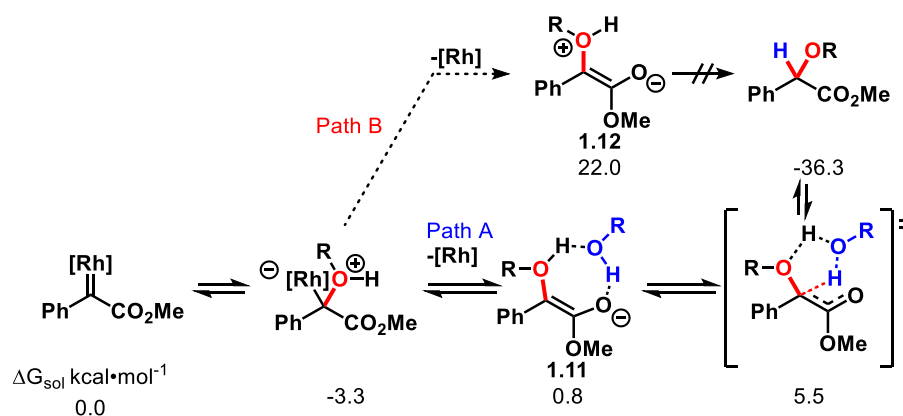
**Figure 1.7.** Select examples of metal-carbene mediated Si–H bond insertion.



**Scheme 1.3.** General mechanism of nucleophilic X–H bond insertions.

In 2014, Xie, Verpoort, Fang and coworkers<sup>8</sup> elaborated on the mechanism of general O–H bond insertions from metal-carbenes<sup>9</sup> through DFT studies. These calculations suggest that formation of enolate **1.11** is plausible, enabled by intermolecular hydrogen-bonding with an equivalent of alcohol (Path A, **Scheme 1.4**). At the

M06/BSI/SMD//B3LYP/BSI level, dissociation of rhodium to form the enolate (**1.12**) requires a high energy barrier of 25.3 kcal•mol<sup>-1</sup> (Path B), while hydrogen-bonding support drastically lowers the activation energy barrier to only 4.1 kcal•mol<sup>-1</sup>, favoring the latter pathway by 21.2 kcal•mol<sup>-1</sup>. This work supports how metal-carbene-mediated O–H bond insertions can occur at room temperature or even lower.<sup>10</sup> The authors stated that while other X–H bond insertions may occur similarly (X = N, S, etc.), they may not necessarily follow the same mechanistic regime and the exact nature of the X–H bond should be considered for subsequent mechanistic studies of new transformations.



**Scheme 1.4.** Mechanistic insights and possible intermediates in the O–H bond insertion.

In 2019, Zhu, Zhou and coworkers<sup>11</sup> utilized a copper-borate (Tp\*Cu) complex along with a chiral amino-thiourea (CAT) catalyst to perform a highly enantioselective N–H insertion into diazo compounds (**Figure 1.8**). The mechanism follows the generally accepted pathway (see **Scheme 1.3**) up until enolate formation, where the proton transfer step is key in generating enantioselectivity (**Scheme 1.5**). According to DFT studies, the transition state (2.8 kcal•mol<sup>-1</sup> versus 7.7 kcal•mol<sup>-1</sup>) in which the thiourea catalyst acts as

a chiral proton donor is favored, obtaining enantioenriched products in high to excellent enantiomeric excess.

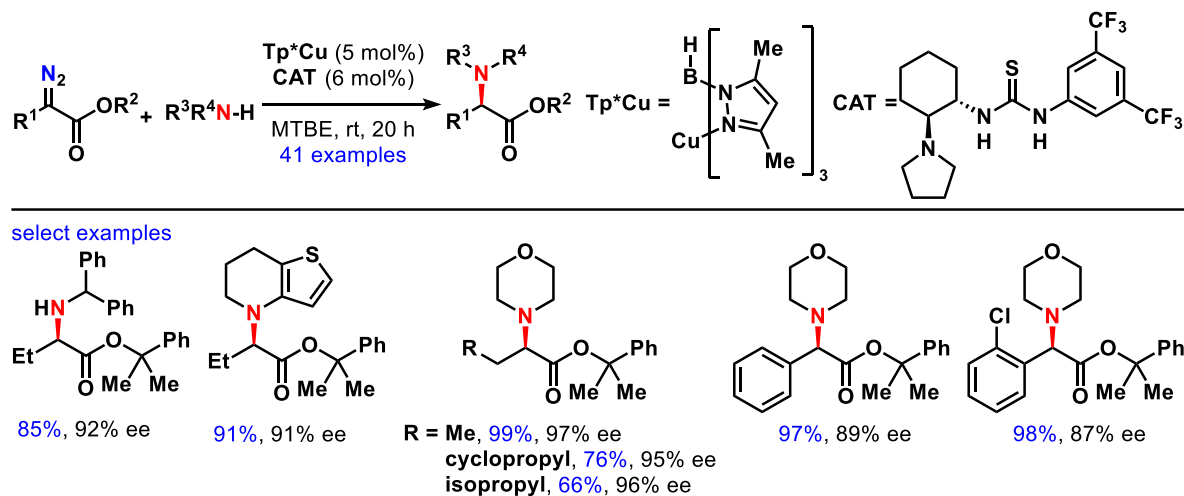
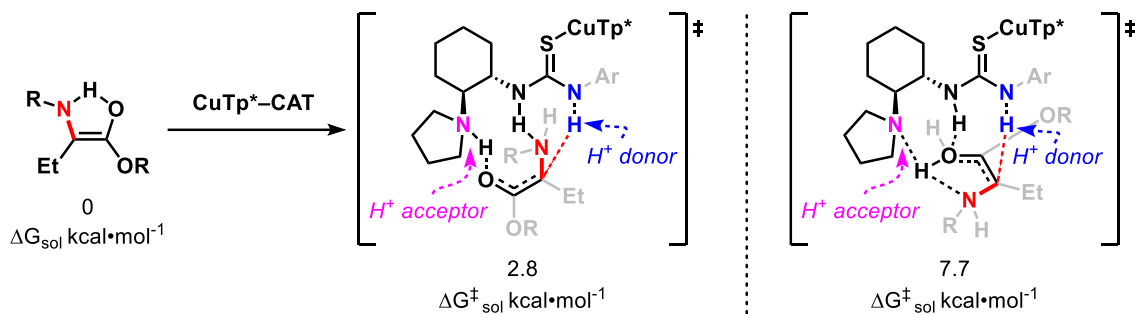


**Figure 1.8.** Select examples of metal-carbene mediated N–H bond insertion.



**Scheme 1.5.** Proposed transition states for proton transfer catalysis.

In 2016, Deng and coworkers<sup>12</sup> demonstrated further application of their methodology in synthesizing diazo-pyranone products. They showed both an example of rhodium-catalyzed N–H and S–H bond insertion in high yields (**Figure 1.9**).

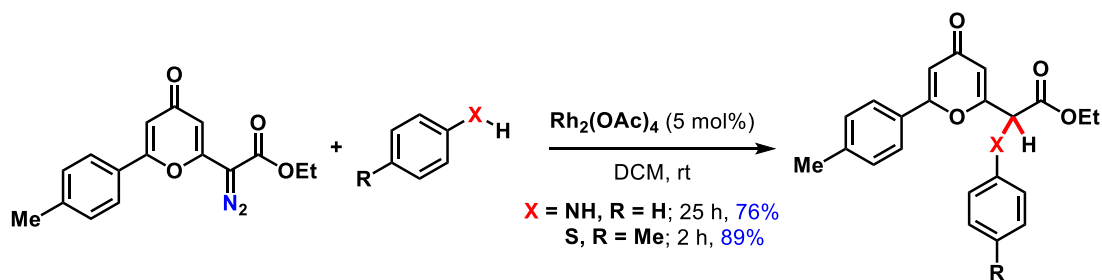


**Figure 1.9.** Examples of N–H and S–H bond insertions.

Activation of olefins toward cyclopropanation is also possible<sup>13</sup> (**Figure 1.10**). As reported by Taber and coworkers in 1982<sup>5</sup> (see **Scheme 1.2**), outcompeting C–H activations over alkene cyclopropanation limits the utility of this application. Epoxidation by carbonyl insertion can be favored over cyclopropanation, depending on the reaction conditions and catalyst<sup>13,14</sup> (**Figure 1.11**).

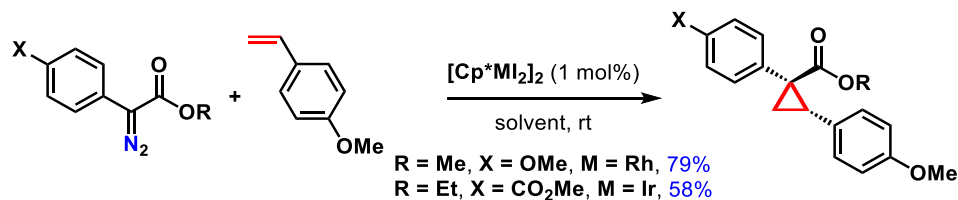


**Figure 1.10.** C=C bond insertions of styrene motifs to cyclopropanate.

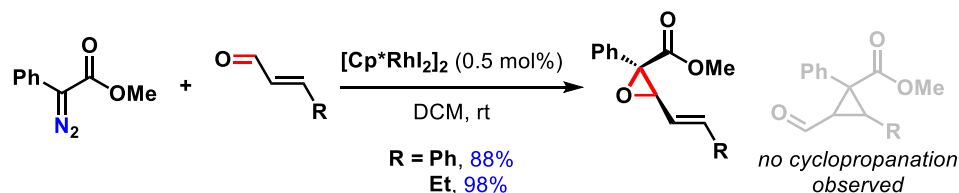


**Figure 1.11.** C=O bond insertion to form epoxides over C=C bond insertion.

Cyclopropanation of alkynes<sup>15</sup> achieves cyclopropenes **1.13** (**Figure 1.12**). Just like with olefins, alkynes suffer from competing reactions depending on the reaction conditions

and the alkyne motif. In some cases, 1,2-hydride shifts may occur (**1.14**) to afford alkenes over cyclopropenation (**1.13**). With different Rh(II) complexes, Hashimoto and coworkers found that they were able to modestly control for C≡C bond insertion versus intramolecular 1,2-hydride shift in overall moderate yields.

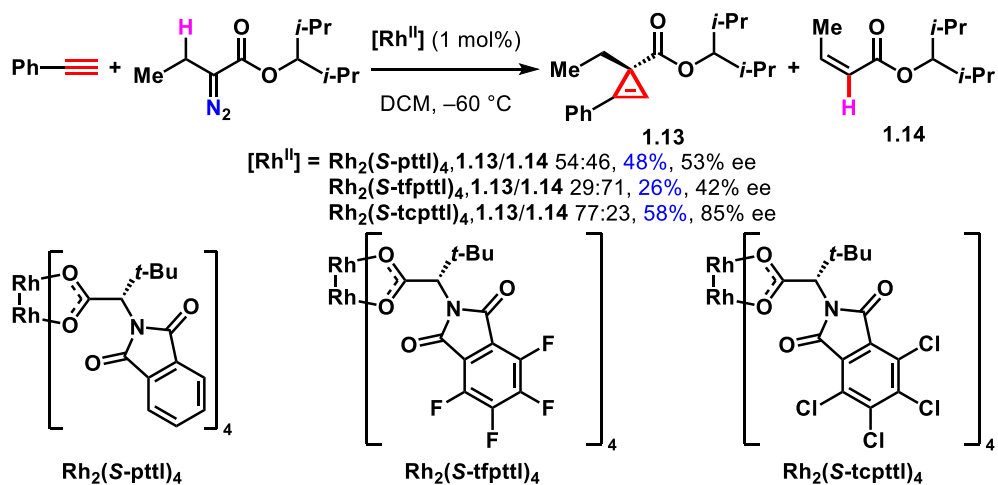


**Figure 1.12.** Competing C≡C bond insertion versus intramolecular 1,2-hydride shift.

C–C single bond activation/insertion is a topic of growing interest but with few ways to achieve.<sup>16–36</sup> Most strategies to formally activate a C–C bond involve rearrangements or activation of less benign X–Y bonds, followed by a variety of rearrangement strategies. Strained rings, namely cyclopropyl or cyclobutyl rings, are also utilized to take advantage of inherently weaker C–C bonds due to their extreme angular strains.

### 1.1.3 C–C single bond activation reactions

Reactions involving diazo compounds performing formal C–C bond insertions have been studied as early as 1885<sup>16</sup> by Büchner, Curtius, and later Schlotterbeck.<sup>17</sup> A

diazoalkane is reacted with an aldehyde or ketone before a 1,2-alkyl or hydride shift occurs to extrude  $N_{2(g)}$ ,<sup>18</sup> which is now known as the Büchner-Curtius-Slotterbeck reaction (**Scheme 1.6**). The scope of compatible ketones and diazo compounds have been improved greatly. For example, in 2020, Krasavin and coworkers<sup>19</sup> utilized a diazo-pyrrolidone to generate spirocyclic pyrrolidones by ring expanding cyclohexanones (**Figure 1.13**). In the case of Boc-protected diazo-pyrrolidones, cleavage of the Boc group occurred over the course of the reaction.

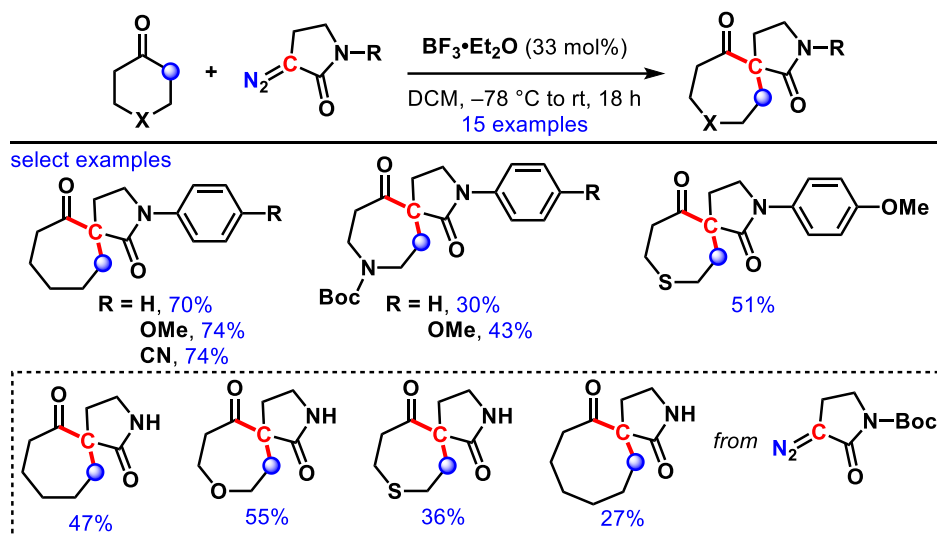
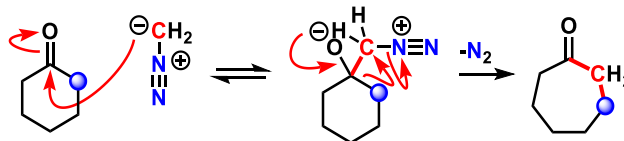


**Figure 1.13.** Diazo-pyrrolidones partaking in an improved Büchner-Curtius-Slotterbeck reaction.



**Scheme 1.6.** General mechanism of the Büchner-Curtius-Slotterbeck reaction.



The Arndt-Eistert synthesis, developed in 1935,<sup>20</sup> effects a one-carbon homologation reaction of carboxylic acids (**Figure 1.14**). The carboxylic acid is converted to an acid chloride before reacting with two equivalents of a diazoalkane, such as diazomethane. Two equivalents are required due to the formation of HCl during the process: one equivalent of the diazoalkane is consumed by the HCl. Alternatively, a weak base such as Et<sub>3</sub>N can be used. With Ag<sub>2</sub>O, a Wolff rearrangement can generate a ketene intermediate, which can be converted to the homologated carboxylic acid with water, to an ester with an alcohol, or to an amide with an amine. Overall, this synthesis demonstrates a formal C–C bond insertion of a carboxylic acid.

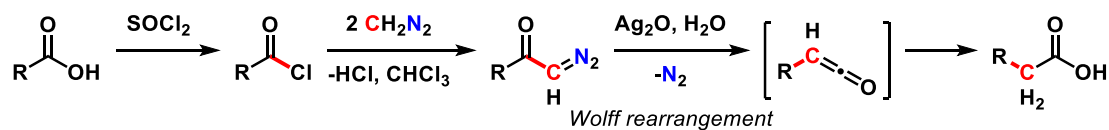
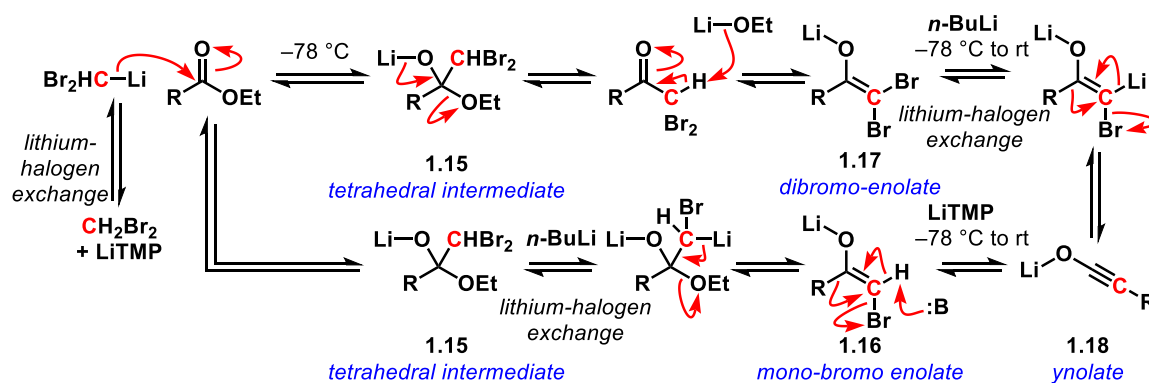


**Figure 1.14.** Arndt-Eistert synthesis for a formal C–C bond insertion of carboxylic acids.

In 1985, Kowalski and coworkers<sup>21</sup> developed a one-step, formal C–C bond insertion of esters (**Scheme 1.7**), known as the Kowalski ester homologation. At  $-78\text{ }^{\circ}\text{C}$ , addition of (dibromomethyl)lithium, which can be prepared *in situ* with methylene bromide and lithium 2,2,6,6-tetramethylpiperidine (LiTMP), to an ester will generate a mixture of intermediates: tetrahedral intermediate **1.15**, mono-enolate **1.16**, and dibromo enolate **1.17**. Tetrahedral intermediate **1.15** can be converted to the mono-bromo enolate **1.16** by rapid lithium-halogen exchange with subsequent addition of *n*-butyllithium. Dibromo-enolate **1.17** can also react with *n*-butyllithium by lithium-halogen exchange and generate ynolate **1.18**. Mono-bromo enolate **1.16** does not readily react at such cold temperatures but can be deprotonated with remaining LiTMP at  $0\text{ }^{\circ}\text{C}$  and will generate the same ynolate **1.18**.

Therefore, to ensure intermediates **1.15**–**1.17** all funnel to ynoate **1.18**, the solution is warmed to rt. The ynoate can generate the product cleanly after the reaction mixture is added to an ice-cold solution of acidic ethanol (prepared by adding acetyl chloride to absolute ethanol), followed by aqueous work-up. If the ethanol solution is added to the reaction mixture, then it is likely that very little product is obtained<sup>22</sup> (**Figure 1.15**). Although thermal control and slow addition of most solutions must be rigorously undertaken throughout the experiment, the resulting product typically does not require purification and accesses the homologation product in one step as opposed to the Arndt-Eistert synthesis that requires several steps.



**Scheme 1.7.** Mechanism of the Kowalski ester homologation for formal C–C bond insertion.

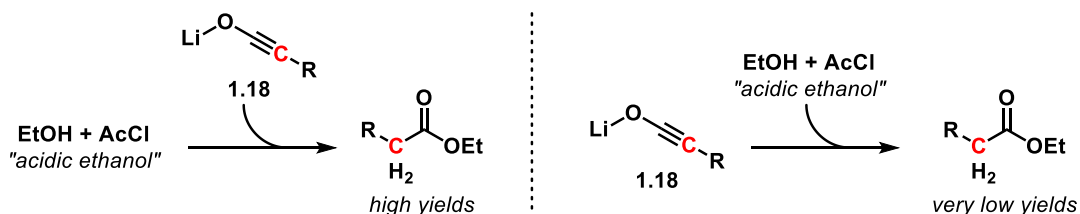
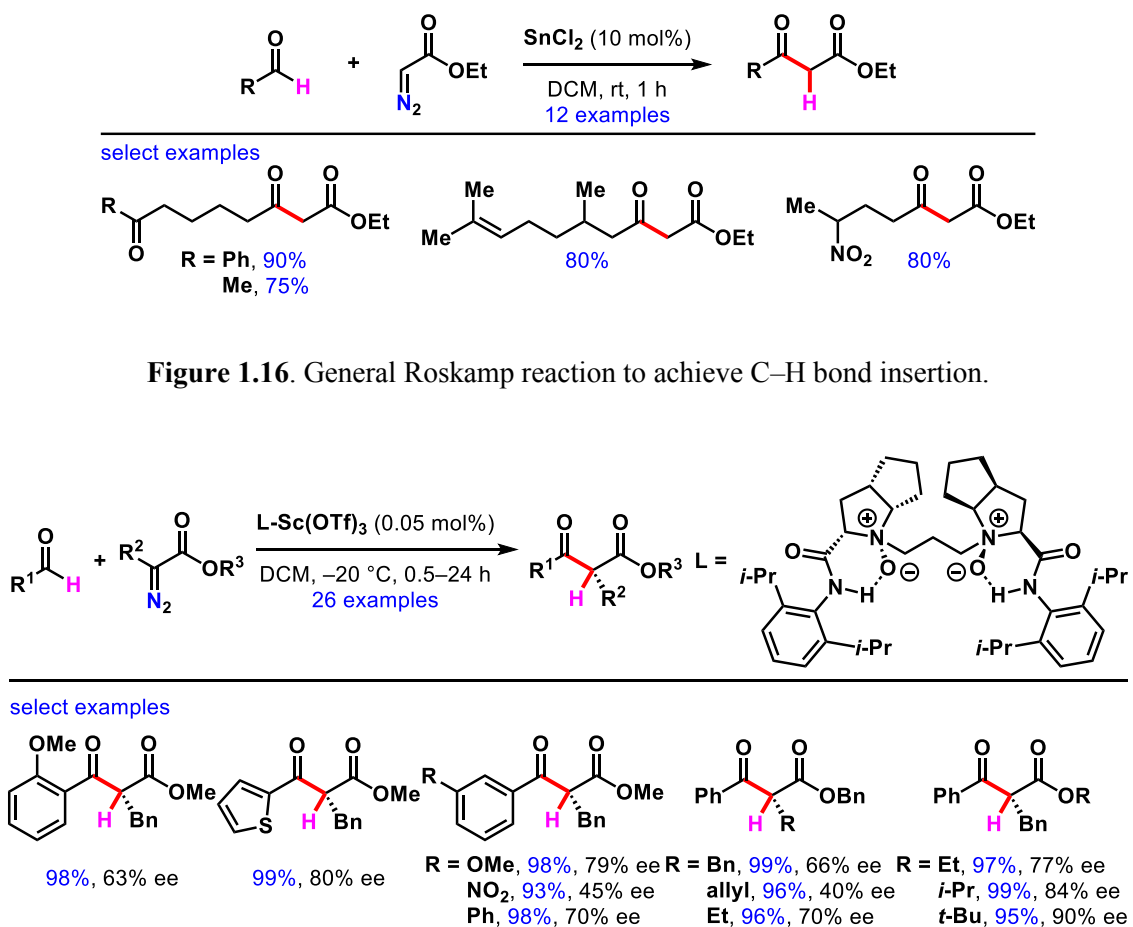


**Figure 1.15.** Importance of adding the ynoate intermediate to acidic ethanol.

In 1989, Roskamp and coworkers<sup>23</sup> developed a tin-catalyzed C–H bond insertion of aldehydes using ethyl diazoacetate (**Figure 1.16**). This work was further developed in 2010 by Feng and coworkers,<sup>24</sup> utilizing more complex diazo compounds to achieve the first asymmetric Roskamp reaction, which is now referred to as the Roskamp-Feng reaction (**Figure 1.17**). Ethyl benzyldiazoacetate or a similar  $\alpha$ -alkyl- $\alpha$ -diazo ester was reacted with an arylaldehyde with  $\text{Sc}(\text{OTf})_3$  and a chiral  $N,N'$ -dioxide ligand to achieve  $\beta$ -ketoesters in high yields and moderate enantioselectivity. This reaction represents a formyl C–H bond insertion.



In 2013, Feng and coworkers<sup>25</sup> expanded the reaction even further to accomplish a formal C–C bond insertion with an yttrium catalyst and a similar chiral *N,N'*-dioxide ligand (**Figure 1.18**). Here, an  $\alpha$ -ketoester and an  $\alpha$ -alkyl- $\alpha$ -diazo ester are utilized, in which the diazo compound attacks the ketone carbonyl. A 1,2-aryl shift to extrude  $N_2(g)$  affords enantioenriched succinate derivatives in moderate to high yields. Finally, in 2023–2024, Ryu and coworkers<sup>26</sup> developed a formal C–C bond insertion of glyoxals (**Figure 1.19**), where they were able to promote a 1,2-acyl shift over a 1,2-hydride shift.<sup>27</sup> This oxazaborolidinium-catalyzed Roskamp-Feng-type reaction<sup>26</sup> results in  $\alpha$ -formyl- $\beta$ -ketoester products. As of now, there is no proposed rationale for why the 1,2-acyl shift was observed over the typical 1,2-hydride shift. One possibility is that after the diazo compound attacks the aldehyde, the hydride is not in an anti-periplanar arrangement and there is limited freedom of rotation due to the extremely bulky nature of the Lewis acid. This could potentially favor shifting of the acyl group over the hydride; however, there remains a lack of mechanistic support.

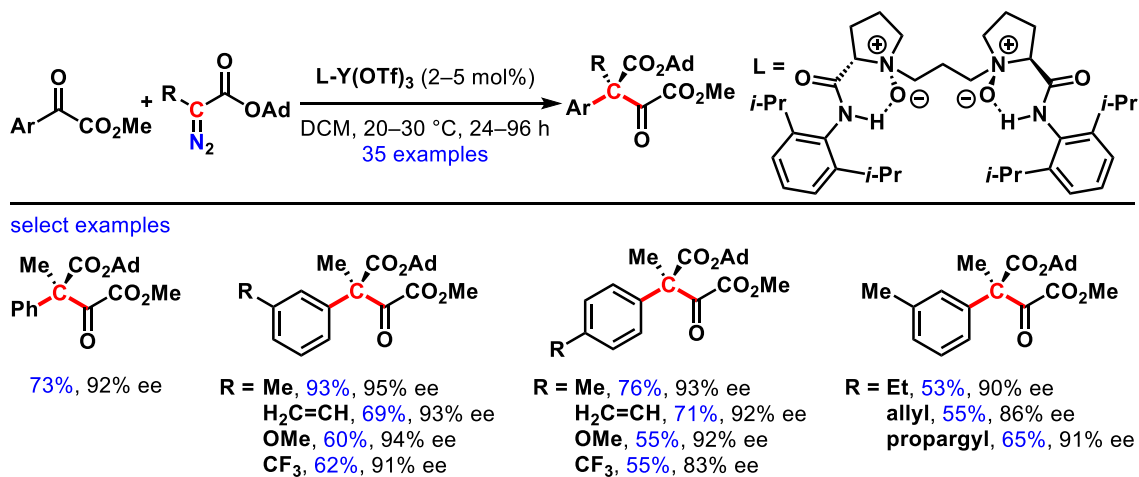


**Figure 1.18.** Enantioselective yttrium-catalyzed formal C–C bond insertion.

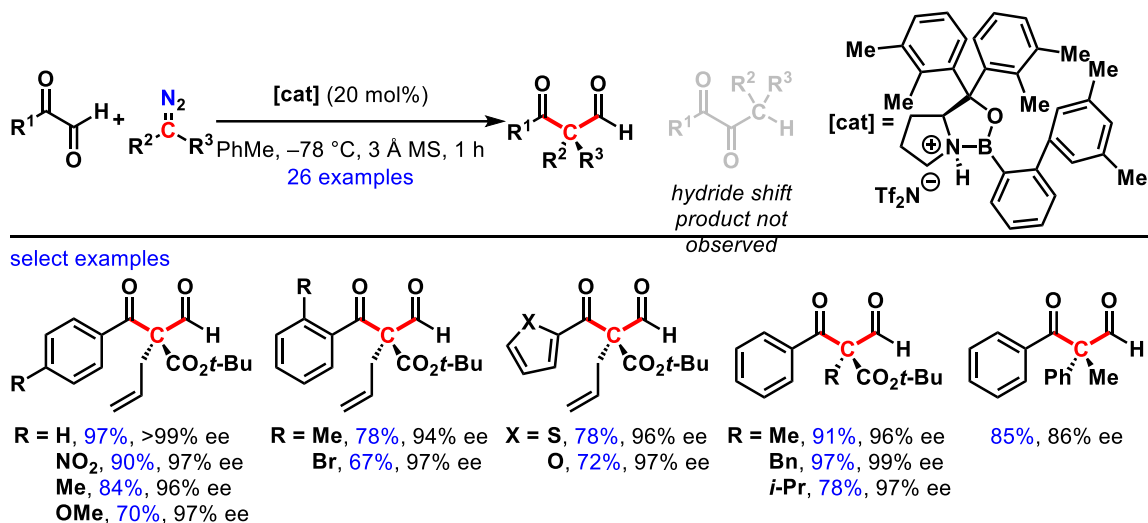


**Figure 1.19.** Oxazaborolidinium-catalyzed formal C–C bond insertion over C–H bond insertion.

Direct oxidative addition of transition metals into C–C bonds is a highly challenging endeavor due to the inertness of most C–C bonds.<sup>28</sup> In most circumstances, the reverse reductive elimination to break two C–transition metal bonds ( $2 \times \sim 30\text{--}40$  kcal/mol) and form a new C–C bond ( $\sim 85\text{--}90$  kcal/mol) is thermodynamically favored (**Figure 1.20**).<sup>29</sup> Methods and techniques to activate C–C bonds include raising the ground state of the starting material containing the target C–C bond, such as by using small, strained rings. Examples of C–C bond activation therefore often involve oxidative addition into strained systems. These methods are used to overcome the unfavorable outcomes arising from cleaving unactivated C–C bonds.

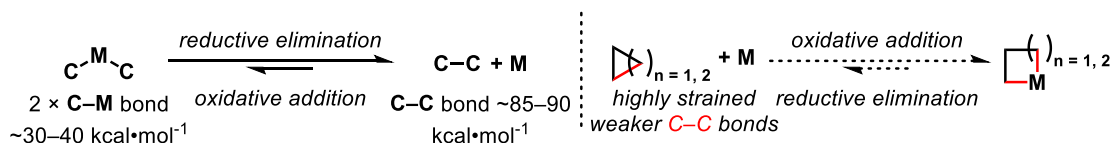


**Figure 1.20.** Normal C–C bonds are inert. Adding strain to the C–C bond can help with oxidative addition.

Direct oxidative addition into a C–C bond was utilized in 2021 by Dong and coworkers<sup>30</sup> in a total synthesis of penicibilaene A and B (**Figure 1.21**). The group took advantage of the strained C–C bond in the cyclobutanone motif, synthesized in three steps. Condensation of an amine as a directing group facilitated rhodium-catalyzed insertion in between the methylene-imine C–C bond (**Scheme 1.8**). This allowed for subsequent migratory insertion of the tethered alkene into the metal-carbon bond, followed by reductive elimination, and hydrolysis of the imine to achieve the desired tricyclic product in moderate yield.

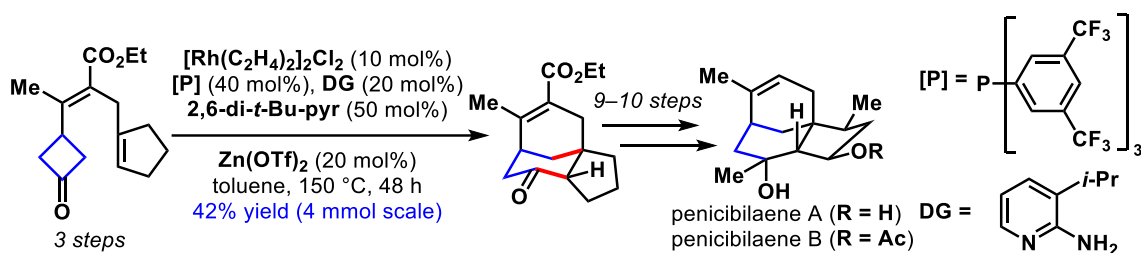
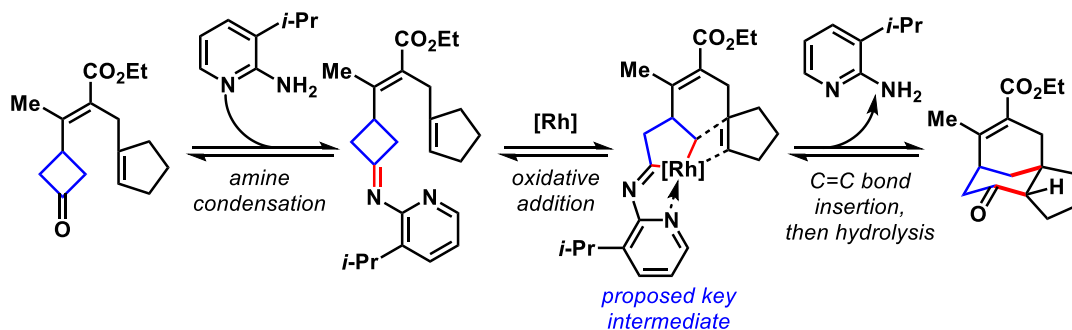


**Figure 1.21.** Total synthesis of two natural products through a key C–C bond insertion step.



**Scheme 1.8.** Proposed mechanism of oxidative addition into strained ring.

A common strategy implemented to achieve formal C–C bond insertion involves cyclobutanone derivatives. In 2012, Murakami and coworkers<sup>31</sup> demonstrated utilizing rhodium-catalyzed formal alkyne insertion between the C–C bond of benzocyclobutanols

to access dihydronaphthalenols (**Figure 1.22**). This method bypasses the unfavorable C–C oxidative addition by taking advantage of a more favorable  $\beta$ -carbon elimination to achieve C–C bond activation. A few years later in 2015, Sarpong and coworkers<sup>32</sup> utilized cyclobutanol-containing bicycles **1.19** for rhodium-catalyzed selective C1–C2 bond cleavage via  $\beta$ -carbon elimination (**Scheme 1.9**). In addition to cyclobutanol's inherent ring strain (1.16), this additional strain imposed by the bicyclic system allows for selective cleavage of the most strained bond in the system.

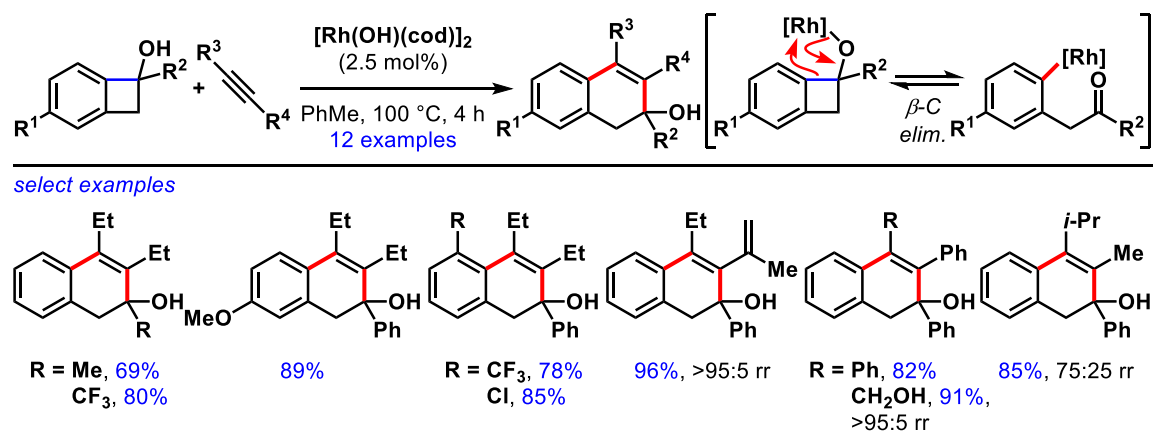
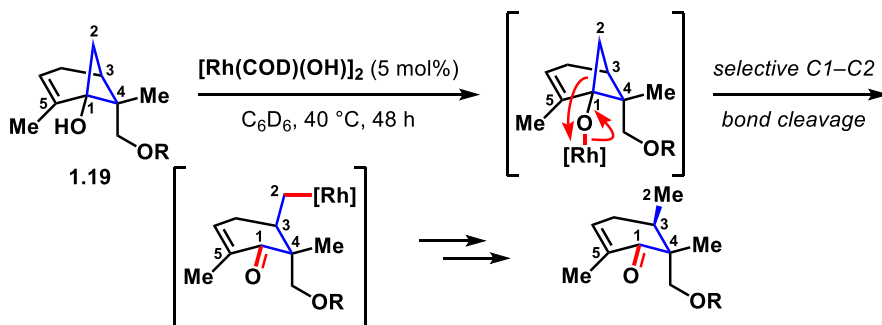


**Figure 1.22.** Formal alkyne insertion between a C–C bond via  $\beta$ -carbon elimination/C–C activation.



**Scheme 1.9.** Selective  $\beta$ -carbon elimination of cyclobutanol-containing bicycles.

Another more recent example in 2022 by Mao, Liu and coworkers<sup>33</sup> takes on a more involved strategy to synthesize oxindoles in a highly efficient manner (**Figure 1.23**). An oxidative addition of palladium into the aryl iodide followed by intramolecular migratory insertion into the alkene leads to ligand exchange with the benzocyclobutanol motif, from which  $\beta$ -carbon elimination/reductive elimination allows for formal C–C bond activation (**Scheme 1.10**). These methods demonstrate a great method to indirectly activate/access high-energy C–C bonds.

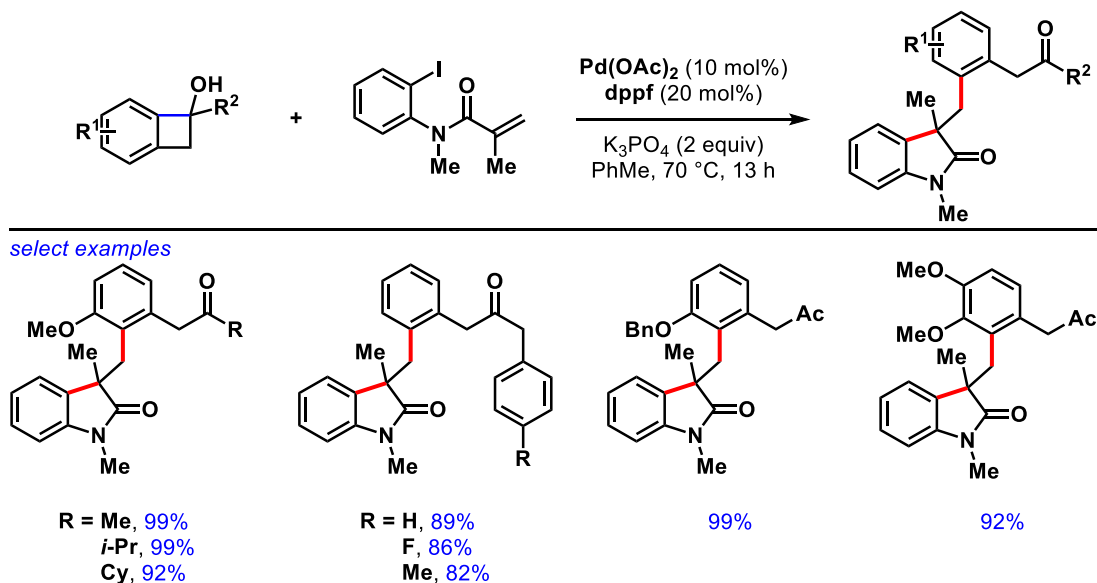
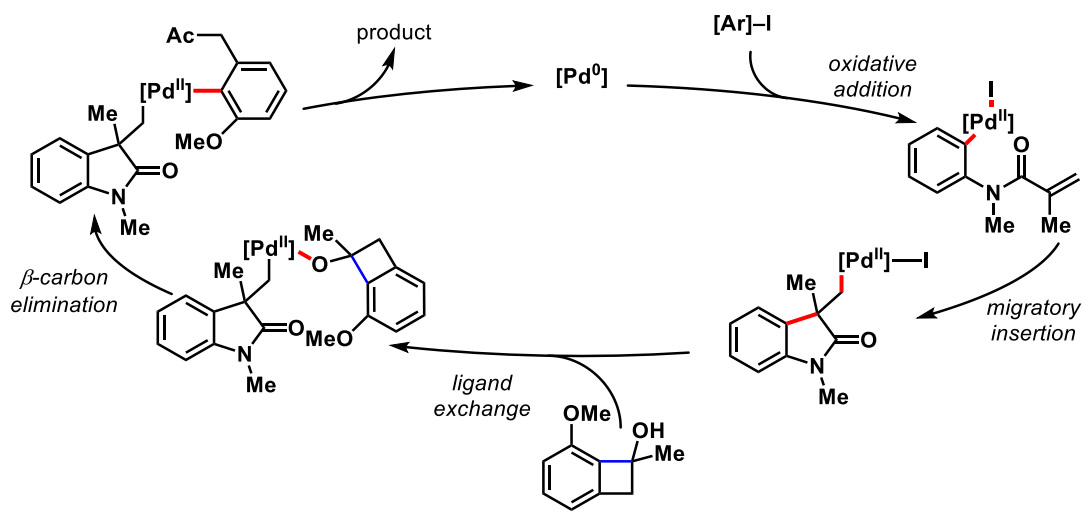


**Figure 1.23.** Synthesis of oxindoles via  $\beta$ -carbon elimination/C–C activation.





**Scheme 1.10.** Proposed mechanism of palladium-catalyzed Heck coupling/C–C bond activation.

Several methods involving metal-carbenes have also been applied to achieve formal C–C bond activation. In a similar strategy to Murakami and coworkers,<sup>31</sup> Wang and coworkers<sup>34</sup> utilized benzocyclobutanols along with diazo compounds to achieve formal C–C bond insertions (**Figure 1.24**). Following  $\beta$ -carbon elimination, the rhodium species can be intercepted by a diazo compound to form a metal-carbenoid complex (**Scheme 1.11**). This initiates migratory insertion of the carbene to form a rhodium-enolate intermediate, which further reacts in an intramolecular aldol addition to form the final indanol product. This method demonstrates a selective, formal C–C bond insertion between the  $C_{\text{aryl}}$ –COH bond.

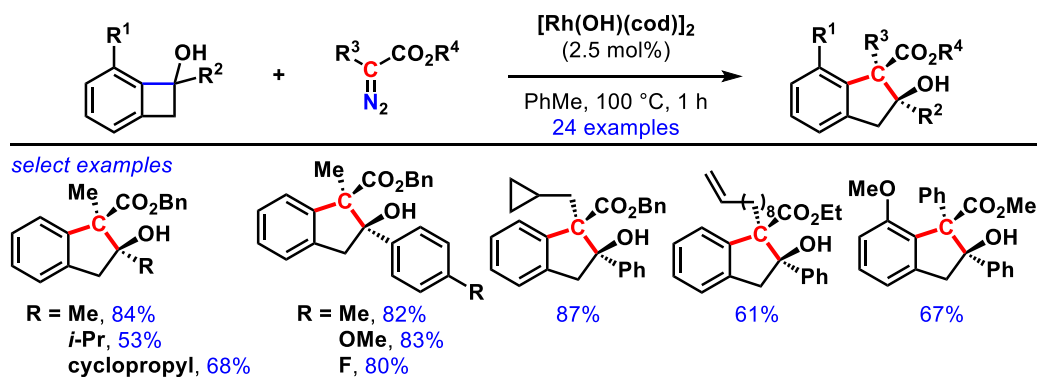
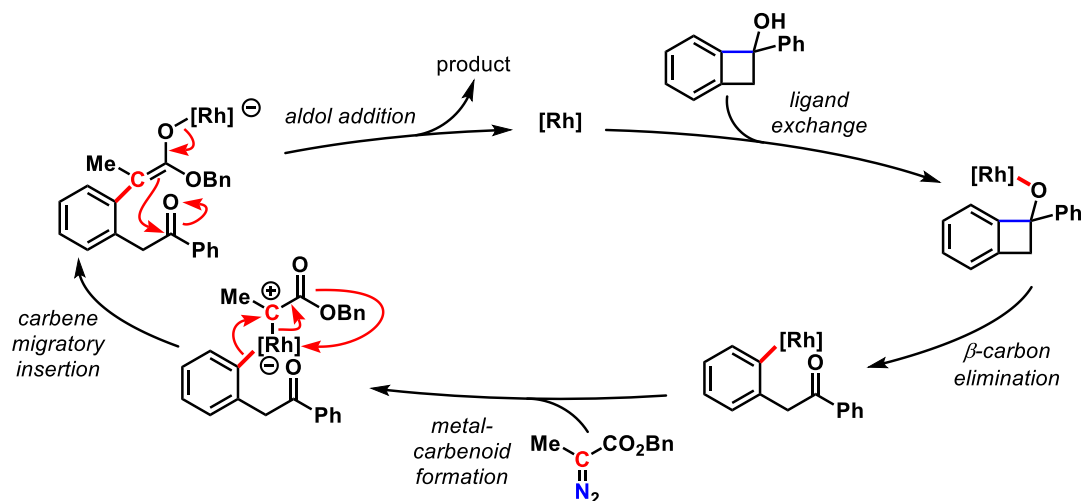


**Figure 1.24.** Formal C–C bond homologation of benzocyclobutanols.



Work by Bi, Anderson and coworkers<sup>35</sup> utilized *N*-nosylhydrazones, AgOTf, and acyclic 1,3-diketones to achieve C–C bond insertion (**Figure 1.25**). Here, an enolizable diketone provides the alkene for the metal-carbene to cyclopropanate. Subsequent ring-opening via a retro-aldol process to achieve formal insertion in between the two ketones. It is important to use acyclic 1,3-diketones since it is proposed that the two oxygens of the carbonyls coordinate to the silver Lewis acid. Cyclic 1,3-diketones do not allow for proper

coordination of both carbonyls to the Lewis acid, thus cyclohexa-1,3-dione proved unsuccessful under these reaction conditions.

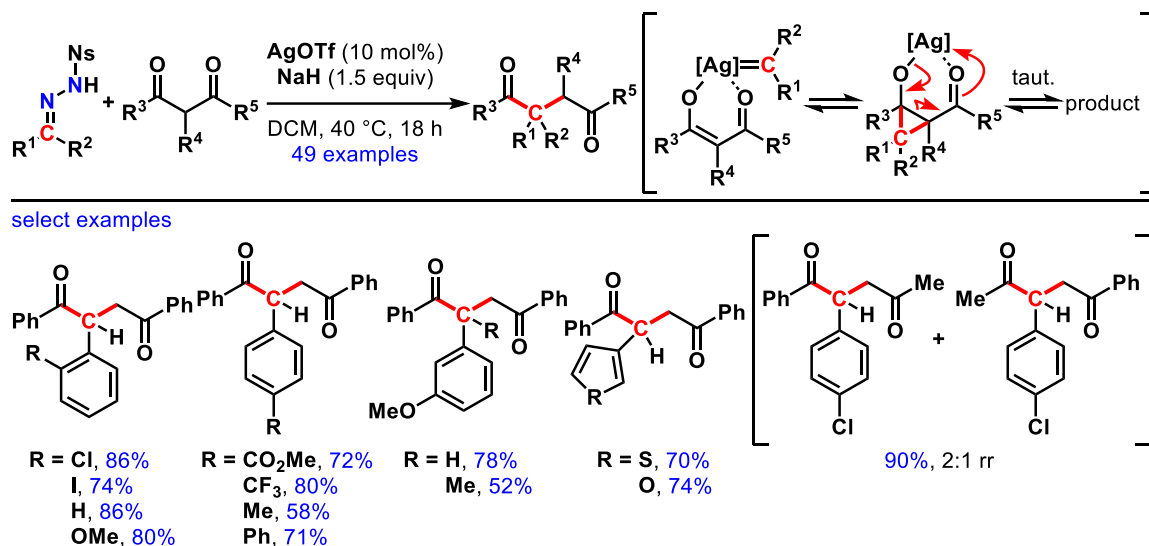


**Figure 1.25.** C–C bond insertion of acyclic 1,3-diketones.

The same research labs utilized alkynyl *N*-nosylhydrazones with 1,3-diketones to achieve C(sp<sup>2</sup>)-homologation<sup>36</sup> (**Figure 1.26**). The transformation inserts a propargyl group adjacent to a ketone, which subsequently tautomerizes to form an allene, resulting in a formal C–C bond insertion of a C(sp<sup>2</sup>)-hybridized carbon group. Unsymmetrical 1,3-diketones typically result in a mixture of two products, where there is a modest preference for the homologation to occur on the more electron-rich side. Although only one  $\beta$ -ketoester was tested, exclusive C–C bond insertion occurred on the side of the ketone instead of the ester.

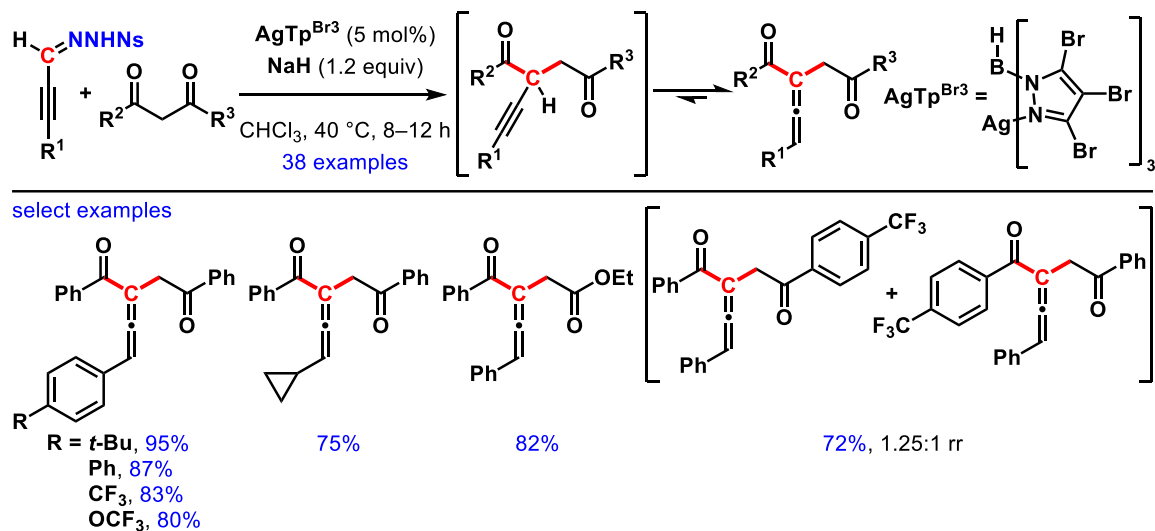
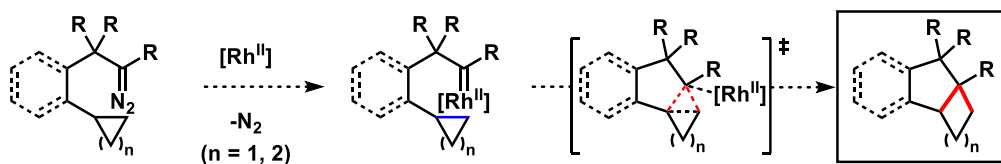


**Figure 1.26.** Formal C–C bond insertion of a C(sp<sup>2</sup>)-hybridized carbon.

### 1.2.1 Strategy for direct C–C bond activation

Although formal C–C bond insertion reactions through these methods continue to expand, there is no precedence for direct C–C bond insertion via carbenes. Herein, we propose a metal-catalyzed carbene insertion into the strained C–C bonds of cyclopropanes or cyclobutanes (**Scheme 1.12**).



**Scheme 1.12.** Target transformation and proposed transition state.

I observed early on in a separate study that cyclopropanation of 2'-bromoacetophenone (**1.20**) led to 2'-cyclopropylacetophenone (**1.21**) in 95% yield (**Figure 1.27**); however, B. Zaki, who was pursuing this substrate, converted 2'-cyclopropylacetophenone (**1.21**) to diazo compound **1.22** bearing a tertiary, benzylic

alcohol, which failed to undergo the desired C–C insertion in producing tricycle **1.23** (Figure 1.28). In the presence of  $\text{Cu}(\text{OTf})_2$  and heat, alcohol **1.22** underwent 1,2-methyl shift to produce  $\alpha$ -methyl **1.24**, or elimination to alkene **1.25**, followed by cycloisomerization to pyrazole **1.26**. Similar pyrazole formation was observed by Padwa and coworkers on a very similar ester.<sup>37</sup> For these reasons, we turned to substrates that lack alcohols adjacent to the diazo functional group (Figure 1.29, 1.27–1.32).

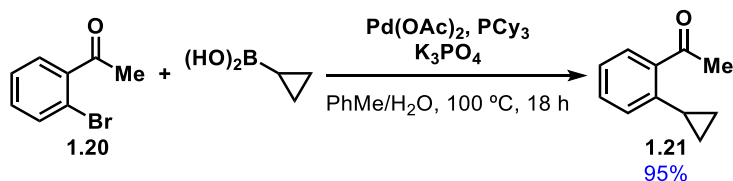


Figure 1.27. Suzuki cross-coupling.

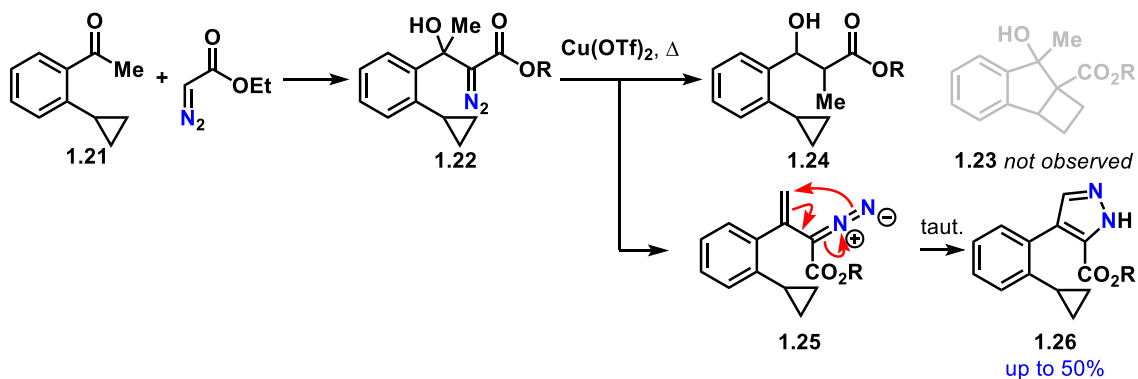


Figure 1.28. Side reaction with unprotected alcohol.

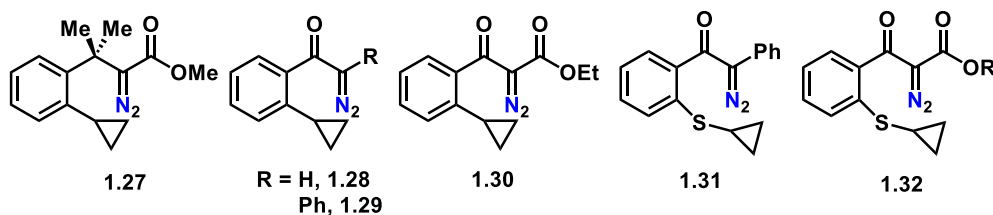


Figure 1.29. Target diazo substrates.

### 1.2.2 Synthesis of *gem*-dimethyl diazo compound **1.27**

**Figure 1.30** shows the synthetic route to obtain the target diazo compound **1.27**. Beginning with Meldrum's acid (**1.33**), Knoevenagel condensation with acetone yielded isopropylidene **1.34**.<sup>38</sup> By using distilled water instead of 5% aqueous NaOH solution for the workup, the isolated yield improved from 44% to 95%. Presumably, isopropylidene **1.34** is unstable and readily hydrolyzes under basic conditions. Control experiments were conducted to investigate this dramatic change in yield. After the reactions were deemed complete by TLC analysis, the mixtures were divided into four equal aliquots. One aliquot was concentrated *in vacuo* and, according to the literature precedence,<sup>38</sup> quenched with 5% aqueous NaOH solution and extracted with methyl *tert*-butyl ether to afford isopropylidene **1.34** in 24% yield. Although not a practical isolated yield, this method turned out to produce the highest purity and conversion to product by NMR analysis of the crude reaction mixture. The next two aliquots were quenched with 5% aqueous NaOH solution before extraction with EtOAc, resulting in 2% and 6% yield. This showed that not only does this method result in poor yields, but there was also poor reproducibility even when performed side-by-side. The final aliquot was concentrated *in vacuo* before quenching with DI water, which after work-up, afforded product in 88% crude yield. Clearly, this method offered the best yield, even though the crude mixture was slightly less pure (about 98% product **1.34**, 2% starting material **1.33**) compared to the method that produced 24% yield.

It is also noteworthy that the reaction did not require anhydrous acetone, adding to both cost- and time-effectiveness in not needing to dry/distill the solvent nor purchase rigorously anhydrous reagent. Moderate improvements were attained with higher

concentrations: it was found that using  $8 \times$  acetone by weight (0.85 M compared to 0.7 M) was most successful in producing isopropylidene **1.34** (95% yield). Any concentrations higher than 0.85 M resulted in lower yields.

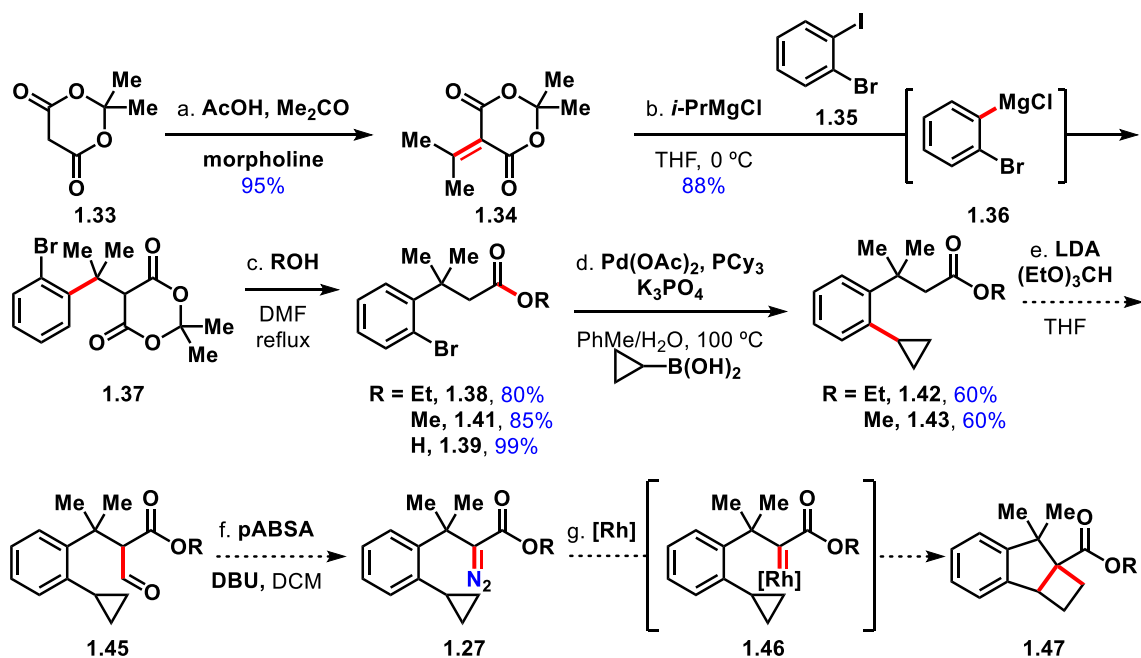


**Figure 1.30.** Synthesis progress of cyclopropyl ester **1.42** and **1.43**.

Conjugate arylation of isopropylidene **1.34** was achieved by its direct reaction with Grignard reagent **1.36**, formed from subjecting 2-bromoiodobenzene (**1.35**) to *i*-PrMgCl, which produced benzylic malonate **1.37**.<sup>39</sup> Improvements from the initial isolation yield of 40% to 88% was accomplished when the Grignard reagent was titrated and determined to be 1.2 M instead of the expected 2 M. Maintaining the reaction at 0 °C for an extended duration (24 h compared to 1 h) showed no improvement in yield. The use of the “turbo-Grignard” reagent *i*-PrMgCl•LiCl did not lead to any improvements over several attempts. Solid magnesium(0) turnings had been tested several times in place of *i*-PrMgCl, however

no product formation was ever observed. Purification of benzylic malonate **1.37** by trituration offered similar yields to column chromatography. During trituration, the mother liquor concentrate was repeated trituated with ether until no product remained by TLC analysis. One advantage of the trituration method was that there was a large amount of crude solid material obtained during this reaction (multi-gram), therefore column chromatography was not optimal.

Ring opening of benzyl malonate **1.37** to produce ester **1.38** proved to be challenging. Some literature procedures<sup>38,40</sup> proceed directly to the subsequent hydrolysis in forming ester **1.38** (**Figure 1.31**), carboxylic acid **1.39**, or malonate<sup>39</sup> **1.40** (undesired but observed in some reactions). Attempts were made with absolute ethanol, as well as in combination with a cosolvent such as benzene to directly produce ethyl ester **1.38**; however, most reactions failed to produce synthetically useful quantities of product. After concluding that this was not an effective pathway, we turned our attention to synthesizing the carboxylic acid first and subsequently esterifying.

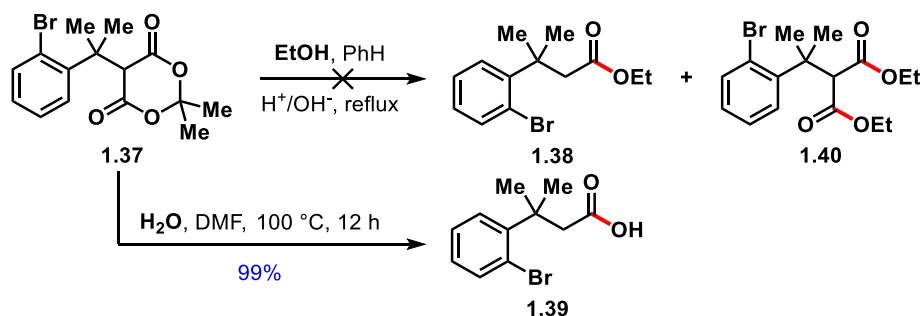


**Figure 1.31.** Unsuccessful ring opening attempts with benzene to produce ester **1.38**. Switching to DMF was significant in successful ring opening to carboxylic acid **1.39**.



The ring opening of benzyl malonate **1.37** to carboxylic acid **1.39** (Figure 1.31) proceeded cleanly using distilled water<sup>38</sup> and DMF instead of benzene as solvent, resulting in quantitative yield. The resultant light-orange solid was pure by NMR analysis, and thus was used directly without additional purification. One drawback of this reaction was the usage of DMF, which was difficult to completely remove; however, the residual DMF may be serendipitously acting as a catalyst in the next step.

Fischer esterification<sup>41</sup> was first attempted to obtain ester **1.41**. Several reaction conditions were attempted, including using a Dean-Stark apparatus setup and toluene as the solvent to promote azeotropic removal of water (Figure 1.32, c<sub>1</sub> reaction). Results of these conditions showed ~76% conversion but with impurities that were difficult to separate. An attempt was made to convert the carboxylic acid to an acid chloride at reflux,<sup>42</sup> followed by esterification with methanol, but this led to a mixture with many impurities even after column chromatography (condition c<sub>2</sub>). A different report suggested conducting the reaction at rt<sup>43</sup> (reaction c<sub>3</sub>); in our case, the results showed improvements in yields (up to 85%) without the presence of impurities. The use of catalytic DMF gave similar results.

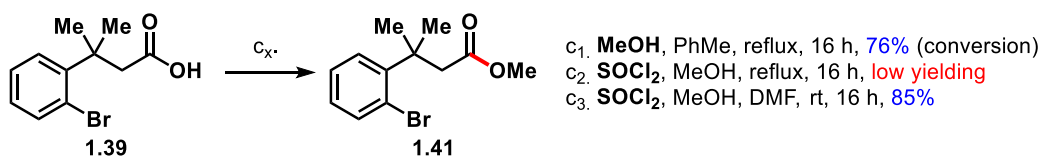
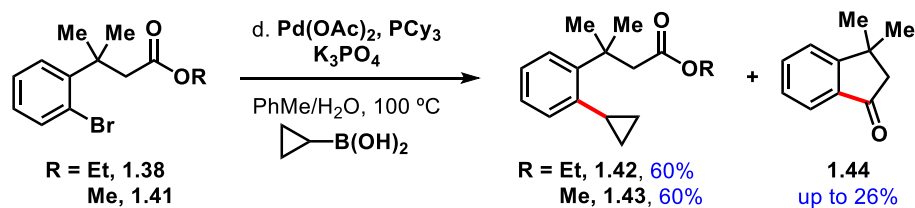


Figure 1.32. Conditions to esterify carboxylic acid **1.39** to ester **1.41**.

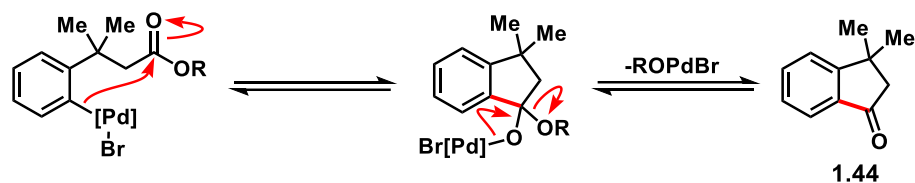
Other attempts to access esters **1.38** or **1.41** proved successful and more straightforward. The substitution of water (see Scheme 1.30) for methanol or ethanol in DMF solvent under otherwise similar conditions for the ring-opening reaction of benzylic

Meldrum's acid **1.37** afforded bromo ethyl-ester **1.38** and bromo methyl-ester **1.41** respectfully, in up to 85% yields with negligible amounts of impurities. In addition to saving a step, purification was also not necessary. The starting material was recovered when DMF was not present, suggesting that a polar, aprotic solvent was required.

The Suzuki reaction<sup>44</sup> (**Figure 1.30**, reaction d) to yield cyclopropyl esters **1.42** or **1.43** was improved from ~25% to 55–60%. Lowering the reaction temperature from 120 °C to 100 °C as well as lowering the concentration contributed to the improvement. It was discovered that a competing reaction was occurring in the Suzuki coupling reaction (**Figure 1.33**), in which migratory insertion of the ester carbonyl into the Ar–Pd intermediate led to a five-membered ring mixed ketal that collapses to 3,3-dimethyl-1-indanone (**1.44**) in up to 26% yield (**Scheme 1.13**). Although not reported in an intramolecular sense, a similar intermolecular reaction involving palladium and a boronic acid has been previously reported.<sup>45</sup> This side reaction resulted in significantly lowered yields of the desired product, even though the indanone was easily separable. Substituting the ester for an amide may mitigate this undesirable pathway.



**Figure 1.33.** Side reaction in the Suzuki cross-coupling.



**Scheme 1.13.** Proposed pathway to indanone **1.44**.

Attempts were made to formylate the  $\alpha$ -position of the ester to synthesize dicarbonyl **1.45** and directly carry out the next diazo transfer in producing diazo ester **1.27** (**Figure 1.30**, reaction e). It was difficult to determine if dicarbonyl **1.45** was formed by NMR analysis of the crude reaction mixtures due to low conversions, although  $^1\text{H}$  and  $^{13}\text{C}$  NMR spectra look promising. It is possible that dicarbonyl **1.45** was produced based on the presence of a deshielded signal at  $\delta$  9.60 in the  $^1\text{H}$  NMR spectrum. There have been a few instances where this signal remained after storing the product in the freezer, alongside evidence of decomposition after a few weeks; thus, its stability is unknown. Due to low crude yields and the unknown stability of aldehyde **1.45**, accessing diazo ester **1.27** directly from the crude mixture of dicarbonyl **1.45** was attempted (**Figure 1.30**, reaction f). However, significant quantities of the desired product were unlikely to have formed based on NMR analysis of the crude reaction mixture.

An alternate route that involves the iron-catalyzed alkylation of a phenolic derivative was attempted (**Figure 1.34**).<sup>46</sup> Ethyl acetate (**1.48**) was successfully transformed to tertiary alcohol **1.49** in 58% yield through an aldol reaction with acetone.<sup>47</sup> The subsequent alkylation step to combine the tertiary alcohol with phenolic **1.50** would form the desired alkylation product **1.51**, which would be triflated to arrive at pseudo-

halide **1.52**, and then cross-coupled with cyclopropylboronic acid to achieve cyclopropyl ester **1.53**.

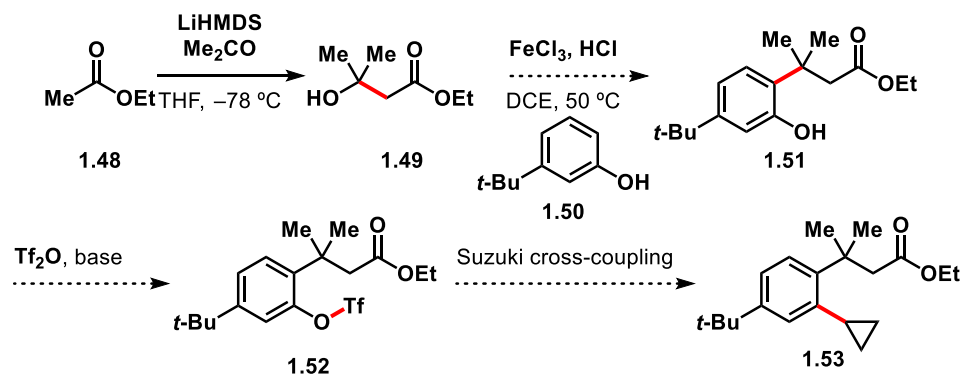


**Figure 1.34.** Alternate synthesis route involving previously developed Fe-catalysis.

Subjecting 3-*tert*-butylphenol (**1.50**) and tertiary alcohol **1.49** to catalytic  $\text{FeCl}_3$  resulted in no reaction. Using one equivalent of  $\text{FeCl}_3$  afforded hydrocoumarin **1.54** in 26% yield (**Figure 1.35**). This was concluded by the loss of the ethyl group by  $^1\text{H}$  NMR spectroscopy and the presence of a strong carbonyl stretch at  $1770\text{ cm}^{-1}$  in the IR spectrum, which is higher in frequency than typical esters and consistent with hydrocoumarins.<sup>48</sup> This method can potentially be optimized to produce hydrocoumarins as an extension to the Friedel-Crafts reactions developed over the course of my dissertation studies (see Chapters 2 and 3).

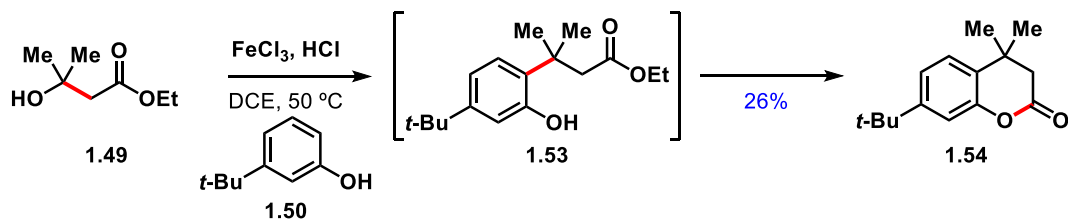


**Figure 1.35.** Coumarin **1.54** from iron-catalyzed coupling reaction.

An alternate route that took advantage of the acidic  $\alpha$ -protons of the 1,3-dicarbonyl present in benzyl malonate **1.37** was pursued (**Figure 1.36**), attempting to perform the diazo transfer directly to access bromo-diazo **1.55**. This route offered a shorter synthesis to the desired intermediate (four steps overall) with most steps already optimized. Unfortunately, no reactivity was observed at room temperature for the diazo transfer reaction. It is possible that the cyclic malonate is unsuitable for a diazo transfer reaction. A possible problem considered was that certain functional groups, especially the potential diazonium intermediate, were not tolerated under these reaction conditions. Another possible issue could be the base being insufficiently basic or too bulky to access the  $\alpha$  protons on the malonate.

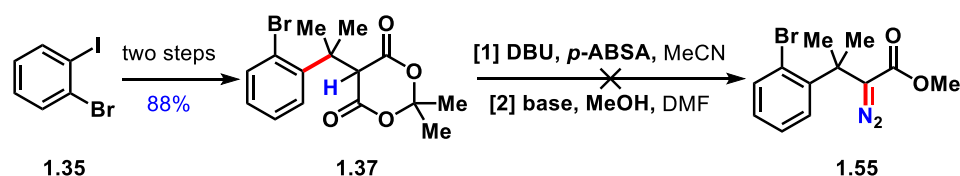


**Figure 1.36.** Unsuccessful attempt utilizing malonate to access diazo **1.55**.

Suzuki cross-coupling of 2-bromoiodobenzene (**1.35**) afforded the desired 1-bromo-2-cyclopropylbenzene (**1.56**) in 61% NMR yield and undesired 1,2-dicyclopropylbenzene (**1.57**) in 30% NMR yield (**Figure 1.37**). This mixture was difficult to separate, thus the use of less boronic acid and its slow addition may keep the concentration of the boronic acid sufficiently low to minimize undesired dialkylation. An interesting observation made was that the NMR spectrum of the crude mixture was cleaner than the usual cross-coupling reaction (*cf.* bromoaryl-methyl ester **1.41** to cyclopropylaryl-methyl ester **1.43**, see **Figure 1.30** and **1.43**), likely due to the simplicity of the starting

material. Had benzyl malonate **1.33** been successfully converted to bromo-diazo **1.45**, 1-bromo-2-cyclopropylbenzene (**1.56**) could undergo Grignard coupling to access cyclopropyl-malonate **1.58** before performing the diazo transfer to access cyclopropyl diazo **1.27**.

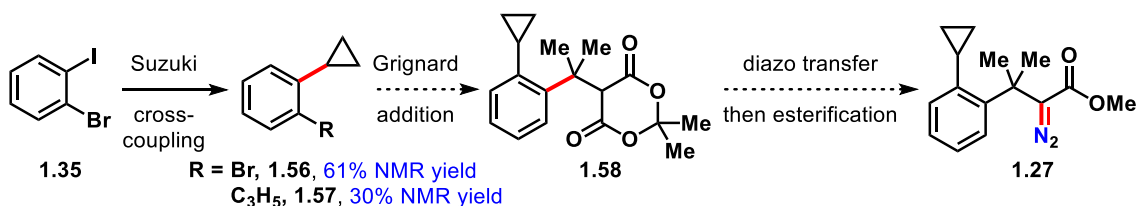


**Figure 1.37.** Shorter synthesis attempt to achieve target diazo compound **1.27**.

### 1.2.3 Syntheses of 2'-cyclopropylbenzoyl diazo compounds **1.28**–**1.32**

To augment substrate options to test the proposed C–C bond insertion, other diazo compounds were synthesized. **Figure 1.38** shows the synthesis route to diazo-acetyl **1.28** in an overall 16% yield over 3 steps. The synthesis began with a Suzuki cross-coupling from 2'-bromoacetophenone (**1.20**) to 2'-cyclopropylacetophenone (**1.21**), which underwent Claisen condensation with 2,2,2-trifluoroethyl trifluoroacetate to access enol **1.59** in 50% yield. Enol **1.59** was reacted with *p*-ABSA and triethylamine to obtain the target diazoacetyl **1.28** in 33% yield after purification. This diazo motif completely decomposed over a period of two months at  $-7\text{ }^{\circ}\text{C}$ , thus the material should be stored at the enol stage (**1.59**) before converting to diazoacetyl **1.28**.

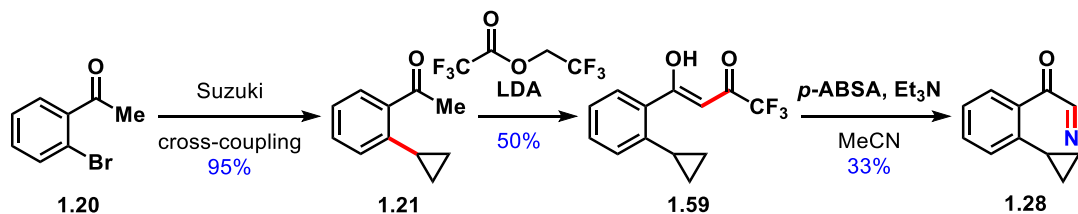


Figure 1.38. Synthesis route to diazoacetyl **1.28**.

Figures 1.39 and 1.40 show the synthesis routes investigated to access diazo-phenylacetophenone **1.29** in an overall yield of 15%. The synthesis began with *N,O*-dimethylamine (**1.60**) and phenylacetyl chloride to generate methoxyamide **1.61** in 92% yield<sup>49</sup> (Figure 1.39). Attempts to react methoxyamide **1.61** with dihalobenzene **1.35** via a Grignard addition to access brominated phenylacetophenone **1.62** proved to be difficult, partially resulting in reduction of methoxyamide **1.61** to *N*-methyl amide **1.63**. Other attempts with 1-bromo-2-cyclopropylbenzene (**1.56**) to form the corresponding Grignard reagent with  $Mg_{(s)}$  and *i*-PrMgCl, followed by addition to methoxyamide **1.61** failed to produce the arylation product **1.64**, regardless of the reaction scale (up to 1 mmol scale tested).

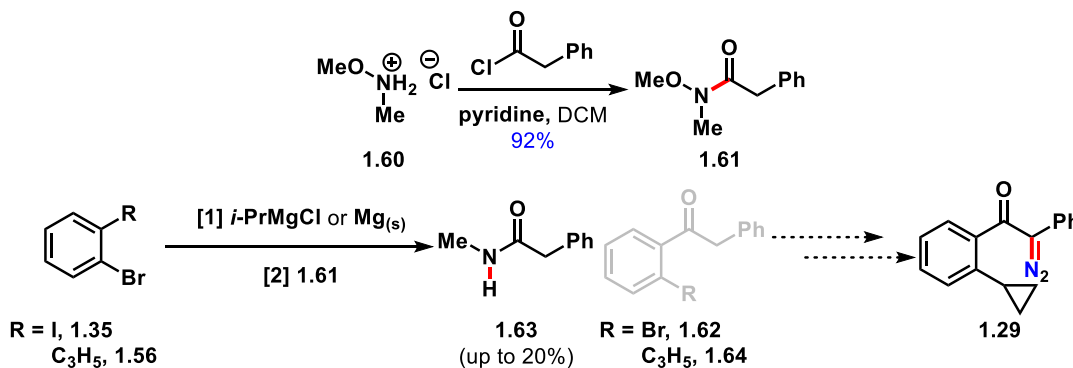
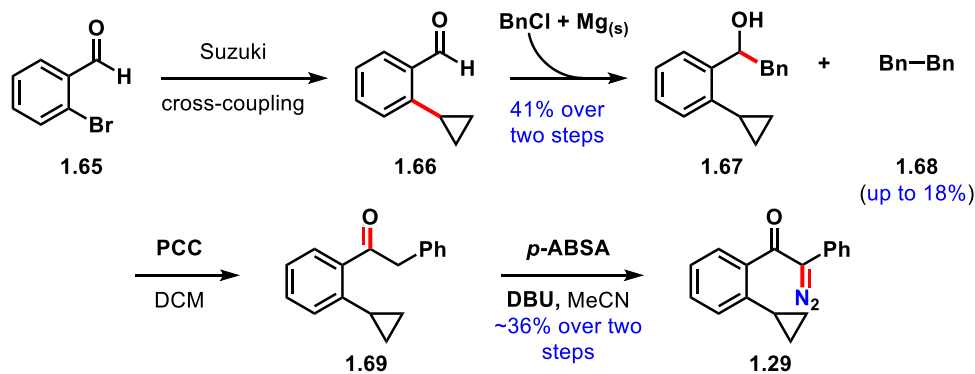


Figure 1.39. Initial attempts diazo-phenylacetophenone **1.29**.

Taking a different approach, 2-bromobenzaldehyde (**1.65**) underwent a Suzuki cross-coupling reaction to achieve 2-cyclopropylbenzaldehyde (**1.66**) in near quantitative yield (**Figure 1.40**). The crude product was treated with benzyl magnesium chloride, which afforded alcohol **1.67** in 41% yield after 2 steps. It was observed that the Grignard reagent homocoupled to form 1,2-diphenylethane (**1.68**) in up to 18% yield, which required the use of an excess of the Grignard reagent (over 2 equivalents) to obtain a synthetically useful yield of alcohol **1.67**. A one-pot, slow addition of benzyl chloride still showed formation of 1,2-diphenylethane (**1.68**), though the reaction works without having to pre-form the Grignard reagent. Alcohol **1.67** was oxidized with PCC to ketone **1.69** in excellent yield if the *purified* alcohol **1.67** was used. If *crude* material was used, the oxidation still proceeds, albeit with a drop in yield to 28%. Ketone **1.69** was converted to phenylacetyl-diazo **1.29** with *p*-ABSA and DBU in <36% yield over two steps; however, purification of this compound proved difficult and clean NMR spectra could not be obtained.



**Figure 1.40.** Tentative successful route to diazo-phenylacetophenone **1.29**.

It was initially hypothesized that the diazo compound (**1.29**) decomposes on silica gel during column chromatography, thus an internal standard (1,3,5-trimethoxybenzene,



0.33 equiv) was added to determine the approximate amount of product in the crude mixture. The  $^1\text{H}$  NMR spectrum of the crude mixture showed that, compared to the internal standard, only about 20% of product was in the crude mixture (however this particular reaction did not fully convert). Therefore, it was concluded that the low yield likely was not due to decomposition during column purification. It was also observed that upon resubjecting the reaction, heating to 50 °C drastically changed the color from bright orange to dark purple in a matter of minutes, though it was unclear what the source of the color was. The color returned to orange overnight, albeit very pasty instead of clear. The reaction failed in the end, therefore it is unrecommended that the reaction be heated for future reference.

2-Cyclopropylacetophenone (**1.21**, **Figure 1.41**) was deprotonated with NaH before reacting with diethyl carbonate via a Claisen condensation<sup>50</sup> to achieve ketoester **1.70**. Initial purification of this crude material was somewhat problematic, thus the material was carried forward to perform a diazo transfer with *p*-ABSA and DBU to obtain ketoester-diazo **1.30** in 54% yield (over 2 steps).

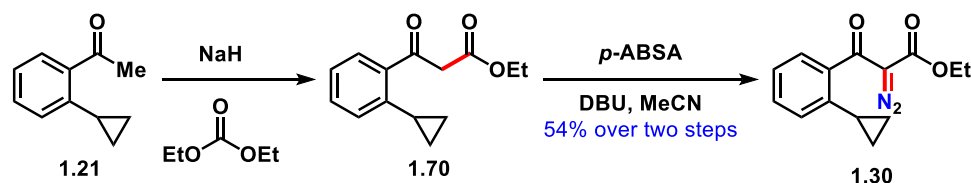


**Figure 1.41.** Synthesis route to ketoester-diazo **1.30**.

**Figure 1.42** shows the synthesis plan to access thio-diazo **1.31**, which was no longer pursued due to undesirable outcomes from metal-carbene studies of other diazo

substrates. The synthesis of thio-diazo **1.31** began with 2-bromothiophenol (**1.71**), which was readily alkylated to furnish cyclopropyl sulfane **1.72** in 80% yield.<sup>43</sup> The remaining plan was to couple *N*-methoxyamide **1.61** via the Grignard reaction to cyclopropyl sulfane **1.72**. A final diazo transfer reaction as previously achieved (*cf.* phenylacetyl **1.69** to diazo-phenylacetophenone **1.30**, see **Figure 1.40**) would provide thio-diazo **1.31**.

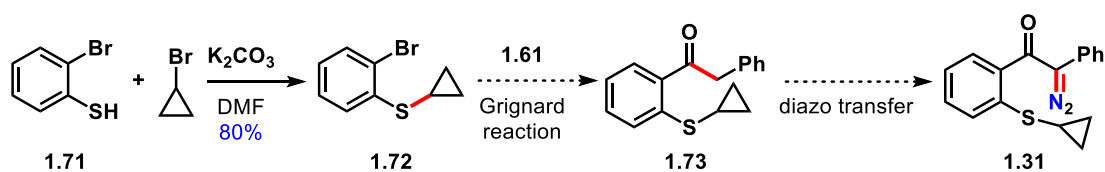


**Figure 1.42.** Synthesis route to thio-diazo **1.31**.

In the presence of  $\text{Rh}_2(\text{OAc})_4$ ,  $\text{Rh}_2(\text{TFA})_4$ ,  $\text{B}(\text{C}_6\text{F}_5)_3$ , or  $\text{Cu}(\text{OTf})_2$  with heating in DCM, diazo ketoester **1.30** undergoes C–H insertion of the benzylic hydrogen to form spiro-cyclopropyl **1.74** (**Figure 1.43**) instead of the desired C–C insertion to **1.47**. Based on these results, re-strategizing the substrate design was necessary, in which a benzylic hydrogen was absent. Therefore, similar substrate designs as the previous cyclopropyl diazo compounds **1.27–1.30** were sought after, where an addition substituent replaces the benzylic hydrogen (**1.75–1.78**, **Figure 1.44**).

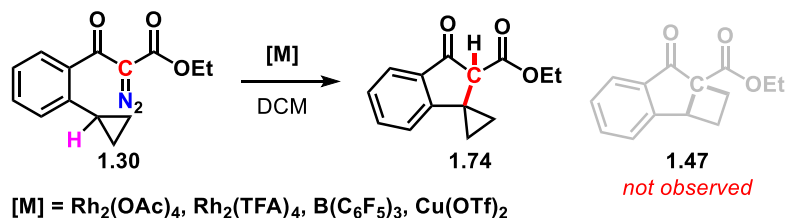


**Figure 1.43.** Observed C–H insertion of metal-carbenoids to spiro-cyclopropyl **1.74** and no desired C–C insertion to cyclobutyl **1.47**.

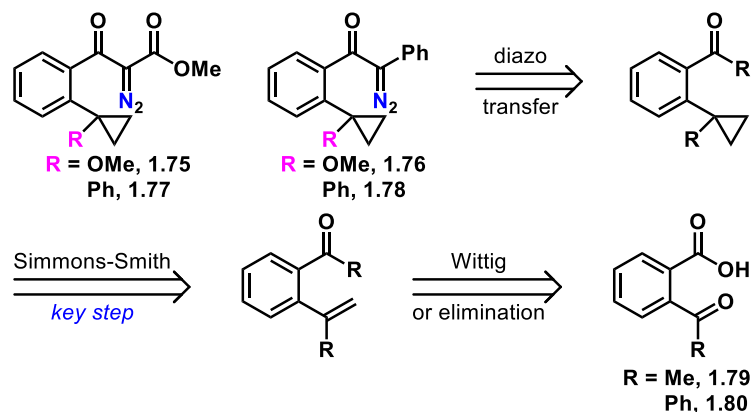


**Figure 1.44.** Re-strategized substrate designs and proposed retrosyntheses.

#### 1.2.4 Syntheses of quaternary-substituted cyclopropyl diazo compounds **1.75–1.78**

The proposed retrosynthesis plans to generate **1.75–1.78** involved a key Simmons–Smith reaction in forming a cyclopropyl group bearing an all-carbon quaternary center (**Figure 1.44**). The olefin can be generated from an acid-catalyzed elimination reaction of a ketal, or a Wittig olefination from the ketone. Thus, the starting material of choice was narrowed down to 2-ketobenzoic acids **1.79** and **1.80** for synthesizing methoxy-cyclopropyl diazos **1.75** and **1.76** and phenyl-cyclopropyl diazos **1.77** and **1.78**.

The route to methoxy-cyclopropyl diazos **1.75** and **1.76** began with methylation of 2-acetylbenzoic acid (**1.79**, **Figure 1.45**) to ester **1.81**, followed by ketalization (**1.82**) and acid-catalyzed elimination to generate vinyl ether **1.83**. The olefin was treated with  $\text{Et}_2\text{Zn}$  and  $\text{CH}_2\text{I}_2$  to form methoxycyclopropane **1.84** in 81% yield over four steps. This intermediate was saponified to carboxylic acid **1.85**. Conversion to the acid chloride *in situ*, followed by treatment with ethyl diazoacetate (EDA) was planned to form ketoester-derived diazo **1.86**. However, upon treatment of carboxylic acid **1.85** with oxalyl chloride,

the resulting intermediate cyclized spontaneously to spirolactone **1.87**. Due to this undesired intramolecular lactonization, methoxy-ketoester diazo **1.75** was accessed through a different approach.

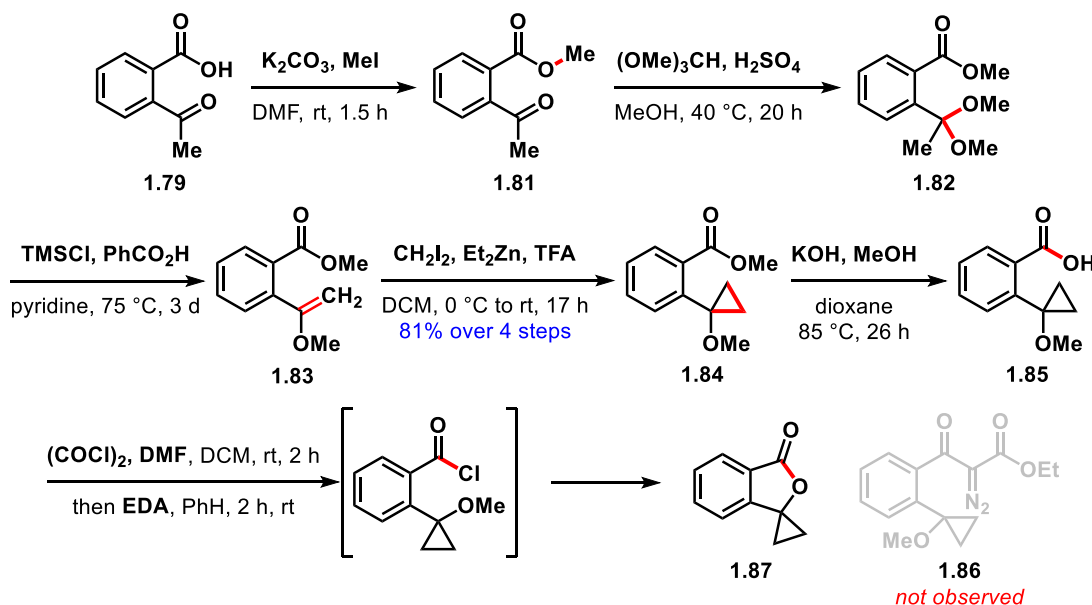


**Figure 1.45.** Synthesis route concluded to lactone **1.87** instead of methoxyketoester diazo **1.86**.

The plan was to selectively reduce ester **1.84** to its corresponding aldehyde (**1.88**), en-route to methoxy-phenyl diazo **1.76**. (**Figure 1.46**). The use of two equivalents of diisobutylaluminum hydride (DIBAL-H) resulted in complete reduction to alcohol **1.89**, while the use of 1 equivalent of DIBAL-H afforded a 1:1 mixture of starting material **1.84** and alcohol **1.89**. These results suggested that selectively arresting at the aldehyde oxidation state was unlikely with ester **1.84**. Therefore, the ester was fully reduced to alcohol **1.89** with  $\text{LiAlH}_4$ , and subsequently oxidized to aldehyde **1.88** by a Swern oxidation in 83% yield over two steps. Aldehyde **1.88** was treated with benzyl magnesium chloride to generate alcohol **1.90** in 73% yield, followed by PCC oxidation of the resultant

alcohol to ketone **1.91** in 89% yield. The diazo group was introduced with *p*-ABSA to achieve methoxy-phenyl diazo **1.76** in 83% crude yield. Formation of the metal-carbene with  $\text{Rh}_2(\text{OAc})_4$ ,  $[(\text{cod})\text{RhCl}]_2$ ,  $(\text{Ph}_3\text{P})_3\text{RhCl}$ , or  $\text{CuOTf}_2\cdot\text{C}_6\text{H}_6$  unfortunately afforded complex mixtures with no observable desired product **1.92**; thus, other diazo compounds were pursued.

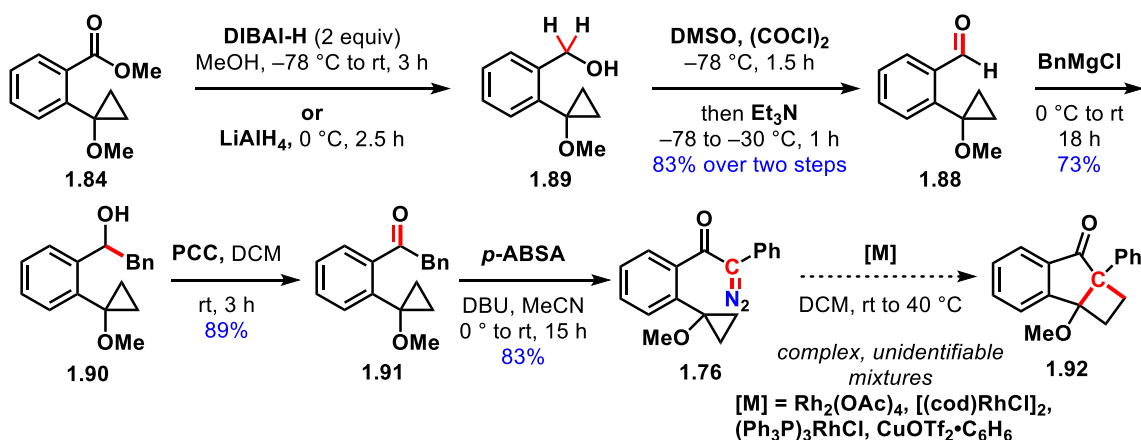


**Figure 1.46.** Synthesis route to methoxy-phenyl diazo **1.76**. Complex mixtures with metal-carbene reactivity.

To access ketoester diazo **1.75** (Figure 1.47), aldehyde **1.88** was treated with methyllithium to afford alcohol **1.93** in 86% yield, followed by a Swern oxidation to achieve ketone **1.94** in 81% yield. Ketone **1.94** underwent a Claisen condensation with dimethyl carbonate to afford ketoester **1.95** in 91% yield. Diazo transfer with *p*-ABSA to access the desired ketoester diazo **1.75** was fulfilled in 98% yield. Along with several Rh(II) catalysts, an abundant amount of different transition metal catalysts tested unfortunately did not afford any desired C–C inserted product. The products that were able to be identified (**1.96–1.98**) can be explained by a Stevens rearrangement-type of reaction

pathway. These results agree with a recent study of proximal methoxy or carbonyl groups to a metal-carbene center.<sup>51</sup>

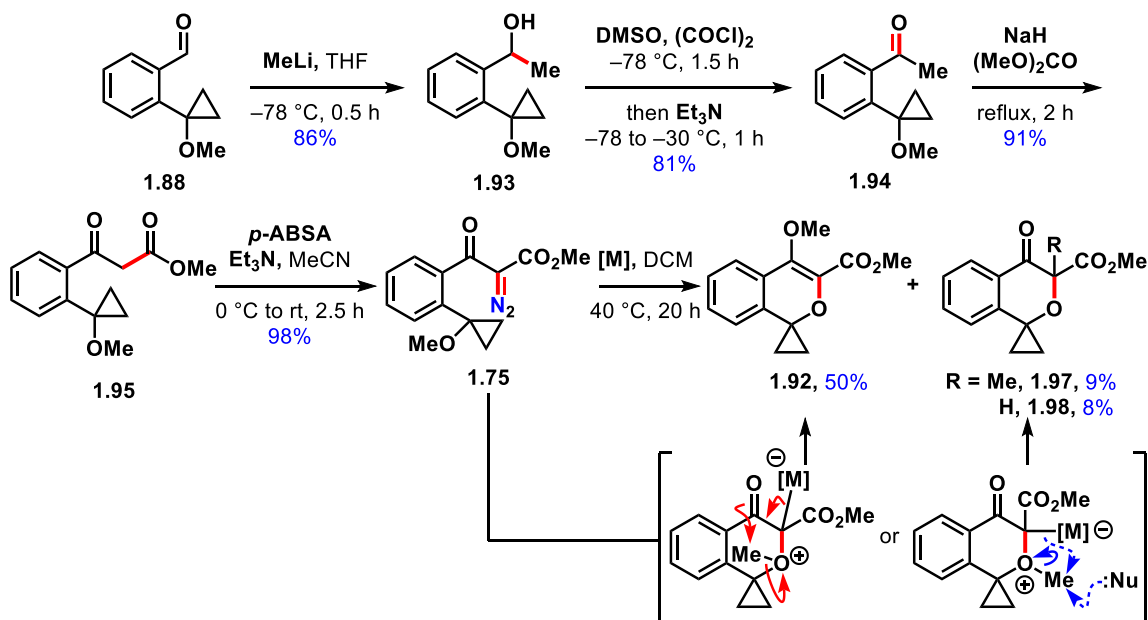


**Figure 1.47.** Synthesis to ketoester diazo **1.75**. Major identifiable products involved in the metal-carbene reactions were Stevens rearrangement-type products.

To further study the carbene reactivity, benzoyl diazo **1.99** was obtained in 23% yield over two steps (**Figure 1.48**). Starting from ketone **1.94**, a Claisen condensation with 2,2,2-trifluoroethyl trifluoroacetate resulted in diketone **1.100** in 37% yield, followed by a similar diazo transfer as before to afford benzoyl diazo **1.99** in 61% yield. A handful of transition-metals that displayed reactivity with diazo **1.75** were examined with benzoyl diazo **1.99**, only to observe similar Stevens rearrangement-type reactivity as with ketoester diazo **1.75** and afford isochromene **1.101** or isochromanes **1.102** and **1.103**.

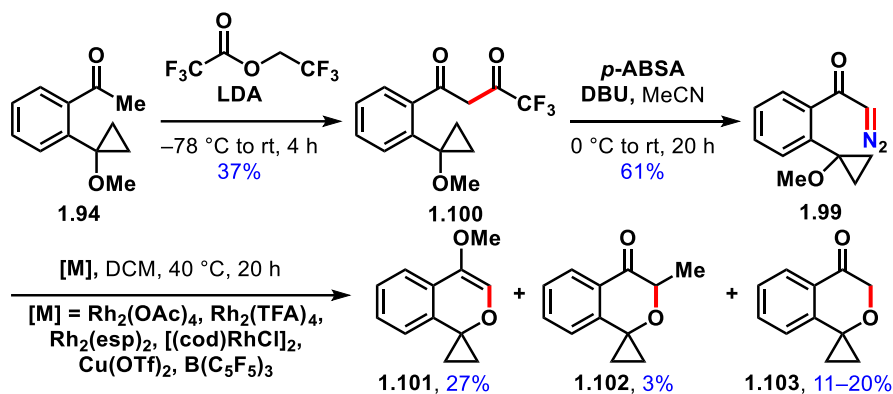


**Figure 1.48.** Metal-carbene reactions with benzoyl diazo **1.99** also observed Stevens rearrangement-type reactivity.

The synthesis route to carboxylic acid cyclopropane **1.104**, en-route to diazos **1.77** and **1.78**, began with a Wittig olefination of carboxylic acid **1.80** to alkene **1.105** in 56% yield (**Figure 1.49**). A Simmons-Smith reaction of alkene **1.105** resulted in cyclopropane **1.104** in 67% yield. Although these two steps occurred in moderate to good yields, purification of these carboxylic acids via column chromatography was impractical, requiring significant time- and solvent-consumptions due to the carboxylic acid's high polarity. Therefore, an alternative pathway was sought in an attempt to increase yield and efficiency, albeit with extra steps.

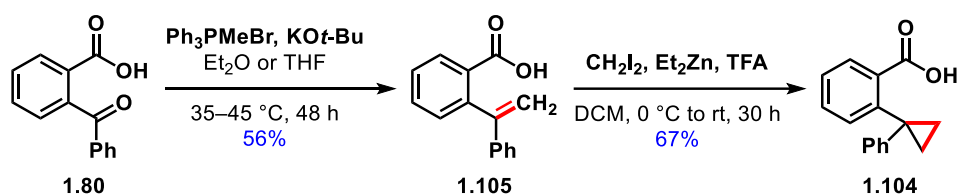


**Figure 1.49.** Synthesis route to carboxylic acid cyclopropane **1.104**.

Carboxylic acid **1.80** was converted to methyl ester **1.106** before a Wittig olefination to afford alkene-ester **1.107** in 21% yield over two steps (**Figure 1.50**). Using

KHMDS as a stronger base did not afford better results. The exact cause of the poor yield was uncertain. Overall, it is likely in the best interest resorting to the carboxylic acid for this Wittig reaction. An initial attempt to cyclopropanate  $\gamma,\delta$ -unsaturated ester **1.107** to cyclopropyl-ester **1.108** was surprisingly well-behaved, resulting in a yield of 94%. Hydrolysis of cyclopropyl-ester **1.108** afforded carboxylic acid **1.104**. Formation of the acid chloride with oxalyl chloride and DMF followed by treatment with EDA was unsuccessful in forming **1.109**, thus other routes were examined.

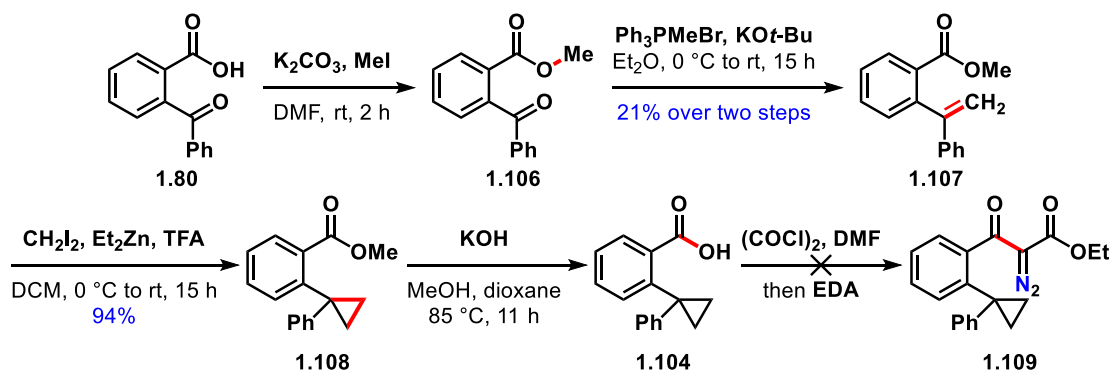


**Figure 1.50.** Alternative synthesis of carboxylic acid-cyclopropane **1.104**. Unsuccessful attempt to access diazo **1.109** from carboxylic acid **1.104** in one step.

Ester **1.108** was reduced with  $LiAlH_4$  to alcohol **1.110**, which was then oxidized with PCC to aldehyde **1.111** in 74% yield over two steps (**Figure 1.51**). Treatment with  $BnMgCl$  afforded secondary alcohol **1.112** in 57% yield, slightly lower than anticipated possibly due to the unfavorable steric interaction imposed by the *ortho*-substituted quaternary carbon bearing the cyclopropane and phenyl ring. Secondary alcohol **1.112** was oxidized to ketone **1.113**. Diazotization of the  $\alpha$ -carbon with *p*-ABSA was surprisingly robust to afford diazo compound **1.78** in 92% yield over two steps. Unfortunately,



treatment with  $\text{Rh}_2(\text{OAc})_4$  afforded either cycloheptatriene **1.114** via Büchner ring expansion or dibenzo-cycloheptane **1.115** via  $\text{C}(\text{sp}^2)\text{-H}$  bond insertion (based on the  $^1\text{H}$  NMR chemical shifts of the involved aryl ring) in 92% yield.  $\text{Rh}_2(\text{TFA})_4$ ,  $\text{CuOTf}_2\cdot\text{C}_6\text{H}_6$ , or  $\text{B}(\text{C}_6\text{F}_5)_3$  afforded similar results with varying yields. Aryl  $\text{C}=\text{C}$  insertion or aryl  $\text{C-H}$  insertion into the aryl ring was more facile than inserting into the cyclopropyl  $\text{C-C}$  bond. Due to this  $\text{C}(\text{sp}^2)\text{-C}(\text{sp}^2)$  or  $\text{C}(\text{sp}^2)\text{-H}$  insertion, further phenyl-cyclopropyl diazo substrates were set aside to pursue other diazo compounds.

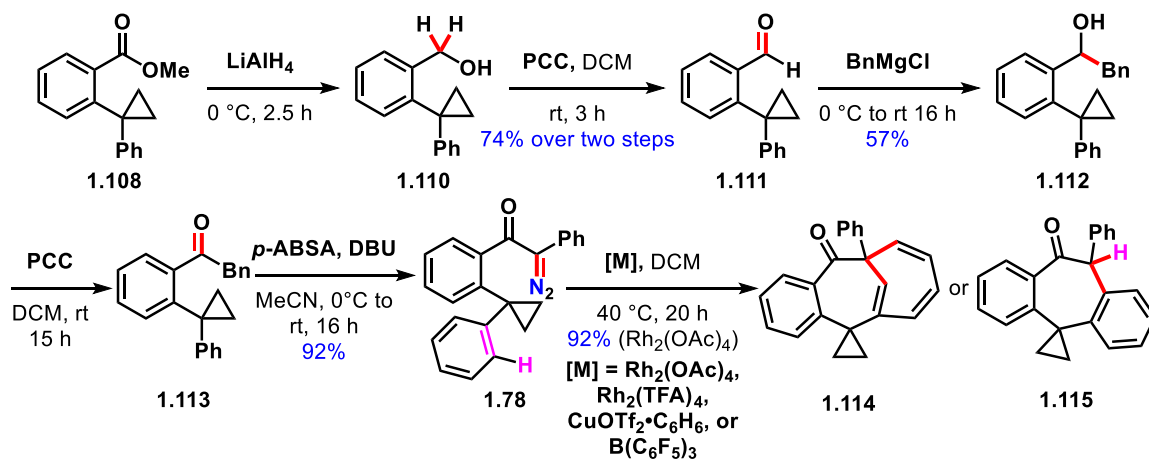


**Figure 1.51.** Synthesis route to diazo **1.78**. Metal-carbene-mediated reactions failed to result in the desired  $\text{C-C}$  bond insertion of the cyclopropyl ring.

### 1.3 Conclusion

Six cyclopropyl-tethered diazo derivatives were synthesized to probe the possibility of a direct insertion into the strained  $\text{C-C}$  bonds. The proximity of the metal carbene to the strained cyclopropane was anticipated to promote the desired reactivity. Instead, compounds bearing or lacking benzylic hydrogens resulted in a variety of undesirable reactivity, including  $\text{C}(\text{sp}^3)\text{-H}$  insertion,  $\text{C}(\text{sp}^2)\text{-H}$  insertion, and Büchner ring expansion.

Adding a non-interfering, electron-donating functional group tethering off the cyclopropyl ring, such as a *tert*-butyl group or deactivated esters/amides, may increase the possibility of direct C–C bond insertion.

#### 1.4 References

1. Bernasconi, C. F.; Sun, W. Physical Organic Chemistry of Transition Metal Carbene Complexes. 8.1 Kinetic and Thermodynamic Acidities of Alkoxyalkylcarbene Pentacarbonyl Complexes of Cr, Mo, and W in Aqueous Acetonitrile. Dependence on Metal, Alkyl Group, and Alkoxy Group. *Organometallics* **1997**, *16*, 1926–1932.
2. Green, S. P.; Wheelhouse, K. M.; Payne, A. D. Hallett, J. P.; Miller, P. W.; Bull, J. A. Thermal Stability and Explosive Hazard Assessment of Diazo Compounds and Diazo Transfer Reagents. *Org. Process. Res. Dev.* **2020**, *24*, 67–84.
3. Dötz, K. H. Carbene Complexes in Organic Synthesis. *Angew. Chem. Int. Ed.* **1984**, *23*, 587–608.
4. (a) Pirrung, M. C.; Liu, H.; Morehead, A. T. Rhodium Chemzymes: Michaelis-Menten Kinetics in Dirhodium(II) Carboxylate-Catalyzed Carbenoid Reactions. *J. Am. Chem. Soc.* **2002**, *9*, 1014–1023. (b) Nakamura, E.; Yoshikai, N.; Yamanaka, M. Mechanism of C-H Bond Activation/C-C Bond Formation Reaction between Diazo Compound and Alkane Catalyzed by Dirhodium Tetracarboxylate. *J. Am. Chem. Soc.* **2002**, *124*, 7181–7192.
5. Taber, D. F.; Petty, E. H. General Route to Highly Functionalized Cyclopentane Derivatives by Intramolecular C–H Insertion. *J. Org. Chem.* **1982**, *47*, 4808–4809.
6. Nouri, D. H.; Tantillo, D. J. Hiscotropic Rearrangements: Hybrids of Electrocyclic and Sigmatropic Reactions. *J. Org. Chem.* **2006**, *71*, 3686–3695.
7. Chen, D.; Zhu, D.-X.; Xu, M.-H. Rhodium(I)-Catalyzed Highly Enantioselective Insertion of Carbenoid into Si–H: Efficient Access to Functional Chiral Silanes. *J. Am. Chem. Soc.* **2016**, *138*, 1498–1501.
8. Xie, Z.-Z.; Liao, W.-J.; Guo, L.-P.; Verpoort, F.; Fang, W. Mechanistic Insight into the Rhodium-Catalyzed O–H Insertion Reaction: A DFT Study. *Organometallics* **2014**, *33*, 2448–2456.

9. Hu, W.; Xu, X.; Zhou, J.; Liu, W.-J.; Huang, H.; Hu, J.; Yang, L.; Gong, L.-Z. Cooperative Catalysis with Chiral Brønsted Acid-Rh<sub>2</sub>(OAc)<sub>4</sub>: Highly Enantioselective Three-Component Reactions of Diazo Compounds with Alcohols and Imines. *J. Am. Chem. Soc.* **2008**, *130*, 7782–7783.
10. Li, Z.; Boyarskikh, V.; Hansen, J. H.; Autschbach, J.; Musaev, D. G.; Davies, H. M. L. Scope and Mechanistic Analysis of the Enantioselective Synthesis of Allenes by Rhodium-Catalyzed Tandem Ylide Formation/[2,3]-Sigmatropic Rearrangement between Donor/Acceptor Carbenoids and Propargylic Alcohols *J. Am. Chem. Soc.* **2012**, *134*, 15497–15504.
11. Li, M.-L.; Yu, J.-H.; Li, Y.-H.; Zhu, S.-F.; Zhou, Q.-L. Highly enantioselective carbene insertion into N–H bonds of aliphatic amines. *Science* **2019**, *366*, 990–994.
12. Wang, F.; Lu, S.; Chen, B.; Zhou, Y.; Yang, Y.; Deng, G. Regioselective Reversal in the Cyclization of 2-Diazo-3,5-dioxo-6-ynoates (Ynones, Ynamide): Construction of  $\gamma$ -Pyrones and 3(2*H*)-Furanones Starting from Identical Materials. *Org. Lett.* **2016**, *18*, 6248–6251
13. Tindall, D. J.; Werlé, C.; Goddard, R.; Phillips, P.; Farès, Fürstner, A. Structure and Reactivity of Half-Sandwich Rh(+3) and Ir(+3) Carbene Complexes. Catalytic Metathesis of Azobenzene Derivatives. *J. Am. Chem. Soc.* **2018**, *140*, 1884–1893.
14. Doyle, M. P.; Hu, W.; Timmons, D. J. Epoxides and Aziridines from Diazoacetates via Ylide Intermediates. *Org. Lett.* **2001**, *3*, 933–935.
15. Goto, T.; Takeda, K.; Shimada, N.; Nambu, H.; Anada, M.; Shiro, M.; Ando, K.; Hashimoto, S. Highly Enantioselective Cyclopropanation Reaction of 1-Alkynes with  $\alpha$ -Alkyl- $\alpha$ -Diazoesters Catalyzed by Dirhodium(II) Carboxylates. *Angew. Chem. Int. Ed.* **2011**, *50*, 6803–6808.
16. Buchner, E.; Curtius, T. Synthese von Ketonsäureäthern aus Aldehyden und Diazoessigäther. *Ber. Dtsch. Chem. Ges.* **1885**, *18*, 2371–2377.
17. Schlotterbeck, F. Umwandlung von Aldehyden in Ketone durch Diazomethan. *Ber. Dtsch. Chem. Ges.* **1907**, *40*, 1826–1827.
18. Zhang, Y.; Wang, J. Recent development of reactions with  $\alpha$ -diazocarbonyl compounds as nucleophiles. *Chem. Commun.* **2009**, 5350–5361.
19. Eremeyeva, M.; Zhukovsky, D.; Dar'in, D.; Krasavin, M. The Use of  $\alpha$ -Diazo- $\gamma$ -butyrolactams in the Büchner–Curtius–Schlotterbeck Reaction of Cyclic Ketones Opens New Entry to Spirocyclic Pyrrolidones. *Synlett* **2020**, *31*, 982–986.

20. Arndt, F.; Eistert, B. Ein Verfahren zur Überführung von Carbonsäuren in ihre höheren Homologen bzw. deren Derivate. *Ber. Dtsch. Chem. Ges. B* **1935**, *68*, 200–208.
21. Kowalski, C. J.; Haque, M. S.; Fields, K. W. Ester Homologation via  $\alpha$ -Bromo  $\alpha$ -Keto Dianion Rearrangement. *J. Am. Chem. Soc.* **1985**, *107*, 1429–1430.
22. Reddy, R. E.; Kowalski, C. J. Ethyl 1-Naphthylacetate: Ester Homologation via Ynolate Anions. *Org. Synth.* **1993**, *71*, 146.
23. Holmquist, C. R.; Roskamp, E. J. A Selective Method for the Direct Conversion of Aldehydes into  $\beta$ -Keto Esters with Ethyl Diazoacetate Catalyzed by Tin(II) Chloride. *J. Org. Chem.* **1989**, *54*, 3258–326.
24. Li, W.; Wang, J.; Hu, X.; Shen, K.; Wang, W.; Chu, Y.; Lin, L.; Liu, X.; Feng, X. Catalytic Asymmetric Roskamp Reaction of  $\alpha$ -Alkyl- $\alpha$ -diazoesters with Aromatic Aldehydes: Highly Enantioselective Synthesis of  $\alpha$ -Alkyl- $\beta$ -keto Esters. *J. Am. Chem. Soc.* **2010**, *132*, 8532–8533.
25. Li, W.; Liu, X.; Tan, F.; Hao, X.; Zheng, J.; Lin, L.; Feng, X. Catalytic Asymmetric Homologation of  $\alpha$ -Ketoesters with  $\alpha$ -Diazoesters: Synthesis of Succinate Derivatives with Chiral Quaternary Centers. *Angew. Chem. Int. Ed.* **2013**, *52*, 10883–10886.
26. Jeong, H.-M.; Lee, J.-W.; Kim, D.-K.; Ryu, D.-H. Catalytic Asymmetric Formal C–C Bond Insertion Reaction of Aldehydes via 1,2-Acyl Shift: Construction of All-Carbon Quaternary Stereocenters with Three Carbonyl Groups. *ACS Catal.* **2024**, *14*, 131–137.
27. Whitemore, F. C. The Common Basis of Intramolecular Rearrangements. *J. Am. Chem. Soc.* **1932**, *54*, 3274–3283.
28. Souillart, L.; Cramer, N. Catalytic C–C Bond Activations via Oxidative Addition to Transition Metals. *Chem. Rev.* **2015**, *115*, 9410–9464.
29. Halpern, J. Determination and Significance of Transition-Metal-Alkyl Bond Dissociation Energies. *Acc. Chem. Res.* **1982**, *15*, 238–244.
30. Xue, Y.; Dong, G. Total Synthesis of Penicibilaenes via C–C Activation-Enabled Skeleton Deconstruction and Desaturation Relay-Mediated C–H Functionalization. *J. Am. Chem. Soc.* **2021**, *143*, 8272–8277.

31. Ishida, N.; Sawano, S.; Masuda, Y.; Murakami, M. Rhodium-Catalyzed Ring Opening of Benzocyclobutenols with Site-Selectivity Complementary to Thermal Ring Opening. *J. Am. Chem. Soc.* **2012**, *134*, 17502–17504.
32. Xia, Y.; Liu, Z.; Liu, Z.; Ge, R.; Ye, F.; Hossain, M.; Zhang, Y.; Wang, J. Formal Carbene Insertion into C–C Bond: Rh(I)-Catalyzed Reaction of Benzocyclobutenols with Diazoesters. *J. Am. Chem. Soc.* **2015**, *137*, 6327–6334.
33. Mao, G.; Meng, C.; Cheng, F.; Wu, W.; Gao, Y.-Y.; Li, G.-W.; Liu, L. A palladium-catalyzed sequential Heck coupling/C–C bond activation approach to oxindoles with all-carbon-quaternary centers. *Org. Biomol. Chem.* **2022**, *20*, 1642–1646.
34. Xia, Y.; Liu, Z.; Liu, Z.; Ge, R.; Ye, F.; Hossain, M.; Zhang, Y.; Wang, J. Formal Carbene Insertion into C–C Bond: Rh(I)-Catalyzed Reaction of Benzocyclobutenols with Diazoesters. *J. Am. Chem. Soc.* **2014**, *136*, 3013–3015.
35. Liu, Z.; Zhang, X.; Virelli, M.; Zanoni, G.; Anderson, E. A.; Bi, X. Silver-Catalyzed Regio- and Stereoselective Formal Carbene Insertion into Unstrained C–C  $\sigma$ -Bonds of 1,3-Dicarbonyls. *iScience* **2018**, *8*, 54–60.
36. Ning, Y.; Song, Q.; Sivaguru, P.; Wu, L.; Anderson, E. A.; Bi, X. Ag-Catalyzed Insertion of Alkynyl Carbenes into C–C Bonds of  $\beta$ -Ketocarbonyls: A Formal C(sp<sup>2</sup>) Insertion. *Org. Lett.* **2022**, *24*, 631–636.
37. Padwa, A.; Kulkarni, Y. S.; Zhang, Z. Reaction of carbonyl compounds with ethyl lithiodiazoacetate. Studies dealing with the rhodium(II)-catalyzed behavior of the resulting adducts. *J. Org. Chem.* **1990**, *55*, 4144–4153.
38. Reeves, J. T.; Fandrick, D. R.; Tan, Z.; Song, J. J.; Rodriguez, S.; Qu, B.; Kim, S.; Niemeier, O.; Li, Z.; Byrne, D.; Campbell, S.; Chitroda, A.; DeCroos, P.; Fachinger, T.; Fuchs, V.; Gonnella, N. C.; Grinberg, N.; Haddad, Z.; Jäger, B.; Lee, H.; Lorenz, J. C.; Ma, S.; Narayanan, B. A.; Nummy, L. J.; Premasiri, A.; Roschangar, F.; Sarvestani, M.; Shen, S.; Spinelli, E.; Sun, X.; Varsolona, R. J.; Yee, N.; Brenner, M.; Senanayake, C. H. *J. Org. Chem.* **2013**, *78*, 3616–3635.
39. Fillion, E.; Wilsily, A.; Fishlock, D. Development of a Large Scale Asymmetric Synthesis of the Glucocorticoid Agonist BI 653048 BS H<sub>3</sub>PO<sub>4</sub>. *J. Org. Chem.* **2009**, *74*, 1259–1267.
40. Fandrick, D. R.; Reeves, J. T.; Song, J. J.; Tan, Z.; Qu, B.; Yee, N.; Rodriguez, S. Synthesis of Certain Trifluoromethyl Ketones. PCT. Int. Appl. WO/2010/141331, 2010.

41. Khopade, T. M.; Mete, T. B.; Arora, J. S.; Bhat, R. G. An Adverse Effect of Higher Catalyst Loading and Longer Reaction Time on Enantioselectivity in an Organocatalytic Multicomponent Reaction. *Chem. Eur. J.* **2018**, *24*, 6036–6040.
42. Herr, R. J.; Junghein, L. N.; McGill, J. M.; Thrasher, K. J.; Valluri, M. Compounds, Methods, and Formulations for the Oral Delivery of a Glucagon like Peptide (GLP)-1 Compound or a Melanocortin 4 Receptor (MC4) Agonist Peptide. PCT. Int. Appl. WO/2005/019184, 2005.
43. Ponra, S.; Nyadanu, A.; Pan, N.; Martinand-Lurin, E.; Savy, A.; Vitale, M.; Kail, L. E.; Grimaud, L. Cyclopropyl Thioethers, New Inputs for Palladium Catalyzed Ring Opening of Cyclopropanes. *Org. Process Res. Dev.* **2020**, *24*, 827–834.
44. Zhou, S. M.; Deng, M. Z.; Xia, L. J.; Tang, M. H. Efficient Suzuki-Type Cross-Coupling of Enantiomerically Pure Cyclopropylboronic Acids. *Angew. Chem. Int. Ed.* **1998**, *37*, 2845–2847.
45. Gao, A.; Liu, X. Y.; Li, H.; Ding, C. H.; Hou, X. L. Synthesis of  $\beta,\beta$ -Disubstituted Indanones via the Pd-Catalyzed Tandem Conjugate Addition/Cyclization Reaction of Arylboronic Acids with  $\alpha,\beta$ -Unsaturated Esters. *J. Org. Chem.* **2017**, *82*, 9988–9994.
46. Pan, A.; Chojnacka, M.; Crowley, R. III; Göttemann, L.; Haines, B. E.; Kou, K. G. M. Synergistic Brønsted/Lewis acid catalyzed aromatic alkylation with unactivated tertiary alcohols or di-*tert*-butylperoxide to synthesize quaternary carbon centers. *Chem. Sci.* **2022**, *13*, 3539–3548.
47. Shi, L.; Li, K.; Cui, P. C.; Li, L. L.; Pan, S. L.; Li, M. Y.; Yu, X. Q. BINOL derivatives with aggression-induced emission. *J. Mater. Chem. B*, **2018**, *6*, 4413–4416.
48. Zaman, M. K.; Khan, S. N.; Cai, Y.; Sun, Z. Decarboxylative Oxidation of Carboxylic Acids Using Photocatalysis and Copper Catalysis. *Synlett* **2023**, *34*, 2029–2033.
49. Chanthamath, S.; Takaki, S.; Shibatomi, K.; Iwasa, S. Highly Stereoselective Cyclopropanation of  $\alpha,\beta$ -Unsaturated Carbonyl Compounds with Methyl (Diazoacetoxy)acetate Catalyzed by a Chiral Ruthenium(II) Complex. *Angew. Chem. Int. Ed.* **2013**, *52*, 5818–5821.
50. Brandhuber, B. J.; Jiang, Y.; Kolakowski, G. R.; Winski, S. L. Thiazolyl and Oxazolyl Urea, Thiourea, Guanidine, and Cyanoguanidine Compounds as TRKA Kinase Inhibitors. PCT. Int. Appl. WO/2014/078322, 2014.

51. Liu, Q.; Ma, Y.-T.; Huang, X.-Y.; Li, Y.-Z.; Yang, F.; Ali, S.; Ji, K.; Chen, Z.-S. Rh(II)-Catalyzed Chemoselective Oxy-alkynylation of Acceptor–Acceptor Carbenes: Synthesis of C2-Quaternary Alkyne-Substituted 3(2*H*)-Furanones. *Org. Lett.* **2023**, *25*, 4044–4049.

## 1.5 Experimental

### 1.5.1 General information

#### *Solvents and reagents*

Unless noted below, commercial reagents were purchased from Sigma Aldrich, Acros Organics, Fisher Scientific, Chem-Impex, Tokyo Chemical Industry (TCI), Oakwood Chemical, and Alfa Aesar, and used without additional purification. Solvents were purchased from Fisher Scientific, Acros Organics, and Sigma Aldrich. Tetrahydrofuran (THF), diethyl ether (Et<sub>2</sub>O), acetonitrile (MeCN), dichloromethane (DCM), 1,4-dioxane, triethylamine (Et<sub>3</sub>N), and toluene were sparged with argon and dried by passing through alumina columns using argon in a solvent purification system. Benzene was freshly distilled over calcium hydride under an N<sub>2</sub> atmosphere prior to each use. Unless noted below, acetone was freshly distilled over calcium sulfate under a N<sub>2</sub> atmosphere prior to each use. Isopropyl magnesium chloride (*i*-PrMgCl) reagents, ethanol (EtOH), dimethylformamide (DMF), dimethyl sulfoxide (DMSO), and dichloroethane (DCE) were purchased in Sure/Seal or AcroSeal, and used directly. Deuterated solvents were obtained from Cambridge Isotope Laboratories, Inc. or MilliporeSigma.

#### *Reaction setup, progress monitoring, and product purification*

Unless otherwise noted in the experimental procedures, reactions were carried out in flame or oven-dried glassware in anhydrous solvents. Reaction temperatures above rt

(19 to 21 °C) were controlled by an IKA<sup>®</sup> temperature modulator. Reaction progresses were monitored using thin-layer chromatography (TLC) on EMD Silica Gel 60 F254 or Macherey–Nagel SIL HD (60 Å mean pore size, 0.75 mL/g specific pore volume, 5–17 µm particle size, with fluorescent indicator) silica gel plates. Visualization of the developed plates was performed under UV-light (254 nm). Purification and isolation of products were performed via silica gel chromatography (both column and preparative thin-layer chromatography). Organic solutions were concentrated under reduced pressure on an IKA<sup>®</sup> temperature-controlled rotary evaporator equipped with an ethylene glycol/water condenser. Solids measured for melting point were dried under high vacuum overnight and not crystallized.

#### *Analytical instrumentation*

Melting points were measured with the MEL-TEMP melting point apparatus.

NMR spectral data were obtained using deuterated solvents obtained from Cambridge Isotope Laboratories, Inc, or Sigma-Aldrich. <sup>1</sup>H NMR, <sup>13</sup>C NMR, and <sup>19</sup>F NMR data were recorded on Bruker Avance NEO-400 MHz spectrometer using CDCl<sub>3</sub> at 22 °C, or Avance 500 or Avance 600 MHz spectrometers using CDCl<sub>3</sub> at 25 °C. Chemical shifts (δ) are reported in ppm relative to the residual solvent signal (δ 7.26 for <sup>1</sup>H NMR, δ 77.16 for <sup>13</sup>C NMR in CDCl<sub>3</sub>).<sup>1</sup> Data for <sup>1</sup>H NMR spectroscopy are reported as follows; chemical shift (δ ppm), multiplicity (s = singlet, d = doublet, t = triplet, q = quartet, m = multiplet, br = broad, dd = doublet of doublets, dt = doublet of triplets, dp = doublet of pentets), coupling constant (Hz), integration.

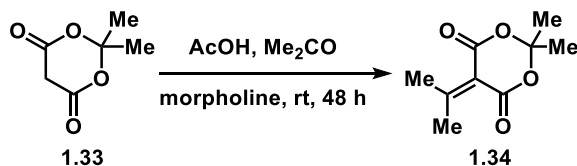


IR spectroscopic data were recorded on a NICOLET 6700 FT-IR spectrophotometer using a diamond attenuated total reflectance (ATR) accessory. Samples were loaded onto the diamond surface either neat or as a solution in organic solvent and the data acquired after the solvent had evaporated.

High resolution accurate mass (ESI) spectral data were obtained from the Analytical Chemistry Instrumentation Facility at the University of California, Riverside, on an Agilent 6545 Q-TOF LC/MS instrument (supported by NSF grant CHE-1828782). High resolution accurate mass (EI) spectral data were obtained from the Mass Spectrometry Facility at the University of California, Irvine, on a ThermoFinnegan TraceMS+ GC EI/CI instrument.

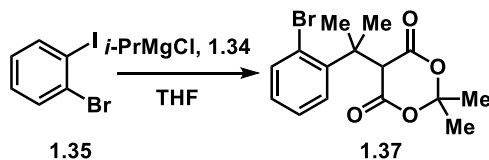
X-ray diffraction data were collected on a Bruker-AXS Apex II diffractometer with an Apex II CCD detector using Mo  $K\alpha$  radiation ( $\lambda = 0.71073 \text{ \AA}$ ) from a fine-focus sealed tube source. CYLview and ORTEP3 were used for graphic rendering.<sup>2,3</sup> Structures were solved by Dr. Veronica Carta (UCR).

## 1.5.2 Experimental Procedures and Characterization Data



### 2,2-Dimethyl-5-(propan-2-ylidene)-1,3-dioxane-4,6-dione (**1.34**)

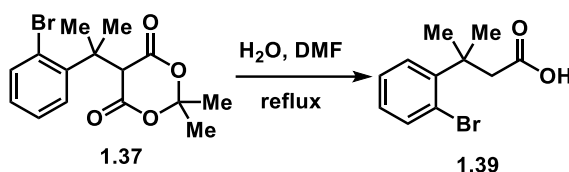
To a 100 mL round-bottomed flask was added Meldrum's acid (**1.33**) (4.9914 g, 34.632 mmol, 1 equiv), followed by acetone (50 mL, 8 × by weight, not anhydrous). The resulting suspension was stirred at rt until the reagents were fully dissolved. To the resultant clear colorless solution was added AcOH (39.8 μL, 0.696 mmol, 0.02 equiv), followed by morpholine (54.6 μL, 0.622 mmol, 0.018 equiv). The reaction mixture was allowed to stir at rt for 48 h. The volatile components were removed under reduced pressure to yield an off-white, light-yellow oil. The resultant residue was diluted with distilled water (20 mL) and then extracted with EtOAc (3 × 20 mL). The combined organic extract was washed with sat. brine (20 mL), dried over anhydrous Na<sub>2</sub>SO<sub>4</sub>, filtered, and concentrated under reduced pressure to yield isopropylidene Meldrum's acid **1.34** as a white solid (6.06 g, 95%). The isolated material contained minor impurities and was advanced without further purification. R<sub>f</sub>: 0.39 (30% EtOAc in hexanes). <sup>1</sup>H NMR (400 MHz, CDCl<sub>3</sub>) δ 2.51 (s, 6H), 1.72 (s, 6H). The spectroscopic data is consistent with those previously reported.<sup>1</sup>



### 5-(2-(2-Bromophenyl)propan-2-yl)-2,2-dimethyl-1,3-dioxane-4,6-dione (1.37)

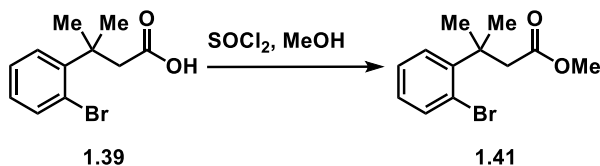
To a flame-dried 100 mL round-bottomed flask equipped with a stir bar was added 2-bromoiodobenzene **1.35** (1.4 mL, 11 mmol, 2 equiv). The flask and its contents were purged with N<sub>2</sub> gas. The flask was chilled to 0 °C and dihalobenzene was added THF (5 mL, 0.5 M), followed by a solution of *i*-PrMgCl in THF (2 M, 5.2 mL, 1.0 × 10<sup>1</sup> mmol, 1.9 equiv) and stirred at 0 °C under N<sub>2</sub> atmosphere for 0.5–1 h. At the same time, to a flask containing isopropylidene Meldrum's acid **1.34** (1.0111 g, 5.4895 mmol, 1 equiv) was added THF (11 mL, 0.5 M) and allowed to stir at 0 °C under N<sub>2</sub> atmosphere until the Grignard reagent formed completely (about 0.5 to 1 h). The solution of Grignard reagent was slowly transferred to the solution containing **1.34** over 5 min and the reaction mixture was left to stir at 0 °C under N<sub>2</sub> atmosphere for 22 h. THF was then removed under reduced pressure to yield a viscous light-yellow solid, which was diluted and quenched with 4 M aqueous HCl (~8 mL) to break up the gelatinous material. The resultant acidified solution was extracted with EtOAc (3 × 10 mL). The combined organic extract was washed with sat brine (11 mL), dried over anhydrous Na<sub>2</sub>SO<sub>4</sub>, filtered, and concentrated under reduced pressure to yield a yellow material that was partially solid. Purification by gradient flash chromatography (eluted with 5–9% EtOAc in hexanes, then 30–35% EtOAc in hexanes) or trituration (with Et<sub>2</sub>O) provided benzyl Meldrum's acid **1.37** as a white solid (1.65 g, 88%). R<sub>f</sub>: 0.36 (15% EtOAc in hexanes). Mp 121–124 °C (lit. 127–129 °C).<sup>2</sup> <sup>1</sup>H NMR (500

MHz, CDCl<sub>3</sub>)  $\delta$  7.58 (dd,  $J$  = 8.1, 1.5 Hz, 1H), 7.55 (dd,  $J$  = 8.0, 1.4 Hz, 1H), 7.33 (dt,  $J$  = 7.4, 1.4 Hz, 1H), 7.09 (dt,  $J$  = 7.4, 1.5 Hz, 1H), 5.74 (s, 1H), 1.87 (s, 3H), 1.79 (s, 6H), 1.73 (s, 3H). The spectroscopic data is consistent with those previously reported.<sup>2</sup>



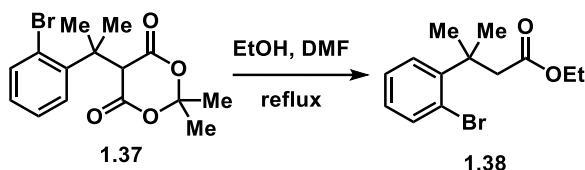
### 3-(2-Bromophenyl)-3-methylbutanoic acid (**1.39**)

To a 100 mL round-bottomed flask was added benzyl Meldrum's Acid **1.37** (2.1533 g, 6.3110 mmol, 1 equiv), followed by DMF (25 mL, 0.25 M) and distilled water (12.5 mL). The clear light-yellow solution was refluxed for 12 h. The solution was allowed to cool to rt before removing DMF under reduced pressure. The resultant orange oil was quenched with 1 M aqueous HCl (25 mL) and extracted with EtOAc (3 × 15 mL). The combined organic extract was washed with sat. brine (20 mL), dried over anhydrous Na<sub>2</sub>SO<sub>4</sub>, filtered, and concentrated under reduced pressure to yield carboxylic acid **1.39** as an orange-red solid (1.53 g, about 94%). The isolated material contained minor impurities and was advanced without further purification. R<sub>f</sub>: 0.29 (30% EtOAc in hexanes). Mp 68–72 °C. <sup>1</sup>H NMR (600 MHz, CDCl<sub>3</sub>)  $\delta$  7.58 (dd,  $J$  = 8.0, 1.4 Hz, 1H), 7.43 (dd,  $J$  = 8.1, 1.5 Hz, 1H), 7.25 (dt,  $J$  = 8.1, 1.5 Hz, 1H), 7.05 (dt,  $J$  = 8.0, 1.5 Hz, 1H), 3.15 (s, 2H), 1.60 (s, 6H). <sup>13</sup>C NMR (126 MHz, CDCl<sub>3</sub>)  $\delta$  176.9, 144.6, 135.7, 128.9, 128.0, 127.3, 122.2, 43.8, 38.5, 28.4. IR (ATR): 2961, 16981 1467, 1414, 1253, 1015, 944, 759, 549, 523, 460 cm<sup>-1</sup>. HRMS (ESI) (m/z): [M-H<sup>-</sup>] calculated for C<sub>11</sub>H<sub>12</sub>BrO<sub>2</sub>: 255.0026; found: 255.0034.



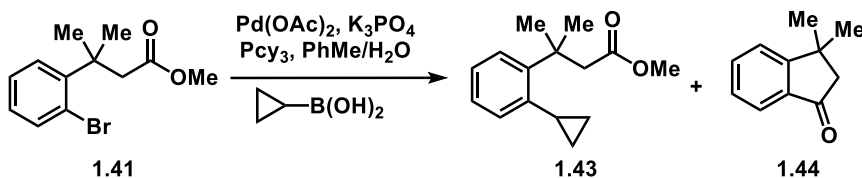
### Methyl 3-(2-bromophenyl)-3-methylbutanoate (**1.41**)

To a 100 mL round-bottomed flask equipped with a stir bar was added the carboxylic acid **1.39** (0.7383 g, 2.871 mmol, 1 equiv), followed by methanol (5.80 mL, 0.5 M) and stirred at 0 °C for 5 min. To the chilled solution was added thionyl chloride (0.42 mL, 5.8 mmol, 2 eq) and stirred at 0 °C for 5 min before removing from ice bath and the clear yellow-orange solution was stirred at rt for 18 h. The reaction was quenched with sat aqueous NaHCO<sub>3</sub> (5 mL), followed by solid NaHCO<sub>3</sub> (about 1 g) to neutralize the solution to about pH 7. The resultant neutralized solution was extracted with Et<sub>2</sub>O (3 × 5 mL) before the combined organic extract was washed with sat brine (11 mL). The organic extract was dried over anhydrous Na<sub>2</sub>SO<sub>4</sub>, filtered, and concentrated under reduced pressure to yield a light-orange liquid. Purification by gradient flash chromatography (eluted with 3–9% EtOAc in hexanes, then 20–25% EtOAc in hexanes) provided methyl ester **1.41** as a clear colorless liquid (0.66 g, 85%). R<sub>f</sub>: 0.27 (5% EtOAc in hexanes). <sup>1</sup>H NMR (400 MHz, CDCl<sub>3</sub>) δ 7.58 (dd, *J* = 8.0, 1.2 Hz, 1H), 7.44 (dd, *J* = 8.0, 1.6 Hz, 1H), 7.26 (dt, *J* = 1.2 Hz, 1H), 7.05 (dt, *J* = 8.0, 1.6 Hz, 1H), 3.50 (s, 3H), 3.13 (s, 2H), 1.60 (s, 6H). <sup>13</sup>C NMR (100 MHz, CDCl<sub>3</sub>) δ 172.2, 145.0, 135.8, 129.0, 128.0, 127.4, 122.4, 51.3, 44.1, 38.8, 28.6. IR (ATR): 2951, 1733, 1468, 1430, 1347, 1202, 1132, 1015, 755, 651, 458 cm<sup>-1</sup>.



### Ethyl 3-(2-bromophenyl)-3-methylbutanoate (**1.38**)

To a 50 mL round-bottom flask equipped with a stir bar was added malonate **1.37** (1.00 g, 2.93 mmol, 1 equiv), followed by *N,N*-dimethylformamide (4.9 mL, 0.5 M), followed by ethanol (5.9 mL, 0.5 M) and refluxed at 100 °C for 16 h. The reaction was quenched with sat aqueous NaHCO<sub>3</sub> (10 mL) and extracted with EtOAc (3 × 10 mL). The combined organic extract was washed with sat brine (3 × 10 mL) and dried over anhydrous Na<sub>2</sub>SO<sub>4</sub>, filtered, and concentrated under reduced pressure to yield ethyl ester **1.38** as a yellow oil (0.70 g, about 84%) The isolated material contained minor impurities and was advanced without further purification. <sup>1</sup>H NMR (500 MHz, CDCl<sub>3</sub>) δ 7.56 (dd, *J* = 7.9, 1.5 Hz, 1H), 7.42 (dd, *J* = 8.0, 1.7 Hz, 1H), 7.24 (dt, *J* = 8.0, 1.5 Hz, 1H), 7.04 (dt, *J* = 7.9, 1.8 Hz, 1H), 3.92 (q, *J* = 7.1 Hz, 2H), 3.09 (s, 2H), 1.59 (s, 6H), 1.01 (t, *J* = 7.1 Hz, 3H). HRMS (ESI) (*m/z*): [M+H]<sup>+</sup> calculated for C<sub>13</sub>H<sub>18</sub>BrO<sub>2</sub>: 285.0485; found: 285.0494.



### Methyl 3-(2-cyclopropylphenyl)-3-methylbutanoate (**1.43**)

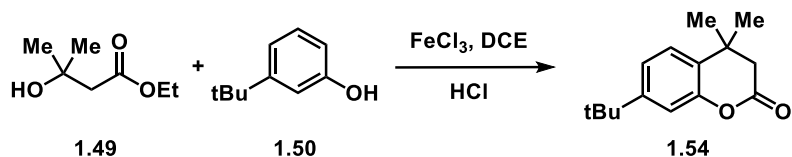
To a 25 mL round-bottomed flask equipped with a stir bar in a glovebox was added Pd(OAc)<sub>2</sub> (13.1 mg, 58.4 μmol, 0.05 equiv), Pcy<sub>3</sub> (25.8 mg, 92.0 μmol, 0.10 equiv), K<sub>3</sub>PO<sub>4</sub> (0.6063 g, 2.856 mmol, 3.5 equiv), cyclopropyl boronic acid (89.3 mg, 1.04 mmol, 1.3

equiv), and methyl ester **1.41** (0.2194 g, 0.8091 mmol, 1 equiv) before removing the flask from the glovebox. To the solids was added toluene:H<sub>2</sub>O solvent (8.1 mL 20:1 toluene:H<sub>2</sub>O, 0.2 M, sparged with N<sub>2</sub> gas) before stirring the translucent dark black reaction at 100 °C for 18 h under inert gas. The reaction was allowed to cool to rt before quenching with distilled water (15 mL), then extracted with EtOAc (3 × 10 mL). The combined organic extract was washed with sat brine (15 mL), dried over anhydrous Na<sub>2</sub>SO<sub>4</sub>, filtered, and concentrated under reduced pressure to yield a dark black liquid. Purification by gradient flash chromatography (eluted with 4–6% EtOAc in hexanes) provided methyl cyclopropyl-ester **1.43** as a clear colorless liquid (0.1120 g, 60%) and 3,3-dimethylindan-1-one **1.44** as a clear colorless liquid (34 mg, 26%).

**Methyl cyclopropyl-ester 1.43:** R<sub>f</sub>: 0.48 (10% EtOAc in hexanes). <sup>1</sup>H NMR (400 MHz, CDCl<sub>3</sub>) δ 7.36 (m, 1H), 7.31 (m, 1H), 7.12 (m, 1H), 6.91 (m, 1H), 3.55 (s, 3H), 2.97 (s, 2H), 2.27 (dp, *J* = 5.4, 2.8 Hz, 1H), 1.62 (s, 6H), 1.03 (dq, *J* = 6.4, 4.7 Hz, 2H), 0.83 (dq, *J* = 5.9, 4.4 Hz, 2H). <sup>13</sup>C NMR (126 MHz, CDCl<sub>3</sub>) δ 172.5, 146.3, 140.9, 126.6, 126.5, 125.6, 125.5, 51.3, 44.2, 38.4, 29.9, 15.1, 10.4. IR (ATR): 2951, 1732 cm<sup>-1</sup>. HRMS (ESI) (m/z): [M+H]<sup>+</sup> calculated for C<sub>15</sub>H<sub>21</sub>O<sub>2</sub>: 233.1536; found: 233.1547.

**3,3-Dimethylindan-1-one 1.44:** R<sub>f</sub>: 0.29 (10% EtOAc in hexanes). <sup>1</sup>H NMR (400 MHz, CDCl<sub>3</sub>) δ 7.71 (d, *J* = 7.6 Hz, 1H), 7.61 (dt, *J* = 7.8, 1.2 Hz, 1H), 7.51 (d, *J* = 7.7 Hz, 1H), 7.37 (dt, *J* = 7.8, 1.0 Hz, 1H), 2.59 (s, 2H), 1.42 (s, 6H). <sup>13</sup>C NMR (126 MHz, CDCl<sub>3</sub>) δ 206.24, 164.02, 135.40, 135.12, 127.54, 123.65, 123.49, 53.06, 38.68, 30.12. IR (ATR): 2957, 2926, 2855, 2360, 2342, 1712, 1603, 1541, 1498, 1471, 1444, 1408, 1384, 1324, 1290, 1244, 1166, 1091, 1070, 1036, 1015, 956, 931, 880, 834, 765, 753, 700, 668, 600,

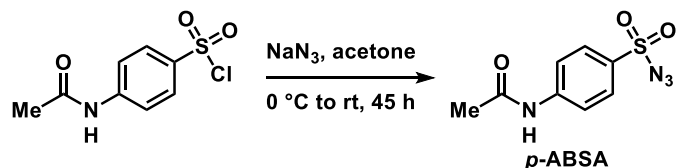
566, 551, 544, 539, 532, 527  $\text{cm}^{-1}$ . HRMS (ESI) (m/z):  $[\text{M}+\text{H}]^+$  calculated for  $\text{C}_{11}\text{H}_{13}\text{O}$ : 161.0961; found: 161.0969.



#### 7-(*tert*-Butyl)-4,4-dimethylchroman-2-one (**1.54**)

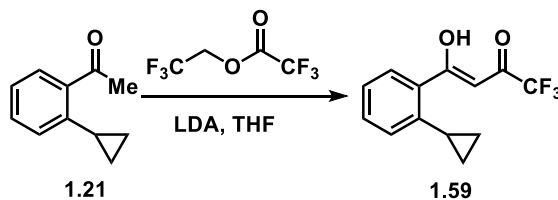
To a 1-dram vial was added 3-*tert* butylphenol (**1.50**) (23.6 mg, 0.157 mmol, 1 equiv) followed by FeCl<sub>3</sub> (25.4 mg, 0.157 mmol, 1 equiv). The solids were diluted in anhydrous DCE (0.63 mL, 0.25 M) and charged with a micro stir bar. To the resultant solution was added conc aqueous HCl (11.7  $\mu\text{L}$ , 0.119 mmol, 0.75 equiv), followed by tertiary alcohol **1.49** (26  $\mu\text{L}$ , 0.17 mmol, 1.1 equiv) and the reaction was allowed to stir airtight at 50 °C for 20 h. The reaction was passed through a silica plug with EtOAc and concentrated under reduced pressure to obtain a reddish brown-black oil. Purification by preparative TLC (eluted with 10% EtOAc in hexanes) afforded **1.54** as a light-yellow oil (7.4 mg, 26%). <sup>1</sup>H NMR (500 MHz, CDCl<sub>3</sub>)  $\delta$  7.23 (d,  $J$  = 8.1 Hz, 1H), 7.17 (dd,  $J$  = 8.1, 2.0 Hz, 1H), 7.08 (d,  $J$  = 2.0 Hz, 1H), 2.61 (s, 2H), 1.34 (s, 6H), 1.31 (s, 9H). <sup>13</sup>C NMR (100 MHz, CDCl<sub>3</sub>)  $\delta$  168.7, 152.2, 150.6, 128.7, 124.1, 121.8, 114.3, 43.9, 34.7, 33.1, 31.3, 27.9. IR (ATR): 2961, 1770  $\text{cm}^{-1}$ . HRMS (ESI) (m/z):  $[\text{M}+\text{H}]^+$  calculated for  $\text{C}_{11}\text{H}_{13}\text{O}_2$ : 233.1536; found: 233.1532.





#### 4-Acetamidobenzenesulfonyl azide (*p*-ABSA)

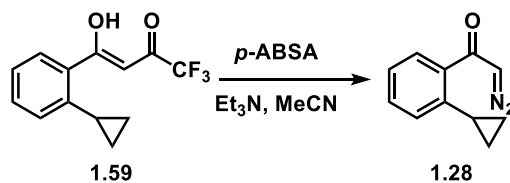
Based on a modified procedure,<sup>3</sup> to a 200 mL round-bottomed flask (not rigorously dried) equipped with a stir bar was added NaN<sub>3</sub> (1.54 g, 23.7 mmol, 1.1 equiv) followed by non-anhydrous acetone (70 mL, 0.3 M) and cooled to 0 °C. To the stirring solution was added slowly in small portions in open air 4-acetamidobenzenesulfonyl chloride (5.02 g, 21.5 mmol, 1 equiv) and allowed the white heterogeneous solution to stir at 0 °C to rt for 45 h. The volatiles in the white solution were removed under reduced pressure. The slurry was diluted in EtOAc (50 mL) and washed with water (3 × 25 mL) and sat brine (25 mL). The organic extract was dried over anhydrous Na<sub>2</sub>SO<sub>4</sub>, filtered, and concentrated under reduced pressure to afford *p*-ABSA as a white solid (4.57 g, about 89%). The isolated material contained minor impurities and was advanced without further purification. <sup>1</sup>H NMR (600 MHz, CDCl<sub>3</sub>) δ 7.91 (dd, *J* = 8.8, 1.3 Hz, 2H), 7.77 (d, *J* = 8.4 Hz, 2H), 7.41 (s, 1H), 2.25 (s, 3H). The spectroscopic data is consistent with those previously reported.<sup>3</sup>



#### (*Z*)-4-(2-Cyclopropylphenyl)-1,1,1-trifluoro-4-hydroxybut-3-en-2-one (1.59)

To a 3-neck round-bottomed flask equipped with a stir bar was added ketone **1.21** (0.55 g, 3.6 mmol, 1 equiv). The flask and its contents were purged with N<sub>2</sub> gas. To the

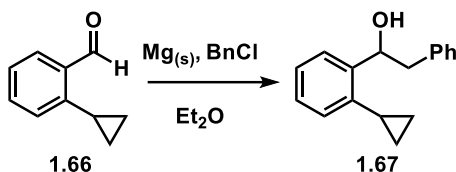
flask was added THF (6.9 mL, 0.5 M) and the reaction was allowed to stir at  $-70\text{ }^{\circ}\text{C}$ . A solution of LDA (2 M in solvent, 1.9 mL, 3.8 mmol, 1.1 equiv) was added and the reaction was stirred at  $-70\text{ }^{\circ}\text{C}$  for 5 min before switching to an ice bath and the reaction stirred for an additional 25 min. To a separate 1-dram vial equipped with a stir bar was added 2,2,2-trifluoroethyl trifluoroacetate (2.3 mL, 17 mmol, 5 equiv). The vial and its contents were purged with  $\text{N}_2$  gas and allowed to stir at  $-70\text{ }^{\circ}\text{C}$ . The enolate solution was transferred to the 2,2,2-trifluoroethyl trifluoroacetate solution dropwise and allowed to stir to  $-70\text{ }^{\circ}\text{C}$  to rt for 4 h. The dark red-orange solution was cooled back to  $0\text{ }^{\circ}\text{C}$  before quenching the reaction with a 5:1 mixture of  $\text{Et}_2\text{O}$  and 5% aqueous HCl (8 mL) before the layers were separated. The aqueous layer was extracted with  $\text{Et}_2\text{O}$  ( $3 \times 3\text{ mL}$ ) and the combined organic extract was washed with sat brine (10 mL), dried over anhydrous  $\text{Na}_2\text{SO}_4$ , filtered, and concentrated under reduced pressure to yield a red-brown oil. Purification by gradient flash chromatography (eluted with 20–30% EtOAc in hexanes) provided **1.59** as a red-orange oil (0.44 g, 50%).  $^1\text{H}$  NMR (400 MHz,  $\text{CDCl}_3$ )  $\delta$  7.58–7.53 (m, 1H), 7.44 (dt,  $J = 7.6, 1.5$  Hz, 1H), 7.31–7.23 (m, 1H), 7.12–7.05 (m, 1H), 6.46 (s, 1H), 2.29 (tt,  $J = 8.6, 5.3$  Hz, 1H), 1.10–0.97 (m, 2H), 0.80–0.71 (m, 2H).  $^{19}\text{F}$  NMR (564 MHz,  $\text{CDCl}_3$ )  $\delta$   $-76.4$  (s, 3F). IR (ATR): 3087, 1601, 1490, 1458, 1272, 1149, 1102, 1083, 1054, 1027, 966, 899, 810, 770, 751, 890, 668, 580, 625, 565, 546, 539, 531  $\text{cm}^{-1}$ . HRMS (ESI) ( $m/z$ ):  $[\text{M}+\text{H}]^+$  calculated for  $\text{C}_{13}\text{H}_{12}\text{F}_3\text{O}_2$ : 257.0784; found: 257.0782.



### 1-(2-Cyclopropylphenyl)-2-diazoethanone (**1.28**)

To a 1-dram vial (not rigorously dried) equipped with a mini stir bar was added enol **1.59** (129.1 mg, 0.5037 mmol, 1 equiv). The vial and its contents were purged with N<sub>2</sub> gas. To the vial was added MeCN (0.5 mL, 1 M), dropwise water (0.5 mL, 1 M) and dropwise Et<sub>3</sub>N (0.65 mL, 0.77 M) and the reaction was allowed to stir at rt. To a separate 1-dram vial was added *p*-ABSA (156.5 mg, 0.6509 mmol, 1.3 equiv) before the vial and its contents were purged with N<sub>2</sub> gas. MeCN (0.65 mL, 1 M) was added and slowly transferred to the black enol solution and the reaction was allowed to stir at rt for 16 h. The orangish solution was quenched with a 6:1 mixture of Et<sub>2</sub>O and 5% aqueous NaOH (3.5 mL) before the layers were separated and the combined organic extract was washed with 5% aqueous NaOH (3 × 1 mL), water (3 × 1 mL), and sat brine (1 mL). The organic extract was dried over anhydrous Na<sub>2</sub>SO<sub>4</sub>, filtered, and concentrated under reduced pressure to afford a red-brown oil. Purification by gradient flash chromatography (eluted with 5–30% EtOAc in hexanes) provided **1.28** as an orange oil (14.2 mg, 33%). <sup>1</sup>H NMR (500 MHz, CDCl<sub>3</sub>) δ 7.38–7.30 (m, 2H), 7.18 (t, *J* = 7.5 Hz, 1H), 6.95 (d, *J* = 7.8 Hz, 1H), 5.66 (s, 1H), 1.05–0.92 (m, 2H), 0.75–0.68 (m, 2H). <sup>13</sup>C NMR (126 MHz, CDCl<sub>3</sub>) δ 190.5, 141.9, 131.0, 128.76, 126.8, 125.5, 125.1, 56.9, 12.9, 9.5. IR (ATR): 3118, 2357, 2102, 1592, 1565, 1488, 1453, 1374, 1332, 1277, 1224, 1201, 1145, 1050, 1031, 1017, 899, 870, 811, 775,

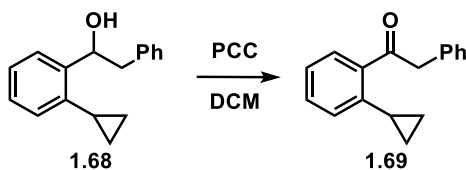
754, 738, 707, 658, 573, 548  $\text{cm}^{-1}$ . HRMS (ESI) (m/z):  $[\text{M}+\text{H}]^+$  calculated for  $\text{C}_{11}\text{H}_{11}\text{N}_2\text{O}$ : 187.0866; found: 187.0874.



### 1-(2-Cyclopropylphenyl)-2-phenylethanol (**1.67**)

To a 10 mL round-bottomed flask (not rigorously dried) equipped with a stir bar was added magnesium turnings (98.3 mg, 4.05 mmol, 2 equiv). The flask containing Mg was flame-dried under vacuum, backfilled with  $\text{N}_2$  gas, and cooled to  $-20$  to  $-10$   $^\circ\text{C}$ . To the chilled flask was added  $\text{Et}_2\text{O}$  (2 mL, 2 M) followed by benzyl chloride (0.23 mL, 2.0 mmol, 2.2 equiv) and the reaction was stirred at  $-20$  to  $-10$   $^\circ\text{C}$  for 30 min. To a separate oven-dried 10 mL round-bottomed flask equipped with a stir bar under inert atmosphere was added aldehyde **1.66** (0.14 mL, 1.0 mmol, 1 equiv) followed by  $\text{Et}_2\text{O}$  (2 mL, 0.5 M) and allowed to stir at rt. The Grignard reagent was added to the aldehyde via cannula and allowed to stir at  $0$   $^\circ\text{C}$  for 30 min. The ice bath was removed, and the reaction mixture stirred at rt for an additional 5 h. The resulting light-brown solution was quenched with a 1:1 mixture of sat aqueous  $\text{NH}_4\text{Cl}$  and  $\text{H}_2\text{O}$  (6 mL). The biphasic mixture was separated, and the aqueous layer was extracted with  $\text{Et}_2\text{O}$  ( $4 \times 4$  mL). The combined organic extract was washed with sat brine (9 mL), dried over anhydrous  $\text{Na}_2\text{SO}_4$ , filtered, and concentrated under reduced pressure to yield a yellow oil. Purification by gradient flash chromatography (eluted with 2–50% DCM in hexanes, then 5% acetone in DCM) afforded **1.67** as a faint yellow oil (97.2 mg, 41%). 7.58 (dd,  $J = 7.6, 1.6$  Hz, 1H), 7.36–7.30 (m, 2H), 7.29–7.24

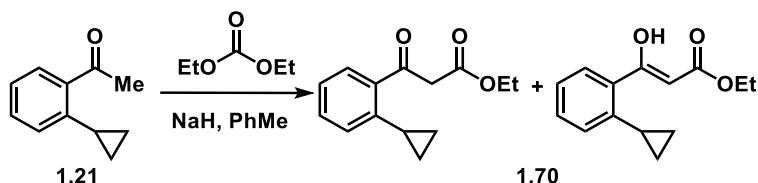
(m, 4H), 7.21 (dt,  $J = 7.5, 1.6$  Hz, 1H), 7.04 (dd,  $J = 7.6, 1.3$  Hz, 1H), 5.53 (dd,  $J = 9.1, 3.8$  Hz, 1H), 3.13 (dd,  $J = 13.8, 3.8$  Hz, 1H), 2.95 (dd,  $J = 13.8, 9.1$  Hz, 1H), 1.92 (tt,  $J = 8.4, 5.4$  Hz, 1H), 0.96 (ddt,  $J = 6.6, 5.0, 3.3$  Hz, 2H), 0.75–0.61 (m, 2H).  $^{13}\text{C}$  NMR (126 MHz,  $\text{CDCl}_3$ )  $\delta$  143.6, 139.2, 138.8, 129.6, 128.7, 127.5, 126.7, 126.5, 126.2, 125.3, 71.5, 45.4, 12.8, 7.5, 7.1. IR (ATR): 3566, 3422, 3061, 3027, 3002, 2921, 2361, 2339, 1746, 1603, 1575, 1494, 1452, 1337, 1286, 1314, 1258, 1187, 1160, 1128, 1075, 1094, 1030, 949, 905, 874, 824, 754, 725, 697, 669, 635, 620, 610, 584, 548, 533, 528  $\text{cm}^{-1}$ . HRMS (ESI) ( $m/z$ ):  $[\text{M}+\text{Na}]^+$  calculated for  $\text{C}_{17}\text{H}_{18}\text{NaO}$ : 261.1255; found: 261.1245.



### 1-(2-Cyclopropylphenyl)-2-phenylethanone (1.69)

To a 50 mL round-bottomed flask (not rigorously dried) equipped with a stir bar was added alcohol **1.68** (1.2497 g, 5.2437 mmol, 1 equiv) followed by non-anhydrous DCM (21 mL, 0.25 M). To the yellow solution was added PCC (1.1155 g, 5.2479 mmol, 1 equiv) and celite (4.01 g), and the brownish-black mixture was allowed to stir at rt for 3 h. The mixture was filtered through a silica plug (eluted with DCM until the brown color nears the end but does not elute out) and concentrated under reduced pressure to afford **1.69** as a yellow oil (0.9383 g, about 76%). The isolated material contained minor impurities and was advanced without further purification.  $^1\text{H}$  (600 MHz,  $\text{CDCl}_3$ )  $\delta$  7.50 (d,  $J = 7.7$  Hz, 1H), 7.37–7.29 (m, 3H), 7.28–7.18 (m, 4H), 7.02 (d,  $J = 7.8$  Hz, 1H), 4.24 (s, 2H), 2.28–2.23 (m, 1H), 0.91 (d,  $J = 6.8$  Hz, 2H), 0.59 (d,  $J = 5.3$  Hz, 2H).  $^{13}\text{C}$  NMR (126

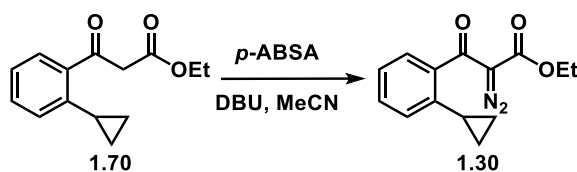
MHz, CDCl<sub>3</sub>)  $\delta$  143.4, 139.0, 138.6, 129.4, 128.5, 127.3, 126.5, 126.3, 126.0, 125.1, 71.3, 45.2, 12.6, 7.3, 6.9. IR (ATR): 3064, 3029, 1683, 1599, 1568, 1494, 1454, 1379, 1325, 1297, 1253, 1199, 1177, 1102, 1074, 1050, 1030, 1018, 985, 932, 899, 863, 841, 824, 782, 752, 715, 695, 656, 644, 622, 602, 582, 575, 553, 539, 531 cm<sup>-1</sup>. [M+H]<sup>+</sup> calculated for C<sub>17</sub>H<sub>17</sub>O: 237.1274; found: 237.1279.



### Ethyl 3-(2-cyclopropylphenyl)-3-oxopropanoate (1.70)

To a 2-neck 25 mL round-bottomed flask equipped with a stir bar was added NaH (0.3940 g, 16.42 mmol, 2.8 equiv). The flask and its contents were purged with N<sub>2</sub> gas and added toluene (3.0 mL, 2 M). To the solution was added diethyl carbonate (1.4 mL, 12 mmol, 2 equiv) and the reaction mixture was stirred at reflux. To a separate 10 mL pear-shaped round-bottomed flask under inert atmosphere was added 2'-cyclopropylacetophenone (**1.21**) (0.9440 g, 5.892 mmol, 1 equiv) followed by toluene (5.9 mL, 2 M) before transferring the solution to the flask containing carbonate via syringe over four min and allowed to reflux for 5 h. The dark brown-black solution was allowed to cool to rt before slowly quenching with acetic acid (1.5 mL). Distilled H<sub>2</sub>O (7–10 mL) was used to assist with transferring the resultant emulsion to a separatory funnel. The biphasic mixture was separated, and the aqueous layer was extracted with Et<sub>2</sub>O (3 × 7 mL). The combined organic extract was washed with sat brine (10 mL), dried over anhydrous Na<sub>2</sub>SO<sub>4</sub>, filtered, and concentrated under reduced pressure to yield a black oil. Purification

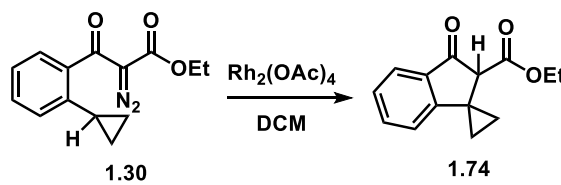
by gradient flash chromatography (eluted with 1–50% EtOAc in hexanes) afforded **1.70** as a 2.5:1 mixture of the ketoester and enol-ester as an orange-yellow oil (0.62 g, 45%). <sup>1</sup>H NMR (500 MHz, CDCl<sub>3</sub>) δ 7.53 (dd, *J* = 7.7, 1.5 Hz, 1H), 7.43–7.35 (m, 1.4H), 7.32 (dt, *J* = 7.6, 1.5 Hz, 0.4H), 7.23 (dt, *J* = 7.5, 1.2 Hz, 1H), 7.19 (dt, *J* = 7.5, 1.3 Hz, 0.4H), 7.09–7.03 (m, 1H), 6.96 (dd, *J* = 7.9, 1.2 Hz, 0.4H), 5.40 (s, 0.4H), 4.27 (q, *J* = 7.1 Hz, 0.8H), 4.19 (q, *J* = 7.1 Hz, 2H), 3.98 (s, 2H), 2.41 (tt, *J* = 8.5, 5.4 Hz, 1H), 2.26 (tt, *J* = 8.5, 5.3 Hz, 0.4H), 1.34 (t, *J* = 7.1 Hz, 1.2H), 1.24 (t, *J* = 7.1 Hz, 3H), 1.04–0.95 (m, 3.2H), 0.73–0.66 (m, 3.2H).



### Ethyl 3-(2-cyclopropylphenyl)-2-diazo-3-oxopropanoate (**1.30**)

To a 25 mL round-bottomed flask was added ketoester **1.70** (1.0757 g, 4.6309 mmol, 1 equiv). The flask and its contents were purged with N<sub>2</sub> gas. MeCN (5.8 mL, 0.8 M) was added and cooled to 0 °C. To the solution was added *p*-ABSA (1.4330 g, 5.9650 mmol, 1.3 equiv) followed by a solution of DBU (0.92 mL, 6.2 mmol 1.33 equiv) in MeCN (1.5 mL, 3 M) and allowed to stir at 0 °C to rt for 17 h. The orange-red-brown solution was quenched with 1 M aqueous NaOH (10 mL) and the resultant dark yellow-orange solution stirred for a few min at rt in open air. The biphasic mixture was separated, and the aqueous layer extracted with Et<sub>2</sub>O (3 × 7 mL). The combined organic extract was washed with a 1:1 mixture of sat brine and sat aqueous NaHCO<sub>3</sub> (12 mL), dried over anhydrous Na<sub>2</sub>SO<sub>4</sub>, filtered, and concentrated under reduced pressure to yield a dark orange-brown oil.

Purification by gradient flash chromatography (eluted with 5–30% EtOAc in hexanes with 1% Et<sub>3</sub>N additive) provided **1.30** as a light-yellow oil (0.65 g, 54%). <sup>1</sup>H NMR (500 MHz, CDCl<sub>3</sub>) δ 7.37–7.30 (m, 1H), 7.19 (d, *J* = 4.2 Hz, 2H), 6.97 (d, *J* = 7.9 Hz, 1H), 4.17 (q, *J* = 7.1 Hz, 2H), 2.01 (tt, *J* = 8.4, 5.2 Hz, 1H), 1.15 (t, *J* = 7.1 Hz, 3H), 0.95–0.88 (m, 2H), 0.72–0.65 (m, 2H). <sup>13</sup>C NMR (126 MHz, CDCl<sub>3</sub>) δ 190.2, 141.9, 139.1, 132.8, 131.0, 128.8, 127.1, 126.8, 125.5, 125.1, 56.9, 12.9, 9.5. IR (ATR): 2933, 2124, 1728, 1696, 1589, 1534, 1490, 1446, 1369, 1303, 1258, 1163, 1122, 1087, 1011, 934, 899, 826, 750, 660, 633, 315, 589, 544, 528 cm<sup>-1</sup>.

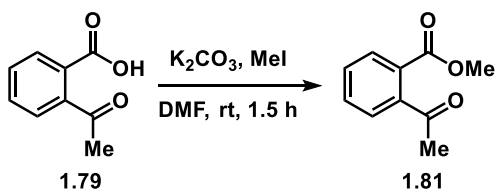


### Ethyl 3'-oxo-2',3'-dihydrospiro[cyclopropane-1,1'-indene]-2'-carboxylate (**1.74**)

To a 1-dram vial equipped with a stir bar in a glovebox was added Rh<sub>2</sub>(OAc)<sub>4</sub> (1.3 mg, 2.9 μmol 0.025 equiv) before the vial was removed from the glovebox and added DCM (0.58 mL, 0.2 M) and gently sparged by N<sub>2</sub> gas. The vial was heated to 40 °C and then added ketoester-diazo **1.30** (30.0 mg, 0.116 mmol, 1 equiv). The resulting blue-green solution was stirred at 40 °C for 16 h. The vial was allowed to cool to rt and concentrated under reduced pressure to afford a green oil. Purification by preparative thin-layer chromatography (eluted with 1% acetone in hexanes × 2) provided **1.74** as a yellow oil (7.2 mg, 27%). <sup>1</sup>H NMR (500 MHz, CDCl<sub>3</sub>) δ 7.78 (d, *J* = 7.7 Hz, 1H), 7.62 (dt, *J* = 7.6, 1.2 Hz, 1H), 7.39–7.32 (m, 1H), 7.00 (d, *J* = 7.8 Hz, 1H), 4.24 (dq, *J* = 10.6, 7.1 Hz, 1H), 4.17–4.08 (m, 2H), 1.68 (ddd, *J* = 10.1, 7.3, 5.0 Hz, 1H), 1.37 (ddd, *J* = 9.8, 7.4, 5.2 Hz, 1H),

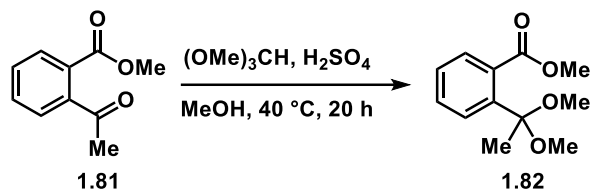


1.14 (t,  $J = 7.1$  Hz, 3H), 1.06 (ddd,  $J = 9.9, 7.3, 5.2$  Hz, 1H), 0.98 (ddd,  $J = 9.7, 7.3, 4.9$  Hz, 1H).  $^{13}\text{C}$  NMR (126 MHz,  $\text{CDCl}_3$ )  $\delta$  200.8, 171.5, 158.1, 136.3, 133.9, 127.0, 124.4, 119.7, 81.6, 62.7, 30.6, 16.8, 14.3, 14.0.



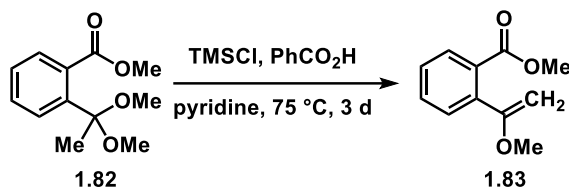
### Methyl 2-acetylbenzoate (1.81)

Based on a modified procedure,<sup>4</sup> a 50 mL round-bottomed flask equipped with a stir bar was added 2-acetylbenzoic acid (**1.79**) (2.00 g, 12.2 mmol, 1 equiv),  $\text{K}_2\text{CO}_3$  (2.50 g, 18.1 mmol, 1.5 equiv), and non-anhydrous DMF (10 mL, 1.2 M, sparged with  $\text{N}_2$  gas), and the resulting mixture was stirred at rt. To the white suspension was added a solution of methyl iodide (2.28 mL, 36.6 mmol, 3 equiv) in non-anhydrous DMF (8.0 mL, 4.5 M, sparged with  $\text{N}_2$  gas) and allowed to stir at rt for 1.5 h. The volatiles in the light-yellow solution were removed by concentration under reduced pressure and the resultant white slurry was diluted in DCM. The solution was vacuum-filtrated, and the filtrate washed with sat brine (10 mL), dried over anhydrous  $\text{MgSO}_4$ , filtered, and concentrated under reduced pressure to afford **1.81** a pale-yellow oil (1.88 g, about 87%). The isolated material contained minor impurities and was advanced without further purification.  $^1\text{H}$  NMR (500 MHz,  $\text{CDCl}_3$ )  $\delta$  7.87 (dd,  $J = 7.7, 1.3$  Hz, 1H), 7.59 (dt,  $J = 7.6, 1.4$  Hz, 1H), 7.52 (dt,  $J = 7.6, 1.4$  Hz, 1H), 7.44 (dd,  $J = 7.5, 1.4$  Hz, 1H), 3.92 (s, 3H), 2.56 (s, 3H). The spectroscopic data is consistent with those previously reported.<sup>4</sup>



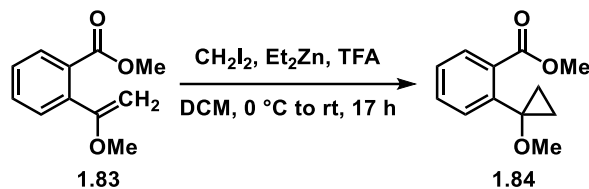
### Methyl 2-(1,1-dimethoxyethyl)benzoate (**1.82**)

Based on a modified procedure,<sup>5</sup> a 10 mL round-bottomed flask equipped with a stir bar was added sequentially in open-air ketone **1.81** (0.7129 g, 4.001 mmol, 1 equiv), trimethyl orthoacetate (0.66 mL, 6.0 mmol, 1.5 equiv), methanol (0.8 mL, 5 M), and conc aqueous H<sub>2</sub>SO<sub>4</sub> (1 drop, catalytic). The red solution was allowed to stir at 40 °C for 20 h. The resultant black solution was allowed to cool to rt before quenching the reaction with Et<sub>3</sub>N (6 mL). The mixture was stirred for a few min before washing the resultant red-orange solution with sat aqueous NaHCO<sub>3</sub> (3 × 15 mL) and a 1:1 mixture of sat brine and sat aqueous NaHCO<sub>3</sub> (10 mL). The organic extract was dried over anhydrous Na<sub>2</sub>SO<sub>4</sub>, filtered, and concentrated under reduced pressure to yield **1.82** as an orange oil (0.8946 g, about 99%). The isolated material contained minor impurities and was advanced without further purification. <sup>1</sup>H NMR (500 MHz, CDCl<sub>3</sub>) δ 7.53–7.47 (m, 1H), 7.42 (ddd, *J* = 7.9, 6.4, 2.3 Hz, 1H), 7.37–7.28 (m, 2H), 3.87 (s, 3H), 3.17 (s, 6H), 1.67 (s, 3H). [M+Na]<sup>+</sup> calculated for C<sub>12</sub>H<sub>16</sub>NaO<sub>4</sub>: 247.0946; found: 247.0939. The spectroscopic data is consistent with those previously reported.<sup>6</sup>



### Methyl 2-(1-methoxyvinyl)benzoate (**1.83**)

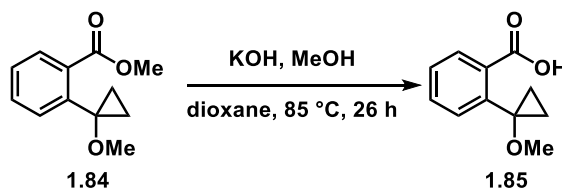
To a 100 mL round-bottomed flask equipped with a stir bar was added benzoic acid (0.50 g, 4.5 mmol, 0.2 equiv) followed by ketal **1.82** (5.01 g, 22.3 mmol, 1 equiv), and the reaction was allowed to slowly stir while the flask and its contents were purged with N<sub>2</sub> gas. To the flask was added pyridine (10 mL, 2.25 M) followed dropwise by TMSCl (9.0 mL, 71 mmol, 3.2 equiv) and the cloudy orange-yellow solution was allowed to stir at 75 °C under inert atmosphere for 3 days. The resultant orange-brown solution was cooled to 0 °C before slowly quenching with ice-cold 15% aqueous NaOH (15 mL) and the mixture was stirred under open air at 0 °C for a few min before the layers were separated. The aqueous layer was extracted with Et<sub>2</sub>O (3 × 10 mL) before the combined organic extract was washed with a 1:1 mixture of sat brine and sat aqueous NaHCO<sub>3</sub> (25 mL). The organic extract was dried over anhydrous Na<sub>2</sub>SO<sub>4</sub>, filtered, and concentrated under reduced pressure to yield **1.83** as a red-orange oil (4.13 g, about 96%). The isolated material contained minor impurities and was advanced without further purification. <sup>1</sup>H NMR (500 MHz, CDCl<sub>3</sub>) δ 7.70–7.64 (m, 1H), 7.48–7.42 (m, 2H), 7.38 (ddd, *J* = 7.6, 6.6, 2.2 Hz, 1H), 4.39 (d, *J* = 2.7 Hz, 1H), 4.29 (d, *J* = 2.7 Hz, 1H), 3.86 (s, 3H), 3.68 (s, 4H). HRMS (ESI) (*m/z*): [M+H]<sup>+</sup> calculated for C<sub>15</sub>H<sub>20</sub>O<sub>2</sub>: 193.0859; found: 193.0869.



### Methyl 2-(1-methoxycyclopropyl)benzoate (**1.84**)

To a 250 mL round-bottomed flask equipped with a stir bar under inert atmosphere was added 1 M Et<sub>2</sub>Zn in hexanes (42 mL, 42 mmol, 2 equiv) and cooled to 0 °C. The solids were diluted in DCM (10 mL, 2 M) followed by dropwise addition of a solution of TFA (3.2 mL, 42 mmol, 2 equiv) in DCM (10 mL, 2 M). To the stirring solution was added CH<sub>2</sub>I<sub>2</sub> (3.4 mL, 42 mmol, 2 equiv) and the flask was stirred at 0 °C for 20 min. To the cooled solution was added a solution of alkene **1.83** (4.0179 g, 20.904 mmol, 1 equiv) in DCM (21 mL, 1 M). The resultant red-black solution was allowed to gradually warm from 0 °C to rt under inert atmosphere for 24 h. The reaction was quenched with 1 M aqueous HCl (30 mL) and the mixture was stirred under open air for a few min before the biphasic orange mixture was separated. The aqueous layer was extracted with DCM (3 × 20 mL) before the combined organic extract was washed with a 1:1 mixture of sat brine and sat aqueous NH<sub>4</sub>Cl (50 mL). The organic extract was dried over anhydrous MgSO<sub>4</sub>, filtered, and concentrated under reduced pressure to yield a dark red oil. Purification by gradient flash chromatography (eluted with 5–20% EtOAc in hexanes) afforded **1.84** as a pale-yellow oil (3.51 g, 81%). <sup>1</sup>H NMR (500 MHz, CDCl<sub>3</sub>) δ 7.70 (d, *J* = 7.3 Hz, 1H), 7.44 (ddd, *J* = 9.0, 6.9, 1.5 Hz, 1H), 7.40–7.30 (m, 2H), 3.93 (d, *J* = 1.2 Hz, 3H), 3.11 (s, 3H), 1.17 (q, *J* = 5.4, 4.9 Hz, 2H), 1.08–0.99 (m, 2H). <sup>13</sup>C NMR (151 MHz, CDCl<sub>3</sub>) δ 169.6, 138.6,

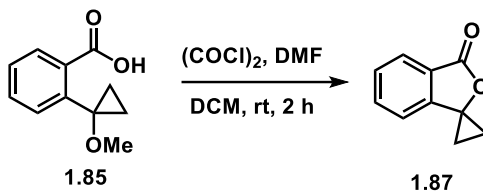
133.1, 130.6, 129.7, 129.1, 127.8, 63.2, 54.9, 52.3, 13.9  $\text{cm}^{-1}$ . HRMS (ESI) (m/z):  $[\text{M}+\text{H}]^+$  calculated for  $\text{C}_{12}\text{H}_{15}\text{O}_2$ : 207.1016; found: 207.1021.



### 2-(1-Methoxycyclopropyl)benzoic acid (**1.85**)

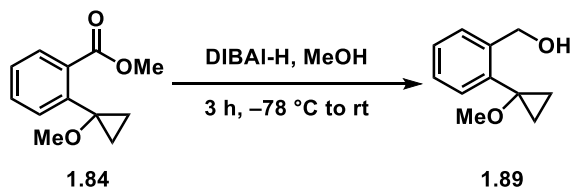
To a 250 mL round-bottomed flask (not rigorously dried) equipped with a stir bar was sequentially added under open air ester **1.84** (2.02 g, 0.80 mmol, 1 equiv), potassium hydroxide (5.30 g, 94.5 mmol, 10 equiv), methanol (32 mL, 0.3 M), and 1,4-dioxane (48 mL, 0.2 M) before equipping the flask with a water condenser. The bright yellow solution was stirred at 85 °C for 26 h. The reaction was cooled to 0 °C and quenched with 6 M aqueous HCl until pH 1 (~20 mL). The volatiles were removed under reduced pressure before diluting the white slurry with water (100 mL) and extracted with EtOAc (3 × 30 mL). The organic extract was washed with a 1:1 mixture of sat brine and sat aqueous  $\text{NH}_4\text{Cl}$  (50 mL), dried over anhydrous  $\text{Na}_2\text{SO}_4$ , filtered, and concentrated under reduced pressure to yield **1.85** as an orange-brown solid (1.6909 g, about 90%). The isolated material contained minor impurities and was advanced without further purification. Mp 88–89 °C.  $^1\text{H}$  NMR (500 MHz,  $\text{CDCl}_3$ )  $\delta$  11.78 (s, 1H), 8.05 (dt,  $J = 7.4, 1.5$  Hz, 1H), 7.54–7.43 (m, 2H), 7.38 (dd,  $J = 7.1, 1.7$  Hz, 1H), 3.28 (d,  $J = 1.1$  Hz, 3H), 1.33–1.28 (m, 2H), 1.07–1.03 (m, 2H).  $^{13}\text{C}$  NMR (151 MHz,  $\text{CDCl}_3$ )  $\delta$  168.6, 135.8, 134.0, 133.2, 133.1, 131.8, 130.1, 129.5, 129.4, 115.1, 64.1, 55.0, 12.8. IR (ATR): 3012, 2826, 2671, 1680, 1605, 1578, 1492, 1455, 1433, 1411, 1305, 1277, 1230, 1189, 1142, 1120, 1079, 1054, 1027, 927, 904, 855,

710, 805, 767, 750, 727, 695, 652, 591, 577, 539, 527  $\text{cm}^{-1}$ . HRMS (ESI) ( $m/z$ ):  $[\text{M}+\text{H}]^+$  calculated for  $\text{C}_{11}\text{H}_{13}\text{O}_3$ : 193.0859; found: 193.0863.



### **3'*H*-Spiro[cyclopropane-1,1'-isobenzofuran]-3'-one (1.87)**

To a 25 mL round-bottomed flask equipped with a stir bar was added carboxylic acid **1.85** (100.7 mg, 0.5237 mmol, 1 equiv). The flask and its contents were purged with  $\text{N}_2$  gas to displace air and create an inert atmosphere. A solution of oxalyl chloride (89.2  $\mu\text{L}$ , 1.04 mmol, 2 equiv) in DCM (0.5 mL, 2 M), followed by one drop of DMF were added, and the resulting yellow solution was stirred for 0.5 h at rt before removing volatiles under reduced pressure. The resultant orange oil was redissolved in benzene (0.9 mL, 0.6 M) followed by addition of a solution of ethyl diazoacetate (0.11 mL, 1.0 mmol, 2 equiv) in benzene (0.9 mL, 0.6 M), and allowed to stir at rt for 2 h. The yellow solution was concentrated under reduced pressure to yield an orange-yellow oil. Purification by gradient flash chromatography (eluted with 2–50% EtOAc in hexanes) afforded **1.87** as a white fluffy solid (78.9 mg, 95%).  $^1\text{H}$  NMR (600 MHz,  $\text{CDCl}_3$ )  $\delta$  7.92 (d,  $J = 7.7$  Hz, 1H), 7.65 (dt,  $J = 7.5, 1.0$  Hz, 1H), 7.52–7.47 (m, 1H), 1.85–1.79 (m, 2H), 1.41–1.37 (m, 2H).  $^{13}\text{C}$  NMR (151 MHz,  $\text{CDCl}_3$ )  $\delta$  170.2, 151.0, 134.3, 128.4, 126.2, 125.8, 118.0, 66.3, 14.2.  $[\text{M}+\text{H}]^+$  calculated for  $\text{C}_{11}\text{H}_{13}\text{O}_3$ : 161.0597; found: 161.0604.

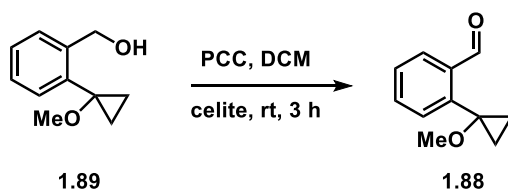


### (2-(1-Methoxycyclopropyl)phenyl)methanol (**1.89**)

To a 50 mL round-bottomed flask equipped with a stir bar was added ester **1.84** (0.5027 g, 2.438 mmol, 1 equiv). The flask and its contents were purged with N<sub>2</sub> gas to displace air and create an inert atmosphere. Anhydrous DCM (4.8 mL, 0.5 M) was added and the solution was allowed to cool to -78 °C. To the stirring solution was added over 1 h via syringe pump a solution of DIBAL-H in hexanes (1 M, 5.3 mL, 5.3 mmol, 2.2 equiv). The colorless solution was stirred for an additional 20 min at -78 °C. The DIBAL-H was slowly quenched over 20 min via syringe pump addition of MeOH (0.22 mL, 5.3 mmol, 2.2 equiv). A 1:1 mixture of sat aqueous Rochelle salt:Et<sub>2</sub>O (1:1, 10 mL) was added and the mixture was gradually allowed to warm from -78 °C to rt, vigorously stirring for an additional 45 min before the layers were separated and extracted with Et<sub>2</sub>O (3 × 3 mL). The combined organic extract was washed with sat brine (9 mL); one drop of 1 M aqueous NaOH was added to break any emulsion. The organic extract was dried over anhydrous Na<sub>2</sub>SO<sub>4</sub>, filtered, and concentrated under reduced pressure to yield a colorless oil. Purification by gradient flash chromatography (eluted with 10–30% EtOAc in hexanes) afforded **1.89** as a colorless oil (0.35 g, 81%).

Alternative approach: To a 250 mL round-bottomed flask (flame-dried, thick 4 cm stir bar) was added LiAlH<sub>4</sub> (0.74 g, 19 mmol, 1 equiv). The flask and its contents were purged with N<sub>2</sub> gas to displace air and create an inert atmosphere. The solids were

suspended in Et<sub>2</sub>O (97 mL, 0.2 M) and the mixture was cooled to 0 °C. To the mixture was added dropwise a solution of ester **1.84** (4 g, 19.4 mmol, 1 equiv) in Et<sub>2</sub>O (17 mL, 1.14 M), which was allowed to stir at 0 °C for 3 h. The reaction was quenched pipette volume-wise with 1:2.5 dH<sub>2</sub>O and sat aqueous NH<sub>4</sub>Cl (60 mL) (slowly until 20 mL when bubbling significantly slowed down, then slowly poured remaining solution). The flask's contents were stirred for a few min under open air and filtered through a celite plug, eluting with EtOAc. The biphasic mixture was separated, and the aqueous layer extracted with EtOAc (3 × 25 mL). The colorless organic extract was washed with sat brine (50 mL), dried over anhydrous Na<sub>2</sub>SO<sub>4</sub>, filtered, and concentrated under reduced pressure to afford **1.89** as a pale-yellow oil (3.24 g, about 94%). The isolated material contained minor impurities and was advanced without further purification. <sup>1</sup>H NMR (600 MHz, CDCl<sub>3</sub>) δ 7.42 (d, *J* = 7.6 Hz, 1H), 7.36–7.32 (m, 2H), 7.28 (t, *J* = 7.4 Hz, 1H), 4.84 (s, 2H), 3.13 (d, *J* = 0.9 Hz, 3H), 1.25–1.20 (m, 3H), 0.96–0.91 (m, 2H). <sup>13</sup>C NMR (151 MHz, CDCl<sub>3</sub>) δ 142.5, 136.7, 130.1, 128.9, 127.4, 64.0, 54.5, 12.6. [M+H]<sup>+</sup> calculated for C<sub>11</sub>H<sub>15</sub>O<sub>2</sub>: 179.1067; found: 179.1013.

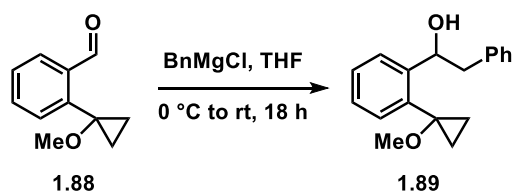


### 2-(1-Methoxycyclopropyl)benzaldehyde (**1.88**)

To a 25 mL round-bottomed flask (not rigorously dried) equipped with a stir bar under open air was added sequentially alcohol **1.89** (180 mg, 1.01 mmol, 1 equiv), DCM (5 mL, 0.2 M), PCC (322.5 mg, 1.496 mmol, 1.5 equiv), and celite (1.3 g). The mixture



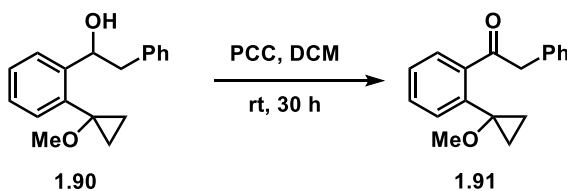
was stirred at rt for 3 h and the dark-brown slush was filtered through a silica plug, eluting with DCM before the solution was concentrated under reduced pressure to afford **1.88** as a colorless oil (127.9 mg, 72%). The isolated material contained minor impurities and was advanced without further purification. <sup>1</sup>H NMR (600 MHz, CDCl<sub>3</sub>) δ 10.83 (s, 1H), 7.98 (d, *J* = 7.6 Hz, 1H), 7.53 (dt, *J* = 7.5, 1.5 Hz, 1H), 7.45 (t, *J* = 7.5 Hz, 1H), 7.39 (d, *J* = 7.6 Hz, 1H), 3.11 (s, 3H), 1.24 (dd, *J* = 4.4, 2.9 Hz, 2H), 1.05–1.00 (m, 2H). <sup>13</sup>C NMR (151 MHz, CDCl<sub>3</sub>) δ 192.8, 141.6, 135.6, 133.2, 129.4, 128.6, 127.9, 61.9, 54.6, 12.7. [M+H]<sup>+</sup> calculated for C<sub>11</sub>H<sub>13</sub>O<sub>2</sub>: 177.0910; found: 177.0910.



### 1-(2-(1-Methoxycyclopropyl)phenyl)-2-phenylethanol (**1.90**)

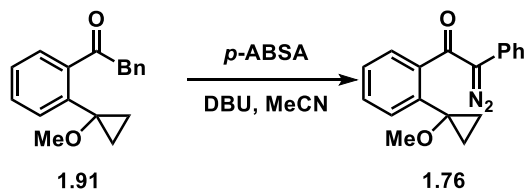
To a 50 mL round-bottomed flask equipped with a stir bar was added aldehyde **1.88** (1.00 g, 5.68 mmol, 1 equiv). The flask and its contents were purged with N<sub>2</sub> gas to displace air and create an inert atmosphere. To the flask was added THF (11 mL, 0.5 M) and the solution stirred at 0 °C. To the stirring solution was added dropwise 1.37 M BnMgCl in THF (8.2 mL, 11.3 mmol, 2 equiv) and the reaction gradually warmed from 0 °C to rt over 14 h. The yellow-golden solution was quenched with sat aqueous NH<sub>4</sub>Cl (15 mL) and allowed to stir for a few min at rt before the solids were filtered off. The biphasic mixture was separated, and the aqueous layer extracted with EtOAc (3 × 10 mL) before the combined organic extract was washed with sat brine (15 mL), dried over anhydrous Na<sub>2</sub>SO<sub>4</sub>, filtered, and concentrated under reduced pressure to afford a pale-yellow oil.

Purification by gradient flash chromatography (eluted with 5–25% EtOAc in hexanes) afforded **1.90** as a colorless oil (1.11 g, 73%). <sup>1</sup>H NMR (600 MHz, CDCl<sub>3</sub>) δ 7.72 (d, *J* = 7.7 Hz, 1H), 7.40–7.31 (m, 5H), 7.28 (t, *J* = 7.5 Hz, 2H), 5.73 (dd, *J* = 9.3, 3.7 Hz, 1H), 3.19 (dd, *J* = 13.6, 3.7 Hz, 1H), 3.12 (s, 3H), 3.02 (dd, *J* = 13.7, 9.3 Hz, 1H), 1.28–1.15 (m, 2H), 0.93 (ddt, *J* = 14.9, 10.7, 5.9 Hz, 2H). <sup>13</sup>C NMR (151 MHz, CDCl<sub>3</sub>) δ 145.3, 139.4, 135.3, 129.8, 129.6, 128.8, 128.5, 126.8, 126.6, 126.4, 70.8, 63.3, 54.3, 44.6, 13.0, 12.6. [M+Na]<sup>+</sup> calculated for C<sub>19</sub>H<sub>20</sub>NaO<sub>3</sub>: 291.1356; found: 291.1360.



### 1-(2-(1-Methoxycyclopropyl)phenyl)-2-phenylethanone (**1.91**)

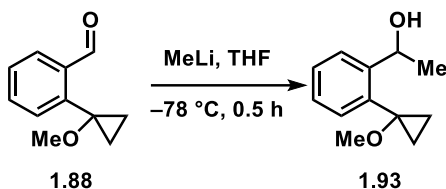
To a 50 mL round-bottomed flask (not rigorously dried) equipped with a stir bar containing alcohol **1.90** (1.11 g, 4.14 mmol, 1 equiv) under open air was added sequentially non-anhydrous DCM (21 mL, 0.2 M), PCC (1.34 g, 6.20 mmol, 1.5 equiv), and celite (5.4 g), and allowed to stir at rt for 30 h. The dark-brown solution was filtered through a silica plug, eluting with EtOAc and concentrated under reduced pressure to afford a yellow oil. Purification by gradient flash chromatography (eluted with 2–20% EtOAc in hexanes) afforded **1.91** as a yellow oil (0.77 g, 89%). <sup>1</sup>H NMR (400 MHz, CDCl<sub>3</sub>) δ 7.38–7.18 (m, 8H), 7.11 (dd, *J* = 7.6, 1.4 Hz, 1H), 4.28 (s, 2H), 3.09 (s, 3H), 1.28–1.22 (m, 2H), 1.15–1.10 (m, 2H). <sup>13</sup>C NMR (101 MHz, CDCl<sub>3</sub>) δ 205.0, 141.8, 136.9, 134.7, 130.0, 129.7, 128.5, 127.8, 127.8, 126.9, 126.5, 62.9, 54.8, 49.9, 14.6. [M+H]<sup>+</sup> calculated for C<sub>18</sub>H<sub>19</sub>O<sub>3</sub>: 267.1380; found: 267.1388.



### 2-Diazo-1-(2-(1-methoxycyclopropyl)phenyl)-2-phenylethanone (**1.76**)

To a 1-dram vial equipped with a mini stir bar was added *p*-ABSA (234.62 mg, 0.41992 mmol, 1.3 equiv) followed by dihydro ketoester **1.91** (209.5 mg, 0.7867 mmol, 1 equiv). The flask and its contents were purged with N<sub>2</sub> gas to displace air and create an inert atmosphere. The flask was cooled to 0 °C before MeCN (0.95 mL) was added and allowed to stir at 0 °C. To the flask was added dropwise a solution of DBU (146 μL, 0.976 mmol, 1.3 equiv) in MeCN (0.33 mL, 3 M) and the resulting yellow solution was gradually allowed to warm from 0 °C to rt over 15 h. The reaction was quenched with 1 M aqueous NaOH (0.75 mL) before the layers were separated and the aqueous layer extracted with EtOAc (3 × 0.5 mL). The combined organic extract was washed with a 1:1 mixture of sat brine and sat aqueous NaHCO<sub>3</sub> (1 mL), dried over anhydrous Na<sub>2</sub>SO<sub>4</sub>, filtered, and concentrated under reduced pressure to afford a bright orange oil. The oil was sent through a short silica plug and eluted with 10% EtOAc in hexanes with 1% Et<sub>3</sub>N additive (10 mL) and concentrated *in vacuo* to afford **1.76** as a bright orange oil (191.6 mg, 83%). R<sub>f</sub>: 0.44 (10% EtOAc in hexanes). <sup>1</sup>H NMR (600 MHz, CDCl<sub>3</sub>) δ 7.66–7.53 (m, 2H), 7.44–7.35 (m, 5H), 7.26–7.21 (m, 2H), 3.14 (s, 3H), 1.14–1.06 (m, 2H), 1.02–0.95 (m, 2H). <sup>13</sup>C NMR (151 MHz, CDCl<sub>3</sub>) δ 190.2, 140.2, 136.5, 129.6, 128.9, 128.5, 128.2, 127.3, 126.6, 125.9, 125.2, 63.1, 54.9, 13.8. IR (ATR): 3061, 2933, 2824, 2070, 1628, 1596, 1575, 1497, 1447, 1414, 1350, 1332, 1286, 1234, 1181, 1159, 1123, 1097, 1060, 1017, 971, 907, 878, 560,

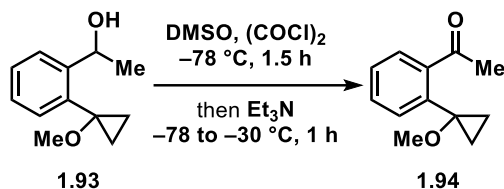
841, 753, 729, 707, 690, 642, 598, 583, 536, 518, 494, 414  $\text{cm}^{-1}$ .  $[\text{M}-\text{N}_2]^+$  calculated for  $\text{C}_{18}\text{H}_{17}\text{O}_2$ : 265.1234; found: 265.1237.



### 1-(2-(1-Methoxycyclopropyl)phenyl)ethanol (**1.93**)

To a 200 mL round-bottomed flask equipped with a stir bar was added aldehyde **1.88** (5.16 g, 29.3 mmol, 1 equiv). The flask and its contents were purged with  $\text{N}_2$  gas to displace air and create an inert atmosphere. The flask was charged with THF (59 mL, 0.5 M) and the solution was allowed to stir at  $-78\text{ }^\circ\text{C}$ . To the solution was added dropwise a solution of methyllithium in  $\text{Et}_2\text{O}$  (1.6 M, 37 mL, 59 mmol, 2 equiv) and allowed to stir at  $-78\text{ }^\circ\text{C}$  for 30 min. The yellow solution was slowly quenched with sat aqueous  $\text{NH}_4\text{Cl}$  (80 mL) (initially bubbled, white precipitate formed) and allowed to stir for a few min at  $0\text{ }^\circ\text{C}$  before the solids were filtered and the biphasic layers separated. The aqueous layer was extracted with  $\text{EtOAc}$  ( $3 \times 40\text{ mL}$ ) before the combined organic extract was washed with sat brine (50 mL), dried over anhydrous  $\text{Na}_2\text{SO}_4$ , filtered, and concentrated under reduced pressure to afford a yellow oil. Purification by gradient flash chromatography (eluted with 10–30%  $\text{EtOAc}$  in hexanes) afforded **1.93** as a light yellow oil (4.89 g, 86%).  $R_f$ : 0.24 (20%  $\text{EtOAc}$  in hexanes).  $^1\text{H}$  NMR (600 MHz,  $\text{CDCl}_3$ )  $\delta$  7.58 (dd,  $J = 7.7, 1.3\text{ Hz}$ , 1H), 7.38 (t,  $J = 7.6\text{ Hz}$ , 1H), 7.31 (dd,  $J = 7.6, 1.4\text{ Hz}$ , 1H), 7.27–7.22 (m, 1H), 5.61 (q,  $J = 6.5\text{ Hz}$ , 1H), 3.10 (s, 3H), 1.57 (d,  $J = 6.5\text{ Hz}$ , 3H), 1.34–1.24 (m, 1H), 1.15–1.08 (m, 1H), 1.02–0.94 (m, 1H), 0.92–0.86 (m, 1H).  $^{13}\text{C}$  NMR (151 MHz,  $\text{CDCl}_3$ )  $\delta$  168.3, 146.1, 144.7, 132.9,

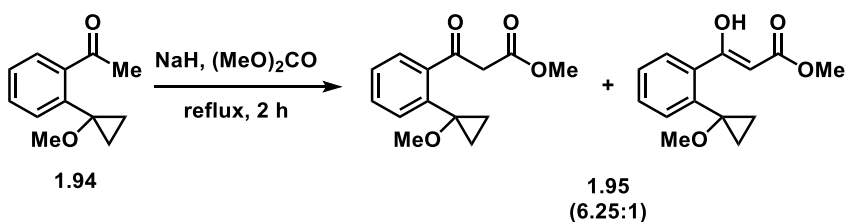
131.6, 130.1, 128.0, 126.9, 125.6, 125.1, 51.9, 28.8, 18.3.  $[M+Na]^+$  calculated for  $C_{12}H_{17}NaO_2$ : 215.1043; found: 215.1042.



### 1-(2-(1-Methoxycyclopropyl)phenyl)ethenone (**1.94**)

To a 100 mL round-bottomed flask equipped with a stir bar under inert atmosphere was added DCM (2.4 mL, 3.5 M) followed by oxalyl chloride (1.1 mL, 12.5 mmol, 1.5 equiv) and cooled to  $-78\text{ }^{\circ}\text{C}$ . To the flask was added dropwise DMSO (1.8 mL, 25 mmol, 3 equiv) (smoked a lot throughout) and the reaction was allowed to stir at  $-78\text{ }^{\circ}\text{C}$  for 15 min. To the flask was added a solution of alcohol **1.93** (1.60 g, 8.32 mmol, 1 equiv) in DCM (40 mL, 0.2 M) and the light yellow solution was stirred at  $-78\text{ }^{\circ}\text{C}$  for 1.5 h.  $\text{Et}_3\text{N}$  (14 mL, 33 mmol, 4 equiv) was added and the solution stirred for 1 h, gradually warming from  $-78$  to  $-30\text{ }^{\circ}\text{C}$ . The reaction was then quenched at about  $-30\text{ }^{\circ}\text{C}$  with a 1:1 solution of  $\text{dH}_2\text{O}:\text{EtOAc}$  (25 mL) and allowed to stir under open air for a few min before the biphasic mixture was separated. The aqueous layer was extracted with EtOAc ( $3 \times 20\text{ mL}$ ), and the combined organic extract was washed with distilled water ( $2 \times 25\text{ mL}$ ), sat aqueous  $\text{NaHCO}_3$  ( $2 \times 75\text{ mL}$ ) and sat brine (30 mL). The organic extract was dried over anhydrous  $\text{Na}_2\text{SO}_4$ , filtered, and concentrated under reduced pressure to yield a yellow oil. Purification by gradient flash chromatography (eluted with 2–30% EtOAc in hexanes) afforded **1.94** as a yellow oil (3.93 g, 81%).  $R_f$ : 0.21 (5% EtOAc in hexanes).  $^1\text{H NMR}$  (600 MHz,  $\text{CDCl}_3$ )  $\delta$  7.38–7.30 (m, 3H), 7.13 (d,  $J = 7.2\text{ Hz}$ , 1H), 3.07 (s, 3H), 2.62 (s, 3H),

1.20–1.15 (m, 2H), 1.10–1.04 (m, 2H).  $^{13}\text{C}$  NMR (151 MHz,  $\text{CDCl}_3$ )  $\delta$  205.3, 142.4, 136.6, 129.7, 127.8, 127.2, 127.0, 62.7, 54.6, 30.7, 14.3.  $[\text{M}+\text{H}]^+$  calculated for  $\text{C}_{12}\text{H}_{15}\text{O}_2$ : 191.1067; found: 191.1075.



### Methyl 3-(2-(1-methoxycyclopropyl)phenyl)-3-oxopropanoate (1.95)

To a 3-neck, 50 mL round-bottomed flask equipped with a stir bar was added 60% NaH in paraffin oil (0.30 g, 7.5 mmol, 1.5 equiv). The flask and its contents were purged with  $\text{N}_2$  gas to displace air and create an inert atmosphere. Dimethyl carbonate (10 mL, 0.5 M) was added and the solution was allowed to stir at rt. A solution of ketone **1.94** (0.95 g, 5.0 mmol, 1 equiv) in dimethyl carbonate (5.0 mL, 1 M) was added and the cloudy light-yellow solution stirred at reflux for 2 h. The red-brown solution was cooled to rt and quenched with 1 M aqueous HCl (9 mL, until pH 1-2). The biphasic mixture was separated and the aqueous layer was extracted with DCM ( $3 \times 5$  mL). The combined organic extract was washed with sat brine (15 mL) and dried over anhydrous  $\text{Na}_2\text{SO}_4$ , filtered, and concentrated under reduced pressure to yield a red-orange oil. Purification by gradient flash chromatography (eluted with 10–40% EtOAc in hexanes) afforded **1.95** as an orange oil (1.13, 91%) in ~6.25:1 ratio of ketoester to enol form. R<sub>f</sub>: 0.22 (10% EtOAc in hexanes).  $^1\text{H}$  NMR (500 MHz,  $\text{CDCl}_3$ )  $\delta$  12.42 (s, 1H, enol-OH), 7.60 (dd,  $J = 6.6, 2.3$  Hz, 1H, enol), 7.45–7.30 (m, 3.6H, enol/ketoester Ar-H), 7.10 (d,  $J = 7.5$  Hz, 1H, ketoester Ar-H), 5.79 (s, 0.16H, enol alkene-H), 4.09 (s, 2H, ketoester alpha-C methylene), 3.80 (s, 0.48H, enol

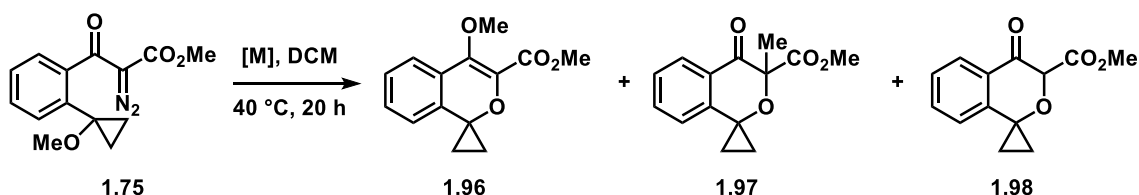
OMe-ester), 3.71 (s, 3H, ketoester OMe-ester), 3.18 (s, 0.48H, enol OMe on cyclopropyl ring), 3.06 (s, 3H, ketoester OMe on cyclopropyl ring), 1.22 (q,  $J = 5.2$  Hz, 2H, ketoester cyclopropyl ring), 1.12 (d,  $J = 6.3$  Hz, 0.32H, enol cyclopropyl ring), 1.08 (q,  $J = 5.2$  Hz, 2H, ketoester cyclopropyl ring), 0.91–0.86 (m, 0.32H, enol cyclopropyl ring).  $^{13}\text{C}$  NMR (151 MHz,  $\text{CDCl}_3$ )  $\delta$  199.3 (ketoester), 173.1 (enol), 168.2 (ketoester), 140.7 (ketoester), 137.1 (ketoester), 136.8 (enol), 131.6 (enol), 130.5 (ketoester), 129.6 (enol), 129.4 (enol), 128.4 (ketoester), 128.2 (enol), 128.0 (ketoester), 126.8 (ketoester), 115.1 (ketoester), 92.5 (enol), 63.1 (enol), 62.7 (ketoester), 54.8 (ketoester), 54.7 (enol), 52.3 (ketoester), 51.5 (enol), 49.1 (ketoester), 14.5 (ketoester), 14.0 (enol).  $[\text{M}+\text{H}]^+$  calculated for  $\text{C}_{14}\text{H}_{17}\text{O}_4$ : 249.1121; found: 249.1127.



### **Methyl 2-diazo-3-(2-(1-methoxycyclopropyl)phenyl)-3-oxopropanoate (1.75)**

To a 100 mL round-bottomed flask equipped with a stir bar was added *p*-ABSA (1.20 g, 5.01 mmol, 1.1 equiv). The flask and its contents were purged with  $\text{N}_2$  gas to displace air and create an inert atmosphere. To the flask was added dihydro ketoester **1.95** (1.13 g, 4.55 mmol, 1 equiv) in MeCN (30 mL, 0.15 M) and allowed to stir at 0 °C. To the solution was added triethylamine (1.9 mL, 14 mmol, 3 equiv) dropwise over 4 min. The resulting bright yellow solution was stirred at 0 °C for 15 min. The water-ice bath was removed and the reaction was stirred at rt until starting material was fully consumed by TLC analysis (2.5 h). The resultant heterogeneous solution was concentrated under reduced

pressure to yield a yellow-white solid. The solids were resuspended in DCM before the precipitate was separated by filtration. The filtrate was concentrated under reduced pressure to afford an orange oil. Purification by gradient flash chromatography (eluted with 10% EtOAc in hexanes in 1% Et<sub>3</sub>N, then 15–30% EtOAc in hexanes) afforded **1.75** as an orange solid (1.22 g, ~98%). The isolated material contained minor impurities and was advanced without further purification. R<sub>f</sub>: 0.31 (20% EtOAc in hexanes). Mp 48–50 °C. <sup>1</sup>H NMR (500 MHz, CDCl<sub>3</sub>) δ 7.37 (dp, *J* = 7.4, 1.6 Hz, 2H), 7.26 (dd, *J* = 6.7, 2.3 Hz, 1H), 7.19 (dd, *J* = 7.1, 1.7 Hz, 1H), 3.71 (s, 3H), 3.06 (s, 3H), 1.10–1.04 (m, 2H), 1.02–0.95 (m, 2H). <sup>13</sup>C NMR (151 MHz, CDCl<sub>3</sub>) δ 189.0, 161.4, 139.7, 136.5, 129.7, 127.7, 126.8, 63.0, 55.0, 52.2, 13.9. [M+H]<sup>+</sup> calculated for C<sub>14</sub>H<sub>15</sub>N<sub>2</sub>O<sub>4</sub>: 275.1026; found: 275.1026.



#### Methyl 4'-methoxyspiro[cyclopropane-1,1'-isochromene]-3'-carboxylate (**1.96**)

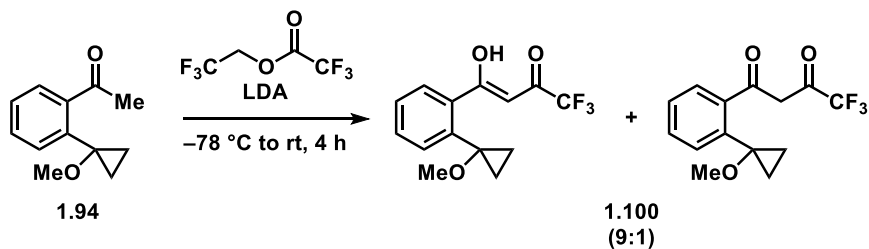
In a glovebox, a 1-dram vial equipped with a stir bar was added diazo **1.75** (9.8 mg, 0.0358 mmol, 1 equiv) followed by Rh<sub>2</sub>(OAc)<sub>4</sub> (0.3 mg, 0.9 μmol, 0.025 equiv) and DCM (0.35 mL, 0.1 M). The vial was capped, removed from the glovebox, and allowed to stir at 40 °C for 20 h. The green-blue solution was allowed to cool to rt and filtered through a short silica pipette plug, eluting with EtOAc, and concentrated under reduced pressure to yield a green-blue oil. Purification by preparative TLC (eluted with 5% EtOAc in hexanes × 2, then 10% EtOAc in hexanes × 2) afforded **1.96** as a white solid (4.8 mg, 50%), **1.97** as a white solid (0.9 mg, 9%) and **1.98** as a colorless oil (0.8 mg, 8%).



**Isochromene ester 1.96:**  $^1\text{H}$  NMR (500 MHz,  $\text{CDCl}_3$ )  $\delta$  7.52–7.48 (m, 1H), 7.33–7.29 (m, 2H), 6.84–6.80 (m, 1H), 3.87 (s, 3H), 3.84 (s, 3H), 1.43–1.38 (m, 2H), 1.04–0.99 (m, 2H).  $^{13}\text{C}$  NMR (151 MHz,  $\text{CDCl}_3$ )  $\delta$  162.6, 149.1, 136.0, 135.5, 130.3, 129.5, 127.6, 122.1, 120.5, 62.3, 60.7, 52.3, 14.6.  $[\text{M}+\text{H}]^+$  calculated for  $\text{C}_{14}\text{H}_{15}\text{O}_4$ : 247.0965; found: 247.0971.

**Methyl isochromane ester 1.97:**  $^1\text{H}$  NMR (600 MHz,  $\text{CDCl}_3$ )  $\delta$  8.09 (d,  $J = 7.8$  Hz, 1H), 7.55–7.49 (m, 1H), 7.36 (t,  $J = 7.6$  Hz, 1H), 6.69 (d,  $J = 7.9$  Hz, 1H), 3.72 (s, 2H), 1.70 (s, 3H), 1.66–1.61 (m, 1H), 1.48–1.42 (m, 1H), 1.34 (dt,  $J = 10.6, 6.9$  Hz, 1H), 1.00 (ddd,  $J = 10.6, 8.1, 5.5$  Hz, 1H).  $^{13}\text{C}$  NMR (151 MHz,  $\text{CDCl}_3$ )  $\delta$  192.0, 171.0, 144.9, 134.4, 128.3, 127.3, 126.7, 120.7, 82.7, 57.3, 52.8, 21.0, 19.0, 16.9.  $[\text{M}+\text{H}]^+$  calculated for  $\text{C}_{14}\text{H}_{15}\text{O}_4$ : 247.0965; found: 247.0971.

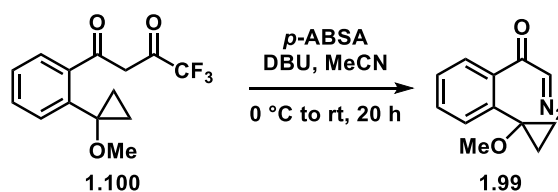
**Isochromane ester 1.98:**  $^1\text{H}$  NMR (500 MHz,  $\text{CDCl}_3$ )  $\delta$  8.07 (d,  $J = 7.9$  Hz, 1H), 7.57 (t,  $J = 7.7$  Hz, 1H), 7.37 (t,  $J = 7.6$  Hz, 1H), 6.73 (d,  $J = 8.0$  Hz, 1H), 4.80 (s, 1H), 3.90 (s, 3H), 1.69 (ddd,  $J = 11.1, 7.9, 5.7$  Hz, 1H), 1.45 (ddd,  $J = 11.1, 8.4, 6.3$  Hz, 1H), 1.39–1.32 (m, 1H), 1.18 (ddd,  $J = 10.5, 8.3, 5.7$  Hz, 1H).  $^{13}\text{C}$  NMR (151 MHz,  $\text{CDCl}_3$ )  $\delta$  187.5, 169.0, 145.3, 135.2, 127.7, 127.4, 127.0, 120.9, 95.2, 56.7, 54.2, 21.1, 15.3.  $[\text{M}+\text{H}]^+$  calculated for  $\text{C}_{13}\text{H}_{13}\text{O}_4$ : 233.0808; found: 233.0791.



#### 4,4,4-Trifluoro-1-(2-(1-methoxycyclopropyl)phenyl)butane-1,3-dione (**1.100**)

To a 50 mL round-bottomed flask equipped with a stir bar was added ketone **1.94** (0.57 g, 3.0 mmol, 1 equiv). The flask and its contents were purged with N<sub>2</sub> gas to displace air and create an inert atmosphere. To the flask was added THF (6 mL, 0.5 M) and the solution was cooled to -78 °C. To the mixture was added dropwise 2 M LDA in THF/heptane/PhEt (1.65 mL, 3.3 mmol, 1.1 equiv) and the resulting yellow solution was allowed to stir at the same temperature for 5 min. The solution was warmed to 0 °C in a water/ice bath and stirred for an additional 25 min. The flask was cooled to -78 °C and added a solution of 2,2,2-trifluoroethyl trifluoroacetate (2.0 mL, 15 mmol, 5 equiv) in THF (3 mL, 5 M) (smoked upon addition). The solution was stirred at -78 °C and gradually allowed to warm to rt over 4 h. The yellow solution was cooled to 0 °C and quenched with a 5:2 mixture of 1 M aqueous HCl and Et<sub>2</sub>O (5 mL), and allowed to stir under open air for a few min before the layers were separated. The aqueous layer was extracted with EtOAc (3 × 3 mL). The combined organic extract was washed with sat brine (5 mL), dried over anhydrous Na<sub>2</sub>SO<sub>4</sub>, filtered, and concentrated under reduced pressure to yield an orange oil. Purification by gradient flash chromatography (eluted with 5–20%, then 50% EtOAc in hexanes) afforded **1.100** as an orange-red oil. R<sub>f</sub>: 0.51 (diketone), 0.32 (keto-enol) (20% EtOAc in hexanes). <sup>1</sup>H NMR (500 MHz, CDCl<sub>3</sub>) δ 7.68 (d, *J* = 7.5 Hz, 1H, enol Ar-H),

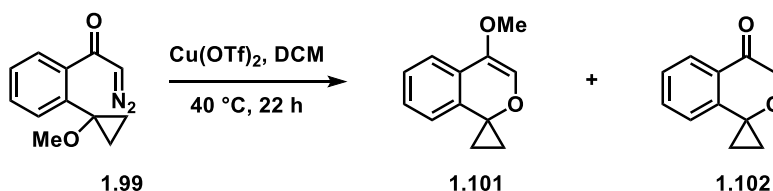
7.52–7.47 (m, 1H, enol Ar-H), 7.47–7.37 (m, 4.2 H, enol/ketoester Ar-H), 7.35 (d,  $J = 7.6$  Hz, 0.1H, ketoester Ar-H), 7.06 (d,  $J = 7.8$  Hz, 0.1H, ketoester Ar-H), 6.84 (s, 1H), 3.44 (s, 0.2H, ketoester alpha-C methylene), 3.16 (s, 3H, enol OMe ester), 3.10 (s, 0.3H, ketoester OMe ester), 1.37–1.32 (m, 0.2H, ketoester cyclopropyl ring), 1.27–1.23 (m, 0.2H, ketoester cyclopropyl ring), 1.19–1.13 (m, 2H enol cyclopropyl ring), 0.95–0.90 (m, 2H, enol cyclopropyl ring).  $^{13}\text{C}$  NMR (151 MHz,  $\text{CDCl}_3$ )  $\delta$  190.4, 137.9, 136.3, 131.5, 130.9, 129.6, 128.5, 98.5, 62.7, 54.8, 14.2.  $[\text{M}+\text{H}]^+$  calculated for  $\text{C}_{14}\text{H}_{14}\text{F}_3\text{O}$ : 287.0890; found: 287.0901.



### 2-Diazo-1-(2-(1-methoxycyclopropyl)phenyl)ethanone (1.99)

To a 1-dram vial equipped with a stir bar was added *p*-ABSA (0.55 g, 2.3 mmol, 1.3 equiv). The flask and its contents were purged with  $\text{N}_2$  gas to displace air and create an inert atmosphere. The vial was cooled to 0 °C and added a solution of diketone **1.100** (0.49862 g, 1.7419 mmol, 1 equiv) in MeCN (2.2 ml, 0.8 M) and dropwise addition of a solution of DBU (0.34 mL, 2.3 mmol, 1.3 equiv) in MeCN (0.75 mL, 3 M). The yellow solution was allowed to gradually warm from 0 °C to rt over 18 h. The dark-red solution was quenched with 1 M aqueous NaOH (3 mL) before the layers were separated. The aqueous layer was extracted with EtOAc (3 × 3 mL). The combined organic extract was washed with sat brine (5 mL), dried over anhydrous  $\text{Na}_2\text{SO}_4$ , filtered, and concentrated under reduced pressure to afford a viscous red residue. Dry-loading in deactivated silica

gel and gradient flash chromatography (eluted with 5–30% acetone in hexanes in 1% Et<sub>3</sub>N) afforded **1.99** as a yellow solid (0.23 g, 61%). R<sub>f</sub>: 0.24 (10% acetone in hexanes). Mp 46–48 °C. <sup>1</sup>H NMR (500 MHz, CDCl<sub>3</sub>) δ 7.62 (s, 1H), 7.44–7.32 (m, 3H), 6.44 (s, 1H), 3.21 (s, 3H), 1.19–1.14 (m, 2H), 0.96–0.90 (m, 2H).



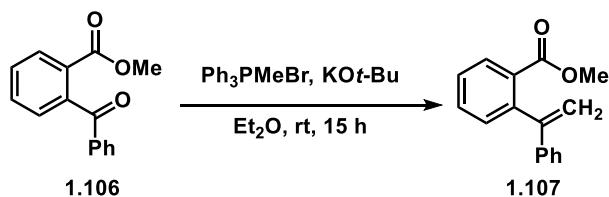
#### 4'-Methoxyspiro[cyclopropane-1,1'-isochromene] (**1.101**)

In a glovebox, a 1-dram vial equipped with a stir bar was added diazo **1.99** (9.7 mg, 0.045 mmol, 1 equiv) followed by Cu(OTf)<sub>2</sub> (1.1 mg, 3.0 μmol, 0.05 equiv) and DCM (0.45 mL, 0.1 M). The vial was capped, removed from the glovebox, and the orange solution stirred at 40 °C for 22 h. The orange-brown solution was allowed to cool to rt and filtered through short silica SiO<sub>2</sub> plug, eluting with EtOAc, and concentrated under reduced pressure to yield an orange-brown oil. Purification by preparative TLC (eluted with 20% EtOAc in hexanes × 2) afforded **isochromene 1.101** as a yellow solid (4.7 mg, 27%) and **isochromane 1.102** as a yellow oil (3.4 mg, 20%).

**Isochromene 1.101**: Mp 103–104 °C. <sup>1</sup>H NMR (500 MHz, CDCl<sub>3</sub>) δ 7.43–7.31 (m, 3H), 7.08 (d, *J* = 7.5 Hz, 1H), 7.03 (s, 1H), 2.97 (s, 3H), 1.07–1.01 (m, 2H), 1.01–0.94 (m, 2H). <sup>13</sup>C NMR (151 MHz, CDCl<sub>3</sub>) δ 197.8, 139.5, 139.3, 138.6, 130.4, 128.4, 127.7, 126.3, 62.7, 54.6, 14.6.

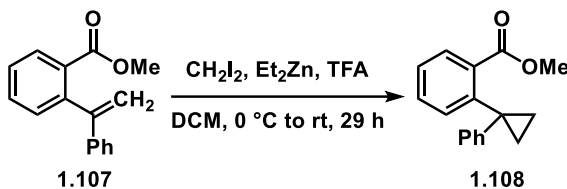
**Isochromane 1.102**: <sup>1</sup>H NMR (500 MHz, CDCl<sub>3</sub>) δ 8.05 (d, *J* = 7.8 Hz, 1H), 7.53 (t, *J* = 7.5 Hz, 1H), 7.36 (t, *J* = 7.6 Hz, 1H), 6.81 (d, *J* = 7.9 Hz, 1H), 4.40 (s, 2H), 1.48–1.41 (m,

2H), 1.17 (q,  $J = 5.4$  Hz, 2H).  $^{13}\text{C}$  NMR (151 MHz,  $\text{CDCl}_3$ )  $\delta$  194.3, 145.2, 134.6, 130.0, 127.0, 126.8, 121.0, 72.2, 59.6, 15.9.



### Methyl 2-(1-phenylvinyl)benzoate (1.107)

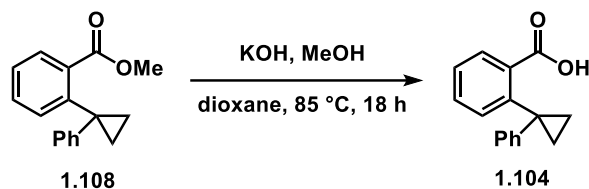
To a 2-neck, 25 mL round-bottomed flask equipped with a stir bar was added  $\text{Ph}_3\text{PMeBr}$  (0.89 g, 2.5 mmol, 1.2 equiv). The flask and its contents were purged with  $\text{N}_2$  gas to displace air and create an inert atmosphere.  $\text{Et}_2\text{O}$  (6.3 mL, 0.4 M) was added, and the pasty-white solution was cooled to  $0^\circ\text{C}$  before adding  $\text{KOt-Bu}$  (0.2909 g, 2.592 mmol, 1.2 equiv). The resultant bright yellow solution was allowed to gradually warm from  $0^\circ\text{C}$  to rt over 15 min. To the stirring mixture was added a solution of ketone **1.106** (0.50 g, 2.2 mmol, 1 equiv) in  $\text{Et}_2\text{O}$  (2 mL, 1.1 M) and the reaction mixture stirred at rt for 15 h. The dark-green solution was filtered through a celite plug and the red filtrate concentrated under reduced pressure to afford a dark red oil. Purification by gradient flash chromatography (eluted with 2–5%  $\text{EtOAc}$  in hexanes) afforded **1.107** as a red-orange oil (110 mg, 21%).  $^1\text{H}$  NMR (500 MHz,  $\text{CDCl}_3$ )  $\delta$  7.83 (d,  $J = 7.7$  Hz, 1H), 7.53 (t,  $J = 7.5$  Hz, 1H), 7.45–7.36 (m, 2H), 7.31–7.22 (m, 5H), 5.69 (s, 1H), 5.27 (s, 1H), 3.51 (s, 3H).  $^{13}\text{C}$  NMR (151 MHz,  $\text{CDCl}_3$ )  $\delta$  168.3, 149.9, 142.5, 141.0, 131.7, 131.4, 131.1, 129.9, 128.2, 127.8, 127.6, 126.7, 114.3, 51.8.  $[\text{M}+\text{H}]^+$  calculated for  $\text{C}_{16}\text{H}_{15}\text{O}_2$ : 239.1067; found: 239.1071.



### Methyl 2-(1-phenylcyclopropyl)benzoate (**1.108**)

To a 2-neck, 25 mL round-bottomed flask equipped with a stir bar under inert atmosphere was added DCM (2.5 mL, 2 M), and the flask was cooled to 0 °C. To the flask was added 1 M Et<sub>2</sub>Zn in hexanes (5 mL, 5 mmol, 2 equiv) (smoked as it was added). To the solution was slowly added a solution of TFA (0.38 mL, 5.0 mmol, 2 equiv) in DCM (2.5 mL, 2 M). To the largely colorless solution was added CH<sub>2</sub>I<sub>2</sub> (0.40 mL, 5.0 mmol, 2 equiv) and the reaction mixture was stirred at 0 °C for 20 min. To the flask was added a solution of olefin **1.107** (2.37 g, 10.7 mmol, 1 equiv), which was then allowed to gradually warm from 0 °C to rt over 29 h. The light-orange solution was quenched with 1 M aqueous HCl (5 mL) and the resultant light-yellow solution was stirred at rt under open air before the layers were separated. The aqueous layer was extracted with DCM (3 × 7 mL). The combined organic extract was washed with sat brine (25 mL), dried over anhydrous Na<sub>2</sub>SO<sub>4</sub>, filtered, and concentrated under reduced pressure to afford **1.108** as an orange-yellow oil (2.45 g, about 94%). The isolated material contained minor impurities and was advanced without further purification. <sup>1</sup>H NMR (600 MHz, CDCl<sub>3</sub>) δ 7.76 (dd, *J* = 7.8, 1.6 Hz, 1H), 7.59 (dd, *J* = 7.8, 1.3 Hz, 1H), 7.50 (dt, *J* = 7.6, 1.5 Hz, 1H), 7.34 (dt, *J* = 7.6, 1.4 Hz, 1H), 7.20 (t, *J* = 7.8 Hz, 2H), 7.13–7.07 (m, 1H), 7.02–6.98 (m, 2H), 3.71 (s, 3H), 1.41–1.34 (m, 2H), 1.33–1.23 (m, 2H). <sup>13</sup>C NMR (151 MHz, CDCl<sub>3</sub>) δ 168.33, 146.12,

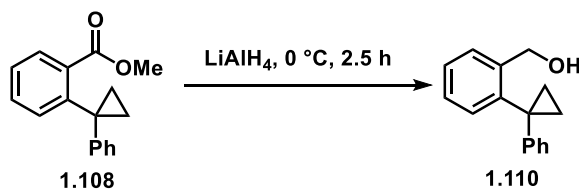
144.71, 133.00, 132.87, 131.57, 130.12, 127.96, 126.87, 125.63, 125.13, 51.89, 28.80, 18.33.  $[M+H]^+$  calculated for  $C_{17}H_{17}O_2$ : 253.1223; found: 253.1234.



### 2-(1-Phenylcyclopropyl)benzoic acid (1.104)

To a 25 round-bottomed flask equipped with a stir bar in open air was sequentially added KOH (0.44 g, 7.84 mmol, 8 equiv), ester **1.108** (239.3 mg, 0.948 mmol, 1 equiv) non-anhydrous MeOH (3.2 mL, 0.3 M), and non-anhydrous dioxane (4.7 mL, 0.2 M), and the reaction mixture was allowed to stir at 85 °C for 11 h. The yellow solution was allowed to cool to 0 °C and slowly quenched with 6 M aqueous HCl to pH 1 (1.4 mL). The resultant white slurry was allowed to stir for a few min at 0 °C before the volatiles were removed under reduced pressure. The white slurry was diluted in H<sub>2</sub>O (2 mL) to dissolve most of the solids and extracted with EtOAc (3 × 1 mL). The combined organic extract was washed with a 1:1 mixture of sat brine and sat aqueous NH<sub>4</sub>Cl (3 mL), dried over anhydrous Na<sub>2</sub>SO<sub>4</sub>, filtered, and concentrated under reduced pressure to afford **1.104** as a white solid (217.9 mg, about 96%). The isolated material contained minor impurities and was advanced without further purification. <sup>1</sup>H NMR (600 MHz, CDCl<sub>3</sub>) δ 7.92 (dd, *J* = 7.8, 1.5 Hz, 1H), 7.63 (dd, *J* = 7.8, 1.3 Hz, 1H), 7.37 (dt, *J* = 7.6, 1.3 Hz, 1H), 7.19 (t, *J* = 7.6 Hz, 2H), 7.10 (t, *J* = 7.3 Hz, 1H), 7.04–6.98 (m, 2H), 1.42 (t, *J* = 3.4 Hz, 2H), 1.37–1.30 (m, 2H). <sup>13</sup>C NMR (151 MHz, CDCl<sub>3</sub>) δ 171.7, 146.0, 145.9, 133.3, 132.6, 131.3, 131.2, 128.1,

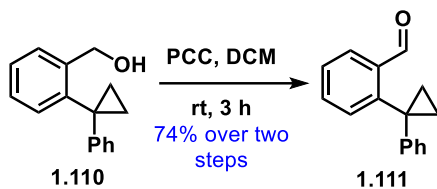
127.1, 125.9, 125.3, 28.9, 18.6.  $[M+H]^+$  calculated for  $C_{16}H_{15}O_2$ : 239.1067; found: 239.1073.



### (2-(1-Phenylcyclopropyl)phenyl)methanol (**1.110**)

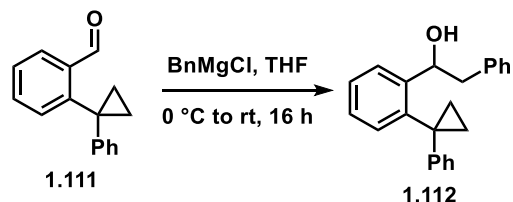
To a 2-neck, 25 mL round-bottomed flask equipped with a stir bar was added  $\text{LiAlH}_4$  (0.39 g, 3.43 mmol, 1 equiv). The flask and its contents were purged with  $\text{N}_2$  gas to displace air and create an inert atmosphere. The solids were suspended in  $\text{Et}_2\text{O}$  (9.7 mL) and the mixture was cooled to  $0\text{ }^\circ\text{C}$ . To the flask was added dropwise a solution of ester **1.108** (2.45 g, 9.71 mmol, 1 equiv) in  $\text{Et}_2\text{O}$  (32 mL) and the mixture was stirred at  $0\text{ }^\circ\text{C}$  for 3 h. The grey solution was slowly quenched with 1:2.5 distilled water and sat aqueous  $\text{NH}_4\text{Cl}$  and allowed to stir for a few min under open air before filtering through a celite plug and eluting with  $\text{EtOAc}$ . The biphasic mixture was separated, and the aqueous layer extracted with  $\text{EtOAc}$  ( $3 \times 15\text{ mL}$ ). The combined organic extract was washed with sat brine (25 mL), dried over anhydrous  $\text{Na}_2\text{SO}_4$ , filtered, and concentrated under reduced pressure to afford **1.110** as a light-yellow oil (1.82 g about 83%). The isolated material contained minor impurities and was advanced without further purification.  $^1\text{H NMR}$  (500 MHz,  $\text{CDCl}_3$ )  $\delta$  7.47 (dd,  $J = 7.3, 1.7\text{ Hz}$ , 1H), 7.34 (ddd,  $J = 9.6, 7.3, 1.7\text{ Hz}$ , 2H), 7.21 (t,  $J = 7.6\text{ Hz}$ , 2H), 7.12 (t,  $J = 7.4\text{ Hz}$ , 1H), 6.96 (d,  $J = 7.7\text{ Hz}$ , 2H), 4.72 (s, 2H), 1.38 (d,  $J = 4.3\text{ Hz}$ , 2H), 1.36–1.31 (m, 2H).  $[M+\text{Na}]^+$  calculated for  $C_{16}H_{16}\text{NaO}$ : 247.1093; found: 247.1088.





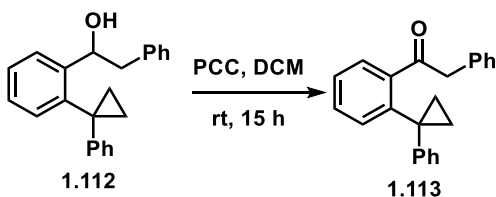
### 2-(1-Phenylcyclopropyl)benzaldehyde (1.111)

To a 100 mL round-bottomed flask equipped with a stir bar containing alcohol **1.110** (1.82 g, 8.11 mmol, 1 equiv) was added sequentially under open air non-anhydrous DCM (41 mL, 0.2 M), PCC (2.62 g, 12.2 mmol, 1.5 equiv), and celite (10.5 g) and allowed to stir at rt lightly capped for 3 h. The brown solution was filtered through a pipette-sized silica plug, eluting with 1:1 hexanes:EtOAc, and the green solution obtained in this manner was concentrated under reduced pressure to afford a green oil (1.70 g, 94%). Purification by gradient column chromatography (eluted with 2–10% EtOAc in hexanes) afforded **1.111** as a pale-yellow oil (1.34 g, 74%). <sup>1</sup>H NMR (600 MHz, CDCl<sub>3</sub>) δ 10.58 (s, 1H), 7.94 (dd, *J* = 7.8, 1.4 Hz, 1H), 7.64–7.57 (m, 2H), 7.43 (dt, *J* = 7.4, 1.6 Hz, 1H), 7.22 (t, *J* = 7.7 Hz, 2H), 7.13 (t, *J* = 7.4 Hz, 1H), 6.98–6.94 (m, 2H), 1.54–1.51 (m, 2H), 1.50–1.43 (m, 2H). <sup>13</sup>C NMR (151 MHz, CDCl<sub>3</sub>) δ 192.5, 147.2, 145.6, 135.3, 134.3, 131.8, 128.5, 128.0, 127.6, 125.8, 125.5, 26.5, 18.1. [M+H]<sup>+</sup> calculated for C<sub>16</sub>H<sub>15</sub>O: 223.1117; found: 223.1118.



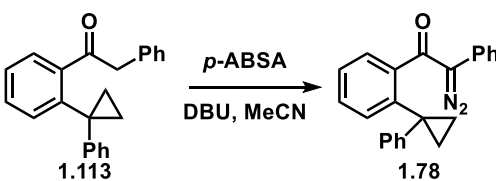
### 2-Phenyl-1-(2-(1-phenylcyclopropyl)phenyl)ethanol (1.112)

To a 25 mL round-bottomed flask equipped with a stir bar was added aldehyde **1.111** (1.00 g, 4.50 mmol, 1 equiv). The flask and its contents were purged with N<sub>2</sub> gas to displace air and create an inert atmosphere. To the flask was added THF (9 mL, 0.5 M) and the solution was allowed to stir at 0 °C. To the flask was added dropwise 1.37 M BnMgCl in THF (6.6 mL, 9.0 mmol, 2 equiv) and allowed to stir at 0 °C rt for 16 h. The yellow-green solution was quenched with sat aqueous NH<sub>4</sub>Cl (13 mL) and the mixture was stirred for a few min before the white solids were separated by filtration. The biphasic filtrate was separated, and the aqueous layer extracted with EtOAc (3 × 7 mL). The combined organic extract was washed with sat brine (15 mL), dried over anhydrous Na<sub>2</sub>SO<sub>4</sub>, filtered, and concentrated under reduced pressure to afford an oil. Purification by gradient flash chromatography (eluted with 5–20% EtOAc in hexanes) afforded **1.112** as a pale-yellow viscous oil (0.80 g, 57%). <sup>1</sup>H NMR (500 MHz, CDCl<sub>3</sub>) δ 7.66 (d, *J* = 7.7 Hz, 1H), 7.46 (d, *J* = 7.5 Hz, 1H), 7.41 (t, *J* = 7.5 Hz, 1H), 7.37–7.31 (m, 1H), 7.25–7.16 (m, 5H), 7.13 (t, *J* = 7.3 Hz, 1H), 6.97 (t, *J* = 8.7 Hz, 4H), 5.34 (dd, *J* = 9.7, 3.2 Hz, 1H), 2.78 (dd, *J* = 13.7, 9.7 Hz, 1H), 2.66 (dd, *J* = 13.7, 3.2 Hz, 1H), 1.54–1.49 (m, 1H), 1.33–1.23 (m, 3H). <sup>13</sup>C NMR (126 MHz, CDCl<sub>3</sub>) δ 145.8, 144.3, 140.9, 139.6, 130.9, 129.3, 128.4, 128.3, 127.7, 126.8, 126.4, 125.4, 125.3, 68.8, 46.7, 27.9, 18.6, 17.5. [M+Na]<sup>+</sup> calculated for C<sub>23</sub>H<sub>22</sub>NaO<sub>3</sub>: 337.1563; found: 337.1560.



### 2-Phenyl-1-(2-(1-phenylcyclopropyl)phenyl)ethenone (1.113)

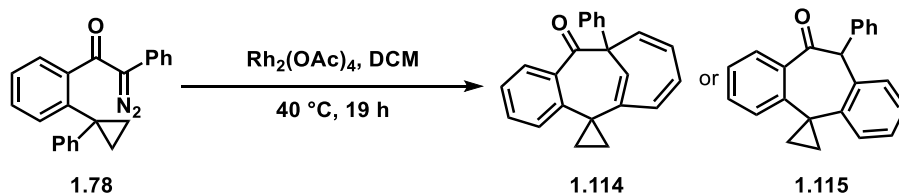
To the 50 mL round-bottomed flask equipped with a stir bar containing alcohol **1.112** (0.35 g in 0.44 g product, 1.11 mmol, 1 equiv) was added sequentially under open air non-anhydrous DCM (13 mL, 0.2 M), PCC (0.36 g, 3.82 mmol, 1.5 equiv), and celite (1.4 g) and the reaction was allowed to stir at rt lightly capped for 15 h. The brown solution was filtered through a silica plug (eluted with EtOAc) and concentrated under reduced pressure to afford **1.113** a yellow oil (0.79 g, about 99%). The isolated material contained minor impurities and was advanced without further purification.  $^1\text{H}$  NMR (600 MHz,  $\text{CDCl}_3$ )  $\delta$  7.57 (d,  $J = 7.7$  Hz, 1H), 7.46 (dt,  $J = 7.5, 1.6$  Hz, 1H), 7.43 (d,  $J = 7.7$  Hz, 1H), 7.34 (t,  $J = 7.5$  Hz, 1H), 7.29–7.19 (m, 5H), 7.14 (t,  $J = 6.9$  Hz, 1H), 7.04–6.94 (m, 4H), 3.91 (s, 2H), 1.39–1.35 (m, 2H), 1.27 (q,  $J = 4.5$  Hz, 2H).  $^{13}\text{C}$  NMR (101 MHz,  $\text{CDCl}_3$ )  $\delta$  203.4, 145.9, 142.3, 142.0, 134.1, 132.9, 130.7, 129.8, 128.5, 128.3, 128.0, 127.0, 126.9, 126.0, 125.5, 49.6, 28.2, 18.7.  $[\text{M}+\text{H}]^+$  calculated for  $\text{C}_{21}\text{H}_{21}\text{O}$ : 313.1587; found: 313.1596.



### 2-Diazo-2-phenyl-1-(2-(1-phenylcyclopropyl)phenyl)ethenone (1.78)

To a 1-dram vial equipped with a mini stir bar was added *p*-ABSA (100.9 mg, 0.41992 mmol, 1.3 equiv) followed by dihydro ketoester **1.113** (101.80 mg, 0.32586 mmol,

1 equiv). The flask and its contents were purged with N<sub>2</sub> gas to displace air and create an inert atmosphere. The flask was cooled to 0 °C and added MeCN (0.4 ml). To the stirring solution was added dropwise a solution of DBU (62 μL, 0.42 mmol, 1.3 equiv) in MeCN (0.14 mL, 3 M) and the yellow solution stirred at 0 °C to rt for 16 h. The slightly dark orange solution was quenched with 1 M aqueous NaOH (0.5 mL) before the layers were separated. The aqueous layer was extracted with EtOAc (3 × 0.3 mL). The combined organic extract was washed with sat brine (1 mL), dried over Na<sub>2</sub>SO<sub>4</sub>, filtered, and concentrated under reduced pressure to afford a bright orange oil. The oil was filtered through a silica plug (2 cm high, monster pipette), eluting with 89:10:1 hexanes:EtOAc:Et<sub>3</sub>N (10 mL) and concentrated *in vacuo* to afford **1.78** as a yellow oil (100 mg, about 92%). The isolated material contained minor impurities and was advanced without further purification. <sup>1</sup>H NMR (400 MHz, CDCl<sub>3</sub>) δ 7.74–7.65 (m, 1H), 7.40–7.33 (m, 4H), 7.30 (dq, *J* = 7.6, 1.7 Hz, 2H), 7.26–7.20 (m, 1H), 7.22–7.10 (m, 4H), 7.13–7.05 (m, 1H), 1.40–1.37 (m, 2H), 1.34–1.27 (m, 2H). <sup>13</sup>C NMR (101 MHz, CDCl<sub>3</sub>) δ 189.7, 144.6, 142.5, 140.6, 131.3, 130.1, 128.9, 128.1, 127.6, 126.9, 126.6, 126.6, 125.8, 125.6, 125.1, 75.3, 28.6, 15.6. [M+H]<sup>+</sup> calculated for C<sub>23</sub>H<sub>21</sub>O: 313.1587; found: 313.1602.



**11'-Phenylspiro[cyclopropane-1,5'-[6,11](metheno)benzo[10]annulene]-12'(11'*H*)-one (1.114) or 11'-Phenylspiro[cyclopropane-1,5'-dibenzo[*a,d*][7]annulene]-10'(11'*H*)-one (1.115)**

To a 1-dram vial was added diazo compound **1.78** (10.1 mg, 0.0298 mmol, 1 equiv) and transferred into a glovebox. To the vial was added  $\text{Rh}_2(\text{OAc})_4$  (0.3 mg, 0.7  $\mu\text{mol}$ , 0.025 equiv) and DCM (0.3 mL, 0.1 M). The vial was sealed using septum-cap, removed from glovebox, and allowed to stir at 40 °C for 19 h. The green-blue solution was cooled to rt, filtered through a short pipette-sized silica plug and concentrated under reduced pressure to afford a green oil. Purification by preparative thin-layer chromatography (eluted with 5% EtOAc in hexanes  $\times$  2) afforded **1.114** or **1.115** as a pale-yellow oil (8.4 mg, 92%).  $^1\text{H}$  NMR (600 MHz,  $\text{CDCl}_3$ )  $\delta$  7.65 (d,  $J = 7.6$  Hz, 1H), 7.50 (t,  $J = 7.7$  Hz, 1H), 7.10 (d,  $J = 7.9$  Hz, 1H), 7.07–6.94 (m, 6H), 6.16 (t,  $J = 7.8$  Hz, 2H), 6.11 (dd,  $J = 9.5, 7.1$  Hz, 1H), 5.45 (d,  $J = 8.6$  Hz, 1H), 1.82 (dt,  $J = 9.8, 6.1$  Hz, 1H), 0.96 (ddd,  $J = 9.9, 6.3, 4.0$  Hz, 1H), 0.92 (ddd,  $J = 10.4, 6.9, 3.9$  Hz, 1H).  $^{13}\text{C}$  NMR (101 MHz,  $\text{CDCl}_3$ )  $\delta$  199.5, 143.6, 137.6, 134.5, 133.9, 129.9, 129.9, 128.7, 128.0, 127.0, 126.9, 126.6, 125.4, 122.1, 119.0, 56.9, 26.1, 23.1, 11.0.  $[\text{M}+\text{H}]^+$  calculated for  $\text{C}_{23}\text{H}_{19}\text{O}$ : 311.1430; found: 311.1441.

### 1.5.3 References

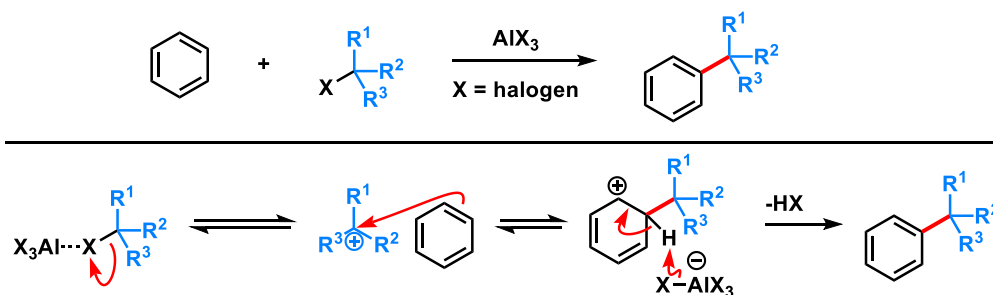
1. Fandrick, D. R.; Reeves, J. T.; Song, J. J.; Tan, Z.; Qu, B.; Yee, N.; Rodriguez, S. Synthesis of Certain Trifluoromethyl Ketones. PCT. Int. Appl. WO/2010/141334, 2010.
2. Fillion, E.; Wilsily, A.; Fishlock, D. Probing Persistent Intramolecular C-H $\cdots$ X (X = O, S, Br, Cl, and F) Bonding in Solution Using Benzyl Meldrum's Acid Derivatives. *J. Org. Chem.* **2009**, *74*, 1259–1267.
3. Keipour, H.; Jalba, A.; Delage-Laurin, L.; Ollevier, T. Copper-Catalyzed Carbenoid Insertion Reactions of  $\alpha$ -Diazoesters and  $\alpha$ -Diazoketones into Si–H and S–H Bonds. *J. Org. Chem.* **2017**, *82*, 3000–3010.
4. Ruthenium-Catalyzed Enantioselective Hydrogenation/Lactonization of 2-Acylarylcarboxylates: Direct Access to Chiral 3-Substituted Phthalides. *Chem. Cat. Chem.* **2017**, *9*, 3989–3996.
5. Liu, J.-L.; Zhu, Z.-F.; Liu, F. Oxycyanation of Vinyl Ethers with 2,2,6,6-Tetramethyl-*N*-oxopiperidinium Enabled by Electron Donor-Acceptor Complex. *Org. Lett.* **2018**, *20*, 720–723.
6. Heaney, H.; Simcox, M. T.; Slawin, A. M. Z.; Giles, R. G. Lanthanide Triflate Catalysed Reactions of Acetals with Primary Amines and Cascade Cyclisation Reactions. *Synlett* **1998**, *6*, 640–642.

## Chapter 2 – Synergistic Brønsted/Lewis Acid Catalyzed Aromatic Alkylation with Unactivated Tertiary Alcohols or di-*tert*-Butylperoxide to Synthesize Quaternary Carbon Centers

### 2.1 Introduction: Friedel–Crafts alkylation

The Friedel–Crafts alkylation reaction has been studied in great depth since its discovery in 1877 to form C(sp<sup>2</sup>)–C(sp<sup>3</sup>) bonds.<sup>1</sup> In this chapter, the focus will be on the C(sp<sup>3</sup>) carbon, where the carbon center is an all-carbon quaternary center.

In a traditional Friedel–Crafts alkylation, an alkyl halide is treated with aluminum trihalide in the presence of an aromatic ring, such as benzene, and results in an alkylated aromatic ring (**Scheme 2.1**). The aluminum trihalide acts as a Lewis acid to extract the halogen from the alkyl group, forming a carbocation intermediate. The nucleophilic arene then engages the carbocation, followed by re-aromatization to result in an alkylated aromatic ring with the release of HX as a byproduct.



**Scheme 2.1.** Traditional Friedel-Crafts reaction and widely accepted mechanism.

Bromides and chlorides are often the common choice of alkyl halides due to their high reactivity, while fluorides and iodides have potential concerns regarding cost and side

reactions. The choice of Lewis acids may vary as well, in which a wide variety may be used, such as iron(III), boron, titanium, etc.<sup>2</sup>

### 2.1.1 Traditional Friedel-Crafts alkylation reactions

The Friedel–Crafts alkylation is a classic example of an electrophilic aromatic substitution (EAS) reaction. Electron-rich aromatic rings tend to be more reactive as long as the electron-donating group does not interfere with the Lewis acid. One such example was demonstrated in 2016 by Moran and coworkers<sup>3</sup> using phenols and anisoles as nucleophiles and alkyl fluorides as electrophiles (**Figure 2.1**). The tertiary alkyl fluoride reacts with borane monohydrate to generate the carbocation, which then reacts with the electron-rich arene (**Scheme 2.2**). Only a small amount of borane catalyst is required due to the formation of HF, which acts as an autocatalyst for the reaction.

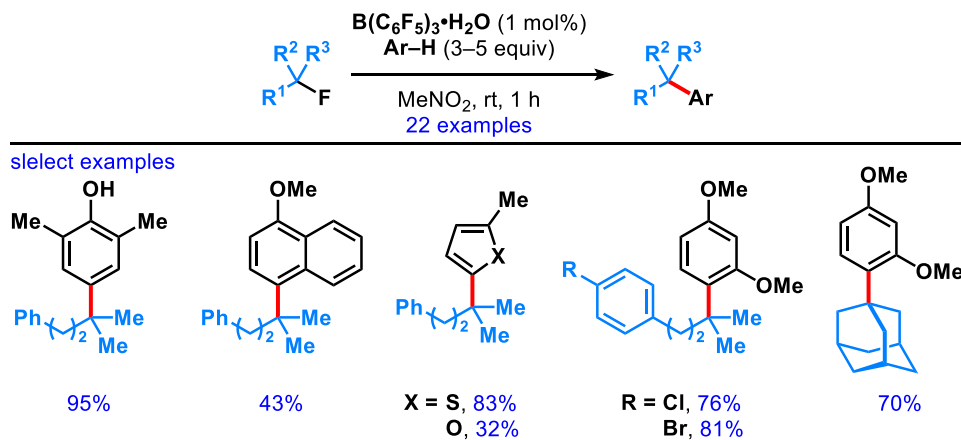
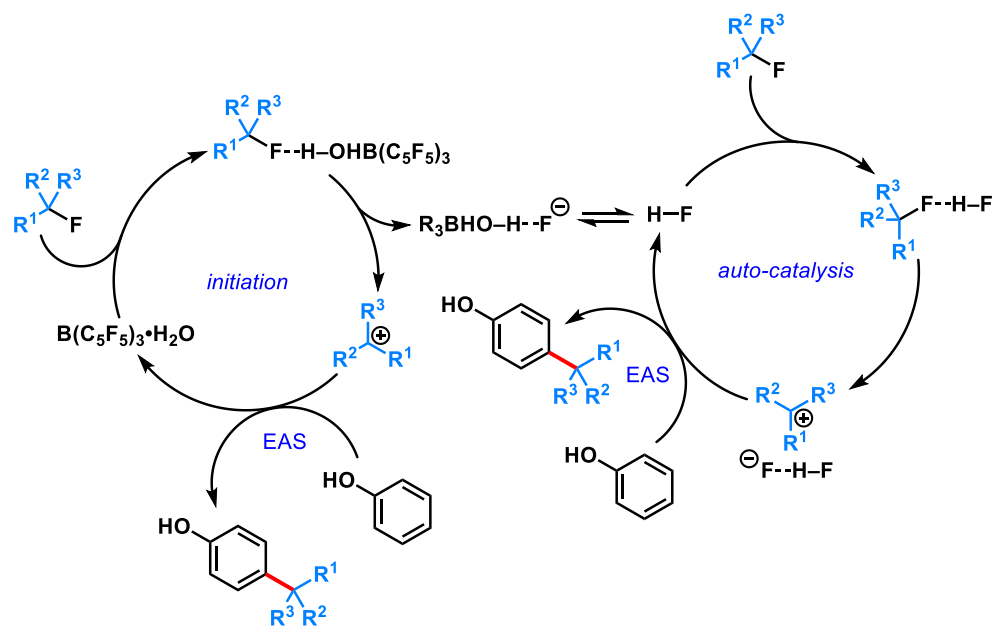


**Figure 2.1.** Friedel–Crafts alkylation with alkyl fluorides and catalytic borane monohydrate to initiate the reaction.





**Scheme 2.2.** Proposed mechanism. Initiation with Lewis acid followed by autocatalysis with HF.

In the same year, Lin and coworkers<sup>4</sup> employed a molybdenum complex/*ortho*-chloranil-catalyzed Friedel–Crafts alkylation reaction of various electron-rich arenes (**Figure 2.2**). Along with other electrophilic alkyl sources, *tert*-butyl alcohol or halides afforded alkylation on the arene in varying yields, with *para*-alkylation being the major or only product. In this method, the authors proposed the *in situ* formation of a chloranil-[Mo] complex **2.1** to be the active catalyst (**Scheme 2.3**). From here, abstraction of the hydroxy or halide by chloranil-[Mo] complex **2.1** generates the carbocation necessary for the Friedel–Crafts reaction.

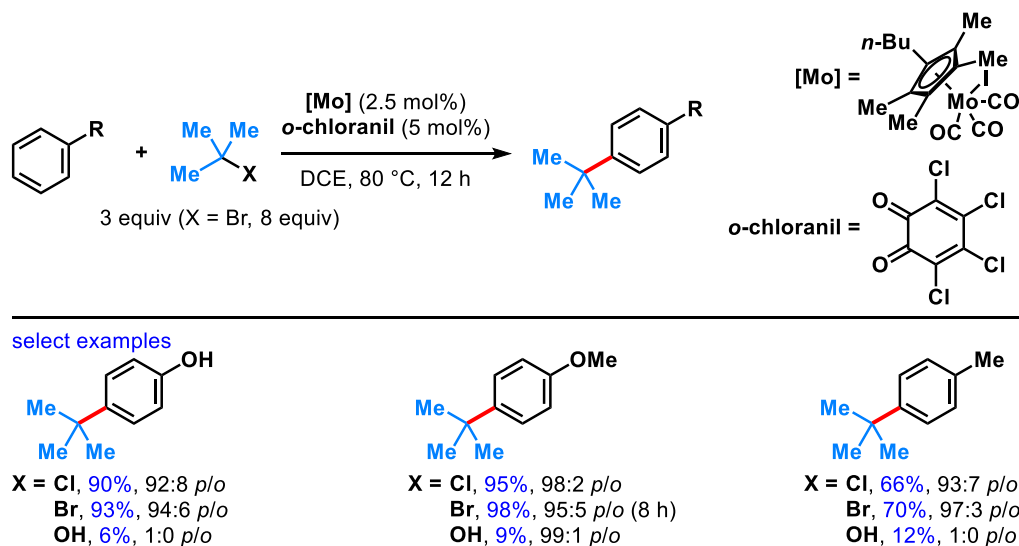
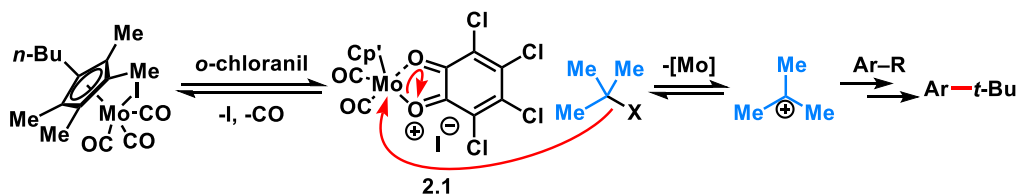


**Figure 2.2.** Friedel–Crafts reaction catalyzed by a molybdenum/chloranil complex.



**Scheme 2.3.** Proposed mechanism of molybdenum/chloranil-catalyzed Friedel–Crafts alkylation.

In 2022, Martin and coworkers<sup>5</sup> developed a unique carborane with a C<sub>2</sub>B<sub>10</sub> icosahedron-shape skeleton (**Figure 2.3**, B(*o*-Cb)<sub>3</sub>). To demonstrate its utility, a Friedel–Crafts alkylation was carried out with 1-fluoroadamantane. B(*o*-Cb)<sub>3</sub> acted as the Lewis acid in this reaction, in which the carbocation is trapped by a hydride source or alkyl benzene nucleophile. In the case of benzene, when B(C<sub>6</sub>F<sub>5</sub>)<sub>3</sub> was used, no reaction was observed. They hypothesized that the fluoride affinity in B(*o*-Cb)<sub>3</sub> is much higher compared to B(C<sub>6</sub>F<sub>5</sub>)<sub>3</sub>.

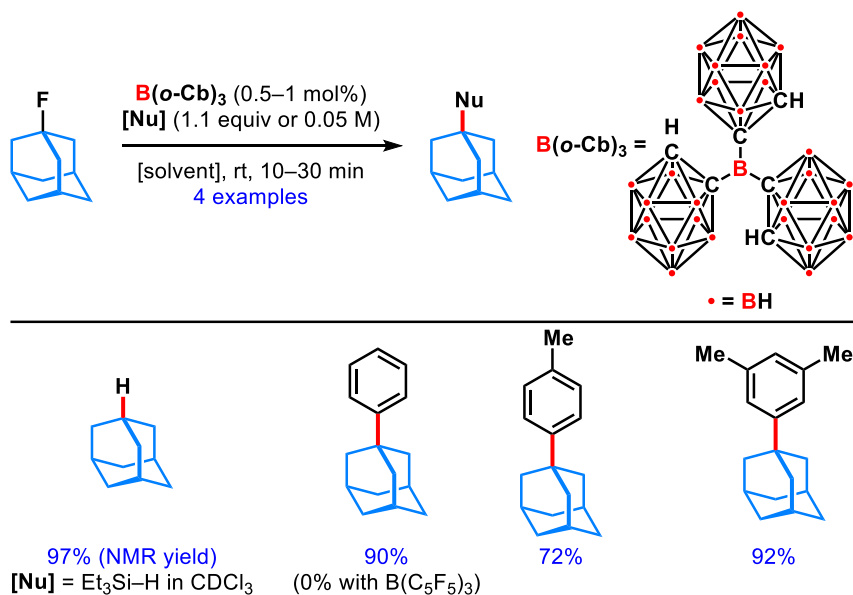


**Figure 2.3.** A Friedel–Crafts alkylation utilizing a unique carborane as the Lewis acid.

Aniline nucleophiles are typically incompatible in Friedel–Crafts reactions due to the facile, strong binding of the Lewis acid to the nitrogen, which deactivates the catalyst. This can be resolved by using certain protecting groups, as illustrated by Shi, Zhao and coworkers<sup>6</sup> in 2023. The *iso*-butyl isomer of the Boc group was used as the protecting group on nitrogen, effectively enabling the majority of substrates to undergo Friedel–Crafts alkylation reactions, though several other protecting groups work as well (**Figure 2.4**). The Brønsted acid, 1,1,1,3,3,3-hexafluoroisopropanol (HFIP), was used as the solvent in place of a catalytic Lewis acid. The fate of the bromide upon departure with HFIP is not known, however, it is believed that the formation of HBr is possible (**Scheme 2.4**).

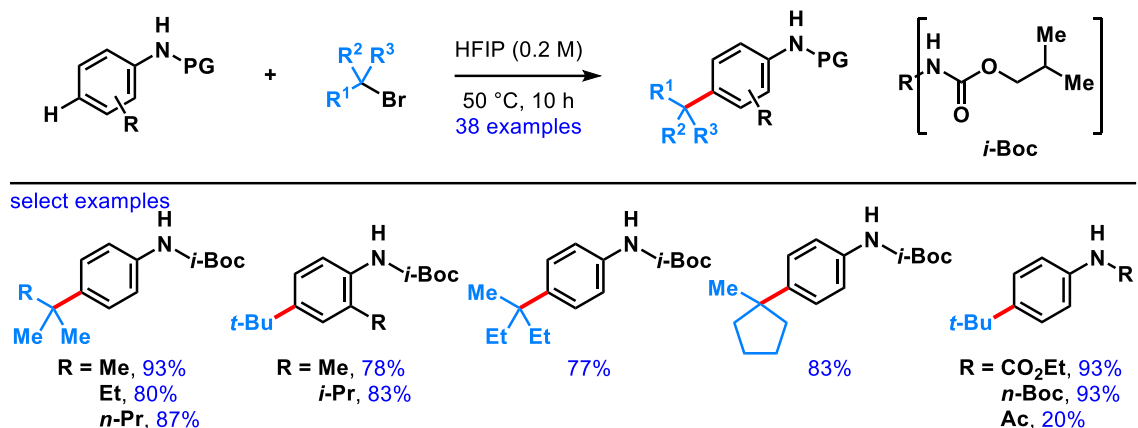
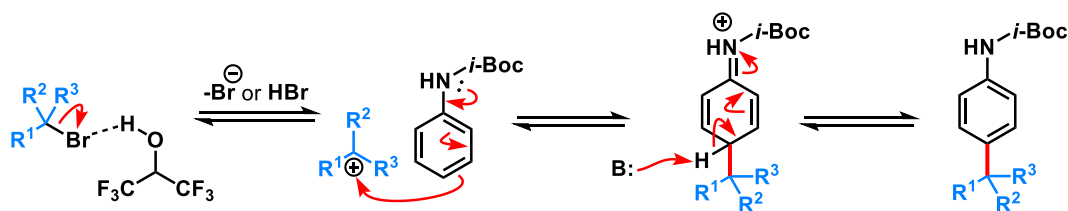


**Figure 2.4.** Friedel–Crafts reaction with a protected aniline.



**Scheme 2.4.** Proposed mechanism, with the possibility of forming HBr assisted by HFIP.

### 2.1.2 Other C(sp<sup>2</sup>)–C(sp<sup>3</sup>) bond forming reactions

Cross-coupling reactions involving transition metals to form C(sp<sup>2</sup>)–C(sp<sup>2</sup>) bonds is a vastly studied and rapidly growing field; however, cross-coupling reactions to form C(sp<sup>2</sup>)–C(sp<sup>3</sup>) bonds are much less developed, often due to facile  $\beta$ -hydride eliminations (**Figure 2.5**). As such, the synthesis of C(sp<sup>2</sup>)–C(sp<sup>3</sup>) bonds through cross-coupling reactions is uncommon. One recent example from 2011 by Glorius and coworkers<sup>7</sup> achieve this via a nickel-catalyzed Kumada–Corriu–Tamao-type cross-coupling reaction. Along with a nucleophilic heterocyclic carbene (NHC) ligand, *t*-BuMgCl is coupled to an aryl bromide, effectively substituting a *tert*-butyl group in place of the bromide (**Figure 2.6**).

This method allows for the formation of C(sp<sup>2</sup>)–C(sp<sup>3</sup>) bonds under mild conditions; however, Grignard reagents are often incompatible with many functional groups, limiting the scope to relatively unfunctionalized coupling partners.

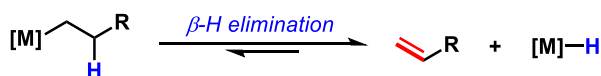


**Figure 2.5.**  $\beta$ -Hydride elimination when a transition metal is on an alkyl group.

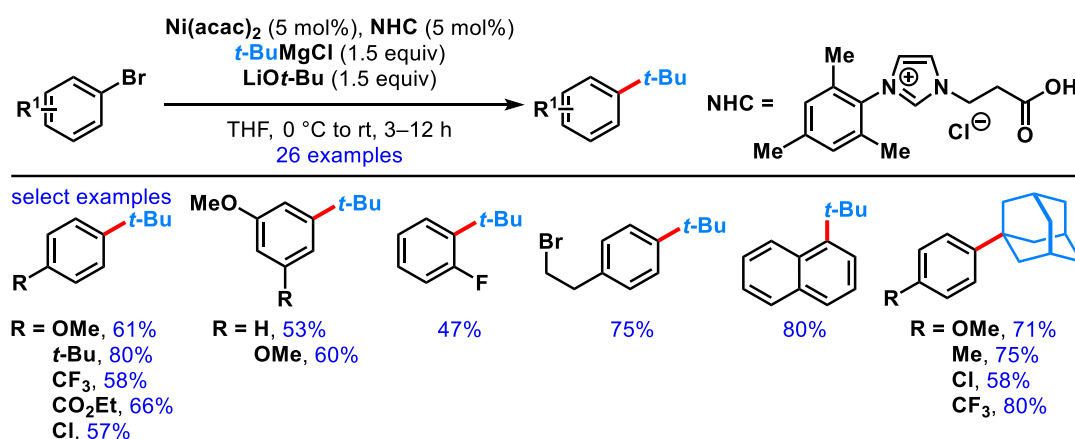


**Figure 2.6.** Nickel-catalyzed Kumada-Corriu-Tamao-type reaction for *tert*-butylation.

Complementing Friedel–Crafts reactions, which involves electron-rich aromatic nucleophiles, is the Minisci reaction, which involves electron-deficient aromatic electrophiles. One recent example developed in 2019 by Overman and coworkers<sup>8</sup> involves cesium- or lithium-oxalate salts as alkylating reagents (**Figure 2.7**). With an iridium(III) photocatalyst, the oxalate decomposes into two equivalents of CO<sub>2(g)</sub> and a tertiary carbon-centered radical, which reacts with electron-poor heteroarenes. Chain propagation is maintained by stoichiometric amounts of ammonium persulfate. The Minisci reaction and the Friedel–Crafts alkylation reaction together cover all types of aromatic alkylation, from electron-rich to electron-poor arenes.

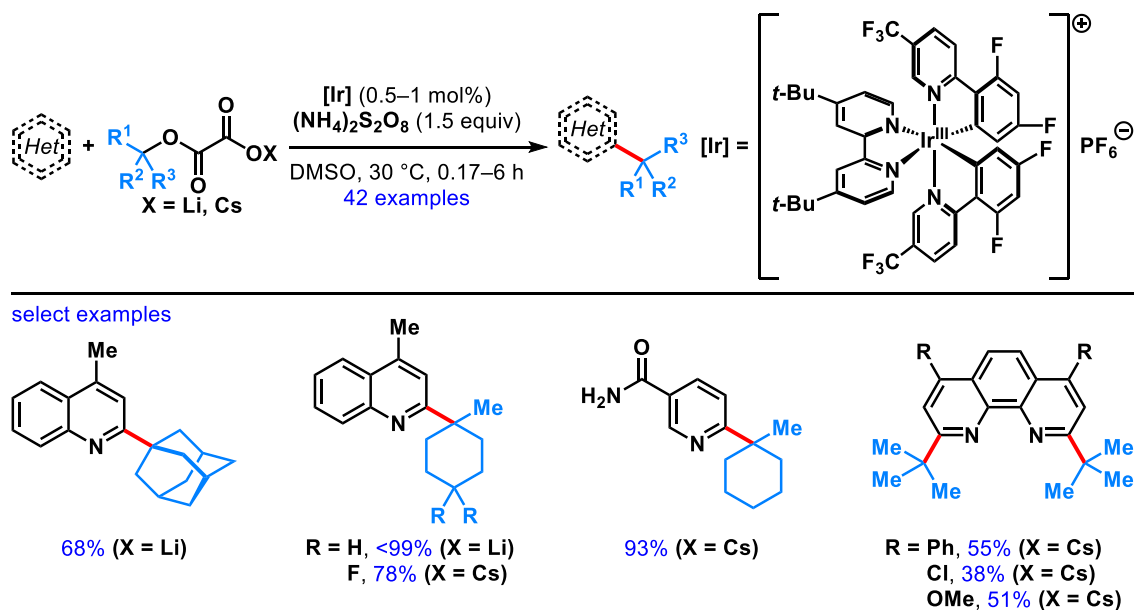


**Figure 2.7.** A Minisci reaction alkylates electron-deficient aromatic rings.

### 2.1.3 Tertiary alcohols in Friedel–Crafts alkylation reactions

Alkyl halides may pose a serious environmental and toxic hazard,<sup>9</sup> especially at an industrial scale, thus safer alternatives are desired. Although comparably less reactive, alkyl alcohols have been developed as alkyl halide substitutes. Methods to increase reactivity, or “activate” alcohols, involve increasing the labile nature of the OH group. This involves functional groups such as benzylic alcohols, propargylic alcohols, and allylic alcohols. Converting the alcohol to a better leaving group by acetylation or sulfonylation is also possible.

A relatively recent example from 2006 is demonstrated by Rueping and coworkers.<sup>10</sup> Along with a variety of primary and secondary benzylic alcohols reacting intermolecularly, two examples of tertiary benzylic alcohols were reported to react intramolecularly to form fluorene products using a bismuth Lewis acid catalyst (**Figure**

2.8). Although limited in substrate scope, this method highlighted the milder conditions as opposed to the traditionally harsh conditions, such as in using super-stoichiometric sulfuric acid in acetic acid solvent at high temperatures.<sup>11</sup>

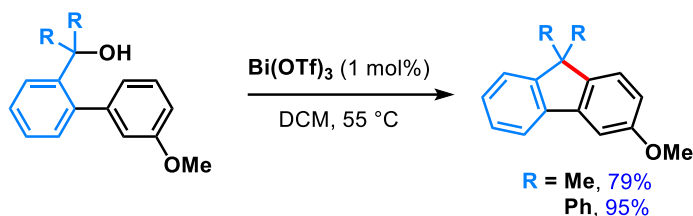


**Figure 2.8.** Tertiary benzylic alcohols undergoing intramolecular alkylation to form fluorenes.

Another bismuth-catalyzed intramolecular cyclization to form tetrahydronaphthalenes and bicyclic heterocycles was established in 2013 by Bunce and coworkers<sup>12</sup> (**Figure 2.9**). This method showcased the use of both activated (benzylic) and non-activated tertiary alcohols in accomplishing cyclization in good to excellent yields. This opened the opportunity to broaden the substrate scope to non-activated tertiary alcohols from the typical scope of activated alcohols.

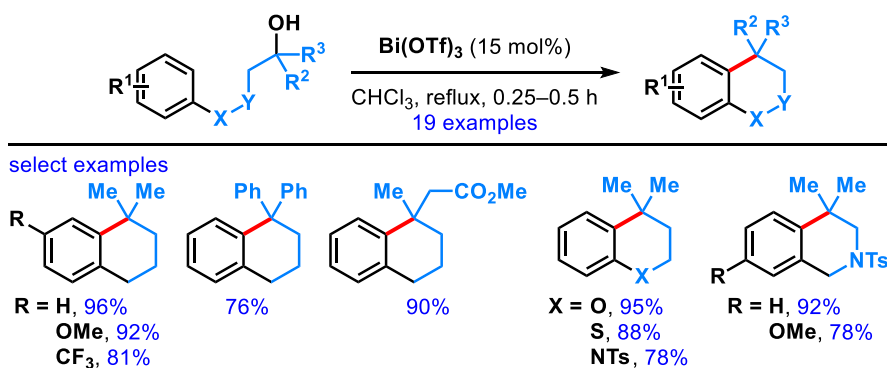


**Figure 2.9.** Intramolecular cyclization of activated and unactivated tertiary alcohols.

In 2010, Niggemann and coworkers optimized a calcium-catalyzed intermolecular alkylation of activated tertiary alcohols<sup>13</sup> (**Figure 2.10**). In the presence of a phase-transfer catalyst ( $\text{Bu}_4\text{NPF}_6$ ), alkylation of nucleophilic arenes proceeded relatively quickly under mild conditions. Calcium is an alkaline earth metal that shows growing potential as a catalyst, as it is nontoxic, sustainable, relatively low costing, and readily available.<sup>14</sup>

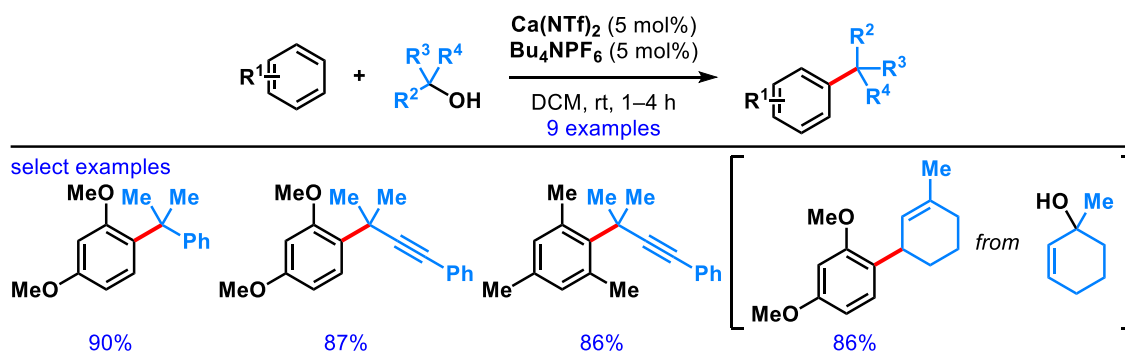


**Figure 2.10.** Calcium-catalyzed alkylation of electron-rich arenes via activated tertiary alcohols.

A Lewis-acid catalyzed Friedel–Crafts alkylation/lactonization method was developed by Zhou and coworkers<sup>15</sup> to form benzofuranones (**Figure 2.11**). Here, a tertiary benzylic alcohol is reacted with a substituted phenol in which, based on NMR studies, a Friedel–Crafts alkylation occurs first and followed by lactonization. Although there is strong support for this mechanistic pathway, it was also observed by NMR that a minor portion of the reaction mixture may lactonize first. The vastly varying reaction times could be reasoned based on the electronic effects of the aromatic ring on the tertiary alcohol. Strong electron-donating groups, such as oxygen, proceeded faster compared to alkyl groups. Electron-withdrawing groups were still tolerated; however, noticeably longer reaction times were required and in some instances, resulted in lower yields.



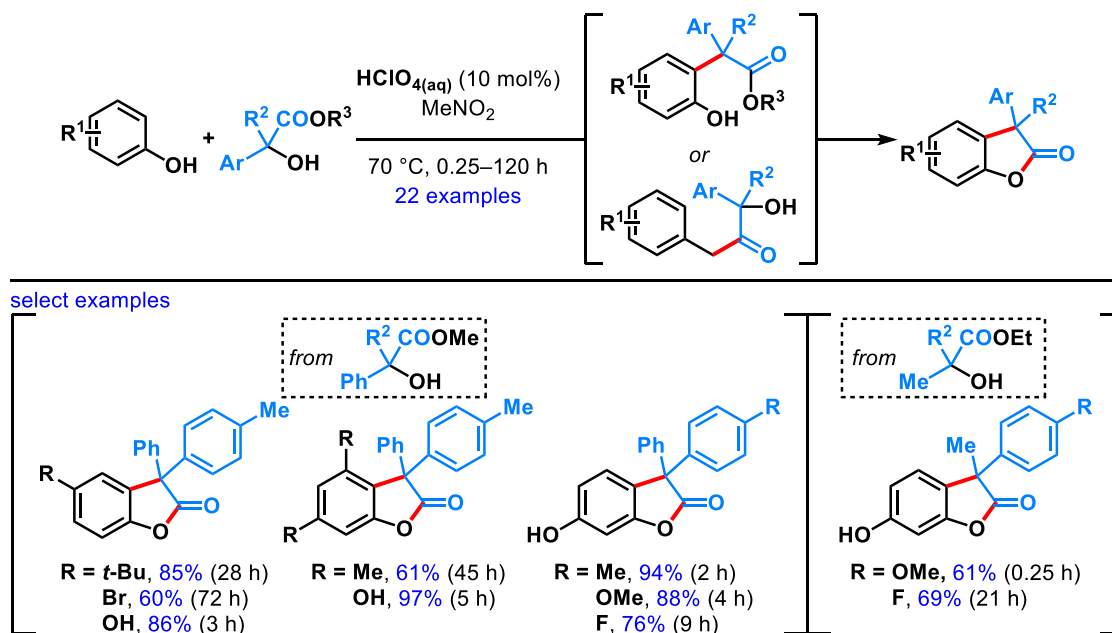


**Figure 2.11.** Tandem Friedel–Crafts alkylation/lactonization to form benzofuranones.

Tertiary allylic alcohols partaking in Friedel–Crafts alkylations can undergo an allylic shift side reaction, possibly due to steric hindrance of the nucleophilic attack. An example of this type of reaction was pursued in 2015 by Hall and coworkers<sup>16</sup> with a distinctly designed boronic acid (**Figure 2.12**). A proposed rationale for the boronic acid design having an *ortho*-hydrogen present instead of fluorine is to promote hydrogen bonding upon complexation to alcohol (**Figure 2.13**). A fluorine present may suffer from repulsive interactions when the tertiary alcohol binds the boron, thereby disfavoring the interaction between the two compounds.

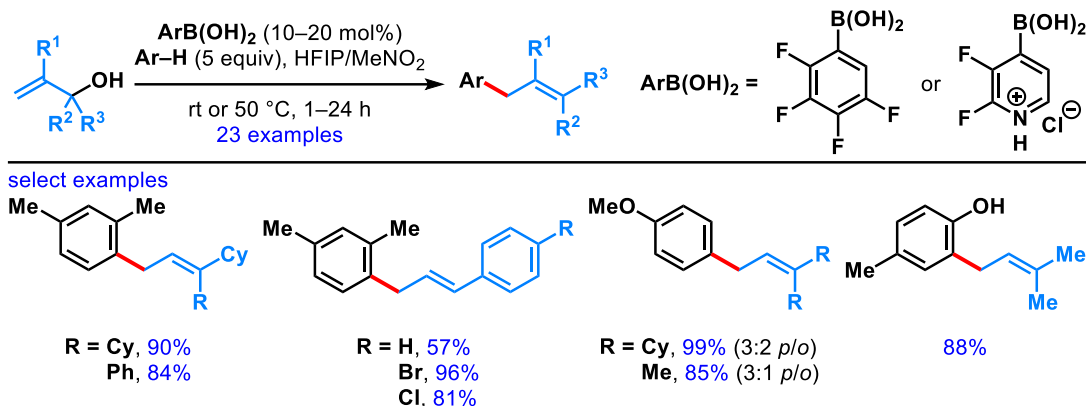


**Figure 2.12.** Tertiary allylic alcohols in Friedel–Crafts alkylation resulting in allylic shift products.

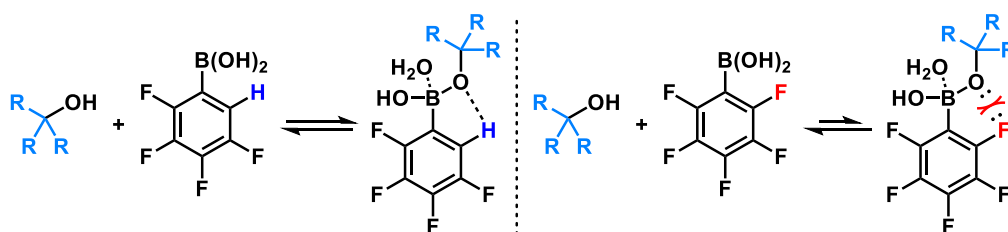


**Figure 2.13.** Possible hydrogen bonding versus electron repulsion when alcohol binds to boronic acid.

The use of inexpensive and readily accessible iron is often regarded as favorable compared to other transition metals that are rare and expensive. An example of an iron-catalyzed Friedel–Crafts alkylation of (hetero)arenes was demonstrated in 2018 by Schneider and coworkers<sup>17</sup> with tertiary oxime alcohols/ethers (**Figure 2.14**). As mentioned previously, unprotected aniline-type arenes usually encounter compatibility issues since the nitrogen can strongly bind and sequester the Lewis acid; however, in this case, indole-derivatives and other (hetero)arenes are alkylated without protecting groups. Oxime ethers were chosen to mitigate possible side reactivity of the nucleophile attacking

the otherwise aldehyde or ketone. Oxime ethers may also contribute to carbocation stabilization by resonance (**Scheme 2.5**).

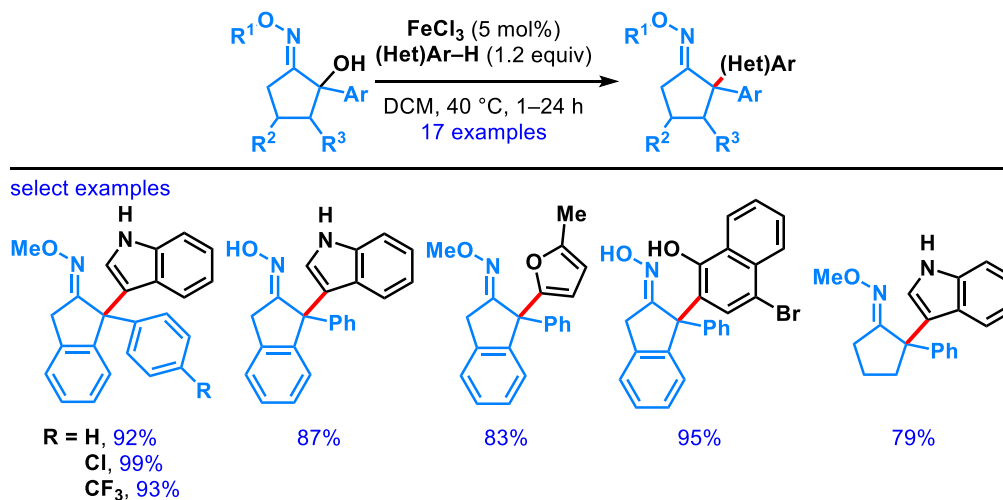
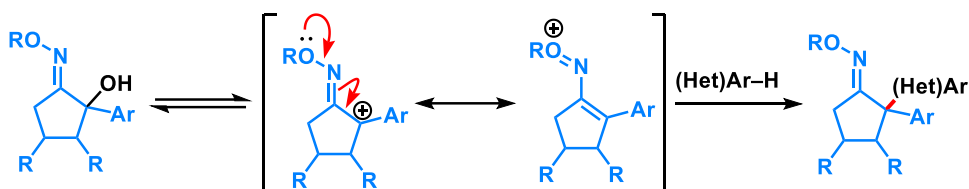


**Figure 2.14.** Unprotected indoles and other arenes partaking in iron-catalyzed Friedel–Crafts alkylation.



**Scheme 2.5.** Possible resonance-stabilization of benzylic tertiary carbocation.

Another example of iron-catalyzed Friedel–Crafts alkylation was studied in 2019 by Cook, Baik and coworkers<sup>18</sup> to form indolines (**Figure 2.15**). Unactivated tertiary alcohols were the main focus of this study. Along with some unactivated secondary alcohols as part of the study, intramolecular alkylation was remarkably achieved with stereoinversion of the carbon center, as opposed to typical racemization of tertiary carbocations. The group proposes that, upon carbocation formation, the iron hydroxide

complex blocks the face it departs from (**Scheme 2.6**). Rapid attack into the carbocation from the opposing face of the iron hydroxide complex achieves stereoinversion through an  $S_N1$  pathway.

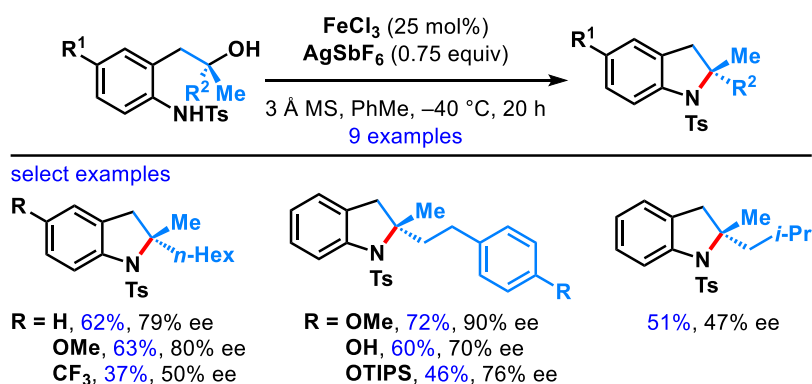
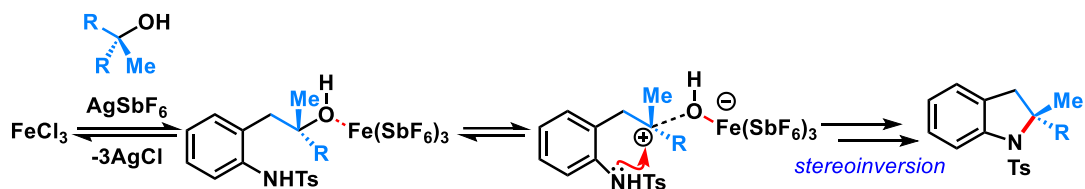


**Figure 2.15.** Intramolecular alkylation of unactivated tertiary alcohol resulted in stereoinverted products.



**Scheme 2.6.** Proposed mechanism. Potential carbocation intermediate retaining stereochemistry.

Heterocyclic quaternary carbon-containing molecules are particularly attractive in the design of biologically relevant molecules.<sup>19</sup> The use of heterocycles bearing tertiary alcohols as alkylating agents to form new  $\text{C}(\text{sp}^2)\text{--C}(\text{sp}^3)$  bonds under mild conditions posed a challenge for the field. Bull and coworkers<sup>20</sup> successfully demonstrated a Friedel–Crafts alkylation with a heterocyclic tertiary benzylic alcohol (**Figure 2.16**). Five- or six-membered oxygen- or nitrogen-containing heterocycles were utilized in this study with several different Lewis acids. In some cases, the additive  $\text{Bu}_4\text{NPF}_6$  was necessary. When

protected with CBz, nitrogen-containing heterocycles are accommodated. Only two nucleophiles were employed, possibly to avoid or minimize site selectivity issues. Overall, these relatively mild conditions afforded moderate to excellent yields for coupling heterocycles to electron-rich arenes.

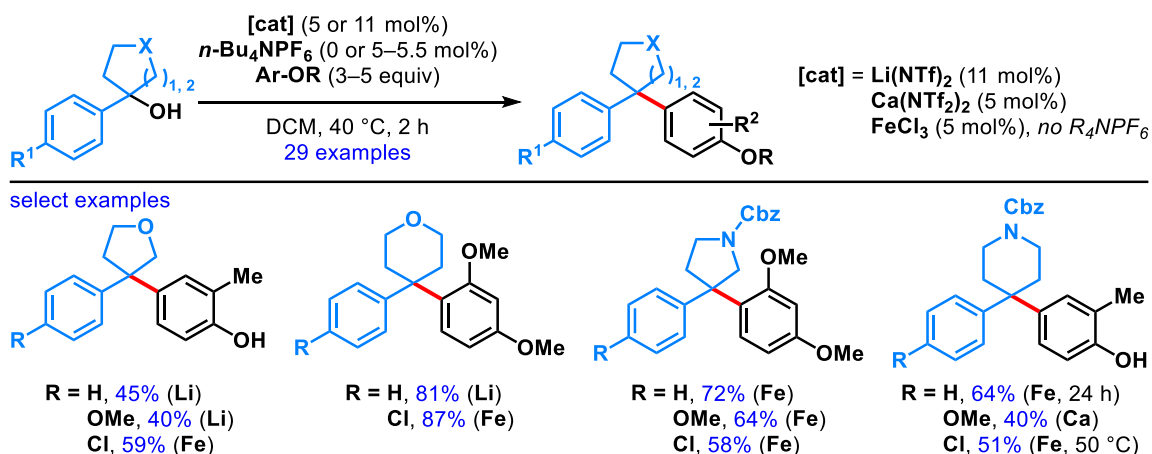


**Figure 2.16.** Heterocyclic tertiary benzylic alcohols partaking in a Friedel–Crafts alkylation reaction.

Another example of heterocyclic tertiary alcohols participating in Friedel–Crafts alkylation was developed in 2020 by Shankaraiah and coworkers<sup>21</sup> with 3-hydroxy oxindoles (**Figure 2.17**). Catalyzed by  $\text{BF}_3 \cdot \text{Et}_2\text{O}$  as a Lewis acid, tertiary, benzylic/propargylic alcohols were coupled to electron-rich arenes to form 3-aryl-3-alkynyl oxindoles via microwave irradiation. *N*-Alkylated oxindole derivatives operated well under the reaction conditions. In the case of aniline-derived nucleophiles, the toluenesulfonyl (Ts) group was utilized was necessary. Electron-withdrawing groups on the nucleophile’s aromatic system typically halted reactivity.

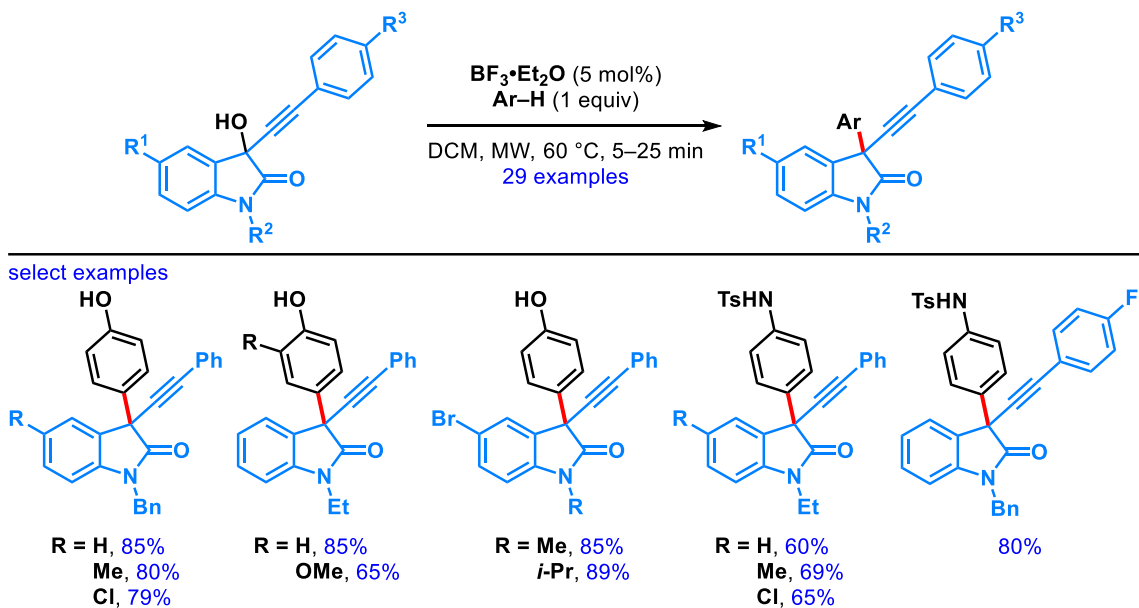


**Figure 2.17.** Coupling of hydroxy-oxindoles to electron-rich arenes under microwave conditions.

In 2022, May and coworkers<sup>22</sup> coupled an aryl boronic acid to a tertiary propargylic alcohol using catalytic  $\text{GaCl}_3$  (**Figure 2.18**). Although electron-rich aryl boronic acids worked well as nucleophiles, electron-poor aryl boronic acids afforded non-synthetically useful yields. At low temperatures, formation of all-carbon quaternary center product was favored over elimination product **2.2** (**Figure 2.19**), although both products were observed to a certain degree. DCE proved to be a superior solvent than DCM, which gave solely elimination product even at low temperatures. At higher temperatures (50 °C), only elimination product was observed with DCE. This method is a good alternative to using expensive transition-metal-catalyzed cross-coupling reactions to form  $\text{C}(\text{sp}^2)\text{--C}(\text{sp}^3)$  bonds.

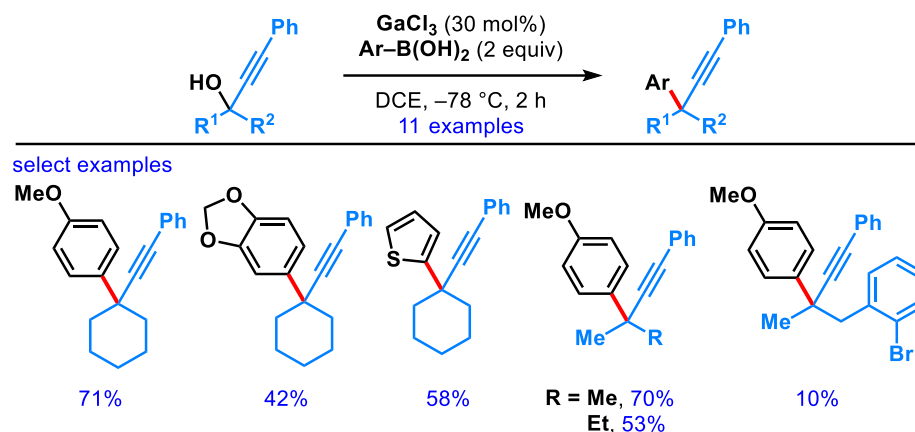


**Figure 2.18.** Transition-metal free coupling of aryl boronic acids to tertiary propargylic alcohols.

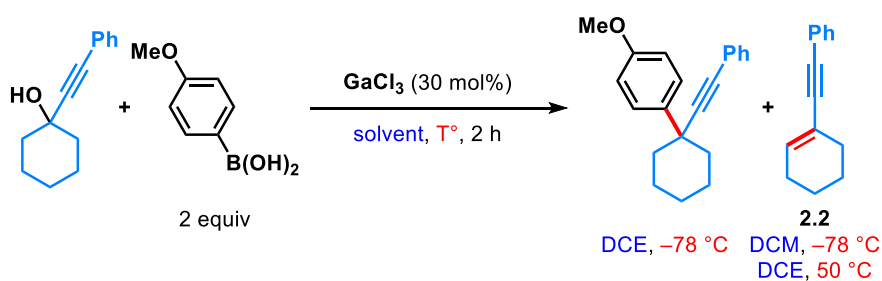


**Figure 2.19.** Elimination side reactivity observed and favored under certain conditions.

*tert*-Butylation reactions are commonly performed with isobutylene in the presence of a strong acid, such as in the synthesis of 2,6-di-*tert*-butyl-4-methylphenol (butylated hydroxytoluene, or BHT).<sup>23</sup> Sartori and coworkers<sup>24</sup> demonstrated a Friedel–Crafts alkylation utilizing a solution of isobutylene in chloroform. They developed a set of conditions to control *para*- versus *ortho*-alkylation (**Figure 2.20**). When using phenol, exclusively *para*-alkylation occurred in 78% yield, whereas potassium phenolate afforded predominantly *ortho*-alkylation. Other examples of exclusive *para*-alkylation occurred with two other alkenes as well.

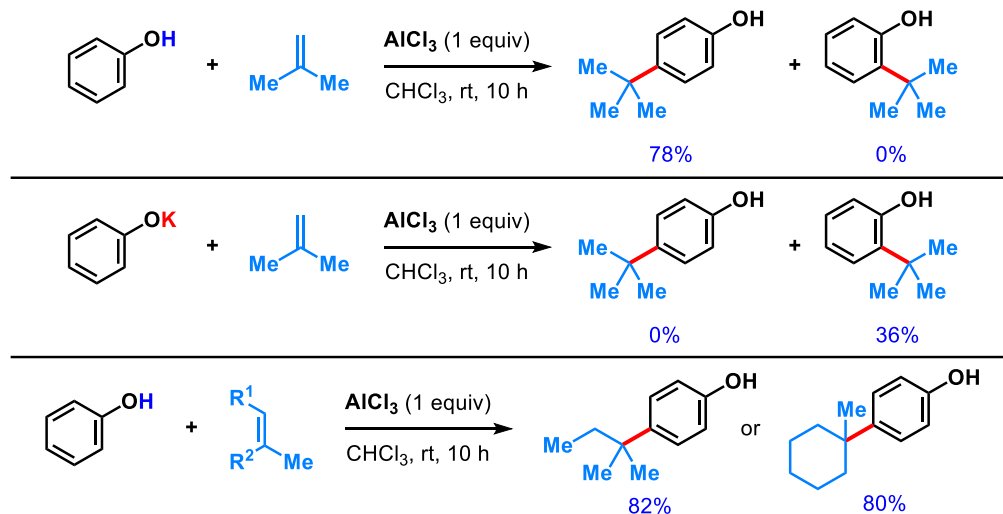


**Figure 2.20.** Conditions for exclusive *para*- or *ortho*-alkylation.

Di-*tert*-butylperoxide (DTBP) as a direct *tert*-butylating agent has not been studied in the Friedel–Crafts reaction, possibly due to the same challenges that unactivated tertiary alcohols face. A patent from 2011 disclosing the invention by Warren<sup>25</sup> utilized DTBP to react with copper complex **2.3** in forming *tert*-butoxy-copper complex **2.4** (**Figure 2.21**), and observed the formation of two equivalents of *tert*-butanol as the byproduct. Among many possible reasons, formation of alkoxy-copper complex **2.4** with DTBP may imply the reduction of the peroxide to its alcohol component, which engages the copper complex, though this was not specified in the invention.

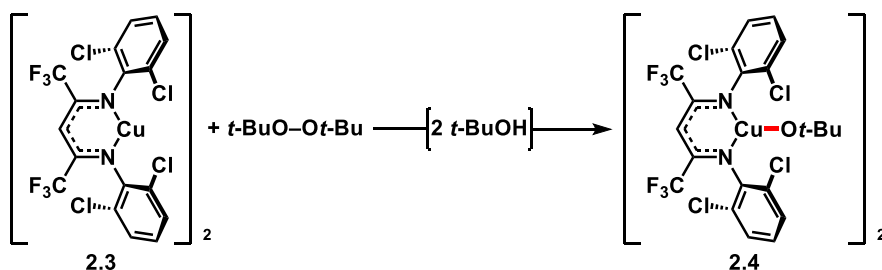


**Figure 2.21.** Example of utilizing DTBP to *tert*-butoxylate a copper complex in a patent.

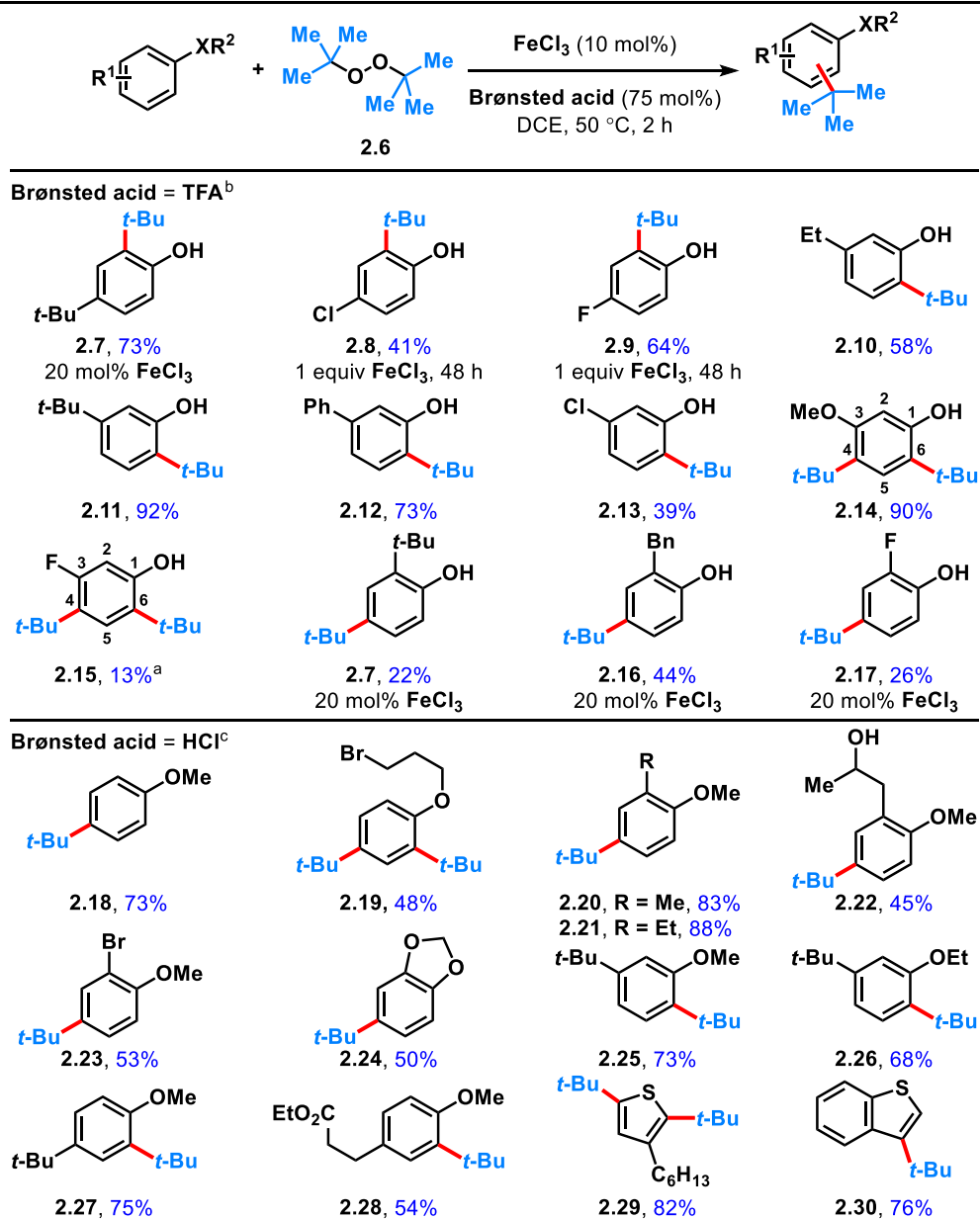


## 2.2 Alkylations with DTBP

Herein, we demonstrate a method for Friedel–Crafts *tert*-alkylation of electron-rich arenes using both DTBP and unactivated *tert*-alkanols via dual Brønsted/Lewis acid catalysis. Their respective mechanisms were also examined. In our investigations of the reactivity of aromatic C–H bonds under Fenton-inspired conditions, it was observed that the treatment of 3-*tert*-butylphenol (**2.5**) and other phenolic substrates with equimolar DTBP (**2.6**), trifluoroacetic acid, and catalytic FeCl<sub>3</sub> led to site-selective C–C bond formations (**Table 2.1**). This dual Brønsted/Lewis acid catalysis exerts considerably enhanced reactivity compared to a related iron-mediated system where the arene reagent was employed as the solvent.<sup>26</sup>

We find that substituted phenolic and anisolic substrates generally alkylate to yield one major isomeric product. Reactions with phenolic substrates were performed along with L. Göttemann. Exposing 4-*tert*-butylphenol to DTBP (**2.6**) in the presence of iron(III) and HCl catalysts yields 73% of 2,4-di-*tert*-butylphenol (**2.7**). 4-Chloro- and 4-fluorophenols require stoichiometric iron salts to proceed and were transformed into their alkylated counterparts **2.8** and **2.9** in 41% and 64% yields, respectively. Under these reaction conditions, overoxidation to benzoquinone-type side-products accounts for some of the mass balance. *meta*-Substituted phenols were alkylated exclusively at the less hindered position(s) *ortho* to the phenolic group. Both 3-ethyl and 3-*tert*-butylphenol were converted to *tert*-butylated **2.10** and **2.11** in 58% and 92% yields, respectively, the latter of which was confirmed by X-ray crystallography by V. Carta.

**Table 2.1.** Scope of *tert*-butylation of phenolic, aryl ether, and thiophene derivatives.



<sup>a</sup> 2-*tert*-Butyl-5-fluorophenol isolated in 5% yield. <sup>b</sup> Combined efforts with L. Gottemann. <sup>c</sup> Work done by M. Chojnacka and R. Crowley III.

3-Phenylphenol was transformed into the corresponding alkylated product (**2.12**) in 73% yield. The phenolic derivative bearing a *meta*-chloro substituent undergoes *tert*-

alkylation to yield phenolic **2.13** in a modest 39% yield. Contrary to products **2.7–2.13** that were monoalkylated at the less hindered *ortho* site, 3-methoxy- and 3-fluorophenol were *tert*-butylated at both the 4- and 6-positions to furnish tetrasubstituted phenols **2.14** and **2.15**, in 90% and 13% yields, respectively, with 1 equivalent of DTBP (**2.6**). *ortho*-Substituted phenolic substrates were considerably less reactive but were selectively *tert*-butylated *para* to the hydroxy group to yield **2.7**, **2.16**, and **2.17** in 22–44% yields using higher iron loadings and extended reaction times.

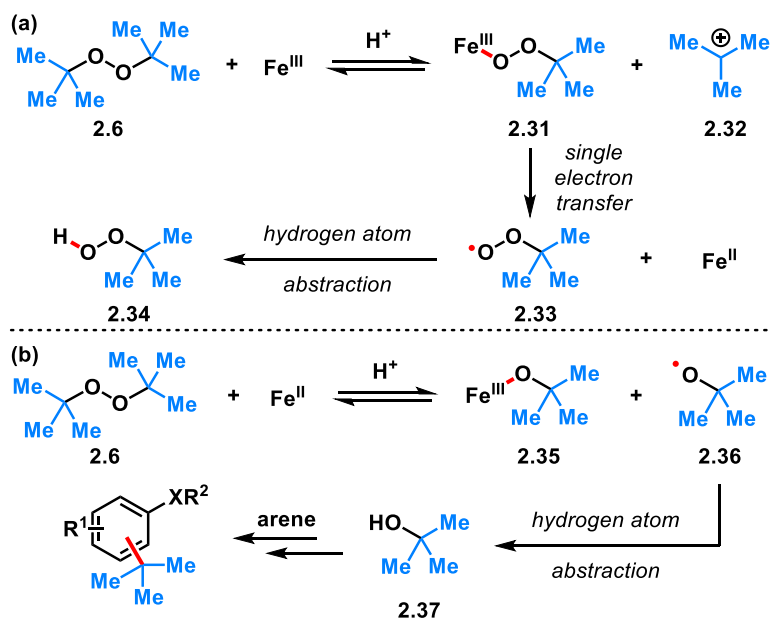
Aryl ether and thiophene derivatives were better behaved in the dual iron(III)/HCl catalyzed *tert*-butylation reaction (**Table 2.1**, reactions performed by M. Chojnacka and R. Crowley III). Anisole was converted to 4-*tert*-butylanisole (**2.18**) in 73% yield. 2,4-Dialkylation occurred with bromopropyl phenyl ether to afford trisubstituted arene **2.29** in 48% yield, with no monoalkylation product observed. *ortho*-Substituted anisole precursors were site-selectively functionalized *para* to the methoxy group. Unlike the 2-alkylphenolic derivatives, which were poorly reactive, 2-methyl- and 2-ethylanisoles undergo *tert*-butylation to give **2.20** and **2.21** in 83% and 88% yields, respectively. Anisole derivatives with an aliphatic alcohol or bromo group at the 2-position were transformed to their corresponding *tert*-butylated products in moderate yields (45% for **2.22** and 53% for **2.23**). New C(sp<sup>2</sup>)–C(sp<sup>3</sup>) bond formation occurred with benzodioxole, albeit less effectively than with anisole, producing **2.24** in 50% yield. 3-Substituted aryl ethers were functionalized selectively to products **2.25** and **2.26** with alkylation at the *ortho* positions in 68–73% yields. Selective mono-*tert*-butylation proceeds with 4-*tert*-butylanisole to deliver 2,4-di-*tert*-butylanisole (**2.27**) in 75% yield.

An anisole derivative bearing a pendant ester group was accommodated and 54% of the alkylated product (**2.28**) was formed. In addition to anisole derivatives, thiophene derivatives also react effectively. Treating 3-hexylthiophene with DTBP (**2.6**) under iron(III)/HCl catalysis favors di-*tert*-butylation at both the 2- and 5-positions (**2.29**, 82%), whereas the analogous reaction with benzothiophene leads to selective *tert*-butylation at the 3-position in 73% yield (**2.30**). In contrast, the phosphoric acid-mediated direct alkylation of thiophene derivatives with *tert*-butanol requires 200 °C to achieve modest yields.<sup>27</sup> Hojo and coworkers<sup>28</sup> were able to achieve similar yields of *tert*-butylated benzothiophene **2.30** with *t*-BuBr, albeit with superstoichiometric amounts of *t*-BuBr (6 equiv)/other additives in CCl<sub>4</sub> at 78 °C.

### 2.2.1 DTBP mechanistic and kinetic studies

The dual Brønsted/Lewis acid catalyzed cross-coupling between electron-rich arenes and DTBP (**2.6**) represents an underexplored site-selective Friedel–Crafts alkylation process. However, the modest reactivity experienced by several substrates and the reliance on DTBP (**2.6**) limit synthetic practicality. We speculate side reaction pathways arising from radical species compromise reactivity and product yields. In a proposed pathway, analogous to that with hydrogen peroxide (**Scheme 2.7a**),<sup>29</sup> DTBP (**2.6**) can react with iron(III) to form iron(III) *tert*-butylperoxide (**2.31**) and *tert*-butyl cation (**2.32**), the latter of which can participate in the desired electrophilic alkylation. Homolysis with the former would lead to iron(II) and *tert*-butylperoxyl radical (**2.33**), which could abstract a hydrogen atom from the solvent or substrate to give *tert*-butyl hydroperoxide (**2.34**), which also

promotes this reaction, albeit less effectively than DTBP (**2.6**). Alternatively, iron(II) produced in this manner, or through reduction of iron(III) by phenol and anisole derivatives,<sup>30,31</sup> can reduce DTBP (**2.6**) in a Fenton-like fashion to generate iron(III) (**2.35**) and *tert*-butoxyl radical (**2.36**, **Scheme 2.7b**). Subsequent hydrogen atom abstraction by the oxygen-centered radical may initiate undesirable side reactions while producing *tert*-butanol (**2.37**), a potential precursor to the desired Friedel–Crafts reaction. We find catalysis with FeCl<sub>2</sub> proceeds similarly to FeCl<sub>3</sub>, which is consistent with a Fenton initiation process.



**Scheme 2.7.** Proposed pathways for the decomposition of DTBP (**2.6**). (a) Fe(III) initiated pathway. (b) Fe(II) initiated pathway.

Along with L. Göttemann, a kinetic analysis was undertaken to derive insight into optimizing the C(sp<sup>2</sup>)–C(sp<sup>3</sup>) cross-coupling reaction. (**Figure 2.22**). 3-*tert*-Butylphenol (**2.5**) was selected as the model substrate to react with DTBP (**2.6**) because no side products

formed over the course of the reaction, thus simplifying the data analysis and interpretation. Initial rates (for *tert*-butylation) were then measured (Figures 2.23–2.26) by varying the concentrations of phenolic 2.5, DTBP (2.6), TFA, and FeCl<sub>3</sub> catalyst (Table 2.2).

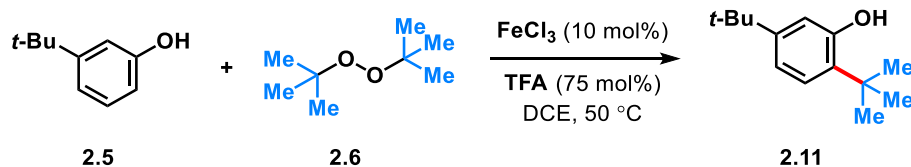


Figure 2.22. Conditions for kinetic analysis. Combined efforts with L. Gottemann.

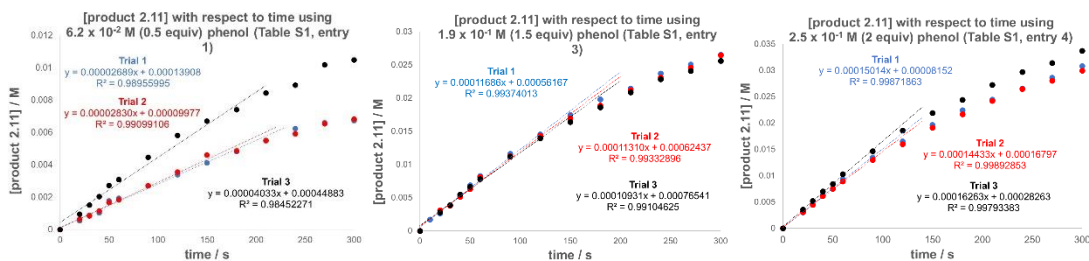


Figure 2.23. Initial rates when varying [phenolic 2.5].

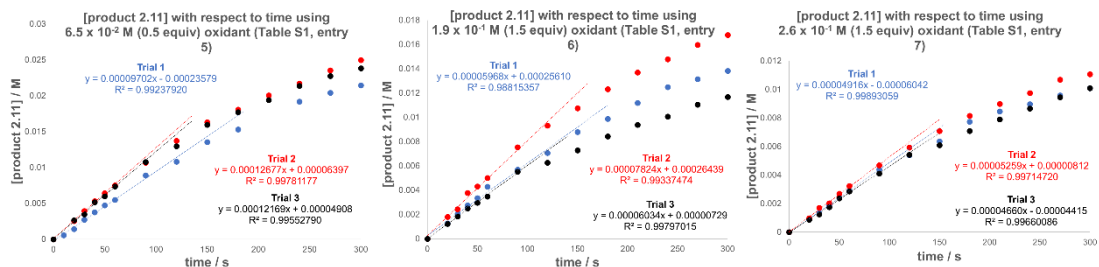


Figure 2.24. Initial rates when varying [peroxide 2.6].

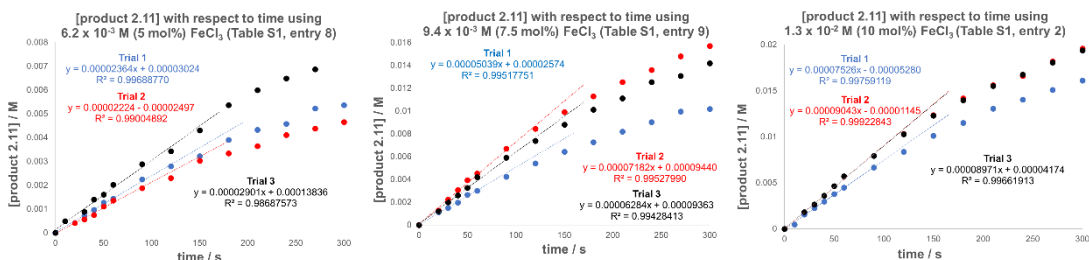


Figure 2.25. Initial rates when varying [FeCl<sub>3</sub>].

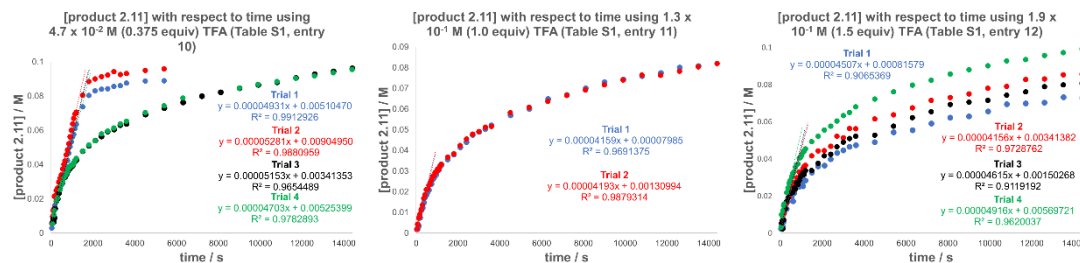


Figure 2.26. Initial rates when varying [TFA].

Table 2.2. Kinetic data for arene alkylation with di-*tert*-butylperoxide.

Entry	[2.5] / M	[2.6] / M	[FeCl <sub>3</sub> ] / M	[TFA] / M	initial rate <sup>a</sup> / M·s <sup>-1</sup>
1	$6.2 \times 10^{-2}$	$1.3 \times 10^{-1}$	$1.3 \times 10^{-2}$	$9.4 \times 10^{-2}$	$0.31_8 \times 10^{-4}$
2	$1.2_5 \times 10^{-1}$	$1.3 \times 10^{-1}$	$1.3 \times 10^{-2}$	$9.4 \times 10^{-2}$	$0.85_1 \times 10^{-4}$
3	$1.9 \times 10^{-1}$	$1.3 \times 10^{-1}$	$1.3 \times 10^{-2}$	$9.4 \times 10^{-2}$	$1.1_3 \times 10^{-4}$
4	$2.5 \times 10^{-1}$	$1.3 \times 10^{-1}$	$1.3 \times 10^{-2}$	$9.4 \times 10^{-2}$	$1.5_2 \times 10^{-4}$
5	$1.2_5 \times 10^{-1}$	$6.5 \times 10^{-2}$	$1.3 \times 10^{-2}$	$9.4 \times 10^{-2}$	$1.1_5 \times 10^{-4}$
6	$1.2_5 \times 10^{-1}$	$1.9 \times 10^{-1}$	$1.3 \times 10^{-2}$	$9.4 \times 10^{-2}$	$0.66_1 \times 10^{-4}$
7	$1.2_5 \times 10^{-1}$	$2.6 \times 10^{-1}$	$1.3 \times 10^{-2}$	$9.4 \times 10^{-2}$	$0.49_5 \times 10^{-4}$
8	$1.2_5 \times 10^{-1}$	$1.3 \times 10^{-1}$	$6.2 \times 10^{-3}$	$9.4 \times 10^{-2}$	$0.25_0 \times 10^{-4}$
9	$1.2_5 \times 10^{-1}$	$1.3 \times 10^{-1}$	$9.4 \times 10^{-3}$	$9.4 \times 10^{-2}$	$0.61_7 \times 10^{-4}$
10	$1.2_5 \times 10^{-1}$	$1.3 \times 10^{-1}$	$1.3 \times 10^{-2}$	$4.7 \times 10^{-2}$	$0.50_2 \times 10^{-4}$ <sup>b</sup>
11	$1.2_5 \times 10^{-1}$	$1.3 \times 10^{-1}$	$1.3 \times 10^{-2}$	$1.3 \times 10^{-1}$	$0.49_5 \times 10^{-4}$ <sup>c</sup>
12	$1.2_5 \times 10^{-1}$	$1.3 \times 10^{-1}$	$1.3 \times 10^{-2}$	$1.9 \times 10^{-1}$	$0.50_2 \times 10^{-4}$ <sup>b</sup>

<sup>a</sup> Average value from 3 independent experiments. <sup>b</sup> Average value from 4 independent experiments. <sup>c</sup> Average value from 2 independent experiments.

A first-order rate dependence on the concentration of phenolic **2.5** was observed (Figure 2.27a). The kinetics experiments revealed a half-order dependence with respect to the concentration of DTBP (**2.6**) (Figure 2.27b), suggestive of **2.6** dissociating into two active fragments and consistent with the mechanistic hypotheses presented in Scheme 2.1. Little change in initial rates was observed with varying TFA concentrations, which was

interpreted as zero-order rate dependence (**Figure 2.27c**). TFA may play a role in forming the active catalyst, potentially as a ligand. With respect to  $\text{FeCl}_3$ , a relatively uncommon second order dependence of rate was observed (**Figure 2.27d**).<sup>32</sup>

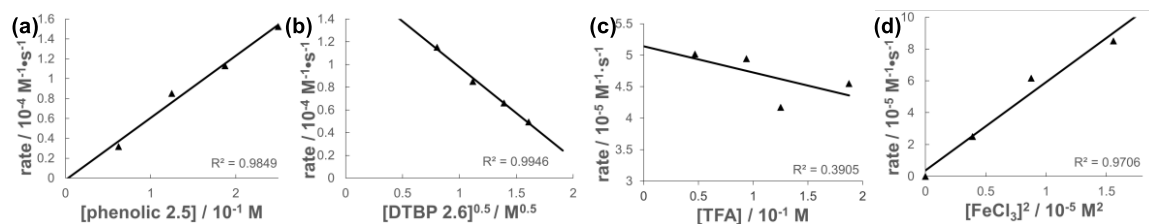


**Figure 2.27.** Plots of initial rates with respect to:

(a) [3-*tert*-butylphenol (**2.5**)] indicating approximate first-order dependence, [DTBP (**2.6**)] = 0.13 M,  $[\text{FeCl}_3] = 0.013$  M, [TFA] = 0.094 M; (b)  $[\text{DTBP} (\mathbf{2.6})]^{0.5}$  indicating half order dependence,  $[\mathbf{2.5}] = 0.12$  M,  $[\text{FeCl}_3] = 0.013$  M, [TFA] = 0.094 M; (c) [TFA] suggestive of zero-order dependence,  $[\mathbf{2.5}] = 0.12$  M, [DTBP (**2.6**)] = 0.13 M,  $[\text{FeCl}_3] = 0.013$  M; (d)  $[\text{FeCl}_3]^2$  indicating second-order dependence,  $[\mathbf{2.5}] = 0.12$  M, [DTBP (**2.6**)] = 0.13 M, [TFA] = 0.094 M. Each data point was measured in triplicate.

Additional evidence for the catalyst order was sought by treating the reaction profile data to graphical analysis using the normalized time scale method.<sup>33</sup> Rather than converting the raw data to rates, the raw concentration data of the entire data sets (*i.e.*  $[\mathbf{2.5}]$ ) were plotted against normalized time scales,  $t[\text{FeCl}_3]^n$ , where  $t$  = time and  $n$  corresponds to the catalyst order when all the curves overlay on one another (**Figure 2.28**). Using the data sets obtained from varying the catalyst loadings, the curves overlay when  $n = 2$ , which support a second order dependence in  $[\text{FeCl}_3]$  and is consistent with a tandem iron-catalyzed process.<sup>34,35</sup> Therein, the catalyst plays distinct roles in transforming DTBP (**2.6**) into the reactive alkylating agent, potentially *tert*-butanol (**2.37**), and further activates it for merger with the arene coupling partner. The latter activation of *tert*-butanol for arene



alkylation is potentially the turnover-limiting step and would be consistent with the rate law,  $k[\text{phenol}]^1[\text{DTBP}]^{0.5}[\text{FeCl}_3]^2[\text{TFA}]^0$ .

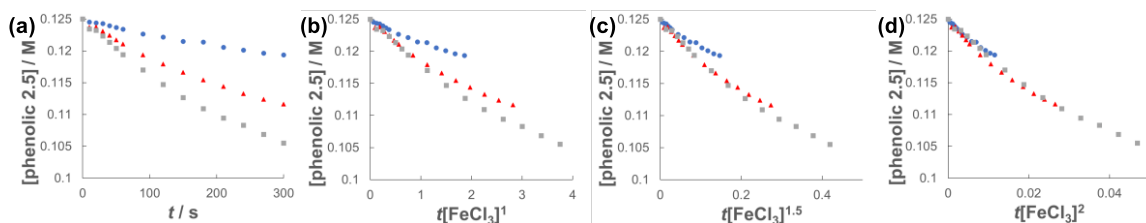


**Figure 2.28.** Plots of the normalized time scale method for determining catalyst order: blue circle = 6.2 mM FeCl<sub>3</sub>, red triangle = 9.4 mM FeCl<sub>3</sub>, grey square = 13 mM FeCl<sub>3</sub>.

### 2.3 Alkylations with *tert*-alkanols

Based on this mechanistic conjecture, DTBP (**2.6**) could be substituted with *tert*-alkanols. While catalytic *tert*-alkylations using allylic, propargylic, and benzylic alcohols are well precedented,<sup>10,12,13,15–17,19–22</sup> few examples exist with unactivated *tert*-alkanols, especially in the context of site-selectivity.<sup>27,36</sup> We envisage that the process involving a synergistic combination of Fe(III) and Brønsted acid catalysts would address the synthetic limitations imposed by using peroxides as coupling reagents, and would provide a simple approach for directly forging C(sp<sup>2</sup>)–C(sp<sup>3</sup>) bonds with quaternary carbon centers.

We targeted the joining of 2-methyl-2-butanol (**2.38**) and 3-*tert*-butylphenol (**2.5**) to investigate our hypothesis (**Table 2.3**). The use of 2.5 mol% FeCl<sub>3</sub> and 75 mol% HCl in DCE solvent afforded 72% yield of target **2.39** (entry 1). Only 10% of the product was formed in the absence of HCl. In contrast to the reactions with DTBP (**2.6**), *tert*-alkylation does not occur with trifluoroacetic acid as the co-catalyst (entry 2), while 66% NMR yield was obtained with HBr (entry 3). Using FeCl<sub>2</sub> instead of FeCl<sub>3</sub> resulted in a significant

drop in conversion to 15% (entry 4). FeBr<sub>3</sub> (entry 5) and FeBr<sub>2</sub> (entry 6) performed similarly to FeCl<sub>3</sub> (70% yields). The use of Fe(OTf)<sub>2</sub> provided modest reactivity when combined with HCl (46%, entry 7), and no reactivity without HCl. Increasing or decreasing the amounts of acid led to inferior 63% and 60% yields, respectively (entries 8 and 9).

Exchanging the solvent for HFIP resulted in only 13% conversion (entry 10). The reaction proceeded similarly in chlorobenzene solvent (75%, entry 11). When performed in toluene, moderate levels of product formation were observed (43%, entry 12); the lower yield is attributed to toluene being reactive, which consumes a significant proportion of the alcohol. Isopropanol and THF solvents do not promote the desired alkylation (entries 13 and 14).

Considering reagent cost and operation simplicity, we elected to use FeCl<sub>3</sub>, HCl, and DCE solvent as the optimal conditions to explore the substrate scope. These reactions can be set up under air. Moisture does not affect reactivity and aqueous HCl can be used as the source of Brønsted acid. The unique reactivity arising from the combination of FeCl<sub>3</sub> and HCl previously observed in a cation- $\pi$  polycyclization has been attributed to the formation of HFeCl<sub>4</sub>.<sup>37</sup>

**Table 2.3.** Survey of conditions for direct Friedel–Crafts alkylation with phenolic **2.5** and alcohol **2.38**.

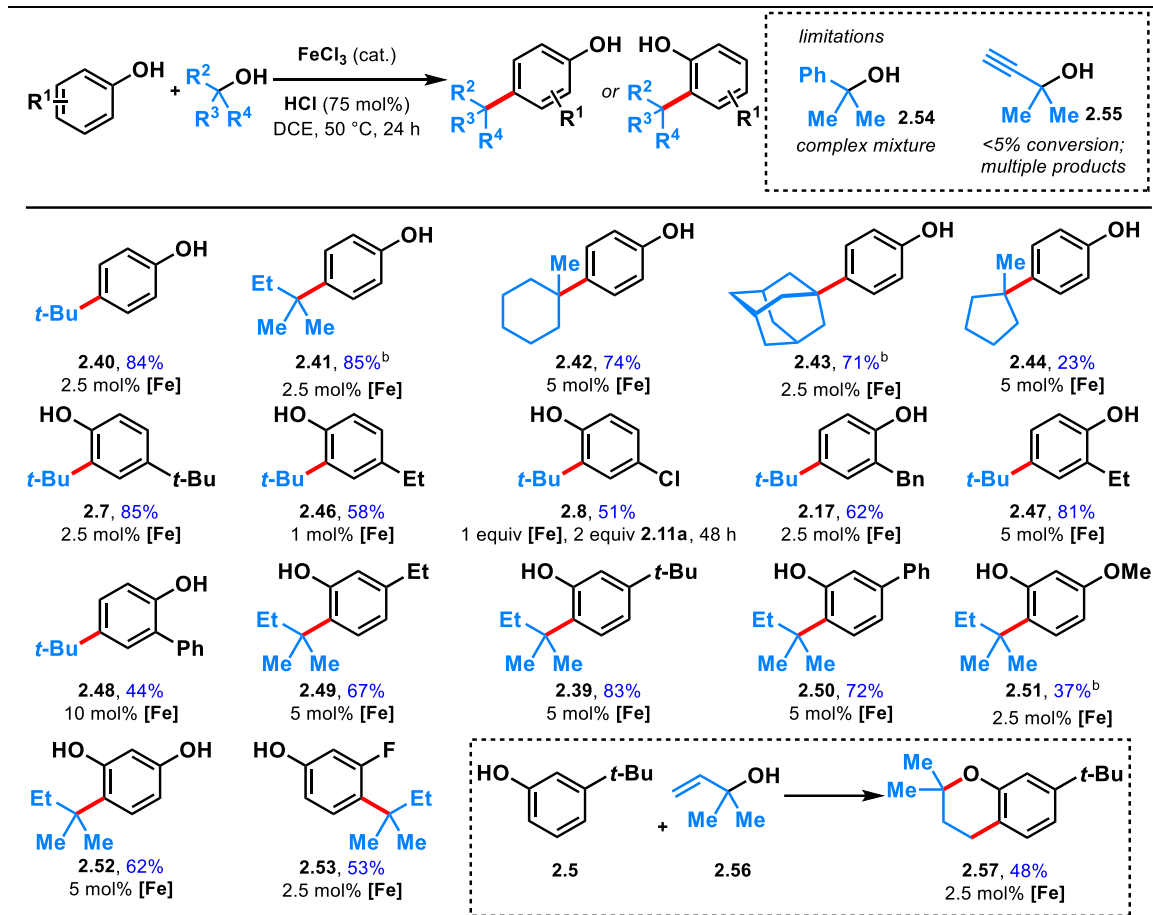
Reaction scheme: Phenolic **2.5** (1 equiv) + Alcohol **2.38** (1.1 equiv)  $\xrightarrow[\text{acid (y mol\%), solvent, 50 }^\circ\text{C, 24 h}]{[\text{FeX}] (2.5 \text{ mol\%})}$  Product **2.39**

	X	acid <sup>a</sup>	y	solvent	% yield <sup>b</sup>		X	acid <sup>a</sup>	y	solvent	% yield <sup>b</sup>
1	Cl <sub>3</sub>	HCl	75	DCE	72 (10) <sup>c</sup>	8	Cl <sub>3</sub>	HCl	50	DCE	63
2	Cl <sub>3</sub>	TFA	75	DCE	0	9	Cl <sub>3</sub>	HCl	100	DCE	60
3	Cl <sub>3</sub>	HBr	75	DCE	66	10	Cl <sub>3</sub>	HCl	75	HFIP	13
4	Cl <sub>2</sub>	HCl	75	DCE	15	11	Cl <sub>3</sub>	HCl	75	PhCl	75
5	Br <sub>3</sub>	HCl	75	DCE	70	12	Cl <sub>3</sub>	HCl	75	PhMe	43
6	Br <sub>2</sub>	HCl	75	DCE	70	13	Cl <sub>3</sub>	HCl	75	IPA	0
7	(OTf) <sub>2</sub>	HCl	75	DCE	46 (<5) <sup>c</sup>	14	Cl <sub>3</sub>	HCl	75	THF	0

All reactions performed on 0.2 mmol scale, phenolic **2.5** (1 equiv), alcohol **2.38** (1.1 equiv), 0.25 M, 50 °C, 24 h. <sup>a</sup> Concentrated aqueous HCl or HBr. <sup>b</sup> Determined by NMR analysis of the crude reaction mixture using 1,3,5-trimethoxybenzene as the internal standard. <sup>c</sup> No HCl.

The ability to use tertiary alcohols enables various alkyl groups to be added (**Table 2.4**). Reactions with phenolic substrates were carried out along with L. Göttemann. Alkylation of phenol (**2.5**) occurred selectively at the *para* position, affording **2.40–2.43** in 71–85% yields (**2.41** and **2.43** by K. G. M. Kou). Adamantane is a privileged structure that has earned the reputation of being a “lipophilic bullet” for enhancing pharmacological activity<sup>38</sup> and various methods have been devised for their derivatization,<sup>39</sup> including a Friedel–Crafts strategy that requires trifluoroacetic acid as the solvent.<sup>40</sup> Here, dual FeCl<sub>3</sub>/HCl catalysis allows arylation of 1-adamantanol under mild reaction conditions.

**Table 2.4.** Scope of dual Brønsted/Lewis acid catalyzed, C(sp<sup>2</sup>)-C(sp<sup>3</sup>) coupling between phenolic and tertiary alcohol derivatives.<sup>a</sup>



<sup>a</sup> Combined efforts with L. Gottmann. <sup>b</sup> Reaction carried out by K. G. M. Kou.

Surprisingly, 1-methylcyclopentanol (**2.44**) turned out to be a poor alkylating agent that only gave 23% yield of *para*-methylcyclopentyl phenol (**2.45**) even with a higher catalyst loading. Analysis of the reaction mixture revealed the major side product to be cyclopentene. Presumably, the dehydration pathway was facile, and the reverse hydration step was unfavorable under the reaction conditions. Using *tert*-butanol (**2.37**), alkylation of 4-*tert*-butylphenol furnishes di-*tert*-butylphenol (**2.7**) in 85% yield, while 4-ethylphenol was alkylated to yield **2.46** in 58% yield at 1 mol% FeCl<sub>3</sub> loading. 4-

Chlorophenol required 1 equivalent of FeCl<sub>3</sub> to achieve 51% yield of **2.8**. 2-Benzyl-, 2-ethyl-, and 2-phenyl-phenol were alkylated in moderate-to-good yields (44–81%) to give **2.16**, **2.47**, and **2.12**, respectively. Some substrates require higher catalyst loadings (*e.g.*, 2-ethylphenol and 2-phenyl-phenol) to achieve high reactivity but absent of a trend. Minor amounts of dialkylation side products were isolated and characterized.

*tert*-Alkylation of *meta*-substituted phenols was examined using 2-methyl-2-propanol (**2.38**). At 5 mol% catalyst loading, 3-ethyl-, 3-*tert*-butyl-, and 3-phenylphenol were converted to disubstituted phenols **2.49**, **2.39**, **2.50** in 67–83% yields. 3-Methoxyphenol was converted by K. G. M. Kou to **2.51** in 37% yield and alkylated resorcinol **2.52** was synthesized in 62% yield. Unlike other *meta*-substituted phenols, 3-fluorophenol was *tert*-alkylated *para* to the hydroxy group in 53% yield (**2.53**). When reacted with phenol, tertiary benzylic (**2.54**) and propargylic (**2.55**) alcohols, normally successful in Friedel–Crafts alkylations, converted to multiple products that could not be purified to homogeneity. With dimethylvinylcarbinol (**2.56**), *C*-alkylation followed by cyclization was observed with 3-*tert*-butylphenol to produce chromane **2.57** in 48% yield.

The desired *tert*-alkylation reactions were not restricted to phenolic compounds, but also to anisolic and electron-neutral arenes, in which cases the combination of FeBr<sub>3</sub> and HBr catalysts were found to be the optimal catalysts (**Table 2.5**). Using 2-methylanisole (**2.58**) for optimization studies, it was discovered by M. Chojnacka that the optimal condition involved FeBr<sub>3</sub> and HBr in DCE solvent, which afforded the product (**2.59**) in 68% NMR yield (entry 1). While the use of FeCl<sub>3</sub> was optimal with phenolic substrates, it decreased the conversion to 47% (entry 2), and FeBr<sub>2</sub> proved even less

effective (31%, entry 3). Adding more HBr co-catalyst reduced product formation to 44% (entry 4). The reaction still proceeded to 66% conversion when the acid additive was absent (entry 5). Chlorobenzene was the only other effective solvent (63%, entries 6–9). Finally, the reaction was run with only the Brønsted (entry 10) or AlCl<sub>3</sub> (entry 11). Both Friedel–Crafts reactions failed, with AlCl<sub>3</sub> inducing low conversion to a complex mixture.

**Table 2.5.** Optimization conditions with 2-methylanisole (**2.58**).

Reaction scheme: 2-methylanisole (**2.58**, 1 equiv) + 2-methylbutan-2-ol (**2.38**, 1 equiv)  $\xrightarrow[\text{solvent, 50 } ^\circ\text{C, 24 h}]{[\text{Fe}] (x \text{ mol}\%), \text{ acid } (y \text{ mol}\%)}$  2-(2-ethyl-2-propylphenyl)-1,3-dimethoxybenzene (**2.59**)

	[Fe]	x	acid	y	solvent	% yield <sup>a</sup>
1	FeBr <sub>3</sub>	30	HBr	15	DCE	68 (33) <sup>b</sup>
2	FeCl <sub>3</sub>	30	HCl	15	DCE	47
3	FeBr <sub>2</sub>	30	HBr	15	DCE	31
4	FeBr <sub>3</sub>	30	HBr	75	DCE	44
5	FeBr <sub>3</sub>	30	HBr	0	DCE	66
6	FeBr <sub>3</sub>	30	HBr	15	<i>i</i> -PrOH	0
7	FeBr <sub>3</sub>	30	HBr	15	HFIP	6
8	FeBr <sub>3</sub>	30	HBr	15	ClC <sub>6</sub> H <sub>5</sub>	63
9	FeBr <sub>3</sub>	30	HBr	15	PhMe	25
10	—	—	HBr	100	DCE	0
11	—	—	AlCl <sub>3</sub>	100	DCE	— <sup>c</sup>

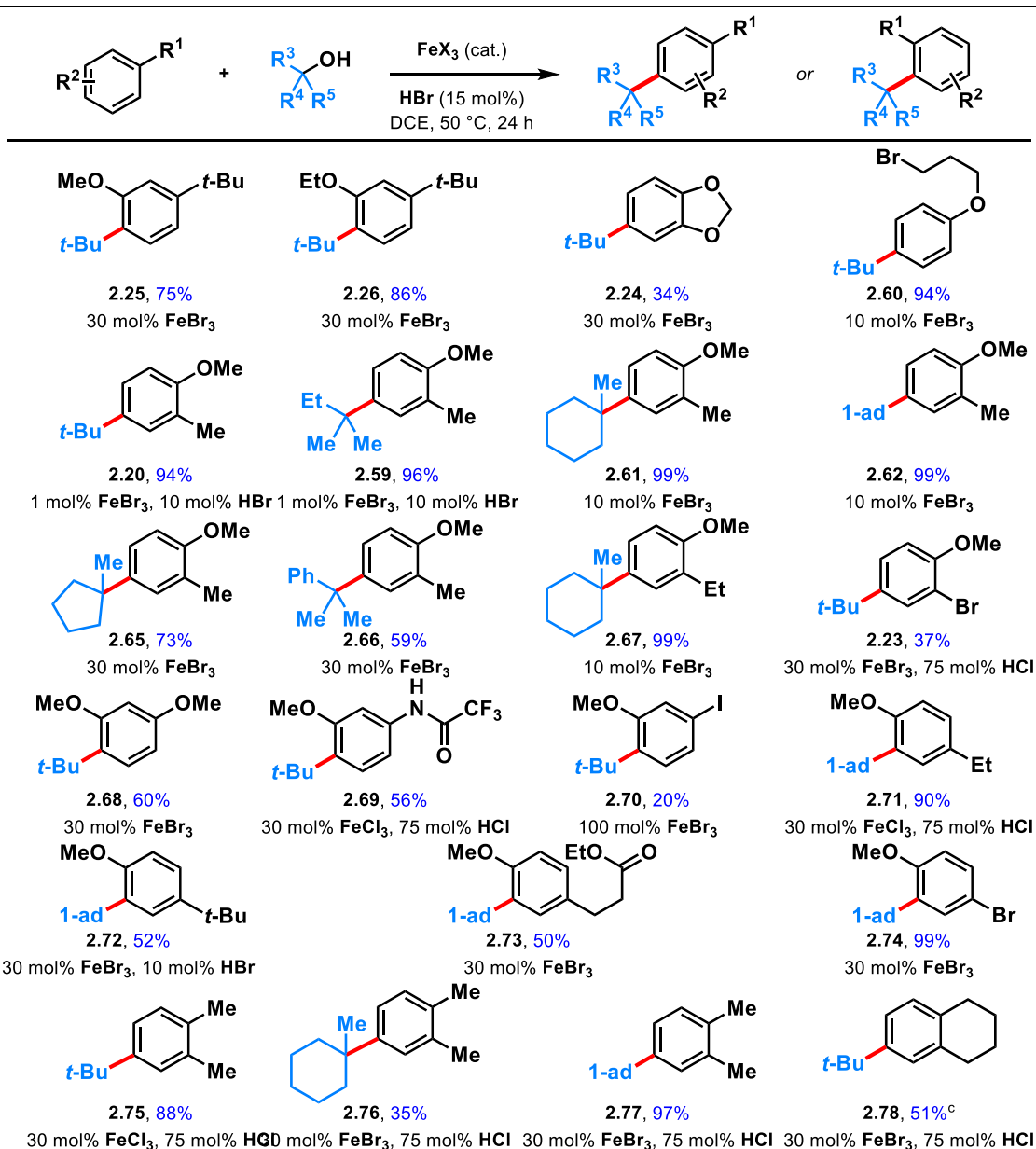
Conditions: All reactions performed by M. Chojnacka on 0.2 mmol scale, anisolic **2.58** (1 equiv), alcohol **2.38** (1 equiv), 0.2 M, 50 °C, 24 h. <sup>a</sup> Determined by NMR analysis of the crude reaction mixture using 1,3,5-trimethoxybenzene as the internal standard. <sup>b</sup> 20 °C. <sup>c</sup>

Low conversion to a complex mixture of products.

M. Chojnacka and R. Crowley III next examined the alkylation of aryl ethers and simple arenes (**Table 2.6**). 3-*tert*-Butylanisole was alkylated at the less sterically encumbered *ortho* position with respect to the methoxy group (**2.25**, 75%). Swapping the methyl ether with an ethyl ether yields product **2.26** in 86%. However, 1,2-benzodioxole (**2.24**) was *tert*-butylated in a modest 34% yield. A primary halide tethered off the ether linkage does not hinder the reaction and resulted in 94% yield of **2.60**. A variety of tertiary alcohols were tested to alkylate 2-methylanisole (**2.58**). Most of the alcohols deliver the alkylated products (**2.20**, **2.59**, **2.61**, **2.62**) in near quantitative yields (94–99%) with low catalyst loadings: 1 mol% for *tert*-butanol (**2.37**) and *tert*-amyl alcohol (**2.38**), and 10 mol% for methylcyclohexanol (**2.63**) and adamantanol (**2.64**). Methylcyclopentanol (**2.44**) and cumyl alcohol (**2.54**), substrates that reacted poorly with phenol (*cf.* **Table 2.4**), require 30 mol% iron and yields alkylated **2.65** and **2.66** in 73% and 59%, respectively. Alkylation of 2-ethylanisole with methylcyclohexanol provided **2.67** in 99% yield. 2-Bromoanisole was considerably less reactive, leading to alkylated **2.23** in 37% yield with a full equivalent of FeBr<sub>3</sub>. While most of the *meta*-substituted anisole derivatives were alkylated to **2.68** and **2.69** in moderate yields (56–60%) with catalytic FeBr<sub>3</sub>, 3-iodo-anisole requires a full equivalent of FeBr<sub>3</sub> and furnished the product (**2.70**) in 20% yield. *tert*-Alkylation of 4-ethylanisole led to product **2.71** in 90% yield, but 4-*tert*-butylanisole turned out to be a more challenging substrate, likely owing to the added steric bulk, forming alkylation product **2.72** in 52% yield. The reaction accommodates esters, providing product **2.73** in 50% yield. In contrast to previously studied halogenated arenes, 4-bromoanisole was

converted to product **2.74** in quantitative yield. Neutral arenes *ortho*-xylene and tetralin were alkylated to provide arenes **2.75–2.78** in 35–97% yields.

**Table 2.6.** Scope of dual Brønsted/Lewis acid-catalyzed, C(sp<sup>2</sup>)-C(sp<sup>3</sup>) coupling between arene and tertiary alcohol derivatives.<sup>a</sup>



<sup>a</sup> Work done by M. Chojnacka and R. Crowley III. <sup>b</sup> Isolated as a 2.6 to 1 mixture of product/starting material. <sup>c</sup> NMR yield.



### 2.3.1 Mechanistic studies through *tert*-butanol kinetic studies

The kinetic profile of the reaction was examined using the method of initial and exponential rates and by varying the concentrations of **2.5**, **2.37**, FeCl<sub>3</sub> catalyst, and conc aqueous HCl (**Table 2.7**). 3-*tert*-Butylphenol (**2.5**) was chosen because little-to-no side products form over the course of the reaction, and no decomposition was observed. The conversions to product **2.11** were monitored by SFC analysis (**Figures 2.29–2.32**).

**Table 2.7.** Kinetic data for arene alkylation with *tert*-butanol.

	[ <b>2.5</b> ] / M	[ <b>2.37</b> ] / M	[FeCl <sub>3</sub> ] / M	[HCl] / M	Induction Period <sup>a</sup> / M·s <sup>-1</sup>	Acceleration Phase <sup>a</sup> / M·s <sup>-1</sup>
1	6.3 × 10 <sup>-2</sup>	1.3 × 10 <sup>-1</sup>	1.3 × 10 <sup>-2</sup>	9.4 × 10 <sup>-2</sup>	2.5 <sub>5</sub> × 10 <sup>-6</sup>	1.5 <sub>9</sub> × 10 <sup>-5</sup>
2	1.3 × 10 <sup>-1</sup>	1.3 × 10 <sup>-1</sup>	1.3 × 10 <sup>-2</sup>	9.4 × 10 <sup>-2</sup>	5.5 <sub>6</sub> × 10 <sup>-6</sup>	3.0 <sub>4</sub> × 10 <sup>-5</sup>
3	2.5 × 10 <sup>-1</sup>	1.3 × 10 <sup>-1</sup>	1.3 × 10 <sup>-2</sup>	9.4 × 10 <sup>-2</sup>	1.9 <sub>3</sub> × 10 <sup>-6</sup>	7.4 <sub>5</sub> × 10 <sup>-5</sup>
4	1.3 × 10 <sup>-1</sup>	6.3 × 10 <sup>-2</sup>	1.3 × 10 <sup>-2</sup>	9.4 × 10 <sup>-2</sup>	9.8 <sub>3</sub> × 10 <sup>-6</sup>	2.1 <sub>0</sub> × 10 <sup>-5</sup>
5	1.3 × 10 <sup>-1</sup>	1.9 × 10 <sup>-1</sup>	1.3 × 10 <sup>-2</sup>	9.4 × 10 <sup>-2</sup>	4.2 <sub>0</sub> × 10 <sup>-6</sup>	2.5 <sub>9</sub> × 10 <sup>-5b</sup>
6	1.3 × 10 <sup>-1</sup>	2.5 × 10 <sup>-1</sup>	1.3 × 10 <sup>-2</sup>	9.4 × 10 <sup>-2</sup>	1.0 <sub>8</sub> × 10 <sup>-6</sup>	1.3 <sub>5</sub> × 10 <sup>-5b</sup>
7	1.3 × 10 <sup>-1</sup>	1.3 × 10 <sup>-1</sup>	3.1 × 10 <sup>-3</sup>	9.4 × 10 <sup>-2</sup>	2.2 <sub>3</sub> × 10 <sup>-6</sup>	2.1 <sub>6</sub> × 10 <sup>-5</sup>
8	1.3 × 10 <sup>-1</sup>	1.3 × 10 <sup>-1</sup>	6.3 × 10 <sup>-3</sup>	9.4 × 10 <sup>-2</sup>	1.7 <sub>8</sub> × 10 <sup>-6</sup>	1.6 <sub>9</sub> × 10 <sup>-5</sup>
9	1.3 × 10 <sup>-1</sup>	1.3 × 10 <sup>-1</sup>	9.4 × 10 <sup>-3</sup>	9.4 × 10 <sup>-2</sup>	4.3 <sub>7</sub> × 10 <sup>-6</sup>	1.7 <sub>8</sub> × 10 <sup>-5</sup>
10	1.3 × 10 <sup>-1</sup>	1.3 × 10 <sup>-1</sup>	1.9 × 10 <sup>-2</sup>	9.4 × 10 <sup>-2</sup>	3.9 <sub>3</sub> × 10 <sup>-6</sup>	2.8 <sub>5</sub> × 10 <sup>-5b</sup>
11	1.3 × 10 <sup>-1</sup>	1.3 × 10 <sup>-1</sup>	1.3 × 10 <sup>-2</sup>	4.7 × 10 <sup>-2</sup>	18.4 × 10 <sup>-6</sup>	3.3 <sub>8</sub> × 10 <sup>-5</sup>
12	1.3 × 10 <sup>-1</sup>	1.3 × 10 <sup>-1</sup>	1.3 × 10 <sup>-2</sup>	1.3 × 10 <sup>-1</sup>	1.9 <sub>2</sub> × 10 <sup>-6</sup>	2.0 <sub>7</sub> × 10 <sup>-5</sup>
13	1.3 × 10 <sup>-1</sup>	1.3 × 10 <sup>-1</sup>	1.3 × 10 <sup>-2</sup>	1.9 × 10 <sup>-1</sup>	1.9 <sub>8</sub> × 10 <sup>-6</sup>	2.3 <sub>6</sub> × 10 <sup>-5</sup>

Average value from: <sup>a</sup> 2 independent experiments. <sup>b</sup> 3 independent experiments.

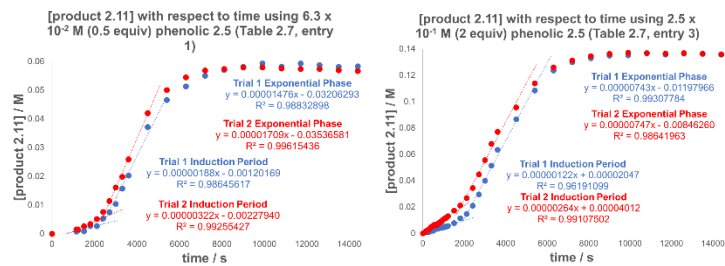


Figure 2.29. Rates of induction period and exponential phase when varying [phenolic 2.5].

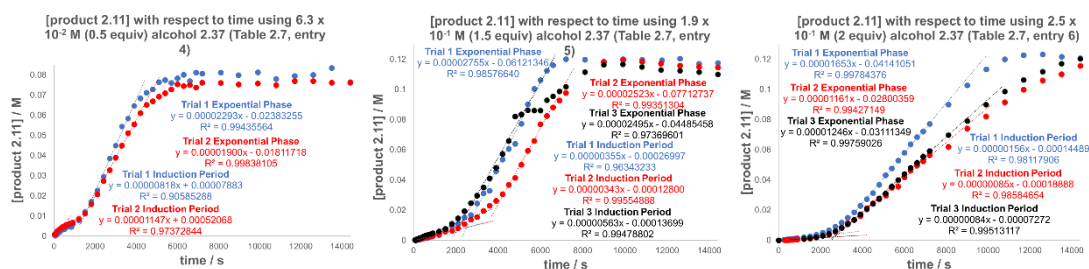


Figure 2.30. Rates of induction period and exponential phase when varying [alcohol 2.37].

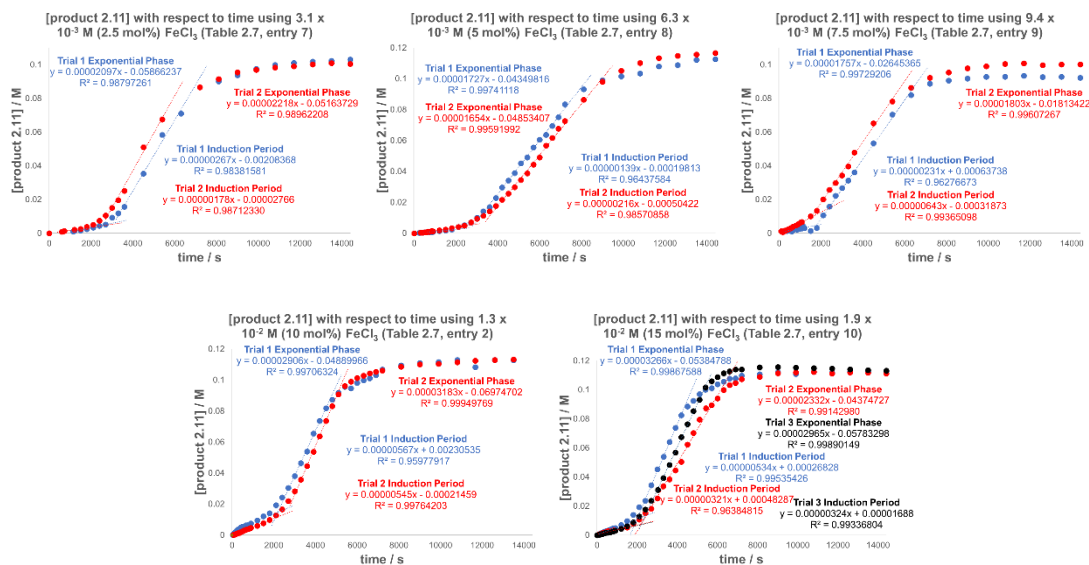
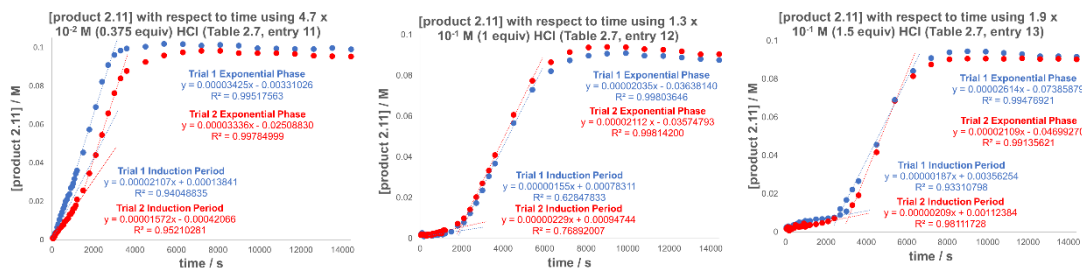


Figure 2.31. Rates of induction period and exponential phase when varying [ $\text{FeCl}_3$ ].



**Figure 2.32.** Rates of induction period and exponential phase when varying [HCl].

While the kinetics for the DTBP (**2.6**) system were well-behaved, the kinetics data obtained for the alkylation process with *tert*-butanol were all complicated by induction periods. This may be due to the heterogeneous nature of the reaction mixtures; the iron catalyst does not completely solubilize. The induction periods were characterized by slow reaction rates and lasted for 2000–4000 s (~30–60 min). They did not follow a trend and were unpredictable. Even those induction periods measured within replicate runs differed 2–3 fold in reaction rates. It was observed that the acceleration phases following the induction periods all displayed constant reaction rates (apparent zero-order dependencies), regardless of varying arene, alcohol, iron, or HCl concentrations. The reaction rates during the acceleration periods following the induction periods were invariably constant and do not appear to be affected by concentrations of  $\text{FeCl}_3$ , HCl, phenolic substrate, or *tert*-butanol, thereby resembling zero-order behaviors in all cases (**Table 2.7**).

Several naturally occurring compounds were subjected to *tert*-alkylation (**Figure 2.33**). Initially, the compounds tested performed poorly due to low solubility in DCE at 50 °C. However, useful yields resulted by changing the solvent to chlorobenzene and heating to 100 °C. Thymol and sesamol were adamantylated to produce functionalized **2.79** and

**2.90** in 38% and 65% yields, respectively. The relatively more complex molecule, estrone, undergoes *tert*-butylation in 40% yield (**2.81**) and adamantylation in 19% yield (**2.82**).

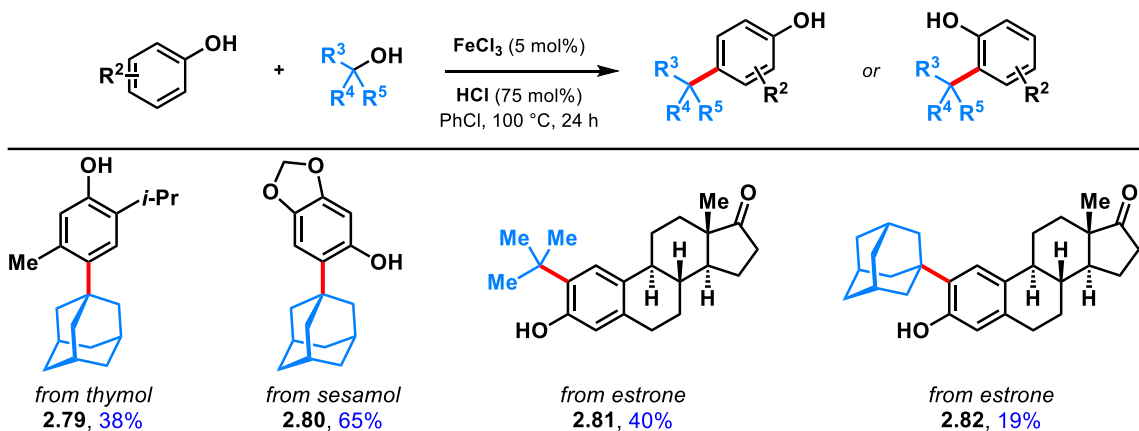


**Figure 2.33.** *tert*-Alkylation of natural products.

To assess the stability of the tertiary alcohol under the reaction conditions, R. Crowley III exposed 1-adamantanol (**2.64**) to dual Brønsted/Lewis acid catalysis conditions (**Figure 34a**). In the absence of the arene substrate, 1-bromoadamantane (**2.83**) was isolated in 28% yield. Subjecting the same reaction to 1 equivalent of  $FeBr_3$  increased the yield to 87%. To probe whether the reaction proceeds through a closed- or open-shell pathway, Crowley investigated the capturing of putative radical intermediates using various Michael acceptors **2.84** (**Figure 34b**). The potential for a 1-electron reduction of the newly formed carbon–halogen bond using an iron(II) catalyst was examined. However, attempts to generate radical species from both 1-adamantanol (**2.64**) and 1-bromoadamantane (**2.83**) were deemed unsuccessful as alkyl addition to the Michael acceptors was not observed. Initially, methyl acrylate and phenyl acrylate were tested, however both proved ineffective, as did others that were investigated.

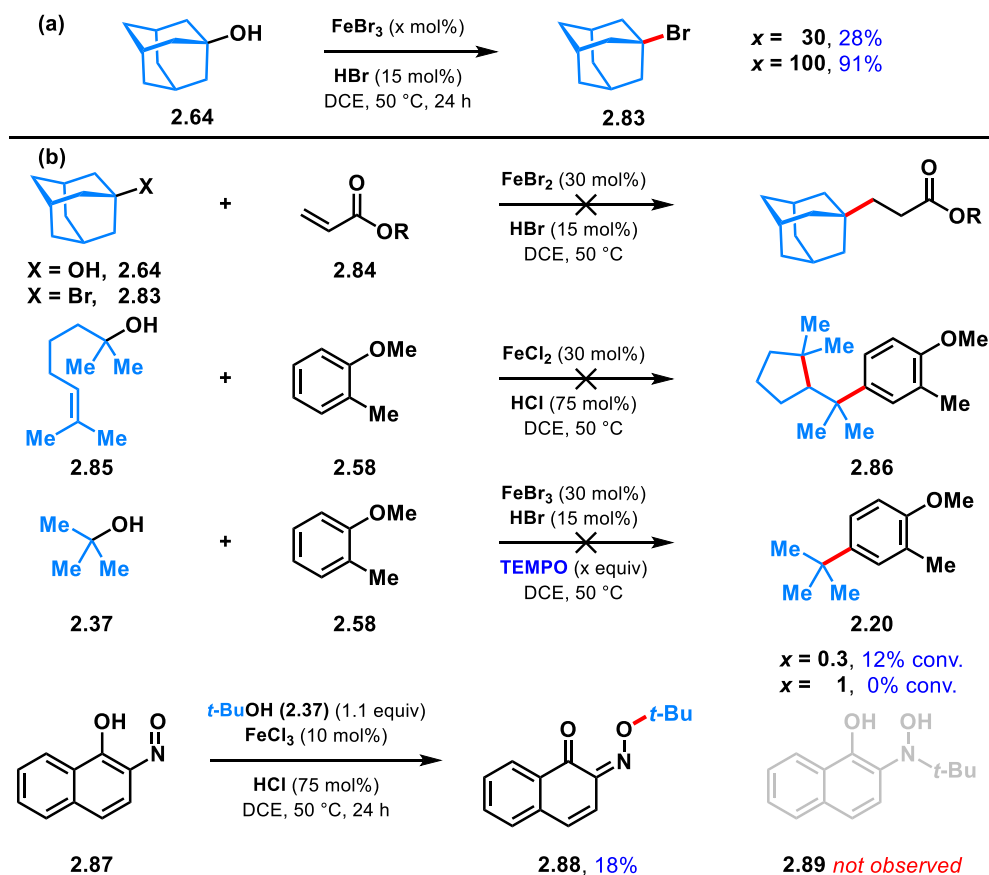


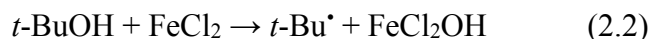
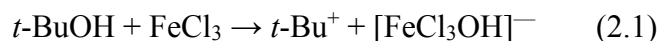
**Figure 2.34.** (a) Fate of the alcohol. (b) Probing for a radical vs. polar pathway.

If a radical intermediate forms from alkenol **2.85**, the resulting tertiary radical could cyclize onto the alkene, but attempts by R. Crowley III to react alkenol **2.85** with 2-methylanisole (**2.58**) resulted in a mixture of products with no indication of cyclization to cyclopentyl **2.86**. Addition of substoichiometric (2,2,6,6-tetramethylpiperidin-1-yl)oxyl (TEMPO) reduced reactivity to 12% conversion and stoichiometric TEMPO halted reactivity. However, in the absence of other compelling data, this was interpreted as a competitive interaction between TEMPO and the iron reagent that led to an inactive Fe(II) species.<sup>41</sup> This was supported by the lack of TEMPO-adducts observed, which were

otherwise expected to form from the quenching of arene or tertiary alkyl radical species. While less common than TEMPO, nitroso compounds exert radical scavenging properties.<sup>42</sup> As such, it was rationalized that 2-nitroso-1-naphthol (**2.87**) could potentially differentiate radical and polar pathways. The donating capacity of the phenolic group could render the nitroso functionality reactive towards polar electrophiles to give oxime ether **2.88**. Alternatively, radical intermediates would engage the nitroso group to arrive at hydroxylamine **2.89**. Under the reaction conditions, only oxime ether **2.88** was formed in 18% yield, with the remainder of the mass balance attributed to unreacted starting materials. Amine **2.89** was not detected in the reaction mixture.

### 2.3.2 Mechanistic studies through computational studies

Prof. B. E. Haines (Westmont College) employed density functional theory (DFT) calculations with energies refined at the B2PLYP-D3/def2-TZVPPD level of theory<sup>43</sup> to assess the thermodynamics of closed- and open-shell pathways for activation of *t*-BuOH (**2.37**) by FeCl<sub>3</sub> through a polar pathway using eqn (2.1) ( $\Delta G^\circ/\Delta H^\circ = 15.8/18.2 \text{ kcal}\cdot\text{mol}^{-1}$ ) or FeCl<sub>2</sub> through a radical pathway using eqn (2.2) ( $\Delta G^\circ/\Delta H^\circ = 42.5/46.7 \text{ kcal}\cdot\text{mol}^{-1}$ ):



The reaction between *t*-BuOH (**2.37**) and FeCl<sub>3</sub> to form *tert*-butyl cation (eqn (2.1)) was computed to be lower in free energy by 26.7 kcal·mol<sup>-1</sup>, suggesting it was far more likely to occur. Considering the reaction is run in the presence of a strong Brønsted acid, Haines also examined how protonation of the alcohol group affects the energetics. First,

protonation of the alcohol group by HCl is predicted to be significantly thermodynamically uphill ( $\Delta G^\circ = 28.8 \text{ kcal}\cdot\text{mol}^{-1}$ ). The free energy for subsequent cleavage of the C–O bond in the presence of FeCl<sub>3</sub> and FeCl<sub>2</sub> were computed using eqn (2.3) ( $\Delta G^\circ/\Delta H^\circ = -5.8/-4.0 \text{ kcal}\cdot\text{mol}^{-1}$ ) and eqn (2.4) ( $\Delta G^\circ/\Delta H^\circ = 40.1/44.1 \text{ kcal}\cdot\text{mol}^{-1}$ ), respectively:



The reaction in eqn (2.3) is lower in free energy than the reaction in eqn (2.4) by  $45.9 \text{ kcal}\cdot\text{mol}^{-1}$ , suggesting that the effect of protonating the alcohol renders the polar pathway even more likely. Based on these studies, we propose this reaction proceeds *via* a polar Friedel–Crafts type mechanism.

From here, Haines next sought to gain insight into the course of the reaction (**Figure 2.35**). He first computed the association complexes between FeCl<sub>3</sub> and other components in the reaction. All attempts to locate a structure for “HFeCl<sub>4</sub>” through coordination of HCl to the iron center of FeCl<sub>3</sub> led to dissociation of the HCl upon optimization. This indicates that HFeCl<sub>4</sub> is not a well-defined minimum on the potential energy surface at this level of theory (in the gas phase). In addition, the formation of the FeCl<sub>3</sub>---Cl–H association complex is uphill ( $\Delta G^\circ/\Delta H^\circ = 5.5/-1.8 \text{ kcal}\cdot\text{mol}^{-1}$ ). Haines found that the most stable 1:1 complex is between *t*-BuOH (**2.37**) and FeCl<sub>3</sub> ( $t\text{-BuOH} + \text{FeCl}_3 \rightarrow t\text{-BuOH}\text{--}\text{FeCl}_3$ ) where  $\Delta G^\circ/\Delta H^\circ = -10.4/-21.7 \text{ kcal}\cdot\text{mol}^{-1}$ . Direct ionization from this complex to form the *tert*-butyl cation is significantly thermodynamically uphill ( $\Delta G^\circ/\Delta H^\circ = 26.2/39.9 \text{ kcal}\cdot\text{mol}^{-1}$ ), which is consistent with how FeCl<sub>3</sub> has not been successful in catalyzing transformations with unactivated *tert*-alkanols.<sup>44–46</sup> Additionally, the role of HCl in this process is unclear.

Alternatively, HCl association with *t*-BuOH (**2.37**) to form a hydrogen bonded complex is slightly unfavored ( $t\text{-BuOH} + \text{HCl} \rightarrow t\text{-BuOH}\cdots\text{HCl}$ ) where  $\Delta G^\circ/\Delta H^\circ = 2.0/-5.4$  kcal $\cdot\text{mol}^{-1}$ . However, putting FeCl<sub>3</sub> near the HCl and optimizing the geometry results in spontaneous protonation of the alcohol to form the  $t\text{-BuOH}_2^+/\text{[FeCl}_4\text{]}^-$  ion pair. The ion pair is lower in free energy than the hydrogen bonded complex by 12.8 kcal $\cdot\text{mol}^{-1}$ , indicating that FeCl<sub>3</sub>-facilitated protonation of the alcohol is competitive with direct coordination of FeCl<sub>3</sub> to *t*-BuOH (**2.37**). From the ion pair, ionization to the *tert*-butyl cation is only 7.7 kcal $\cdot\text{mol}^{-1}$  uphill. Thus, the combination of FeCl<sub>3</sub> and HCl provides a low energy pathway to the formation of the reactive *tert*-butyl cation.

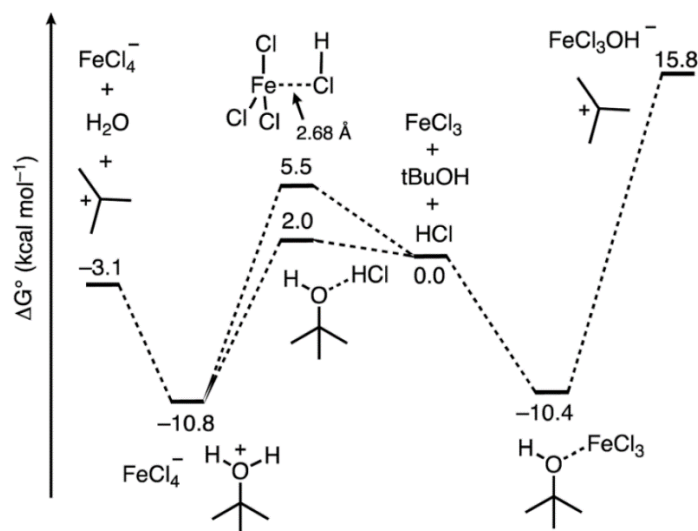


**Figure 2.35.** Free energy profile computed using DFT calculations for the course of ionization of *t*-BuOH (**2.37**) in the presence of the FeCl<sub>3</sub>/HCl acid pair and FeCl<sub>3</sub>.

The results in **Figure 2.35** imply that the FeCl<sub>3</sub> Lewis acid additive increases the Brønsted acidity of HCl despite the lack of a discrete structure for “HFeCl<sub>4</sub>”. This is reminiscent of the HF/BF<sub>3</sub> pair that is sometimes referred to as HBF<sub>4</sub>, for which there is no



expected discrete structure but can be qualified as a super acid.<sup>47</sup> Haines next sought to quantify the extent of increased Brønsted acidity imparted by the inclusion of the Lewis acid additive for several Brønsted acid/Lewis acid (HA/L) pairs. He used the reaction shown in eqn (2.5), where HA is the Brønsted acid, L represents the Lewis acid additive, and HA-L represents a complex formed between them:



The HA/L pairs studied were HCl/FeCl<sub>3</sub>, HBr/FeBr<sub>3</sub>, CF<sub>3</sub>COOH/ FeCl<sub>3</sub>, as well as HF/BF<sub>3</sub> (**Table 2.8**). It should be noted that for the binary mineral acids studied, the HA-L is not stable relative to the separated HA and L species and so the energy calculated from eqn (5) corresponds with the complexation energy between A<sup>-</sup> and L.

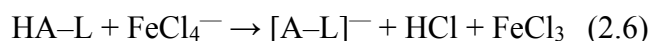
**Table 2.8.** Free energy calculated from eqn (2.5) to estimate the increased Brønsted acid/Lewis acid pairs (HA/L) discussed in this study.

HA/L	$\Delta G^\circ$ eqn (2.5) (kcal•mol <sup>-1</sup> )	$\Delta pK_a$
HCl/FeCl <sub>3</sub>	-31.4	23
HBr/FeBr <sub>3</sub>	-28.6	21
CF <sub>3</sub> COOH/FeCl <sub>3</sub>	-24.7	18
HF/BF <sub>3</sub>	-47.5	35

The data in **Table 2.8** show that the added Lewis acid has a substantial effect on the acidity of the Brønsted acids. FeCl<sub>3</sub> provides more stabilization to the chloride ion than to trifluoroacetate ( $\Delta\Delta G^\circ = -6.7$  kcal•mol<sup>-1</sup>) and more stabilization than FeBr<sub>3</sub> provides to the bromide ion ( $\Delta\Delta G^\circ = -2.8$  kcal•mol<sup>-1</sup>). In addition, the largest increase is achieved for

the HF/BF<sub>3</sub> pair. These results suggest a synergistic effect between the conjugate base and Lewis acid may be a significant factor for determining the increase in Brønsted acidity.

Haines next used eqn (2.6) to gain a better sense for the acidity of the HA/L pairs relative to HCl/FeCl<sub>3</sub> to assess their overall reactivity:



For the HBr/FeBr<sub>3</sub> pair,  $\Delta G^\circ/\Delta H^\circ = -2.9/-3.2 \text{ kcal}\cdot\text{mol}^{-1}$ , which is consistent with our experimental results suggesting this pair to be more reactive. However, this value is about half as much as one would expect based on the relative p*K*<sub>a</sub> values of HCl and HBr in DCE, ( $\Delta\text{p}K_{\text{a}}[\text{DCE}], \text{HBr} - \text{HCl} = 4.5$ ).<sup>48</sup> The other two combinations are predicted to be less reactive than HCl/FeCl<sub>3</sub>, where the CF<sub>3</sub>COOH/FeCl<sub>3</sub> and HF/BF<sub>3</sub> combinations give  $\Delta G^\circ/\Delta H^\circ = 8.4/16.8$  and  $7.5/7.1 \text{ kcal}\cdot\text{mol}^{-1}$ , respectively. The former case is consistent with experimental results from **Table 2.3** (entry 2) showing no product formation with the CF<sub>3</sub>COOH/FeCl<sub>3</sub> pair. The use of HBF<sub>4</sub> (2.5 mol%) as the catalyst resulted in only trace product formation (<5% by <sup>1</sup>H NMR analysis). These results suggest that the pairing of a Lewis acid with a Brønsted acid generally increases the Brønsted acidity significantly in organic media, and that careful choice of the pairing could provide a level of control over the overall reactivity of the pair.

## 2.4 Conclusion

We have detailed mild and operationally simple reaction conditions to achieve *tert*-alkylations of aromatic systems with di-*tert*-butylperoxide (**2.6**) and *tert*-alkanols in forming all-carbon quaternary centers through synergistic Brønsted/Lewis acid catalysis.

These reactions fill a gap in the Friedel–Crafts alkylation literature by enabling the use of tertiary aliphatic alcohols that lack stabilizing aryl, alkenyl, and alkynyl substituents. We expect that this approach will prove to be practical in installing quaternary carbon centers when orchestrated into synthesis plans that take advantage of C–O bonds (*e.g.*, triflyl and methoxy groups) for cross-coupling applications.<sup>49</sup> The use of cost-effective and readily-available iron, alcohol and arene reagents render this methodology advantageous for all-carbon quaternary center and C(sp<sup>2</sup>)–C(sp<sup>3</sup>) bond synthesis.

## 2.5 References

1. Friedel, C.; Crafts, J. M. A New General Synthetical Method of Producing Hydrocarbons, &c. *J. Chem. Soc.* **1877**, 32, 725–791.
2. Augustine, J. K.; Naik, Y. A.; Mandal, A. B.; Alagarsamy, P.; Akabote, V. Novel and Highly Regioselective Friedel–Crafts Alkylation of 3,5-Dimethoxyaniline Using an Aldehyde and Triethylsilane as Reducing Agent. *Syn. Lett.* **2008**, 16, 2429–2432.
3. Dryzhakov, M.; Moran, J. Autocatalytic Friedel–Crafts Reactions of Tertiary Aliphatic Fluorides Initiated by B(C<sub>6</sub>F<sub>5</sub>)<sub>3</sub>·H<sub>2</sub>O. *ACS Catal.* **2016**, 6, 3670–3673.
4. Ma, Z.-H.; Lv, L.-Q.; Wang, H.; Han, Z.-G.; Zheng, X.-Z.; Lin, J. Synthesis and catalytic reactivity of mononuclear substituted tetramethylcyclopentadienyl molybdenum carbonyl complexes. *Transition Met. Chem.* **2016**, 41, 225–233
5. Akram, M. O.; Tidwell, J. R.; Dutton, J. L.; Martin, C. D. Tris(*ortho*-carboranyl)borane: An Isolable, Halogen-Free, Lewis Superacid. *Angew. Chem. Int. Ed.* **2022**, 61, e202212073.
6. Huang, P.; Jiang, X.; Gao, D.; Wang, C.; Shi, D.-Q.; Zhao, Y. HFIP-promoted *para*-selective alkylation of anilines and phenols with tertiary alkyl bromides. *Org. Chem. Front.* **2023**, 10, 2476–2481.
7. Lohre, C.; Dröge, T.; Wang, C.; Glorius, F. Nickel-Catalyzed Cross-Coupling of Aryl Bromides with Tertiary Grignard Reagents Utilizing Donor-Functionalized N-Heterocyclic Carbenes (NHCs). *Chem. Eur. J.* **2011**, 17, 6052–6055.

8. Pitre, S. P.; Muuronen, M.; Fishman, D. A.; Overman, L. E. Tertiary Alcohols as Radical Precursors for the Introduction of Tertiary Substituents into Heteroarenes. *ACS Catal.* **2019**, *9*, 3413–3418.
9. Weber, L. W. D.; Boll, M.; Stampfl, A. Hepatotoxicity and Mechanism of Action of Haloalkanes: Carbon Tetrachloride as a Toxicological Model. *Crit. Rev. Toxicol.* **2008**, *33*, 105–136.
10. Rueping, M.; Nachtsheim, B. J.; Ieawsuwan, W. An Effective Bismuth-Catalyzed Benzoylation of Arenes and Heteroarenes. *Adv. Synth. Catal.* **2006**, *348*, 1033–1037.
11. Setayesh, S.; Grimsdale, A. C.; Weil, T.; Enkelmann, V.; Müllen, K.; Meghdadi, F.; List, E. J. W.; Leising, G. Polyfluorenes with Polyphenylene Dendron Side Chains: Toward Non-Aggregating, Light-Emitting Polymers. *J. Am. Chem. Soc.* **2001**, *123*, 946–953.
12. Nammalwar, B.; Bunce, R. A. Friedel–Crafts cyclization of tertiary alcohols using bismuth(III) triflate. *Tetrahedron Lett.* **2013**, *54*, 4330–4332.
13. Niggemann, M.; Meel, M. J. Calcium-Catalyzed Friedel–Crafts Alkylation at Room Temperature. *Angew. Chem. Int. Ed.* **2010**, *49*, 3684–3687.
14. Kazmaier, U. Direct Michael, Aldol, and Mannich Additions Catalyzed by Alkaline Earth Metals. *Angew. Chem. Int. Ed.* **2009**, *48*, 5790–5792.
15. Chen, L.; Zhou, F.; Shi, T.-D.; Zhou, J. Metal-Free Tandem Friedel–Crafts/Lactonization Reaction to Benzofuranones Bearing a Quaternary Center at C3 Position. *J. Org. Chem.* **2012**, *77*, 4354–4362.
16. Ricardo, C. L.; Mo, X.; McCubbin, J. A.; Hall, D. G. A Surprising Substituent Effect Provides a Superior Boronic Acid Catalyst for Mild and Metal-Free Direct Friedel–Crafts Alkylations and Prenylations of Neutral Arenes. *Chem. Eur. J.* **2015**, *21*, 4218–4223.
17. Schlegel, M.; Schneider, C. Lewis acid-catalyzed Friedel–Crafts reactions toward highly versatile,  $\alpha$ -quaternary oxime ethers. *Chem. Commun.* **2018**, *54*, 11124–11127.
18. Marcyk, P. T.; Jefferies, L. R.; AbuSalim, D. I.; Pink, M.; Baik, M.-H.; Cook, S. P. Stereoinversion of Unactivated Alcohols by Tethered Sulfonamides. *Angew. Chem. Int. Ed.* **2019**, *58*, 1727–1731.

19. (a) Cho, K.; Ando, M.; Kobayashi, K.; Miyazoe, H.; Tsujino, T.; Ito, S.; Suzuki, T.; Tanaka, T.; Tokita, S.; Sato, N. Design, synthesis and evaluation of a novel cyclohexanamine class of neuropeptide Y Y1 receptor antagonists. *Bioorg. Med. Chem. Lett.* **2009**, *19*, 4781–4785. (b) Liras, S.; McHardy, S. F.; Allen, M. P.; Segelstein, B. E.; Heck, S. D.; Bryce, D. K.; Schmidt, A. W.; Vanase-Frawley, M.; Callegari, E.; McLean, S. Biaryl piperidines as potent and selective delta opioid receptor ligands. *Bioorg. Med. Chem. Lett.* **2010**, *20*, 503–507.
20. Croft, R. A.; Dubois, M. A. J.; Boddy, A. J.; Denis, C.; Lazaridou, A.; Voisin-Chiret, A. S.; Bureau, R.; Choi, C.; Mousseau, J. J.; Bull, J. A. Catalytic Friedel-Crafts Reactions on Saturated Heterocycles and Small Rings for  $sp^3$ - $sp^2$  Coupling of Medicinally Relevant Fragments. *Eur. J. Org. Chem.* **2019**, 5385–5395.
21. Laxmikeshav, K.; Sakla, A. P.; Rasane, S.; John, S. E.; Shankaraiah, N. Microwave-Assisted Regioselective Friedel–Crafts Arylation by  $BF_3 \cdot OEt_2$ : A Facile Synthetic Access to 3-Substituted-3-Propargyl Oxindole Scaffolds. *ChemistrySelect* **2020**, *5*, 7004–7012.
22. Donald, C. P.; Boylan, A.; Nguyen, T. N.; Chen, P.-A.; May, J. A. Quaternary and Tertiary Carbon Centers Synthesized via Gallium-Catalyzed Direct Substitution of Unfunctionalized Propargylic Alcohols with Boronic Acids. *Org. Lett.* **2022**, *24*, 6767–6771.
23. Wang, Y.-J.; Bao, Y.-F.; Lu, X.-J.; Dong, J.-Q.; Liu, D.-H. High-efficiency catalyst  $CuSO_4/SBA-15$  toward butylated hydroxytoluene synthesis in a heterogeneous system. *RSC Adv.* **2023**, *13*, 3033–3038.
24. Sartori, G.; Bigi, F.; Maggi, R.; Arienti, A. Acidity effect in the regiochemical control of the alkylation of phenol with alkenes. *J. Chem. Soc., Perkin Trans. 1.* **1997**, 257–260.
25. Warren, T. H. Transition Metal-Catalyzed C–H Amination Using Unactivated Amines. US2011/213146, 2011, A1.
26. Liguori, L.; Bjørsvik, H.-R.; Fontana, F.; Bosco, D.; Galimberti, L.; Minisci, F. Electrophilic Aromatic Alkylation by Hydroperoxides. Competition between Ionic and Radical Mechanisms with Phenols. *J. Org. Chem.* **1999**, *64*, 8812–8815.
27. Kutz, W. M.; Corson, B. B. Alkylation of Thiophene by Olefins and Alcohols. *J. Am. Chem. Soc.* **1946**, *68*, 1477–1479.
28. Kamitori, Y.; Hojo, M.; Masuda, R.; Izumi, T.; Tsukamoto, S. Silica Gel as an Effective Catalyst for the Alkylation of Phenols and Some Heterocyclic Aromatic Compounds. *J. Org. Chem.* **1984**, *49*, 4161–4165.

29. Perez-Benito, J. F. Iron(III)–Hydrogen Peroxide Reaction: Kinetic Evidence of a Hydroxyl-Mediated Chain Mechanism. *J. Phys. Chem. A* **2004**, *108*, 4853–4858.
30. Shalit, H.; Libman, A.; Pappo, D. *meso*-Tetraphenylporphyrin Iron Chloride Catalyzed Selective Oxidative Cross-Coupling of Phenols. *J. Am. Chem. Soc.* **2017**, *139*, 13404–13413.
31. Horibe, T.; Ohmura, S.; Ishihara, K. Structure and Reactivity of Aromatic Radical Cations Generated by FeCl<sub>3</sub>. *J. Am. Chem. Soc.* **2019**, *141*, 1877–1881.
32. Albright, H.; Riehl, P. S.; McAtee, C. C.; Reid, J. P.; Ludwig, J. R.; Karp, L. A.; Zimmerman, P. M.; Sigman, M. S.; Schindler, C. S. Catalytic Carbonyl-Olefin Metathesis of Aliphatic Ketones: Iron(III) Homo-Dimers as Lewis Acidic Superelectrophiles. *J. Am. Chem. Soc.* **2019**, *141*, 1690–1700.
33. Burés, J. A Simple Graphical Method to Determine the Order in Catalyst. *Angew. Chem. Int. Ed.* **2016**, *55*, 2028–2031.
34. Fogg, D. E.; dos Santos, E. N. Tandem catalysis: a taxonomy and illustrative review. *Coord. Chem. Rev.* **2004**, *248*, 2365–2379.
35. (a) Kou, K. G. M.; Dong, V. M. Tandem rhodium catalysis: exploiting sulfoxides for asymmetric transition-metal catalysis. *Org. Biomol. Chem.* **2015**, *13*, 5844–5847; (b) Dornan, P. K.; Kou, K. G. M.; Houk, K. N.; and Dong, V. M. Dynamic Kinetic Resolution of Allylic Sulfoxides by Rh-Catalyzed Hydrogenation: A Combined Theoretical and Experimental Mechanistic Study. *J. Am. Chem. Soc.* **2014**, *136*, 291–298.
36. Liu, Y.; Kim, B.; Taylor, S. D. Synthesis of 4-Formyl Estrone Using a Positional Protecting Group and Its Conversion to Other C-4-Substituted Estrogens. *J. Org. Chem.* **2007**, *72*, 8824–8830.
37. Elkin, M.; Szewczyk, S. M.; Scruse, A. C. Newhouse, T. R. Total Synthesis of (±)-Berkeleyone A. *J. Am. Chem. Soc.* **2017**, *139*, 1790–1793.
38. Wanka, L.; Iqbal K.; Schreiner, P. R. The Lipophilic Bullet Hits the Targets: Medicinal Chemistry of Adamantane Derivatives. *Chem. Rev.* **2013**, *113*, 3516–3604.

39. (a) Lao, Y.-X.; Wu, J.-Q.; Chen, Y.; Zhang, S.-S.; Li, Q.; Wang, H. Palladium-catalyzed methylene C(sp<sup>3</sup>)-H arylation of the adamantyl scaffold. *Org. Chem. Front.* **2015**, *2*, 1374–1378; (b) Yang, H.-B.; Feceu, A.; Martin, D. B. C. Catalyst-Controlled C–H Functionalization of Adamantanes Using Selective H-Atom Transfer. *ACS Catal.* **2019**, *9*, 5708–5715; (c) Weigel III, W. K.; Dang, H. T.; Yang, H.-B.; Martin, D. B. C. Synthesis of amino-diamantoid pharmacophores via photocatalytic C–H aminoalkylation. *Chem. Commun.* **2020**, *56*, 9699–9702.
40. (a) Lu, D.; Meng, Z.; Thakur, G. A.; Fan, P.; Steed, J.; Tartal, C. L.; Hurst, D. P.; Reggio, P. H.; Deschamps, J. R.; Parrish, D. A.; George, C.; Järbe, T. U. C.; Lamb, R. J.; Makriyannis, A. Adamantyl Cannabinoids: A Novel Class of Cannabinergic Ligands. *J. Med. Chem.* **2005**, *48*, 4576–4585; (b) Stepakov, A. V.; Molchanov, A. P.; Kostikov, R. R. Alkylation of aromatic compounds with adamantan-1-ol. *Russ. J. Org. Chem.* **2007**, *43*, 538–543; (c) Tominaga, M.; Masu, H.; Azumaya, I. Construction and Charge-Transfer Complexation of Adamantane-Based Macrocycles and a Cage with Aromatic Ring Moieties. *J. Org. Chem.* **2009**, *74*, 8754–8760; (d) Cho, J.-C.; Rho, H. S.; Joo, Y. H.; Lee, C. S.; Lee, J.; Ahn, S. M.; Kim, E.; Shin, S. S.; Park, Y. H.; Suh, K.-D.; Park, S. N. Depigmenting activities of kojic acid derivatives without tyrosinase inhibitory activities. *Bioorg. Med. Chem. Lett.* **2012**, *22*, 4159–4162.
41. Van Humbeck, J. F.; Simonovich, S. P.; Knowles, R. R.; MacMillan, D. W. C. Concerning the Mechanism of the FeCl<sub>3</sub>-Catalyzed  $\alpha$ -Oxyamination of Aldehydes: Evidence for a Non-SOMO Activation Pathway. *J. Am. Chem. Soc.* **2010**, *132*, 10012–10014.
42. de Boer, T. J. Spin-trapping in early and some recent nitroso chemistry. *Can. J. Chem.* **1982**, *60*, 1602–1609.
43. Energies were computed at the B2PLYPD3/def2-TZVPPD// M15L/def2-SVP level of theory. Refined energies include solvation effects with the IEF-PCM model with 1,2-dichloroethane as the solvent and were corrected to a 1 M standard state. See ESI† for full description of computational methods.
44. For reviews of the Friedel–Crafts alkylation, see: (a) Rueping, M.; Nachtsheim, B. J. *Beilstein J. Org. Chem.* **2010**, *6*, DOI: 10.3762/bjoc6.6; (b) Chen, L.; Yin, X.-P.; Wang, C.-H.; Zhou, J. Catalytic functionalization of tertiary alcohols to fully substituted carbon centres. *Org. Biomol. Chem.* **2014**, *12*, 6033–6048.

45. Qin, Q.; Xie, Y.; Floreancig, P. E. Diarylmethane synthesis through  $\text{Re}_2\text{O}_7$ -catalyzed bimolecular dehydrative Friedel–Crafts reactions. *Chem. Sci.* **2018**, *9*, 8528–8534.
46. Bauer, I.; Knölker, H.-J. Iron Catalysis in Organic Synthesis. *Chem. Rev.* **2015**, *115*, 3170–3387.
47. (a) Juhasz, M.; Hoffmann, S.; Stoyanov, E.; Kim, K.-C.; Reed, C. A. The Strongest Isolable Acid. *Angew. Chem. Int. Ed.* **2004**, *43*, 5352–5355; (b) *J. Chem. Soc., Faraday Trans.* 1997, *93*, 2161–2165.
48. (a) Kütt, A.; Rodima, T.; Saame, J.; Raamat, E.; Mäemets, V.; Kaljurand, I.; Koppel, I. A.; Garlyauskayte, R. Y.; Yagupolskii, L.; Yagupolskii, L. M.; Bernhardt, E.; Willner, H.; Leito, I. Equilibrium Acidities of Superacids. *J. Org. Chem.* **2011**, *76*, 391–395; (b) Paenurk, E.; Kaupmees, K.; Himmel, D.; Kütt, A.; Kaljurand, I.; Koppel, I. A.; Krossing, I.; Leito, I. A unified view to Brønsted acidity scales: do we need solvated protons? *Chem. Sci.* **2017**, *8*, 6964–6973.
49. (a) Rosen, B. M.; Quasdorf, K. W.; Wilson, D. A.; Zhang, N.; Resmerita, M.; Garg, N. K.; Percec, V. Nickel-Catalyzed Cross-Couplings Involving Carbon–Oxygen Bonds. *Chem. Rev.* **2011**, *111*, 1346–1416; (b) Tobisu, M.; Chatani, N. Cross-Couplings Using Aryl Ethers via C–O Bond Activation Enabled by Nickel Catalysts. *Acc. Chem. Res.* **2015**, *48*, 1717–1726.

## 2.6 Experimental

### 2.6.1 General Information

See section 1.5.1 for general information.

#### *Reaction setup, progress monitoring, and product purification*

In general, the catalytic reactions were not air- or moisture-sensitive; however, the iron salts are hygroscopic and quickly change color when being weighed and added to the reaction vessel. This influenced how much metal catalyst was being added because their molecular weights increase on hydration. For consistency and rigor, the iron salts were



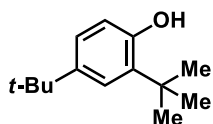
weighed and added to vials inside a nitrogen-filled glovebox. For phenols, mild oxidation during preparatory plate in open air occurred, which may discolor the final product. Unless otherwise noted, products purified by preparatory plate were pure by NMR analysis. Solids and amorphous solids measured for melting point were dried under high vacuum overnight and not crystallized. Substrates **2.18–2.30**, **2.58**, and **2.61–2.79** were prepared by M. Chojnacka or R. C. Crowley III and are not listed in the experimental section.

## 2.6.2 Dual Brønsted/Lewis acid-Catalyzed Friedel–Crafts *tert*-Alkylation

### General Procedure A: Alkylations with di-*tert*-butylperoxide (DTBP)

A one-dram vial equipped with a stirring bar was sequentially added FeCl<sub>3</sub> (0.02–0.06 mmol, 10–30 mol%), arene derivative (0.2 mmol, 1 equiv), DCE (0.8 mL, 0.25 M), DTBP (37 μL, 0.2 mmol, 1 equiv), and TFA (11.5 μL, 0.15 mmol, 75 mol%). The reaction mixture was heated at 50 °C for 2 h, then filtered through a 5” pipette plug of silica gel (approximately half-filled) and eluted with hexanes/EtOAc (1:1) or hexanes/Et<sub>2</sub>O (1:1). The solution was concentrated *in vacuo* and purified via silica gel chromatography to obtain the alkylation product.

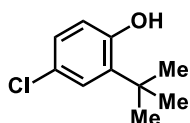
### 2,4-Di-*tert*-butylphenol (2.7)



Prepared using General Procedure A with 4-*tert*-butylphenol (34.0 mg, 0.200 mmol, 1 equiv), FeCl<sub>3</sub> (6.5 mg, 0.04 mmol, 0.02 equiv), DCE (0.8 mL, 0.25 M), DTBP (37 μL, 0.20 mmol, 1 equiv), and TFA (11.5 μL, 0.15 mmol, 0.75 equiv) for 18 h. Purification by preparative TLC (eluted with 19:1 hexanes/EtOAc) afforded **2.7** (9.1 mg, 22%) as a light-orange solid. <sup>1</sup>H NMR (CDCl<sub>3</sub>, 500 MHz): δ 7.30 (d,

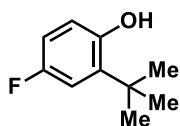
$J = 2.4$  Hz, 1H), 7.08 (dd,  $J = 8.2, 2.4$  Hz, 1H), 6.60 (d,  $J = 8.2$  Hz, 1H), 4.63 (s, 1H), 1.42 (s, 9H), 1.29 (s, 9H). HRMS (ESI<sup>-</sup>):  $m/z$  [M-H]<sup>-</sup> calculated for C<sub>14</sub>H<sub>21</sub>O: 205.1598; found: 205.1608. The spectral data recorded are consistent with those previously reported.<sup>4</sup>

### 2-*tert*-Butyl-4-chlorophenol (**2.8**)



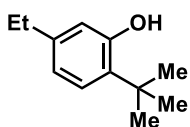
Prepared using General Procedure A with 4-chlorophenol (25.7 mg, 0.200 mmol, 1 equiv), FeCl<sub>3</sub> (32.4 mg, 0.20 mmol, 1 equiv), DCE (0.8 mL, 0.25 M), DTBP (37 μL, 0.20 mmol, 1 equiv), and TFA (11.5 μL, 0.15 mmol, 0.75 equiv) for 48 h. Purified via preparative TLC (eluted with 19:1 hexanes/EtOAc) afforded **2.8** (15.1 mg, 41%) as colorless oil. R<sub>f</sub>: 0.23 (19:1 hexanes/EtOAc). <sup>1</sup>H NMR (CDCl<sub>3</sub>, 600 MHz): δ 7.21 (d,  $J = 3.0$  Hz, 1H), 7.02 (dd,  $J = 8.4, 2.4$ , 1H), 6.60 (d,  $J = 8.4$  Hz, 1H), 4.77 (br s, 1H), 1.38 (s, 9H). <sup>13</sup>C NMR (CDCl<sub>3</sub>, 101 MHz): δ 152.9, 138.2, 127.5, 126.7, 125.58, 117.7, 34.9, 29.5. HRMS (ESI<sup>-</sup>):  $m/z$  [M-H]<sup>-</sup> calculated for C<sub>10</sub>H<sub>12</sub>ClO: 183.0582; found: 183.0590. The spectral data recorded are consistent with those previously reported.<sup>5</sup>

### 2-*tert*-Butyl-4-fluorophenol (**2.9**)



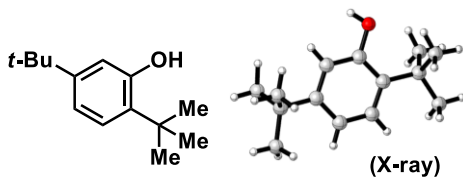
Prepared using General Procedure A with 4-fluorophenol (22.4 mg, 0.200 mmol, 1 equiv), FeCl<sub>3</sub> (32.4 mg, 0.20 mmol, 1 equiv), DCE (0.8 mL, 0.25 M), DTBP (37 μL, 0.20 mmol, 1 equiv), and TFA (11.5 μL, 0.15 mmol, 0.75 equiv) for 48 h. Purified via preparative TLC (eluted with 19:1 hexanes/EtOAc) afforded **2.9** (21.5 mg, 64%) as yellow oil. R<sub>f</sub>: 0.43 (19:1 hexanes/EtOAc). <sup>1</sup>H NMR (CDCl<sub>3</sub>, 600 MHz): δ 6.97 (dd,  $J = 10.8, 3.0$  Hz, 1H), 6.75 (dt,  $J = 8.4, 3.0$  Hz, 1H), 6.59 (dd,  $J = 8.4, 3.0$  Hz, 1H), 4.68 (br s, 1H), 1.39 (s, 9H). The spectral data recorded are consistent with those previously reported.<sup>5</sup>

### 2-*tert*-Butyl-5-ethylphenol (**2.10**)



Prepared using General Procedure A with 3-ethylphenol (24.8  $\mu$ L, 0.200 mmol, 1 equiv), FeCl<sub>3</sub> (3.2 mg, 0.020 mmol, 0.1 equiv), DCE (0.8 mL, 0.25 M), DTBP (37  $\mu$ L, 0.20 mmol, 1 equiv), and TFA (11.5  $\mu$ L, 0.15 mmol, 0.75 equiv). Purification by preparative TLC (eluted with 19:1 hexanes/EtOAc) afforded **2.10** (20.7 mg, 58%) as a yellow oil. R<sub>f</sub>: 0.36 (19:1 hexanes/EtOAc). <sup>1</sup>H NMR (CDCl<sub>3</sub>, 500 MHz):  $\delta$  7.12 (d,  $J$  = 2.3 Hz, 1H), 6.93 (dd,  $J$  = 7.9, 2.2 Hz, 1H), 6.61 (d,  $J$  = 7.9 Hz, 1H), 4.69 (br s, 1H), 2.60 (q,  $J$  = 7.6 Hz, 3H), 1.44 (s, 9H), 1.24 (t,  $J$  = 7.6 Hz, 3H). <sup>13</sup>C NMR (CDCl<sub>3</sub>, 126 MHz):  $\delta$  152.2, 136.2, 135.9, 126.8, 126.0, 116.5, 34.6, 29.8, 28.4, 16.1. IR (ATR): 3515, 2960, 1651, 1461, 1362, 728 cm<sup>-1</sup>. HRMS (ESI<sup>-</sup>):  $m/z$  [M-H]<sup>-</sup> calculated for C<sub>12</sub>H<sub>17</sub>O: 177.1285; found: 177.1293.

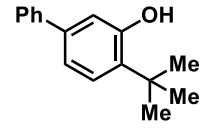
### 2,5-Di-*tert*-butylphenol (**2.11**)



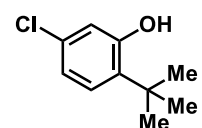
Prepared using General Procedure A with 3-*tert*-butylphenol (30.0 mg, 0.200 mmol, 1 equiv), FeCl<sub>3</sub> (3.2 mg, 0.020 mmol, 0.1 equiv), DCE (0.8 mL, 0.25 M), DTBP (37  $\mu$ L, 0.2 mmol, 1 equiv), and TFA (11.5  $\mu$ L, 0.15 mmol, 0.75 equiv). Purification by preparative TLC (eluted with 19:1 hexanes/EtOAc) afforded **2.11** (37.9 mg, 92%) as a light orange-white amorphous solid. R<sub>f</sub>: 0.44 (19:1 hexanes/EtOAc). Mp 103–106 °C. <sup>1</sup>H NMR (CDCl<sub>3</sub>, 600 MHz):  $\delta$  7.23 (d,  $J$  = 8.2 Hz, 1H), 6.92 (dd,  $J$  = 8.1, 2.0 Hz, 1H), 6.71 (d,  $J$  = 2.0 Hz, 1H), 4.80 (br s, 1H), 1.44 (s, 9H), 1.32 (s, 9H). <sup>13</sup>C NMR (CDCl<sub>3</sub>, 151 MHz):  $\delta$  153.8, 150.5, 133.1, 126.75, 117.5, 114.0, 34.2, 31.4, 29.8. IR (ATR): 3509, 2954, 1611, 1360, 700 cm<sup>-1</sup>. HRMS (ESI<sup>-</sup>):  $m/z$  [M-H]<sup>-</sup> calculated for C<sub>14</sub>H<sub>21</sub>O: 205.1598;

found: 205.1608. The site-selectivity is unambiguously confirmed by single crystal X-ray diffraction. Crystals were grown with a hexanes/EtOAc mixture.

### 3-*tert*-Butyl-5-phenylphenol (**2.12**)

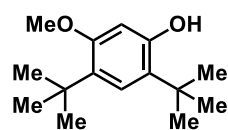
 Prepared using General Procedure A with 3-phenylphenol (34.0 mg, 0.200 mmol, 1 equiv), FeCl<sub>3</sub> (3.2 mg, 0.020 mmol, 0.1 equiv), DCE (0.8 mL, 0.25 M), DTBP (37 μL, 0.20 mmol, 1 equiv), and TFA (11.5 μL, 0.15 mmol, 0.75 equiv). Purification by preparative TLC (eluted with 19:1 hexanes/EtOAc) afforded **2.12** (33.0 mg, 73%) as a red amorphous solid. R<sub>f</sub>: 0.26 (19:1 hexanes/EtOAc). Mp 74–77 °C. <sup>1</sup>H NMR (CDCl<sub>3</sub>, 500 MHz): δ 7.62–7.53 (m, 2H), 7.44 (t, *J* = 7.7 Hz, 2H), 7.36 (dd, *J* = 7.8, 3.2 Hz, 2H), 7.14 (dd, *J* = 8.0, 1.9 Hz, 1H), 6.90 (d, *J* = 1.9 Hz, 1H), 4.96 (br s, 1H), 1.48 (s, 9H). <sup>13</sup>C NMR (CDCl<sub>3</sub>, 126 MHz): δ 154.5, 140.5, 140.4, 135.4, 128.8, 127.7, 127.4, 127.0, 119.4, 115.3, 34.54, 29.8. IR (ATR): 3531, 2953, 1614, 1447, 1360, 700 cm<sup>-1</sup>. HRMS (ESI<sup>-</sup>): *m/z* [M-H]<sup>-</sup> calculated for C<sub>16</sub>H<sub>17</sub>O: 225.1285; found: 225.1285.

### 2-*tert*-Butyl-5-chlorophenol (**2.13**)

 Prepared using General Procedure A with 3-chlorophenol (21.1 μL, 0.200 mmol, 1 equiv), FeCl<sub>3</sub> (3.2 mg, 0.020 mmol, 0.1 equiv), DCE (0.8 mL, 0.25 M), DTBP (37 μL, 0.20 mmol, 1 equiv), and TFA (11.5 μL, 0.15 mmol, 0.75 equiv). Purification by preparative TLC (3 × elutions with 49:1 hexanes/EtOAc) afforded **2.13** (15.1 mg, 41%) as a yellow oil. R<sub>f</sub>: 0.49 (9:1 hexanes/EtOAc). <sup>1</sup>H NMR (CDCl<sub>3</sub>, 500 MHz): δ 7.17 (d, *J* = 8.4 Hz, 1H), 6.84 (dd, *J* = 8.5, 2.2 Hz, 1H), 6.69 (d, *J* = 2.2 Hz, 1H), 5.02 (br s, 1H), 1.38 (s, 9H). <sup>13</sup>C NMR (CDCl<sub>3</sub>, 126 MHz): δ 154.9, 135.0, 131.9, 128.2,

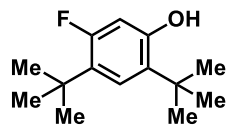
120.7, 116.7, 34.5, 29.6. IR (ATR): 3547, 2958, 1653, 1465, 1363, 704  $\text{cm}^{-1}$ . HRMS (ESI<sup>-</sup>):  $m/z$  [M-H]<sup>-</sup> calculated for C<sub>10</sub>H<sub>12</sub>ClO: 183.0582; found: 183.0584.

### 2,4-Di-*tert*-butyl-5-methoxyphenol (**2.14**)



Prepared using General Procedure A with 3-methoxyphenol (21.7  $\mu\text{L}$ , 0.200 mmol, 1 equiv), FeCl<sub>3</sub> (3.2 mg, 0.020 mmol, 0.1 equiv), DCE (0.8 mL, 0.25 M), DTBP (37  $\mu\text{L}$ , 0.20 mmol, 1 equiv), and TFA (11.5  $\mu\text{L}$ , 0.15 mmol, 0.75 equiv). Purification by preparative TLC (3 elutions with 4:1 hexanes/EtOAc) afforded **2.14** (42.5 mg, 90%) as an orange amorphous solid. R<sub>f</sub>: 0.39 (7:3 hexanes/EtOAc). Mp 95–98 °C. <sup>1</sup>H NMR (CDCl<sub>3</sub>, 500 MHz):  $\delta$  7.15 (s, 1H), 6.26 (s, 1H), 4.61 (br s, 1H), 3.78 (s, 3H), 1.39 (s, 9H), 1.34 (s, 9H). <sup>13</sup>C NMR (CDCl<sub>3</sub>, 126 MHz):  $\delta$  157.2, 152.7, 129.7, 126.6, 125.4, 101.5, 55.2, 34.6, 34.2, 30.2. IR (ATR): 3386, 2948, 1598, 1443, 1358, 724  $\text{cm}^{-1}$ . HRMS (ESI<sup>-</sup>):  $m/z$  [M-H]<sup>-</sup> calculated for C<sub>15</sub>H<sub>23</sub>O<sub>2</sub>: 235.1704; found: 235.1711.

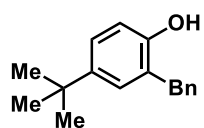
### 2,4-Di-*tert*-butyl-5-fluorophenol (**2.15**)



Prepared using General Procedure A with 3-methoxyphenol (21.7  $\mu\text{L}$ , 0.200 mmol, 1 equiv), FeCl<sub>3</sub> (3.2 mg, 0.020 mmol, 0.1 equiv), DCE (0.8 mL, 0.25 M), DTBP (37  $\mu\text{L}$ , 0.20 mmol, 1 equiv), and TFA (11.5  $\mu\text{L}$ , 0.15 mmol, 0.75 equiv). With no silica pipette filtration, direct purification by preparative TLC (eluted with 9:1 hexanes/EtOAc) afforded **2.15** (27.8 mg, 62%) as a colorless oil. R<sub>f</sub>: 0.44 (9:1 hexanes/EtOAc). <sup>1</sup>H NMR (CDCl<sub>3</sub>, 500 MHz):  $\delta$  7.15 (d,  $J$  = 9.7 Hz, 1H), 6.38 (d,  $J$  = 12.8 Hz, 1H), 4.79 (br s, 1H), 1.39 (s, 9H), 1.34 (s, 9H). <sup>13</sup>C NMR (CDCl<sub>3</sub>, 126 MHz):  $\delta$  161.0, 159.00, 152.9 (d,  $J$  = 10.3 Hz), 130.9, 128.1, 125.5 (d,  $J$  = 7.4 Hz), 105.0 (d,  $J$  = 27.0 Hz), 34.54, 34.0 (d,  $J$  = 3.0 Hz), 30.3 (d,  $J$  = 3.3 Hz), 29.9. <sup>19</sup>F NMR (CDCl<sub>3</sub>, 376 MHz): 114.2

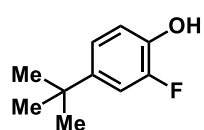
(t,  $J = 11.1$  Hz). IR (ATR): 3544, 2957, 1618, 1469, 1363, 717  $\text{cm}^{-1}$ . HRMS (ESI<sup>-</sup>):  $m/z$  [M-H]<sup>-</sup> calculated for C<sub>14</sub>H<sub>20</sub>FO: 223.1504; found: 223.1512.

#### 2-Benzyl-4-*tert*-butylphenol (2.16)



Prepared using General Procedure A with 2-benzylphenol (36.8 mg, 0.200 mmol, 1 equiv), FeCl<sub>3</sub> (6.5 mg, 0.040 mmol, 0.2 equiv), DCE (0.8 mL, 0.25 M), DTBP (37  $\mu\text{L}$ , 0.20 mmol, 1 equiv), and TFA (11.5  $\mu\text{L}$ , 0.15 mmol, 0.75 equiv) for 18 h. Purification by preparative TLC (eluted with 19:1 hexanes/EtOAc) afforded **2.16** (21.1 mg, 44%) as a yellow oil.  $R_f$ : 0.42 (19:1 hexanes/EtOAc). <sup>1</sup>H NMR (CDCl<sub>3</sub>, 500 MHz):  $\delta$  7.30 (t,  $J = 7.6$  Hz, 2H), 7.23 (d,  $J = 7.4$  Hz, 2H), 7.20 (d,  $J = 7.3$  Hz, 2H), 7.16–7.10 (m, 2H), 6.75–6.68 (m, 1H), 4.52 (br s, 1H), 4.00 (s, 1H), 1.28 (s, 9H). <sup>13</sup>C NMR (CDCl<sub>3</sub>, 126 MHz):  $\delta$  151.6, 143.8, 140.2, 128.74, 128.2, 126.4, 126.2, 124.7, 115.4, 37.0, 34.2, 31.7. IR (ATR): 3525, 3027, 2960, 1602, 1453, 1363, 728  $\text{cm}^{-1}$ . HRMS (ESI<sup>-</sup>):  $m/z$  [M-H]<sup>-</sup> calculated for C<sub>17</sub>H<sub>19</sub>O: 239.1441; found: 239.1447.

#### 4-*tert*-Butyl-2-fluorophenol (2.17)

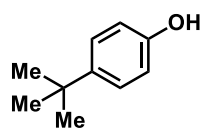


Prepared using General Procedure A with 2-fluorophenol (18.0  $\mu\text{L}$ , 0.200 mmol, 1 equiv), FeCl<sub>3</sub> (32.4 mg, 0.20 mmol, 1 equiv), DCE (0.8 mL, 0.25 M), DTBP (37  $\mu\text{L}$ , 0.20 mmol, 1 equiv), and TFA (11.5  $\mu\text{L}$ , 0.15 mmol, 0.75 equiv) for 48 h. Purified via preparative TLC (eluted with 9:1 hexanes/EtOAc) afforded **2.17** (8.7 mg, 26%) as a light-yellow oil.  $R_f$ : 0.56 (9:1 hexanes/EtOAc). <sup>1</sup>H NMR (CDCl<sub>3</sub>, 500 MHz):  $\delta$  7.12 (dd,  $J = 12.6, 2.4$  Hz, 1H), 7.06 (d,  $J = 7.2$  Hz, 1H), 6.95 (t,  $J = 9.6$ , 1H), 4.98 (br s, 1H), 1.31 (s, 9H). <sup>19</sup>F NMR (CDCl<sub>3</sub>, 564 MHz):  $\delta$  -141.2 (s). The spectral data recorded are consistent with those previously reported.<sup>6</sup>

### General Procedure B – Friedel–Crafts Alkylations with tertiary alcohols

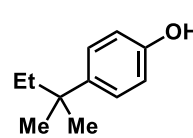
A one-dram vial was charged with a stirring bar and phenol derivative (0.2 mmol, 1 equiv) and brought into a glovebox. To the vial was added iron(III) chloride (0.005 mmol, 0.025 equiv) and DCE (0.8 mL, 0.25 M). The vial was closed with a septum screw-cap and removed from the glovebox and added sequentially in open air alcohol (0.22 mmol, 1.1 equiv) and conc aqueous HCl (37 %, 12.5  $\mu$ L, 0.15 mmol, 0.75 equiv), and heated at 50  $^{\circ}$ C for 24 h. The solution was filtered through a 5" pipette silica plug (approximately half-filled) and eluted with 1:1 hexanes/EtOAc. The solution was concentrated *in vacuo* before purification via preparative TLC (19:1 or 9:1 hexanes/EtOAc) to afford the desired product.

#### 4-*tert*-Butylphenol (2.40)

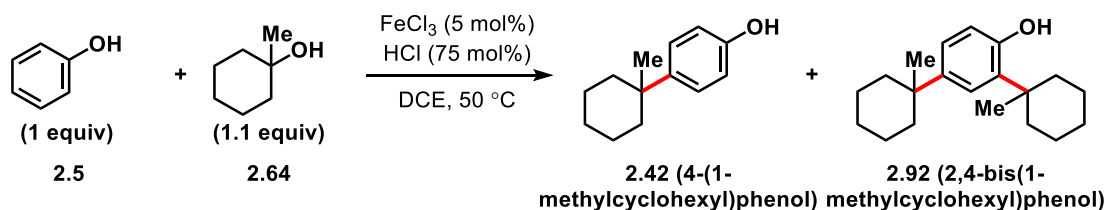


Prepared using General Procedure B with phenol (18.8 mg, 0.200 mmol, 1 equiv), FeCl<sub>3</sub> (0.8 mg, 0.005 mmol, 0.025 equiv), DCE (0.8 mL, 0.25 M), *tert*-butanol (21  $\mu$ L, 0.22 mmol, 1.1 equiv), and conc aqueous HCl (37%, 12.5  $\mu$ L, 0.15 mmol, 0.75 equiv). Purification by preparative TLC (eluted with 19:1 hexanes/EtOAc) afforded **2.40** (25.2 mg, 84%) as a light yellow-white amorphous solid.  $R_f$ : 0.12 (19:1 hexanes/EtOAc). Mp 90–92  $^{\circ}$ C.  $^1\text{H}$  NMR (CDCl<sub>3</sub>, 500 MHz):  $\delta$  7.26 (d,  $J$  = 7.6 Hz, 2H), 6.77 (d,  $J$  = 8.6 Hz, 2H), 4.54 (br s, 1H), 1.29 (s, 9H).  $^{13}\text{C}$  NMR (CDCl<sub>3</sub>, 126 MHz):  $\delta$  153.2, 143.7, 126.6, 114.9, 34.2, 31.7. IR (ATR): 3230, 2959, 1613, 1447, 1361, 722  $\text{cm}^{-1}$ . HRMS (ESI<sup>-</sup>):  $m/z$  [M-H]<sup>-</sup> calculated for C<sub>10</sub>H<sub>13</sub>O: 149.0972; found: 149.0978. The spectral data recorded are consistent with those previously reported.<sup>7</sup>

#### 4-*tert*-Amylphenol (**2.41**)

 Prepared using General Procedure B with phenol (18.8 mg, 0.200 mmol, 1 equiv), FeCl<sub>3</sub> (0.8 mg, 0.005 mmol, 0.025 equiv), DCE (0.8 mL, 0.25 M), 2-methyl-2-butanol (24 μL, 0.22 mmol, 1.1 equiv), and conc aqueous HCl (37%, 12.5 μL, 0.15 mmol, 0.75 equiv). Purification by preparative TLC (eluted with 19:1 hexanes/EtOAc) afforded **2.41** (27.9 mg, 85%) as a pale yellow-white amorphous solid. R<sub>f</sub>: 0.18 (19:1 hexanes/EtOAc). Mp 91–92 °C. <sup>1</sup>H NMR (CDCl<sub>3</sub>, 400 MHz): δ 7.27–7.07 (m, 2H), 6.85–6.67 (m, 2H), 4.84 (br s, 1H), 1.61 (q, *J* = 7.5 Hz, 2H), 1.26 (s, 9H), 0.68 (t, *J* = 7.5 Hz, 3H). <sup>13</sup>C NMR (CDCl<sub>3</sub>, 101 MHz): δ 153.1, 141.9, 127.3, 114.9, 37.4, 37.1, 28.7, 9.3. IR (ATR): 3251, 2963, 1599, 1448, 1375, 705 cm<sup>-1</sup>. HRMS (ESI<sup>-</sup>): *m/z* [M-H]<sup>-</sup> calculated for C<sub>11</sub>H<sub>15</sub>O: 163.1128; found: 163.1134.

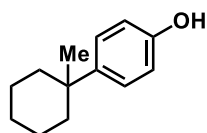
#### **2.42** and **2.92**



The reaction was performed following General Procedure B with phenol (18.8 mg, 0.200 mmol, 1 equiv), FeCl<sub>3</sub> (0.8 mg, 0.005 mmol, 0.025 equiv), DCE (0.8 mL, 0.25 M), 1-methylcyclohexanol (**2.64**, 25.1 mg, 0.22 mmol, 1.1 equiv), and conc aqueous HCl (37%, 12.5 μL, 0.15 mmol, 0.75 equiv). Purification by preparative TLC (eluted with 19:1hexanes/EtOAc) afforded **2.42** (28.2 mg, 74%) as a pale orange-white amorphous solid and **2,4-bis(1-methylcyclohexyl)phenol** (**2.92**, 10.0 mg, 17%) as an orange oil.

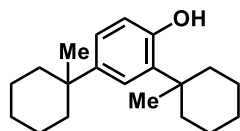


#### 4-(1-Methylcyclohexyl)phenol (**2.42**)



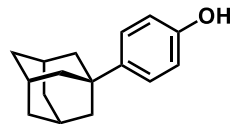
R<sub>f</sub>: 0.15 (19:1 hexanes/EtOAc). Mp 106–108 °C. <sup>1</sup>H NMR (CDCl<sub>3</sub>, 500 MHz): δ 7.24 (d, *J* = 8.2 Hz, 1H), 6.80 (d, *J* = 8.6 Hz, 1H), 4.81 (br s, 1H), 1.99–1.91 (m, 2H), 1.54 (dt, *J* = 7.6, 3.8 Hz, 4H), 1.47–1.36 (m, 4H), 1.16 (s, 3H). <sup>13</sup>C NMR (CDCl<sub>3</sub>, 126 MHz): δ 153.0, 142.5, 127.2, 115.1, 38.2, 37.4, 30.8, 26.5, 22.8. IR (ATR): 3228, 2927, 1598, 1444, 1370, 724 cm<sup>-1</sup>. HRMS (ESI<sup>-</sup>): *m/z* [M-H]<sup>-</sup> calculated for C<sub>13</sub>H<sub>17</sub>O: 189.1285; found: 189.1294.

#### 2,4-Bis(1-methylcyclohexyl)phenol (**2.92**)



R<sub>f</sub>: 0.38 (19:1 hexanes/EtOAc). <sup>1</sup>H NMR (CDCl<sub>3</sub>, 500 MHz): δ 7.30 (d, *J* = 2.4 Hz, 1H), 7.05 (dd, *J* = 8.2, 2.4 Hz, 1H), 6.61 (d, *J* = 8.2 Hz, 1H), 4.72 (br s, 1H), 2.22–2.15 (m, 2H), 1.97–1.90 (m, 2H), 1.73–1.37 (m, 16H), 1.34 (s, 3H), 1.18 (s, 3H). <sup>13</sup>C NMR (CDCl<sub>3</sub>, 126 MHz): δ 151.9, 142.0, 134.6, 125.9, 123.9, 116.5, 38.3, 37.5, 37.2, 26.8, 26.6, 23.0, 22.8. IR (ATR): 3529, 2922, 1605, 1447, 1374, 706 cm<sup>-1</sup>. HRMS (ESI<sup>-</sup>): *m/z* [M-H]<sup>-</sup> calculated for C<sub>20</sub>H<sub>29</sub>O: 285.2224; found: 285.2233.

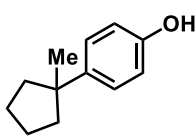
#### 4-(1-Adamantyl)phenol (**2.43**)



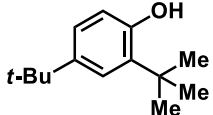
Prepared using General Procedure B with phenol (18.8 mg, 0.200 mmol, 1 equiv), FeCl<sub>3</sub> (0.8 mg, 0.005 mmol, 0.025 equiv), DCE (0.8 mL, 0.25 M), 1-adamantanol (33.5 mg, 0.22 mmol, 1.1 equiv), and conc aqueous HCl (37%, 12.5 μL, 0.15 mmol, 0.75 equiv). Purification by preparative TLC (eluted with 19:1 hexanes/EtOAc) afforded **2.43** (32.4 mg, 71%) as a white amorphous solid. R<sub>f</sub>: 0.18 (19:1 hexanes/EtOAc). Mp 176–179 °C. <sup>1</sup>H NMR (CDCl<sub>3</sub>, 400 MHz): δ 7.24 (dd, *J* = 9.2, 2.8

Hz, 2H), 6.80 (d,  $J = 8.6$  Hz, 2H), 4.84 (br s, 1H), 2.12–2.06 (m, 3H), 1.89 (d,  $J = 3.1$  Hz, 6H), 1.83–1.70 (m, 6H).  $^{13}\text{C}$  NMR ( $\text{CDCl}_3$ , 101 MHz):  $\delta$  153.3, 144.1, 126.2, 115.0, 43.5, 36.9, 35.7, 29.1. IR (ATR): 3248, 2900, 1597, 1446, 1367, 721  $\text{cm}^{-1}$ . HRMS (ESI $^-$ ):  $m/z$   $[\text{M}-\text{H}]^-$  calculated for  $\text{C}_{16}\text{H}_{19}\text{O}$ : 227.1441; found: 227.1448. The spectral data recorded are consistent with those previously reported.<sup>8</sup>

#### 4-(1-Methylcyclopentyl)phenol (**2.45**)

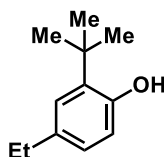
 Prepared using General Procedure B with phenol (18.8 mg, 0.20 mmol, 1 equiv),  $\text{FeCl}_3$  (0.8 mg, 0.005 mmol, 0.025 equiv), DCE (0.8 mL, 0.25 M), 1-methylcyclopentanol (22.0 mg, 0.22 mmol, 1.1 equiv), and conc aqueous HCl (37%, 12.5  $\mu\text{L}$ , 0.15 mmol, 0.75 equiv). Purification by preparative TLC (eluted with 19:1 hexanes/EtOAc) afforded a 1:3 mixture of **2.45**/phenol (22.6 mg, 23% yield of **2.45**) as a yellow oil.  $^1\text{H}$  NMR ( $\text{CDCl}_3$ , 500 MHz): 7.20 (d,  $J = 8.5$  Hz, 2H), 6.77 (d,  $J = 8.5$  Hz, 2H), 5.01 (br s, 1H), 4.93 (br s, 1H), 1.91–1.63 (m, 8H), 1.22 (s, 3H).  $^{13}\text{C}$  NMR ( $\text{CDCl}_3$ , 126 MHz):  $\delta$  153.2, 143.9, 127.3, 114.9, 40.0, 38.9, 29.7, 23.8; PhOH 155.7, 129.8, 120.8, 115.5.

#### 2,4-Di-*tert*-butylphenol (**2.7**)

 Prepared using General Procedure B with 4-*tert*-butylphenol (34.0 mg, 0.200 mmol, 1 equiv),  $\text{FeCl}_3$  (0.8 mg, 0.005 mmol, 0.025 equiv), DCE (0.8 mL, 0.25 M), *tert*-butanol (21  $\mu\text{L}$ , 0.22 mmol, 1.1 equiv), and conc aqueous HCl (37%, 12.5  $\mu\text{L}$ , 0.15 mmol, 0.75 equiv). Purification by preparative TLC (eluted with 19:1 hexanes/EtOAc) afforded **2.7** (35.1 mg, 85%) as a light-orange amorphous solid.  $^1\text{H}$  NMR ( $\text{CDCl}_3$ , 500 MHz):  $\delta$  7.30 (d,  $J = 2.4$  Hz, 1H), 7.08 (dd,  $J = 8.2, 2.4$  Hz, 1H), 6.60 (d,  $J =$

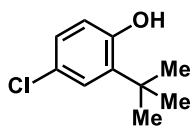
8.2 Hz, 1H), 4.63 (s, 1H), 1.42 (s, 9H), 1.29 (s, 9H). HRMS (ESI<sup>-</sup>):  $m/z$  [M-H]<sup>-</sup> calculated for C<sub>14</sub>H<sub>21</sub>O: 206.1671; found: 206.1680. The spectral data recorded are consistent with those previously reported.<sup>4</sup>

### 2-*tert*-Butyl-4-ethylphenol (**2.46**)



Prepared using General Procedure B with 4-ethylphenol (24.4 mg, 0.200 mmol, 1 equiv), FeCl<sub>3</sub> (0.3 mg, 0.002 mmol, 0.01 equiv), DCE (0.8 mL, 0.25 M), *tert*-butanol (21 μL, 0.22 mmol, 1.1 equiv), and conc aqueous HCl (37%, 12.5 μL, 0.15 mmol, 0.75 equiv). Purification by preparative TLC (eluted with 19:1 hexanes/EtOAc) afforded **2.46** (20.7 mg, 58%) as an orange oil. R<sub>f</sub>: 0.28 (19:1 hexanes/EtOAc). <sup>1</sup>H NMR (CDCl<sub>3</sub>, 500 MHz): δ 7.12 (d,  $J$  = 2.2 Hz, 1H), 6.93 (dd,  $J$  = 7.9, 2.2 Hz, 1H), 6.61 (d,  $J$  = 7.8 Hz, 1H), 4.70 (br s, 1H), 2.60 (q,  $J$  = 7.6 Hz, 2H), 1.44 (s, 9H), 1.24 (t,  $J$  = 7.6 Hz, 3H). <sup>13</sup>C NMR (CDCl<sub>3</sub>, 151 MHz): δ 152.3, 136.1, 135.9, 126.8, 126.0, 116.5, 34.6, 29.8, 28.4, 16.1. IR (ATR): 3528 (br.), 2960, 1608, 1460, 1362, 688 cm<sup>-1</sup>. HRMS (ESI<sup>-</sup>):  $m/z$  [M-H]<sup>-</sup> calculated for C<sub>12</sub>H<sub>17</sub>O: 178.1285; found: 177.1292.

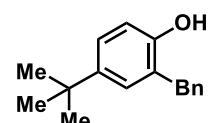
### 2-*tert*-Butyl-4-chlorophenol (**2.8**)



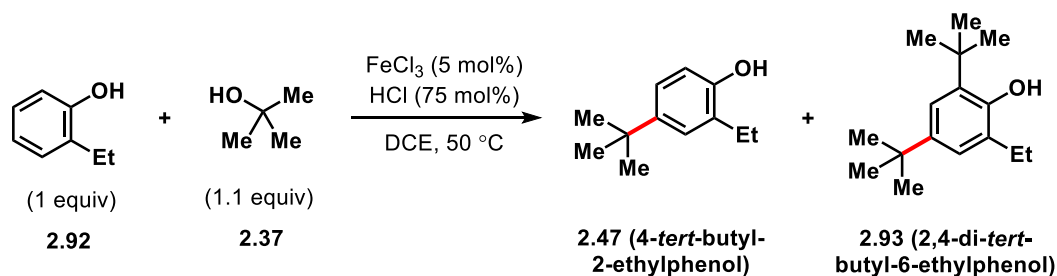
Prepared using General Procedure B with 4-chlorophenol (25.7 mg, 0.200 mmol, 1 equiv), FeCl<sub>3</sub> (32.4 mg, 0.2 mmol, 1 equiv), DCE (0.8 mL, 0.25 M), *tert*-butanol (21 μL, 0.22 mmol, 1.1 equiv), and conc aqueous HCl (37%, 12.5 μL, 0.15 mmol, 0.75 equiv). Purification by preparative TLC (eluted with 19:1 hexanes/EtOAc) afforded **2.8** (18.8 mg, 51%) as a pale-yellow oil. R<sub>f</sub>: 0.23 (19:1 hexanes/EtOAc). <sup>1</sup>H NMR (CDCl<sub>3</sub>, 600 MHz): δ 7.21 (d,  $J$  = 3.0 Hz, 1H), 7.02 (dd,  $J$  = 8.4, 2.4, 1H), 6.60 (d,  $J$  = 8.4 Hz, 1H), 4.77 (br s, 1H), 1.38 (s, 9H). <sup>13</sup>C NMR (CDCl<sub>3</sub>, 101 MHz): δ 152.9, 138.2, 127.5,

126.7, 125.58, 117.7, 34.9, 29.5. HRMS (ESI<sup>-</sup>):  $m/z$   $[M-H]^-$  calculated for C<sub>10</sub>H<sub>12</sub>ClO: 183.0582; found: 183.0590. The spectral data recorded are consistent with those previously reported.<sup>5</sup>

#### 4-*tert*-Butyl-2-benzylphenol (**2.16**)

 Prepared using General Procedure B with 2-benzylphenol (36.8 mg, 0.200 mmol, 1 equiv), FeCl<sub>3</sub> (0.8 mg, 0.005 mmol, 0.025 equiv), DCE (0.8 mL, 0.25 M), *tert*-butanol (21 μL, 0.22 mmol, 1.1 equiv), and conc aqueous HCl (37%, 12.5 μL, 0.15 mmol, 0.75 equiv). Purification by preparative TLC (eluted with 19:1 hexanes/EtOAc) afforded **2.16** (29.8 mg, 62%) as an orange oil. R<sub>f</sub>: 0.34 (19:1 hexanes/EtOAc). <sup>1</sup>H NMR (500 MHz, CDCl<sub>3</sub>) δ 7.33–7.26 (m, 2H), 7.23 (d, *J* = 7.4 Hz, 2H), 7.20 (d, *J* = 7.3 Hz, 1H), 7.17–7.11 (m, 2H), 4.52 (s, 1H), 4.00 (s, 2H), 1.28 (s, 9H). <sup>13</sup>C NMR (101 MHz, CDCl<sub>3</sub>) δ 151.6, 143.8, 140.2, 128.7, 128.2, 126.4, 126.2, 124.7, 115.4, 37.0, 34.2, 31.7. IR (ATR): 3425 (br.), 2960, 1602, 1452, 1363, 697 cm<sup>-1</sup>. HRMS (ESI<sup>-</sup>):  $m/z$   $[M-H]^-$  calculated for C<sub>17</sub>H<sub>19</sub>O: 239.1441; found: 239.1447.

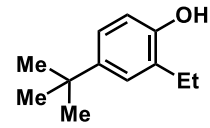
#### 2.47 and 2.93



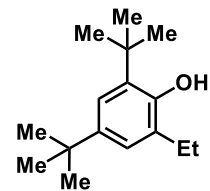
The reaction was performed following General Procedure B with 2-ethylphenol (23.6 μL, 0.200 mmol, 1 equiv), FeCl<sub>3</sub> (1.6 mg, 0.010 mmol, 0.05 equiv), DCE (0.8 mL, 0.25 M), *tert*-butanol (**2.37**, 21 μL, 0.22 mmol, 1.1 equiv), and conc aqueous HCl (37%, 12.5 μL,

0.15 mmol, 0.75 equiv). Purification by preparative TLC (eluted with 19:1 hexanes/EtOAc) afforded **2.47** in 31.1 mg (30.7 mg, 86%) as a light yellow oil and **2,4-di-tert-butyl-6-ethylphenol (2.93)** in 3.1 mg (1.4 mg, 3%) as a yellow oil.

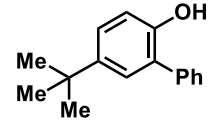
#### 4-tert-Butyl-2-ethylphenol (**2.47**)

 R<sub>f</sub>: 0.28 (19:1 hexanes/EtOAc). <sup>1</sup>H NMR (CDCl<sub>3</sub>, 600 MHz): δ 7.16 (d, *J* = 2.5 Hz, 1H), 7.10 (dd, *J* = 8.3 2.5 Hz, 1H), 6.71 (d, *J* = 8.4 Hz, 1H), 4.63 (br s, 1H), 2.65 (q, *J* = 7.6 Hz, 2H), 1.31 (s, 9H), 1.26 (t, 7.6 Hz, 3H). <sup>13</sup>C NMR (CDCl<sub>3</sub>, 151 MHz): δ 151.1, 143.7, 129.3, 126.5, 123.8, 114.8, 34.2, 31.9, 31.8, 31.7, 23.5, 14.4. IR (ATR): 3397, 2962, 1610, 1462, 1363, 752 cm<sup>-1</sup>. HRMS (ESI<sup>-</sup>): *m/z* [M-H]<sup>-</sup> calculated for C<sub>12</sub>H<sub>17</sub>O: 177.1285; found: 177.1292.

#### 2,4-Di-tert-butyl-6-ethylphenol (**2.93**)

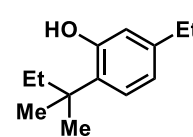
 R<sub>f</sub>: 0.49 (19:1 hexanes/EtOAc). <sup>1</sup>H NMR (CDCl<sub>3</sub>, 600 MHz): δ 7.20 (d, *J* = 2.5 Hz, 1H), 7.04 (d, *J* = 2.4 Hz, 1H), 4.28 (br s, 1H), 2.61 (q, *J* = 7.5 Hz, 2H), 1.44 (s, 9H), 1.31 (s, 9H), 1.29 (t, *J* = 7.7 Hz, 3H). <sup>13</sup>C NMR (CDCl<sub>3</sub>, 151 MHz): 150.0, 142.4, 135.0, 128.4, 123.6, 122.1, 34.9, 34.5, 31.8, 30.1, 23.5, 14.1. IR (ATR): 2956, 1653, 1457, 1445, 1361, 721 cm<sup>-1</sup>. HRMS (ESI<sup>-</sup>): *m/z* [M-H]<sup>-</sup> calculated for C<sub>26</sub>H<sub>25</sub>O: 233.1911; found: 234.1918.

#### 4-tert-Butyl-2-phenylphenol (**2.48**)

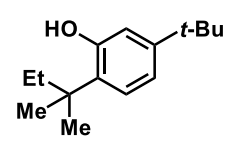
 Prepared using General Procedure B with 2-phenylphenol (34.0 mg, 0.200 mmol, 1 equiv), FeCl<sub>3</sub> (3.2 mg, 0.02 mmol, 0.1 equiv), DCE (0.8 mL, 0.25 M), *tert*-butanol (21 μL, 0.22 mmol, 1.1 equiv), and conc aqueous HCl (37%, 12.5 μL, 0.15 mmol, 0.75 equiv). Purification by preparative TLC (eluted with 97:3

hexanes/EtOAc  $\times$  4) afforded **2.48** (15.0 mg, 44%) as an orange oil. R<sub>f</sub>: 0.14 (97:3 hexanes/EtOAc). <sup>1</sup>H NMR (500 MHz, CDCl<sub>3</sub>)  $\delta$  7.53–7.46 (m, 4H), 7.43–7.38 (m, 1H), 7.30 (dd,  $J$  = 8.5, 2.4 Hz, 1H), 7.25 (d,  $J$  = 2.5 Hz, 1H), 6.93 (d,  $J$  = 8.5 Hz, 1H), 5.08 (s, 1H), 1.33 (s, 9H). <sup>13</sup>C NMR (126 MHz, CDCl<sub>3</sub>)  $\delta$  150.2, 143.7, 137.8, 129.4, 129.3, 127.9, 127.5, 127.3, 126.2, 115.4, 34.3, 31.7. IR (ATR): 3415 (br.), 2956, 1600, 1463, 1363, 699 cm<sup>-1</sup>. HRMS (ESI<sup>-</sup>):  $m/z$  [M-H]<sup>-</sup> calculated for C<sub>16</sub>H<sub>17</sub>O: 225.1285; found: 225.1292.

### 2-*tert*-Amyl-5-ethylphenol (**2.49**)

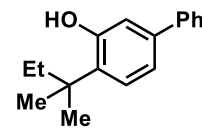
 Prepared using General Procedure B with 3-ethylphenol (24.4  $\mu$ L, 0.200 mmol, 1 equiv), FeCl<sub>3</sub> (1.6 mg, 0.010 mmol, 0.05 equiv), DCE (0.8 mL, 0.25 M), 2-methyl-2-butanol (24  $\mu$ L, 0.22 mmol, 1.1 equiv), and conc aqueous HCl (37%, 12.5  $\mu$ L, 0.15 mmol, 0.75 equiv). Purification by preparative TLC (eluted with 19:1 hexanes/EtOAc) afforded **2.49** (25.8 mg, 67%) as a yellow oil. R<sub>f</sub>: 0.45 (19:1 hexanes/EtOAc). <sup>1</sup>H NMR (CDCl<sub>3</sub>, 600 MHz):  $\delta$  7.13 (d,  $J$  = 7.9 Hz, 1H), 6.73 (dd,  $J$  = 7.9, 1.8 Hz, 1H), 6.51 (d,  $J$  = 1.8 Hz, 1H), 4.76 (br s, 1H), 2.59 (d,  $J$  = 7.6 Hz, 2H), 1.86 (q,  $J$  = 7.5 Hz, 2H), 1.37 (s, 6H), 1.23 (t,  $J$  = 7.6 Hz, 3H), 0.70 (t,  $J$  = 7.5 Hz, 3H). <sup>13</sup>C NMR (CDCl<sub>3</sub>, 151 MHz):  $\delta$  154.1, 143.3, 131.6, 128.4, 120.0, 116.1, 37.9, 33.5, 28.1, 27.9, 15.3, 9.7. IR (ATR): 3530, 2963, 1617, 1460, 1362, 727 cm<sup>-1</sup>. HRMS (ESI<sup>-</sup>):  $m/z$  [M-H]<sup>-</sup> calculated for C<sub>13</sub>H<sub>19</sub>O: 191.1441; found: 191.1450.

### 2-*tert*-Amyl-5-*tert*-butylphenol (**2.39**)

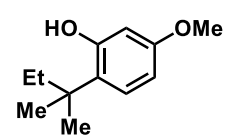
 Prepared using General Procedure B with 3-*tert*-butylphenol (30.0 mg, 0.200 mmol, 1 equiv), FeCl<sub>3</sub> (1.6 mg, 0.010 mmol, 0.05 equiv), DCE (0.8 mL, 0.25 M), 2-methyl-2-butanol (24  $\mu$ L, 0.22 mmol, 1.1 equiv), and conc aqueous

HCl (37%, 12.5  $\mu$ L, 0.15 mmol, 0.75 equiv). Purification by preparative TLC (eluted with 19:1 hexanes/EtOAc) afforded **2.39** (36.6 mg, 83%) as a yellow-white amorphous solid.  $R_f$ : 0.42 (19:1 hexanes/EtOAc). Mp 56–57  $^{\circ}$ C.  $^1\text{H}$  NMR ( $\text{CDCl}_3$ , 600 MHz):  $\delta$  7.15 (d,  $J$  = 8.2 Hz, 1H), 6.90 (dd,  $J$  = 8.2, 2.1 Hz, 1H), 6.68 (d,  $J$  = 2.1 Hz, 1H), 4.76 (br s, 1H), 1.87 (q,  $J$  = 7.5 Hz, 2H), 1.38 (s, 6H), 1.31 (s, 9H), 0.71 (t,  $J$  = 7.5 Hz, 3H).  $^{13}\text{C}$  NMR ( $\text{CDCl}_3$ , 151 MHz):  $\delta$  153.8, 150.4, 131.4, 128.0, 117.4, 113.9, 37.8, 34.2, 33.5, 31.4, 27.8, 9.7. IR (ATR): 3473 (br.), 2961, 1608, 1460, 1361, 706  $\text{cm}^{-1}$ . HRMS (ESI $^-$ ):  $m/z$   $[\text{M}-\text{H}]^-$  calculated for  $\text{C}_{15}\text{H}_{23}\text{O}$ : 219.1754; found: 219.1764.

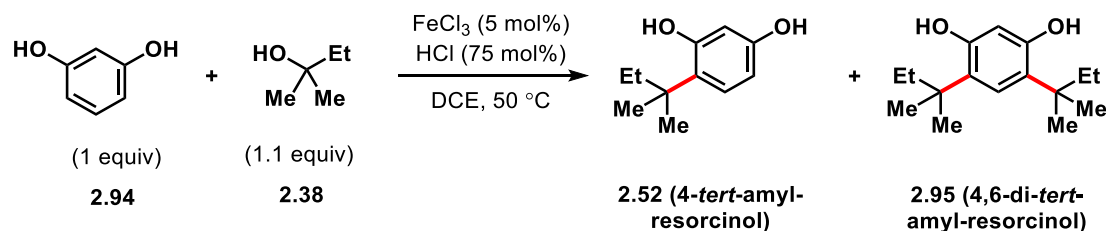
### 2-*tert*-Amyl-5-phenylphenol (**2.50**)

 Prepared using General Procedure B with 3-phenylphenol (34.0 mg, 0.200 mmol, 1 equiv),  $\text{FeCl}_3$  (1.6 mg, 0.010 mmol, 0.05 equiv), DCE (0.8 mL, 0.25 M), 2-methyl-2-butanol (24  $\mu$ L, 0.22 mmol, 1.1 equiv), and conc aqueous HCl (37%, 12.5  $\mu$ L, 0.15 mmol, 0.75 equiv). Purification by preparative TLC (eluted with 19:1 hexanes/EtOAc) afforded **2.50** (34.6 mg, 72%) as an orange-white amorphous solid.  $R_f$ : 0.29 (19:1 hexanes/EtOAc). Mp 63–65  $^{\circ}$ C.  $^1\text{H}$  NMR ( $\text{CDCl}_3$ , 600 MHz):  $\delta$  7.59 (dd,  $J$  = 8.1, 1.4 Hz, 2H), 7.44 (t,  $J$  = 7.6 Hz, 2H), 7.38–7.34 (m, 1H), 7.31 (d,  $J$  = 8.0 Hz, 1H), 7.15 (dd,  $J$  = 8.1, 1.9 Hz, 1H), 6.89 (d,  $J$  = 1.9 Hz, 1H), 4.91 (br s, 1H), 1.93 (d,  $J$  = 7.5 Hz, 2H), 1.44 (s, 6H), 0.75 (t,  $J$  = 7.5 Hz, 3H).  $^{13}\text{C}$  NMR ( $\text{CDCl}_3$ , 151 MHz):  $\delta$  154.5, 140.5, 140.2, 133.7, 129.0, 128.8, 127.3, 127.0, 119.3, 115.1, 38.2, 33.4, 27.8, 9.7. IR (ATR): 3541 (br.), 2960, 1601, 1461, 1360, 721  $\text{cm}^{-1}$ . HRMS (ESI $^-$ ):  $m/z$   $[\text{M}-\text{H}]^-$  calculated for  $\text{C}_{17}\text{H}_{19}\text{O}$ : 239.1441; found: 239.1450.

### 2-*tert*-Amyl-5-methoxyphenol (**2.51**)

 Prepared using General Procedure B with 3-methoxyphenol (24.8 mg, 0.200 mmol, 1 equiv), FeCl<sub>3</sub> (0.8 mg, 0.005 mmol, 0.025 equiv), DCE (0.8 mL, 0.25 M), 2-methyl-2-butanol (24 μL, 0.22 mmol, 1.1 equiv), and conc aqueous HCl (37%, 12.5 μL, 0.15 mmol, 0.75 equiv). Purification by preparative TLC (eluted with 19:1 hexanes/EtOAc) afforded **2.51** (14.4 mg, 37%) as an orange-peach amorphous solid. R<sub>f</sub>: 0.29 (9:1 hexanes/EtOAc). Mp 33–34 °C. <sup>1</sup>H NMR (CDCl<sub>3</sub>, 400 MHz): δ 7.10 (d, *J* = 8.6 Hz, 1H), 6.43 (dd, *J* = 8.6, 2.6 Hz, 1H), 6.26 (d, *J* = 2.6 Hz, 1H), 4.84 (br s, 1H), 3.76 (s, 3H), 1.82 (q, *J* = 7.5 Hz, 2H), 1.31 (s, 6H), 0.67 (t, *J* = 7.5 Hz, 3H). <sup>13</sup>C NMR (CDCl<sub>3</sub>, 151 MHz): δ 158.7, 155.1, 129.1, 127.0, 105.0, 103.1, 55.4, 37.7, 33.6, 29.9, 28.1, 9.7. IR (ATR): 3411, 2960, 1613, 1416, 1376, 737 cm<sup>-1</sup>. HRMS (ESI<sup>-</sup>): *m/z* [M-H]<sup>-</sup> calculated for C<sub>12</sub>H<sub>17</sub>O<sub>2</sub>: 193.1234; found: 193.1241.

### **2.52** and **2.95**

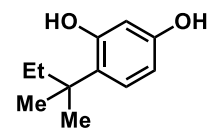


The reaction was performed following General Procedure B with resorcinol (22.0 mg, 0.200 mmol, 1 equiv), FeCl<sub>3</sub> (1.6 mg, 0.010 mmol, 0.05 equiv), DCE (0.8 mL, 0.25 M), 2-methyl-2-butanol (**2.38**, 24 μL, 0.22 mmol, 1.1 equiv), and conc aqueous HCl (37%, 12.5 μL, 0.15 mmol, 0.75 equiv). Purification by preparative TLC (eluted with 19:1

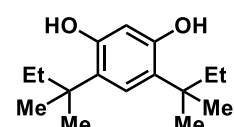


hexanes/EtOAc) afforded **2.52** (22.2 mg, 62%) as an orange oil and **4,6-di-tert-amyl-resorcinol (2.95)**, 10.9 mg, 22%) as a colorless oil.

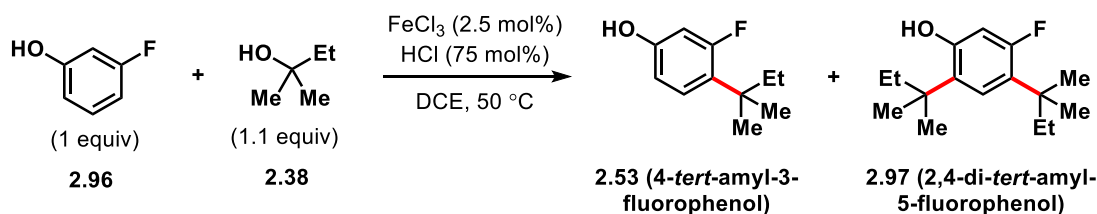
#### 4-tert-Amyl-resorcinol (**2.52**)

 R<sub>f</sub>: 0.39 (7:3 hexanes/EtOAc). <sup>1</sup>H NMR (CDCl<sub>3</sub>, 600 MHz): δ 7.03 (d, *J* = 8.5 Hz, 1H), 6.35 (dd, *J* = 8.5, 2.6 Hz, 1H), 6.23 (d, *J* = 2.6 Hz, 1H), 5.20 (br s, 1H), 1.80 (q, *J* = 7.5 Hz, 2H), 1.32 (s, 6H), 0.65 (t, *J* = 7.5 Hz, 3H). <sup>13</sup>C NMR (CDCl<sub>3</sub>, 151 MHz): δ 155.3, 154.4, 129.3, 127.2, 107.1, 104.1, 37.7, 33.5, 28.0, 9.6. IR (ATR): 3365, 2963, 1600, 1439, 1374, 704 cm<sup>-1</sup>. HRMS (ESI<sup>-</sup>): *m/z* [M-H]<sup>-</sup> calculated for C<sub>11</sub>H<sub>15</sub>O<sub>2</sub>: 179.1078; found: 179.1082.

#### 4,6-Di-tert-amyl-resorcinol (**2.95**)

 R<sub>f</sub>: 0.37 (7:3 hexanes/EtOAc). <sup>1</sup>H NMR (CDCl<sub>3</sub>, 600 MHz): δ 6.98 (s, 1H), 6.05 (s, 1H), 4.57 (s, 1H), 1.78 (q, *J* = 7.5 Hz, 4H), 1.33 (s, 12H), 0.66 (t, *J* = 7.5 Hz, 6H). <sup>13</sup>C NMR (CDCl<sub>3</sub>, 151 MHz): δ 152.6, 128.4, 125.6, 105.4, 37.8, 33.9, 28.1, 9.6. IR (ATR): 3523, 3354, 2959, 1611, 1403, 1376, 703 cm<sup>-1</sup>. HRMS (ESI<sup>-</sup>): *m/z* [M-H]<sup>-</sup> calculated for C<sub>16</sub>H<sub>25</sub>O<sub>2</sub>: 249.1860; found: 249.1865.

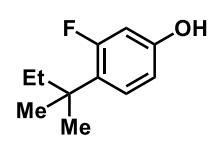
#### 2.53 and 2.97



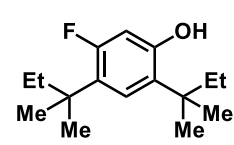
The reaction was performed following General Procedure B with 3-fluorophenol (18.1 μL, 0.200 mmol, 1 equiv), FeCl<sub>3</sub> (0.8 mg, 0.005 mmol, 0.025 equiv), DCE (0.8 mL, 0.25 M), 2-methyl-2-butanol (**2.38**, 24 μL, 0.22 mmol, 1.1 equiv), and conc aqueous HCl (37%, 12.5

$\mu\text{L}$ , 0.15 mmol, 0.75 equiv). Purification by preparative TLC (eluted with 19:1 hexanes/EtOAc) afforded **2.53** (19.3 mg, 53%) as a white amorphous solid and **2,4-di-tert-amyl-5-fluorophenol (2.97)**, 8.1 mg, 16%) as a colorless oil.

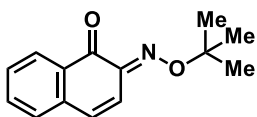
#### 4-tert-Amyl-3-fluorophenol (2.53)


 $R_f$ : 0.26 (9:1 hexanes/EtOAc). Mp 72–74 °C.  $^1\text{H}$  NMR ( $\text{CDCl}_3$ , 500 MHz):  $\delta$  7.07 (t,  $J = 9.1$  Hz, 1H), 6.59–6.46 (m, 2H), 4.72 (br s, 1H), 1.76–1.67 (m, 2H), 1.29 (s, 6H), 0.66 (t,  $J = 7.5$  Hz, 3H).  $^{13}\text{C}$  NMR ( $\text{CDCl}_3$ , 126 MHz):  $\delta$  163.2, 161.2, 154.8 (d,  $J = 12.0$  Hz), 129.1 (d,  $J = 8.1$  Hz), 110.4 (d,  $J = 3.0$  Hz), 104.1 (d,  $J = 27.9$  Hz), 37.5 (d,  $J = 3.4$  Hz), 34.4 (d,  $J = 4.1$  Hz), 28.0 (d,  $J = 2.9$  Hz), 9.5.  $^{19}\text{F}$  NMR ( $\text{CDCl}_3$ , 564 MHz):  $\delta$  107.6 (t,  $J = 12.1$  Hz). IR (ATR): 3256, 2966, 1623, 1444, 1377, 738  $\text{cm}^{-1}$ . HRMS (ESI $^-$ ):  $m/z$   $[\text{M}-\text{H}]^-$  calculated for  $\text{C}_{11}\text{H}_{14}\text{FO}$ : 181.1034; found: 181.1040.

#### 2,4-Di-tert-amyl-5-fluorophenol (2.97)


 $R_f$ : 0.44 (9:1 hexanes/EtOAc).  $^1\text{H}$  NMR ( $\text{CDCl}_3$ , 500 MHz):  $\delta$  7.01 (d,  $J = 9.6$  Hz, 1H), 6.34 (d,  $J = 12.9$  Hz, 1H), 4.76 (br s, 1H), 1.80 (q,  $J = 7.5$  Hz, 2H), 1.70 (q,  $J = 7.5$  Hz, 2H), 1.34 (s, 6H), 1.30 (s, 6H), 0.66 (q,  $J = 7.5$  Hz, 6H).  $^{13}\text{C}$  NMR ( $\text{CDCl}_3$ , 126 MHz):  $\delta$  158.9, 152.8 (d,  $J = 10.2$  Hz), 129.0, 128.1 (d,  $J = 7.6$  Hz), 126.2, 104.8 (d,  $J = 27.2$  Hz), 38.1, 37.6 (d,  $J = 3.5$  Hz), 34.7 (d,  $J = 3.7$  Hz), 33.5, 28.1 (d,  $J = 3.0$  Hz), 28.0, 9.5 (d,  $J = 10.2$  Hz).  $^{19}\text{F}$  NMR ( $\text{CDCl}_3$ , 564 MHz):  $\delta$  114.3 (t,  $J = 11.3$  Hz). IR (ATR): 3262, 1617, 1590, 1462, 1377, 703  $\text{cm}^{-1}$ . HRMS (ESI $^-$ ):  $m/z$   $[\text{M}-\text{H}]^-$  calculated for  $\text{C}_{16}\text{H}_{24}\text{FO}$ : 251.1817; found: 251.1824.

**(E)-2-(tert-Butoxyimino)naphthalen-1(2H)-one (2.89)**



Prepared using General Procedure B with 2-nitroso-1-naphthol (34.7 mg, 0.201 mmol, 1 equiv), FeCl<sub>3</sub> (3.4 mg, 0.021 mmol, 0.10 equiv), DCE (0.8 mL, 0.25 M), *tert*-butanol (21 μL, 0.22 mmol, 1.1 equiv), and conc aqueous HCl (37%, 12.5 μL, 0.15 mmol, 0.75 equiv). Purification by preparative TLC (eluted with 4:1 hexanes/EtOAc × 2) afforded **2.89** (8.2 mg, 18%) as a bright yellow oil. R<sub>f</sub>: 0.50 (17:3 hexanes/EtOAc). <sup>1</sup>H NMR (CDCl<sub>3</sub>, 500 MHz): δ = 8.20 (d, *J* = 7.8 Hz, 1H), 7.56 (t, *J* = 7.4 Hz, 1H), 7.41 (t, *J* = 7.6 Hz, 1H), 7.30 (d, *J* = 7.7 Hz, 1H), 7.10 (d, *J* = 10.1 Hz, 1H), 6.81 (d, *J* = 10.0 Hz, 1H), 1.45 (s, 9H). <sup>13</sup>C NMR (CDCl<sub>3</sub>, 151 MHz): δ = 182.1, 147.2, 136.7, 134.3, 132.1, 130.7, 129.0, 128.5, 128.2, 117.1, 83.5, 27.8. IR (ATR): 2977, 1672, 1613, 1592, 1450, 964, 680 cm<sup>-1</sup>. HRMS (ESI): *m/z* [M+H]<sup>+</sup> calculated for C<sub>14</sub>H<sub>16</sub>NO<sub>2</sub>: 230.1176; found: 230.1174.

2.6.3 References

1. (a) Gottlieb, H. E.; Kotlyar, V.; Nudelman, A. *J. Org. Chem.* **1997**, *62*, 7512–7515; (b) G. R. Fulmer, A. J. M. Miller, N. H. Sherden, H. E. Gottlieb, A. Nudelman, B. M. Stoltz, J. E. Bercaw, K. I. Goldberg, *Organometallics* **2010**, *29*, 2176–2179.
2. CYLview, 1.0b, Legault, C. Y.; Université de Sherbrooke, 2009 (<http://www.cylview.org>)
3. Farrugia, L. J. *J. Appl. Cryst.* **2012**, *45*, 849–854.
4. (a) Rolff, M.; Schottenheim, J.; Peters, G.; Tuzcek, F. *Angew. Chem. Int. Ed.* **2010**, *49*, 6438–6442; *Angew. Chem.* **2010**, *122*, 6583–6587. (b) Kalaichelvan, S.; Sundaraganesan, N.; Dereli, O.; Sayin, U. *Spectrochim. Acta A* **2012**, *85*, 198–209.
5. Nemoto, H.; Nishiyama, T. Akai, S. *Org. Lett.* **2011**, *13*, 2714–2717.

6. Nizovtsev, A.V.; Scheurer, A.; Kosog, B.; Heinemann, F. W.; Meyer, K. *Eur. J. Inorg. Chem.* **2013**, *14*, 2538–2548.
7. H.-L. Qi, D.-S. Chen, J.-S. Ye, J.-M. Huang, *J. Org. Chem.* **2013**, *78*, 7482–7487.

## Chapter 3 – Direct Phenolic Alkylation of Unactivated Secondary Alcohols by Dual Zinc/CSA-Catalyzed Friedel–Crafts Reactions

### 3.1.1 Friedel–Crafts alkylations with secondary benzyl/acyl alcohols or silyl ethers

Chapter 2 discussed the fundamental Friedel–Crafts reaction,<sup>1</sup> as well as examples in forming new all-carbon quaternary centers. In this chapter, the focus will be on Friedel–Crafts alkylations with unactivated secondary alcohols.

Secondary alkyl alcohols can be activated by associating the oxygen to a functional group that increases its ability as a leaving group. One example is converting the alcohol into an ester by acylation, as described in 2005 by Beller and coworkers.<sup>2</sup> Benzylic acetates undergo Friedel–Crafts alkylations when treated with catalytic iron(III) chloride and an excess amount of electron-rich or neutral arene (**Figure 3.1**). In some instances, the secondary benzylic alcohol was also able to react with similar yields (**Figure 3.2**). Although yields for most examples were excellent, a large excess of nucleophilic arene, sometimes in solvent quantities, was required. Overall, this reaction tolerated a variety of functional groups, which can be further derivatized if needed.

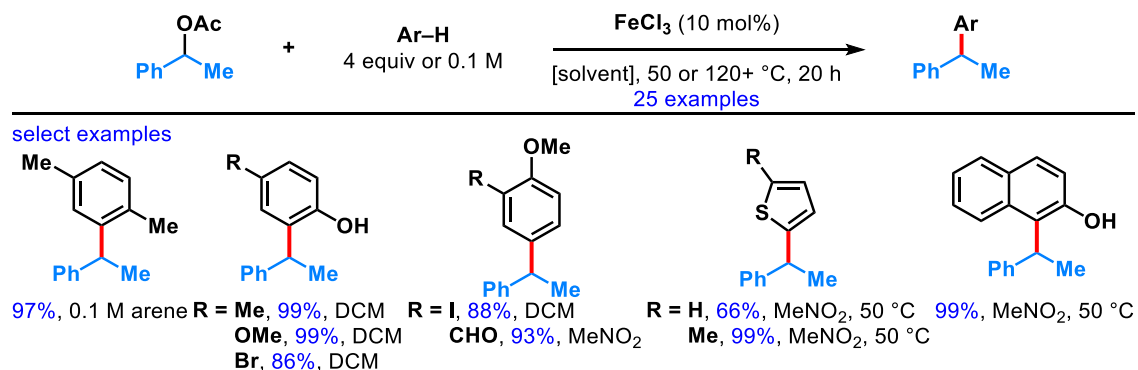


**Figure 3.1.** Friedel–Crafts alkylation of acyl benzyl ethers to nucleophilic arenes.

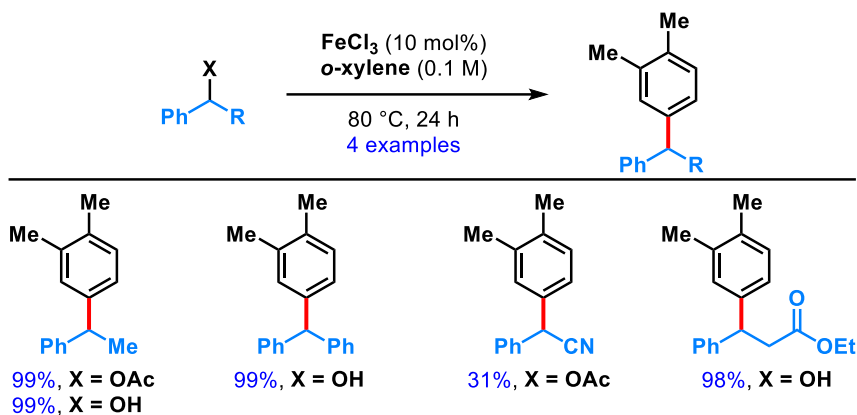


**Figure 3.2.** Benzylic acetates and secondary alcohols for Friedel–Crafts reactions.

Another class of electrophiles reactive to Friedel–Crafts alkylation are trimethylsilyl (TMS)-protected alcohols, demonstrated by Sawama, Sajiki and coworkers.<sup>3</sup> In this method, a benzyl silyl ether was reacted with catalytic  $\text{FeCl}_3$  and a nucleophilic arene to perform a Friedel–Crafts alkylation across a wide range of reaction times (**Figure 3.3**). In general, the electron-rich arenes took considerably less time to react compared to less electron-rich or neutral arenes. Less activated benzyl silyl ethers required longer reaction times, sometimes accompanied by a large drop in yields. Nucleophiles generally alkylate *para* to the electron-donating group, likely due to steric hindrance at the *ortho* position. Although less effective, unsilylated secondary alcohols were also compatible using this method.

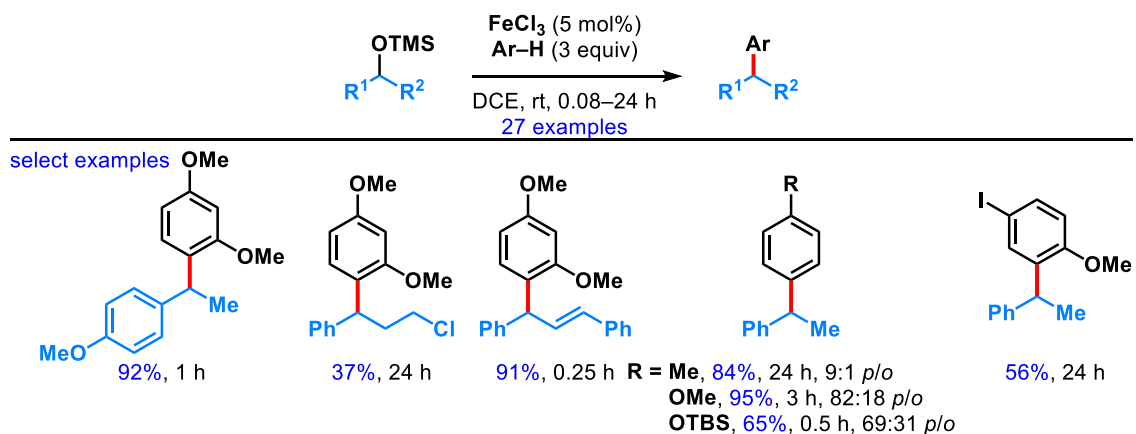


**Figure 3.3.** Friedel–Crafts alkylation with benzyl silyl ethers.

### 3.1.2 Friedel–Crafts alkylations with activated secondary alcohols

Activated secondary alcohols, such as benzylic alcohols, are commonly used in Friedel–Crafts alkylations due to facile carbocation formation arising from resonance stabilization. Along with tertiary alcohols (see chapter 2, **Figure 2.12** and **2.13**), Hall and coworkers<sup>4</sup> utilized two different benzylic alcohols in their tetrafluorophenylboronic acid catalysis (**Figure 3.4**). In both cases with *m*-xylene, substitution occurred at the more sterically accessible position *ortho* to the methyl group (**3.1**), with miniscule amounts (<5%) of alkylation observed in between the methyl groups (**3.2**). This method represents a Friedel–Crafts alkylation using simple secondary benzylic alcohols that operate under mild conditions and short reaction times.

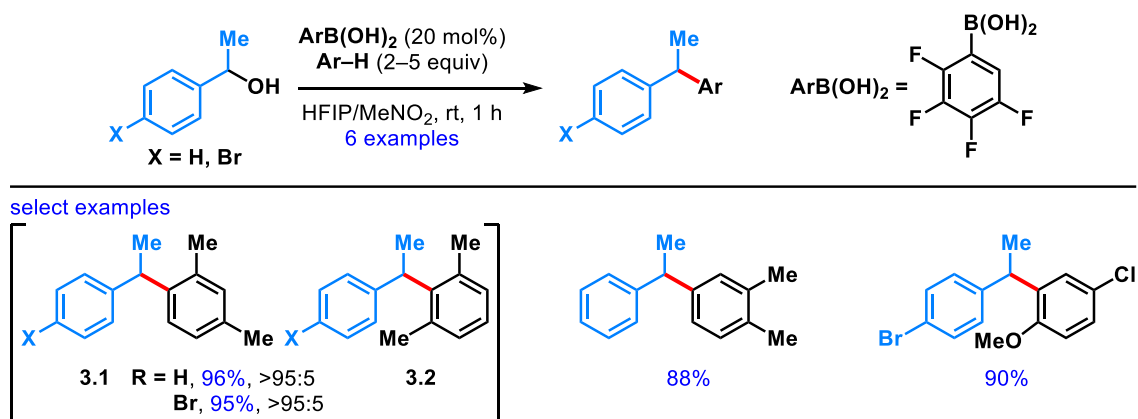


**Figure 3.4.** Tetrafluorophenylboronic acid-catalyzed Friedel–Crafts alkylation with secondary benzylic alcohols.

The principles of green chemistry are highly desirable and can generally apply to all chemical subdisciplines. In 2016, Xiao, Shao, and coworkers<sup>5</sup> demonstrated a green Friedel–Crafts alkylation utilizing water as the solvent to couple secondary benzylic or indolyl alcohols to indoles or other electron-rich arenes (**Figure 3.5**). This astonishing Friedel–Crafts reaction is Lewis/Brønsted acid-free, a rare feature in any electrophilic aromatic substitution reaction. The proposed rationale for the reactivity in the absence of acid is that at 80 °C, the  $\text{pK}_a$  of  $\text{H}_2\text{O}$  is about 6.5, thus generating a weak acid *in situ*, which can protonate the alcohol to promote the formation of the carbocation intermediate. The nucleophilic arene is also only in modest excess with 2–3 equivalents used. In particular, this method is compatible with unprotected indoles, which is sometimes a concern since certain acids may react with indole derivatives.



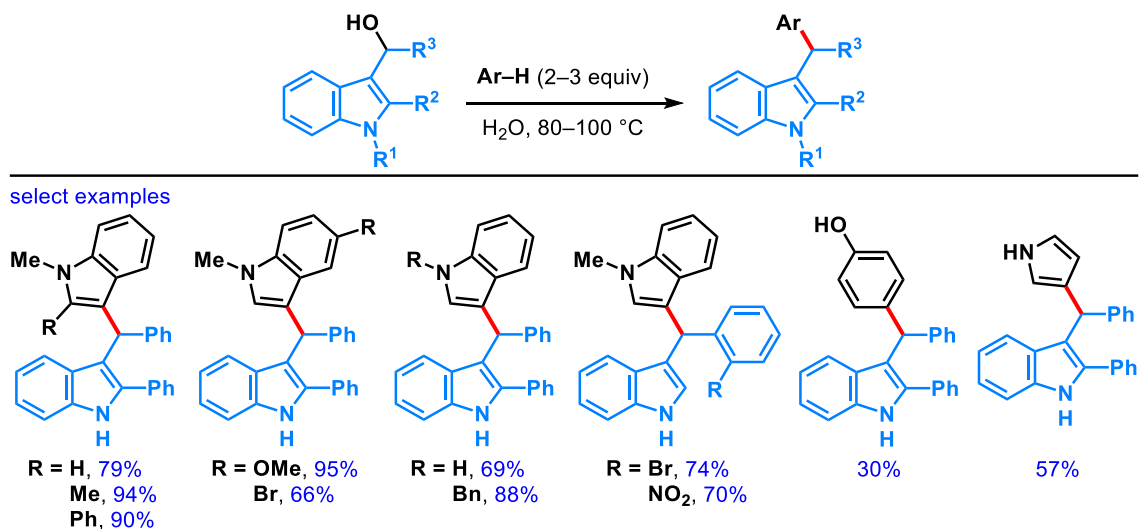


**Figure 3.5.** A green Friedel–Crafts alkylation method utilizing water as a green solvent.

In 2022, Hazra and coworkers<sup>6</sup> developed a method to alkylate electron-rich nucleophiles with secondary benzylic alcohols containing a cyclopropyl motif via Brookhart's acid  $[\text{H}(\text{OEt})_2]^+[\text{BARF}^4]^-$ , a unique acid generated *in situ* (**Figure 3.6**). Under mild conditions, this remarkably fast 5-minute reaction allows for the generation of a carbocation adjacent to a cyclopropyl group, which typically susceptible to competing ring-opening or ring-expansion to form other products.<sup>7</sup> Alcohols containing a strongly electron-withdrawing group at the *para* position, such as **3.3**, exhibited sluggish reactivity and required higher temperatures and reaction times. They proposed that carbocation formation is involved in the rate-determining step, supported by a Hammett study of various *para*-substituted phenyl cyclopropylmethanols.

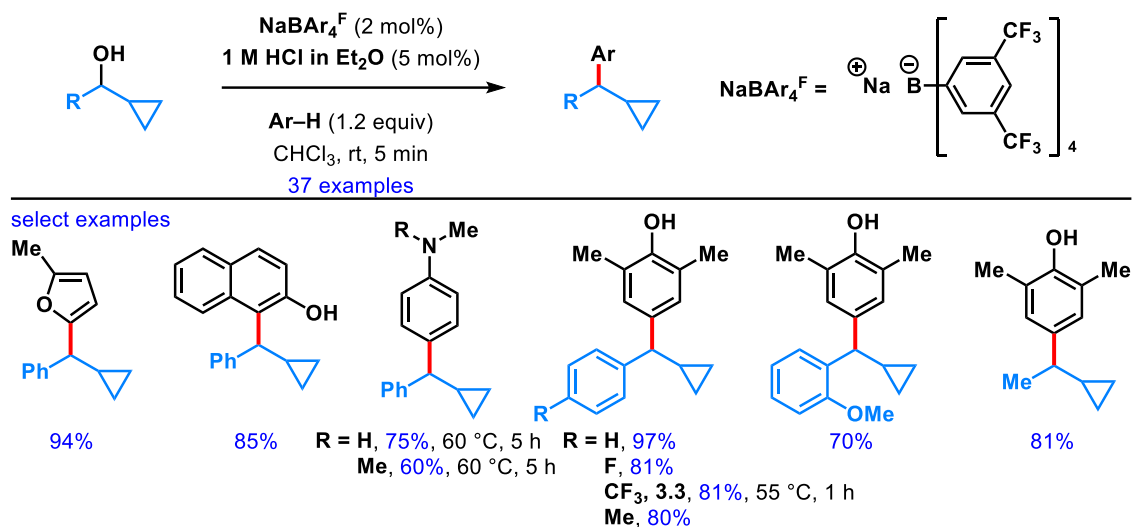
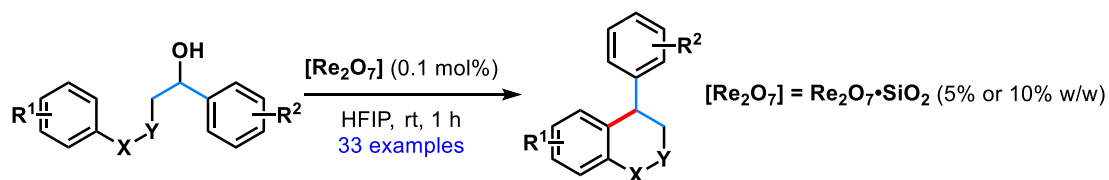


**Figure 3.6.** Cyclopropyl-containing secondary alcohols quickly reacting in a Friedel–Crafts alkylation.

Later in 2022, Xie and coworkers<sup>8</sup> demonstrated a rhenium(VII) oxide-catalyzed intramolecular Friedel–Crafts alkylation from secondary benzylic alcohols to form benzo-fused bicyclic systems (**Figure 3.7**). Under an extremely low catalyst loading (0.02 mol%),  $\text{Re}_2\text{O}_7$  supported on silica gel (5 or 10 w/w%) was utilized to catalyze this intramolecular dehydrative cyclization within 1 hour reaction times (longer if electron-withdrawing substituents were present on the aromatic rings). As opposed to strongly acidic and corrosive trifluoromethanesulfonic acid (TfOH),  $\text{Re}_2\text{O}_7 \cdot \text{SiO}_2$  allowed for acid-sensitive functional groups to be tolerated (**Figure 3.8**). Although rhenium(VII) oxide can be expensive, low catalyst loadings as low as 0.02 mol% can be utilized to catalyze this mild Friedel–Crafts alkylation.



select examples

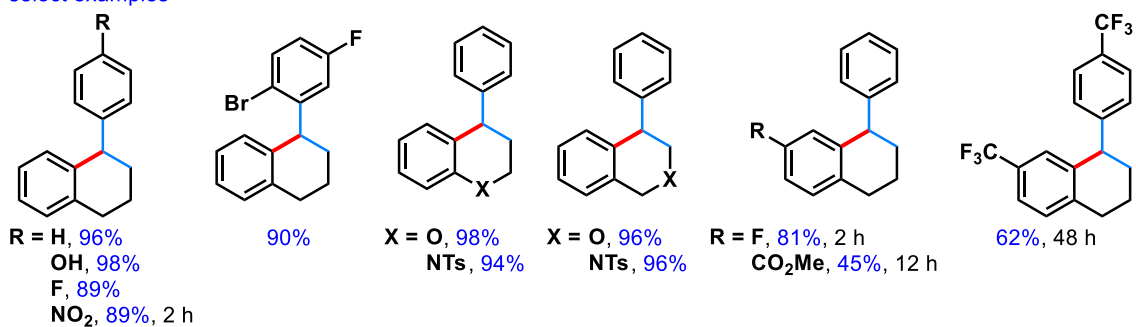


**Figure 3.7.** Substrate scope of rhenium-catalyzed Friedel–Crafts intramolecular cyclization.

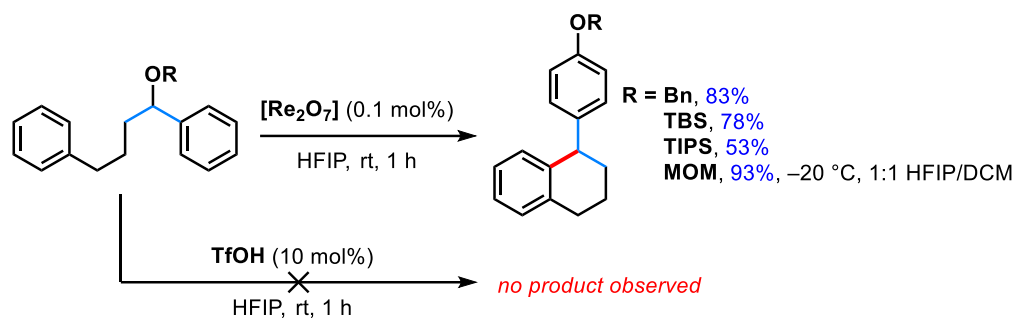


**Figure 3.8.** Scope of acid-sensitive functional groups in the presence of rhenium catalyst versus TfOH.

### 3.1.3 Friedel–Crafts alkylations with unactivated secondary alcohols

There is a large limitation in substrate scope if unactivated secondary alcohols cannot be used in Friedel–Crafts alkylation reactions; therefore, methods to include unactivated secondary alcohols are highly sought after. A challenge for unactivated alkylating reagents involves the large barrier to form a non-stabilized secondary carbocation, which requires either high temperatures or unique catalysts. A method

developed in 2014 by Cook and coworkers<sup>9</sup> utilize cycloalkanols as the non-activated secondary alcohols (**Figure 3.9**). In the case of *para*-xylene, cycloheptanol and cyclododecanol were also successful alcohols to afford **3.4** and **3.5**, respectively. Mono-substituted aryl nucleophiles afforded a mixture of *para* and *ortho* products that were poorly selective (~1:1 mixtures), consistent with previous Friedel–Crafts reactions.<sup>10</sup> A drawback of this method was the necessity of super-stoichiometric nucleophilic arene (15 equivalents), which significantly limits the scope to simple arenes.

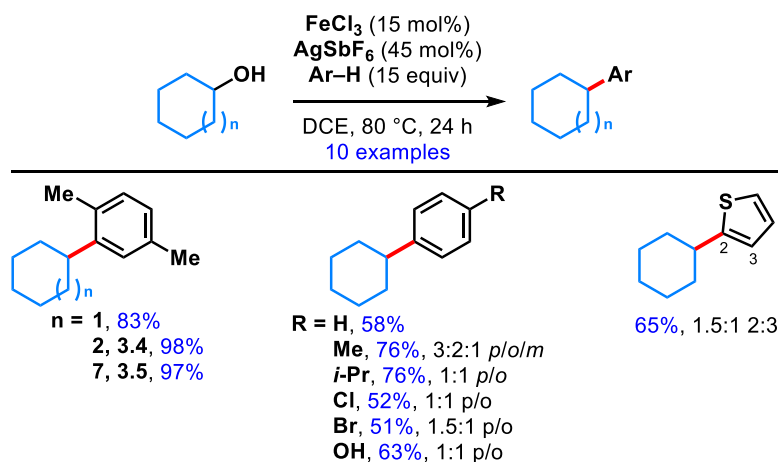


**Figure 3.9.** Unactivated cycloalkyl alcohols undergoing iron-catalyzed Friedel–Crafts alkylations.

In addition to intermolecular Friedel–Crafts alkylations with unactivated secondary alcohols, the group also developed an intramolecular Friedel–Crafts alkylations starting from unactivated secondary alcohols (**Figure 3.10**). This intramolecular reaction resolves the drawback of their intermolecular conditions in which only one equivalent of alcohol, which implies one equivalent of arene, is needed instead of the previously required 15 equivalents of arene. The reaction time was consistently kept at 24 h, however it was noted

that more electron-rich arenes finished within a few hours and resulted in higher yields as expected for Friedel–Crafts alkylations. Although limited in the scope of secondary alcohols, this method opened the doors to reacting unactivated alcohol-based electrophiles in the Friedel–Crafts alkylation under mild conditions, tolerant of air and moisture.

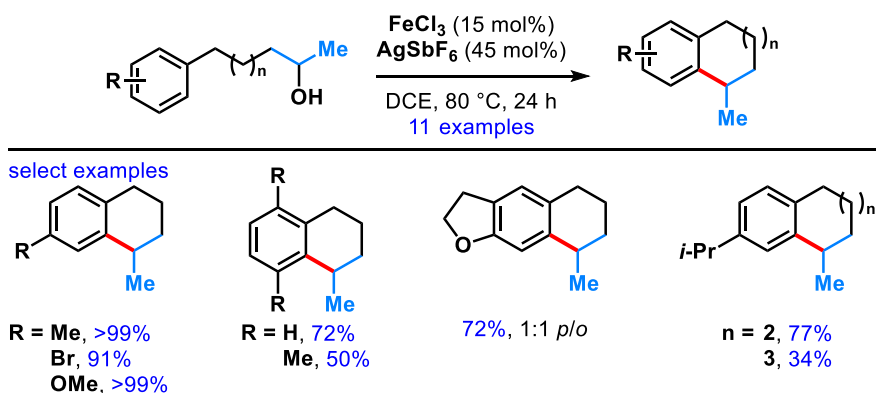


**Figure 3.10.** Intramolecular Friedel–Crafts alkylations with unactivated secondary alcohols.

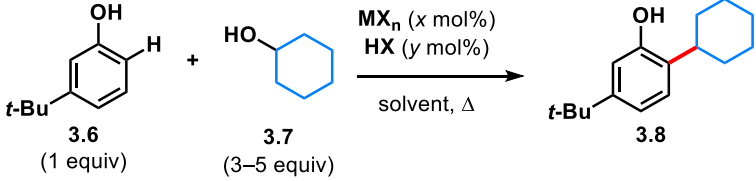
Although it has been well known that unactivated secondary alcohols are capable of alkylating arenes,<sup>11</sup> methods that can control alkylation in a consistent manner without harsh conditions are far and few between. Herein, we report a site-selective Friedel–Crafts alkylation of phenolic derivatives with unactivated secondary alcohols through dual  $\text{ZnCl}_2$  and camphorsulfonic acid (CSA) catalysis.

### 3.2.1 Development and optimization studies for the coupling of 3-*tert*-butylphenol and cyclohexanol

Our previous research has demonstrated the ability of Lewis acids to enhance the acidity of Brønsted acids.<sup>12</sup> Building on this finding, we hypothesized that this co-catalysis approach could be applied to Friedel–Crafts alkylations using unactivated secondary alcohols. This method offers several advantages over existing approaches, including the

use of cost-effective and readily accessible reagents: chlorobenzene instead of HFIP solvent<sup>4,8</sup> and Zn/CSA instead of Fe/Ag as catalysts.<sup>9</sup> 3-*tert*-Butylphenol (**3.6**) and cyclohexanol (**3.7**, CyOH) were selected to test for reactivity since they were readily available and conversion to product could be conveniently quantified by NMR analysis (**Table 3.1**). Catalytic amounts of Fe(III) salts (2.5 mol%) were initially examined with stoichiometric quantities of HCl (2 equiv) at 140 °C. The desired alkylation product (**3.8**) was formed in 50–57% NMR yields (entries 1–2). Using Lewis acid ZnCl<sub>2</sub> performed the best, providing the product in 63% yield (entry 3). Lowering the temperature from 140 °C to 120 °C was detrimental to yield (39%, entry 4), and increasing the ZnCl<sub>2</sub> loading to 5 mol% enhanced product formation (71%, entry 5). However, further increasing the amount of Zn-catalyst to 30 mol% does not improve the reaction outcome (entry 6). CSA was found to be effective at supporting this transformation, albeit providing a lower yield even when cyclohexanol (**3.7**) was employed as the solvent (39%, entry 7). Solid CSA was desirable because it addresses the concern of volatile HCl escaping from the reaction vessels at high temperature. Reducing the amount of alkylating agent in the reaction mixture from solvent quantities to 5 equiv improved the yield to 68% (entry 8). The reactivity was maintained by reducing the amount of CSA from 2 equiv to 0.75 equiv, which resulted in an isolated 74% yield of **3.8** when using 3 equiv of alcohol **3.7**. However, reducing the amount of acid to 50 mol% reduced the NMR yield to 52%.

**Table 3.1.** Survey of conditions for direct Friedel–Crafts alkylation.



Reaction scheme: Phenol **3.6** (1 equiv) + Cyclohexanol **3.7** (3–5 equiv)  $\xrightarrow[\text{solvent, } \Delta]{\text{MX}_n (x \text{ mol\%}), \text{HX} (y \text{ mol\%})}$  Product **3.8**

	MX <sub>n</sub>	x	HX	y	solvent	temp (°C)	% yield <sup>a</sup>
1	FeCl <sub>3</sub>	2.5	HCl	200	PhCl	140	50
2	FeBr <sub>3</sub>	2.5	HCl	200	PhCl	140	57
3	ZnCl <sub>2</sub>	2.5	HCl	200	PhCl	140	63
4	ZnCl <sub>2</sub>	2.5	HCl	200	PhCl	120	39
5	ZnCl <sub>2</sub>	5	HCl	200	PhCl	140	71
6	ZnCl <sub>2</sub>	30	HCl	200	PhCl	140	61
7	ZnCl <sub>2</sub>	5	( <i>R</i> )-CSA•H <sub>2</sub> O	200	CyOH	140	39
8	ZnCl <sub>2</sub>	5	( <i>R</i> )-CSA•H <sub>2</sub> O	200	PhCl	140	68
9	ZnCl <sub>2</sub>	5	( <i>R</i> )-CSA•H <sub>2</sub> O	75	PhCl	140	(74) <sup>b,c</sup>
10	ZnCl <sub>2</sub>	5	( <i>R</i> )-CSA•H <sub>2</sub> O	50	PhCl	140	52

Conditions: reactions performed on 0.1 mmol scale, phenol **3.6** (1 equiv), alcohol **3.7** (5 equiv), 18 h. CSA = camphorsulfonic acid, PhCl = chlorobenzene, CyOH = cyclohexanol. <sup>a</sup> Determined by NMR analysis of the crude reaction mixture using 1,3,5-trimethoxybenzene as internal standard. <sup>b</sup> With 3 equiv **3.7**. <sup>c</sup> Isolated yield.

Further optimization was attempted, reacting with 3 equivalents of cyclohexanol (**3.7**) instead of 5 equivalents (**Table 3.2**). FeCl<sub>3</sub>, FeBr<sub>3</sub>, and Zn(OAc)<sub>2</sub> as Lewis acids afforded lower yields of 54%–64% (entries 1–3), while the absence of any Lewis acid provided product in 50% yield (entry 4). Without both the Lewis acid and Brønsted acid, the reaction did not proceed (entry 5). Increasing or decreasing the mol% of ZnCl<sub>2</sub> did not

improve the yield (entries 6–7). An increase of CSA to 1 equivalent at 1 mol% ZnCl<sub>2</sub> (entry 8) was unideal relative to optimal conditions (**Table 3.1**, entry 9).

**Table 3.2.** Optimization of the reaction conditions.

Reaction scheme: 3-*tert*-butylphenol (**3.6**, 1 equiv) + cyclohexanol (**3.7**, 3 equiv)  $\xrightarrow[\text{PhCl, 140 }^\circ\text{C, 18 h}]{[\text{catalyst}] (x \text{ mol\%}), (R)\text{-CSA}\cdot\text{H}_2\text{O} (y \text{ mol\%})}$  3-*tert*-butyl-1-cyclohexylphenol (**3.8**)

Entry	[catalyst]	<i>x</i>	acid	<i>y</i>	% yield <sup>a</sup>
1	FeCl <sub>3</sub>	5	( <i>R</i> )-CSA·H <sub>2</sub> O	75	64
2	FeBr <sub>3</sub>	5	( <i>R</i> )-CSA·H <sub>2</sub> O	75	54
3	Zn(OAc) <sub>2</sub>	5	( <i>R</i> )-CSA·H <sub>2</sub> O	75	62
4	—	—	( <i>R</i> )-CSA·H <sub>2</sub> O	75	50 <sup>b</sup>
5	—	—	—	—	0
6	ZnCl <sub>2</sub>	1	( <i>R</i> )-CSA·H <sub>2</sub> O	75	52
7	ZnCl <sub>2</sub>	10	( <i>R</i> )-CSA·H <sub>2</sub> O	75	68
8	ZnCl <sub>2</sub>	1	( <i>R</i> )-CSA·H <sub>2</sub> O	100	66

Conditions: All reactions performed on 0.2 mmol scale, 3-*tert*-butylphenol **3.6** (1 equiv), cyclohexanol **3.7** (3 equiv), 1 M PhCl, 140 °C, 18 h. <sup>a</sup> Determined by NMR analysis of the crude reaction mixture using 1,3,5-trimethoxybenzene as the internal standard, unless otherwise specified. <sup>b</sup> Isolated yield.

### 3.2.2 Substrate scope

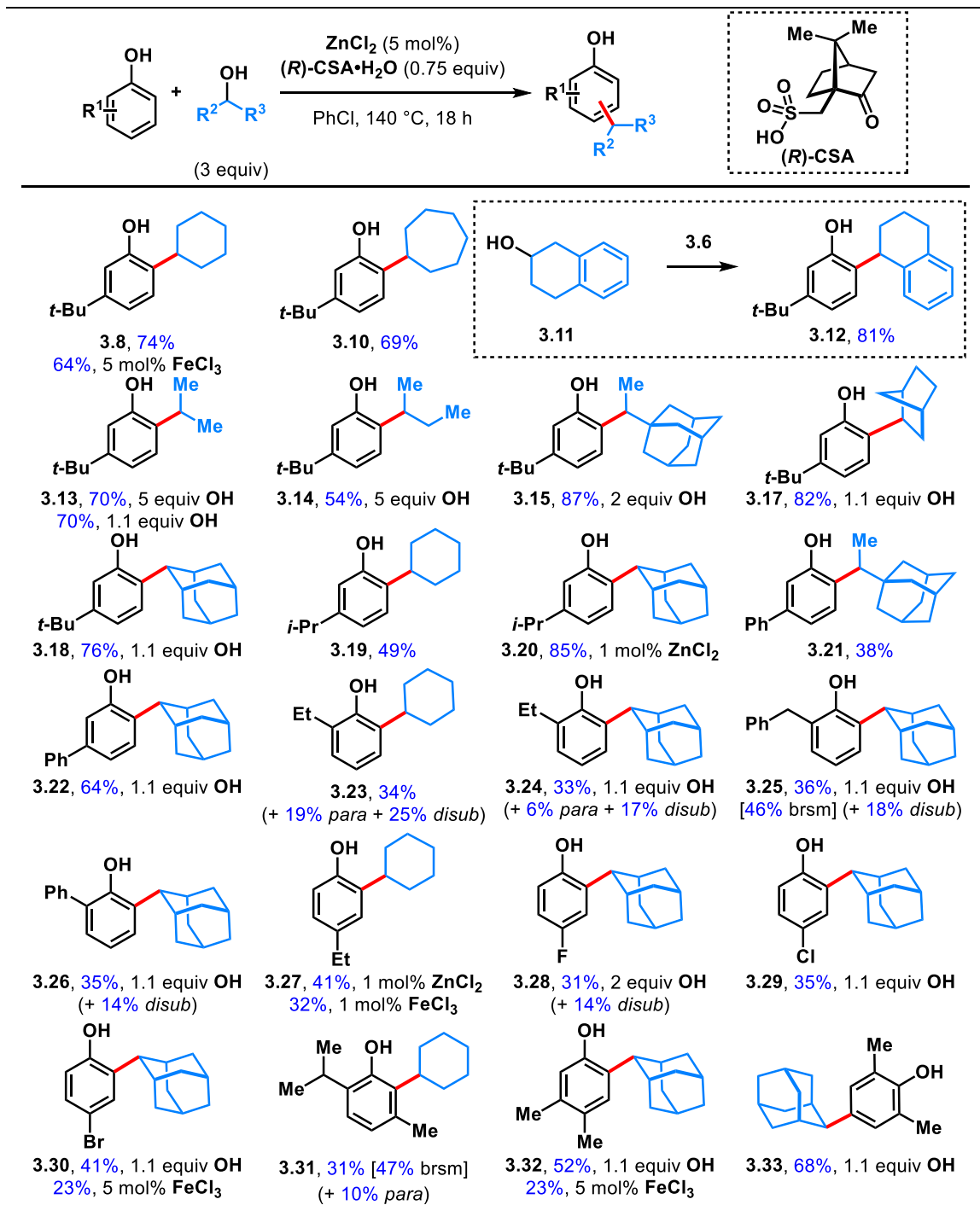
Reactions were carried out in a combined effort along with V. K. Nguyen, L. Rangel, and C. Fan. Cyclohexanol (**3.7**) and cycloheptanol (**3.9**, synthesized by C. Fan) combine with 3-*tert*-butylphenol (**3.6**) to forge alkylated **3.8** and **3.10** in good yields (69–74%, **Table 3.3**). The secondary carbocation generated from tetrahydronaphthalen-2-ol



(**3.11**, synthesized by C. Fan) undergoes 1,2-hydride shift to the corresponding benzylic carbocation under the reaction conditions, which proceeds to diarylmethane derivative **3.12** in 81% yield. Acyclic secondary alcohols isopropanol, 2-butanol, and 1-adamantyl-1-ethanol were converted to arylated products **3.13–3.15** in 54–87% yields. On a larger 1 mmol scale, the reaction proceeds with nearly equimolar alkylating agent (*i.e.*, 1.1 equiv of isopropanol (**3.16**)), leading to isopropylated **3.13** in 70% yield. Strained alcohols such as norborneol and 2-adamantanol were found to be excellent alkylating agents for this catalysis: equimolar quantities of reactants lead to substitution at the *ortho*-position of 3-*tert*-butylphenol (**3.6**) in 82% (**3.17**) and 76% (**3.18**) yields, respectively. 3-Isopropylphenol reacts with cyclohexanol in 49% yield and 2-adamantanol in 85% yield to arrive at alkylated arenes **3.19** and **3.20**. Likewise, 3-phenylphenol was alkylated with 1-adamantyl-1-ethanol in 38% yield (**3.21**) and with 2-adamantanol in 64% yield (**3.22**). In general, reactions with strained secondary alcohols performed better. Substrates bearing heteroatoms, as in those derived from tetrahydropyran or piperidine, represent limitations in this method. Presumably, the heteroatoms can associate with the ZnCl<sub>2</sub> catalyst, sequestering it from reactivity.

The modest preference for *ortho*-alkylation extends to *ortho*-substituted phenolic precursors that display a more sterically accessible *para*-site. Reaction of 2-ethylphenol with 1-adamantyl-1-ethanol modestly favors *ortho*-alkylation, albeit in 34% yield of **3.23**, along with 25% *ortho/para*-dialkylation and 19% *para*-alkylation side products. A similar reactivity pattern was observed between 2-ethylphenol and 2-adamantanol, which gave rise to 33% of phenolic **3.24**. *ortho/para*-Dialkylated (17%) and *para*-substituted (6%) phenols

**Table 3.3.** Scope of Friedel–Crafts alkylations with unactivated secondary alcohols.<sup>a</sup>



Conditions: phenolic compound (0.2 mmol), alcohol (0.6 mmol), ZnCl<sub>2</sub> (0.01 mmol), (*R*)-CSA (0.15 mmol), PhCl (0.2 mL, 1 M), 140 °C, 18 h. <sup>a</sup> Reactions were carried out with combined efforts with V. K. Nguyen, L. Rangel, and C. Fan.

were formed as minor products. Both 2-benzylphenol and 2-phenylphenol alkylate at their *ortho*-sites with 2-adamantanol to afford *ortho/ortho*-dialkylphenols **3.25** and **3.26** in 36% and 35% isolated yields, respectively, along with a minor disubstitution of side products. In these cases, the *para*-substituted isomers were not isolated nor observed by <sup>1</sup>H NMR analysis of the crude reaction mixtures.

*para*-Substituted (including halogenated) phenolic precursors were mono-alkylated in modest 31–41% yields (**3.27–3.30**). Sterically-encumbered thymol alkylates with cyclohexanol in 31% yield (47% brsm) predominantly at the most hindered *ortho*-position (**3.31**, 31%) over the *para*-position (10%). In contrast, with two available *ortho*-sites, the flavoring agent 3,4-xylene undergoes alkylation at the less hindered 6-position to furnish 2-adamantyl-4,5-dimethylphenol (**3.32**) in 52% yield. This selectivity is consistent with all the *meta*-substituted phenolic precursors containing two unsymmetrical *ortho*-sites. With both *ortho*-sites blocked, as in 2,6-xylene, *para*-alkylation resulted in **3.33** in 68% yield.

This chemistry can be applied to the alkylation of more complex molecules like estrone (**3.34**). As examples, its treatment with isopropanol and cyclohexanol furnishes a mixture of **3.35/3.36** in 31% (1:1.5 C4/C2 selectivity) favoring alkylation at the more sterically encumbered *ortho*-site and **3.37/3.38** in 60% yield (2.3:1 C4/C2 selectivity) favoring alkylation at the less hindered *ortho*-site (**Figure 3.11a**). We further demonstrate derivatization of the alkylated phenolic compound (**3.18**) with 2-fluoropyridine (**3.39**) in a nucleophilic aromatic substitution to access pyridylaryl ether **3.40** in 86% yield (**Figure 3.11b**).

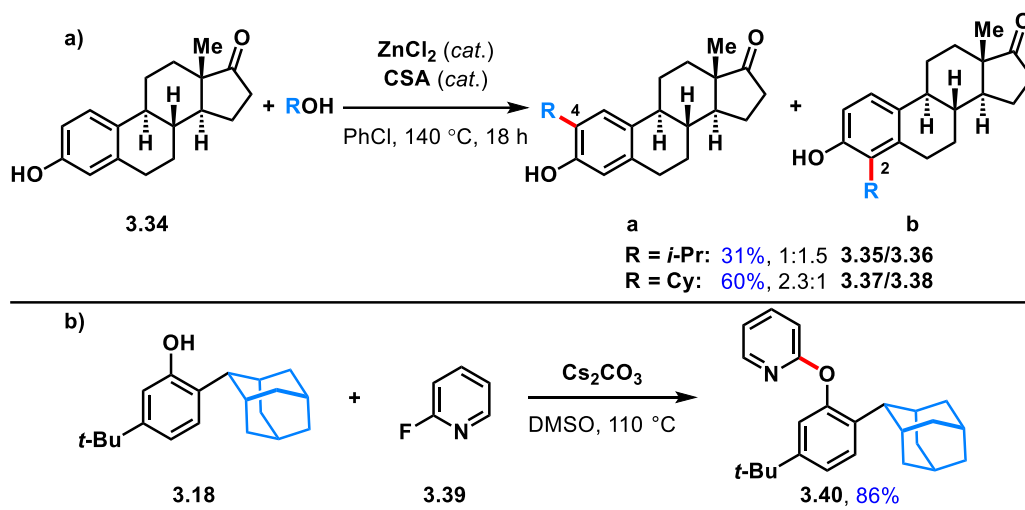


**Figure 3.11.** Application to late-stage derivatization:

a) Direct alkylation of estrone (3.34). b) Derivatization of substituted phenol by S<sub>N</sub>Ar.

### 3.2.3 Mechanistic studies to probe the origin of site-selectivity

The *ortho*-selectivity, albeit only modest, under Zn/CSA-catalysis conditions was similarly observed between unsubstituted phenol (3.41) and 2-adamantanol (3.42) where a mixture of alkylated products formed, with *o*-alkylation occurring as the major product (3.43, 25%), followed by *o,o*-dialkylation (3.44, 14%), and *p*-alkylation (3.45, 8%) (Figure 3.12a). This contrasts from the *para*-selectivity observed in the analogous Fe/HCl-catalyzed Friedel–Crafts alkylation with tertiary alcohols<sup>12</sup> and HFIP-mediated alkylation with tertiary alkyl bromides.<sup>13</sup> On the other hand, we found that the catalytic Zn/CSA system favors *ortho*-selectivity (>16:1 3.46 to 3.47) over 3.48, even with the more hindered *tert*-butanol (3.50) at 80 °C, although with lower reactivity compared to the previously reported Fe/HCl system (Figure 3.12b). At 140 °C, the site-selectivity reverses to favor 3.48 (40% yield, 13:1 *p/o*). Therefore, the site-selectivity was not simply determined by

steric factors, but rather by the catalyst systems. The Zn/CSA catalyst system inherently favors *ortho*-selectivity. The site-selectivity was lost when CSA was substituted for HCl. The Zn/HCl co-catalyzed reaction between 2-ethylphenol (**3.49**) and 2-adamantanol (**3.42**) resulted in a 1:1.2 mixture of **3.51/3.52**, slightly favoring *para*-substitution (**Figure 3.12c**).

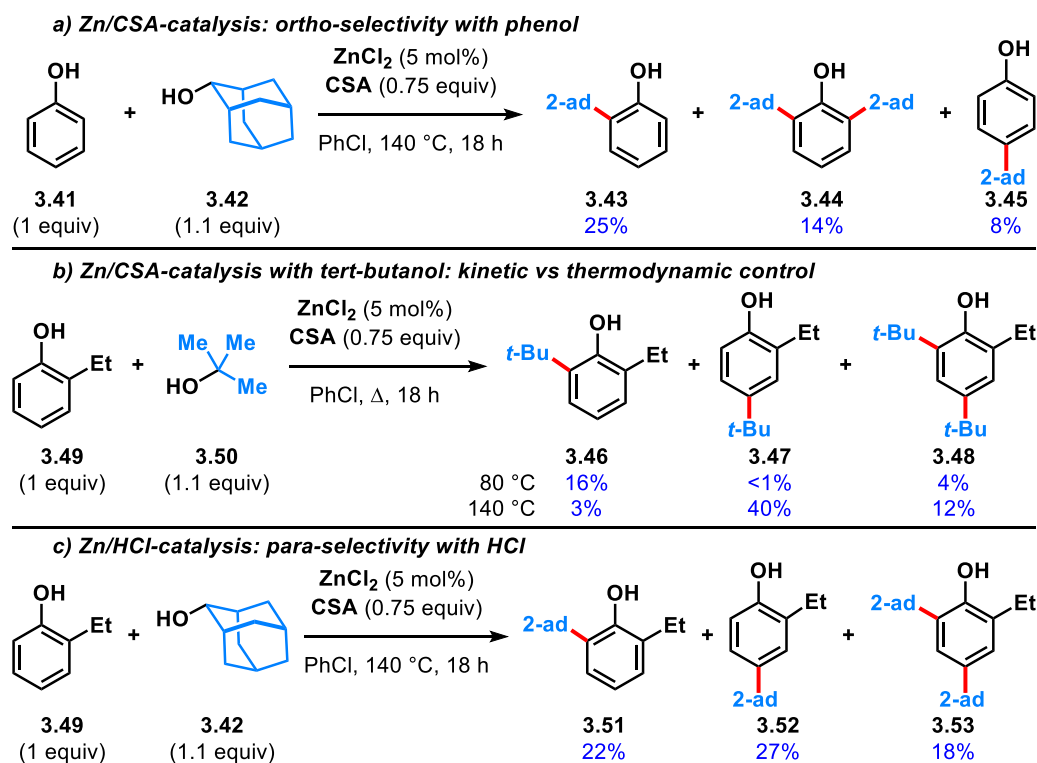


**Figure 3.12.** Mechanistic studies:

- a) Preference for *ortho*-selectivity in Zn/CSA-catalyzed Friedel–Crafts alkylation. b) Insight on kinetic versus thermodynamic control. c) Poor selectivity with Zn/HCl catalysis.

Reaction progress monitoring via SFC analysis was performed using 2-ethylphenol (**3.49**) to corroborate the site-selectivities (**Figure 3.13**). We found that under Zn/CSA catalysis, the initial rate of *ortho*-alkylation was significantly greater than that of *para*-

alkylation (**Figure 3.2a**). In contrast, *ortho*- and *para*-alkylation products formed at similar rates under Zn/HCl catalysis (**Figure 3.2b**).

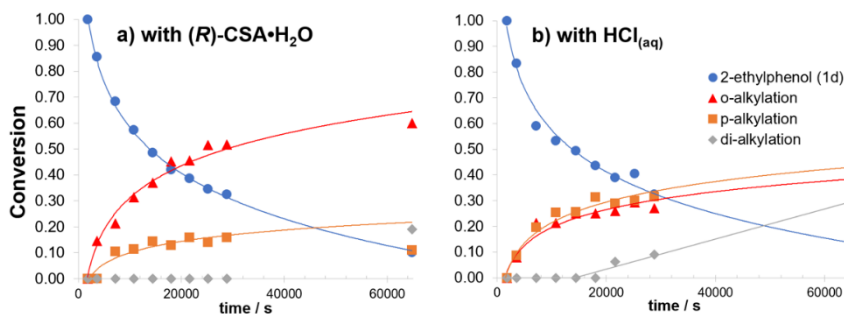


**Figure 3.13.** Reaction progress monitoring of:

- a) Zn/CSA-catalyzed alkylation of 2-ethylphenol (**3.49**) and b) Zn/HCl-catalyzed alkylation of 2-ethylphenol (**3.49**) by SFC analysis. SFC = supercritical fluid chromatography.

These data sets were supportive of the selectivity arising from the catalyst and not simply from substrate bias. We postulate that the Zn and CSA catalysts play roles in templating reactivity and that the phenolic group directs reactivity (through a zinc phenolate species). Upon subjecting anisole (**3.54**) to the catalysis conditions, V. K. Nguyen found that only a small amount of the *para*-alkylated product (**3.55**) was observed by NMR analysis (**Figure 3.14a**). This observation emphasizes the importance of the free phenolic group in directing both reactivity and selectivity. To probe the substitution mechanism of the reaction, a non-racemic mixture of 1-adamantyl-1-ethanol (**3.57**) was subjected to Friedel–Crafts alkylation with 3-*tert*-butylphenol (**3.6**) (**Figure 14b**). The loss of enantiomeric excess in forming the chiral racemic product (**3.15**) (**Table 3.4**) strongly suggests involvement of an  $S_N1$  pathway under the dual  $ZnCl_2/CSA$  catalysis conditions, which was distinct from the  $S_N2$  pathway promoted by TfOH in HFIP.<sup>14</sup>

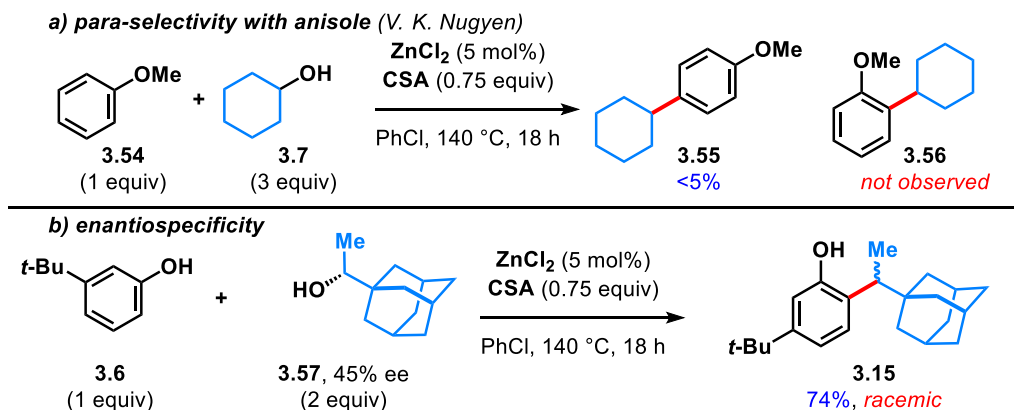
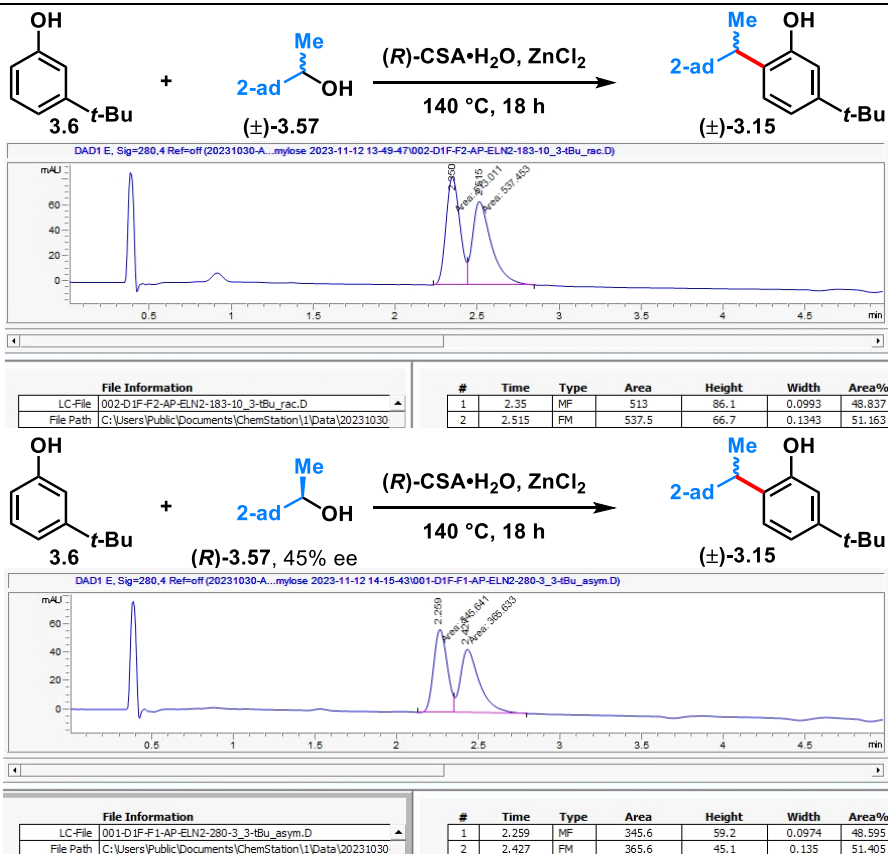


**Figure 3.14.** Mechanistic studies:

a) Alkylation of anisole. *Work done by V. K. Nguyen.* b) Probing enantiospecificity.

**Table 3.4.** Racemic or enantioenrich alcohol **3.57** result in racemic product (±)-**3.15**.



We turned to kinetics studies to derive a rate law for this transformation using 3-*tert*-butylphenol (**3.6**) and 2-adamantanol (**3.42**) as the model system. Initial rates of the alkylation reaction were measured by varying the concentrations of ZnCl<sub>2</sub>, CSA, phenolic **3.6**, alcohol **3.42**, ZnCl<sub>2</sub>, and CSA (Table 3.5) and plotted (Figures 3.16–3.20). These experiments revealed the rate to be largely independent of the concentration of ZnCl<sub>2</sub>, suggestive of saturation kinetics and sequestration by substrate (Figure 3.15).

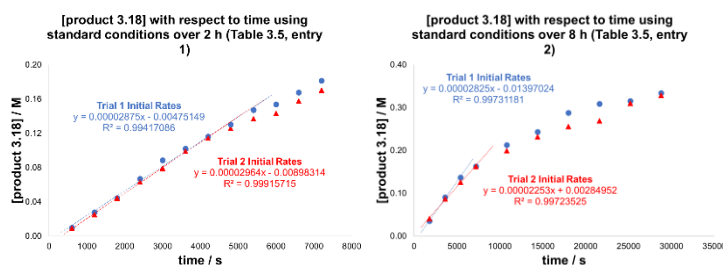


Figure 3.16. Initial rates under standard conditions.

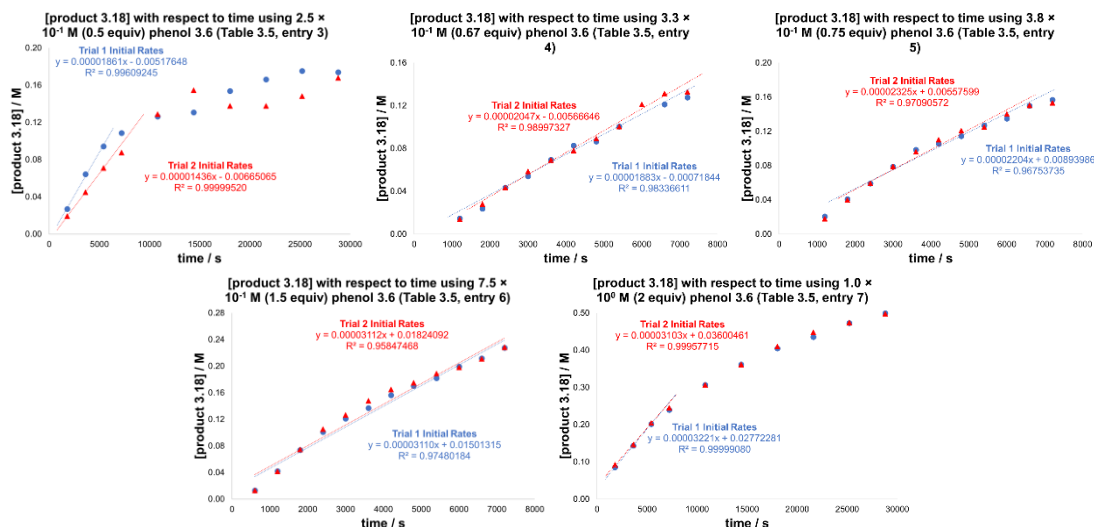


Figure 3.17. Initial rates varying [phenolic 3.6].



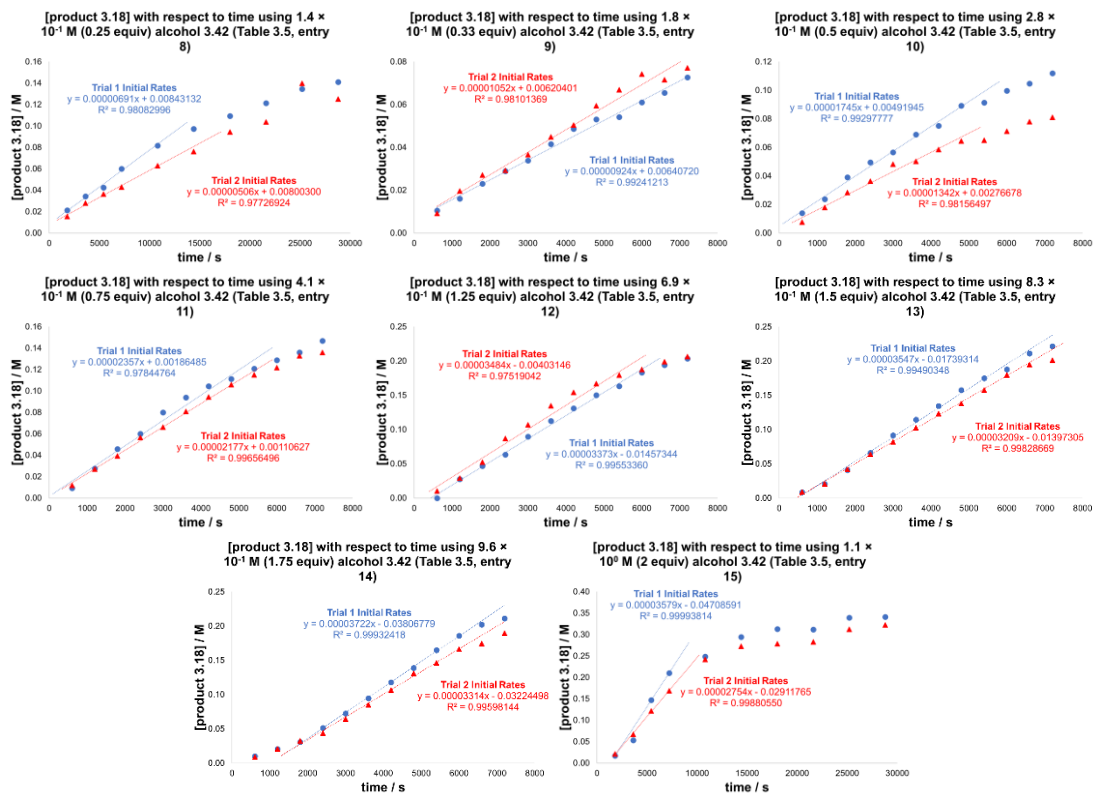


Figure 3.18. Initial rates varying [alcohol 3.42].

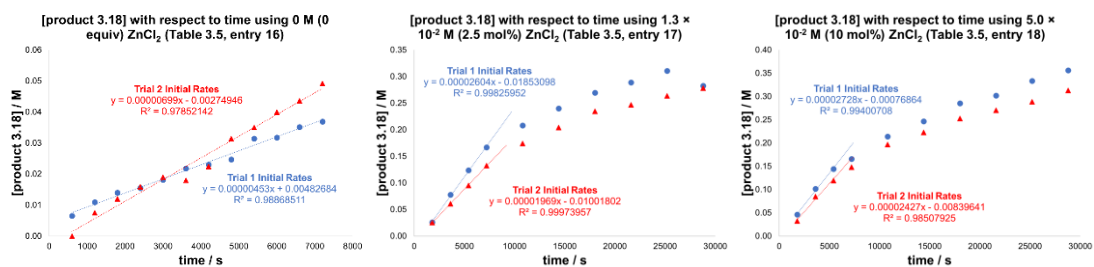


Figure 3.19. Initial rates varying  $[\text{ZnCl}_2]$ .

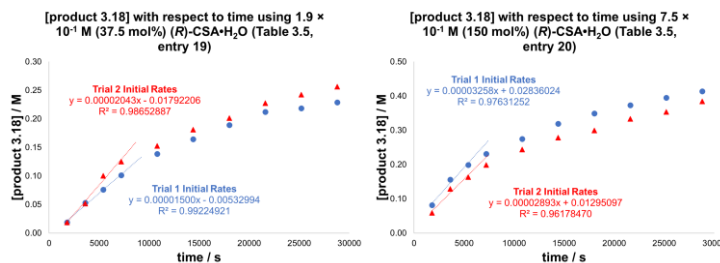


Figure 3.20. Initial rates varying [(R)-CSA·H<sub>2</sub>O].

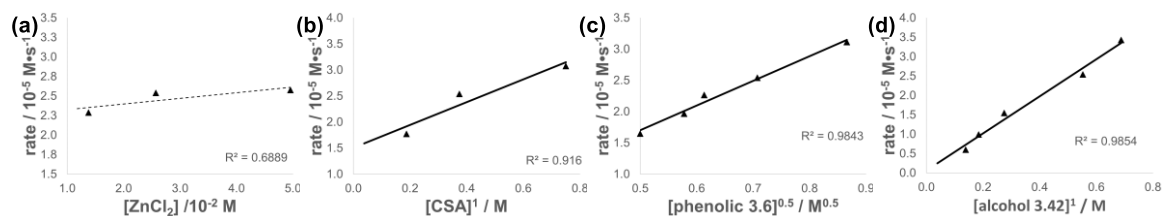


Figure 3.15. Plots of initial rates with respect to:

(a)  $[\text{ZnCl}_2]$  indicating pseudo-zero order dependence,  $[\text{CSA}] = 3.8 \times 10^{-1} \text{ M}$ ,  $[\text{phenolic } 3.6] = 5.0 \times 10^{-1} \text{ M}$ ,  $[\text{alcohol } 3.42] = 5.5 \times 10^{-1} \text{ M}$ ; (b)  $[\text{CSA}]$  indicating first-order dependence,  $[\text{ZnCl}_2] = 2.5 \times 10^{-2} \text{ M}$ ,  $[\text{phenol } 3.6] = 5.0 \times 10^{-1} \text{ M}$ ,  $[\text{alcohol } 3.42] = 5.5 \times 10^{-1} \text{ M}$ ; (c)  $[\text{phenol } 3.6]$  indicating half-order dependence,  $[\text{ZnCl}_2] = 2.5 \times 10^{-2} \text{ M}$ ,  $[\text{CSA}] = 3.8 \times 10^{-1} \text{ M}$ ,  $[\text{alcohol } 3.42] = 5.5 \times 10^{-1} \text{ M}$ ; (d)  $[\text{alcohol } 3.42]$  indicating first-order dependence,  $[\text{ZnCl}_2] = 2.5 \times 10^{-2} \text{ M}$ ,  $[\text{CSA}] = 3.8 \times 10^{-1} \text{ M}$ ,  $[\text{phenol } 3.6] = 5.0 \times 10^{-1} \text{ M}$ .

**Table 3.5.** Kinetic data for arene alkylation with adamant-2-ol.

Entry	[ <b>3.6</b> ] / M	[ <b>3.42</b> ] / M	[ZnCl <sub>2</sub> ] / M	[( <i>R</i> )-CSA•H <sub>2</sub> O] / M	initial rate <sup>a</sup> / M•s <sup>-1</sup>
1	$5.0 \times 10^{-1}$	$5.5 \times 10^{-1}$	$2.5 \times 10^{-2}$	$3.8 \times 10^{-1}$	$2.9_2 \times 10^{-5}$
2 <sup>[b]</sup>	$5.0 \times 10^{-1}$	$5.5 \times 10^{-1}$	$2.5 \times 10^{-2}$	$3.8 \times 10^{-1}$	$2.5_4 \times 10^{-5}$
3	$2.5 \times 10^{-1}$	$5.5 \times 10^{-1}$	$2.5 \times 10^{-2}$	$3.8 \times 10^{-1}$	$1.6_5 \times 10^{-5}$
4	$3.3 \times 10^{-1}$	$5.5 \times 10^{-1}$	$2.5 \times 10^{-2}$	$3.8 \times 10^{-1}$	$1.9_7 \times 10^{-5}$
5	$3.8 \times 10^{-1}$	$5.5 \times 10^{-1}$	$2.5 \times 10^{-2}$	$3.8 \times 10^{-1}$	$2.2_6 \times 10^{-5}$
6	$7.5 \times 10^{-1}$	$5.5 \times 10^{-1}$	$2.5 \times 10^{-2}$	$3.8 \times 10^{-1}$	$3.1_1 \times 10^{-5}$
7 <sup>b</sup>	$1.0 \times 10^0$	$5.5 \times 10^{-1}$	$2.5 \times 10^{-2}$	$3.8 \times 10^{-1}$	$3.1_6 \times 10^{-5}$
8 <sup>b</sup>	$5.0 \times 10^{-1}$	$1.4 \times 10^{-1}$	$2.5 \times 10^{-2}$	$3.8 \times 10^{-1}$	$5.9_9 \times 10^{-6}$
9	$5.0 \times 10^{-1}$	$1.8 \times 10^{-1}$	$2.5 \times 10^{-2}$	$3.8 \times 10^{-1}$	$9.8_8 \times 10^{-6}$
10	$5.0 \times 10^{-1}$	$2.8 \times 10^{-1}$	$2.5 \times 10^{-2}$	$3.8 \times 10^{-1}$	$1.5_4 \times 10^{-5}$
11	$5.0 \times 10^{-1}$	$4.1 \times 10^{-1}$	$2.5 \times 10^{-2}$	$3.8 \times 10^{-1}$	$2.2_7 \times 10^{-5}$
12	$5.0 \times 10^{-1}$	$6.9 \times 10^{-1}$	$2.5 \times 10^{-2}$	$3.8 \times 10^{-1}$	$3.4_3 \times 10^{-5}$
13	$5.0 \times 10^{-1}$	$8.3 \times 10^{-1}$	$2.5 \times 10^{-2}$	$3.8 \times 10^{-1}$	$3.3_8 \times 10^{-5}$
14	$5.0 \times 10^{-1}$	$9.6 \times 10^{-1}$	$2.5 \times 10^{-2}$	$3.8 \times 10^{-1}$	$3.5_2 \times 10^{-5}$
15 <sup>b</sup>	$5.0 \times 10^{-1}$	$1.1 \times 10^0$	$2.5 \times 10^{-2}$	$3.8 \times 10^{-1}$	$3.1_7 \times 10^{-5}$
16	$5.0 \times 10^{-1}$	$5.5 \times 10^{-1}$	0	$3.8 \times 10^{-1}$	$5.7_6 \times 10^{-6}$
17 <sup>b</sup>	$5.0 \times 10^{-1}$	$5.5 \times 10^{-1}$	$1.3 \times 10^{-2}$	$3.8 \times 10^{-1}$	$2.2_9 \times 10^{-5}$
18 <sup>b</sup>	$5.0 \times 10^{-1}$	$5.5 \times 10^{-1}$	$5.0 \times 10^{-2}$	$3.8 \times 10^{-1}$	$2.5_8 \times 10^{-5}$
19 <sup>b</sup>	$5.0 \times 10^{-1}$	$5.5 \times 10^{-1}$	$2.5 \times 10^{-2}$	$1.9 \times 10^{-1}$	$1.7_7 \times 10^{-5}$
20 <sup>b</sup>	$5.0 \times 10^{-1}$	$5.5 \times 10^{-1}$	$2.5 \times 10^{-2}$	$7.5 \times 10^{-1}$	$3.0_8 \times 10^{-5}$

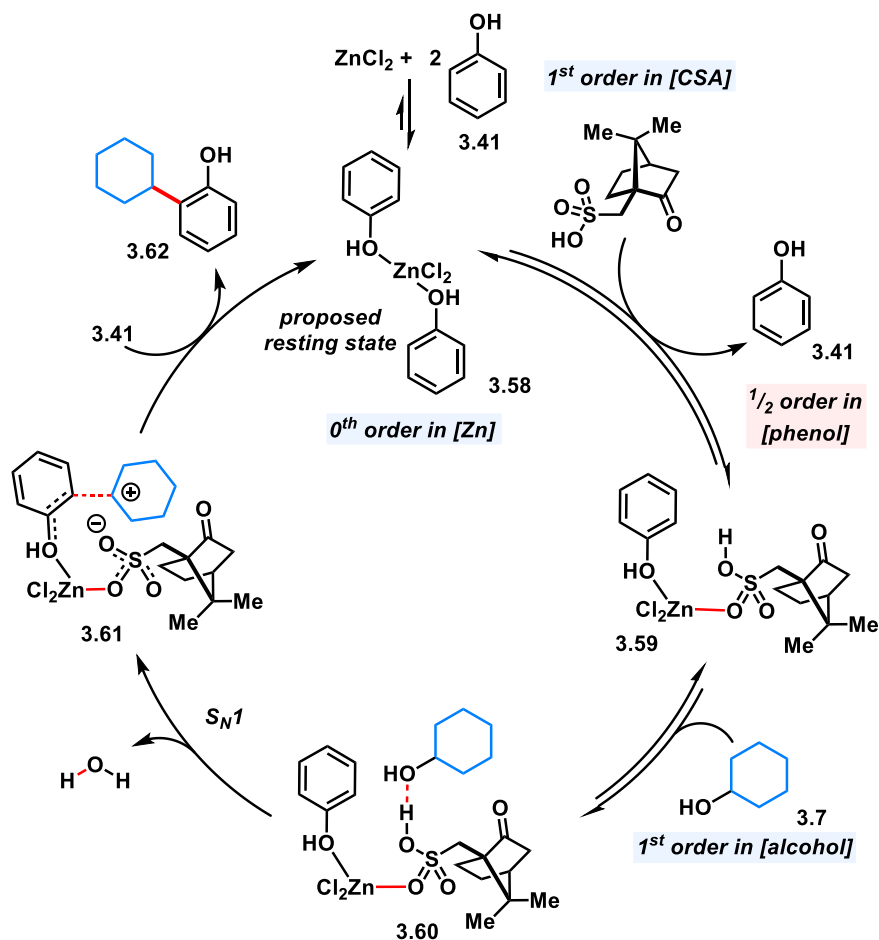
<sup>a</sup> Average value from 2 independent experiments. <sup>b</sup> Experiments ran for 8 h.

In the absence of ZnCl<sub>2</sub>, the initial rate deviates significantly (4.3-fold slower) from the trendline in **Figure 3.15a** (see **Table 3.2**, entry 4) and was indicative of background reactivity proceeding through a different ZnCl<sub>2</sub>-free mechanism. The initial rates (eqn

(3.1)) follow a first-order dependence on the concentration of CSA, half-order dependence on the concentration of phenolic **3.6**, and first-order dependence on the concentration of 2-adamantanol (**3.42**), giving the rate law:

$$rate = k_{obs}[ZnCl_2]^0[CSA]^1[phenolic \text{ 3.6}]^{0.5}[alcohol \text{ 3.42}]^1 \quad (3.1)$$

Based on the experimentally-derived rate law, the zinc catalyst is believed to be saturated with phenol ligands in the form of complex **3.58** (Scheme 3.1).



Scheme 3.1. Proposed mechanism.

We therefore propose it to be the resting state of the catalytic cycle. Alcohols are likely to be competitive ligands for zinc; however, our past study with FeCl<sub>3</sub> revealed that its binding to alcohols poorly facilitates ionization and likely forms unproductive intermediates.<sup>12</sup> For the reaction to proceed, one of the phenolic ligands must dissociate from zinc in exchange for CSA to coordinate, leading to complex **3.59**; hence the half-order dependence on [phenol **3.41**] and first-order dependence on [CSA]. Complexation of the Brønsted acid to zinc effectively enhances its acidity, enabling it to activate alcohol **3.7** toward Friedel–Crafts alkylation (**3.60**). Ionization, as part of the S<sub>N</sub>1 pathway determined via stereochemical studies (**Figure 3.14b**), leads to loss of water and an ion-pair that can potentially proceed via transition state **3.61**. The relatively non-polar PhCl solvent favors formation of a tight ion-pair and accounts for the *ortho*-selectivity. The modest levels of site-selectivity observed is believed to be a consequence of the high temperature that is currently needed, which acts to disrupt the proposed organized network in intermediate **3.61**, thereby allowing the non-directed intermolecular pathway that leads to *para*-substituted products to be competitive. Release of product **3.62** in the presence of excess phenolic substrate turns over the zinc catalyst.

### 3.3 Conclusion

In summary, the combination of zinc and CSA catalysts promotes the first direct *ortho*-selective Friedel–Crafts alkylation of phenolic derivatives with unactivated secondary alcohols. The free phenolic group was found to be important for reactivity and site-selectivity, which was rationalized through zinc-mediated templation that biases

alkylation at the *ortho*-position over the generally more accessible *para*-position. The current catalysis conditions provide a good foundation for developing green and cost-effective conditions for catalytic Friedel–Crafts reactions using readily accessible alcohols as direct alkylating agents.

### 3.4 References

1. Friedel, C.; Crafts, J. M. A New General Synthetical Method of Producing Hydrocarbons. *J. Chem. Soc.* **1877**, *32*, 725–791.
2. Iovel, I.; Mertins, K.; Kischel, J.; Zapf, A.; Beller, M. An Efficient and General Iron-Catalyzed Arylation of Benzyl Alcohols and Benzyl Carboxylates. *Angew. Chem. Int. Ed.* **2005**, *44*, 3913–3917.
3. Sawama, Y.; Shishido, Y.; Kawajiri, T.; Goto, R.; Monguchi, Y.; Sajiki, Hironao. Iron-Catalyzed Friedel–Crafts Benzylation with Benzyl TMS Ethers at Room Temperature. *Chem. Eur. J.* **2014**, *20*, 510–516.
4. Ricardo, C. L.; Mo, X.; McCubbin, J. A.; Hall, D. G. A Surprising Substituent Effect Provides a Superior Boronic Acid Catalyst for Mild and Metal-Free Direct Friedel–Crafts Alkylations and Prenylations of Neutral Arenes. *Chem. Eur. J.* **2015**, *21*, 4218–4223.
5. Xiao, J.; Wen, H.; Wang, L.; Xu, L.; Hao, Z.; Shao, C.-L.; Wang, C.-Y. Catalyst-free dehydrative S<sub>N</sub>1-type reaction of indolyl alcohols with diverse nucleophiles “on water”. *Green Chem.* **2016**, *18*, 1032–1037.
6. Yadav, N.; Khan, J.; Tyagi, A.; Singh, S.; Hazra, C. K. Rapid Access to Arylated and Allylated Cyclopropanes via Brønsted Acid-Catalyzed Dehydrative Coupling of Cyclopropylcarbinols. *J. Org. Chem.* **2022**, *87*, 6886–6901.
7. (a) Franco, M.; Rosenbach, N.; Ferreira, G. B.; Guerra, A. C. O.; Kover, W. B.; Turci, C. C.; Mota, C. J. A. Rearrangement, Nucleophilic Substitution, and Halogen Switch Reactions of Alkyl Halides over NaY Zeolite: Formation of the Bicyclobutonium Cation Inside the Zeolite Cavity. *J. Am. Chem. Soc.* **2008**, *130*, 1592–1600. (b) Mo, Y.; Schleyer, P. R.; Jiao, H.; Lin, Z. Quantitative evaluation of hyperconjugation in the cyclopropylcarbinyl cation and in cyclopropylborane.

- Chem. Phys. Lett.* **1997**, *280*, 439–443.
8. Zheng, Y.; Fang, X.; Deng, W.-H.; Zhao, B.; Liao, R.-Z.; Xie, Y. Direct activation of alcohols via perrhenate ester formation for an intramolecular dehydrative Friedel–Crafts reaction. *Org. Chem. Front.* **2022**, *9*, 4277–4286.
  9. Jefferies, L. R.; Cook, S. P. Iron-Catalyzed Arene Alkylation Reactions with Unactivated Secondary Alcohols. *Org. Lett.* **2014**, *16*, 2026–2029.
  10. Kotsuki, H.; Oshisi, T.; Inoue, M. Scandium(III) Trifluoromethanesulfonate-Catalyzed Friedel–Crafts Alkylation of Aromatic Compounds with Secondary Alcohol Methanesulfonates. *Org. Chem. Front.* **2022**, *9*, 4277–4286.
  11. Huston, R. C.; Kaye, I. A. The Condensation of Some Secondary Aliphatic Alcohols with Benzene in the Presence of Aluminum Chloride. *J. Am. Chem. Soc.* **1942**, *64*, 1576–1580.
  12. Pan, A.; Chojnacka, M.; Crowley, R. III; Göttemann, L.; Haines, B. E.; Kou, K. G. M. Synergistic Brønsted/Lewis acid catalyzed aromatic alkylation with unactivated tertiary alcohols or di-*tert*-butylperoxide to synthesize quaternary carbon centers. *Chem. Sci.* **2022**, *13*, 3539–3548.
  13. Huang, P.; Jiang, X.; Gao, D.; Wang, C.; Shi, D.-Q.; Zhao, Y. HFIP-promoted *para*-selective alkylation of anilines and phenols with tertiary alkyl bromides. *Org. Chem. Front.* **2023**, *10*, 2476–2481.
  14. Zhang, S.; Vayer, M.; Noël, F.; Vuković, V. D.; Golushko, A.; Rezajooei, N.; Rowley, C. N.; Leboëf, D.; Moran, J. Unlocking the Friedel–Crafts arylation of primary aliphatic alcohols and epoxides driven by hexafluoroisopropanol. *Chem.* **2021**, *7*, 3425–3441.

### 3.5 Experimental

#### 3.5.1 General Information

See section 1.5.1 for general information.

*Reaction setup, progress monitoring, and product purification*

In general, the catalytic reactions were not air- or moisture-sensitive; however, the iron and zinc salts are hygroscopic and quickly change color when being weighed and added to the reaction vessel. This influenced how much metal catalyst was being added because their molecular weights increase on hydration. For consistency and rigor, the iron and zinc salts were weighed and added to vials inside a nitrogen-filled glovebox. For phenols, mild oxidation during preparatory plate in open air occurred, which may discolor the final product. Unless otherwise noted, products purified by preparatory plate were pure by NMR analysis.

### 3.5.2 Experimental Procedures: Preparation of Secondary Alcohols

#### **General Procedure A:** Reductions of Ketones with $\text{LiAlH}_4$

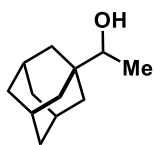
According to a modified procedure of Marino and coworkers,<sup>1</sup> To a 50 mL round-bottomed flask (flame-dried and equipped with a stirring bar) was added  $\text{LiAlH}_4$  (1 equiv). The flask and its contents were purged with  $\text{N}_2$  gas and added dry  $\text{Et}_2\text{O}$  (to produce a 0.2 M suspension). The mixture was cooled to 0 °C and added dropwise a solution of ketone (1 equiv) in dry  $\text{Et}_2\text{O}$  (1 M). The resulting suspension was allowed to stir at 0 °C for 4 h. The reaction mixture was quenched via the Fieser–Fieser workup conditions: diluted with  $\text{Et}_2\text{O}$  (30 mL), then cooled to 0 °C and dropwise added distilled water ( $\text{dH}_2\text{O}$ ) (2 equiv), 15% (w/v) aqueous  $\text{NaOH}$  (2 equiv), and  $\text{dH}_2\text{O}$  (3 equiv). The mixture was warmed to room temperature and stirred for 15 min, then added anhydrous  $\text{MgSO}_4$  was and stirred for an additional 15 min. The solids were removed by filtration and the filtrate was



concentrated under reduced pressure to obtain the secondary alcohol product. The alcohol was subsequently used without further purification.

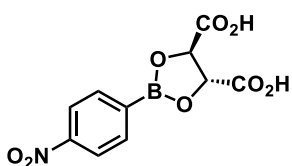
Although synthesized by General Procedure A, cycloheptanol (**3.9**), 1,2,3,4-tetrahydronaphthalen-2-ol (**3.11**), and norborneol (**3.64**) are commercially available and are not listed in the experimental section.

### 1-(Adamant-1-yl)ethanol (**3.57**)



Prepared using General Procedure A with LiAlH<sub>4</sub> (0.19 g, 5 mmol, 1 equiv), Et<sub>2</sub>O (25 mL, 0.2 M), and adamant-1-yl methyl ketone (0.89 g, 5 mmol, 1 equiv) in Et<sub>2</sub>O (5 mL, 1 M) to afford **3.57** (470.0 mg, 63%) as a colorless solid. <sup>1</sup>H NMR (500 MHz, CDCl<sub>3</sub>) δ 3.24 (q, *J* = 6.5 Hz, 1H), 1.96 (s, 3H), 1.68 (d, *J* = 12.3 Hz, 3H), 1.65–1.52 (m, 6H), 1.45 (d, *J* = 12.3 Hz, 3H), 1.06 (d, *J* = 6.6 Hz, 3H). The spectral data recorded are consistent with those previously reported.<sup>2</sup>

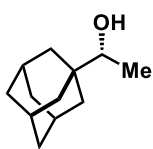
### TarB-NO<sub>2</sub> (**3.65**)



According to a modified procedure of Suri and coworkers,<sup>3</sup> an oven-dried 50 mL round bottom flask equipped with a stirring bar was added tartaric acid (0.75 g, 5 mmol, 1 equiv) followed by (4-nitrophenyl)boronic acid (0.83 g, 5 mmol, 1 equiv). The flask and its contents were purged with N<sub>2</sub> gas to displace air and create an inert atmosphere. The cap was briefly opened to add CaH<sub>2</sub> (0.42 g, 10 mmol, 2 equiv) before the flask was re-purged with N<sub>2</sub> and added dry THF (12.5 mL, 0.4 M). The flask was equipped with a water condenser and was heated to 80 °C and stirred for 1 h. The solution was cooled to rt and the solids were vacuum filtered,

rinsed with Et<sub>2</sub>O, and concentrated under reduced pressure to afford **3.65** (1.14 g, 1.1 to 1 boronic ester to 4-(nitrophenyl)boronic acid as yellow-white solids. The flask was purged with N<sub>2</sub> before diluting in dry THF (10 mL, 0.5 M) and transferring via cannula to an oven-dried, N<sub>2</sub> purged scintillation vial and stored in the freezer. <sup>1</sup>H NMR (400 MHz, THF-d<sub>8</sub>) δ 8.25–8.17 (m, 2H), 8.05–7.96 (m, 2H), 5.09 (s, 2H).

**(R)-1-(Adamant-1-yl)ethanol ((R)-3.57)**



According to a modified procedure of Suri and coworkers,<sup>6</sup> an oven-dried 2-neck round bottom flask equipped with a stir bar was added 1-adamantyl methyl ketone (0.45 g, 2.5 mmol, 1 equiv). The flask and its contents were purged with N<sub>2</sub> gas to displace air and create an inert atmosphere. To the flask was added via syringe a solution of TarB-NO<sub>2</sub> (**3.65**) in dry THF (0.5 M, 5 mL, 0.5 mmol, 1 equiv) and allowed to stir at rt for 10 minutes before cooling to 0 °C. The flask was briefly opened to air to add NaBH<sub>4</sub> (0.19 g, 5 mmol, 2 equiv) and allowed to stir at 0 °C for 0.5 h under N<sub>2</sub> with a vent needle. Light yellow solution slowly bubbles (H<sub>2</sub> formation). The reaction was slowly quenched with distilled water until bubbling stops upon addition (~4 mL). The reaction was alkalized with solid NaOH until pH of 12 (~6 normal-sized pellets) and allowed to stir for a few minutes. The orange biphasic mixture was diluted in pentane (35 mL) and the solution was washed with 2.5 M aqueous NaOH (20 mL) and sat brine (20 mL). The organic extract was dried over anhydrous MgSO<sub>4</sub>, filtered, and concentrated under reduced pressure to afford a yellow solid. Purification by flash chromatography (eluted with 2–20% EtOAc in hexanes, TLCs stained with KMnO<sub>4</sub> and heated until yellow spot appears) afforded **(R)-3.57** (0.37 g, 82%) as a white solid. R<sub>f</sub>: 0.20 (9:1

hexanes/EtOAc).  $^1\text{H}$  NMR (500 MHz,  $\text{CDCl}_3$ )  $\delta$  3.28 (q,  $J = 6.4$  Hz, 1H), 1.99 (p,  $J = 3.2$  Hz, 3H), 1.72 (d,  $J = 12.8$  Hz, 3H), 1.66–1.56 (m, 6H), 1.52–1.44 (m, 3H), 1.09 (d,  $J = 6.4$  Hz, 3H). The spectral data recorded are consistent with those previously reported.<sup>2</sup>  $[\alpha]_D^{19} = +0.850$  ( $c$  1.1,  $\text{CHCl}_3$ , ee ~45%); lit.<sup>4</sup>  $[\alpha]_D^{19} = +1.26$  ( $c$  0.95,  $\text{CHCl}_3$ , ee = 68%).

### 3.5.3 Reactions of Unactivated Secondary Alcohols

#### **General Procedure B:** Alkylations with cyclohexanol

To a one-dram vial equipped with a stirring bar was sequentially added  $\text{ZnCl}_2$  or  $\text{FeCl}_3$  (2–10  $\mu\text{mol}$ , 1–5 mol%), arene derivative (0.2 mmol, 1 equiv),  $\text{PhCl}$  (0.2 mL, 1 M), cyclohexanol (62.5  $\mu\text{L}$ , 0.6 mmol, 3 equiv), and (*R*)-camphorsulfonic acid monohydrate ((*R*)-CSA• $\text{H}_2\text{O}$ ) (37.6 mg, 0.15 mmol, 75 mol%) or (*S*)-camphorsulfonic acid ((*S*)-CSA) (35 mg, 0.15 mmol, 75 mol%). The reaction mixture was heated at 140 °C for 18 h. The solution was filtered through a 5” pipette plug of silica gel (approximately one-third filled) and eluted with hexanes/EtOAc (3:1). The solution was concentrated *in vacuo* and purified via silica gel chromatography to obtain the alkylation product.

#### **General Procedure C:** Alkylations with 2-adamantanol

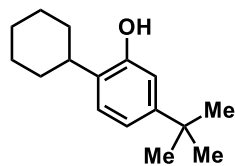
To a one-dram vial equipped with a stirring bar was sequentially added  $\text{ZnCl}_2$  or  $\text{FeCl}_3$  (10  $\mu\text{mol}$ , 5 mol%), arene derivative (0.2 mmol, 1 equiv),  $\text{PhCl}$  (0.2 mL, 1 M), 2-adamantanol (33.5 mg, 0.22 mmol, 1.1 equiv), (*R*)-camphor sulfonic acid monohydrate ((*R*)-CSA• $\text{H}_2\text{O}$ ) (37.6 mg, 0.15 mmol, 75 mol%) or (*S*)-camphor sulfonic acid ((*S*)-CSA) (35 mg, 0.15 mmol, 75 mol%). The reaction mixture was heated at 140 °C for 18 h. The solution was filtered through a silica gel plug (packed in a 5” glass pipette, approximately

one-third filled) and eluted with hexanes/EtOAc (3:1). The solution was concentrated *in vacuo* and purified via silica gel chromatography to obtain the alkylation product.

#### General Procedure D: Alkylations with other secondary alcohols

To a one-dram vial equipped with a stirring bar was sequentially added ZnCl<sub>2</sub> (0.01 mmol, 5 mol%), 3-*tert*-butylphenol (0.2 mmol, 1 equiv), PhCl (0.2 mL, 1 M), secondary alcohol (0.22–1.0 mmol, 1.1–5 equiv), and (*R*)-camphor sulfonic acid monohydrate ((*R*)-CSA•H<sub>2</sub>O) (37.6 mg, 0.15 mmol, 75 mol%). The reaction mixture was heated at 140 °C for 18 h. The solution was filtered through a silica gel plug (packed in a 5" glass pipette, approximately one-third filled) and eluted with hexanes/EtOAc (9:1) or EtOAc. The solution was concentrated *in vacuo* and purified via silica gel chromatography to obtain the alkylation product.

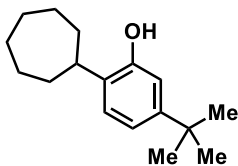
#### 5-(*tert*-Butyl)-2-cyclohexylphenol (**3.8**)



Prepared using General Procedure B with 3-*tert*-butylphenol (30.2 mg, 0.2 mmol, 1 equiv), ZnCl<sub>2</sub> (1.5 mg, 0.055 mmol, 0.05 equiv), PhCl (0.2 mL, 1.0 M), cyclohexanol (62.5 μL, 0.6 mmol, 3 equiv), and CSA•H<sub>2</sub>O (37.6 mg, 0.150 mmol, 0.75 equiv). Purification by preparative TLC (eluted with 9:1 hexanes/EtOAc) afforded **3.8** (34.5 mg, 74%) as a yellow-orange oil. R<sub>f</sub>: 0.33 (19:1 hexanes/EtOAc). <sup>1</sup>H NMR (500 MHz, CDCl<sub>3</sub>) δ 7.12 (d, *J* = 8.1 Hz, 1H), 6.95 (dd, *J* = 8.1, 2.0 Hz, 1H), 6.81 (d, *J* = 2.2 Hz, 1H), 4.74 (s, 1H), 2.77 (qt, *J* = 6.3, 2.5 Hz, 1H), 1.94–1.83 (m, 5H), 1.82–1.74 (m, 1H), 1.51–1.38 (m, 4H), 1.31 (s, 9H). <sup>13</sup>C NMR (151 MHz, CDCl<sub>3</sub>) δ 152.4, 150.2, 130.5, 126.5, 118.0, 112.7, 37.2, 34.4, 33.3, 31.4, 27.2, 26.4. IR

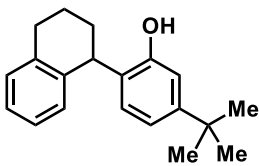
(ATR): 3342, 2925, 2852, 1414, 738  $\text{cm}^{-1}$ . HRMS (ESI+):  $m/z$   $[\text{M}+\text{H}]^+$  calculated for  $\text{C}_{16}\text{H}_{25}\text{O}$ : 233.1900; found: 233.1902.

### 5-(*tert*-Butyl)-2-cycloheptylphenol (**3.10**)



Prepared using General Procedure D with 3-*tert*-butylphenol (30.2 mg, 0.201 mmol, 1 equiv),  $\text{ZnCl}_2$  (1.7 mg, 0.012 mmol, 0.05 equiv),  $\text{PhCl}$  (0.2 mL, 1.0 M), cycloheptanol (69.6 mg, 0.609 mmol, 3 equiv), and  $\text{CSA}\cdot\text{H}_2\text{O}$  (37.8 mg, 0.151 mmol, 0.75 equiv). Purification by preparative TLC (eluted with 19:1 hexanes/ $\text{EtOAc}$   $\times$  2) afforded **3.10** (34.0 mg, 69%) as an orange oil.  $^1\text{H}$  NMR (500 MHz,  $\text{CDCl}_3$ )  $\delta$  7.09 (d,  $J$  = 8.0 Hz, 1H), 6.91 (dd,  $J$  = 8.1, 1.5 Hz, 1H), 6.78 (d,  $J$  = 2.0 Hz, 1H), 2.95–2.83 (m, 1H), 1.96–1.87 (m, 2H), 1.85–1.77 (m, 2H), 1.72–1.52 (m, 8H), 1.28 (s, 9H).  $^{13}\text{C}$  NMR (101 MHz,  $\text{CDCl}_3$ )  $\delta$  151.8, 150.0, 132.4, 126.8, 118.0, 112.7, 39.3, 35.5, 34.4, 31.5, 28.1, 27.6. IR (ATR): 3380, 2923, 2855, 1617, 1577, 1504, 1460, 1415, 1362, 1292, 1264, 1233, 1203, 1168, 1128, 1089, 931, 863, 814, 738, 705, 651, 576, 554, 485, 458, 451, 440, 404  $\text{cm}^{-1}$ . HRMS (ESI+):  $m/z$   $[\text{M}+\text{H}]^+$  calculated for  $\text{C}_{17}\text{H}_{27}\text{O}$ : 247.2056; found: 247.2061.

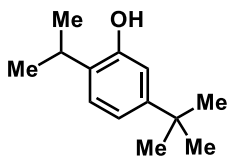
### 5-(*tert*-Butyl)-2-(1,2,3,4-tetrahydronaphthalen-1-yl)phenol (**3.12**)



Prepared using General Procedure D with 3-*tert*-butylphenol (30.2 mg, 0.201 mmol, 1 equiv),  $\text{ZnCl}_2$  (1.5 mg, 0.011 mmol, 0.05 equiv),  $\text{PhCl}$  (0.2 mL, 1.0 M), 2-tetralol (**3.11**) (53.5  $\mu\text{L}$ , 0.399 mmol, 2 equiv), and  $\text{CSA}\cdot\text{H}_2\text{O}$  (37.5 mg, 0.150 mmol, 0.75 equiv). Purification by preparative TLC (eluted with 19:1 hexanes/ $\text{EtOAc}$ ) afforded **3.12** (45.4 mg, 81%) as an orange oil.  $R_f$ : 0.27 (19:1 hexanes/ $\text{EtOAc}$ ).  $^1\text{H}$  NMR (600 MHz,  $\text{CDCl}_3$ )  $\delta$  7.18–7.12 (m, 2H), 7.10–7.04 (m,

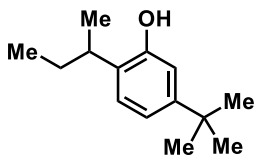
1H), 6.98 (d,  $J = 7.8$  Hz, 1H), 6.89–6.84 (m, 2H), 6.81 (d,  $J = 1.8$  Hz, 1H), 4.48 (s, 1H), 4.28 (dd,  $J = 8.8, 5.7$  Hz, 1H), 2.97–2.80 (m, 2H), 2.17–2.08 (m, 1H), 1.99–1.90 (m, 2H), 1.82–1.73 (m, 1H), 1.29 (s, 9H).  $^{13}\text{C}$  NMR (151 MHz,  $\text{CDCl}_3$ )  $\delta$  152.9, 151.0, 138.3, 137.9, 130.5, 129.6, 129.5, 129.5, 126.5, 126.3, 117.9, 113.6, 40.9, 34.5, 31.5, 30.9, 29.9, 21.7. IR (ATR): 3312, 2971, 1379, 1087, 1045, 879, 653  $\text{cm}^{-1}$ . HRMS (ESI $^-$ ):  $m/z$   $[\text{M}-\text{H}]^-$  calculated for  $\text{C}_{20}\text{H}_{23}\text{O}$ : 279.1754; found 279.1765.

### 5-(*tert*-Butyl)-2-isopropylphenol (**3.13**)



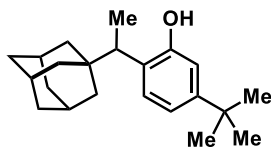
Prepared using General Procedure D with 3-*tert*-butylphenol (30.1 mg, 0.2 mmol, 1 equiv),  $\text{ZnCl}_2$  (1.5 mg, 0.011 mol, 0.05 equiv),  $\text{PhCl}$  (0.2 mL, 1.0 M), isopropanol (76.5  $\mu\text{L}$ , 1.0 mmol, 5 equiv), and  $\text{CSA}\cdot\text{H}_2\text{O}$  (37.5 mg, 0.15 mmol, 0.75 equiv). Purification by preparative TLC (eluted with 19:1 hexanes/EtOAc) afforded **3.13** (26.7 mg, 70%) as a light-yellow-white solid. Mp 53–56  $^\circ\text{C}$ .  $R_f$ : 0.34 (19:1 hexanes/EtOAc).  $^1\text{H}$  NMR (500 MHz,  $\text{CDCl}_3$ )  $\delta$  7.15 (d,  $J = 8.0$  Hz, 1H), 6.97 (dd,  $J = 8.0, 2.0$  Hz, 1H), 6.81 (d,  $J = 1.9$  Hz, 1H), 4.69 (s, 1H), 3.18 (h,  $J = 6.9$  Hz, 1H), 1.32 (s, 9H), 1.28 (d,  $J = 6.9$  Hz, 6H).  $^{13}\text{C}$  NMR (151 MHz,  $\text{CDCl}_3$ )  $\delta$  152.4, 150.3, 131.3, 126.0, 118.0, 112.7, 34.4, 31.5, 26.9, 22.8. IR (ATR): 3349, 2960, 2869, 1415, 1156, 1082, 932, 817, 739  $\text{cm}^{-1}$ . HRMS (ESI $^+$ ):  $m/z$   $[\text{M}+\text{H}]^+$  calculated for  $\text{C}_{13}\text{H}_{21}\text{O}$ : 193.1587; found: 193.1583.

### 2-(*sec*-Butyl)-5-(*tert*-butyl)phenol (**3.14**)



Prepared by L. Rangel using General Procedure D with 3-*tert*-butylphenol (30.1 mg, 0.2 mmol, 1 equiv), ZnCl<sub>2</sub> (1.5 mg, 0.011 mol, 0.05 equiv), PhCl (0.2 mL, 1.0 M), *sec*-butanol (92.0 μL, 1 mmol, 5 equiv), and CSA•H<sub>2</sub>O (37.5 mg, 0.15 mmol, 0.75 equiv). Purification by preparative TLC (eluted with 19:1 hexanes/EtOAc) afforded **3.14** (22.1 mg, 54%) as a colorless oil. <sup>1</sup>H NMR (600 MHz, CDCl<sub>3</sub>) δ 7.07 (d, *J* = 8.0 Hz, 1H), 6.92 (dt, *J* = 8.0, 1.5 Hz, 1H), 6.78 (t, *J* = 1.5 Hz, 1H), 4.57 (s, 1H), 2.89 (sextet, *J* = 7.0 Hz, 1H), 1.70–1.63 (m, 1H), 1.58 (dq, *J* = 13.9, 6.9 Hz, 2H), 1.29 (s, 9H), 1.23 (dd, *J* = 6.9, 1.1 Hz, 3H), 0.88 (dt, *J* = 7.4, 1.1 Hz, 3H). <sup>13</sup>C NMR (151 MHz, CDCl<sub>3</sub>) δ 157.2, 152.7, 150.2, 126.7, 118.0, 112.7, 34.4, 33.9, 31.5, 30.0, 20.5, 12.4. IR (ATR): 3311, 2968, 1417, 1087, 1045, 879, 655 cm<sup>-1</sup>. HRMS (ESI<sup>-</sup>): *m/z* [M-H]<sup>-</sup> calculated for C<sub>14</sub>H<sub>23</sub>O: 205.1598; found: 205.1601.

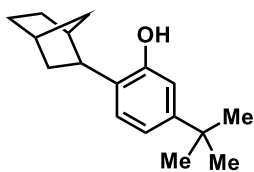
### 2-(1-Adamant-1-yl)ethyl)-5-(*tert*-butyl)phenol (**3.15**)



Prepared using General Procedure D with 3-*tert*-butylphenol (30.0 mg, 0.2 mmol, 1 equiv), ZnCl<sub>2</sub> (1.4 mg, 0.01 mmol, 0.05 equiv), PhCl (0.2 mL, 1.0 M), 1-(adamant-1-yl)ethanol (**3.57**) or (*R*)-1-(adamant-1-yl)ethanol (**(R)-3.57**) (72.2 mg, 0.40 mmol, 2 equiv), and CSA•H<sub>2</sub>O (37.5 mg, 0.15 mmol, 0.75 equiv). Purification by preparative TLC (eluted with 19:1 hexanes/EtOAc) or flash chromatography (eluted with 0–10% EtOAc in hexanes) afforded **3.15** (46.5–54.7 mg, 74–87%) as an orange oil. R<sub>f</sub>: 0.37 (19:1 hexanes/EtOAc). <sup>1</sup>H NMR (600 MHz, CDCl<sub>3</sub>) δ 7.02 (d, *J* = 8.1 Hz, 1H), 6.92–6.87 (m, 1H), 6.78 (d, *J* = 2.1 Hz, 1H), 4.60 (s, 1H), 2.74 (q, *J* = 7.3 Hz, 1H), 1.93 (s, 3H), 1.67–1.62 (m, 5H), 1.57 (d, *J* = 12.6 Hz, 4H), 1.50–1.45

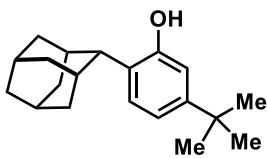
(m, 3H), 1.29 (s, 9H), 1.18 (d,  $J = 7.2$  Hz, 3H).  $^{13}\text{C}$  NMR (151 MHz,  $\text{CDCl}_3$ )  $\delta$  153.0, 150.0, 129.0, 127.0, 117.3, 112.4, 41.0, 39.8, 37.3, 36.3, 34.4, 31.5, 28.9, 14.4. IR (ATR): 3314, 2971, 1379, 1087, 1045, 879, 657  $\text{cm}^{-1}$ . HRMS (ESI $^-$ ):  $m/z$   $[\text{M}-\text{H}]^-$  calculated for  $\text{C}_{22}\text{H}_{31}\text{O}$ : 311.2380; found 311.2395.

### 2-(Norborn-2-yl)-5-(*tert*-butyl)phenol (**3.17**)



Prepared by L. Rangel using General Procedure D with 3-*tert*-butylphenol (30 mg, 0.2 mmol, 1 equiv),  $\text{ZnCl}_2$  (1.5 mg, 0.055 mmol, 0.05 equiv),  $\text{PhCl}$  (0.2 mL, 1.0 M), norbornan-2-ol (24.7 mg, 0.22 mmol, 1.1 equiv), and  $\text{CSA}\cdot\text{H}_2\text{O}$  (37.6 mg, 0.15 mmol, 0.75 equiv). Purification by preparative TLC (eluted with 9:1 hexanes/EtOAc) afforded **3.17** (40.2 mg, 82%) as a yellow-orange oil.  $^1\text{H}$  NMR (400 MHz,  $\text{CDCl}_3$ )  $\delta$  7.14 (d,  $J = 8.1$  Hz, 1H), 6.93 (dd,  $J = 8.1, 2.0$  Hz, 1H), 6.84 (d,  $J = 2.0$  Hz, 1H), 4.73 (s, 1H), 2.82 (dd,  $J = 9.1, 5.3$  Hz, 1H), 2.45–2.24 (m, 2H), 1.81 (ddd,  $J = 11.7, 8.8, 2.3$  Hz, 1H), 1.75–1.51 (m, 4H), 1.47–1.35 (m, 2H), 1.31 (s, 9H), 1.24 (ddd,  $J = 9.7, 2.3, 1.5$  Hz, 1H).  $^{13}\text{C}$  NMR (151 MHz,  $\text{CDCl}_3$ )  $\delta$  153.1, 150.2, 129.9, 125.7, 117.4, 112.7, 41.1, 40.4, 38.2, 37.0, 36.3, 34.4, 31.5, 30.4, 29.2. IR (ATR): 3341, 2949, 2867, 1573, 1413, 1295, 1234, 1092, 932, 814  $\text{cm}^{-1}$ . HRMS (ESI $^+$ ):  $m/z$   $[\text{M}+\text{H}]^+$  calculated for  $\text{C}_{17}\text{H}_{25}\text{O}$ : 245.1900; found: 245.1901.

### 2-(Adamantan-2-yl)-5-(*tert*-butyl)phenol (**3.18**)

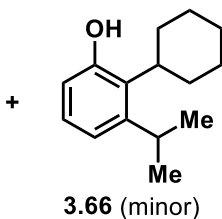
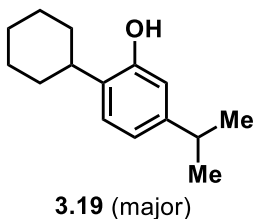


Prepared using General Procedure C with 3-*tert*-butylphenol (30.1 mg, 0.2 mmol, 1 equiv),  $\text{ZnCl}_2$  (1.5 mg, 0.011 mol, 0.05 equiv),  $\text{PhCl}$  (0.2 mL, 1.0 M), adamantan-2-ol (33.9 mg, 0.223 mmol, 1.1 equiv), and  $\text{CSA}\cdot\text{H}_2\text{O}$  (37.48 mg, 0.15 mmol, 0.75 equiv). Purification by preparative TLC



(eluted with 9:1 hexanes/EtOAc) afforded **3.18** (43 mg, 76%) as a pale-yellow-white solid. Mp 135–139 °C. R<sub>f</sub>: 0.35 (19:1 hexanes/EtOAc). <sup>1</sup>H NMR (500 MHz, CDCl<sub>3</sub>) δ 7.37 (d, *J* = 8.1 Hz, 1H), 6.94 (dd, *J* = 8.1, 2.0 Hz, 1H), 6.78 (d, *J* = 2.0 Hz, 1H), 4.67 (s, 1H), 3.15 (s, 1H), 2.38–2.33 (m, 2H), 2.05 (dd, *J* = 12.8, 2.9 Hz, 2H), 2.02–1.92 (m, 5H), 1.88 (p, *J* = 3.2 Hz, 1H), 1.82–1.77 (m, 2H), 1.68–1.63 (m, 2H), 1.30 (s, 9H). <sup>13</sup>C NMR (151 MHz, CDCl<sub>3</sub>) δ 153.6, 150.2, 128.5, 127.9, 117.3, 113.0, 43.9, 40.1, 38.1, 34.3, 33.0, 31.4, 31.2, 28.3, 27.9. IR (ATR): 3301, 2899, 2849, 1615, 1450, 1411, 1192, 1092, 935, 859, 827, 731, 650 cm<sup>-1</sup>. HRMS (ESI<sup>+</sup>): *m/z* [M+H]<sup>+</sup> calculated for C<sub>20</sub>H<sub>29</sub>O: 285.2213; found 285.2223.

### 2-Cyclohexyl-5-isopropylphenol (**3.19**)



Prepared by V. K. Nguyen using General Procedure B with 3-isopropylphenol (27.5 μL, 0.2 mmol, 1 equiv), ZnCl<sub>2</sub> (1.4 mg, 0.01 mmol, 0.05 equiv), PhCl (0.2 mL, 1.0 M), cyclohexanol

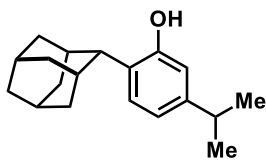
(62.5 μL, 0.6 mmol, 3 equiv), and CSA•H<sub>2</sub>O (37.4 mg, 0.15 mmol, 0.75 equiv).

Purification by preparative TLC (eluted with 9:1 hexanes/EtOAc) afforded a 9:1 mixture of both *ortho*-substituted **3.19** and **3.66** (21.5 mg, 49%) as an orange oil. R<sub>f</sub>: 0.27 (9:1 hexanes/EtOAc).

<sup>1</sup>H NMR (500 MHz, CDCl<sub>3</sub>) δ 7.10 (d, *J* = 7.9 Hz, 1H), 6.79 (dd, *J* = 7.9, 1.8 Hz, 1H), 6.64 (t, *J* = 2.0 Hz, 1H), 4.74 (s, 1H), 2.84 (h, *J* = 6.9 Hz, 1H), 2.79–2.70 (m, 1H), 1.93–1.81 (m, 4H), 1.81–1.72 (m, 1H), 1.49–1.35 (m, 4H), 1.34–1.24 (m, 1H), 1.23 (d, *J* = 6.9 Hz, 6H). <sup>13</sup>C NMR (151 MHz, CDCl<sub>3</sub>) δ 152.7, 147.8, 130.9, 126.8, 119.1, 113.5, 37.2, 33.7, 33.3, 27.2, 26.5, 24.1. IR (ATR): 3390, 2923, 2850, 1579, 1423, 738 cm<sup>-1</sup>.

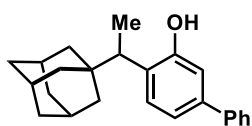
<sup>1</sup>. HRMS (ESI<sup>+</sup>): *m/z* [M+H]<sup>+</sup> calculated for C<sub>15</sub>H<sub>23</sub>O: 219.1743; found: 219.1744.

### 2-(Adamant-2-yl)-5-isopropylphenol (**3.20**)



Prepared using General Procedure C with 3-isopropylphenol (27.5  $\mu\text{L}$ , 0.2 mmol, 1 equiv),  $\text{ZnCl}_2$  (1.7 mg, 0.012 mmol, 0.05 equiv),  $\text{PhCl}$  (0.2 mL, 1.0 M), adamantan-2-ol (33.6 mg, 0.22 mmol, 1.1 equiv), and  $\text{CSA}\cdot\text{H}_2\text{O}$  (37.6 mg, 0.15 mmol, 0.75 equiv). Purification by preparative TLC (eluted with 9:1 hexanes/EtOAc) afforded **3.20** (46.0 mg, 85%) as a yellow-white solid. Mp 115–118  $^\circ\text{C}$ . R<sub>f</sub>: 0.41 (9:1 hexanes/EtOAc).  $^1\text{H}$  NMR (500 MHz,  $\text{CDCl}_3$ )  $\delta$  7.34 (d,  $J$  = 7.9 Hz, 1H), 6.78 (dd,  $J$  = 7.8, 1.2 Hz, 1H), 6.62 (d,  $J$  = 1.4 Hz, 1H), 4.59 (s, 1H), 3.13 (s, 1H), 2.83 (dt,  $J$  = 13.4, 6.3 Hz, 1H), 2.33 (s, 2H), 2.03 (d,  $J$  = 12.4 Hz, 2H), 1.96 (d,  $J$  = 5.4 Hz, 5H), 1.78 (s, 2H), 1.64 (d,  $J$  = 12.7 Hz, 2H), 1.23 (d,  $J$  = 6.9 Hz, 6H).  $^{13}\text{C}$  NMR (151 MHz,  $\text{CDCl}_3$ )  $\delta$  153.9, 147.9, 128.9, 128.1, 118.5, 113.7, 44.0, 40.2, 38.2, 33.6, 33.0, 31.3, 28.3, 27.9, 24.1. IR (ATR): 3411, 2901, 2844, 1619, 1420, 1210, 1094, 1056, 947, 854, 830, 729, 645  $\text{cm}^{-1}$ . HRMS (ESI<sup>-</sup>):  $m/z$   $[\text{M}-\text{H}]^-$  calculated for  $\text{C}_{19}\text{H}_{25}\text{O}$ : 269.1911; found 269.1922.

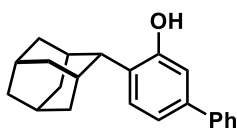
### 2-(1-Adamant-1-yl)ethyl)-5-phenylphenol (**3.21**)



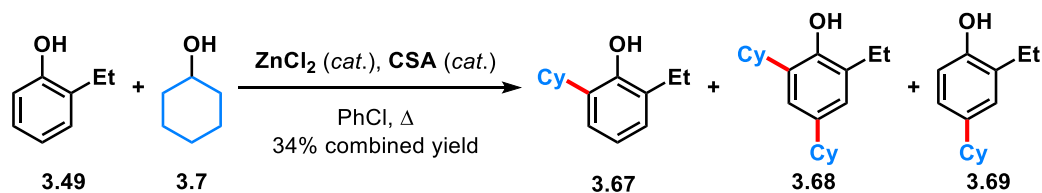
Prepared using General Procedure B with 3-phenylphenol (90% technical grade, 38.1 mg, 0.201 mmol, 1 equiv),  $\text{ZnCl}_2$  (1.5 mg, 0.011 mmol, 0.05 equiv),  $\text{PhCl}$  (0.2 mL, 1.0 M), 1-(adamant-1-yl)ethanol (**3.57**) (72.4 mg, 0.401 mmol, 2 equiv), and  $\text{CSA}\cdot\text{H}_2\text{O}$  (37.7 mg, 0.151 mmol, 0.75 equiv). Purification by two cycles of preparative TLC (eluted with 19:1 hexanes/EtOAc) afforded **3.21** (25.1 mg, 38%) as an orange-white solid. Mp 160–162  $^\circ\text{C}$ . R<sub>f</sub>: 0.19 (19:1 hexanes/EtOAc).  $^1\text{H}$  NMR (500 MHz,  $\text{CDCl}_3$ )  $\delta$  7.61–7.52 (m, 2H), 7.42 (t,  $J$  = 7.5 Hz, 2H), 7.32 (t,  $J$  = 7.4 Hz, 1H), 7.20–

7.11 (m, 2H), 7.02 (d,  $J = 1.9$  Hz, 1H), 4.73 (s, 1H), 2.84 (q,  $J = 7.3$  Hz, 1H), 1.95 (s, 4H), 1.71–1.48 (m, 11H), 1.22 (d,  $J = 7.2$  Hz, 3H).  $^{13}\text{C}$  NMR (151 MHz,  $\text{CDCl}_3$ )  $\delta$  153.8, 140.7, 139.7, 129.9, 129.6, 128.8, 127.3, 127.0, 119.1, 113.8, 41.1, 39.8, 37.3, 36.4, 28.9, 14.4. IR (ATR): 3556, 2903, 2885, 2845, 1484, 1447, 1407, 1310, 1220, 1184, 1176, 1115, 1106, 1029, 901, 855, 932, 760, 745, 712, 697, 673, 647, 623, 509  $\text{cm}^{-1}$ . HRMS (ESI+):  $m/z$   $[\text{M}+\text{H}]^+$  calculated for  $\text{C}_{24}\text{H}_{28}\text{O}$ : 333.2213; found 333.2200.

### 2-(Adamant-2-yl)-5-phenylphenol (**3.22**)



Prepared using General Procedure C with 3-phenylphenol (90% technical grade, 37.9 mg, 0.200 mmol, 1 equiv),  $\text{ZnCl}_2$  (1.3 mg, 9.5  $\mu\text{mol}$ , 0.05 equiv),  $\text{PhCl}$  (0.2 mL, 1.0 M), adamantan-2-ol (33.6 mg, 0.221 mmol, 1.1 equiv), and  $\text{CSA}\cdot\text{H}_2\text{O}$  (37.8 mg, 0.151 mmol, 0.75 equiv). Purification by flash chromatography (eluted with 0–20% EtOAc in hexanes) afforded **3.22** (43.0 mg, 64%) as a light orange-white solid. Mp 104–107  $^\circ\text{C}$ .  $R_f$ : 0.34 (9:1 hexanes/EtOAc).  $^1\text{H}$  NMR (500 MHz,  $\text{CDCl}_3$ )  $\delta$  7.60–7.55 (m, 2H), 7.50 (d,  $J = 8.0$  Hz, 1H), 7.42 (t,  $J = 7.6$  Hz, 2H), 7.32 (t,  $J = 7.3$  Hz, 1H), 7.16 (dd,  $J = 8.8, 1.1$  Hz, 1H), 6.99 (d,  $J = 1.9$  Hz, 1H), 4.77 (s, 1H), 3.22 (s, 1H), 2.39 (s, 2H), 2.07 (d,  $J = 12.8$  Hz, 2H), 2.01–1.98 (m, 4H), 1.90 (s, 1H), 1.80 (s, 2H), 1.68 (d,  $J = 12.5$  Hz, 2H), 1.25 (s, 1H).  $^{13}\text{C}$  NMR (151 MHz,  $\text{CDCl}_3$ )  $\delta$  154.3, 140.7, 139.9, 130.8, 128.8, 128.7, 127.3, 127.0, 119.2, 114.3, 44.1, 40.1, 38.1, 33.0, 31.3, 28.3, 27.9. IR (ATR): 3510, 2897, 2845, 1563, 1485, 1448, 1406, 1172, 1108, 857, 758, 694  $\text{cm}^{-1}$ . HRMS (ESI–):  $m/z$   $[\text{M}-\text{H}]^-$  calculated for  $\text{C}_{22}\text{H}_{23}\text{O}$ : 303.1765; found 303.1765.



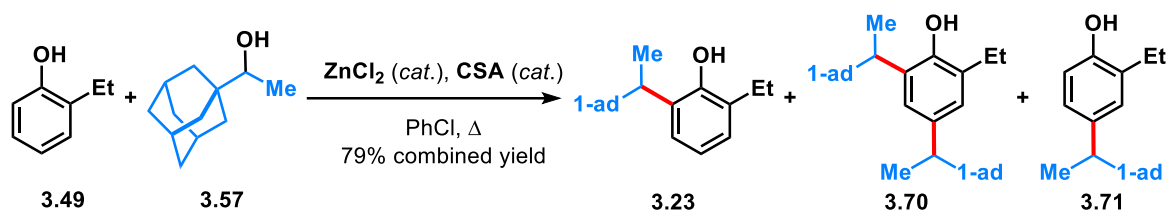
The reaction was performed by V. K. Nguyen using General Procedure B with 2-ethylphenol (23.5  $\mu$ L, 0.20 mmol, 1 equiv), ZnCl<sub>2</sub> (1.4 mg, 0.01 mmol, 0.05 equiv), PhCl (0.2 mL, 1.0 M), cyclohexanol (62.5  $\mu$ L, 0.6 mmol, 3 equiv), and CSA (35 mg, 0.15 mmol, 0.75 equiv). Purification by preparative TLC (eluted with 19:1 hexanes/EtOAc) afforded an inseparable 3:1 mixture of **3.67** (8.7 mg, 21%, 25% brsm) and dialkylated **3.68** (3.7 mg, 6%, 8% brsm) with compound **3.67** being the major product. The mono-*para*-substituted **3.69** (7%, 9% brsm) was observed as a minor product.

**2-Cyclohexyl-6-ethylphenol (3.67):** The NMR data can be extracted from the NMR spectra of the mixture: <sup>1</sup>H NMR (600 MHz, CDCl<sub>3</sub>)  $\delta$  7.06 (dd,  $J$  = 7.7, 1.7 Hz, 1H), 7.00 (dd,  $J$  = 7.4, 1.7 Hz, 1H), 6.87 (t,  $J$  = 7.7 Hz, 1H), 4.71 (s, 1H), 2.77 (dq,  $J$  = 7.2, 3.2 Hz, 1H), 2.63 (q,  $J$  = 7.6 Hz, 2H), 2.07–1.91 (m, 4H), 1.84–1.70 (m, 2H), 1.49–1.35 (m, 4H), 1.26 (t,  $J$  = 7.6 Hz, 3H). <sup>13</sup>C NMR (151 MHz, CDCl<sub>3</sub>)  $\delta$  150.7, 133.1, 129.2, 126.4, 124.5, 120.7, 37.7, 33.4, 27.2, 26.4, 23.3, 14.0. IR (ATR): 3574, 3038, 2963, 1448, 1187, 774 cm<sup>-1</sup>. HRMS (ESI<sup>+</sup>):  $m/z$  [M+H]<sup>+</sup> calculated for C<sub>14</sub>H<sub>21</sub>O: 205.1587; found: 205.1579.

**2,4-Dicyclohexyl-6-ethylphenol (3.68):** The NMR data can be extracted from the NMR spectra of the mixture: <sup>1</sup>H NMR (600 MHz, CDCl<sub>3</sub>)  $\delta$  6.89 (d,  $J$  = 2.2 Hz, 1H), 6.84 (d,  $J$  = 2.2 Hz, 1H), 4.56 (s, 1H), 2.80 (dq,  $J$  = 7.2, 3.2 Hz, 2H), 2.77 (dq,  $J$  = 7.2, 3.2 Hz, 1H), 2.63 (q,  $J$  = 7.6 Hz, 2H), 2.07–1.91 (m, 4H), 1.84–1.70 (m, 2H), 1.49–1.35 (m, 4H), 1.26 (t,  $J$  = 7.6 Hz, 3H). <sup>13</sup>C NMR (151 MHz, CDCl<sub>3</sub>)  $\delta$  148.7, 140.3, 132.8, 128.8, 124.7, 122.8,

44.3, 37.8, 35.0, 33.4, 27.3, 27.2, 26.5, 26.4, 23.5, 14.1. IR (ATR): 3574, 3038, 2963, 1448, 1187, 774  $\text{cm}^{-1}$ . HRMS (ESI+):  $m/z$   $[\text{M}+\text{H}]^+$  calculated for  $\text{C}_{20}\text{H}_{31}\text{O}$ : 287.2369; found: 287.2359.

**4-Cyclohexyl-2-ethylphenol-4-cyclohexyl-2-ethylphenol (3.69):** Isolated as an inseparable 2:1 mixture of **3.49/3.69** with compound **3.49** being the major product. The  $^1\text{H}$  NMR data can be extracted from the NMR spectrum of the mixture:  $^1\text{H}$  NMR (600 MHz,  $\text{CDCl}_3$ )  $\delta$  6.98 (d,  $J = 2.2$  Hz, 1H), 6.92 (dd,  $J = 8.1, 2.2$  Hz, 1H), 6.69 (d,  $J = 8.1$  Hz, 1H), 4.53 (s, 1H), 2.63 (q,  $J = 7.6$  Hz, 2H) 2.41 (d,  $J = 10.9$  Hz, 1H), 1.88–1.79 (m, 2H), 1.73 (d,  $J = 13.3$  Hz, 2H), 1.62 (d,  $J = 25.8$  Hz, 2H), 1.49–1.35 (m, 4H), 1.26 (t,  $J = 7.6$  Hz, 3H).



The reaction was performed using General Procedure D with 2-ethylphenol (24.0  $\mu\text{L}$ , 0.20 mmol, 1 equiv),  $\text{ZnCl}_2$  (1.5 mg, 0.011 mmol, 0.05 equiv),  $\text{PhCl}$  (0.2 mL, 1.0 M), 1-(adamant-1-yl)ethanol (72.7 mg, 0.403 mmol, 2 equiv), and  $\text{CSA}\cdot\text{H}_2\text{O}$  (37.8 mg, 0.151 mmol, 0.75 equiv). Purification by preparative TLC (eluted with 19:1 hexanes/ $\text{EtOAc}$ ) afforded an inseparable 1.33:1 mixture of **3.23** (19.3 mg, 34%) and dialkylated **3.70** (22.7 mg, 25%) as a light yellow oil, with compound **3.23** being the major product. The mono-*para*-substituted **3.71** (19%) was observed as a pale yellow oil as a minor product.

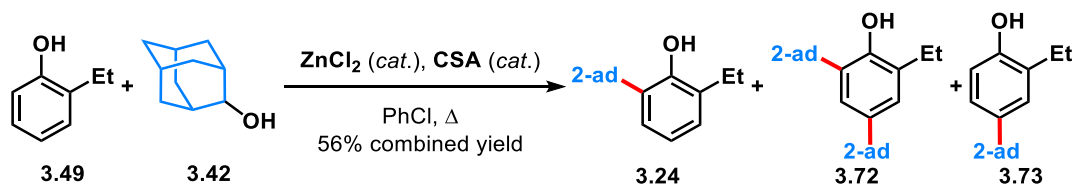
**2-(2-(Adamant-1-yl)ethyl)-6-ethylphenol (3.23):**  $R_f$ : 0.45 (19:1 hexanes/ $\text{EtOAc}$ ). the  $^1\text{H}$  NMR data can be extracted from the NMR spectrum of the mixture:  $^1\text{H}$  NMR (600 MHz,  $\text{CDCl}_3$ )  $\delta$  6.99 (t,  $J = 7.5$  Hz, 1H), 6.85 (t,  $J = 7.5$  Hz, 1H), 6.73 (d,  $J = 10.6$  Hz, 1H), 4.56

(s, 1H), 2.82–2.73 (m, 1H), 2.70–2.58 (m, 2H), 1.96–1.91 (m, 3H) 1.70–1.38 (m, 12H) 1.32–1.23 (m, 3H), 1.21 (d,  $J = 7.0$  Hz, 3H). indistinguishable mixture of **3.23** and two diastereomers of **3.70**:  $^{13}\text{C}$  NMR (101 MHz,  $\text{CDCl}_3$ )  $\delta$  151.4, 149.3, 135.3, 135.1, 129.7, 129.1, 128.6, 128.5, 128.0, 127.7, 127.6, 127.4, 127.0, 126.8, 126.5, 126.2, 119.7, 50.5, 50.4, 41.6, 41.5, 41.4, 40.3, 40.0, 39.9, 39.8, 37.4, 37.3, 37.2, 36.5, 36.3, 35.5, 29.0, 28.9, 28.9, 23.8, 23.7, 23.6, 14.6, 14.6, 14.5, 14.4, 14.2, 14.2, 14.0. IR (ATR): 3608, 2966, 2901, 2847, 1451, 1378, 1361, 1345, 1312, 1264, 1183, 1148, 1107, 1075, 889, 829, 816, 797, 738, 705, 606, 567, 420  $\text{cm}^{-1}$ . HRMS (ESI $^-$ ):  $m/z$   $[\text{M}-\text{H}]^-$  calculated for  $\text{C}_{20}\text{H}_{28}\text{O}$ : 283.2067; found: 283.2094.

**2,4-Bis-(2-(adamant-1-yl)ethyl)-6-ethylphenol (3.70)**:  $R_f$ : 0.45 (19:1 hexanes/EtOAc). the  $^1\text{H}$  NMR data can be extracted from the NMR spectrum of the mixture:  $^1\text{H}$  NMR (600 MHz,  $\text{CDCl}_3$ )  $\delta$  6.99 (s, 1H), 6.70 (s, 1H), 4.74 (s, 1H), 2.82–2.73 (m, 1H), 2.70–2.58 (m, 2H), 2.28 (q,  $J = 7.2$  Hz, 1H), 1.96–1.91 (m, 6H) 1.70–1.38 (m, 24H) 1.32–1.23 (m, 6H), 1.20–1.18 (d,  $J = 7.0$  Hz, 3H). indistinguishable mixture of **3.23** and two diastereomers of **3.70**:  $^{13}\text{C}$  NMR (101 MHz,  $\text{CDCl}_3$ )  $\delta$  151.4, 149.3, 135.3, 135.1, 129.7, 129.1, 128.6, 128.5, 128.0, 127.7, 127.6, 127.4, 127.0, 126.8, 126.5, 126.2, 119.7, 50.5, 50.4, 41.6, 41.5, 41.4, 40.3, 40.0, 39.9, 39.8, 37.4, 37.3, 37.2, 36.5, 36.3, 35.5, 29.0, 28.9, 28.9, 23.8, 23.7, 23.6, 14.6, 14.6, 14.5, 14.4, 14.2, 14.2, 14.0. IR (ATR): 3608, 2966, 2901, 2847, 1451, 1378, 1361, 1345, 1312, 1264, 1183, 1148, 1107, 1075, 889, 829, 816, 797, 738, 705, 606, 567, 420  $\text{cm}^{-1}$ . HRMS (ESI $^-$ ):  $m/z$   $[\text{M}-\text{H}]^-$  calculated for  $\text{C}_{32}\text{H}_{46}\text{O}$ : 445.3476; found: 445.3516.

**4-(2-(Adamant-1-yl)ethyl)-2-ethylphenol (3.71)**:  $^1\text{H}$  NMR (600 MHz,  $\text{CDCl}_3$ )  $\delta$  6.86 (s, 1H), 6.82 (d,  $J = 8.2$  Hz, 1H), 6.66 (d,  $J = 8.1$  Hz, 1H), 4.49 (s, 1H), 2.62 (q,  $J = 7.6$  Hz,

2H), 2.28 (q,  $J = 7.3$  Hz, 1H), 1.94–1.90 (m, 3H), 1.63 (d,  $J = 12.1$  Hz, 3H), 1.57–1.50 (m, 6H), 1.43–1.38 (m, 3H), 1.23 (t,  $J = 7.5$  Hz, 3H), 1.18 (d,  $J = 7.3$  Hz, 3H).  $^{13}\text{C}$  NMR (151 MHz,  $\text{CDCl}_3$ )  $\delta$  151.4, 136.8, 130.3, 128.6, 127.5, 114.2, 50.2, 40.1, 37.3, 35.3, 28.9, 23.2, 14.5, 14.3. IR (ATR): 3423, 2967, 2901, 2847, 1610, 1505, 1448, 1377, 1360, 1345, 1313, 1264, 1178, 1116, 1047, 895, 821, 798, 737, 704, 654, 602, 473, 451, 411  $\text{cm}^{-1}$ . HRMS (ESI $^-$ ):  $m/z$   $[\text{M}+\text{HCOO}]^-$  calculated for  $\text{C}_{20}\text{H}_{28}\text{O}$ : 329.2122; found: 329.2125.



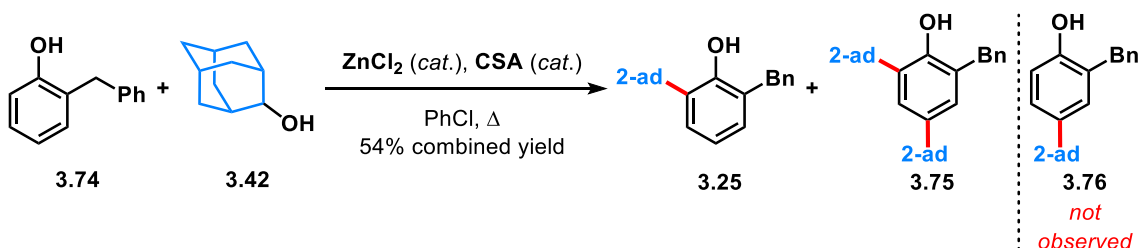
The reaction was performed using General Procedure C with 2-ethylphenol (23.5  $\mu\text{L}$ , 0.20 mmol, 1 equiv),  $\text{ZnCl}_2$  (1.4 mg, 0.01 mmol, 0.05 equiv), PhCl (0.2 mL, 1.0 M), 2-adamantanol (33.5 mg, 0.22 mmol, 1.1 equiv), and CSA (35 mg, 0.15 mmol, 0.75 equiv). Purification by preparative TLC (eluted with 19:1 hexanes/EtOAc) afforded an inseparable 2:1 mixture of **3.24** (16.9 mg, 33%) and dialkylated **3.72** (13.2 mg, 17%) with compound **3.24** being the major product. The mono-*para*-substituted **3.73** (<6%) was observed as a minor product.

**2-(Adamantan-2-yl)-6-ethylphenol (3.24):** The NMR data can be extracted from the NMR spectra of the mixture:  $^1\text{H}$  NMR (500 MHz,  $\text{CDCl}_3$ )  $\delta$  7.32 (d,  $J = 7.8$  Hz, 1H), 7.03 (d,  $J = 7.5$  Hz, 1H), 6.87 (t,  $J = 7.6$  Hz, 1H), 4.70 (s, 1H), 3.17 (s, 1H), 2.62 (q,  $J = 7.6$  Hz, 2H), 2.34 (s, 2H), 2.08–1.93 (m, 7H), 1.92–1.84 (m, 2H), 1.79 (s, 2H), 1.67 (d,  $J = 12.6$  Hz, 2H), 1.25 (t,  $J = 7.5$  Hz, 3H).  $^{13}\text{C}$  NMR (151 MHz,  $\text{CDCl}_3$ )  $\delta$  150.7, 131.1, 129.2, 126.5, 125.8, 120.0, 44.4, 40.3, 38.2, 33.0, 31.4, 28.3, 27.9, 23.2, 14.0. IR (ATR): 3600, 3046,

2901, 1450, 1187, 735  $\text{cm}^{-1}$ . HRMS (ESI+):  $m/z$   $[\text{M}+\text{H}]^+$  calculated for  $\text{C}_{18}\text{H}_{25}\text{O}$ : 257.1900; found: 257.1892.

**2,4-(Diadamantan-2-yl)-6-ethylphenol (3.72):** The NMR data can be extracted from the NMR spectra of the mixture:  $^1\text{H}$  NMR (500 MHz,  $\text{CDCl}_3$ )  $\delta$  7.29 (d,  $J = 2.2$  Hz, 1H), 6.98 (d,  $J = 2.2$  Hz, 1H), 4.55 (s, 1H), 3.17 (s, 1H), 2.96 (s, 1H), 2.62 (q,  $J = 7.6$  Hz, 2H), 2.34 (s, 4H), 2.08–1.93 (m, 16H), 1.79 (s, 4H), 1.67 (d,  $J = 12.6$  Hz, 4H) 1.25 (t,  $J = 7.5$  Hz, 3H).  $^{13}\text{C}$  NMR (151 MHz,  $\text{CDCl}_3$ )  $\delta$  149.2, 135.4, 130.5, 128.6, 124.9, 124.2, 46.5, 44.5, 40.3, 39.4, 38.2, 33.2, 33.0, 32.1, 31.5, 31.4, 28.4, 28.3, 28.0, 27.9, 23.7, 14.3. IR (ATR): 3600, 3046, 2901, 1450, 1187, 735  $\text{cm}^{-1}$ . HRMS (ESI+):  $m/z$   $[\text{M}+\text{H}]^+$  calculated for  $\text{C}_{28}\text{H}_{39}\text{O}$ : 391.2995; found: 391.2985.

**4-(Adamantan-2-yl)-2-ethylphenol (3.73):** Isolated as an inseparable 1:1 mixture of an unidentifiable product and **3.70**. The  $^1\text{H}$  NMR data can be extracted from the NMR spectrum of the mixture:  $^1\text{H}$  NMR (500 MHz,  $\text{CDCl}_3$ )  $\delta$  7.10 (d,  $J = 2.4$  Hz, 1H), 7.05 (dd,  $J = 8.5, 2.2$  Hz, 1H), 6.73 (d,  $J = 8.2$  Hz, 1H), 4.51 (s, 1H), 2.93 (s, 1H), 2.63 (q,  $J = 7.6$  Hz, 2H), 2.41 (s, 2H), 2.18–1.90 (m, 11H), 1.76 (s, 4H), 1.54 (d,  $J = 12.8$  Hz, 4H), 1.24 (t,  $J = 7.6$  Hz, 3H).



Prepared by V. K. Nguyen using General Procedure C with 2-benzylphenol (36.8 mg, 0.20 mmol, 1 equiv),  $\text{ZnCl}_2$  (1.4 mg, 0.01 mmol, 0.05 equiv), PhCl (0.2 mL, 1.0 M), 2-



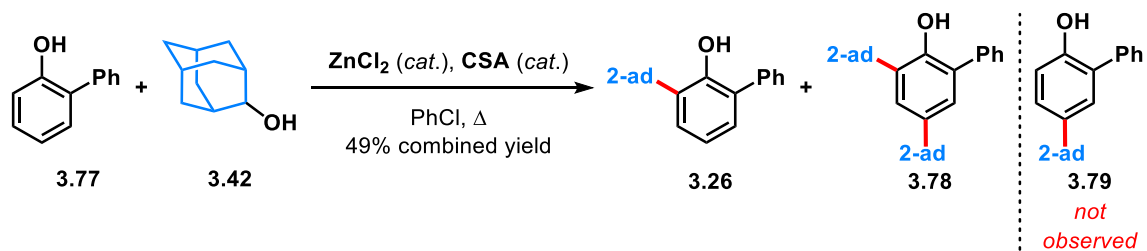
adamantanol (33.5 mg, 0.22 mmol, 1.1 equiv), and CSA (35 mg, 0.15 mmol, 0.75 equiv). Purification by preparative TLC (eluted with 19:1 hexanes/Et<sub>2</sub>O) afforded an inseparable 2:1 mixture (54% overall yield, 38.7 mg) of **3.25** (22.6 mg, 36%, 46% brsm) and dialkylated **3.75** (16.1 mg, 18%, 23% brsm) with compound **3.25** being the major product. The *para*-substituted product **3.76** was not observed by NMR analysis of the crude reaction mixture nor isolated.

### **2-(Adamantan-2-yl)-6-benzylphenol (3.25)**

The NMR data can be extracted from the NMR spectra of the mixture: <sup>1</sup>H NMR (400 MHz, CDCl<sub>3</sub>) δ 7.38 (dd, *J* = 7.6, 1.4 Hz, 1H), 7.33–7.27 (m, 2H), 7.24–7.18 (m, 3H), 7.01 (dd, *J* = 7.4, 1.7 Hz, 1H), 6.89 (t, *J* = 7.6 Hz, 1H), 4.65 (s, 1H), 4.00 (s, 2H), 3.14 (s, 1H), 2.30 (q, *J* = 2.9 Hz, 2H), 2.14–1.92 (m, 7H), 1.88 (dt, *J* = 6.5, 3.2 Hz, 1H), 1.78 (d, *J* = 3.3 Hz, 2H), 1.65 (dtt, *J* = 12.7, 2.5, 1.2 Hz, 2H). <sup>13</sup>C NMR (101 MHz, CDCl<sub>3</sub>) δ 152.4, 139.7, 132.0, 128.9, 128.7, 128.5, 126.7, 126.6, 126.4, 120.1, 44.3, 40.2, 38.1, 37.2, 33.0, 31.4, 28.3, 27.8. IR (ATR): 3544, 2898, 1449, 1187, 730 cm<sup>-1</sup>. HRMS (ESI<sup>+</sup>): *m/z* [M+H]<sup>+</sup> calculated for C<sub>23</sub>H<sub>27</sub>O: 319.2056; found: 319.2055.

### **2,4-Diadamantan-2-yl-6-benzylphenol (3.75)**

The <sup>1</sup>H NMR data can be extracted from the NMR spectrum of the mixture: <sup>1</sup>H NMR (500 MHz, CDCl<sub>3</sub>) δ 7.36 (s, 1H), 7.33–7.27 (m, 2H), 7.24–7.18 (m, 3H), 7.04 (s, 1H), 4.67 (s, 1H), 4.00 (s, 2H), 3.14 (s, 2H), 2.30 (q, *J* = 2.9 Hz, 4H), 2.08–1.92 (m, 14H), 1.90 (dt, *J* = 6.5, 3.2 Hz, 2H), 1.78 (d, *J* = 3.3 Hz, 4H), 1.65 (dtt, *J* = 12.7, 2.5, 1.2 Hz, 4H).



Prepared by V. K. Nguyen using General Procedure C with 2-phenylphenol (34 mg, 0.20 mmol, 1 equiv),  $\text{ZnCl}_2$  (1.4 mg, 0.01 mmol, 0.05 equiv), PhCl (0.2 mL, 1.0 M), 2-adamantanol (33.5 mg, 0.22 mmol, 1.1 equiv), and CSA (35 mg, 0.15 mmol, 0.75 equiv). Purification by preparative TLC (eluted with 19:1 hexanes/ $\text{Et}_2\text{O}$ ) afforded an inseparable 5:2 mixture (49% overall yield, 33.9 mg) of **3.26** (21.5 mg, 35%) and dialkylated **3.78** (12.4 mg, 14%) with compound **3.26** being the major product. The *para*-substituted product **3.79** was not observed by NMR analysis of the crude reaction mixture.

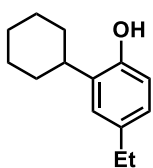
### 2-(Adamantan-2-yl)-6-phenylphenol (**3.26**)

The NMR data can be extracted from the NMR spectra of the mixture:  $^1\text{H}$  NMR (400 MHz,  $\text{CDCl}_3$ )  $\delta$  7.53–7.43 (m, 5H), 7.40 (t,  $J = 7.0$  Hz, 1H), 7.09 (dd,  $J = 7.5, 1.7$  Hz, 1H), 6.97 (t,  $J = 7.6$  Hz, 1H), 5.32 (s, 1H), 3.31 (s, 1H), 2.30 (q,  $J = 2.9$  Hz, 2H), 2.14–1.92 (m, 7H), 1.88 (dt,  $J = 6.5, 3.2$  Hz, 3H), 1.78 (d,  $J = 3.3$  Hz, 1H), 1.65 (dtt,  $J = 12.7, 2.5, 1.2$  Hz, 1H).  $^{13}\text{C}$  NMR (151 MHz,  $\text{CDCl}_3$ )  $\delta$  150.7, 137.6, 132.4, 129.5, 128.0, 127.9, 127.5, 126.3, 125.8, 119.9, 44.4, 40.2, 38.2, 33.2, 31.3, 28.4, 28.0. IR (ATR): 3547, 2900, 2847, 1467, 1196, 907, 733  $\text{cm}^{-1}$ . HRMS (ESI+):  $m/z$   $[\text{M}-\text{H}]^+$  calculated for  $\text{C}_{22}\text{H}_{23}\text{O}$ : 303.1754; found: 303.1753.

### 2,4-Diadamantan-2-yl-6-phenylphenol (3.78)

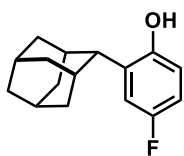
The  $^1\text{H}$  NMR data can be extracted from the NMR spectrum of the mixture:  $^1\text{H}$  NMR (400 MHz,  $\text{CDCl}_3$ )  $\delta$  7.53–7.43 (m, 5H), 7.37 (s, 1H), 7.05 (s, 1H), 5.18 (s, 1H), 3.30 (s, 2H), 2.40 (q,  $J = 2.9$  Hz, 4H), 2.11–2.05 (m, 14H), 2.01–1.88 (dt,  $J = 6.5, 3.2$  Hz, 6H), 1.80 (d,  $J = 5.0$  Hz, 2H), 1.68 (ddt,  $J = 12.8, 2.9, 1.4$  Hz, 2H).

### 2-Cyclohexyl-4-ethylphenol (3.27)



Prepared using General Procedure B with 4-ethylphenol (25.3 mg, 0.2022 mmol, 1 equiv),  $\text{ZnCl}_2$  (0.3 mg, 2.2  $\mu\text{mol}$ , 0.01 equiv),  $\text{PhCl}$  (0.2 mL, 1.0 M), cyclohexanol (62.5  $\mu\text{L}$ , 0.6 mmol, 3 equiv), and  $\text{CSA}\cdot\text{H}_2\text{O}$  (37.6 mg, 0.150 mmol, 0.75 equiv). Purification by preparative TLC (eluted with 19:1 hexanes/ $\text{EtOAc}$ ) afforded **3.27** (16.9 mg, 41%) as a yellow oil.  $R_f$ : 0.26 (19:1 hexanes/ $\text{EtOAc}$ ).  $^1\text{H}$  NMR (500 MHz,  $\text{CDCl}_3$ )  $\delta$  7.03 (d,  $J = 2.2$  Hz, 1H), 6.91 (dd,  $J = 8.1, 2.2$  Hz, 1H), 6.70 (d,  $J = 8.1$  Hz, 1H), 4.75 (s, 1H), 2.81 (tt,  $J = 11.5, 3.0$  Hz, 1H), 2.59 (q,  $J = 7.6$  Hz, 2H), 1.93–1.84 (m, 4H), 1.82–1.76 (m, 1H), 1.52–1.39 (m, 4H), 1.35–1.26 (m, 1H), 1.23 (t,  $J = 7.6$  Hz, 3H).  $^{13}\text{C}$  NMR (151 MHz,  $\text{CDCl}_3$ )  $\delta$  150.7, 136.7, 133.5, 126.5, 125.8, 115.3, 37.5, 33.3, 28.4, 27.2, 26.5, 16.1. IR (ATR): 3341, 2923, 2850, 1504, 1447, 813  $\text{cm}^{-1}$ . HRMS (ESI+):  $m/z$   $[\text{M}+\text{H}]^+$  calculated for  $\text{C}_{14}\text{H}_{21}\text{O}$ : 205.1587; found: 205.1581.

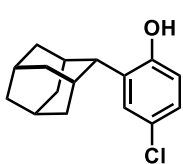
### 2-(Adamant-2-yl)-4-fluorophenol (3.28)



Prepared using General Procedure C with 3-phenylphenol (22.5 mg, 0.200 mmol, 1 equiv),  $\text{ZnCl}_2$  (1.7 mg, 0.012 mmol, 0.05 equiv),  $\text{PhCl}$  (0.2 mL, 1.0 M), adamantan-2-ol (33.7 mg, 0.221 mmol, 1.1 equiv), and  $\text{CSA}\cdot\text{H}_2\text{O}$  (37.4 mg, 0.150 mmol, 0.75 equiv). Purification by preparatory TLC (eluted with 9:1

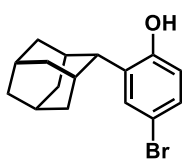
hexanes/EtOAc) afforded **3.28** (15.2 mg, 31%) as a yellow solid. Mp 90–93 °C. R<sub>f</sub>: 0.32 (9:1 hexanes/EtOAc). <sup>1</sup>H NMR (500 MHz, CDCl<sub>3</sub>) δ 7.15 (dd, *J* = 10.6, 3.0 Hz, 1H), 6.76 (dt, *J* = 8.2, 3.1 Hz, 1H), 6.66 (dd, *J* = 8.7, 5.0 Hz, 1H), 4.60 (s, 1H), 3.14 (s, 1H), 2.32 (s, 2H), 2.09 (d, *J* = 11.6 Hz, 1H), 2.00–1.95 (m, 6H), 1.88 (s, 1H), 1.78 (s, 2H), 1.65 (d, *J* = 12.8 Hz, 2H). <sup>13</sup>C NMR (151 MHz, CDCl<sub>3</sub>) δ 157.4 (d, *J* = 236.7 Hz), 149.9, 133.6, 115.9 (d, *J* = 8.3 Hz), 115.3 (d, *J* = 23.8 Hz), 112.5 (d, *J* = 23.2 Hz), 44.3, 40.0, 38.0, 32.8, 31.1, 28.2, 27.7. <sup>19</sup>F NMR (564 MHz, CDCl<sub>3</sub>) δ –124.0. IR (ATR): 3406, 2900, 2847, 1698, 1502, 1427, 1341, 1252, 1178, 1165, 1115, 983, 956, 871, 821, 803, 746, 570, 473 cm<sup>-1</sup>. HRMS (ESI<sup>-</sup>): *m/z* [M–H]<sup>-</sup> calculated for C<sub>16</sub>H<sub>18</sub>FO: 245.1347; found 245.1359.

### 2-(Adamant-2-yl)-4-chlorophenol (**3.29**)



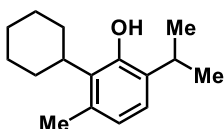
Prepared using General Procedure C with 4-chlorophenol (26.1 mg, 0.203 mmol, 1 equiv), ZnCl<sub>2</sub> (1.4 mg, 0.10 mmol, 0.05 equiv), chlorobenzene (0.2 mL, 1.0 M), adamantan-2-ol (33.6 mg, 0.221 mmol, 1.1 equiv), and CSA•H<sub>2</sub>O (37.8 mg, 0.151 mmol, 0.75 equiv). Purification by flash chromatography (eluted with 0–20% EtOAc in hexanes) afforded **3.29** (21.4 mg, 41%) as a yellow oil. R<sub>f</sub>: 0.30 (9:1 hexanes/EtOAc). <sup>1</sup>H NMR (500 MHz, CDCl<sub>3</sub>) δ 7.37 (d, *J* = 2.5 Hz, 1H), 7.04 (dd, *J* = 8.5, 2.5 Hz, 1H), 6.66 (d, *J* = 8.4 Hz, 1H), 4.70 (s, 1H), 3.13 (s, 1H), 2.32 (s, 2H), 2.01–1.94 (m, 7H), 1.89 (s, 1H), 1.78 (s, 2H), 1.65 (d, *J* = 12.8 Hz, 2H). <sup>13</sup>C NMR (151 MHz, CDCl<sub>3</sub>) δ 153.3, 134.0, 128.3, 126.1, 124.8, 116.4, 44.1, 40.0, 38.1, 32.9, 30.9, 28.2, 27.8. IR (ATR): 3411, 2898, 2847, 1697, 1491, 1409, 1341, 1212, 1166, 1111, 919, 972, 806, 721, 676, 657, 472 cm<sup>-1</sup>. HRMS (ESI<sup>-</sup>): *m/z* [M–H]<sup>-</sup> calculated for C<sub>16</sub>H<sub>18</sub>ClO: 261.1052; found 261.1063.

### 2-(Adamant-2-yl)-4-bromophenol (**3.30**)



Prepared using General Procedure C with 4-bromophenol (34.7 mg, 0.200 mmol, 1 equiv), ZnCl<sub>2</sub> (1.5 mg, 0.11 mmol, 0.05 equiv), chlorobenzene (0.2 mL, 1.0 M), adamantan-2-ol (33.7 mg, 0.221 mmol, 1.1 equiv), and CSA•H<sub>2</sub>O (37.4 mg, 0.150 mmol, 0.75 equiv). Purification by preparative TLC (eluted with 9:1 hexanes/EtOAc) afforded **3.30** (18.6 mg, 35%) as an orange-brown oil. R<sub>f</sub>: 0.38 (9:1 hexanes/EtOAc). <sup>1</sup>H NMR (600 MHz, CDCl<sub>3</sub>) δ 7.50 (d, *J* = 2.5 Hz, 1H), 7.20–7.15 (m, 1H), 6.62 (dd, *J* = 8.6, 1.6 Hz, 1H), 4.68 (s, 1H), 3.14 (s, 1H), 2.32 (s, 2H), 2.02–1.92 (m, 7H), 1.89 (s, 1H), 1.78 (s, 2H), 1.65 (d, *J* = 12.7 Hz, 2H). <sup>13</sup>C NMR (151 MHz, CDCl<sub>3</sub>) δ 153.2, 134.2, 131.3, 129.4, 117.2, 113.0, 44.2, 40.0, 38.0, 32.8, 31.0, 28.1, 27.7. IR (ATR): 3299, 2900, 1411, 1087, 1045, 879, 627 cm<sup>-1</sup>. HRMS (ESI<sup>-</sup>): *m/z* [M-H]<sup>-</sup> calculated for C<sub>16</sub>H<sub>18</sub>BrO: 305.0547; found 305.0551.

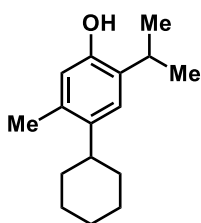
### 2-Cyclohexyl-6-isopropyl-3-methylphenol (**3.31**)



Prepared by V. K. Nguyen using General Procedure B with thymol (30 mg, 0.20 mmol, 1 equiv), ZnCl<sub>2</sub> (1.4 mg, 0.01 mmol, 0.05 equiv), chlorobenzene (0.2 mL, 1.0 M), cyclohexanol (62.5 μL, 0.6 mmol, 3.0 equiv), and CSA (35 mg, 0.15 mmol, 0.75 equiv). Purification by preparative TLC (eluted with 19:1 hexanes/EtOAc) afforded **3.31** (14.5 mg, 31%, 47% brsm) as a colorless oil. The mono-*para*-substituted product **3.80** was observed as a minor product (10%, 16% brsm). <sup>1</sup>H NMR (500 MHz, CDCl<sub>3</sub>) δ 6.94 (d, *J* = 7.9 Hz, 1H), 6.73 (d, *J* = 7.7 Hz, 1H), 4.84 (s, 1H), 3.05 (p, *J* = 6.8 Hz, 1H), 2.90 (s, 1H), 2.32 (s, 3H), 2.04 (q, *J* = 9.9 Hz, 2H), 1.86 (d, *J* = 12.5 Hz, 2H), 1.74 (dd, *J* = 24.5, 12.1 Hz, 3H), 1.38 (q, *J* = 12.5 Hz, 3H), 1.26 (d, *J* = 6.8 Hz,

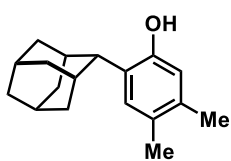
6H).  $^{13}\text{C}$  NMR (151 MHz,  $\text{CDCl}_3$ )  $\delta$  152.0, 134.7, 132.2, 130.9, 123.1, 120.6, 39.9, 34.4, 30.3, 27.0, 26.5, 22.9, 21.0. IR (ATR): 3620, 2922, 1574, 1486, 767  $\text{cm}^{-1}$ . HRMS (ESI+):  $m/z$   $[\text{M}+\text{H}]^+$  calculated for  $\text{C}_{16}\text{H}_{25}\text{O}$ : 233.1900; found: 233.1908.

#### 4-(Cyclohexyl)-2-isopropyl-5-methylphenol (**3.80**)



Isolated as an inseparable 3:1 mixture of thymol and **3.80**, with thymol being the major product. The  $^1\text{H}$  NMR data can be extracted from the NMR spectrum of the mixture (600 MHz,  $\text{CDCl}_3$ ) 7.03 (s, 1H), 6.55 (s, 1H), 4.57 (s, 1H), 3.05 (p,  $J = 6.8$  Hz, 1H), 2.90 (s, 1H), 2.62 (m, 1H), 2.25 (s, 3H), 1.85 (m, 1H), 1.78 (m, 2H), 1.66 (dd,  $J = 24.5, 12.1$  Hz, 3H), 1.38 (q,  $J = 12.5$  Hz, 3H), 1.26 (d,  $J = 6.8$  Hz, 6H).

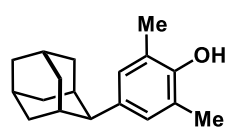
#### 2-(Adamant-2-yl)-4,5-dimethylphenol (**3.32**)

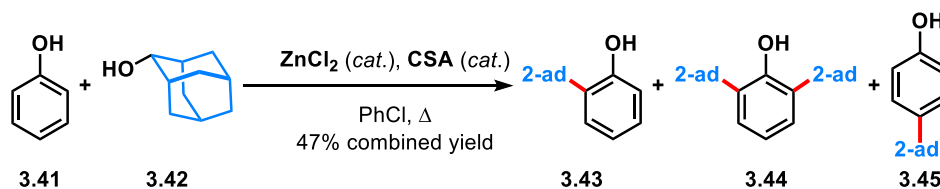


Prepared using General Procedure C with 3,4-xyleneol (24.5 mg, 0.200 mmol, 1 equiv),  $\text{ZnCl}_2$  (1.3 mg, 9.5  $\mu\text{mol}$ , 0.05 equiv), chlorobenzene (0.2 mL, 1.0 M), adamantan-2-ol (33.6 mg, 0.221 mmol, 1.1 equiv), and  $\text{CSA}\cdot\text{H}_2\text{O}$  (37.5 mg, 0.150 mmol, 0.75 equiv). Purification by preparative TLC (eluted with 9:1 hexanes/EtOAc) afforded **3.32** (26.9 mg, 52%) as a light brown-white solid. Mp 105–107  $^\circ\text{C}$ .  $R_f$ : 0.38 (19:1 hexanes/EtOAc).  $^1\text{H}$  NMR (500 MHz,  $\text{CDCl}_3$ )  $\delta$  7.17 (s, 1H), 6.55 (s, 1H), 4.42 (s, 1H), 3.13 (s, 1H), 2.34–2.30 (m, 2H), 2.20 (s, 3H), 2.18 (s, 3H), 2.07–2.01 (m, 2H), 1.99–1.94 (m, 5H), 1.88–1.86 (m, 1H), 1.78 (s, 2H), 1.64 (d,  $J = 12.6$  Hz, 2H).  $^{13}\text{C}$  NMR (151 MHz,  $\text{CDCl}_3$ )  $\delta$  151.8, 134.7, 129.5, 128.7, 128.0, 117.0, 43.9, 40.2, 38.2, 33.0, 31.3, 28.3, 27.9, 19.4, 19.3. IR (ATR): 3313, 2898, 2847, 1617, 1449, 1407,

1275, 1198, 1084, 1044, 878, 576, 474  $\text{cm}^{-1}$ . HRMS (ESI+):  $m/z$   $[\text{M}+\text{H}]^+$  calculated for  $\text{C}_{18}\text{H}_{25}\text{O}$ : 257.1900; found 257.1898.

#### 4-(Adamant-2-yl)-2,6-dimethylphenol (**3.33**)

 Prepared using General Procedure C with 2,6-xyleneol (24.6 mg, 0.201 mmol, 1 equiv),  $\text{ZnCl}_2$  (1.3 mg, 9.5  $\mu\text{mol}$ , 0.05 equiv), chlorobenzene (0.2 mL, 1.0 M), adamantan-2-ol (33.6 mg, 0.221 mmol, 1.1 equiv), and  $\text{CSA}\cdot\text{H}_2\text{O}$  (37.7 mg, 0.151 mmol, 0.75 equiv). Purification by flash chromatography (eluted with 0–20% EtOAc in hexanes) afforded **3.33** (34.2 mg, 68%) as a white solid. Mp 135–139  $^\circ\text{C}$ . R<sub>f</sub>: 0.44 (9:1 hexanes/EtOAc).  $^1\text{H}$  NMR (500 MHz,  $\text{CDCl}_3$ )  $\delta$  6.95 (s, 2H), 4.45 (s, 1H), 2.89 (s, 1H), 2.40 (s, 2H), 2.25 (s, 6H), 2.16 (d,  $J = 7.9$  Hz, 1H), 1.98 (d,  $J = 13.0$  Hz, 3H), 1.88 (dd,  $J = 22.6, 12.6$  Hz, 4H), 1.76 (d,  $J = 7.8$  Hz, 3H), 1.52 (s, 1H).  $^{13}\text{C}$  NMR (151 MHz,  $\text{CDCl}_3$ )  $\delta$  149.8, 136.1, 127.1, 122.6, 46.2, 39.3, 38.1, 32.1, 31.2, 28.2, 28.0, 16.3. IR (ATR): 3379, 2897, 2844, 1486, 1447, 1200, 1144, 869, 765, 699, 631  $\text{cm}^{-1}$ . HRMS (ESI–):  $m/z$   $[\text{M}-\text{H}]^-$  calculated for  $\text{C}_{18}\text{H}_{23}\text{O}$ : 255.1754; found 255.1764.



The reaction was performed using General Procedure C with phenol (19.1 mg, 0.203 mmol, 1 equiv),  $\text{ZnCl}_2$  (1.4 mg, 0.10 mmol, 0.05 equiv), chlorobenzene (0.2 mL, 1.0 M), adamantan-2-ol (33.7 mg, 0.221 mmol, 1.1 equiv), and  $\text{CSA}\cdot\text{H}_2\text{O}$  (37.7 mg, 0.151 mmol, 0.75 equiv). Purification by preparatory TLC (eluted with 9:1 hexanes/EtOAc) afforded

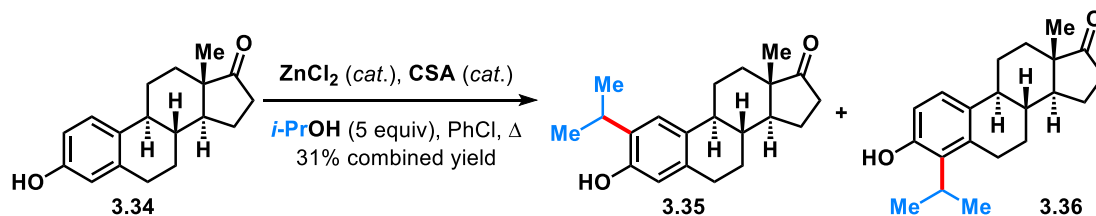
47% overall yield of three products with **3.43** (12.8 mg, 25%) as an orange oil, **3.44** (10.1 mg, 14%) as a yellow-white solid, and **3.45** (4.3 mg, 8%) as a light tan solid.

**2-(Adamant-2-yl)phenol (3.43):**  $^1\text{H}$  NMR (500 MHz,  $\text{CDCl}_3$ )  $\delta$  7.44 (d,  $J = 7.7$  Hz, 1H), 7.11–7.06 (m, 1H), 6.91 (t,  $J = 7.6$  Hz, 1H), 6.75–6.72 (m, 1H), 4.69 (s, 1H), 3.18 (s, 1H), 2.35 (s, 2H), 2.05–1.93 (m, 8H), 1.87 (s, 1H), 1.79 (s, 2H), 1.65 (d,  $J = 12.6$  Hz, 2H).  $^{13}\text{C}$  NMR (151 MHz,  $\text{CDCl}_3$ )  $\delta$  154.0, 131.7, 128.4, 126.8, 120.5, 115.6, 44.1, 40.1, 38.1, 33.0, 31.2, 28.3, 27.9. The spectral data recorded are consistent with those previously reported.<sup>4</sup>

**2,6-Bis(adamant-2-yl)phenol (3.44):**  $^1\text{H}$  NMR (500 MHz,  $\text{CDCl}_3$ )  $\delta$  7.33 (d,  $J = 7.7$  Hz, 2H), 6.90 (t,  $J = 7.7$  Hz, 1H), 4.76 (s, 1H), 3.13 (s, 2H), 2.33–2.29 (m, 4H), 2.05 (d,  $J = 12.9$  Hz, 4H), 2.01–1.95 (m, 10H), 1.90–1.86 (m, 2H), 1.78 (s, 4H), 1.65 (d,  $J = 12.7$  Hz, 4H).  $^{13}\text{C}$  NMR (151 MHz,  $\text{CDCl}_3$ )  $\delta$  152.3, 131.0, 125.5, 119.5, 44.5, 40.3, 38.1, 33.0, 31.5, 28.3, 27.8. IR (ATR): 3589, 2899, 2847, 1732, 1467, 1451, 1437, 1359, 1340, 1316, 1249, 1217, 1183, 1165, 1116, 1095, 1086, 1061, 1048, 995, 953, 934, 877, 840, 826, 802, 767, 752, 735, 698, 638, 627, 559, 539  $\text{cm}^{-1}$ . HRMS (ESI+):  $m/z$   $[\text{M}+\text{H}]^+$  calculated for  $\text{C}_{26}\text{H}_{35}\text{O}$ : 363.2682; found 363.2672.

**4-(Adamant-2-yl)phenol (3.45):**  $^1\text{H}$  NMR (500 MHz,  $\text{CDCl}_3$ )  $\delta$  7.21 (d,  $J = 8.3$  Hz, 2H), 6.80 (d,  $J = 8.3$  Hz, 2H), 4.63 (s, 1H), 2.93 (s, 1H), 2.40 (s, 2H), 2.02–1.88 (m, 8H), 1.83 (d,  $J = 12.8$  Hz, 2H), 1.76 (s, 2H). The spectral data recorded are consistent with those previously reported.<sup>5</sup>





The reaction was performed using General D with estrone (54.3 mg, 0.201 mmol, 1 equiv),  $\text{ZnCl}_2$  (1.5 mg, 0.011 mmol, 0.05 equiv), PhCl (0.2 mL, 1.0 M), isopropanol (76.5  $\mu\text{L}$ , 1.0 mmol, 5 equiv), and CSA (37.6 mg, 0.150 mmol, 0.75 equiv). Purification by flash chromatography (eluted with 5–30% EtOAc in hexanes) afforded 31% overall yield of two alkylation products with **3.35** being the minor product (7.9 mg, 13%) and **3.36** (11.9 mg, 19%) as the major product. The di-alkylated product was not observed.

**(8*R*,9*S*,13*S*,14*S*)-3-Hydroxy-2-isopropyl-13-methyl-6,7,8,9,11,12,13,14,15,16-**

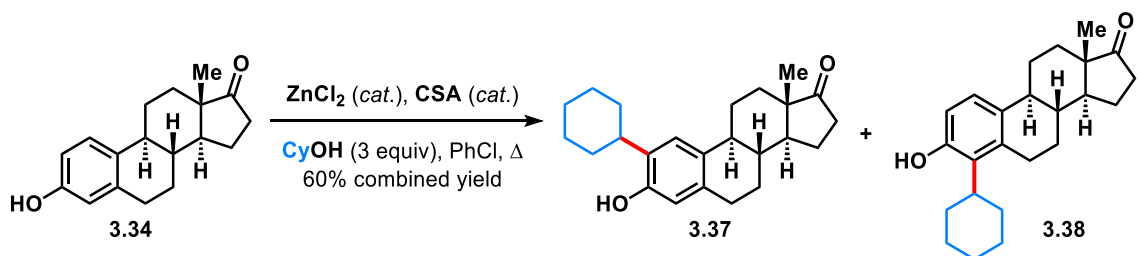
**decahydro-17*H*-cyclopenta[*a*]phenanthren-17-one (3.35):** Mp 137–140 °C.  $R_f$ : 0.56

(4:1 hexanes/EtOAc).  $^1\text{H}$  NMR (400 MHz,  $\text{CDCl}_3$ )  $\delta$  7.12 (s, 1H), 6.50 (s, 1H), 3.16 (p,  $J$  = 6.9 Hz, 1H), 2.86–2.74 (m, 2H), 2.50 (dd,  $J$  = 18.8, 8.7 Hz, 1H), 2.46–2.40 (m, 1H), 2.30–2.20 (m, 1H), 2.19–2.09 (m, 1H), 2.09–1.92 (m, 3H), 1.67–1.39 (m, 6H), 1.25 (dd,  $J$  = 6.9, 5.9 Hz, 6H), 0.91 (s, 3H).  $^{13}\text{C}$  NMR (101 MHz,  $\text{CDCl}_3$ )  $\delta$  221.8, 151.1, 134.9, 132.1, 131.8, 123.4, 115.5, 50.5, 48.2, 44.3, 38.6, 36.0, 31.7, 29.2, 27.2, 26.7, 26.1, 22.9, 21.7, 14.0. IR (ATR): 3317, 2929, 2869, 1720, 1614, 1586, 1510, 1454, 1421, 1375, 1357, 1337, 1264, 1233, 1208, 1162, 1087, 1055, 1034, 1012, 912, 889, 820, 800, 734, 703, 580, 519, 493, 474, 450, 429, 417, 403  $\text{cm}^{-1}$ . HRMS (ESI+):  $m/z$   $[\text{M}+\text{H}]^+$  calculated for  $\text{C}_{21}\text{H}_{29}\text{O}_2$ : 313.2162; found 313.2175.

**(8*R*,9*S*,13*S*,14*S*)-3-Hydroxy-4-isopropyl-13-methyl-6,7,8,9,11,12,13,14,15,16-**

**decahydro-17*H*-cyclopenta[*a*]phenanthren-17-one (3.36):** Mp 137–140 °C.  $R_f$ : 0.56

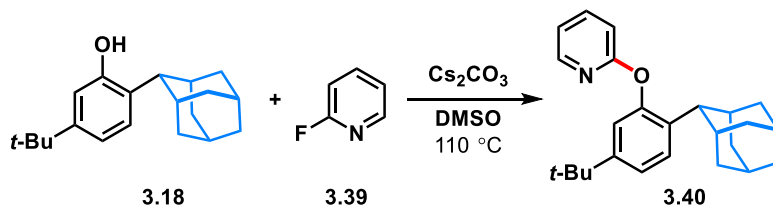
(4:1 hexanes/EtOAc).  $^1\text{H}$  NMR (400 MHz,  $\text{CDCl}_3$ )  $\delta$  7.04 (d,  $J = 8.6$  Hz, 1H), 6.55 (d,  $J = 8.4$  Hz, 1H), 3.31 (q,  $J = 7.1$  Hz, 1H), 2.86–2.74 (m, 2H), 2.50 (dd,  $J = 18.8, 8.7$  Hz, 1H), 2.40–2.34 (m, 1H), 2.30–2.20 (m, 1H), 2.19–2.10 (m, 1H), 2.09–1.92 (m, 3H), 1.67–1.39 (m, 6H), 1.36 (dd,  $J = 7.1, 2.0$  Hz, 6H), 0.90 (s, 3H).  $^{13}\text{C}$  NMR (101 MHz,  $\text{CDCl}_3$ )  $\delta$  214.9, 153.0, 151.1, 135.2, 132.3, 131.7, 123.8, 114.2, 50.6, 48.1, 48.0, 44.7, 37.4, 36.1, 27.5, 27.1, 26.4, 22.9, 21.7, 20.4, 13.9. IR (ATR): 3317, 2929, 2869, 1720, 1614, 1586, 1510, 1454, 1421, 1375, 1357, 1337, 1264, 1233, 1208, 1162, 1087, 1055, 1034, 1012, 912, 889, 820, 800, 734, 703, 580, 519, 493, 474, 450, 429, 417, 403  $\text{cm}^{-1}$ . HRMS (ESI+):  $m/z$   $[\text{M}+\text{H}]^+$  calculated for  $\text{C}_{21}\text{H}_{29}\text{O}_2$ : 313.2162; found 313.2175.



The reaction was performed using General Procedure B with estrone (54.2 mg, 0.201 mmol, 1 equiv),  $\text{ZnCl}_2$  (1.5 mg, 0.011 mmol, 0.05 equiv),  $\text{PhCl}$  (0.2 mL, 1.0 M), cyclohexanol (62.5  $\mu\text{L}$ , 0.6 mmol, 3 equiv), and CSA (37.7 mg, 0.151 mmol, 0.75 equiv). Purification by flash chromatography (eluted with 5–30% EtOAc in hexanes) afforded 60% overall yield of a mixture of two alkylation products with **3.37** being the major product (29.6 mg, 42%) and **3.38** (12.9 mg, 18%) as the minor product. The di-alkylated product was not observed.

**(8R,9S,13S,14S)-2-Cyclohexyl-3-hydroxy-13-methyl-6,7,8,9,11,12,13,14,15,16-decahydro-17H-cyclopenta[*a*]phenanthren-17-one (3.37):** Mp 126–129 °C. R<sub>f</sub>: 0.31 (7:3 hexanes/EtOAc). <sup>1</sup>H NMR (600 MHz, CDCl<sub>3</sub>) δ 7.10 (s, 1H), 6.51 (s, 1H), 4.52 (s, 1H), 2.87–2.80 (m, 3H), 2.50 (dd, *J* = 19.1, 8.7 Hz, 1H), 2.45–2.40 (m, 1H), 2.28–2.22 (m, 1H), 2.18–2.10 (m, 1H), 2.09–1.92 (m, 3H), 1.89–1.81 (m, 4H), 1.78–1.70 (m, 1H), 1.68–1.23 (m, 11H), 0.91 (s, 3H). <sup>13</sup>C NMR (101 MHz, CDCl<sub>3</sub>) δ 221.5, 150.9, 134.9, 132.0, 131.3, 124.0, 115.5, 50.5, 48.2, 44.3, 38.6, 37.4, 36.0, 33.4, 31.7, 29.2, 27.2, 26.7, 26.4, 26.2, 21.7, 14.0. IR (ATR): 3408, 2926, 2852, 1727, 1614, 1508, 1450, 1420, 1374, 1341, 1264, 1207, 1189, 1088, 1054, 1036, 1008, 909, 882, 870, 816, 647, 581, 534, 479, 451, 417, 402 cm<sup>-1</sup>. HRMS (ESI<sup>+</sup>): *m/z* [M+NH<sub>4</sub>]<sup>+</sup> calculated for C<sub>24</sub>H<sub>36</sub>NO<sub>2</sub>: 370.2741; found 370.2740.

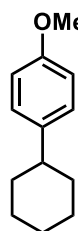
**(8R,9S,13S,14S)-4-Cyclohexyl-3-hydroxy-13-methyl-6,7,8,9,11,12,13,14,15,16-decahydro-17H-cyclopenta[*a*]phenanthren-17-one (3.38):** Mp 126–129 °C. R<sub>f</sub>: 0.31 (7:3 hexanes/EtOAc). <sup>1</sup>H NMR (600 MHz, CDCl<sub>3</sub>) δ 7.03 (d, *J* = 8.5 Hz, 1H), 6.54 (d, *J* = 8.4 Hz, 1H), 4.52 (s, 1H), 2.87–2.80 (m, 3H), 2.50 (dd, *J* = 19.1, 8.7 Hz, 1H), 2.40–2.33 (m, 1H), 2.28–2.22 (m, 1H), 2.18–2.10 (m, 1H), 2.09–1.92 (m, 3H), 1.89–1.81 (m, 4H), 1.78–1.70 (m, 1H), 1.68–1.23 (m, 11H), 0.91 (s, 3H). IR (ATR): 3408, 2926, 2852, 1727, 1614, 1508, 1450, 1420, 1374, 1341, 1264, 1207, 1189, 1088, 1054, 1036, 1008, 909, 882, 870, 816, 647, 581, 534, 479, 451, 417, 402 cm<sup>-1</sup>. HRMS (ESI<sup>+</sup>): *m/z* [M+NH<sub>4</sub>]<sup>+</sup> calculated for C<sub>24</sub>H<sub>36</sub>NO<sub>2</sub>: 370.2741; found 370.2740.



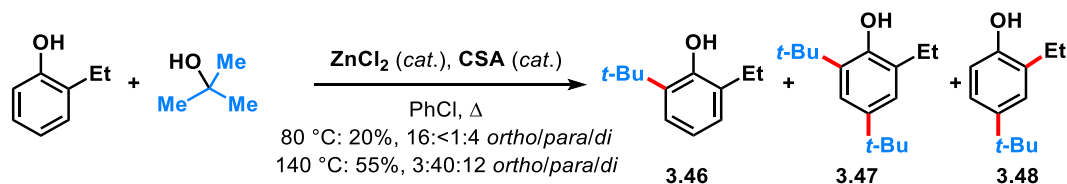
To a one-dram vial (oven-dried, 1.5 × 8 mm stir bar) was added phenol **3.18** (28.7 mg, 0.101 mmol, 1 equiv) followed by Cs<sub>2</sub>CO<sub>3</sub> (39.4 mg, 0.121 mmol, 1.2 equiv) and the vial was brought into a glovebox. To the solids were added via auto-pipette DMSO (170. μL, 0.6 M) and 2-fluoropyridine (10.0 μL, 0.116 mmol, 1.15 equiv) before capping and removing from the glovebox. The solution was allowed to stir at 80 °C for 16 h. Initial white solid (Cs<sub>2</sub>CO<sub>3</sub>) stirring in a light-yellow solution turns into a yellow-orange heterogeneous solution. The reaction was diluted in DCM (0.5 mL) and the solution was washed with water (3 × 0.5 mL) and sat brine (0.5 mL). The organic extract was dried over anhydrous MgSO<sub>4</sub>, filtered, and concentrated under reduced pressure to afford **3.40** (31.2 mg, 86%) as a pale yellow/colorless oil. <sup>1</sup>H NMR (600 MHz, CDCl<sub>3</sub>) δ 8.19 (d, *J* = 5.0 Hz, 1H), 7.64 (tt, *J* = 8.3, 1.6 Hz, 1H), 7.51 (d, *J* = 8.2 Hz, 1H), 7.21 (dt, *J* = 8.1, 1.6 Hz, 1H), 7.03 (t, *J* = 1.7 Hz, 1H), 6.95 (dd, *J* = 7.1, 5.0 Hz, 1H), 6.76 (d, *J* = 8.3 Hz, 1H), 3.02 (s, 1H), 2.33 (s, 2H), 2.04 (d, *J* = 12.8 Hz, 2H), 1.84 (d, *J* = 14.2 Hz, 4H), 1.74 (d, *J* = 8.8 Hz, 4H), 1.61 (d, *J* = 12.7 Hz, 2H), 1.29 (s, 9H). <sup>13</sup>C NMR (151 MHz, CDCl<sub>3</sub>) δ 164.0, 152.3, 150.1, 148.1, 139.3, 134.6, 128.3, 121.8, 119.6, 117.9, 110.6, 44.0, 40.0, 38.1, 34.5, 32.9, 31.4, 31.3, 28.1, 27.9. IR (ATR): 3053, 2902, 2849, 1596, 1574, 1501, 1467, 1451, 1428, 1403, 1362, 1343, 1285, 1264, 1244, 1223, 1206, 1190, 1135, 1099, 1092, 1069, 1036, 990, 969, 943, 910, 887, 851, 831, 813, 776, 734, 703, 679, 627, 598, 513, 475, 443, 413 cm<sup>-1</sup>. HRMS (ESI+): *m/z* [M+H]<sup>+</sup> calculated for C<sub>25</sub>H<sub>32</sub>NO: 362.2478; found 362.2494.

### 3.5.4 Mechanistic Studies

#### 1-(Cyclohexyl)-4-methoxybenzene (3.55)



Prepared by V. K. Nguyen using General Procedure B with anisole (22  $\mu$ L, 0.20 mmol, 1 equiv),  $\text{ZnCl}_2$  (1.4 mg, 0.01 mmol, 0.05 equiv), chlorobenzene (0.2 mL, 1.0 M), cyclohexanol (62.5  $\mu$ L, 0.6 mmol, 3.0 equiv), and CSA (35 mg, 0.15 mmol, 0.75 equiv). Purification by flash chromatography (eluted with 0–20% EtOAc in hexanes) afforded **3.55** (2.0 mg, 5%) as a colorless oil.  $^1\text{H}$  NMR (500 MHz,  $\text{CDCl}_3$ )  $\delta$  7.15 (d,  $J = 8.7$  Hz, 2H), 6.86 (d,  $J = 8.6$  Hz, 2H), 3.81 (s, 3H), 2.47 (t, 1H), 1.86 (dd,  $J = 11.5$ , 7.6 Hz, 4H), 1.76 (d,  $J = 13.1$  Hz, 1H), 1.48–1.35 (m, 4H), 0.92–0.83 (m, 2H). The spectral data recorded are consistent with those previously reported.<sup>6</sup>



80 °C: A one-dram vial equipped with a stirring bar was sequentially added  $\text{ZnCl}_2$  (1.4 mg, 0.010 mmol, 5 mol%), 2-ethylphenol (24.0  $\mu$ L, 0.200 mmol, 1 equiv), PhCl (0.2 mL, 1 M), *tert*-butanol (21.0  $\mu$ L, 0.22 mmol, 1.1 equiv), and (*R*)-camphor sulfonic acid monohydrate ((*R*)-CSA $\cdot$ H<sub>2</sub>O) (37.5 mg, 0.150 mmol, 75 mol%). The reaction mixture was heated at 80 °C for 18 h. The solution was filtered through a silica gel plug (packed in a 5" glass pipette, approximately one-third filled) and eluted with hexanes/EtOAc (9:1), and the solution was concentrated *in vacuo*. Purification by preparatory TLC (19:1 hexanes/EtOAc) afforded mixtures of a 4:1 ratio of **3.46** to **3.47** (7.5 mg, 20%) as a pale-yellow oil, and a 1.25:1 ratio of **3.48** to 2-ethylphenol (0.5 mg, <1%) as a yellow oil.

140 °C: A one-dram vial equipped with a stirring bar was sequentially added ZnCl<sub>2</sub> (1.3 mg, 9.5 μmol, 5 mol%), 2-ethylphenol (24.0 μL, 0.200 mmol, 1 equiv), PhCl (0.2 mL, 1 M), *tert*-butanol (21.0 μL, 0.22 mmol, 1.1 equiv), and (*R*)-camphor sulfonic acid monohydrate ((*R*)-CSA•H<sub>2</sub>O) (37.8 mg, 0.151 mmol, 75 mol%). The reaction mixture was heated at 140 °C for 18 h. The solution was filtered through a silica gel plug (packed in a 5" glass pipette, approximately one-third filled) and eluted with hexanes/EtOAc (9:1), and the solution was concentrated *in vacuo*. Purification by preparatory TLC (19:1 hexanes/EtOAc × 2) afforded mixtures of a 1:3.4 ratio of **3.46** to **3.47** (6.8 mg, 15%) as a bright yellow oil, and 6.7:1 **3.48** to 2-ethylphenol (15.7 mg, 40%) as a bright yellow-orange oil.

**2-*tert*-Butyl-6-ethylphenol (3.46)**: R<sub>f</sub>: 0.45 (19:1 hexanes/EtOAc). <sup>1</sup>H NMR (600 MHz, CDCl<sub>3</sub>) δ 7.17 (dd, *J* = 7.9, 1.6 Hz, 1H), 7.03 (d, *J* = 7.5 Hz, 1H), 6.84 (t, *J* = 7.7 Hz, 1H), 4.86 (s, 1H), 2.61 (q, *J* = 7.6 Hz, 2H), 1.43 (s, 9H), 1.28 (t, *J* = 7.6 Hz, 3H). <sup>13</sup>C NMR (101 MHz, CDCl<sub>3</sub>) δ 152.4, 135.8, 129.1, 126.7, 125.0, 120.2, 34.7, 30.0, 23.0, 13.9. IR (ATR): 3618, 2959, 2871, 1654, 1591, 1479, 1437, 1391, 1361, 1318, 1283, 1265, 1248, 1190, 1150, 1128, 1106, 1060, 932, 877, 834, 820, 794, 763, 746, 721, 649, 597, 573 cm<sup>-1</sup>. HRMS (ESI<sup>-</sup>): *m/z* [M-H]<sup>-</sup> calculated for C<sub>12</sub>H<sub>17</sub>O: 177.1285; found 177.1287.

**2,4-Di-*tert*-butyl-6-ethylphenol (3.47)**: R<sub>f</sub>: 0.45 (19:1 hexanes/EtOAc). <sup>1</sup>H NMR (600 MHz, CDCl<sub>3</sub>) δ 7.20 (d, *J* = 2.5 Hz, 1H), 7.03 (d, *J* = 7.6 Hz, 1H), 4.72 (s, 1H), 2.64–2.59 (m, 2H), 1.44 (s, 9H), 1.31 (s, 9H), 1.29 (t, *J* = 7.6 Hz, 3H). <sup>13</sup>C NMR (101 MHz, CDCl<sub>3</sub>) δ 150.0, 142.4, 135.0, 128.4, 123.6, 122.1, 34.9, 34.5, 31.8, 30.1, 23.5, 14.1. IR (ATR): 3618, 2959, 2871, 1654, 1591, 1479, 1437, 1391, 1361, 1318, 1283, 1265, 1248, 1190, 1150,

1128, 1106, 1060, 932, 877, 834, 820, 794, 763, 746, 721, 649, 597, 573  $\text{cm}^{-1}$ . HRMS (ESI<sup>-</sup>):  $m/z$   $[\text{M}-\text{H}]^-$  calculated for  $\text{C}_{16}\text{H}_{25}\text{O}$ : 233.1911; found 233.1915. The spectral data recorded are consistent with those previously reported.<sup>6</sup>

**4-tert-Butyl-2-ethylphenol (3.48)**: R<sub>f</sub>: 0.25 (19:1 hexanes/EtOAc). <sup>1</sup>H NMR (600 MHz,  $\text{CDCl}_3$ )  $\delta$  7.16 (d,  $J = 2.4$  Hz, 1H), 7.10 (dd,  $J = 8.3, 2.3$  Hz, 1H), 6.70 (d,  $J = 8.4$  Hz, 1H), 4.59 (s, 1H), 2.64 (q,  $J = 7.6$  Hz, 2H), 1.30 (s, 9H), 1.25 (t,  $J = 7.6$  Hz, 3H). The spectral data recorded are consistent with those previously reported.<sup>7</sup>

### 3.5.5 References

1. Marino, J. P.; Jaén, J. C. *J. Am. Chem. Soc.* **1982**, *104*, 3165–3172.
2. Cheang, D. M. J.; Armstrong, R. J.; Akhtar, W. M.; Donohoe, T.J. *Chem. Commun.* **2020**, *56*, 3543–3546.
3. Suri, J. T.; Vu, T.; Hernandez, A.; Congdon, J.; Singaram, B. *Tetrahedron Lett.* **2002**, *43*, 3649–3652.
4. Hoang, H. N.; Nagashima, Y.; Mori, S.; Kagechika, H. *Tetrahedron* **2017**, *73*, 2984–2989.
5. Arredondo, Y.; Moreno-Mañas, M.; Pleixats, R. *Synth. Commun.* **1996**, *26*, 3885–3895.
6. Rago, A. J.; Vasilopoulos, A.; Dombrowski, A. W.; Wang, Y. *Org. Lett.* **2022**, *24*, 8487–8496.
7. Pan, A.; Chojnacka, M.; Crowley, R. III; Göttemann, L.; Haines, B. E.; and Kou, K. G. M. *Chem. Sci.* **2022**, *13*, 3539–3948.

## 4.1 Appendix: NMR Spectra

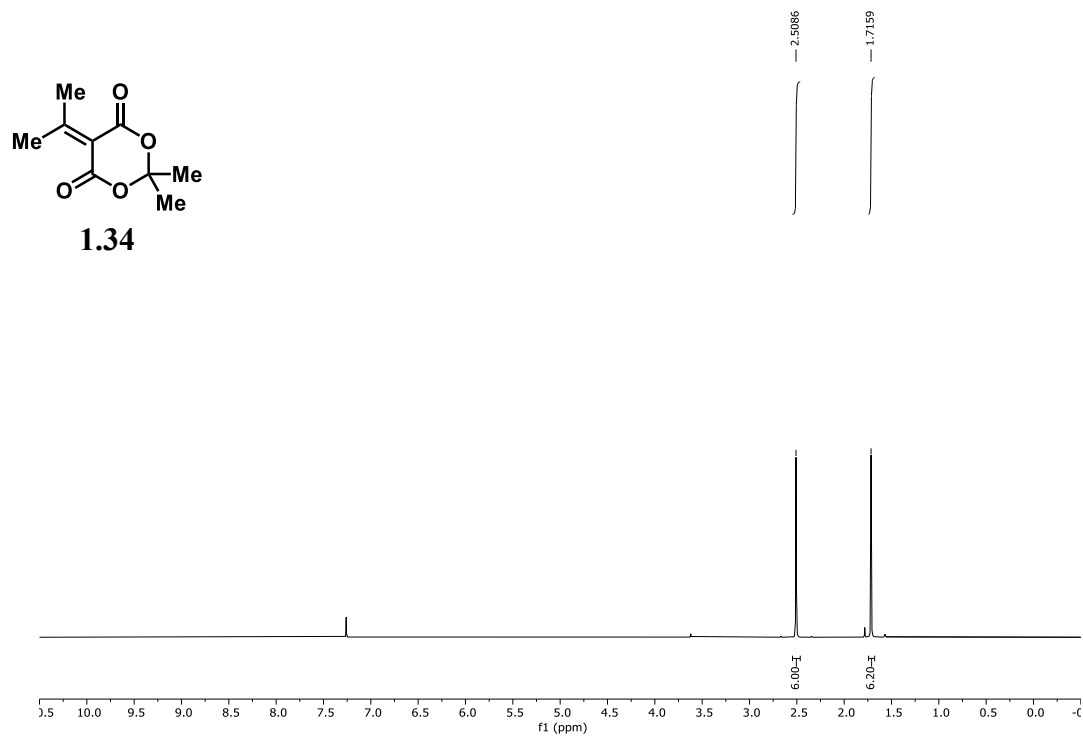


**Figure 4.1.**  $^1\text{H}$  NMR spectrum of **1.34** (400 MHz, 295 K,  $\text{CDCl}_3$ ).



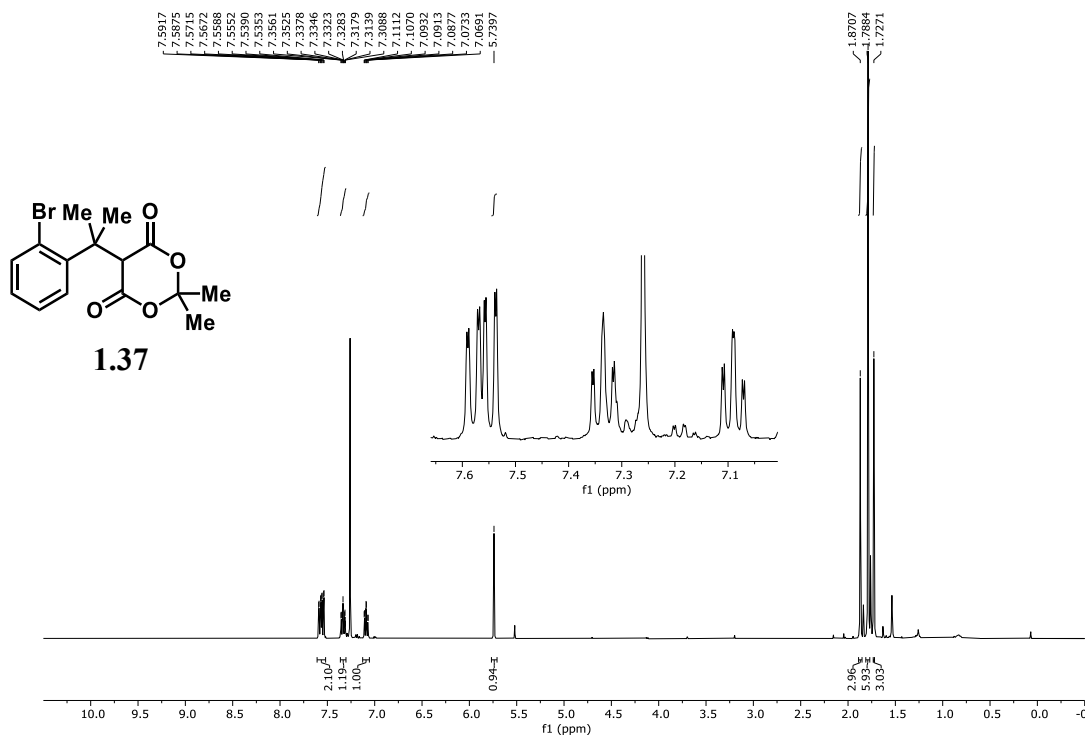


Figure 4.2. <sup>1</sup>H NMR spectrum of **1.37** (400 MHz, 295 K, CDCl<sub>3</sub>).

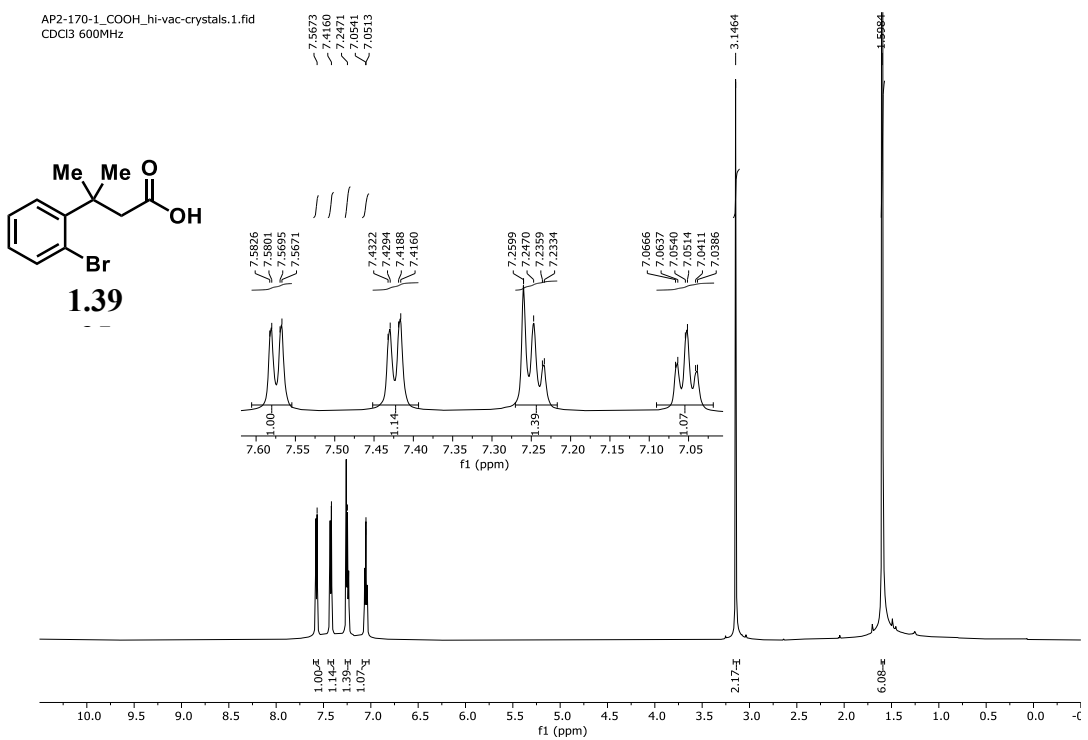


Figure 4.3. <sup>1</sup>H NMR spectrum of **1.39** (400 MHz, 295 K, CDCl<sub>3</sub>).

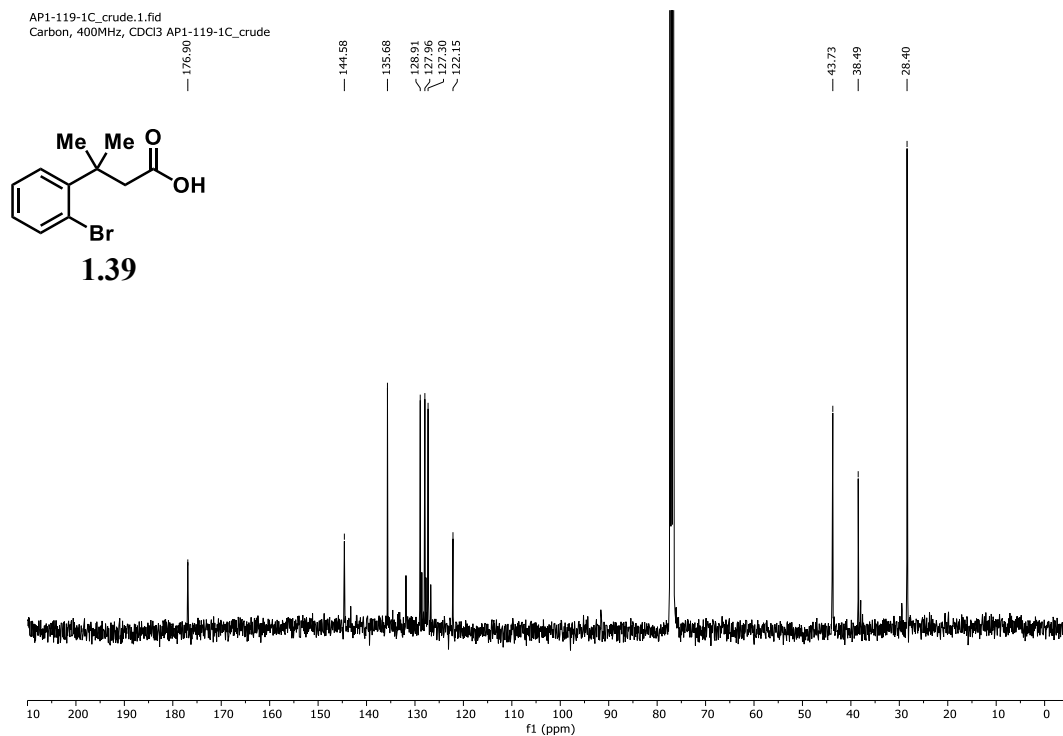


Figure 4.4. <sup>13</sup>C NMR spectrum of **1.39** (101 MHz, 295 K, CDCl<sub>3</sub>).

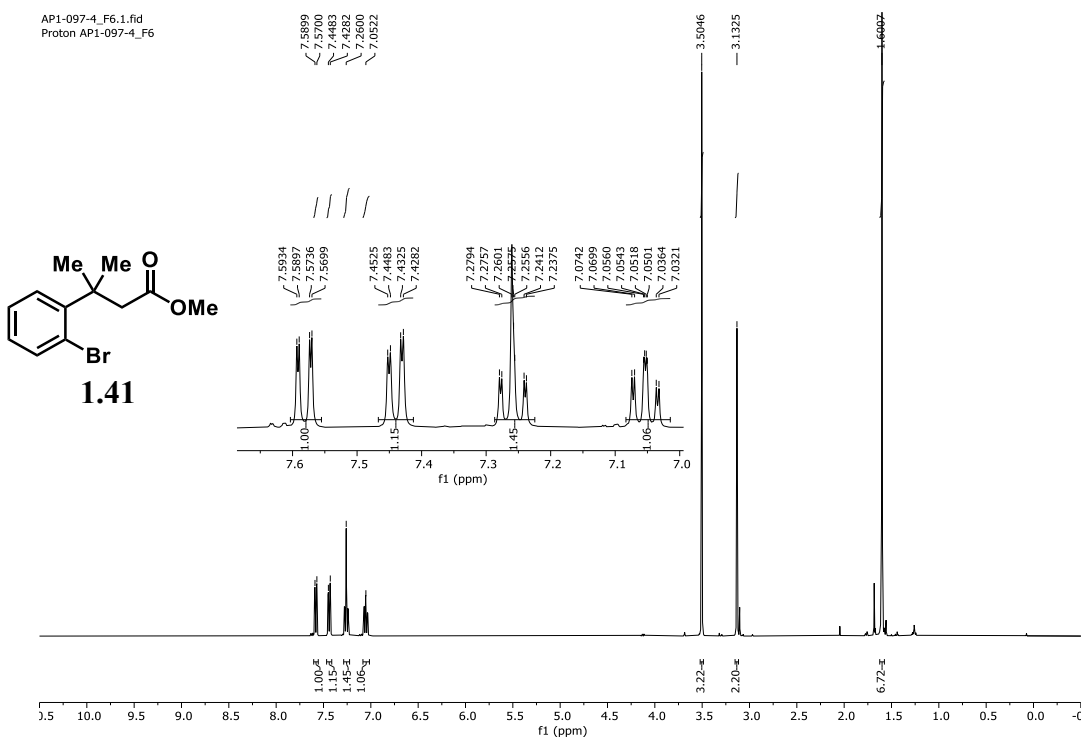


Figure 4.5. <sup>1</sup>H NMR spectrum of **1.41** (400 MHz, 295 K, CDCl<sub>3</sub>).

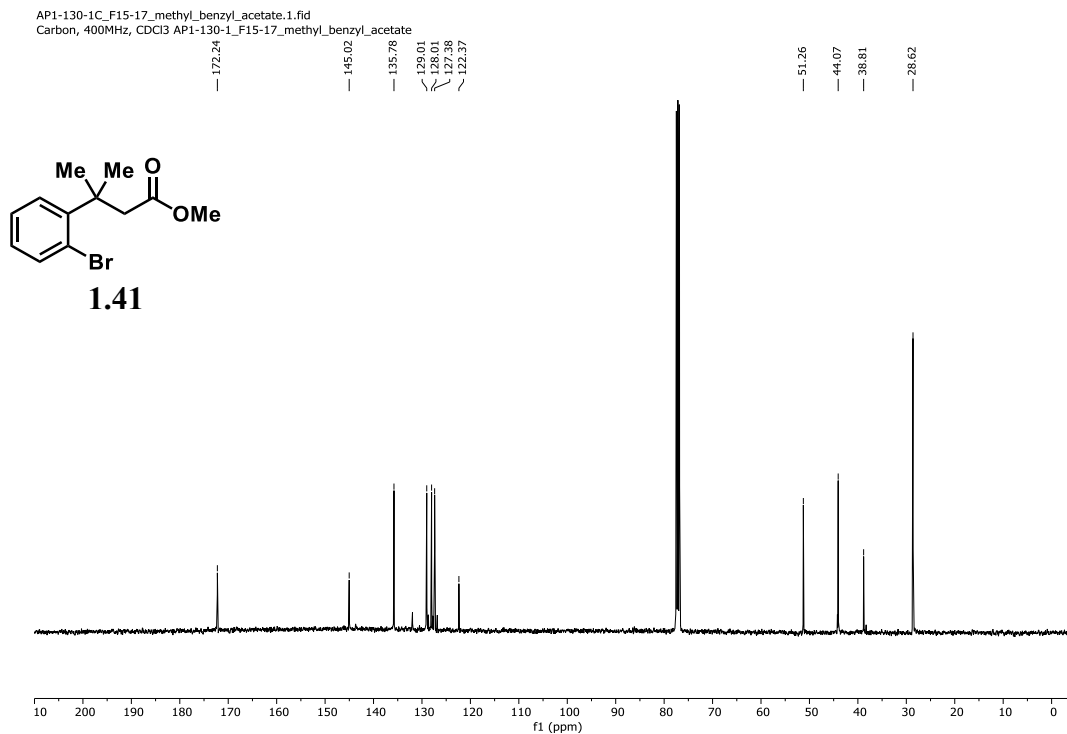


Figure 4.6.  $^{13}\text{C}$  NMR spectrum of **1.41** (101 MHz, 295 K,  $\text{CDCl}_3$ ).

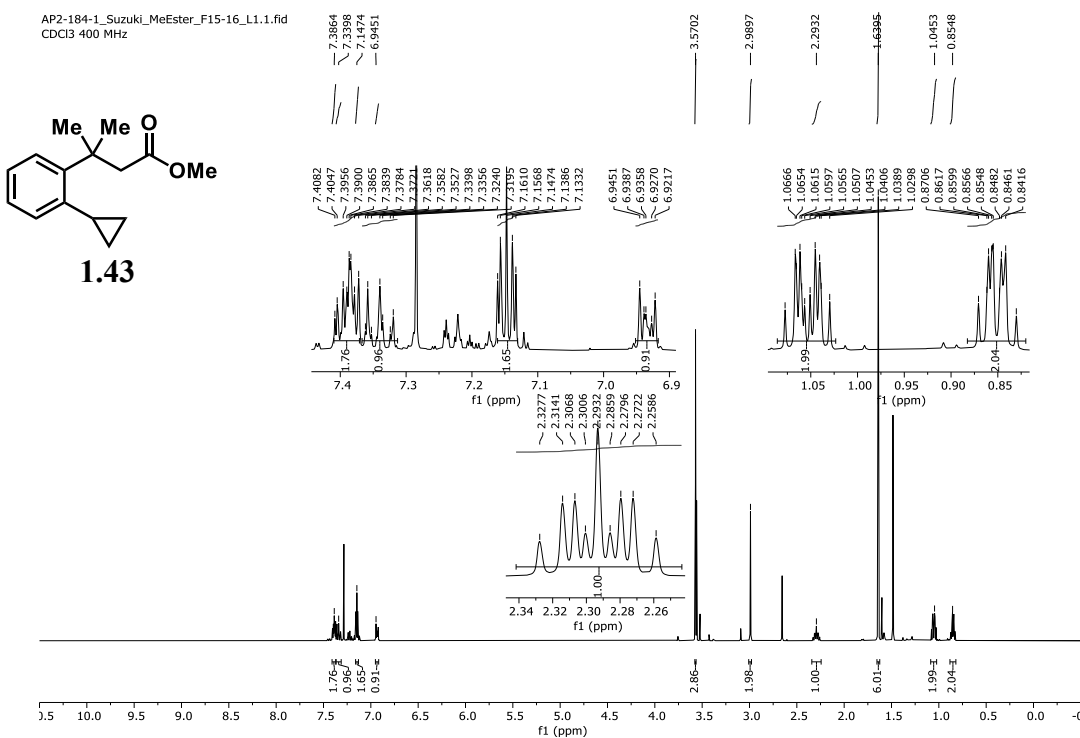


Figure 4.7.  $^1\text{H}$  NMR spectrum of **1.43** (600 MHz, 298 K,  $\text{CDCl}_3$ ).

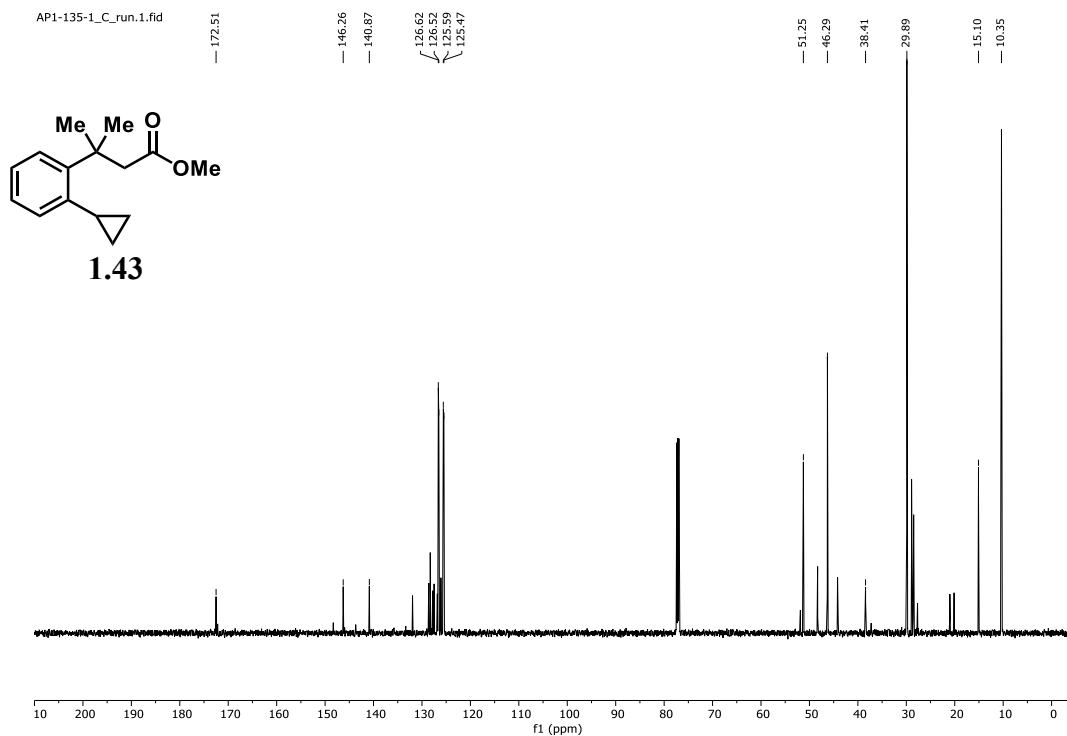


Figure 4.8.  $^{13}\text{C}$  NMR spectrum of **1.43** (151 MHz, 298 K,  $\text{CDCl}_3$ ).

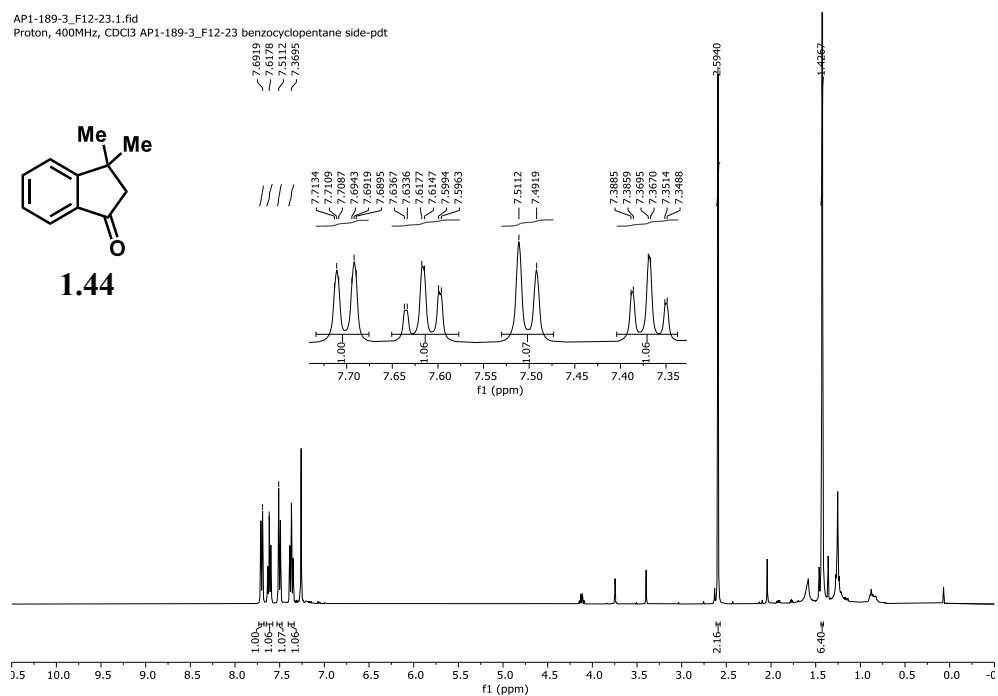
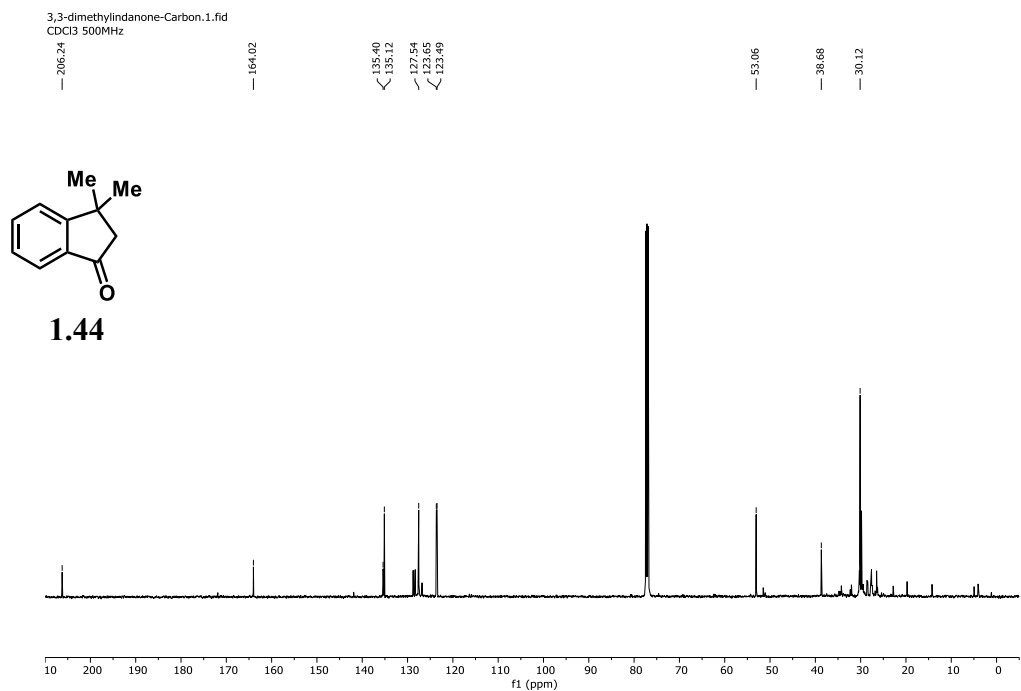
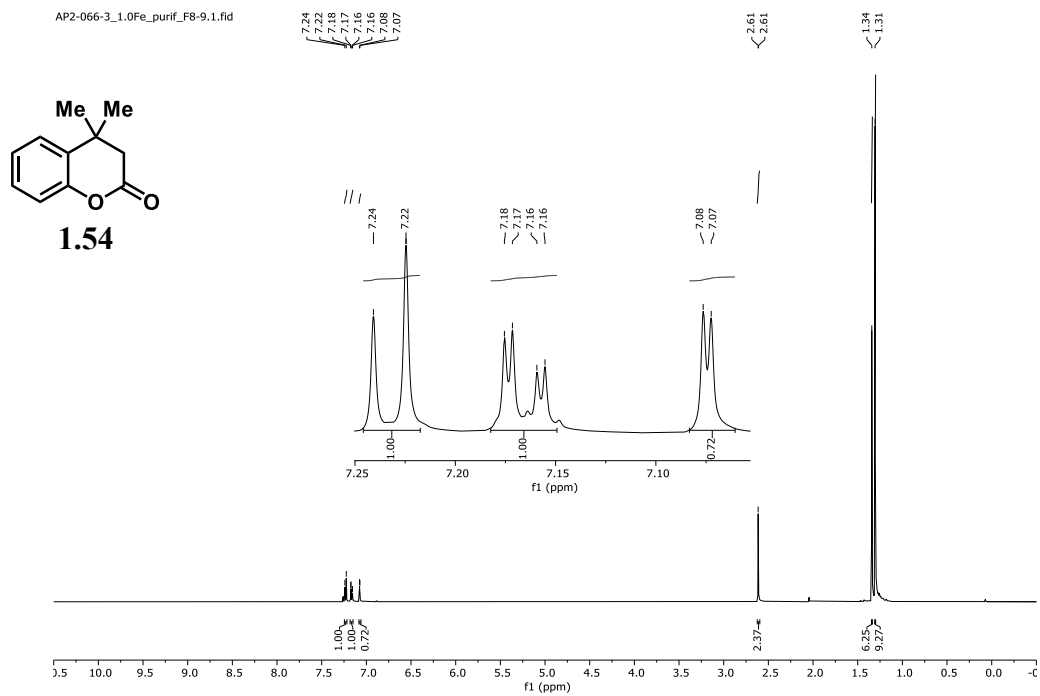


Figure 4.9.  $^1\text{H}$  NMR spectrum of **1.44** (400 MHz, 295 K,  $\text{CDCl}_3$ ).



**Figure 4.10.** <sup>13</sup>C NMR spectrum of **1.44** (126 MHz, 298 K, CDCl<sub>3</sub>).



**Figure 4.11.** <sup>1</sup>H NMR spectrum of **1.54** (500 MHz, 298 K, CDCl<sub>3</sub>).

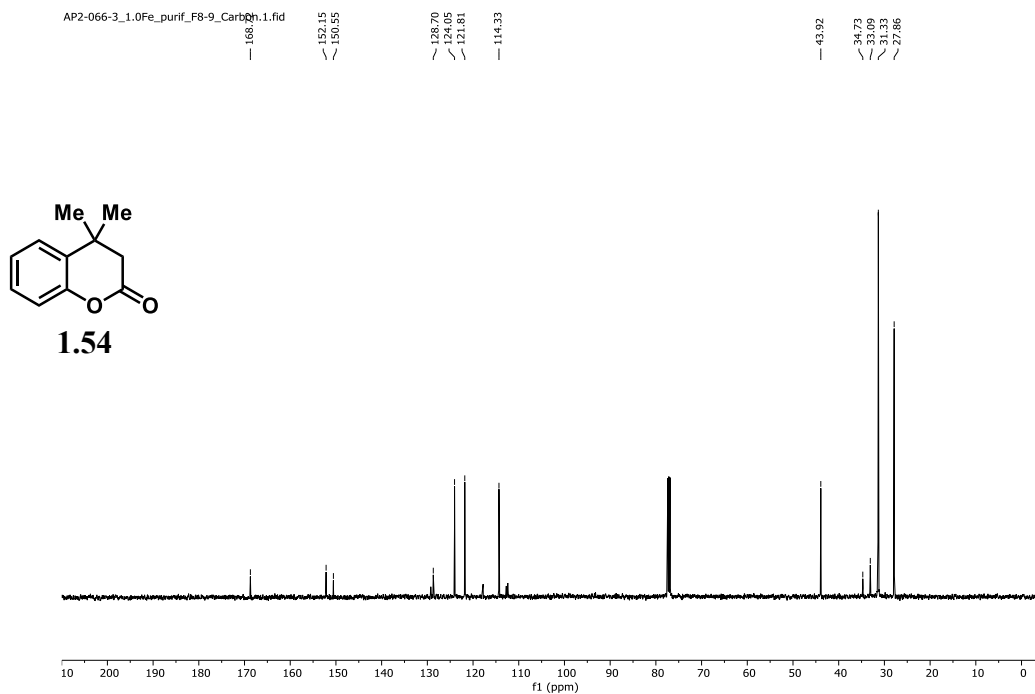


Figure 4.12.  $^{13}\text{C}$  NMR spectrum of **1.54** (126 MHz, 298 K,  $\text{CDCl}_3$ ).

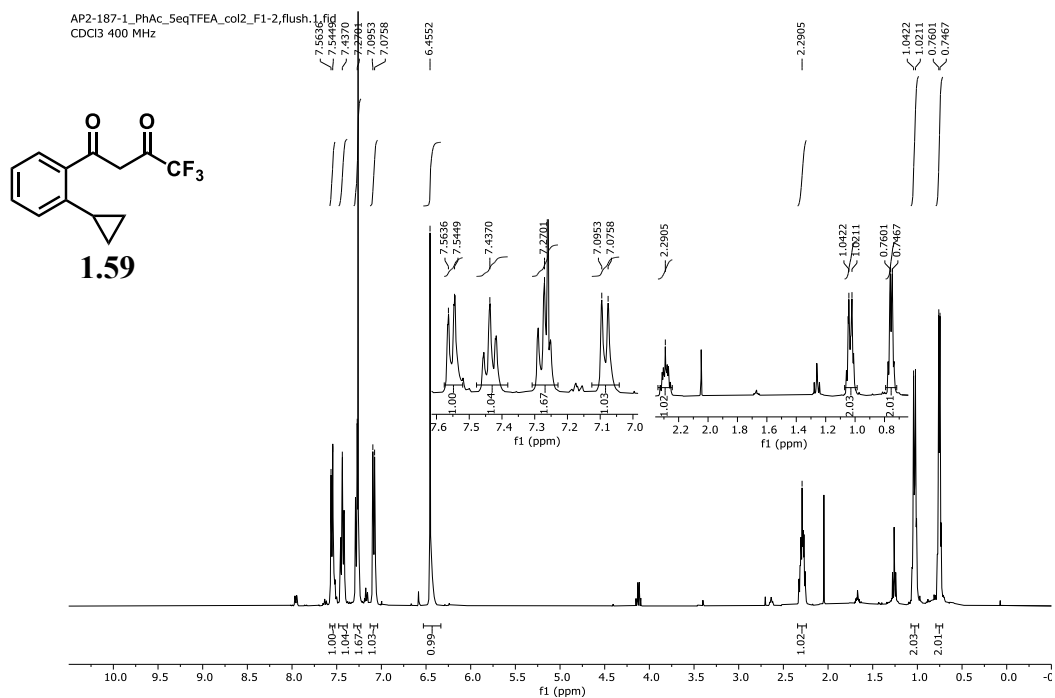


Figure 4.13.  $^1\text{H}$  NMR spectrum of **1.59** (400 MHz, 295 K,  $\text{CDCl}_3$ ).

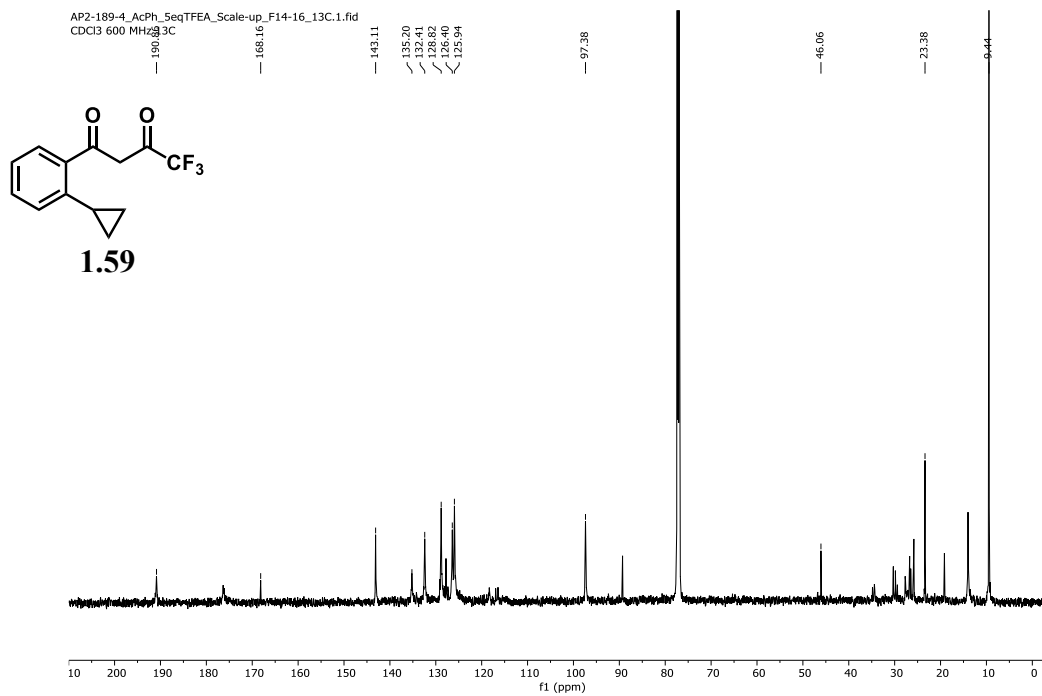


Figure 4.14.  $^{13}\text{C}$  NMR spectrum of **1.59** (151 MHz, 298 K,  $\text{CDCl}_3$ ).

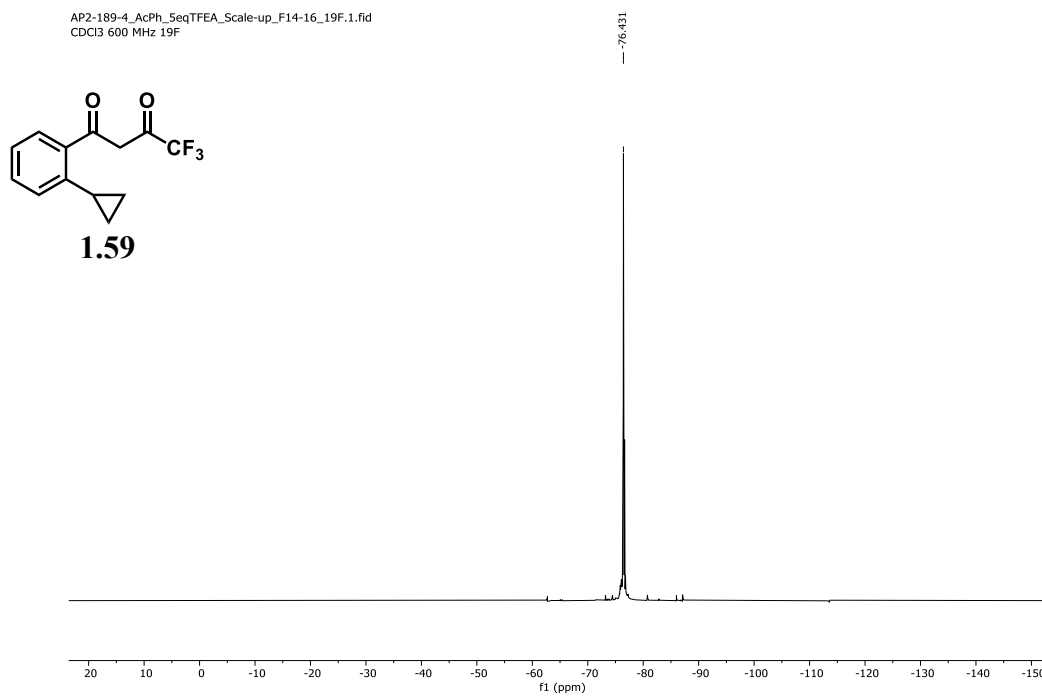


Figure 4.15.  $^{19}\text{F}$  NMR spectrum of **1.59** (564 MHz, 298 K,  $\text{CDCl}_3$ ).

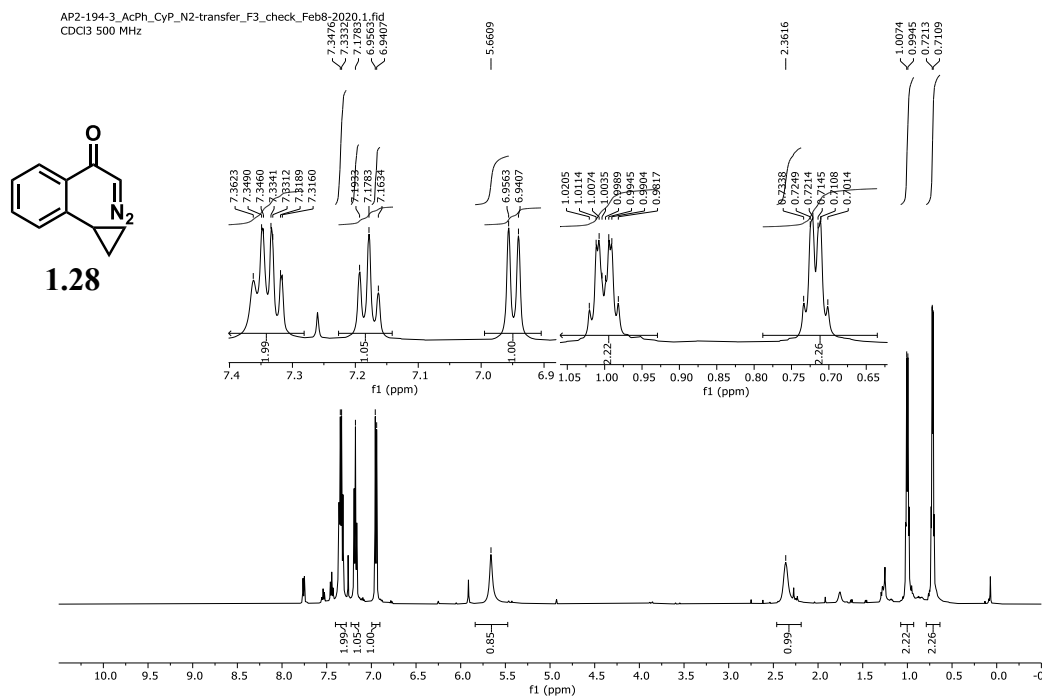


Figure 4.16. <sup>1</sup>H NMR spectrum of **1.28** (500 MHz, 298 K, CDCl<sub>3</sub>).

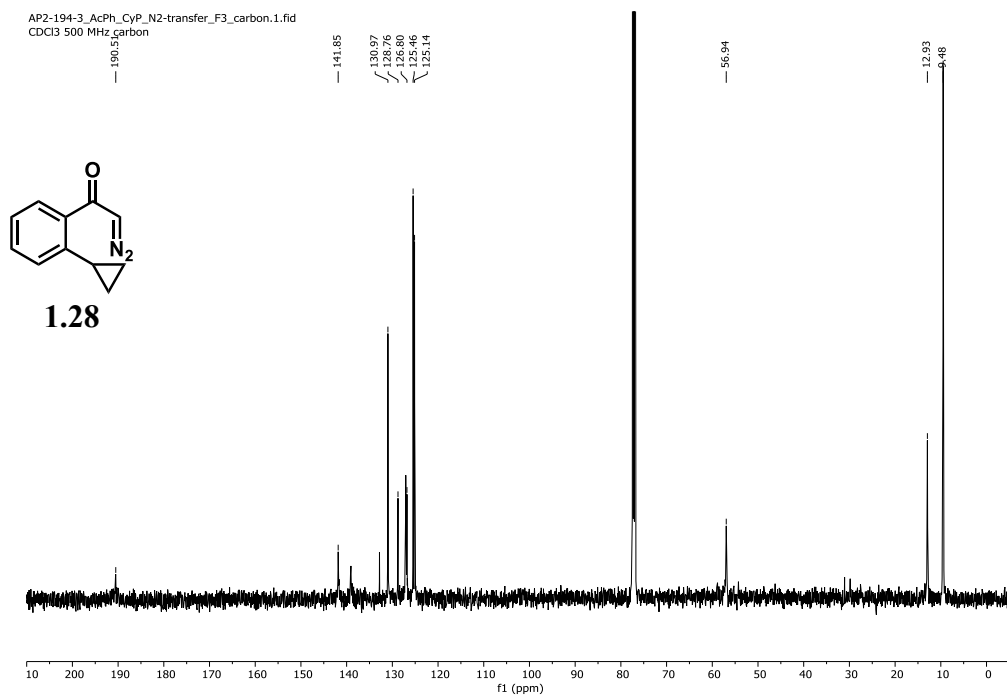


Figure 4.17. <sup>13</sup>C NMR spectrum of **1.28** (151 MHz, 298 K, CDCl<sub>3</sub>).



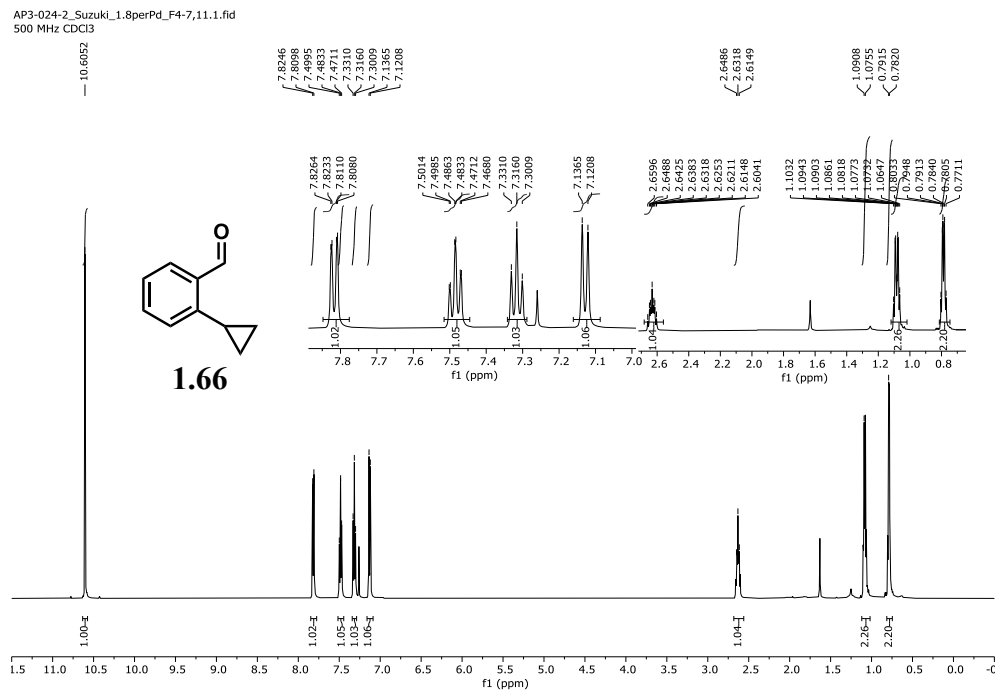


Figure 4.18. <sup>1</sup>H NMR spectrum of **1.66** (500 MHz, 298 K, CDCl<sub>3</sub>).

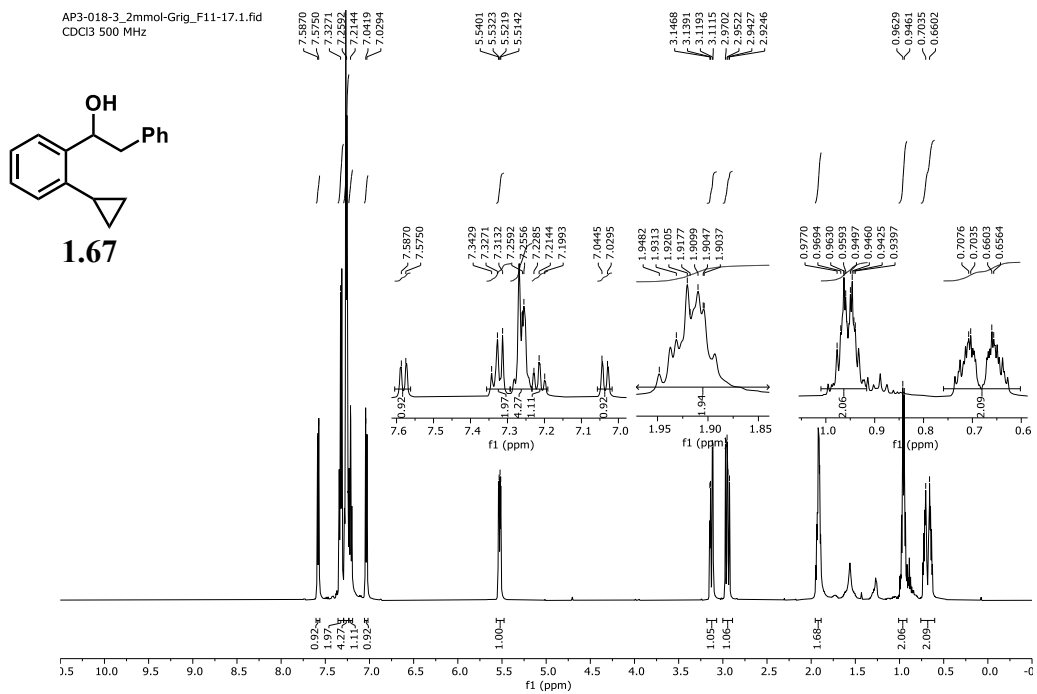


Figure 4.19. <sup>1</sup>H NMR spectrum of **1.67** (500 MHz, 298 K, CDCl<sub>3</sub>).

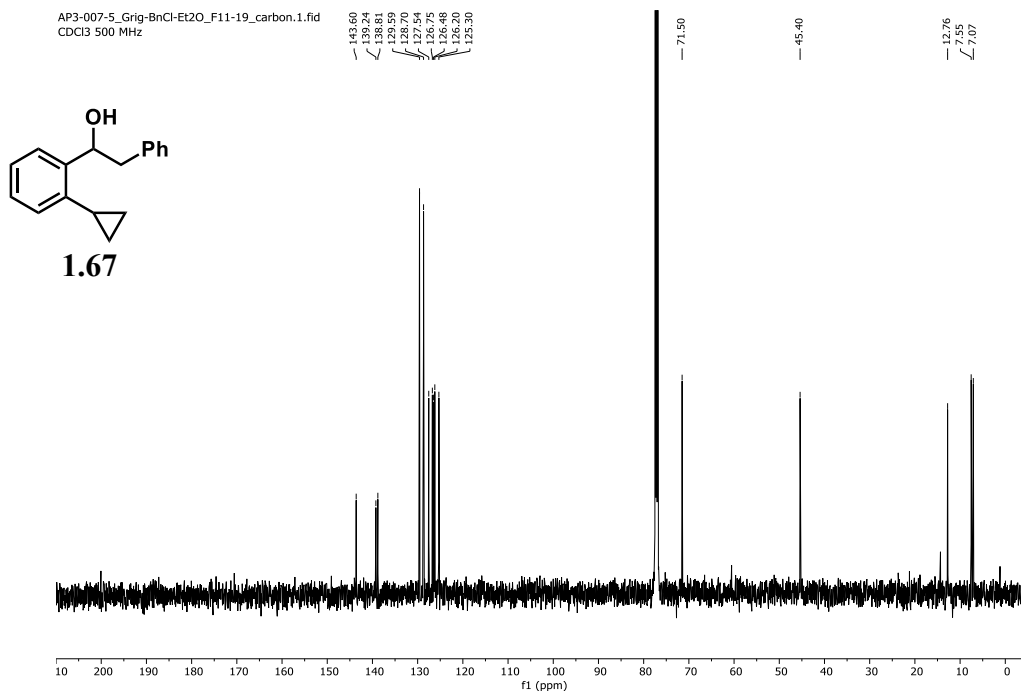


Figure 4.20. <sup>13</sup>C NMR spectrum of **1.67** (126 MHz, 298 K, CDCl<sub>3</sub>).

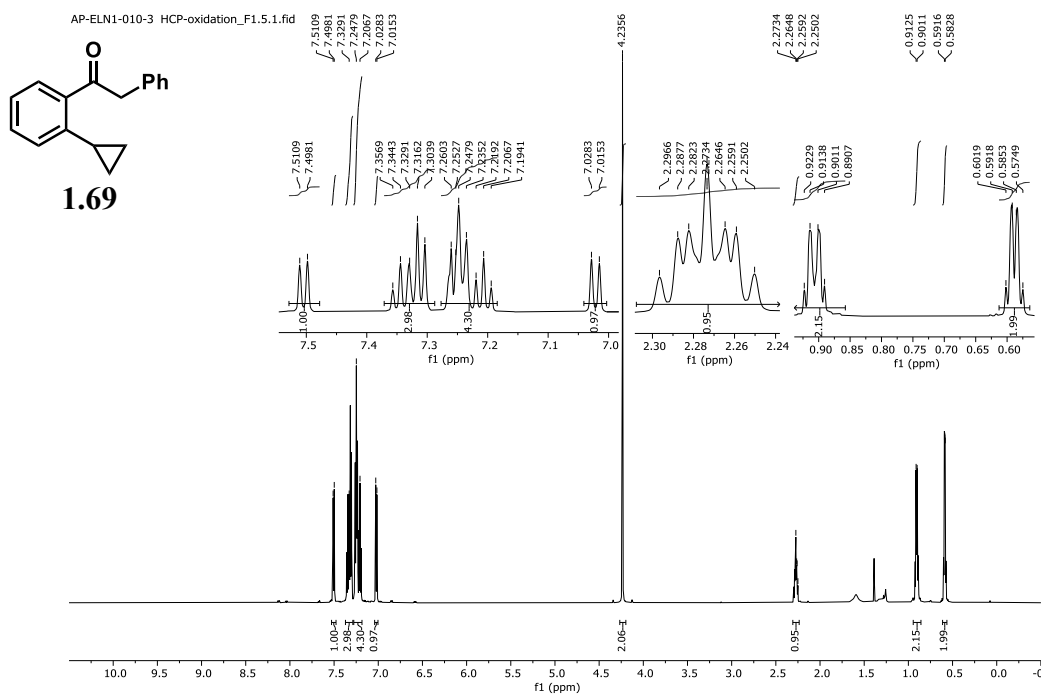


Figure 4.21. <sup>1</sup>H NMR spectrum of **1.69** (500 MHz, 298 K, CDCl<sub>3</sub>).

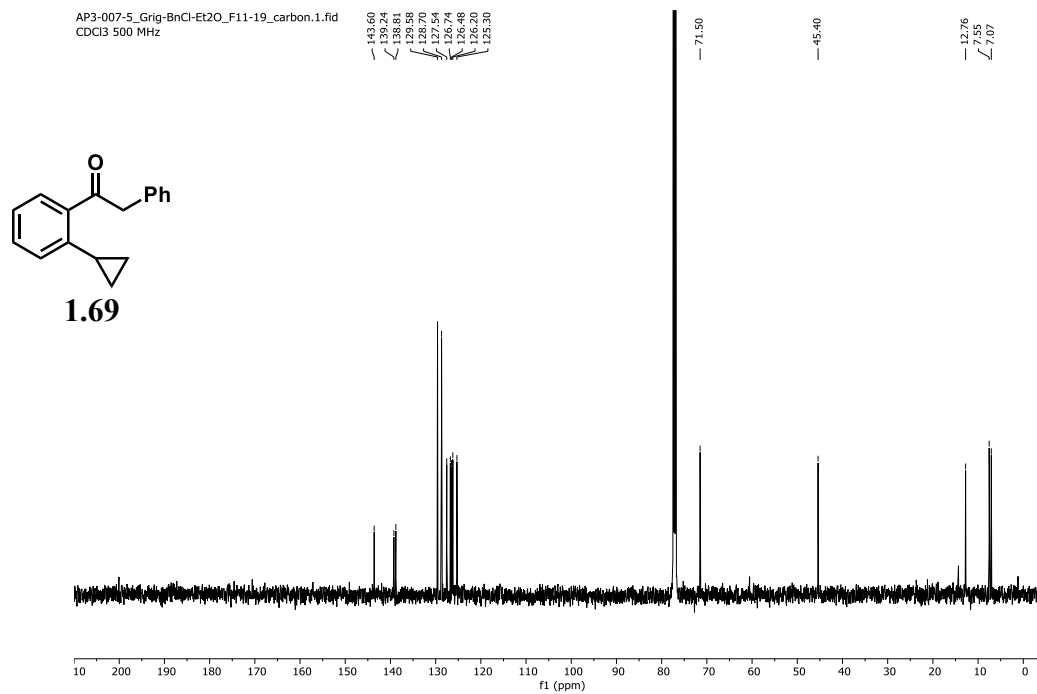


Figure 4.22. <sup>13</sup>C NMR spectrum of **1.69** (126 MHz, 298 K, CDCl<sub>3</sub>).

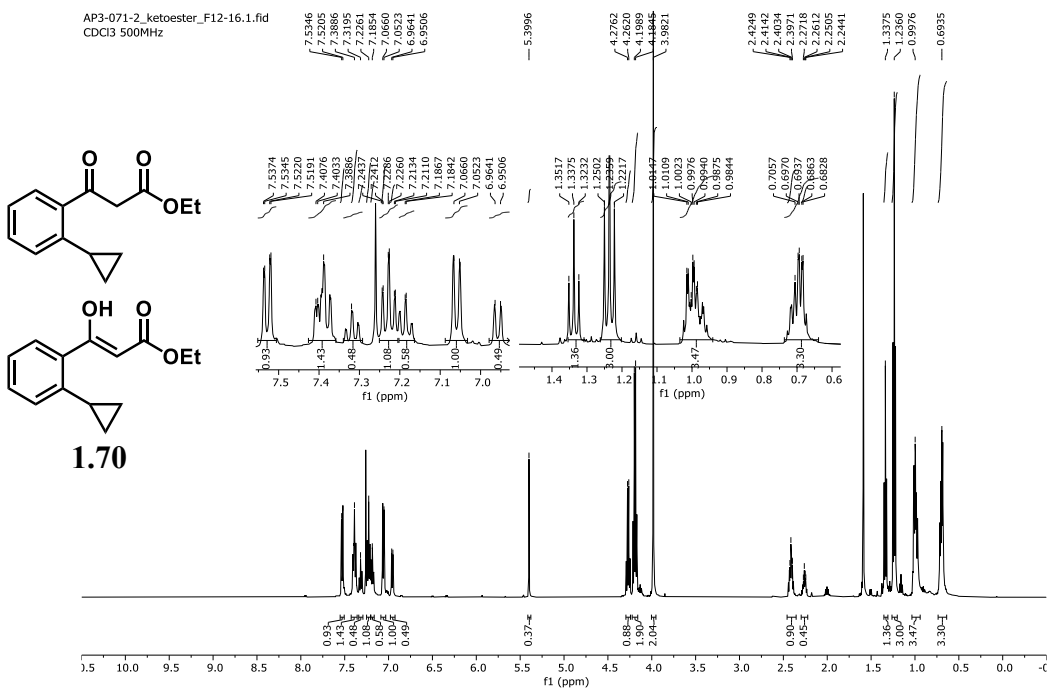


Figure 4.23. <sup>1</sup>H NMR spectrum of **1.70** (500 MHz, 298 K, CDCl<sub>3</sub>).

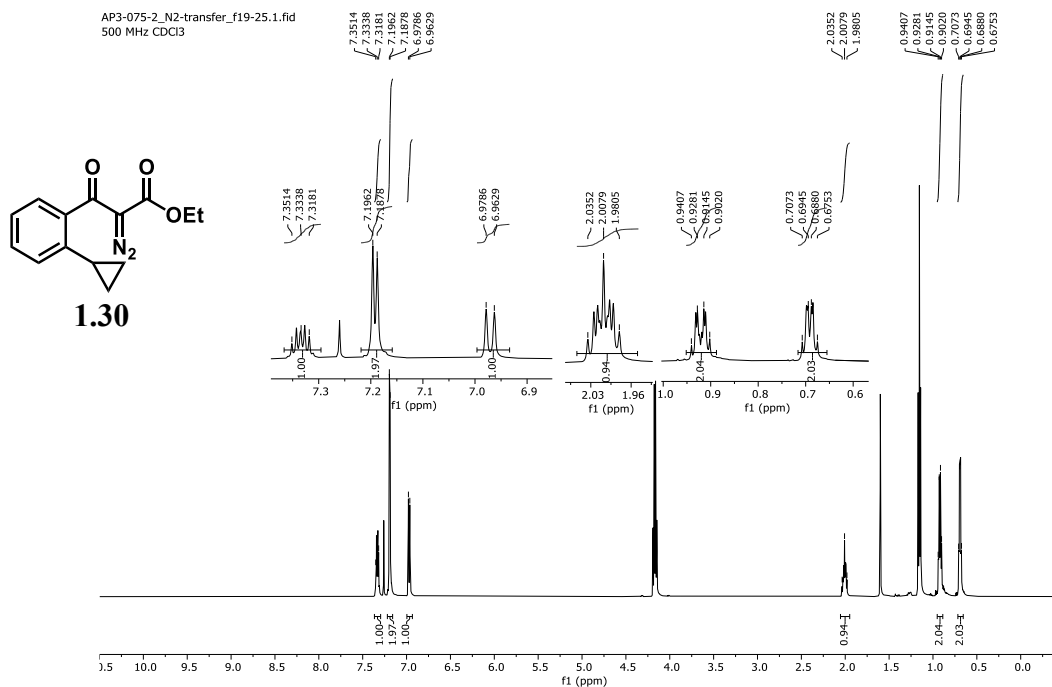


Figure 4.24. <sup>1</sup>H NMR spectrum of **1.30** (500 MHz, 298 K, CDCl<sub>3</sub>).

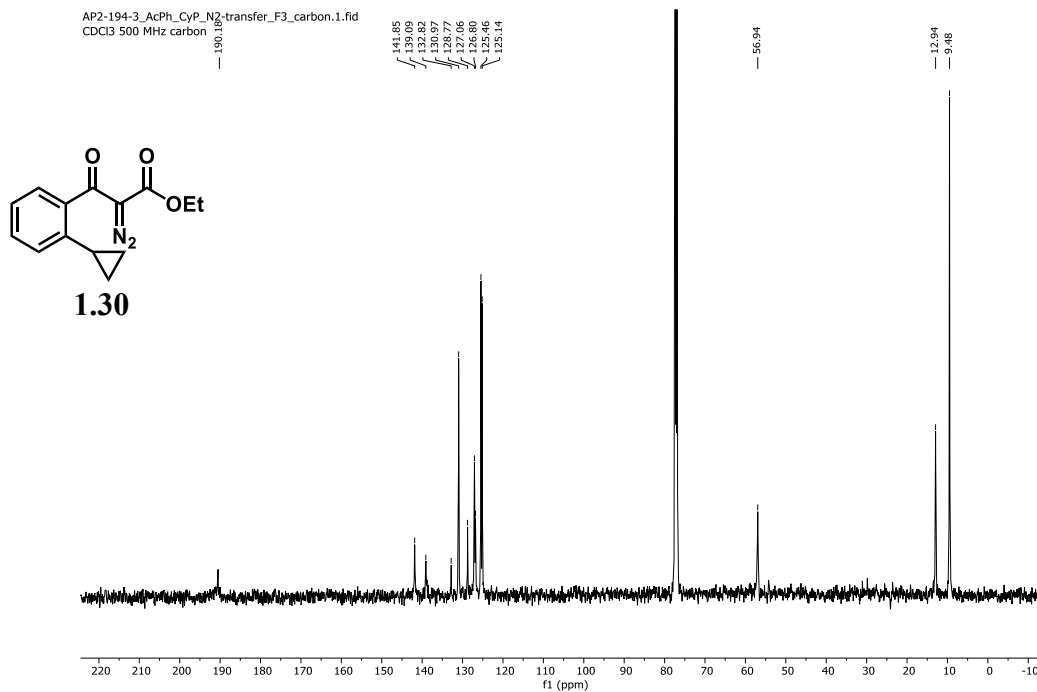


Figure 4.25. <sup>13</sup>C NMR spectrum of **1.30** (126 MHz, 298 K, CDCl<sub>3</sub>).

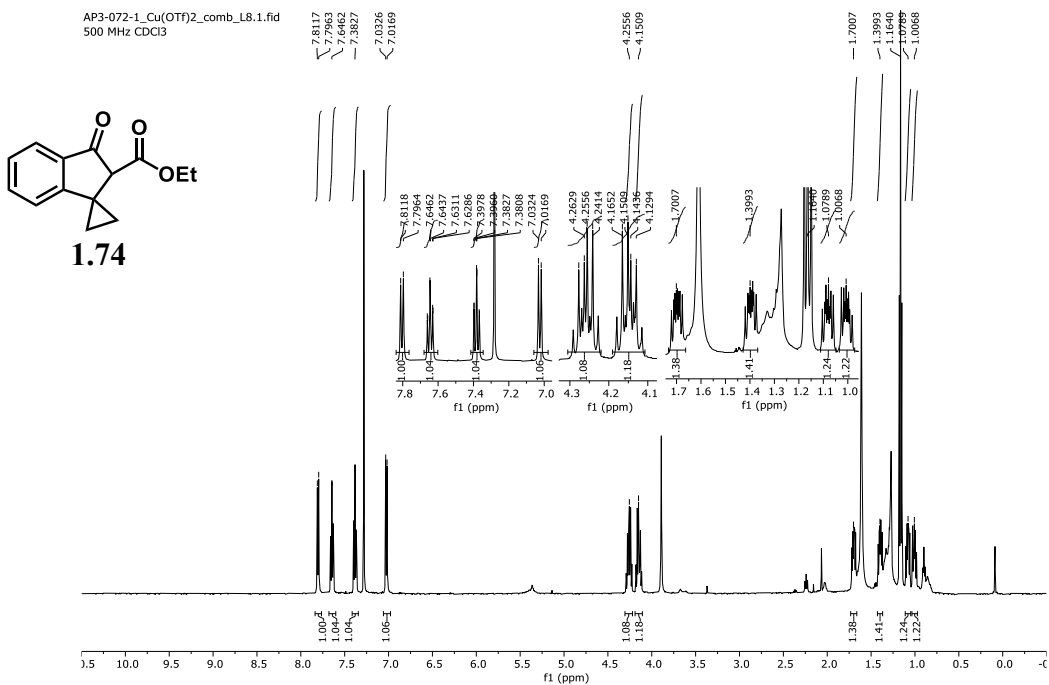


Figure 4.26. <sup>1</sup>H NMR spectrum of **1.74** (500 MHz, 298 K, CDCl<sub>3</sub>).

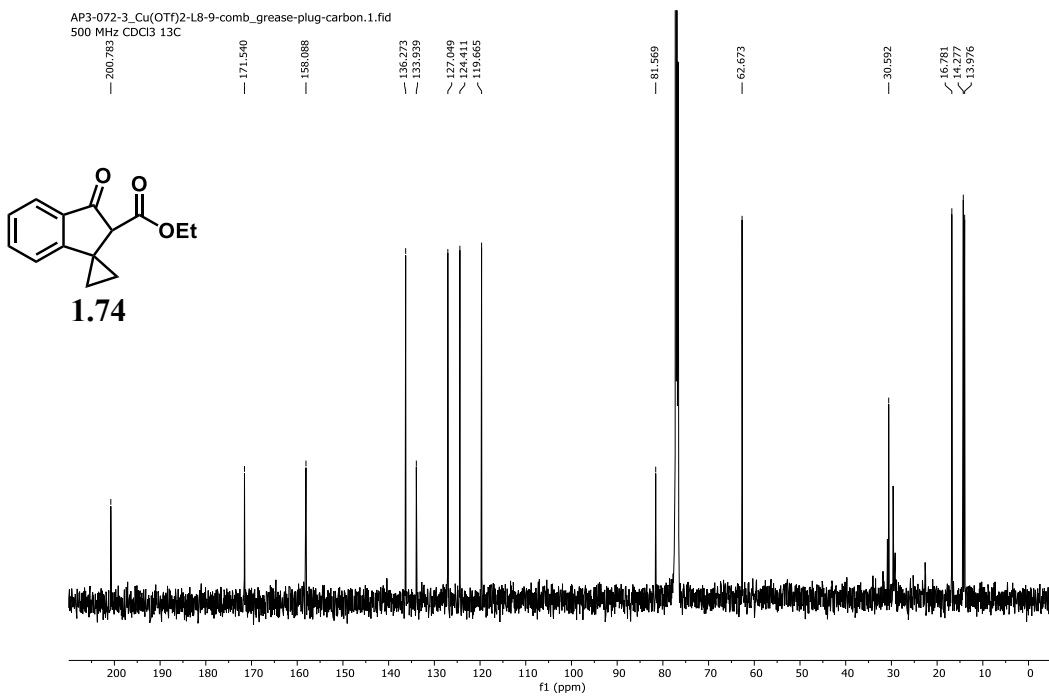


Figure 4.27. <sup>13</sup>C NMR spectrum of **1.74** (126 MHz, 298 K, CDCl<sub>3</sub>).

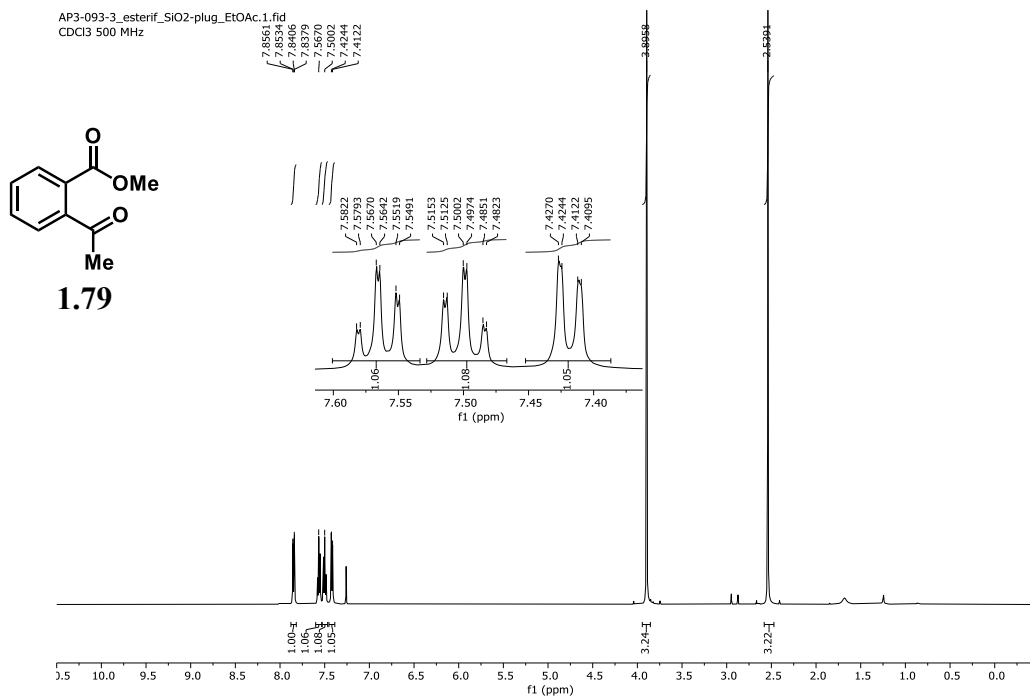


Figure 4.28. <sup>1</sup>H NMR spectrum of **1.79** (500 MHz, 298 K, CDCl<sub>3</sub>).

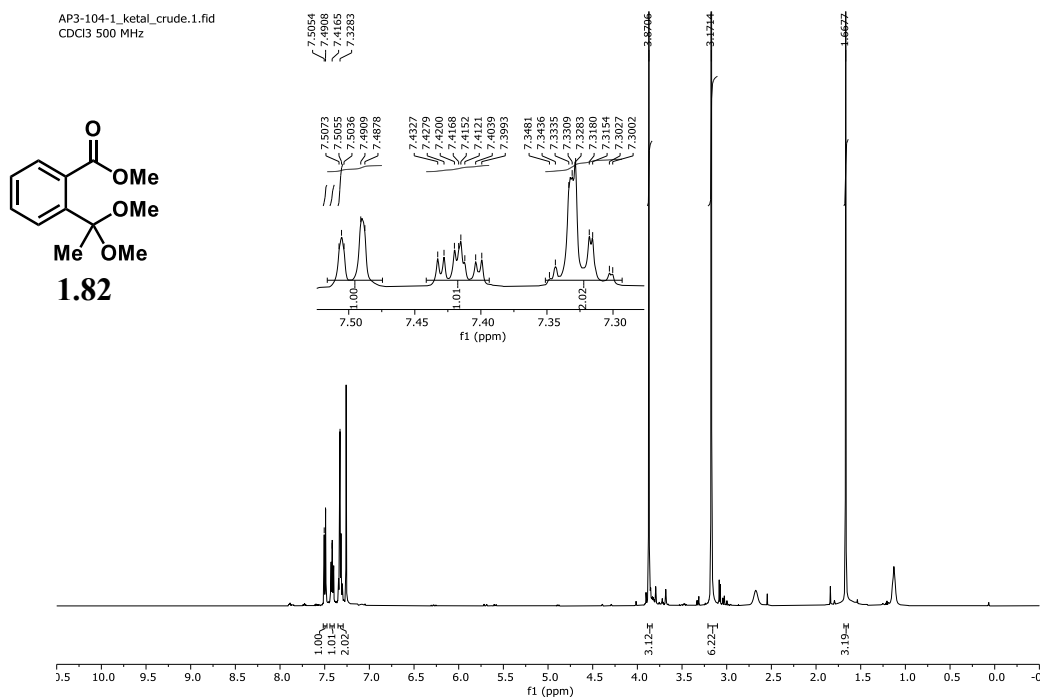


Figure 4.29. <sup>1</sup>H NMR spectrum of **1.82** (500 MHz, 298 K, CDCl<sub>3</sub>).

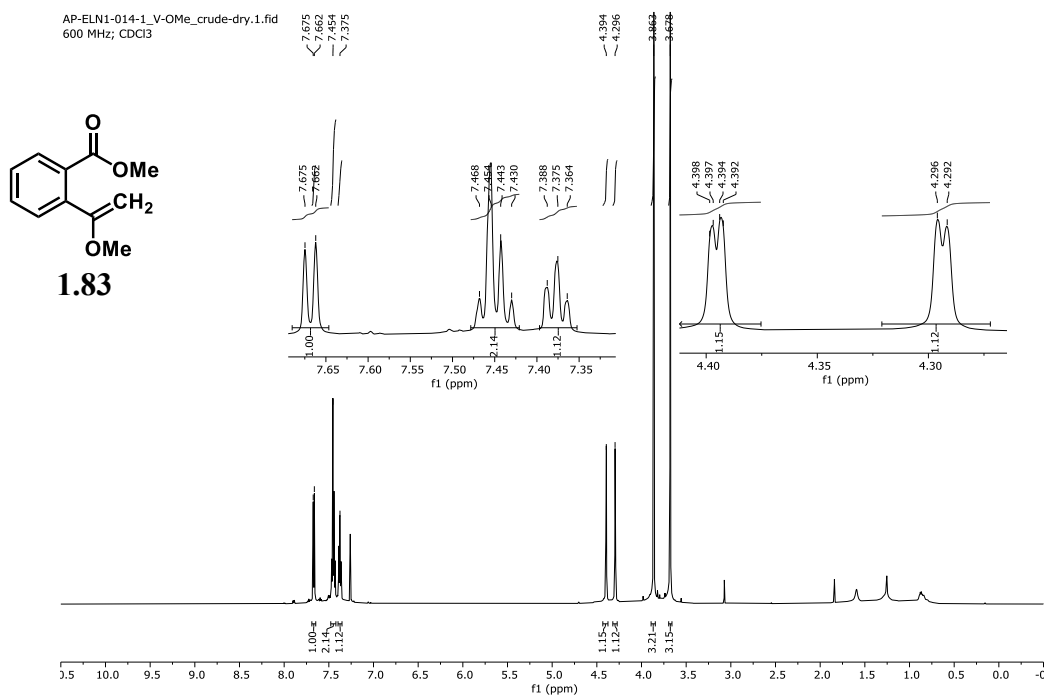


Figure 4.30. <sup>1</sup>H NMR spectrum of **1.83** (600 MHz, 298 K, CDCl<sub>3</sub>).

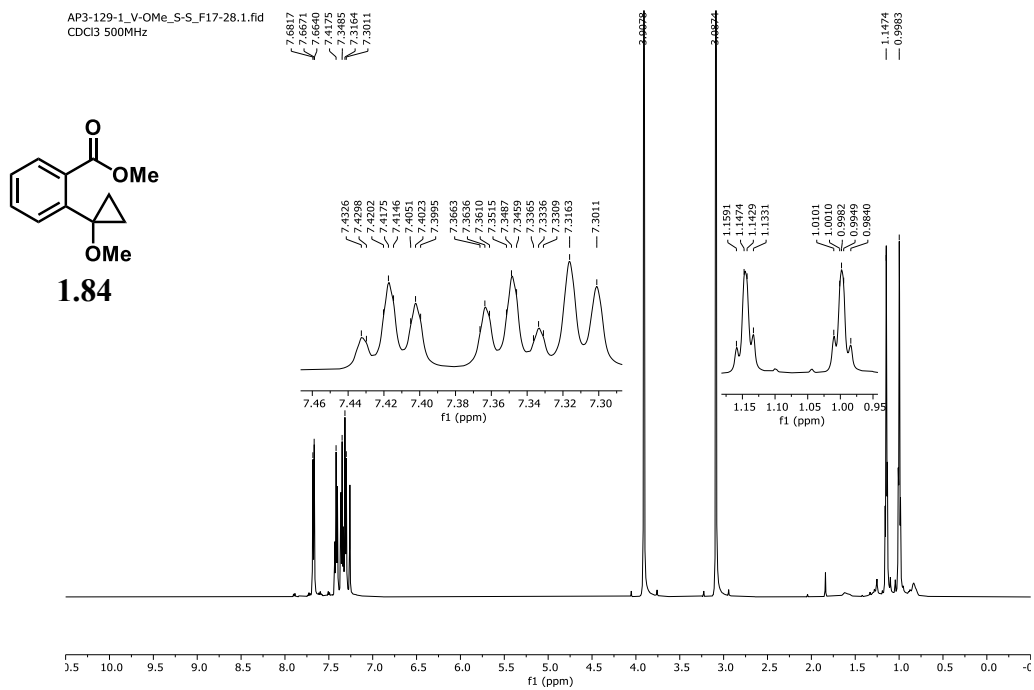


Figure 4.31. <sup>1</sup>H NMR spectrum of **1.84** (500 MHz, 298 K, CDCl<sub>3</sub>).

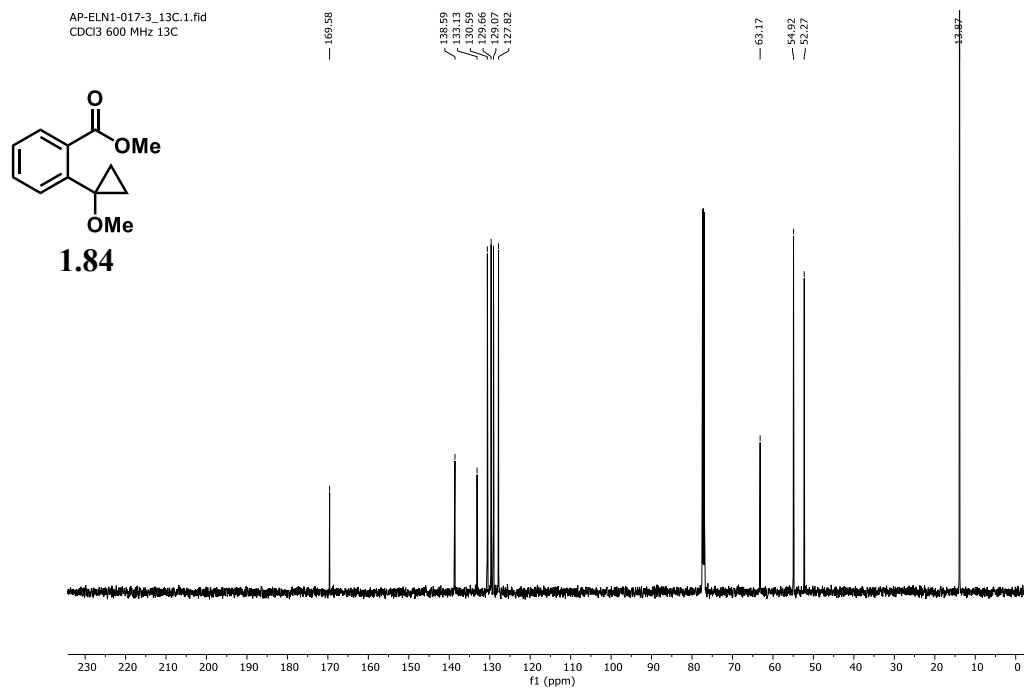


Figure 4.32.  $^{13}\text{C}$  NMR spectrum of **1.84** (151 MHz, 298 K,  $\text{CDCl}_3$ ).

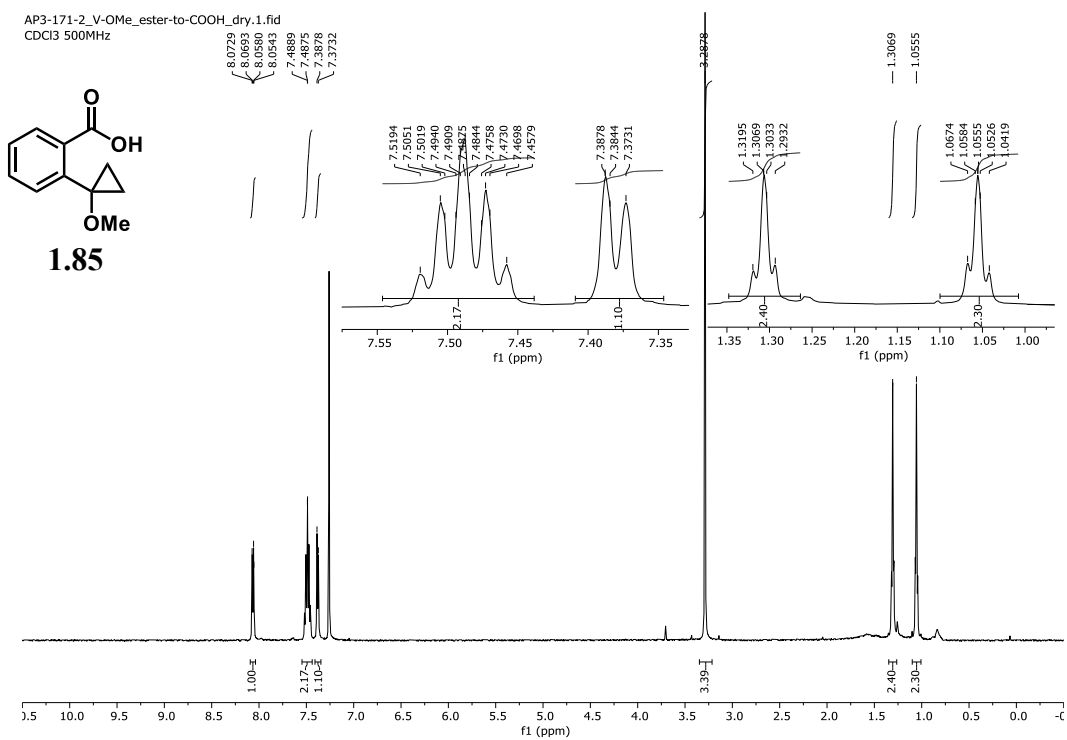


Figure 4.33.  $^1\text{H}$  NMR spectrum of **1.85** (500 MHz, 298 K,  $\text{CDCl}_3$ ).



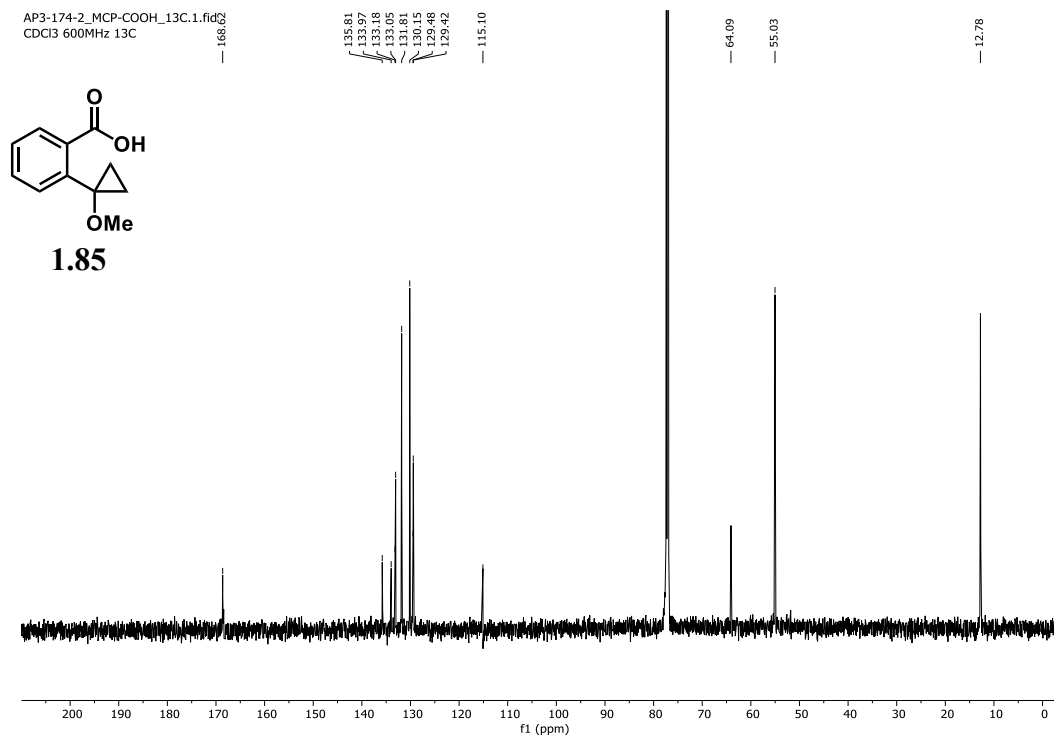


Figure 4.34. <sup>13</sup>C NMR spectrum of **1.85** (151 MHz, 298 K, CDCl<sub>3</sub>).

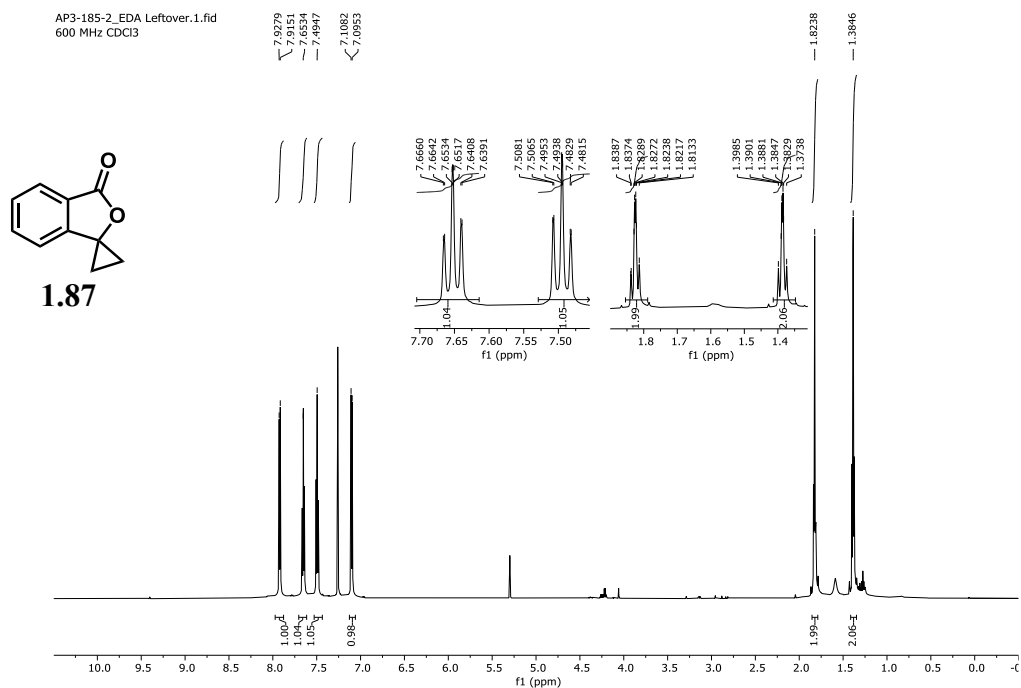


Figure 4.35. <sup>1</sup>H NMR spectrum of **1.87** (600 MHz, 298 K, CDCl<sub>3</sub>).

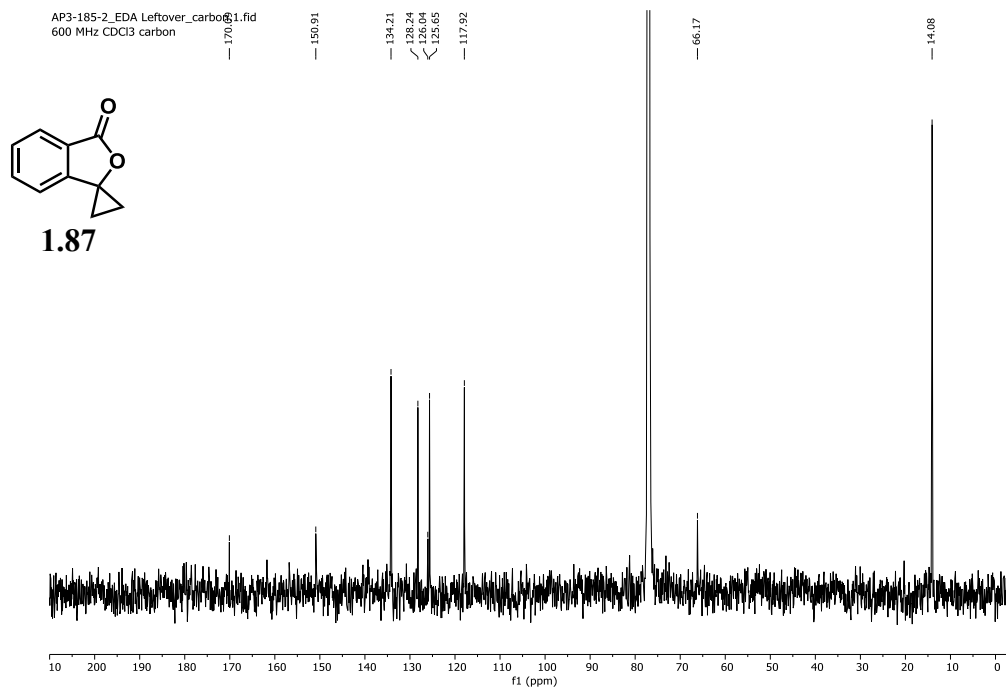


Figure 4.36. <sup>13</sup>C NMR spectrum of **1.87** (151 MHz, 298 K, CDCl<sub>3</sub>).

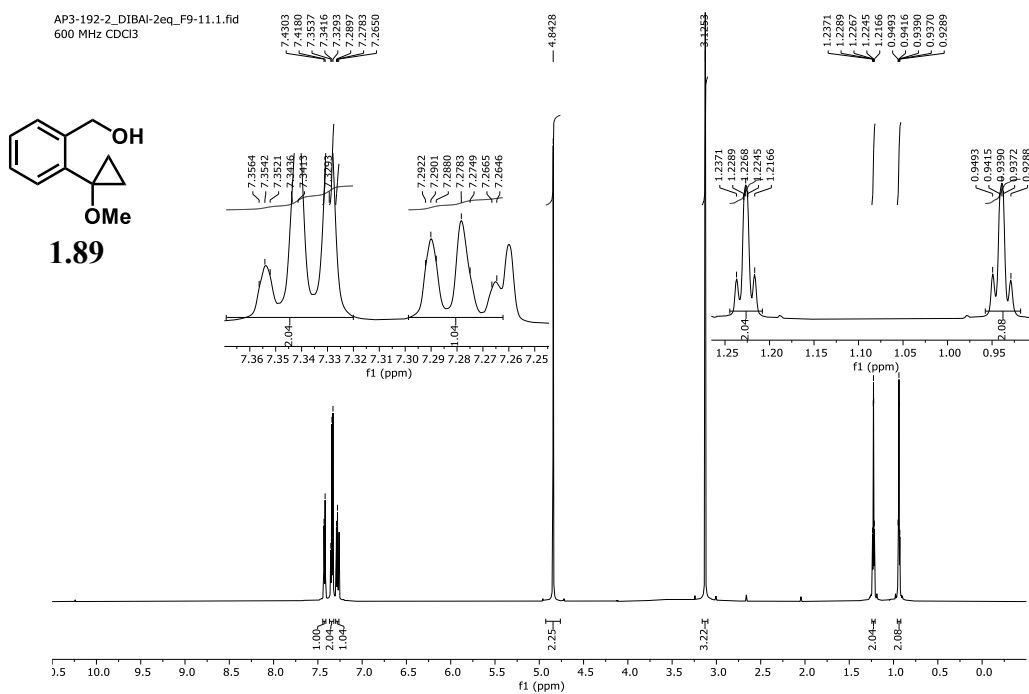


Figure 4.37. <sup>1</sup>H NMR spectrum of **1.89** (600 MHz, 298 K, CDCl<sub>3</sub>).

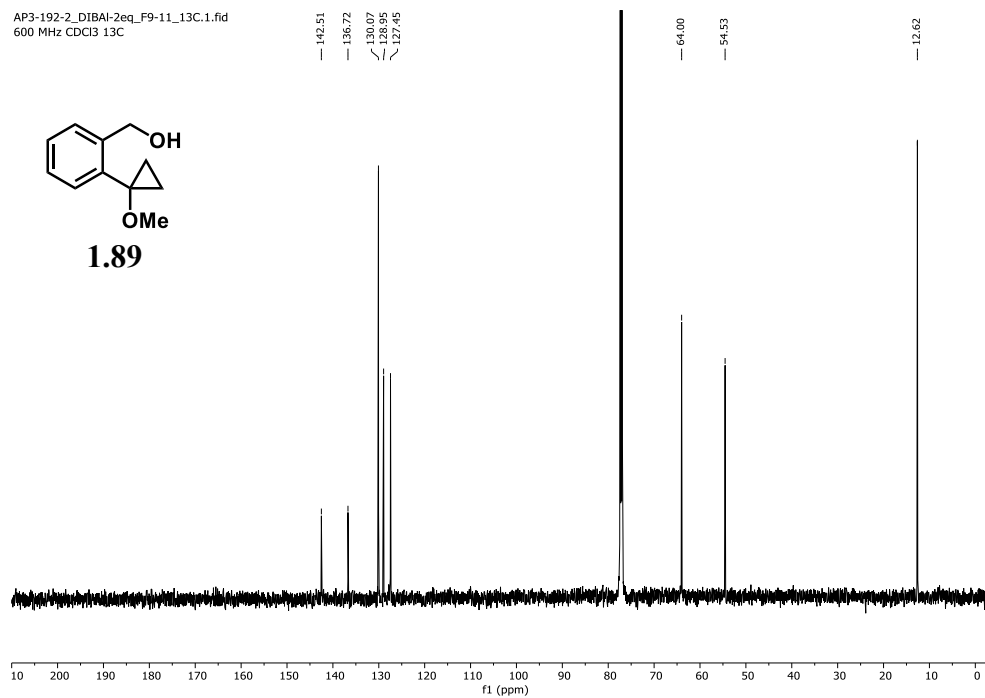


Figure 4.38. <sup>13</sup>C NMR spectrum of **1.89** (151 MHz, 298 K, CDCl<sub>3</sub>).

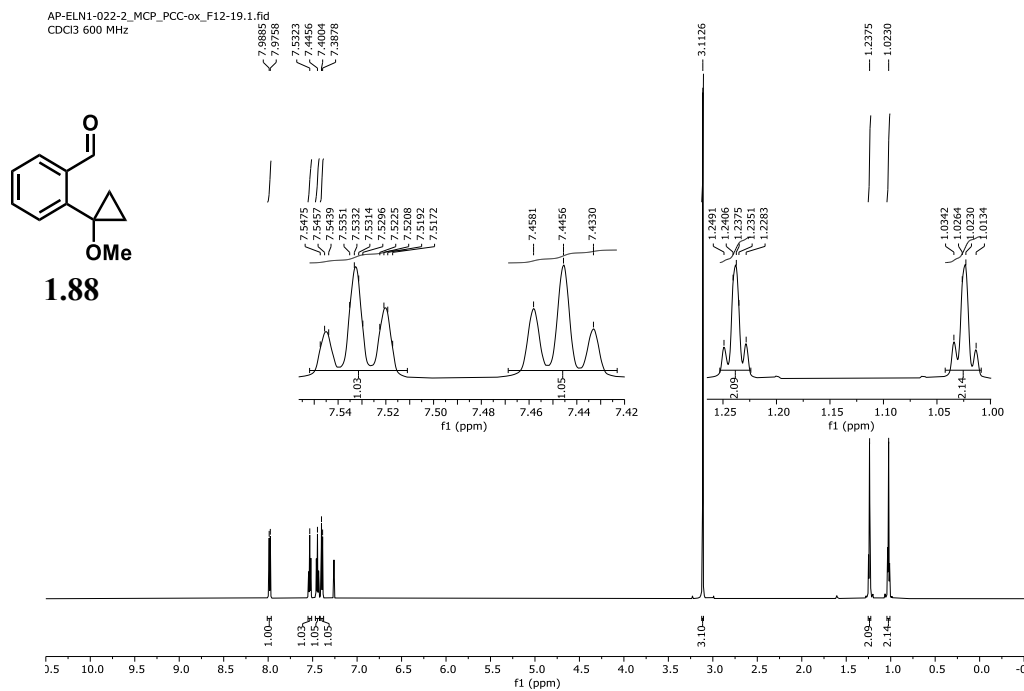


Figure 4.39. <sup>1</sup>H NMR spectrum of **1.88** (600 MHz, 298 K, CDCl<sub>3</sub>).

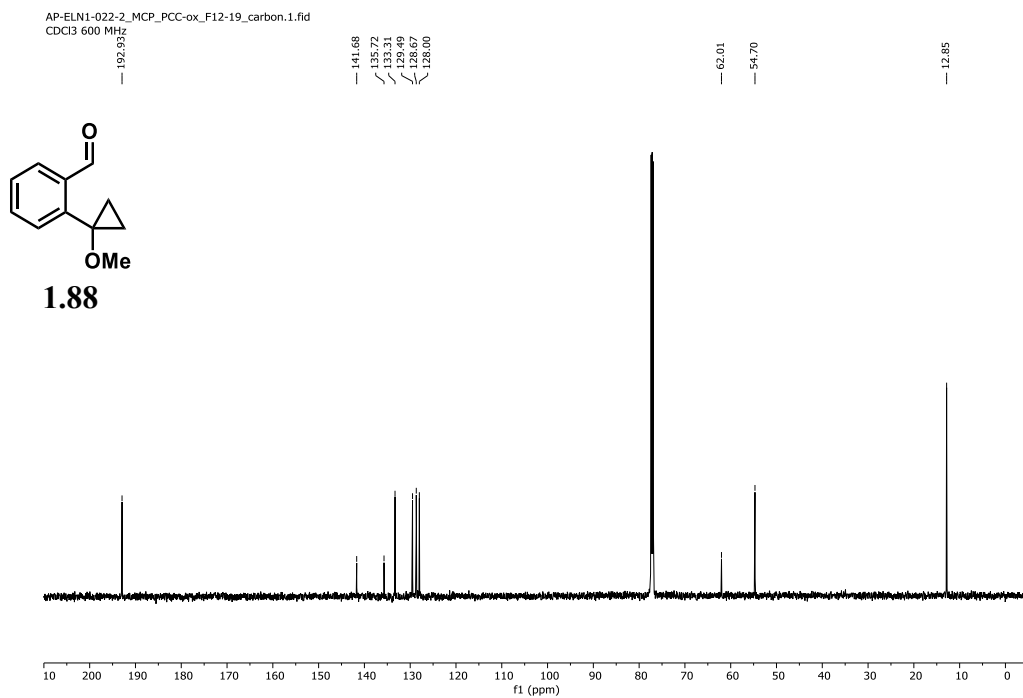


Figure 4.40. <sup>13</sup>C NMR spectrum of **1.88** (151 MHz, 298 K, CDCl<sub>3</sub>).

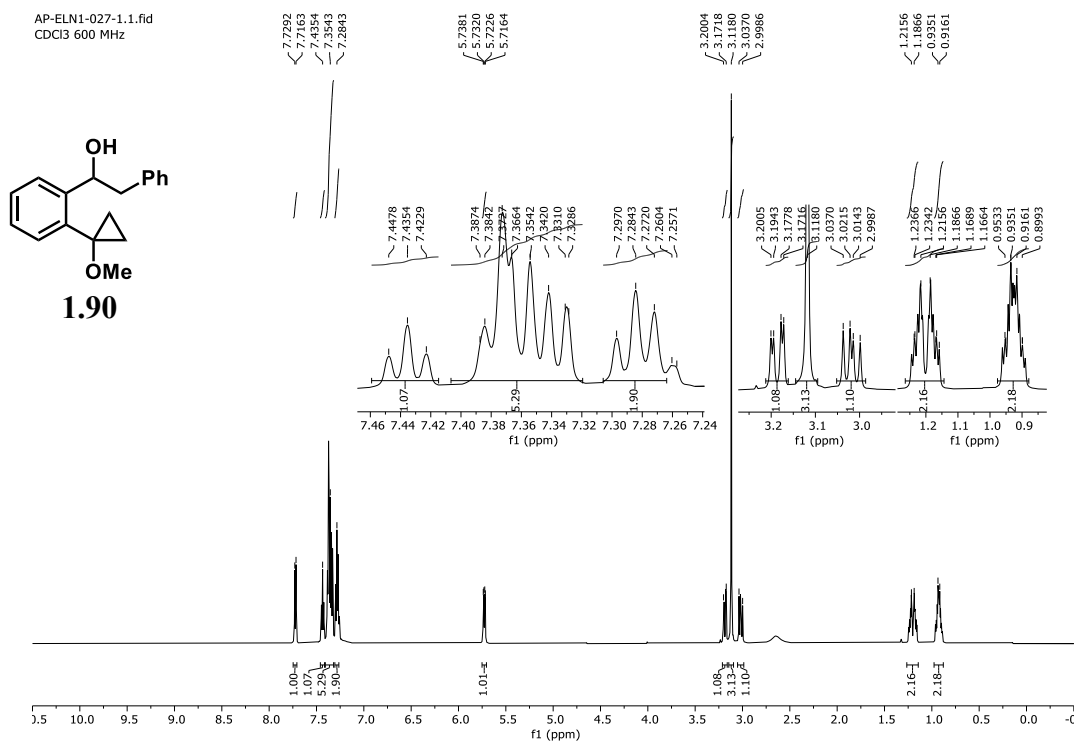


Figure 4.41. <sup>1</sup>H NMR spectrum of **1.90** (600 MHz, 298 K, CDCl<sub>3</sub>).

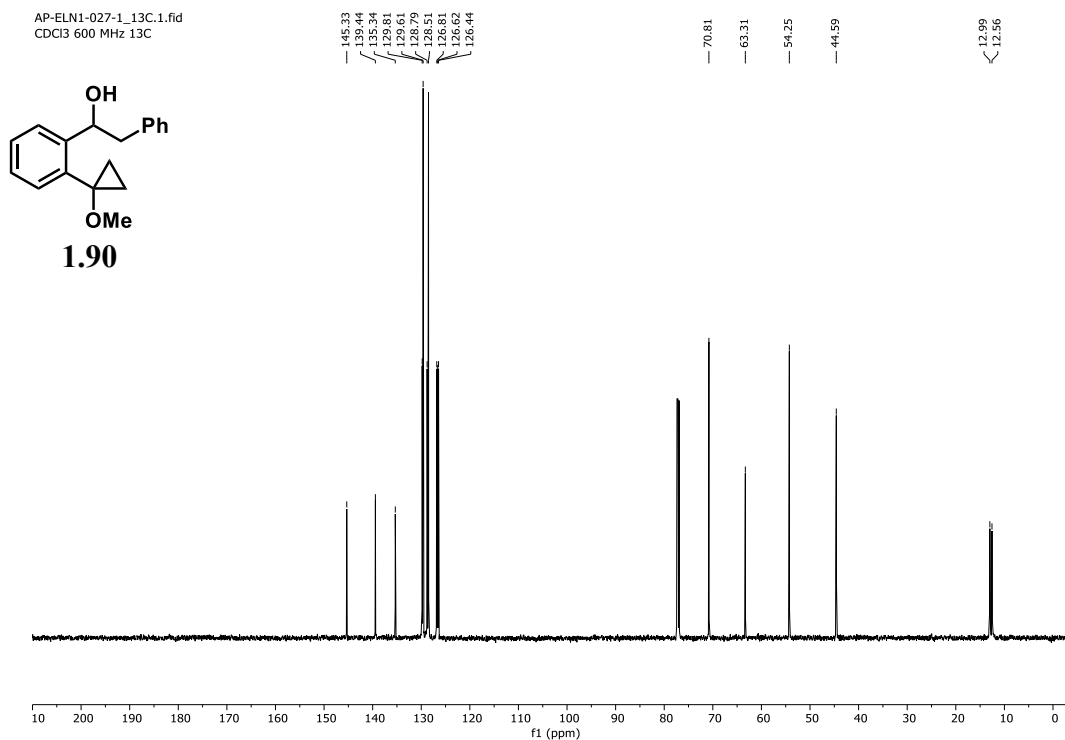


Figure 4.42. <sup>13</sup>C NMR spectrum of **1.90** (151 MHz, 298 K, CDCl<sub>3</sub>).

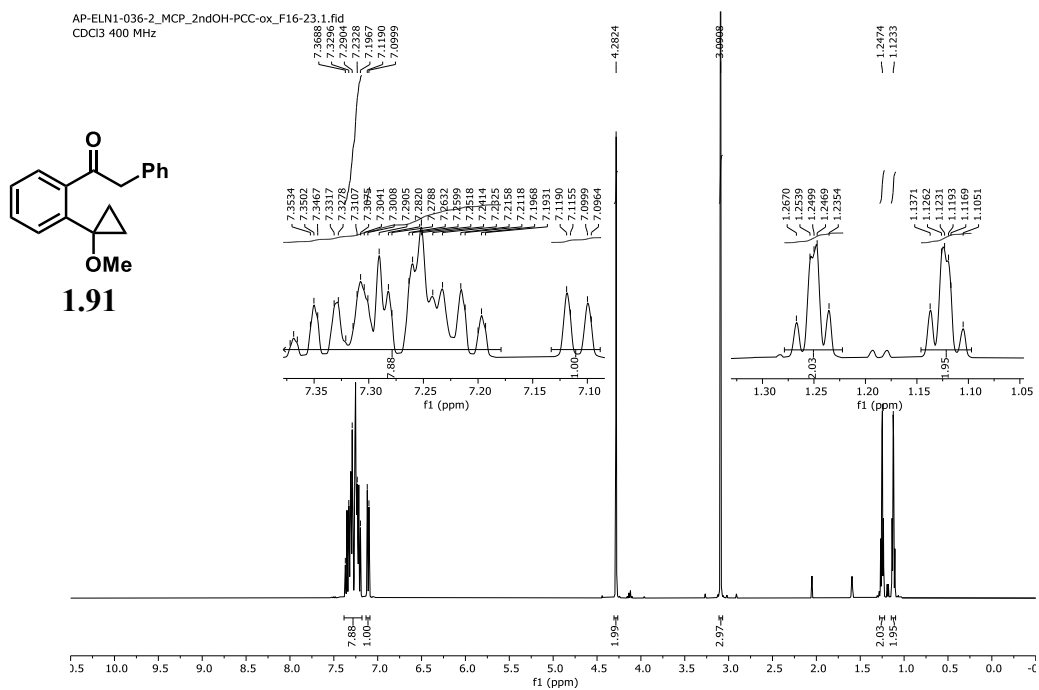


Figure 4.43. <sup>1</sup>H NMR spectrum of **1.91** (400 MHz, 295 K, CDCl<sub>3</sub>).

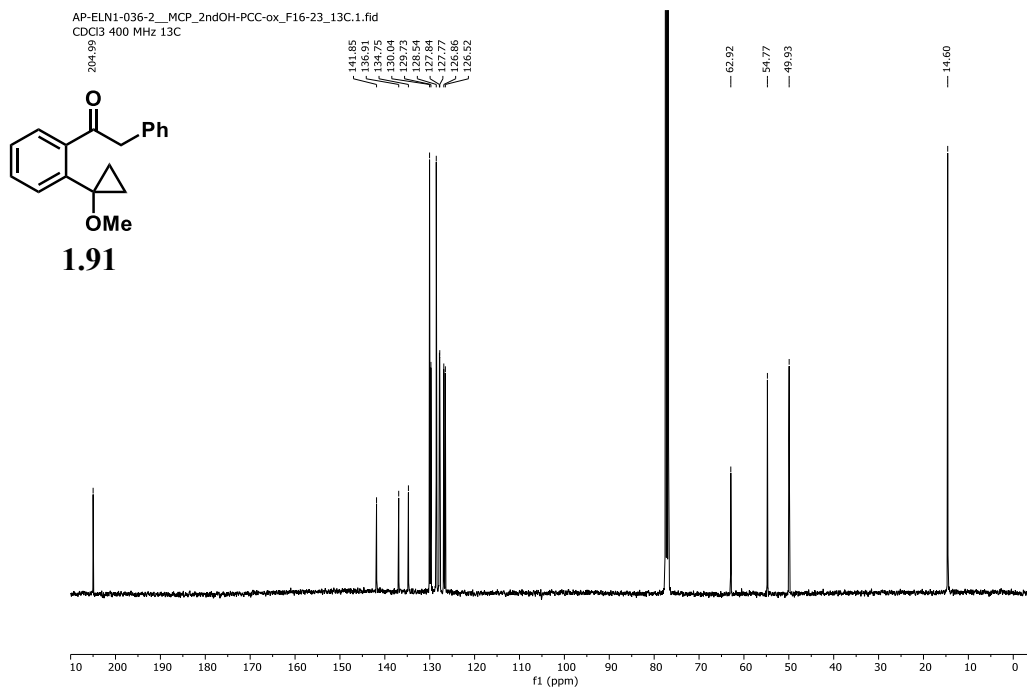


Figure 4.44. <sup>13</sup>C NMR spectrum of **1.91** (101 MHz, 295 K, CDCl<sub>3</sub>).

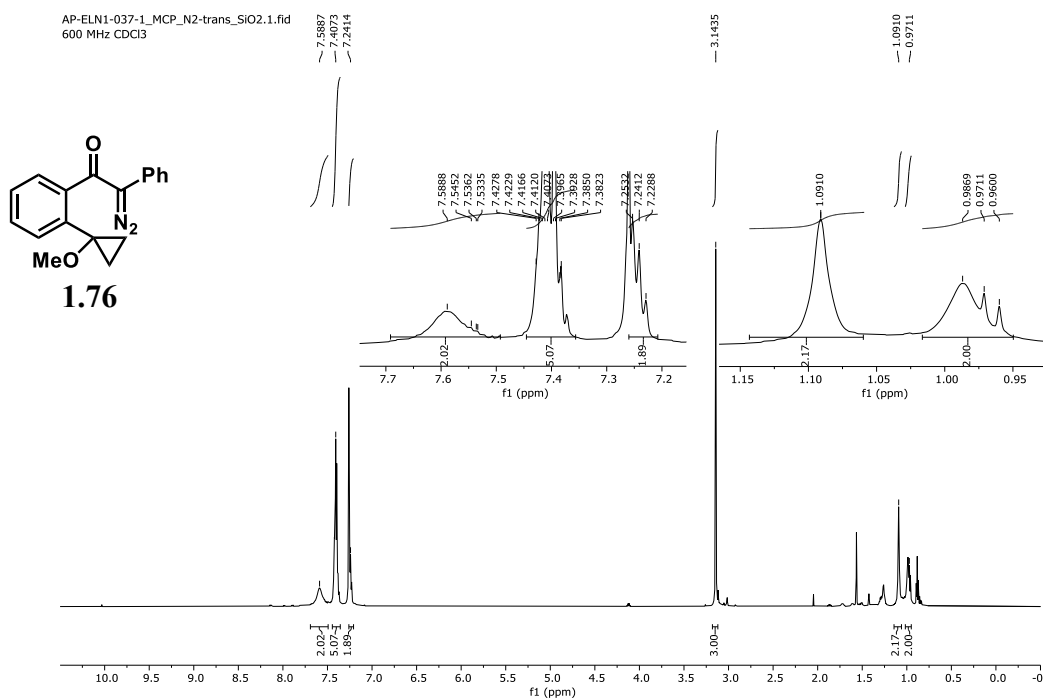


Figure 4.45. <sup>1</sup>H NMR spectrum of **1.76** (600 MHz, 298 K, CDCl<sub>3</sub>).

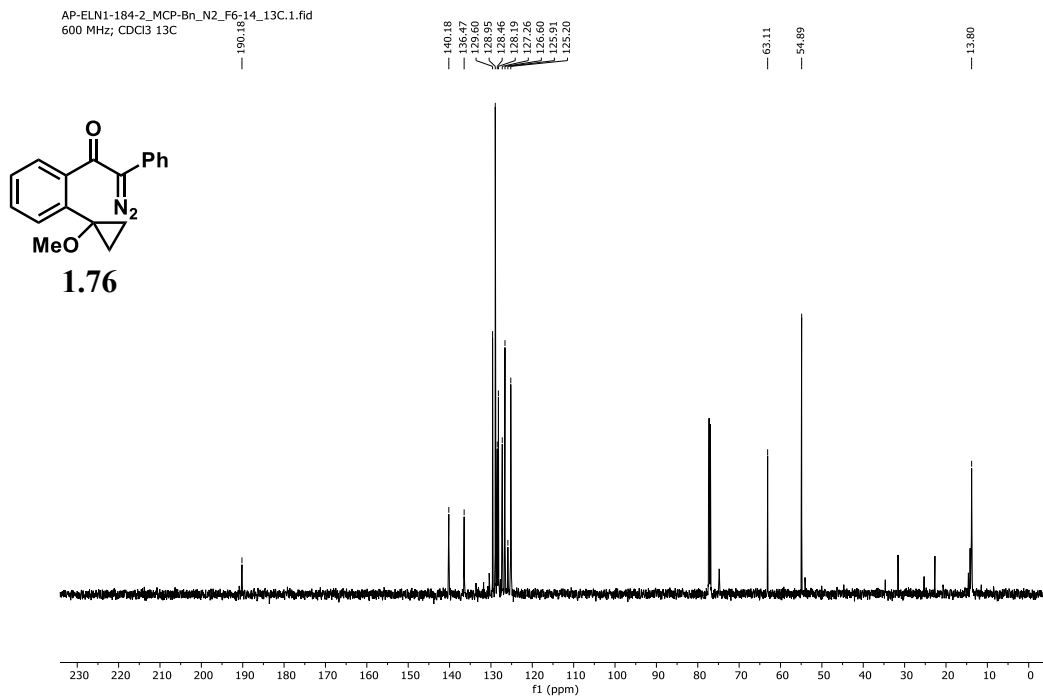


Figure 4.46. <sup>1</sup>H NMR spectrum of **1.76** (151 MHz, 298 K, CDCl<sub>3</sub>).

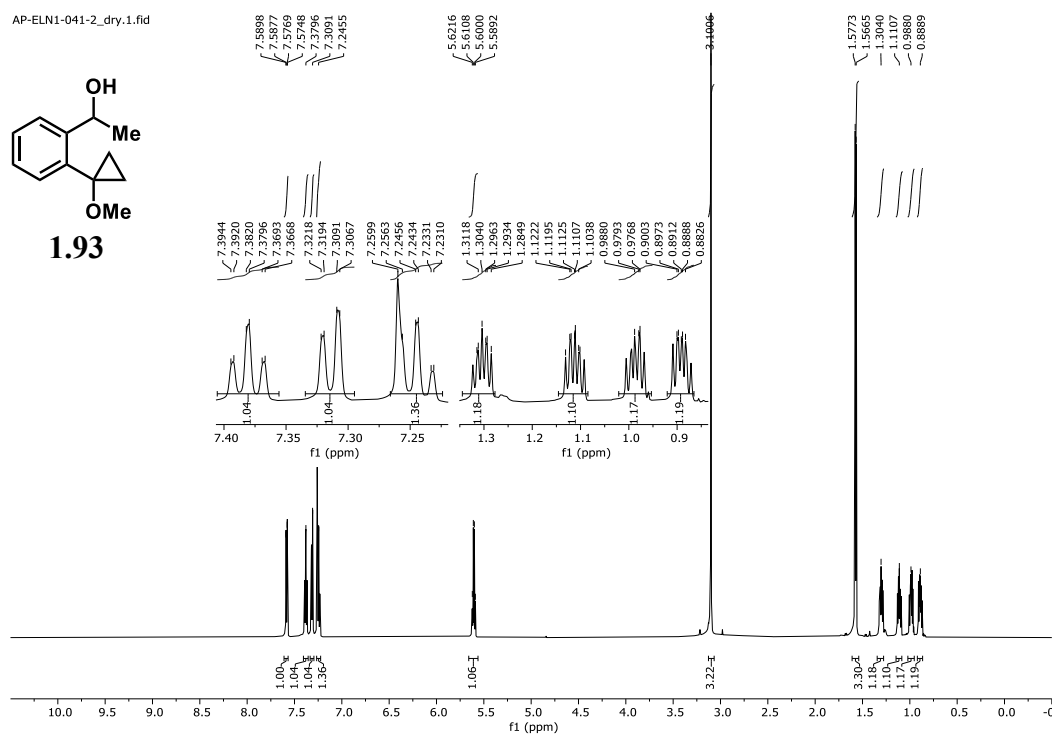
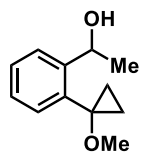


Figure 4.47. <sup>1</sup>H NMR spectrum of **1.93** (600 MHz, 298 K, CDCl<sub>3</sub>).

AP-ELN1-041-2\_dry\_13C.1.fid  
CDCl<sub>3</sub> 600 MHz

146.53  
135.26  
129.92  
128.81  
126.64  
125.99  
65.11  
63.36  
54.18  
22.72  
13.61  
11.83



**1.93**

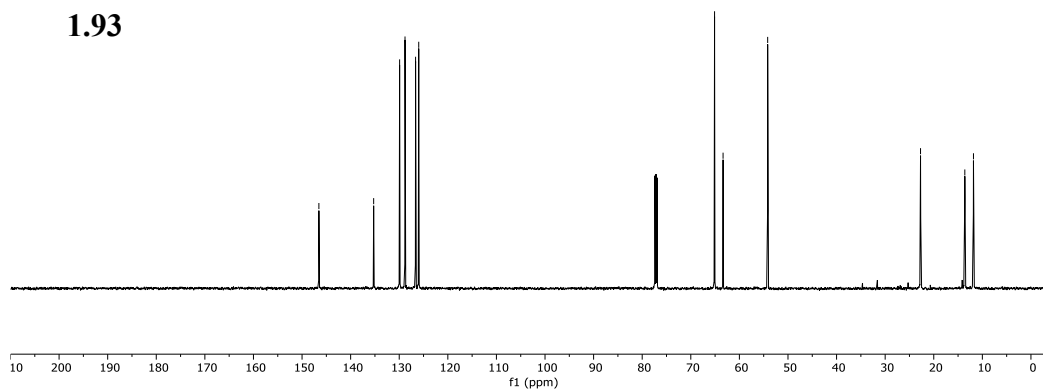
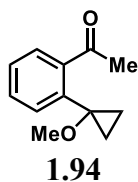


**Figure 4.48.** <sup>13</sup>C NMR spectrum of **1.93** (151 MHz, 298 K, CDCl<sub>3</sub>).

AP-ELN1-056-5\_MCP\_2ndOH-ox\_F26-35.1.fid  
600 MHz CDCl<sub>3</sub>



**1.94**

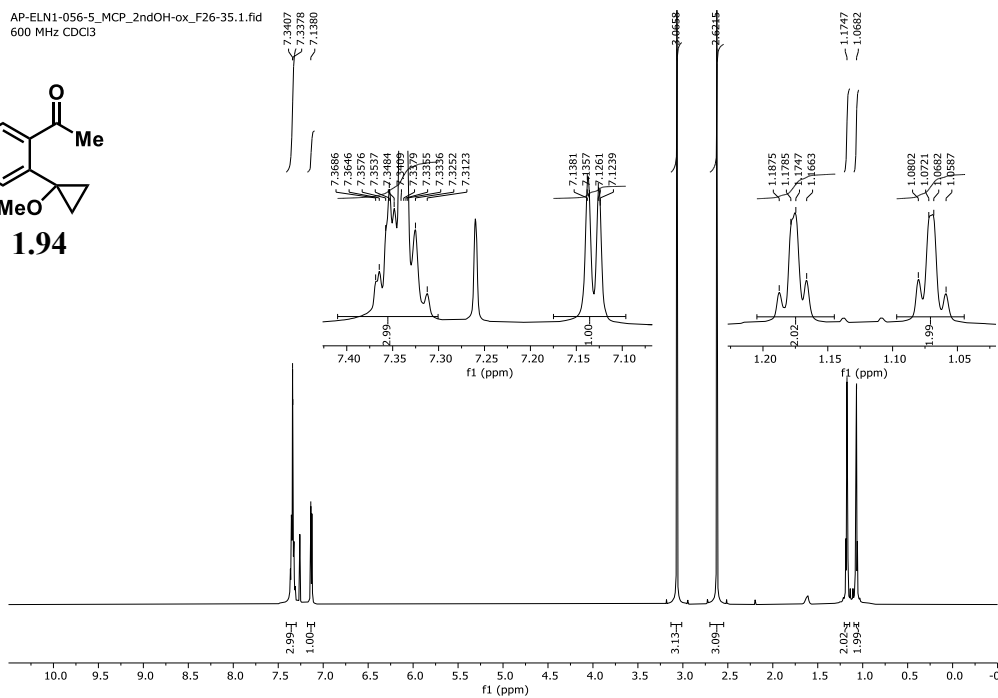


**Figure 4.49.** <sup>1</sup>H NMR spectrum of **1.94** (600 MHz, 298 K, CDCl<sub>3</sub>).



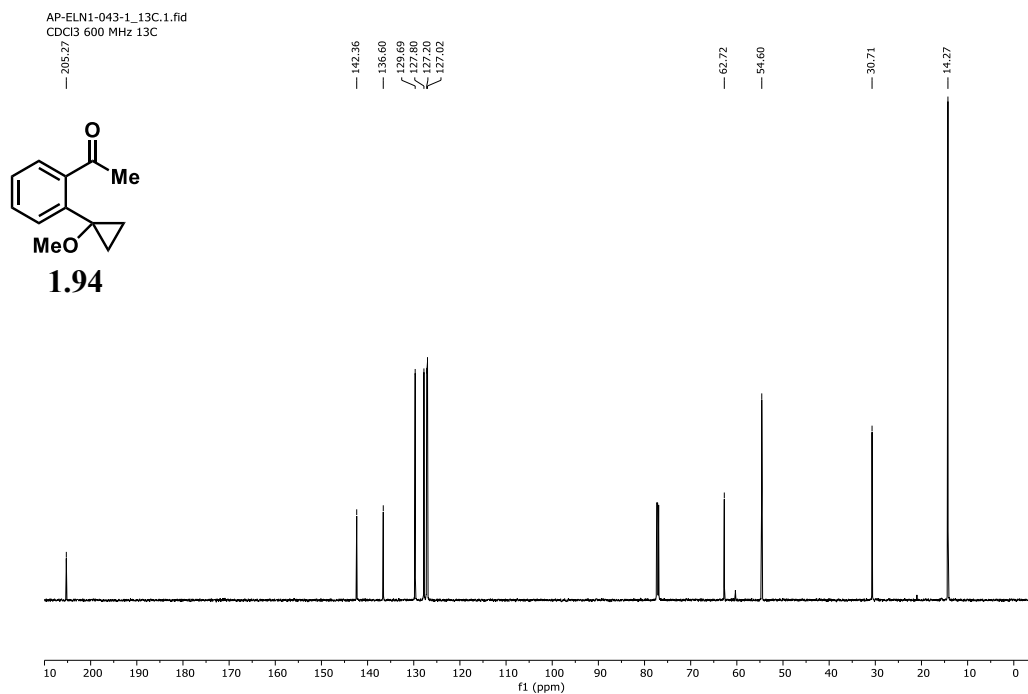


Figure 4.50. <sup>13</sup>C NMR spectrum of **1.94** (151 MHz, 298 K, CDCl<sub>3</sub>).

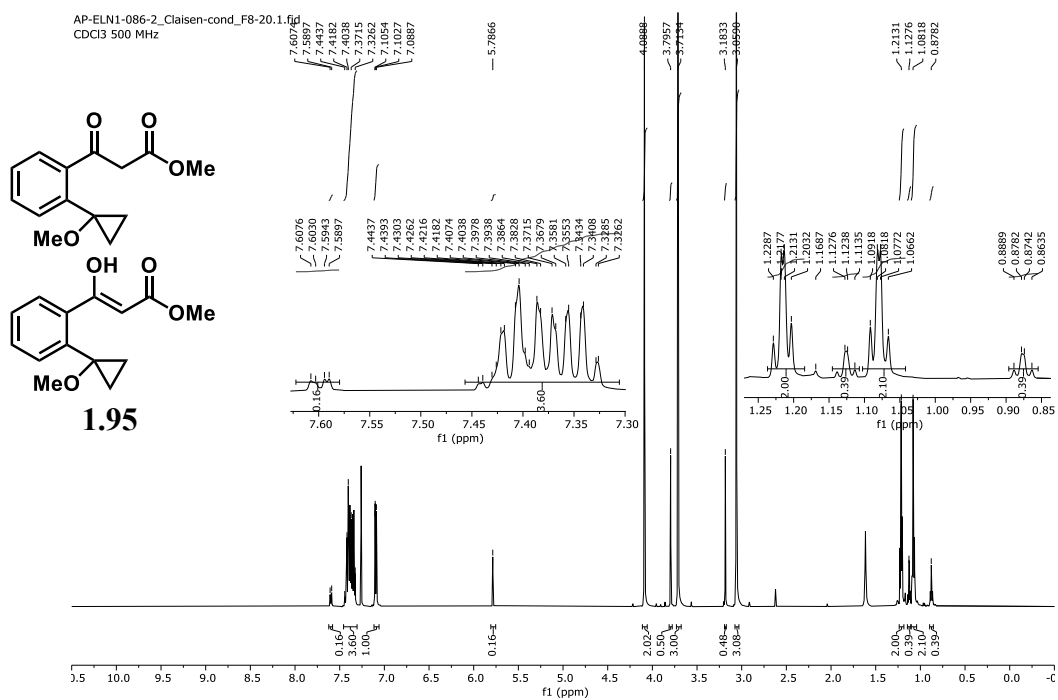


Figure 4.51. <sup>1</sup>H NMR spectrum of **1.95** (500 MHz, 298 K, CDCl<sub>3</sub>).

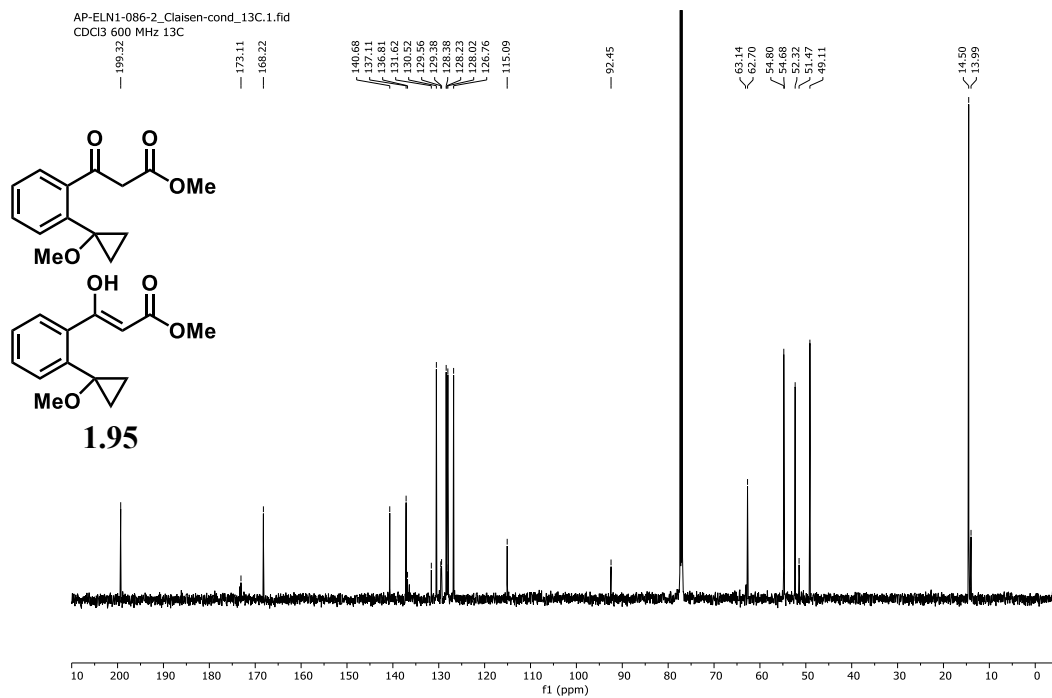


Figure 4.52. <sup>13</sup>C NMR spectrum of **1.95** (151 MHz, 298 K, CDCl<sub>3</sub>).

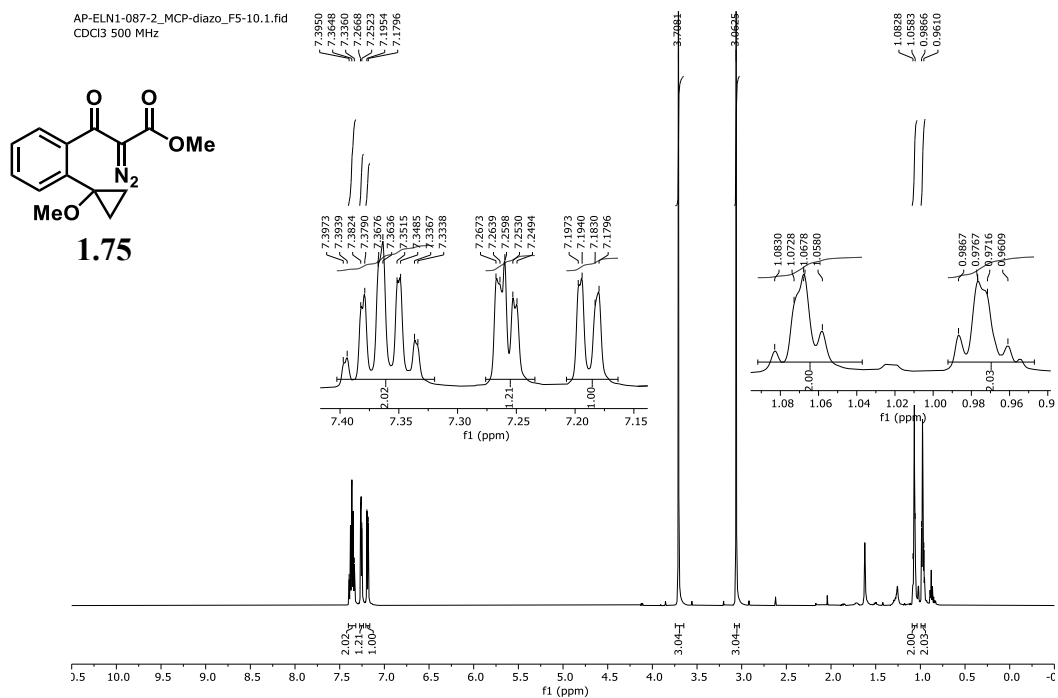


Figure 4.53. <sup>1</sup>H NMR spectrum of **1.75** (500 MHz, 298 K, CDCl<sub>3</sub>).

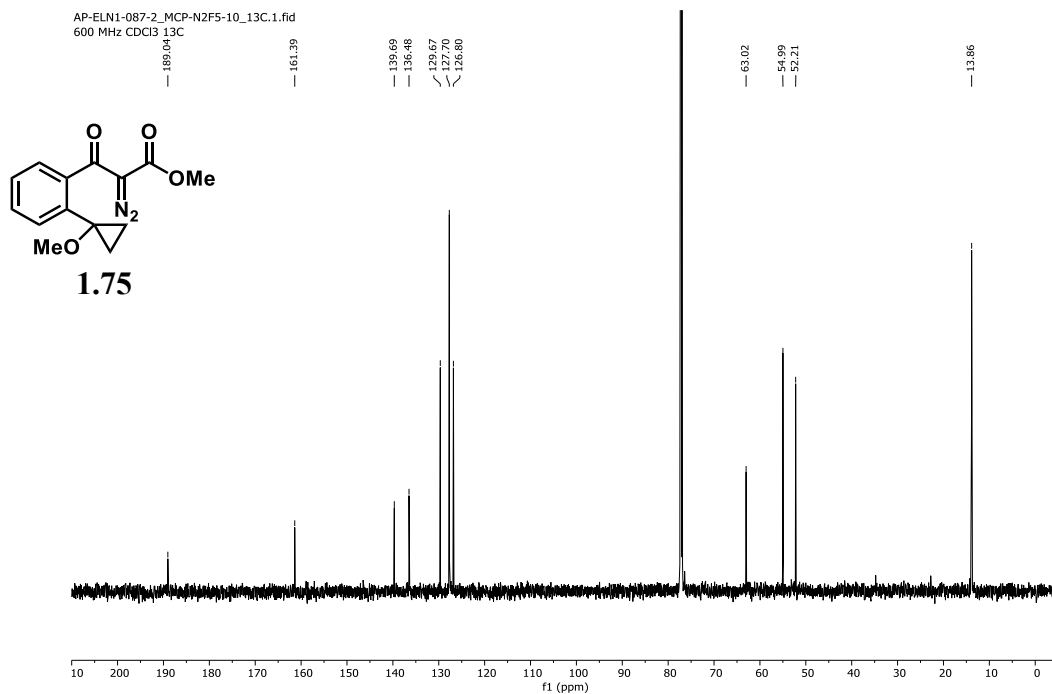


Figure 4.54. <sup>13</sup>C NMR spectrum of **1.75** (151 MHz, 298 K, CDCl<sub>3</sub>).

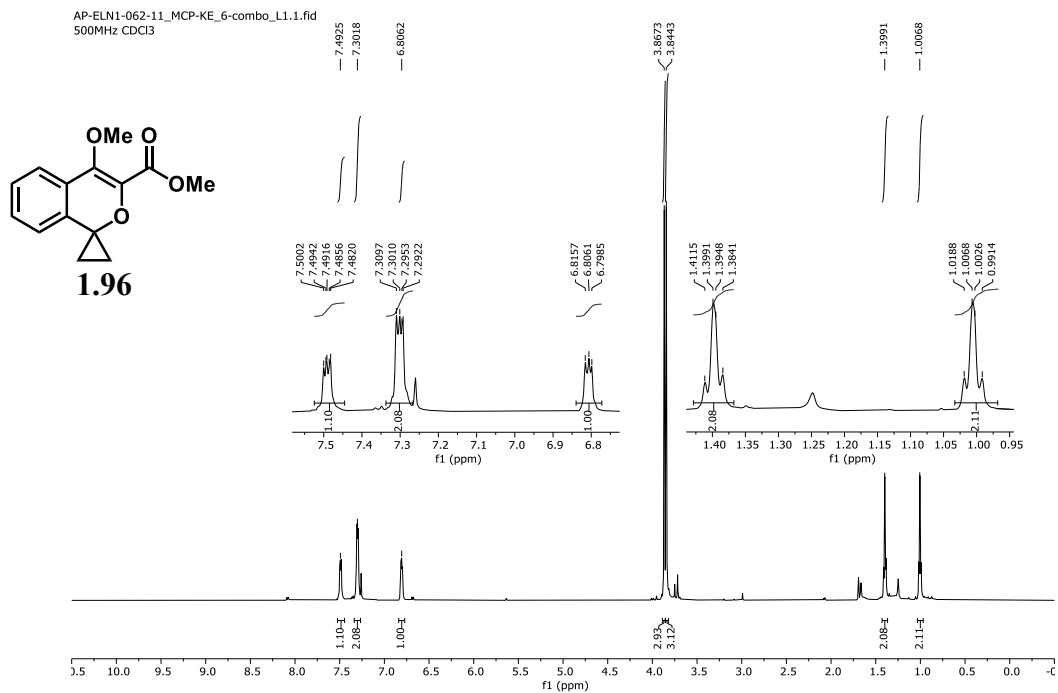


Figure 4.55. <sup>1</sup>H NMR spectrum of **1.96** (500 MHz, 298 K, CDCl<sub>3</sub>).

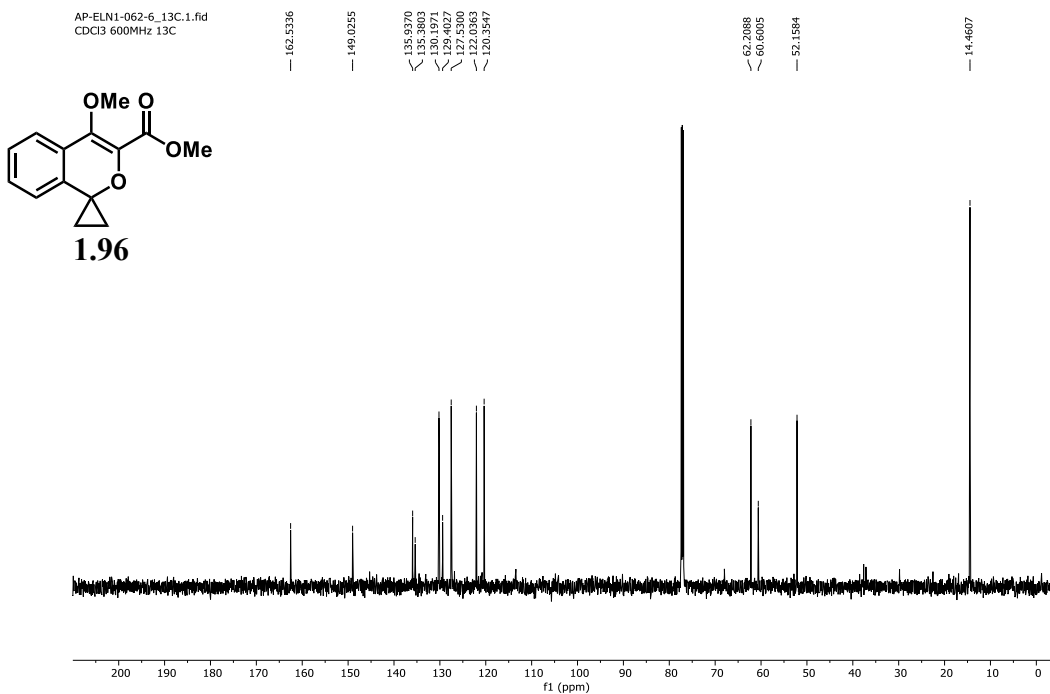


Figure 4.56. <sup>13</sup>C NMR spectrum of **1.96** (151 MHz, 298 K, CDCl<sub>3</sub>).

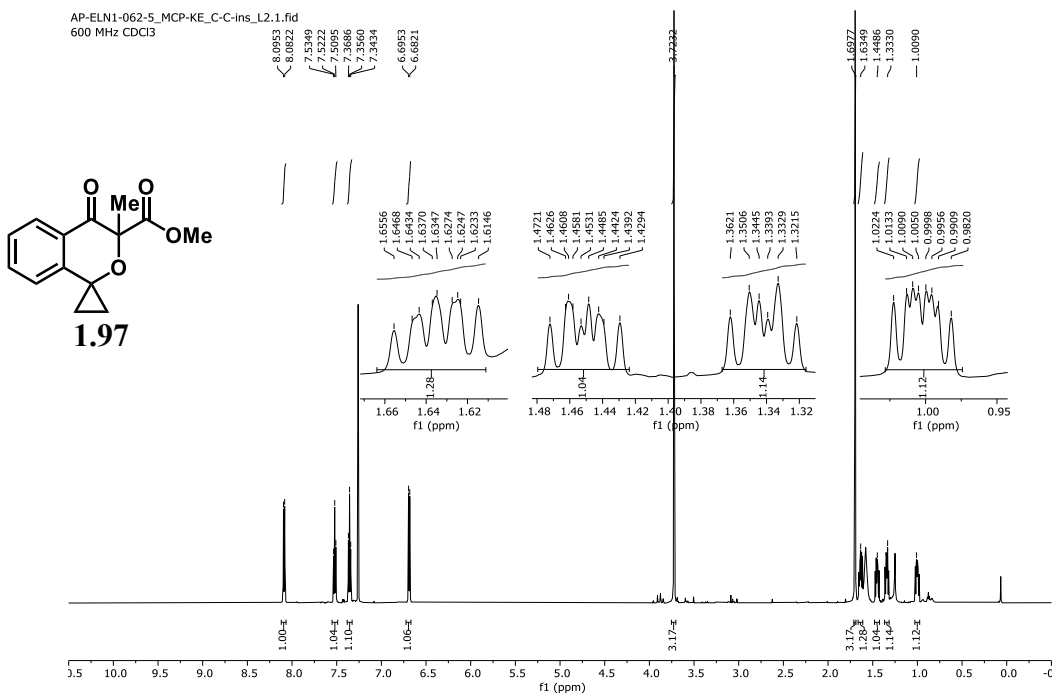


Figure 4.57. <sup>1</sup>H NMR spectrum of **1.97** (600 MHz, 298 K, CDCl<sub>3</sub>).

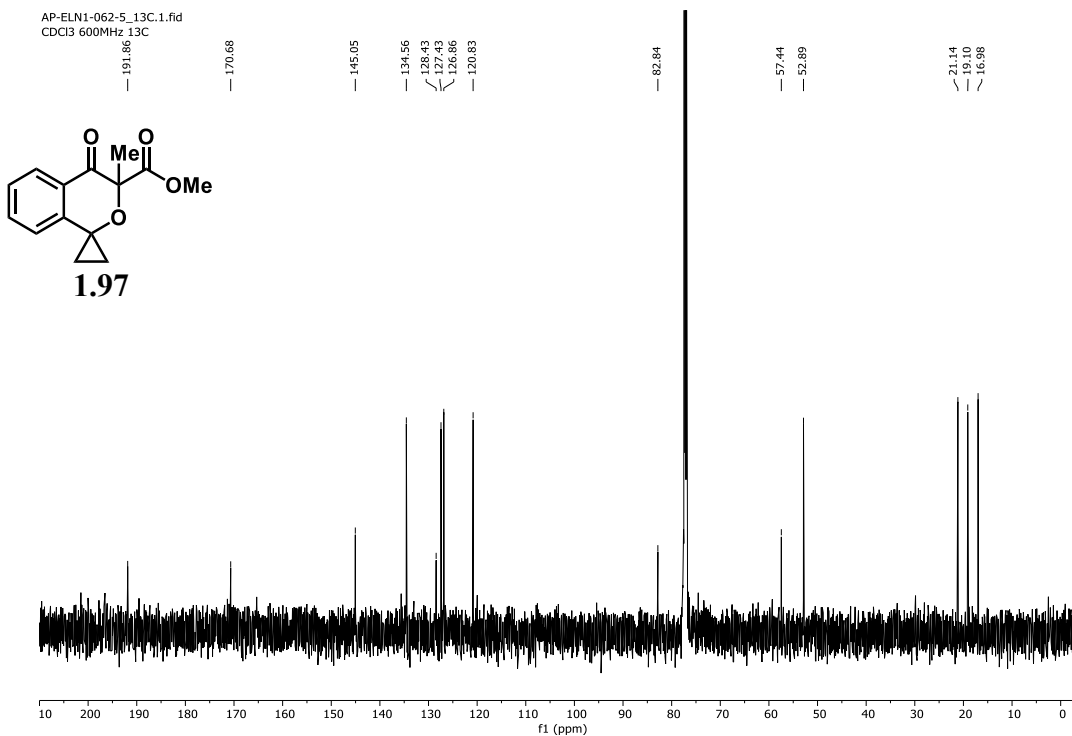


Figure 4.58. <sup>13</sup>C NMR spectrum of **1.97** (151 MHz, 298 K, CDCl<sub>3</sub>).

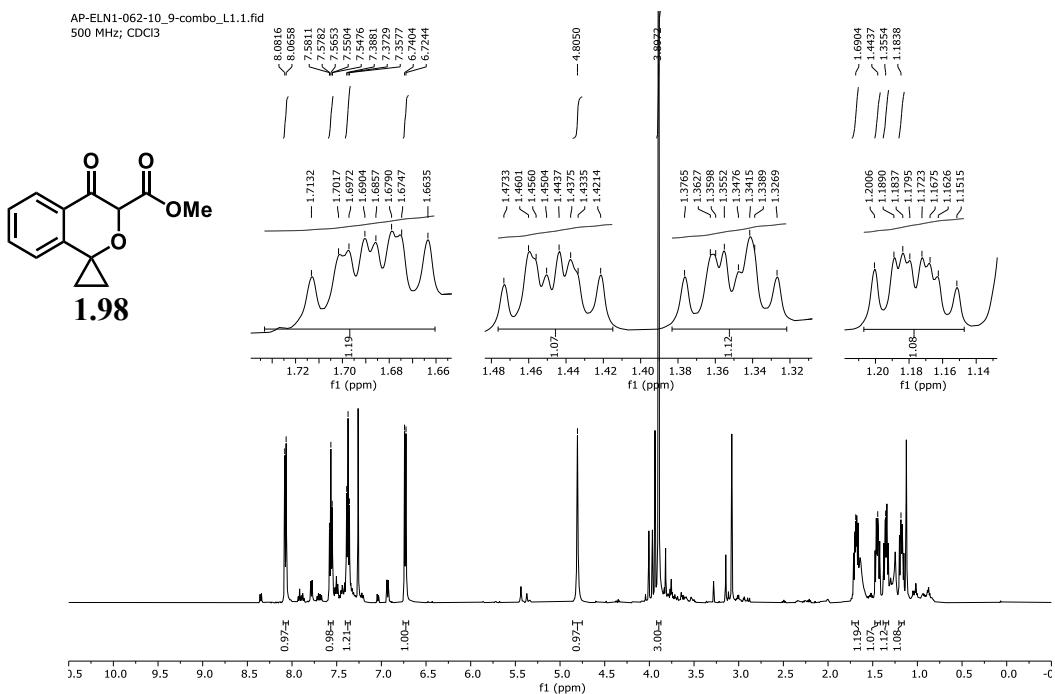


Figure 4.59. <sup>1</sup>H NMR spectrum of **1.98** (500 MHz, 298 K, CDCl<sub>3</sub>).

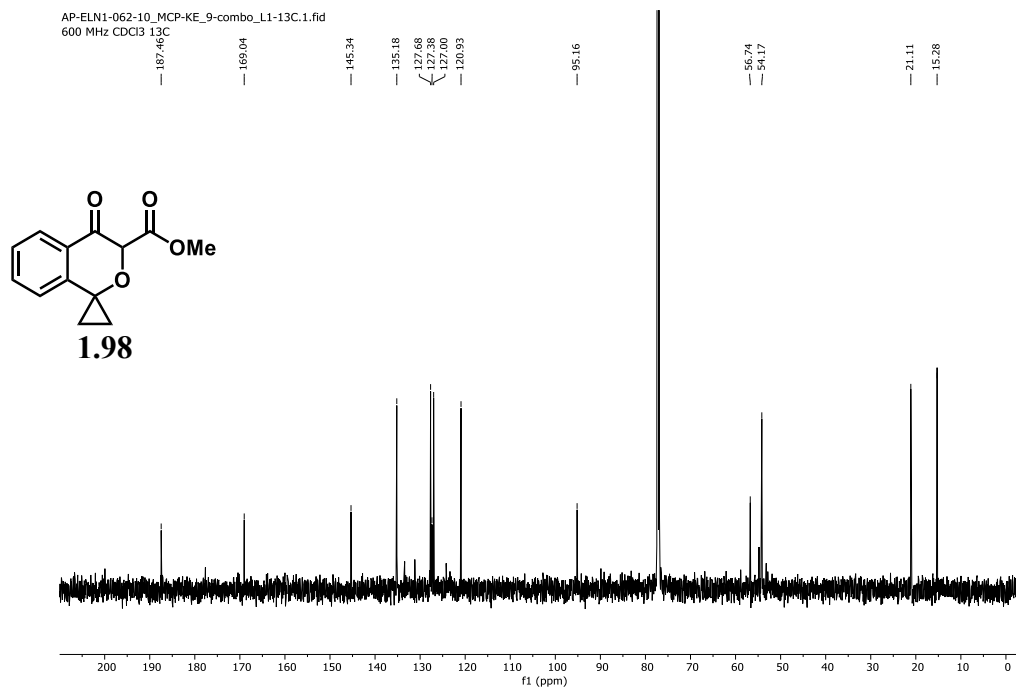


Figure 4.60. <sup>13</sup>C NMR spectrum of **1.98** (151 MHz, 298 K, CDCl<sub>3</sub>).

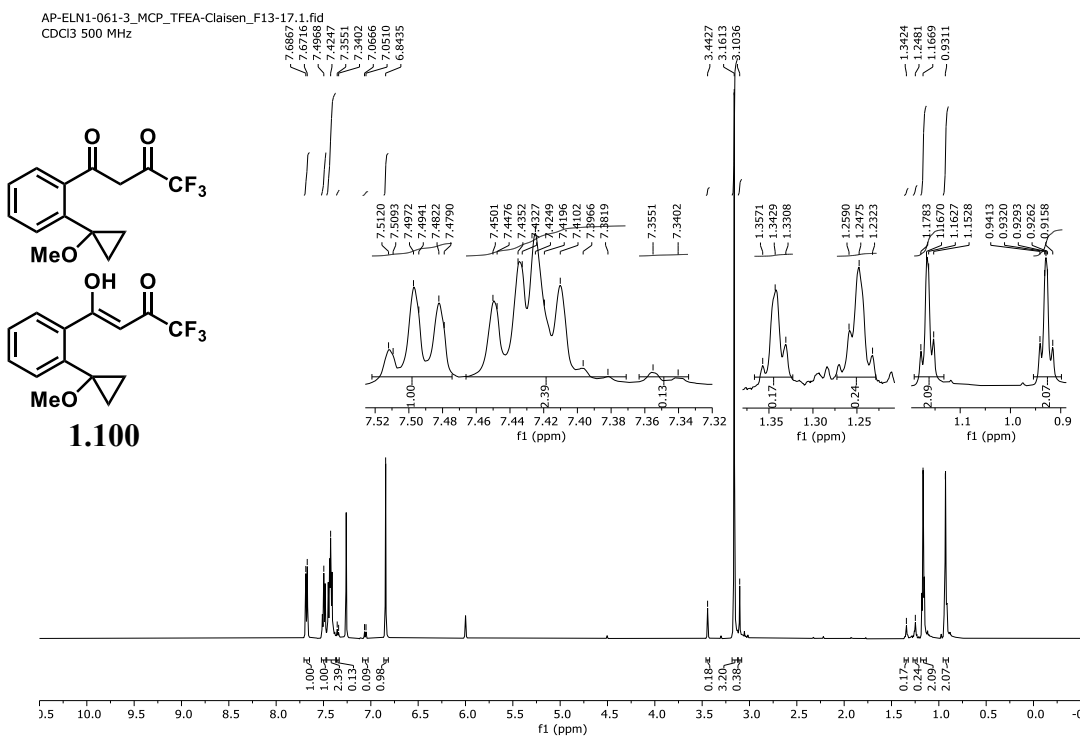


Figure 4.61. <sup>1</sup>H NMR spectrum of **1.100** (500 MHz, 298 K, CDCl<sub>3</sub>).

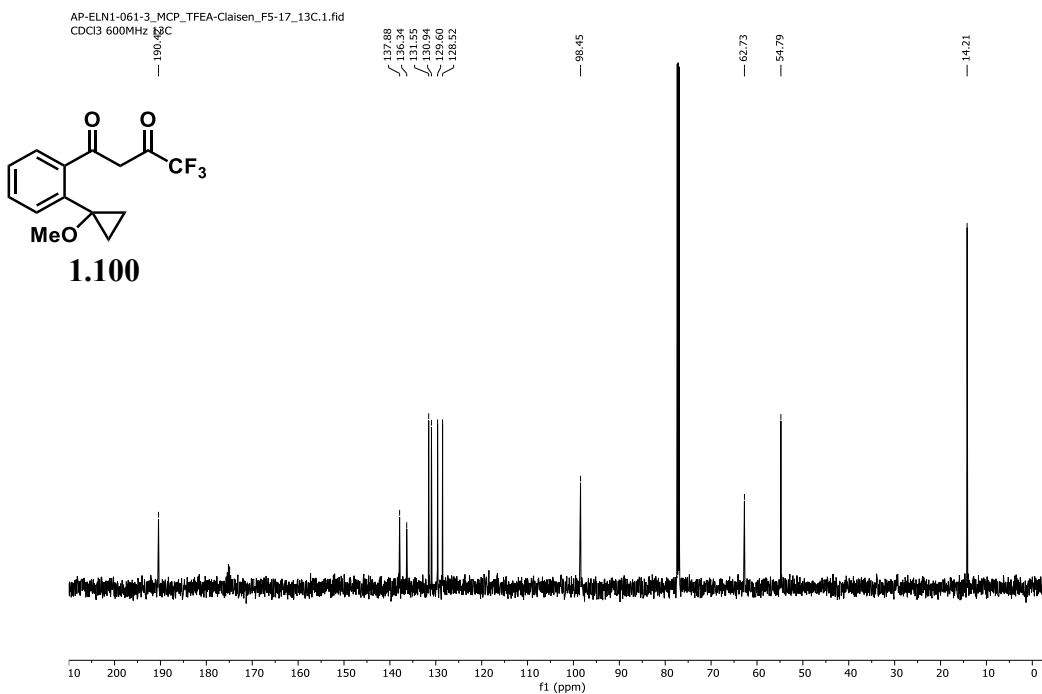


Figure 4.62.  $^{13}\text{C}$  NMR spectrum of **1.100** (151 MHz, 298 K,  $\text{CDCl}_3$ ).

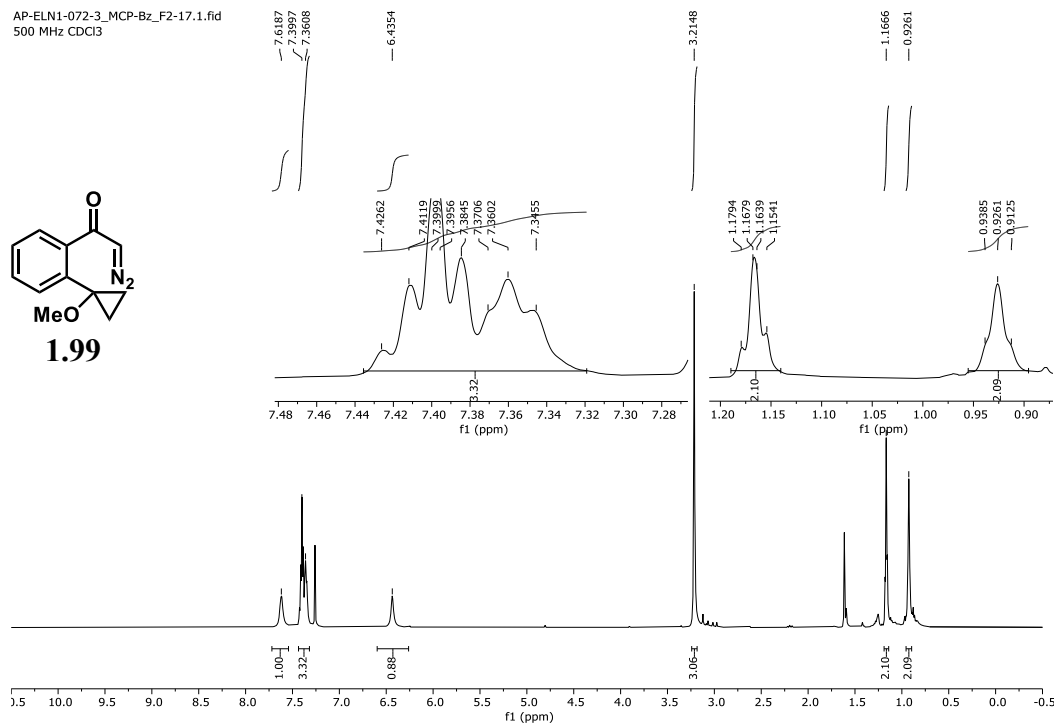


Figure 4.63.  $^1\text{H}$  NMR spectrum of **1.99** (500 MHz, 298 K,  $\text{CDCl}_3$ ).

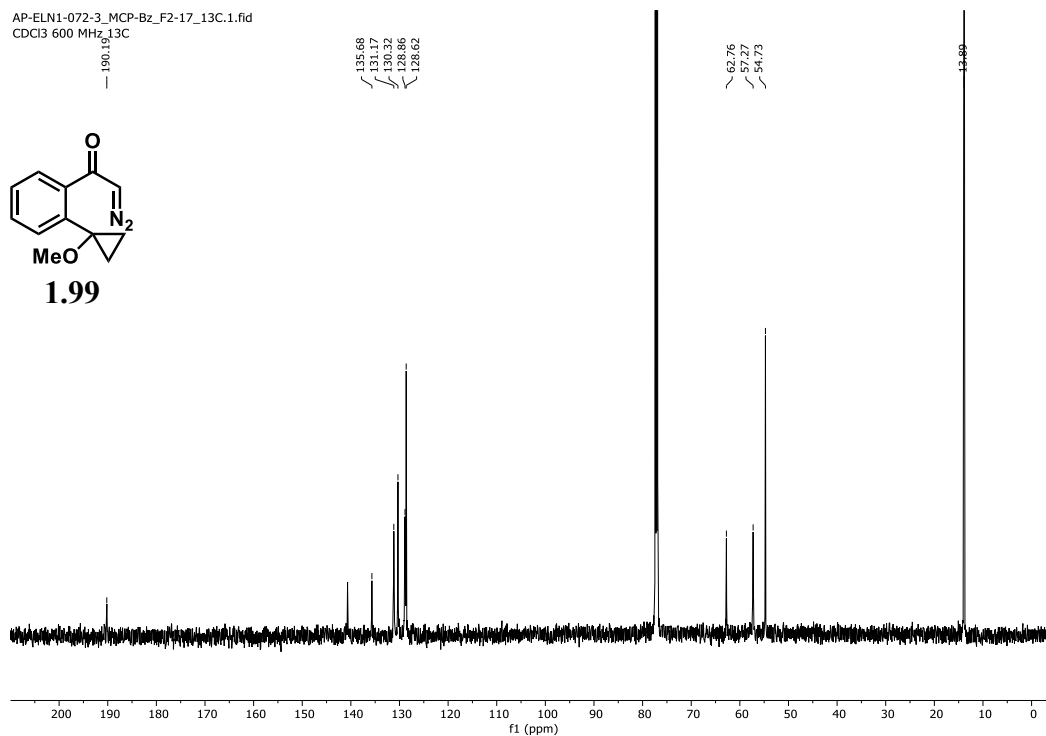


Figure 4.64. <sup>13</sup>C NMR spectrum of **1.99** (151 MHz, 298 K, CDCl<sub>3</sub>).

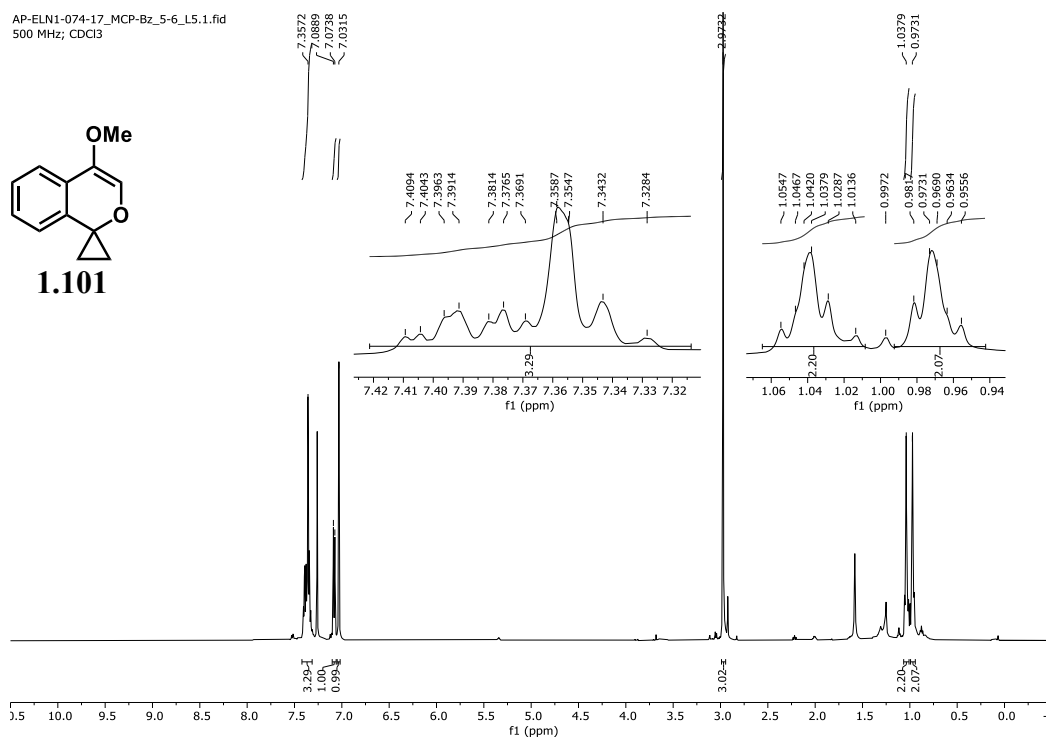


Figure 4.65. <sup>1</sup>H NMR spectrum of **1.101** (500 MHz, 298 K, CDCl<sub>3</sub>).



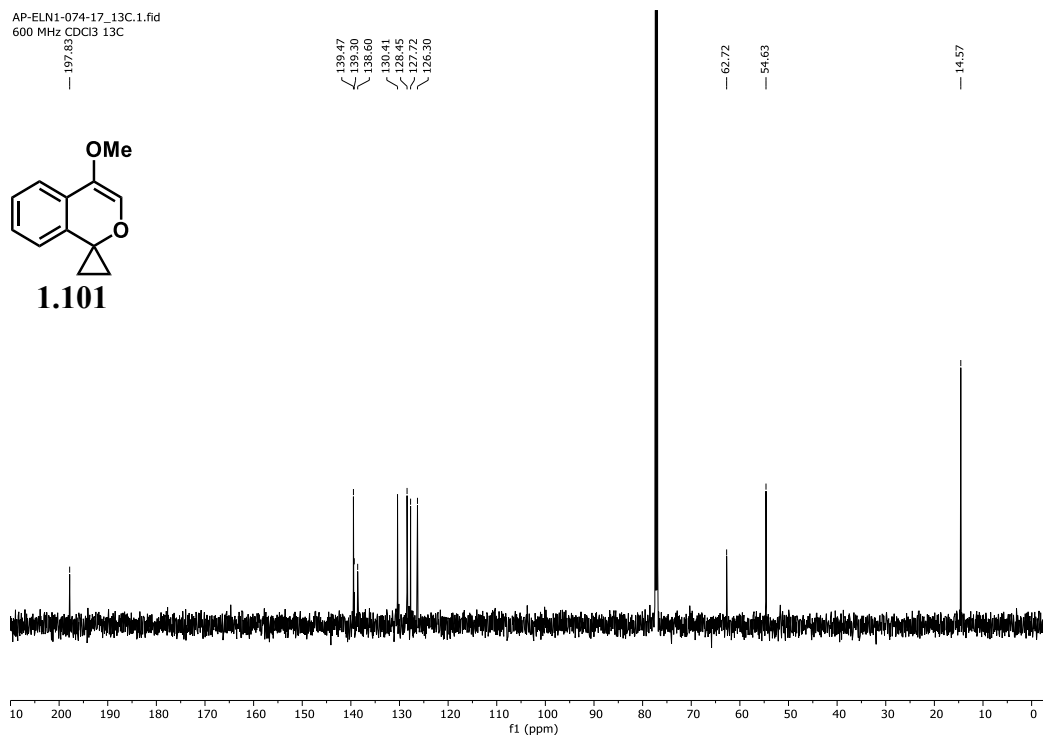


Figure 4.66. <sup>13</sup>C NMR spectrum of **1.101** (151 MHz, 298 K, CDCl<sub>3</sub>).

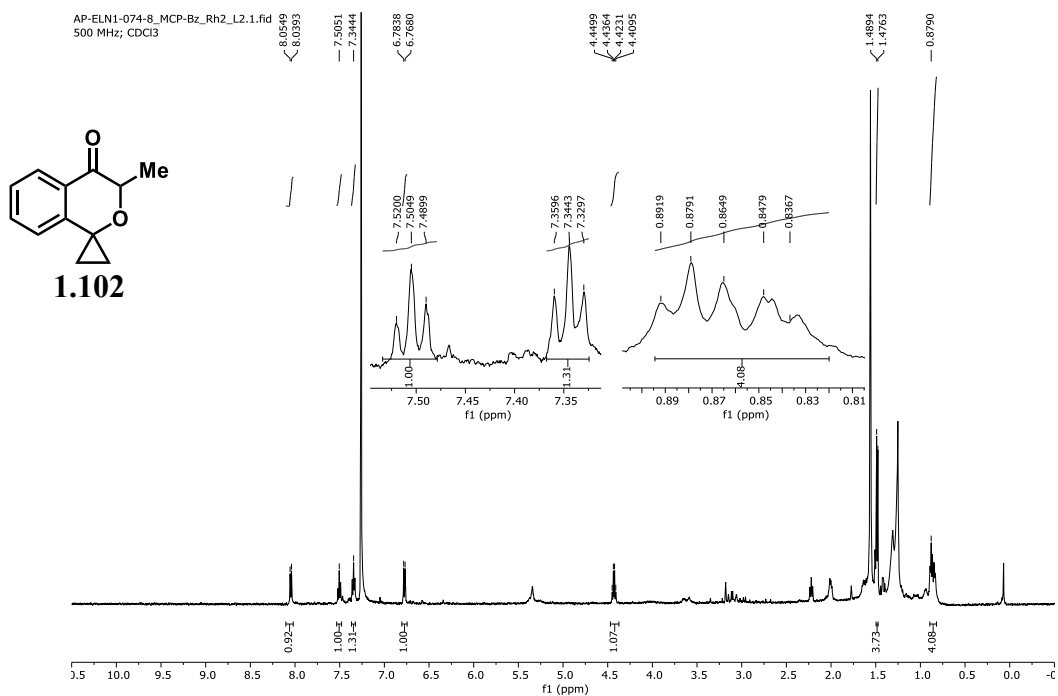
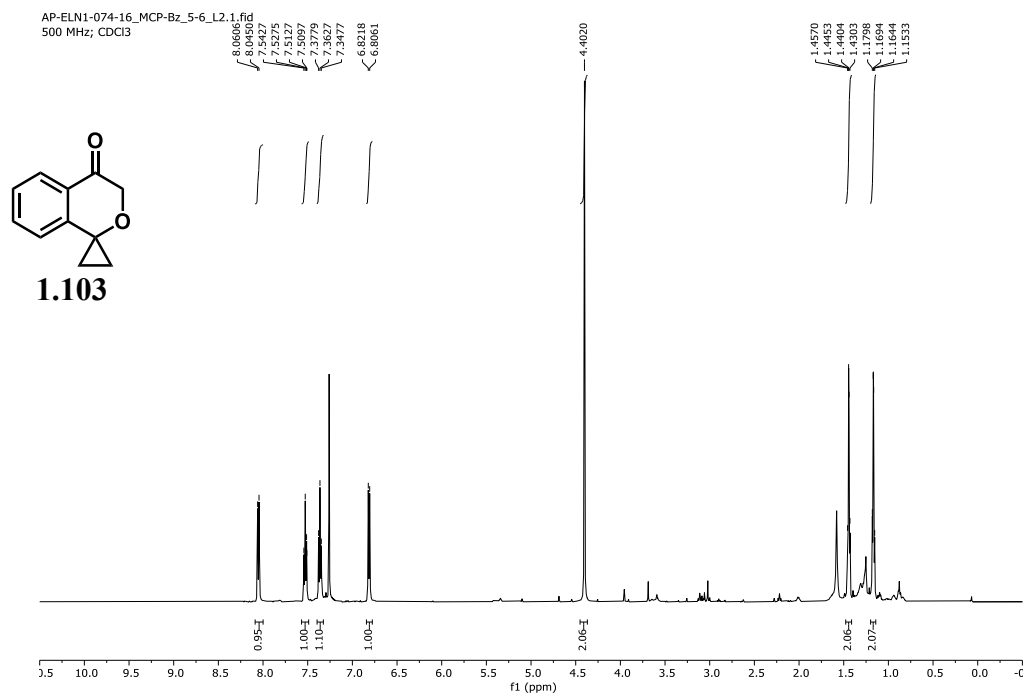
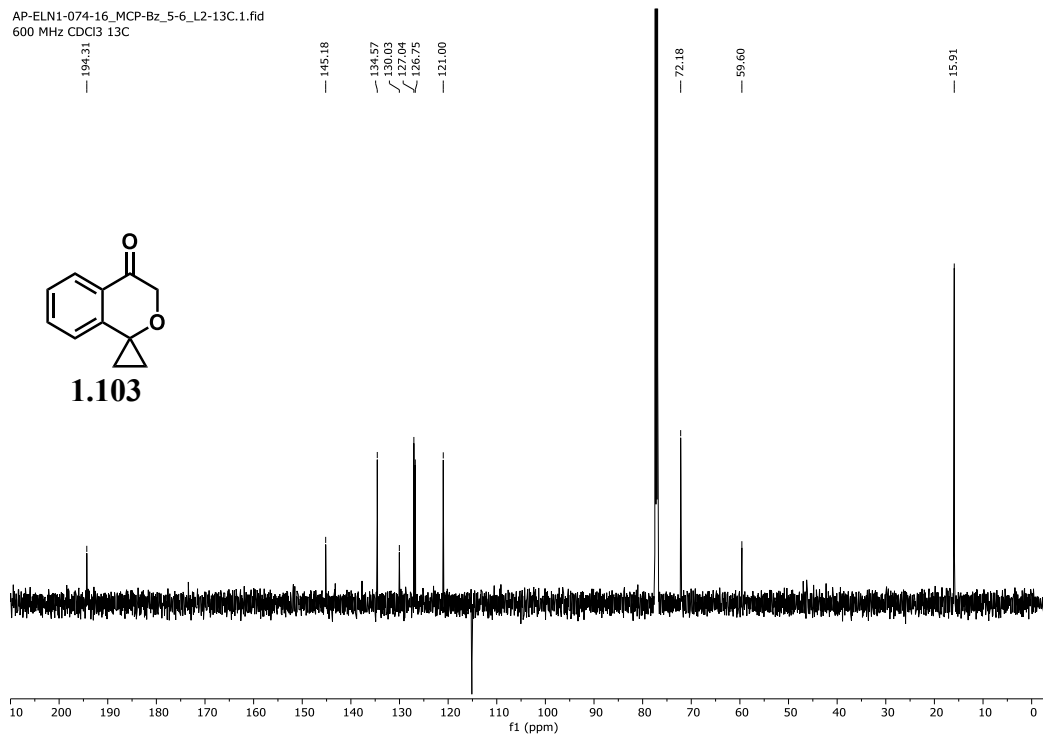


Figure 4.67. <sup>1</sup>H NMR spectrum of **1.102** (500 MHz, 298 K, CDCl<sub>3</sub>).



**Figure 4.68.** <sup>1</sup>H NMR spectrum of **1.103** (500 MHz, 298 K, CDCl<sub>3</sub>).



**Figure 4.69.** <sup>13</sup>C NMR spectrum of **1.103** (151 MHz, 298 K, CDCl<sub>3</sub>).

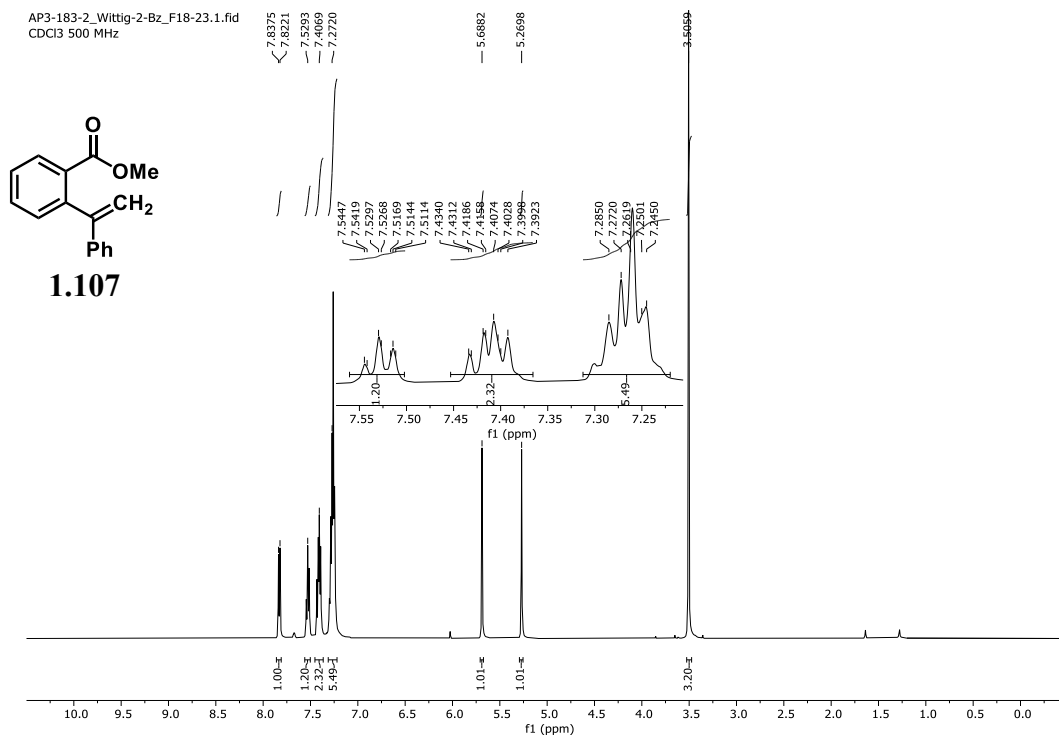


Figure 6.70. <sup>1</sup>H NMR spectrum of **1.107** (500 MHz, 298 K, CDCl<sub>3</sub>).

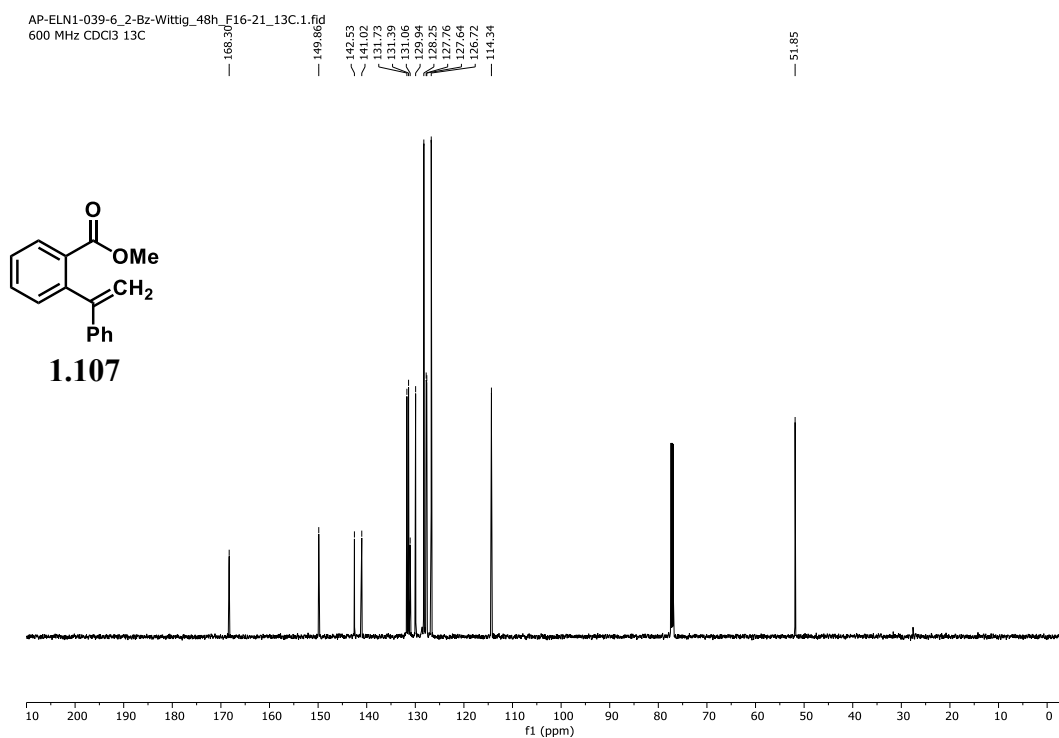


Figure 4.71. <sup>13</sup>C NMR spectrum of **1.107** (151 MHz, 298 K, CDCl<sub>3</sub>).

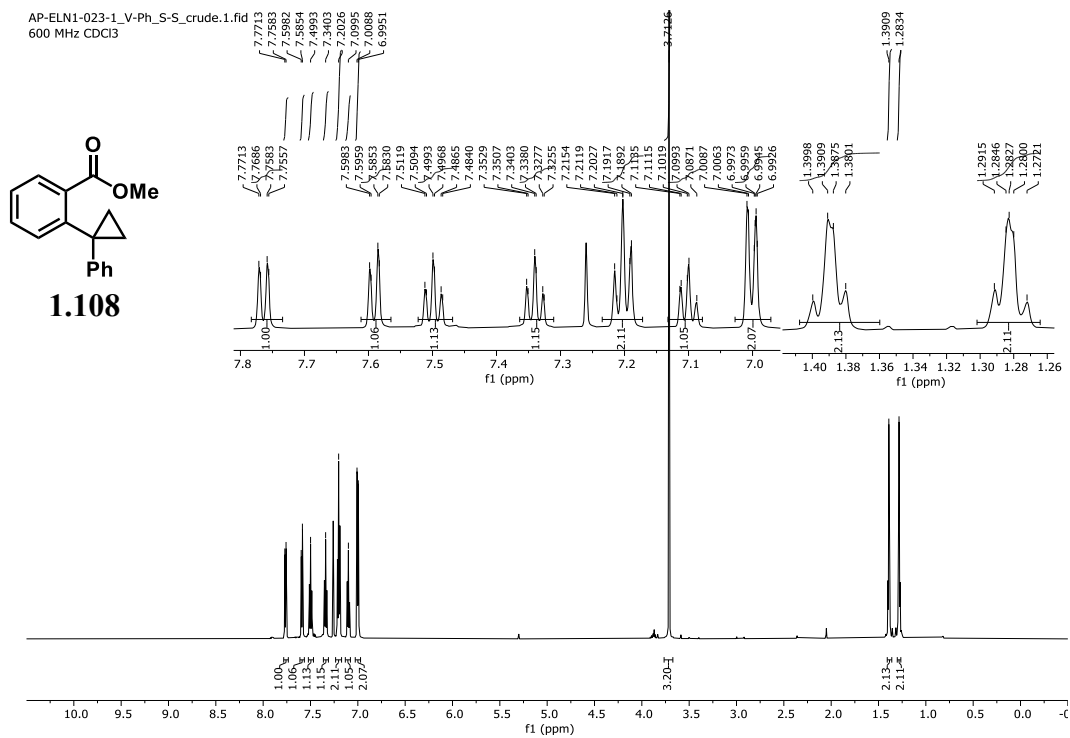


Figure 4.72. <sup>1</sup>H NMR spectrum of **1.108** (600 MHz, 298 K, CDCl<sub>3</sub>).

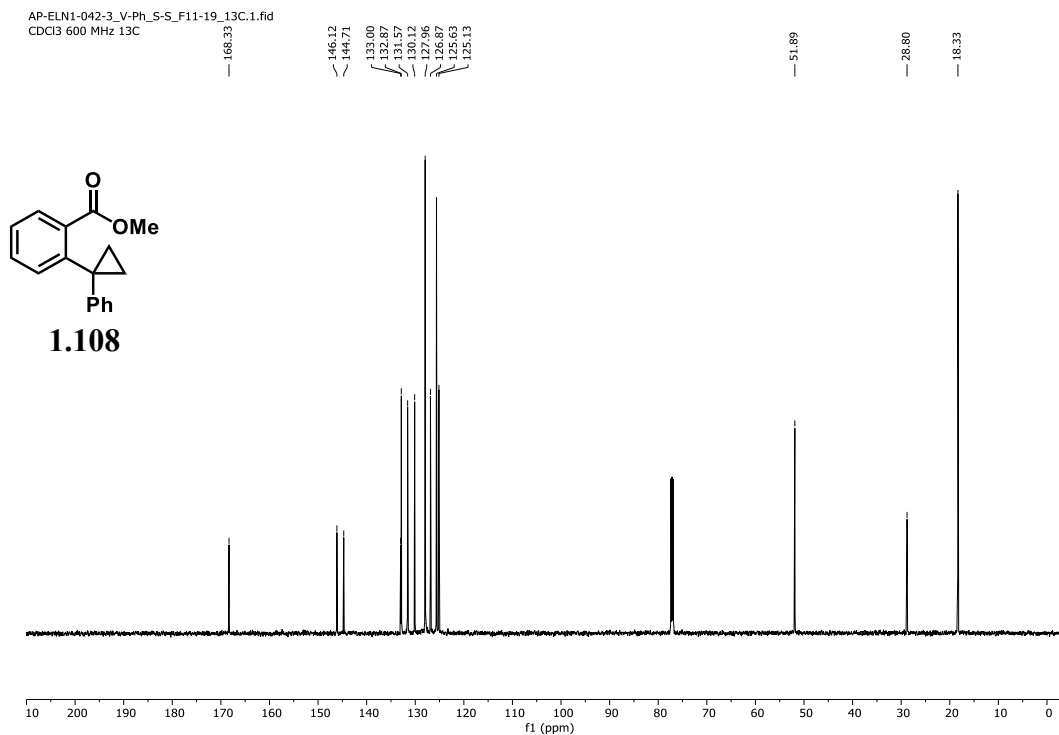


Figure 4.73. <sup>13</sup>C NMR spectrum of **1.108** (151 MHz, 298 K, CDCl<sub>3</sub>).

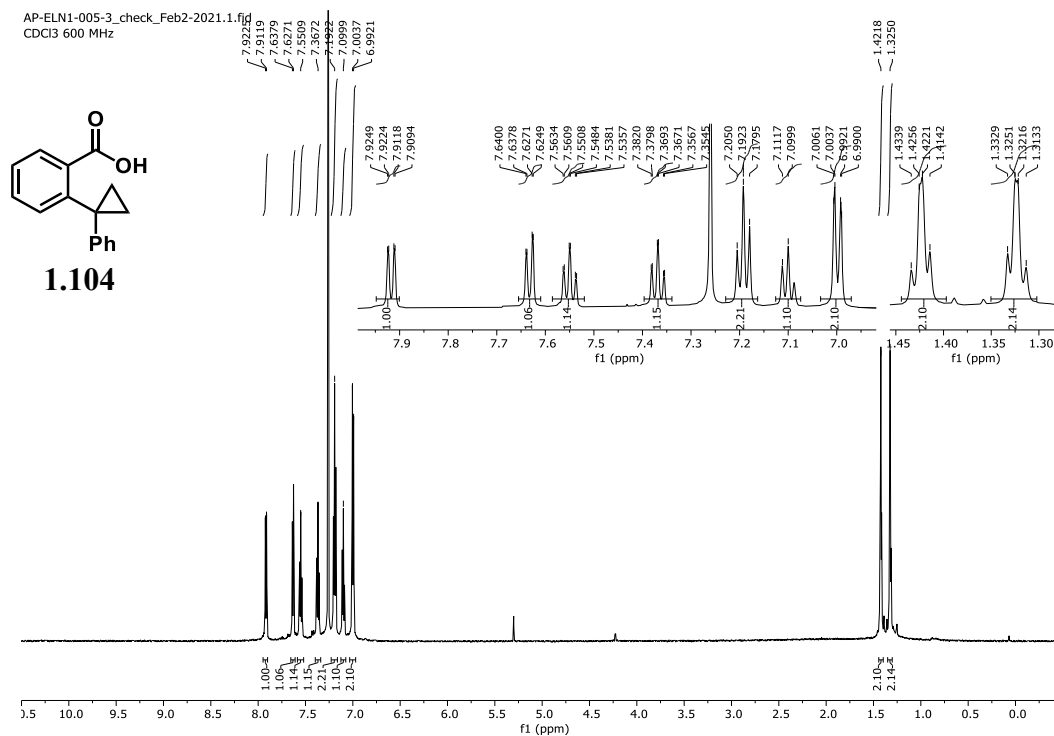


Figure 4.74. <sup>1</sup>H NMR spectrum of **1.104** (600 MHz, 298 K, CDCl<sub>3</sub>).

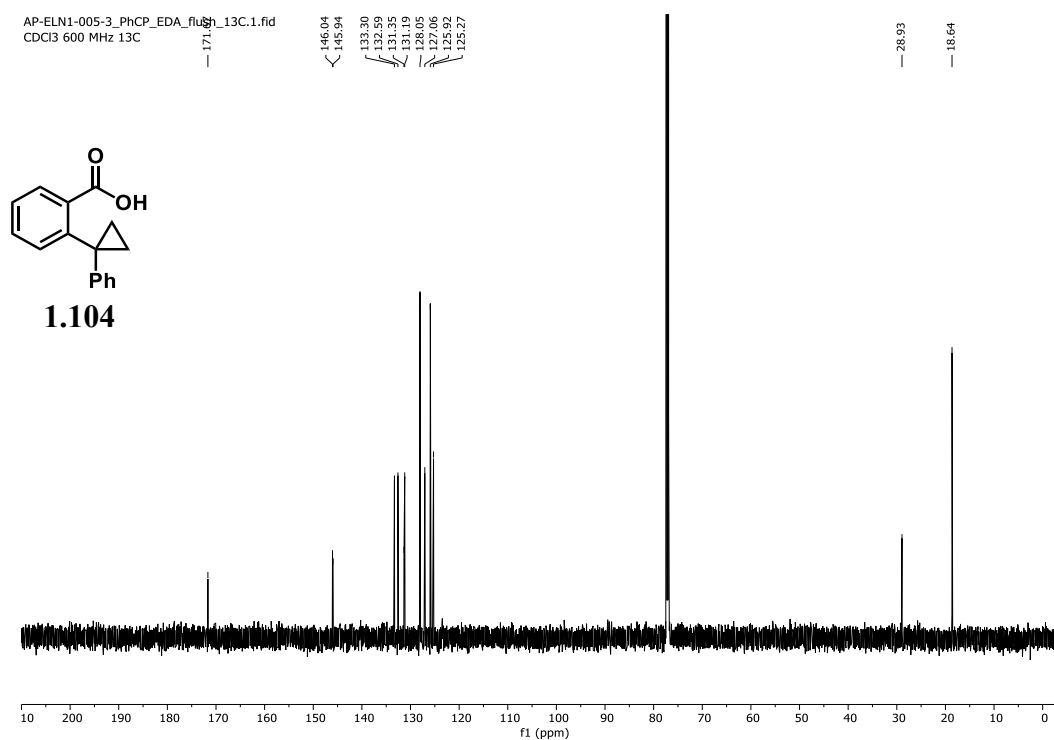


Figure 4.75. <sup>13</sup>C NMR spectrum of **1.104** (151 MHz, 298 K, CDCl<sub>3</sub>).

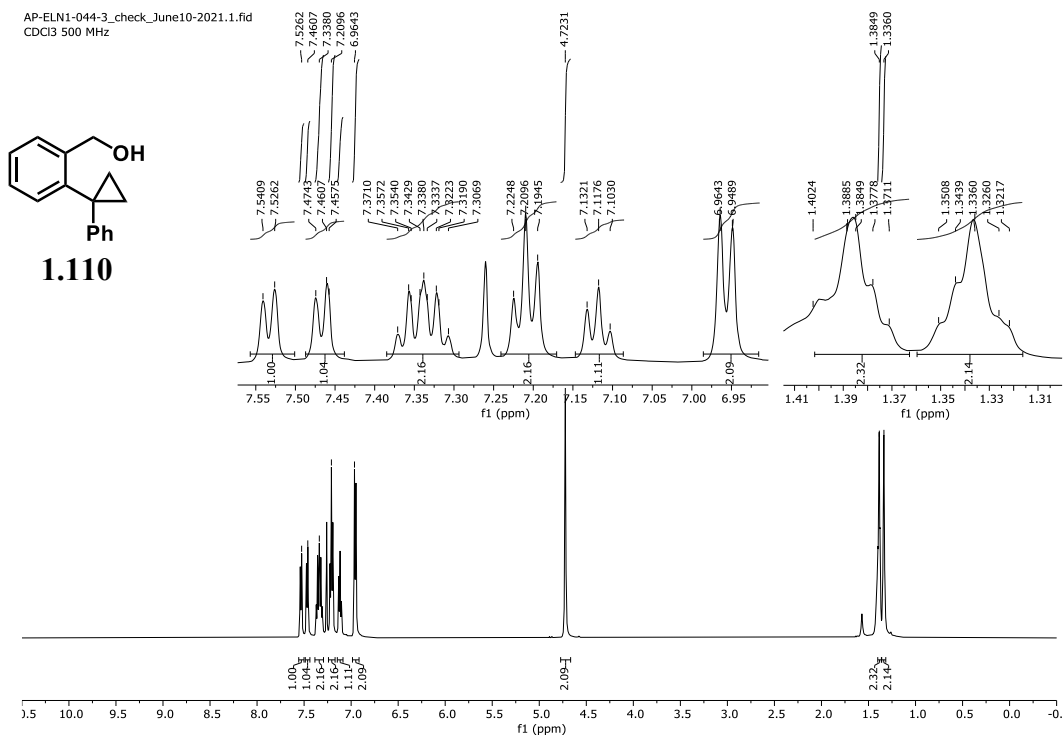


Figure 4.76. <sup>1</sup>H NMR spectrum of **1.110** (600 MHz, 298 K, CDCl<sub>3</sub>).

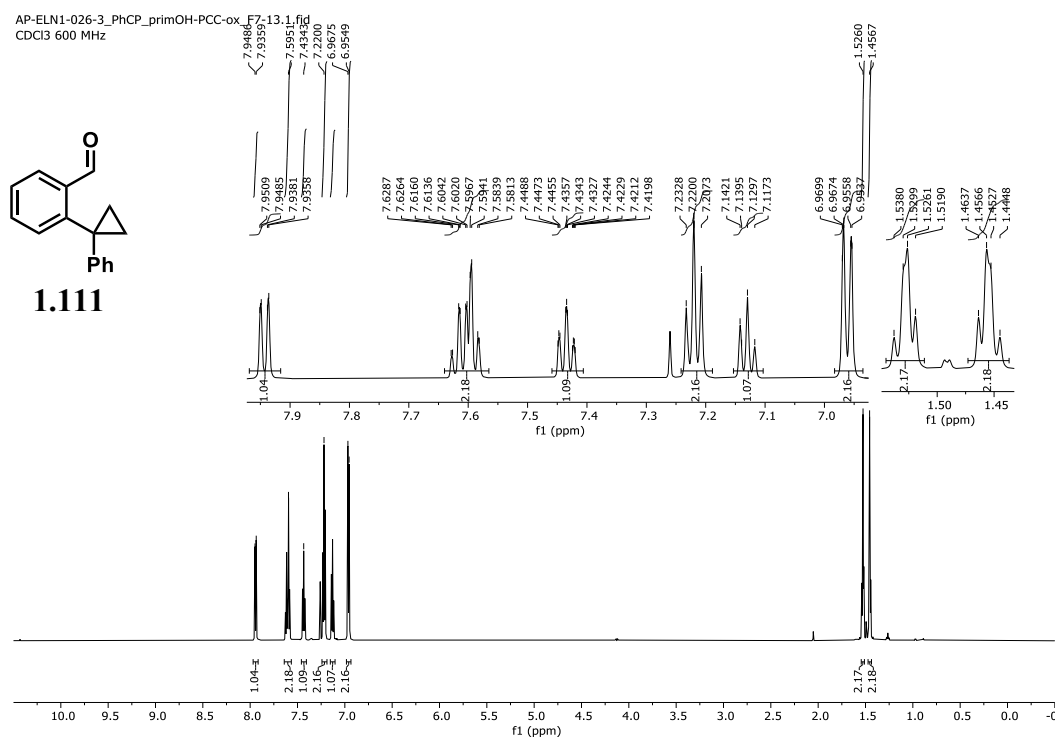


Figure 4.77. <sup>1</sup>H NMR spectrum of **1.111** (600 MHz, 298 K, CDCl<sub>3</sub>).

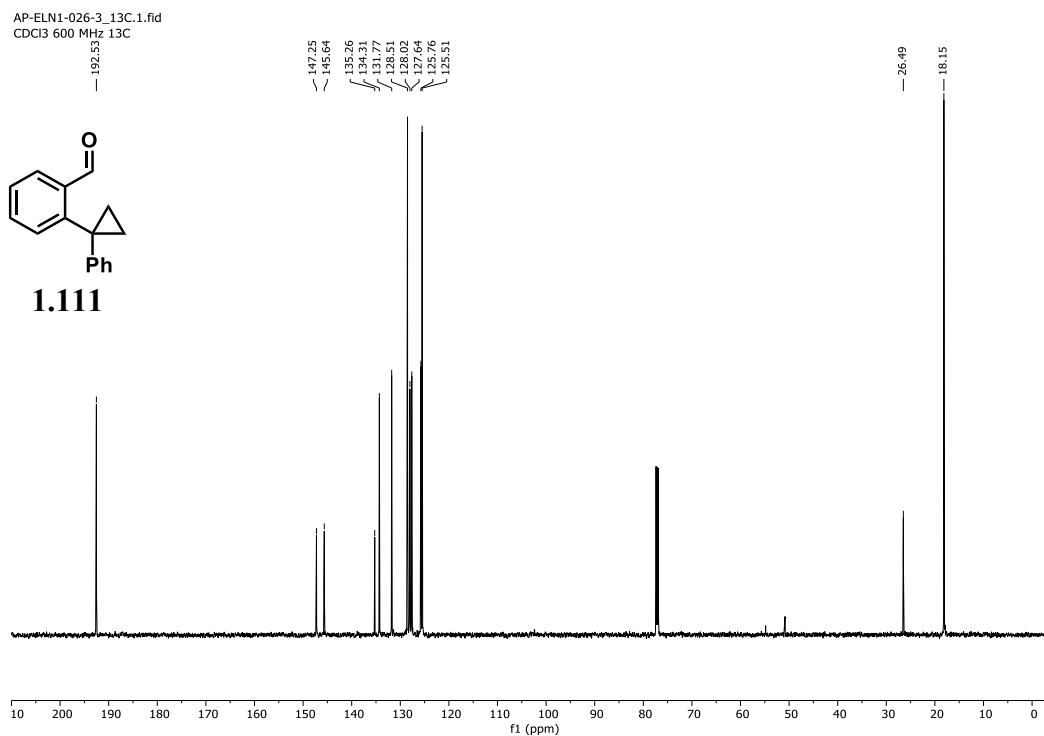


Figure 4.78. <sup>13</sup>C NMR spectrum of **1.111** (151 MHz, 298 K, CDCl<sub>3</sub>).

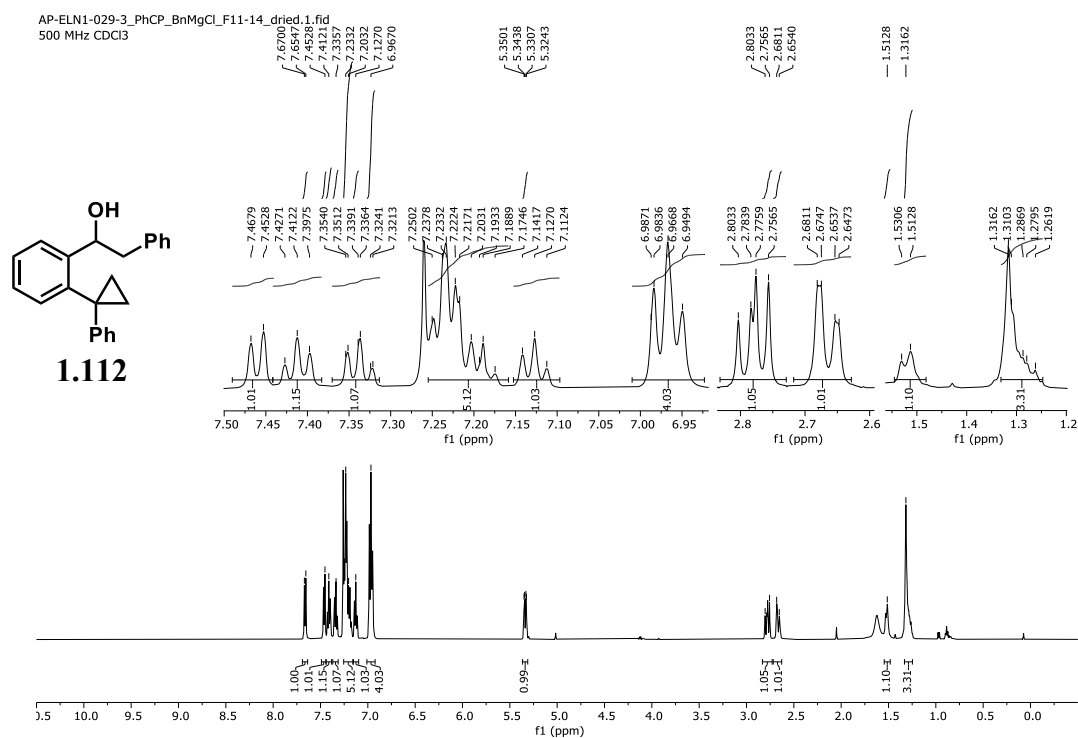


Figure 4.79. <sup>1</sup>H NMR spectrum of **1.112** (500 MHz, 298 K, CDCl<sub>3</sub>).

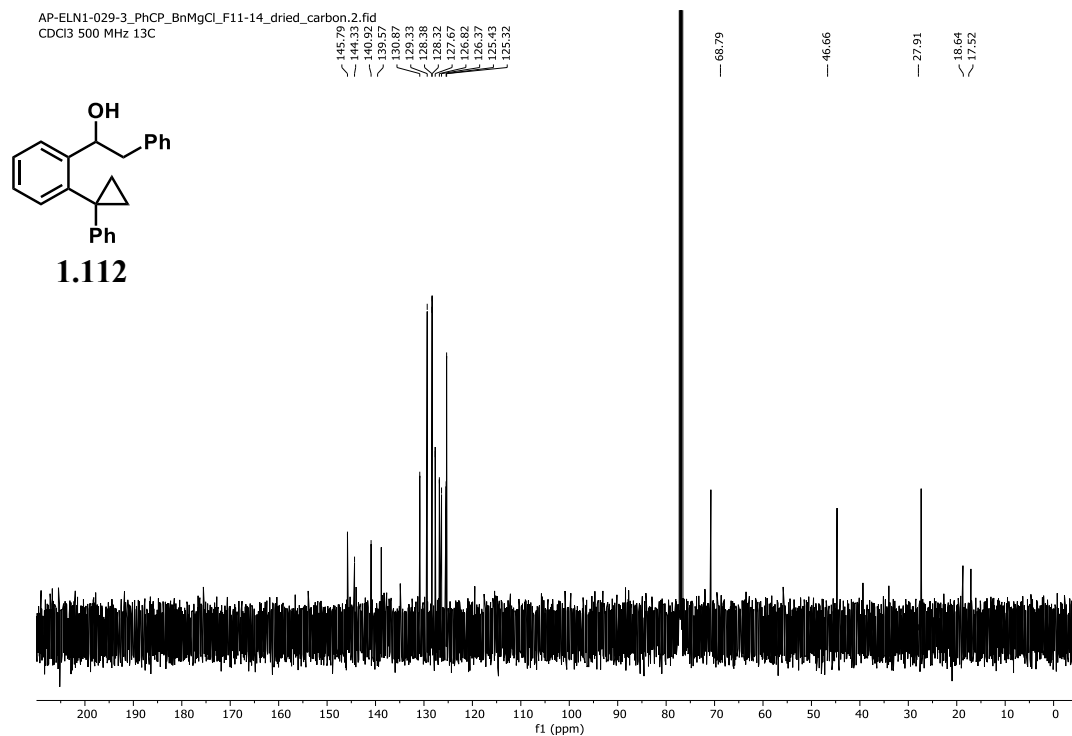


Figure 4.80. <sup>13</sup>C NMR spectrum of **1.112** (126 MHz, 298 K, CDCl<sub>3</sub>).

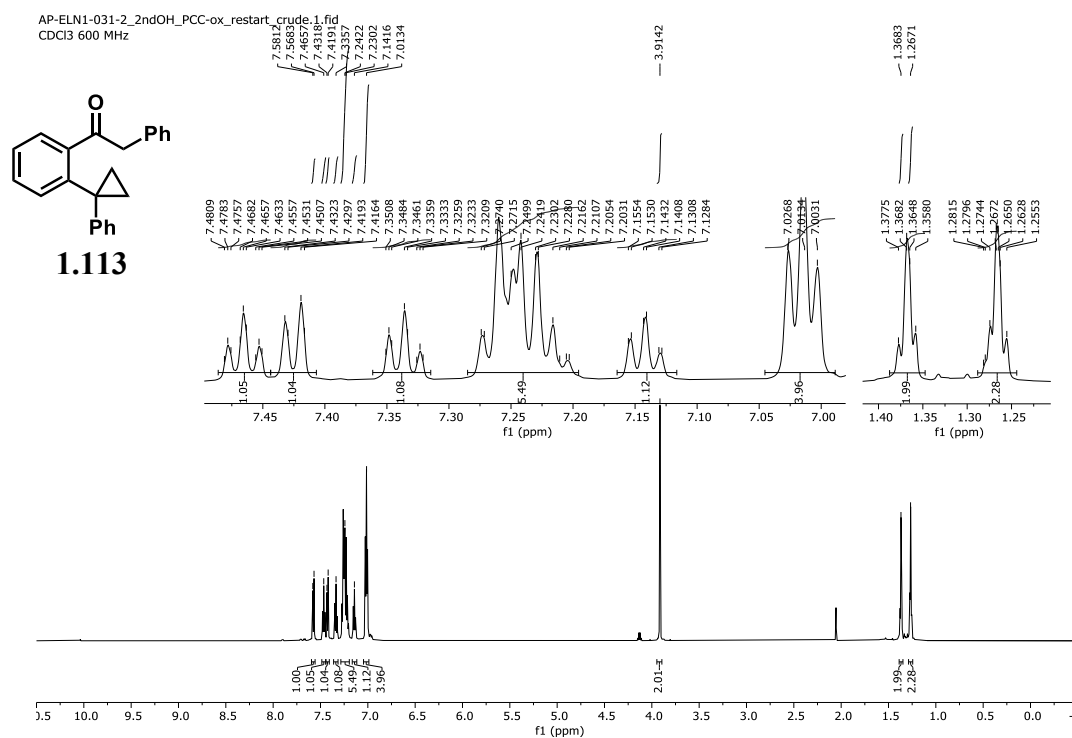


Figure 4.81. <sup>1</sup>H NMR spectrum of **1.113** (600 MHz, 298 K, CDCl<sub>3</sub>).



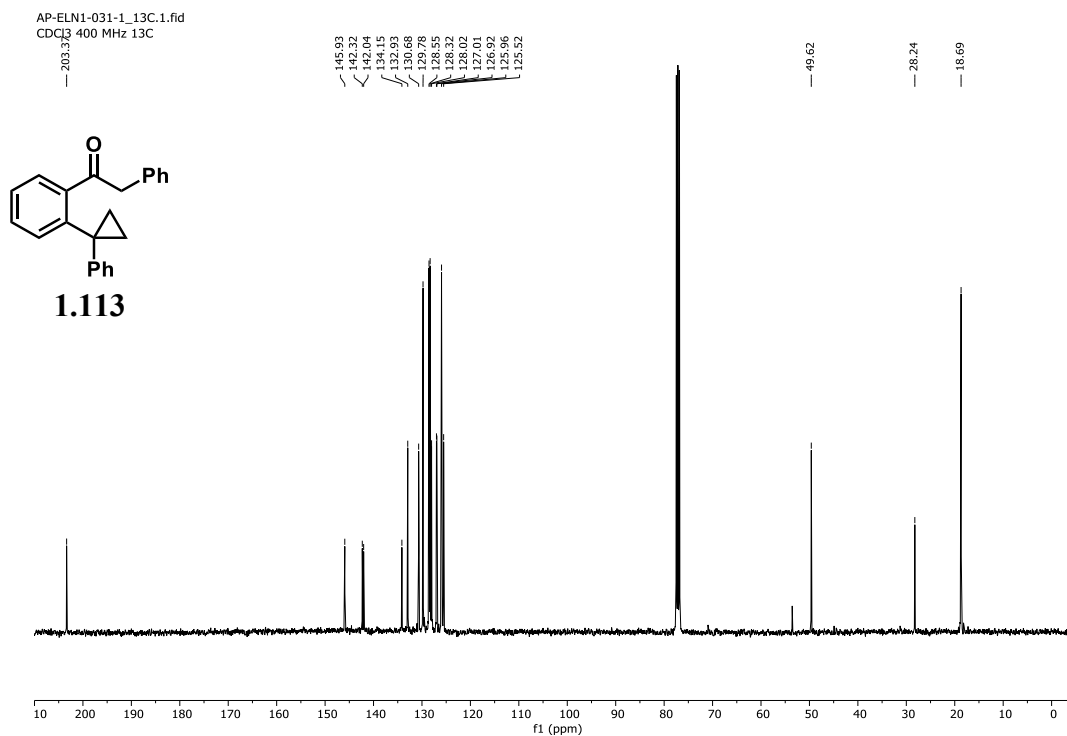


Figure 4.82. <sup>13</sup>C NMR spectrum of **1.113** (101 MHz, 295 K, CDCl<sub>3</sub>).

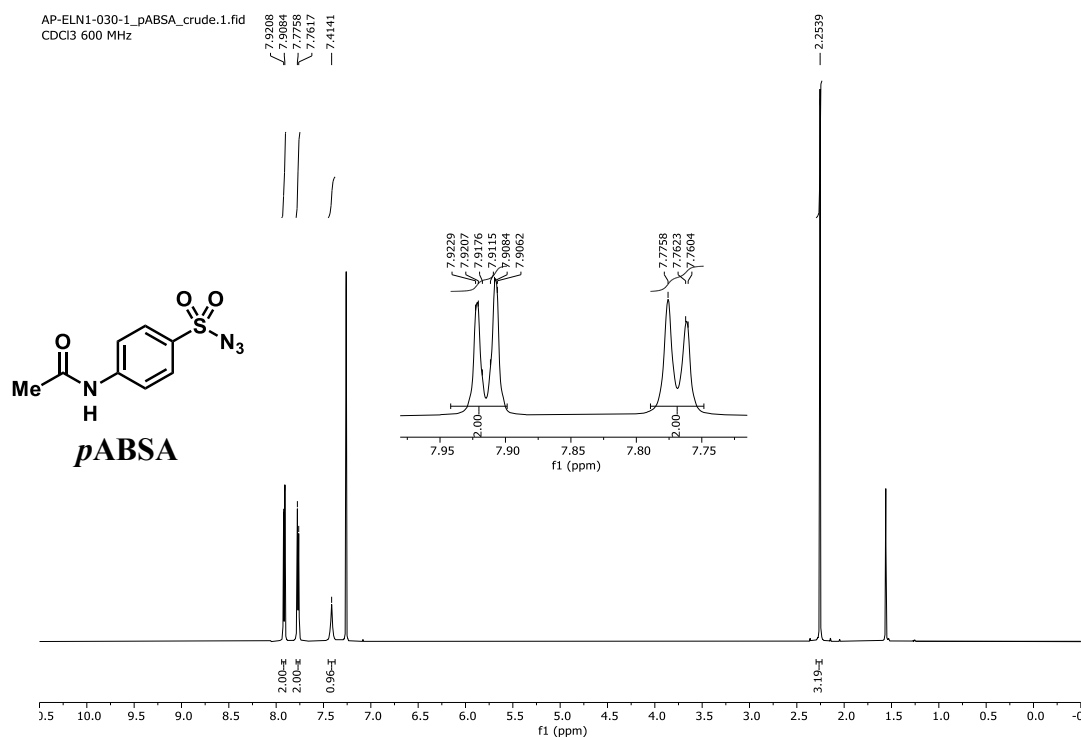


Figure 4.83. <sup>1</sup>H NMR spectrum of *p*ABSA (600 MHz, 298 K, CDCl<sub>3</sub>).

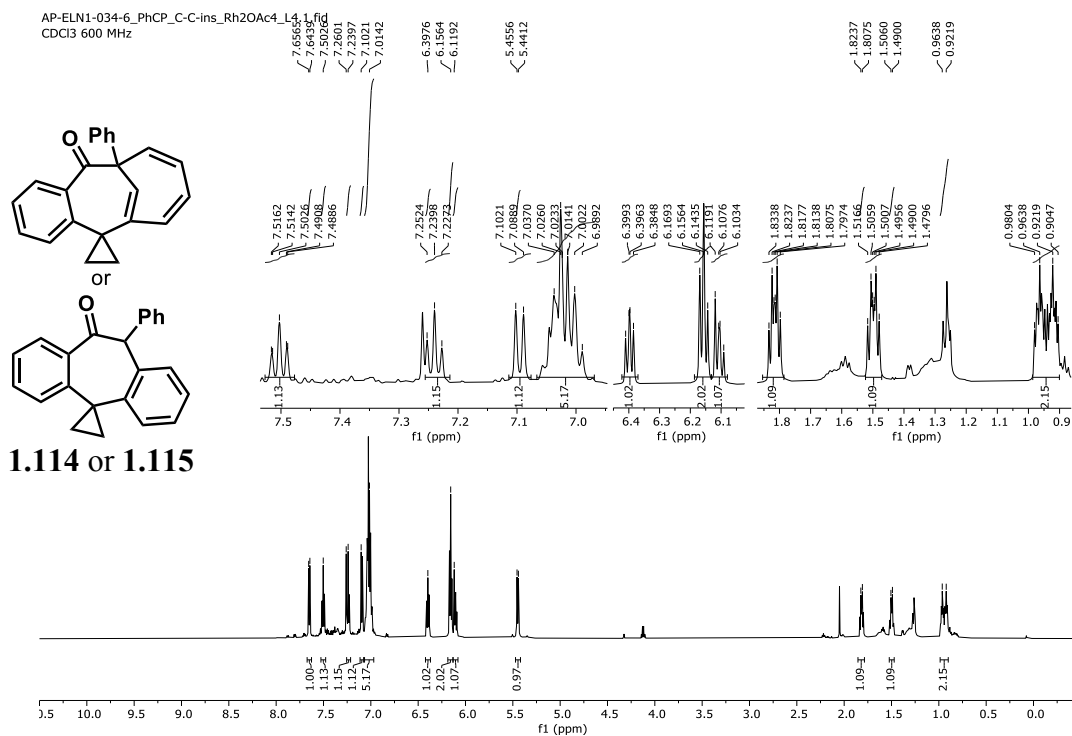


Figure 4.84. <sup>1</sup>H NMR spectrum of 1.114 or 1.115 (600 MHz, 298 K, CDCl<sub>3</sub>).

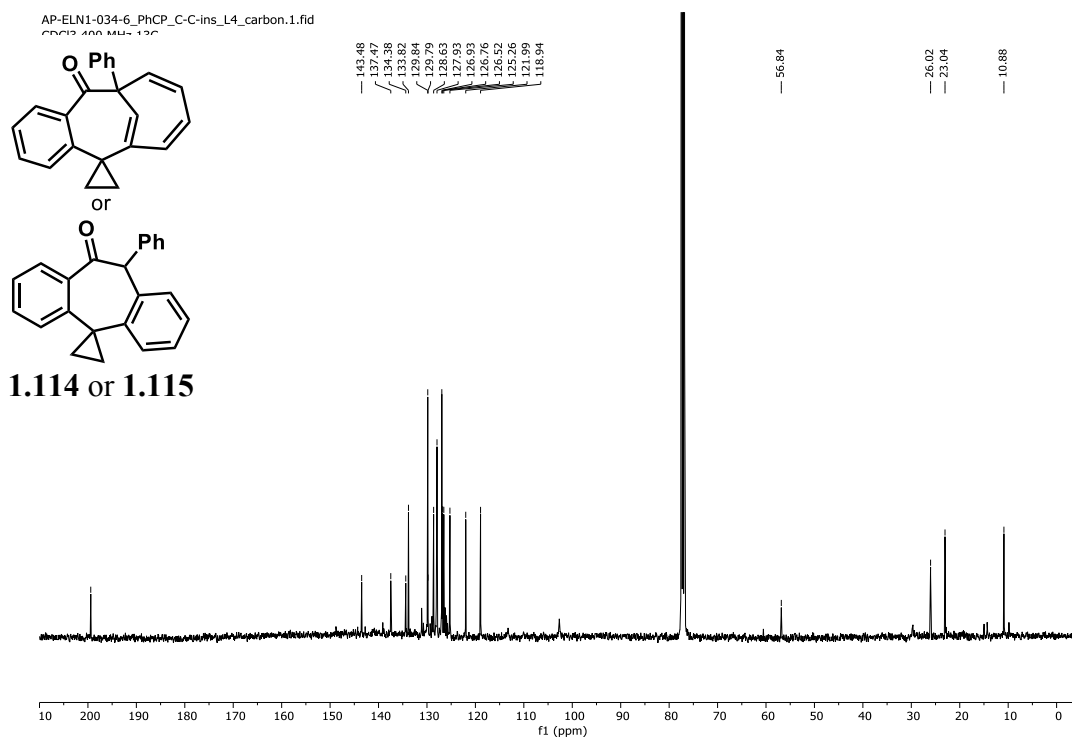


Figure 4.85. <sup>13</sup>C NMR spectrum of 1.114 or 1.115 (101 MHz, 295 K, CDCl<sub>3</sub>).

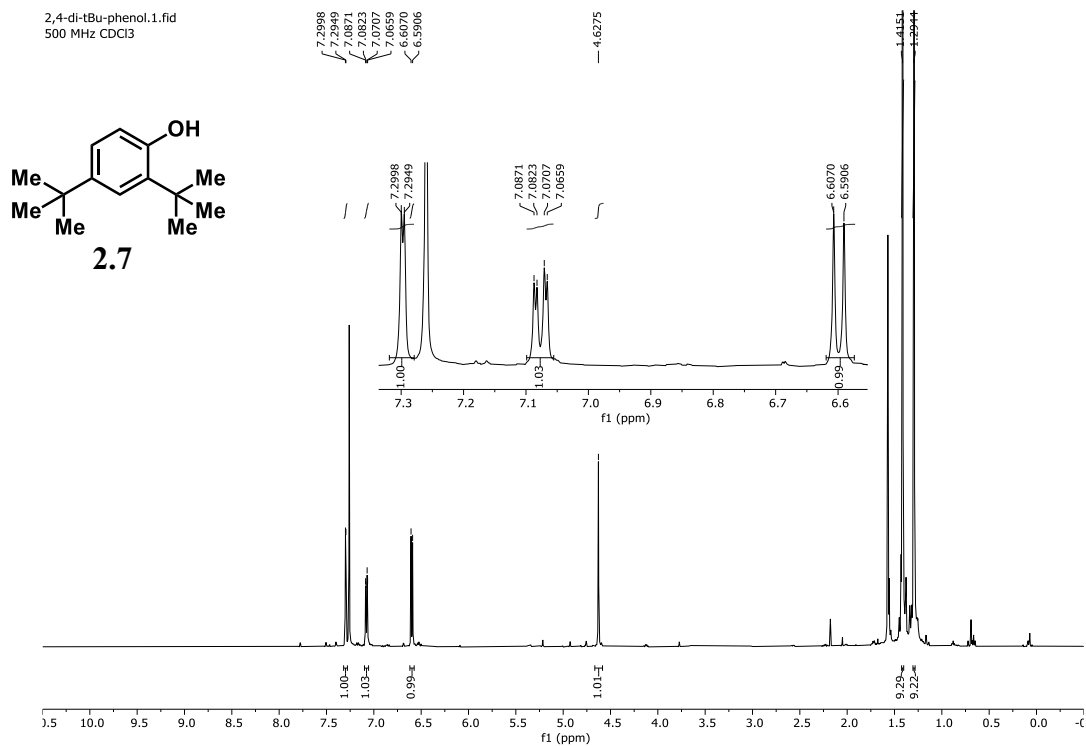


Figure 4.86. <sup>1</sup>H NMR spectrum of **2.7** (500 MHz, 298 K, CDCl<sub>3</sub>).

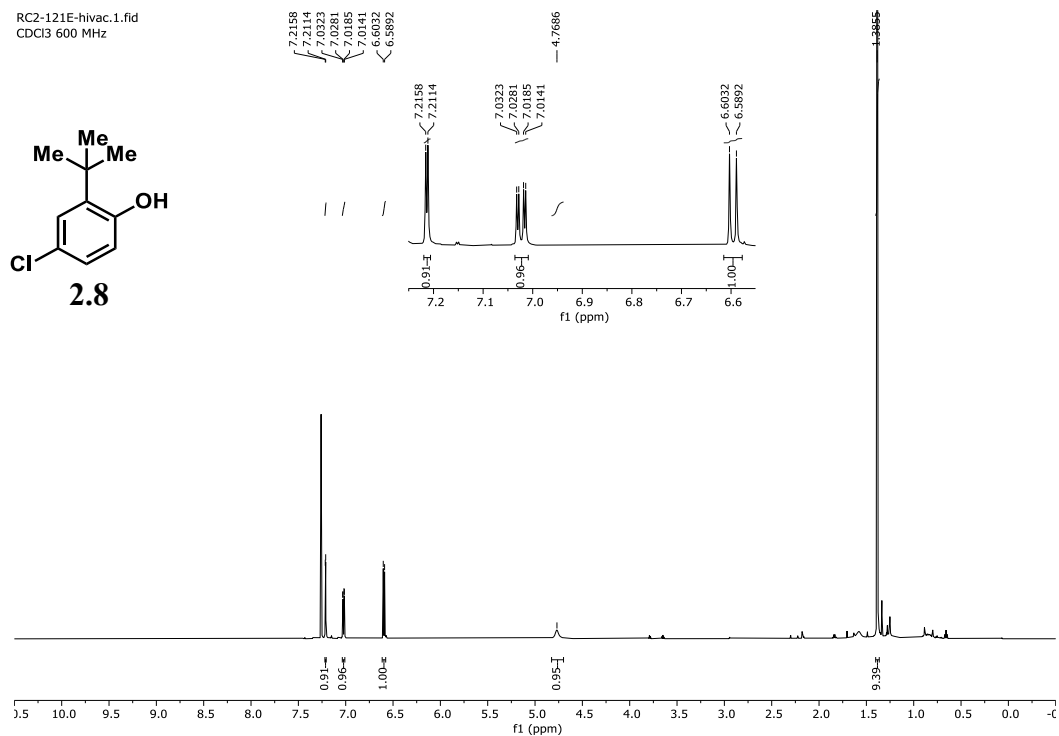


Figure 4.87. <sup>1</sup>H NMR spectrum of **2.8** (600 MHz, 298 K, CDCl<sub>3</sub>).

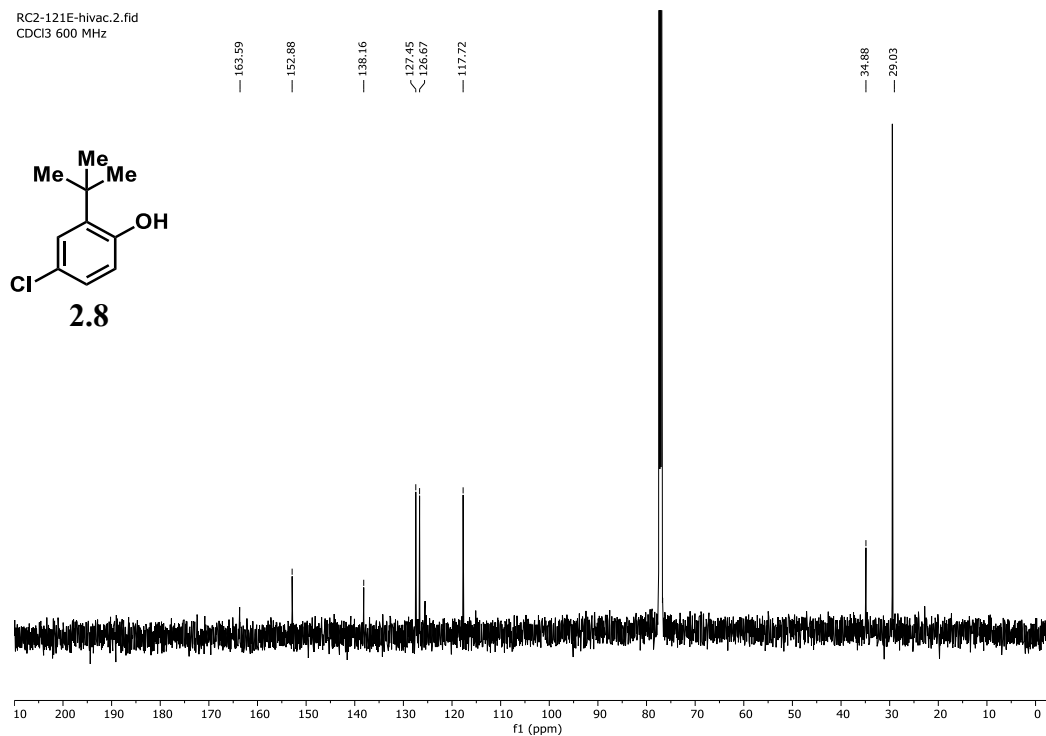


Figure 4.88. <sup>13</sup>C NMR spectrum of **2.8** (151 MHz, 298 K, CDCl<sub>3</sub>).

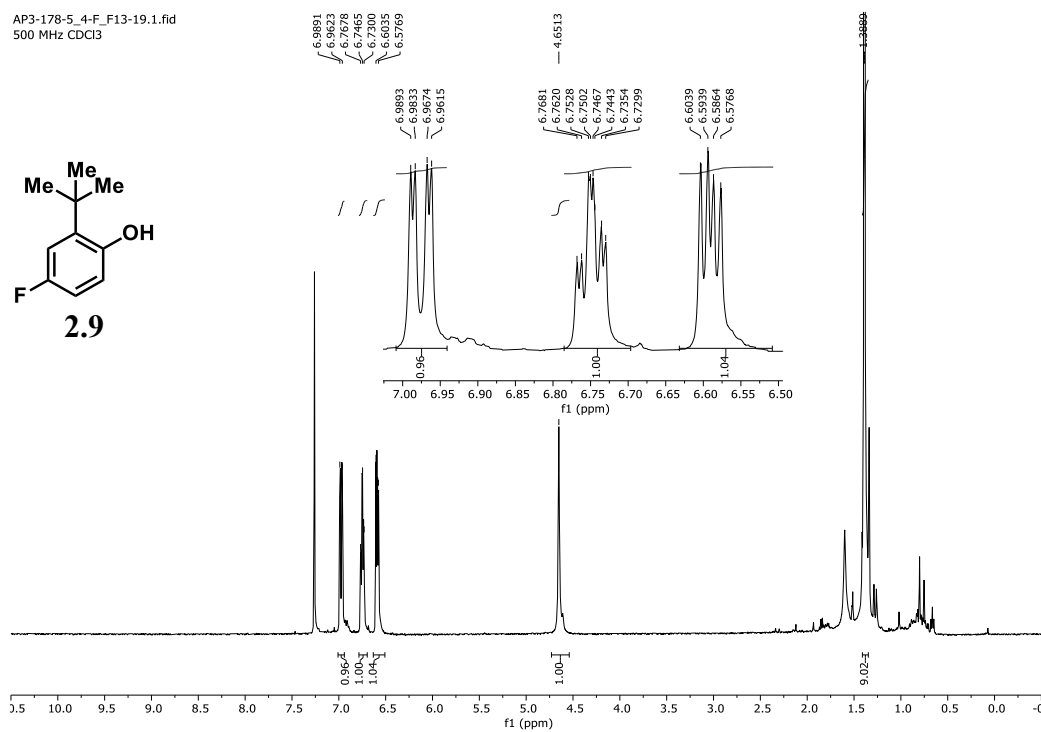


Figure 4.89. <sup>1</sup>H NMR spectrum of **2.9** (500 MHz, 298 K, CDCl<sub>3</sub>).

RC2-123A.10.fid

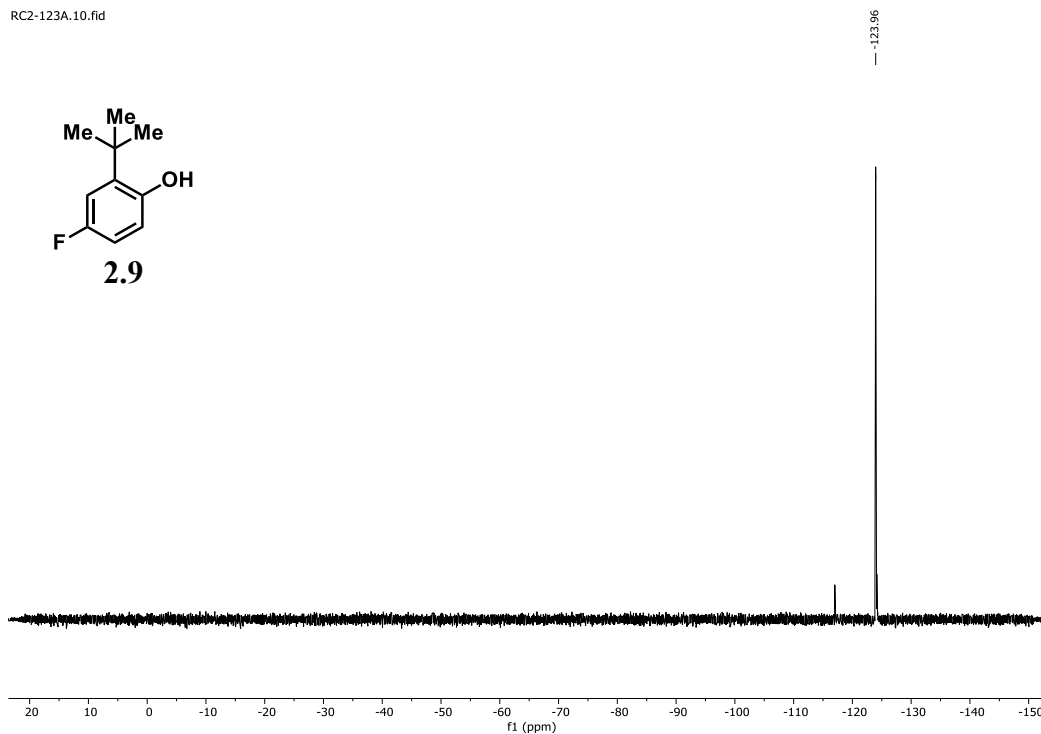


Figure 4.90.  $^{19}\text{F}$  NMR spectrum of **2.9** (564 MHz, 298 K,  $\text{CDCl}_3$ ).

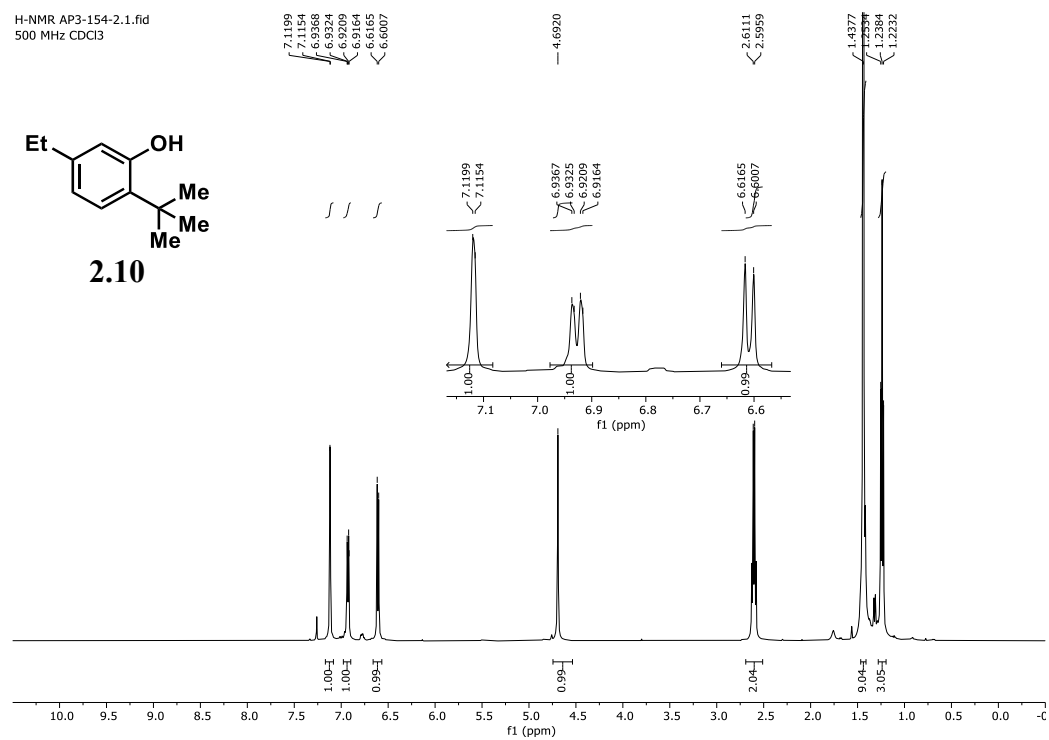


Figure 4.91.  $^1\text{H}$  NMR spectrum of **2.10** (500 MHz, 298 K,  $\text{CDCl}_3$ ).

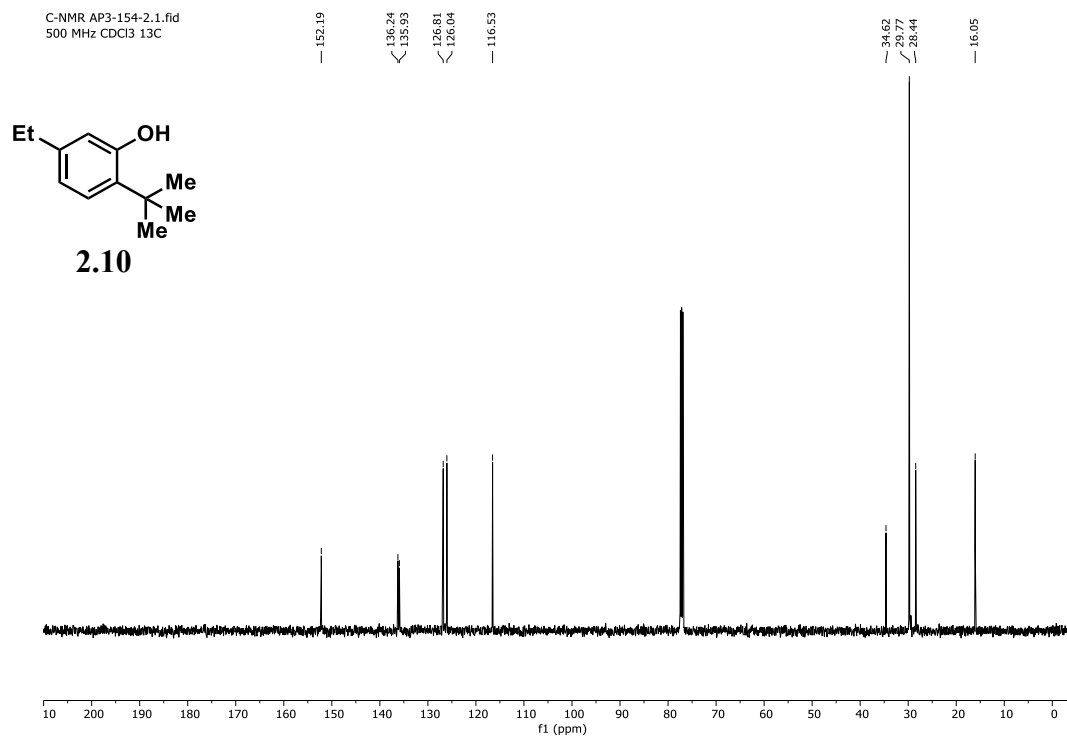


Figure 4.92. <sup>13</sup>C NMR spectrum of **2.10** (126 MHz, 298 K, CDCl<sub>3</sub>).

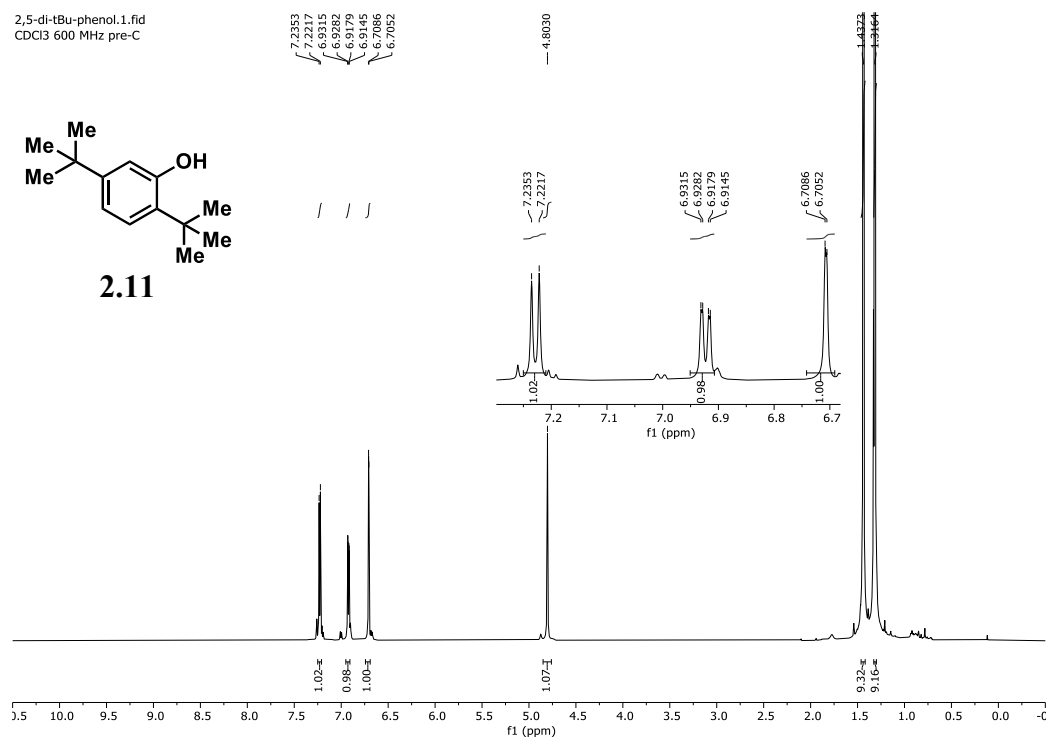
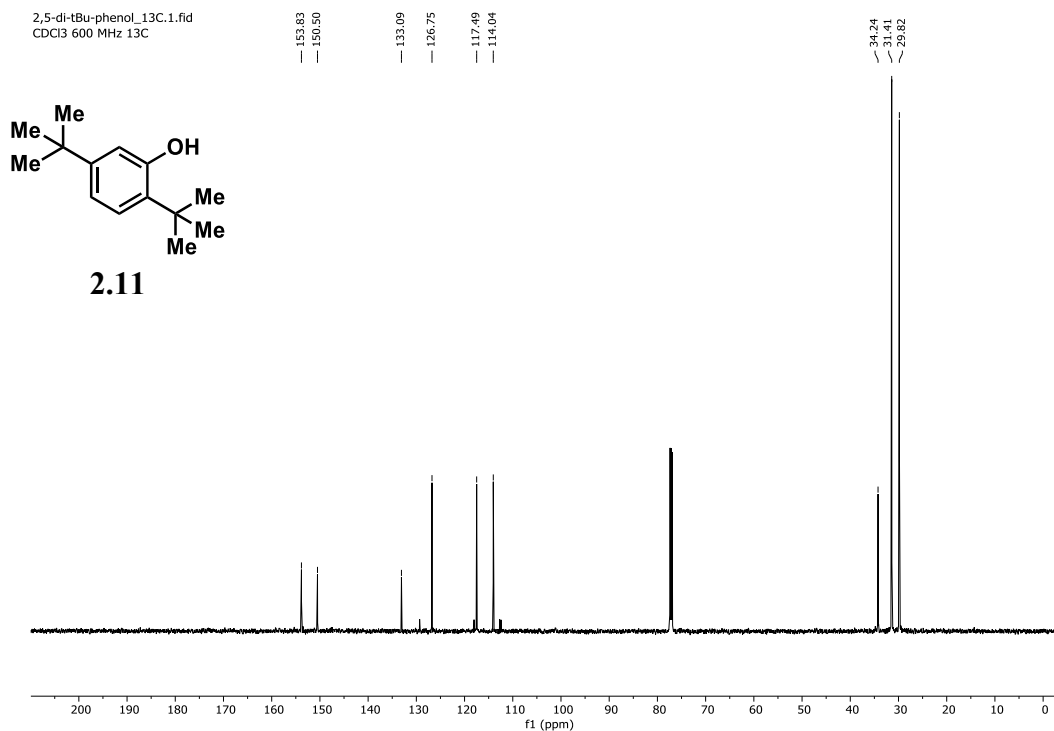
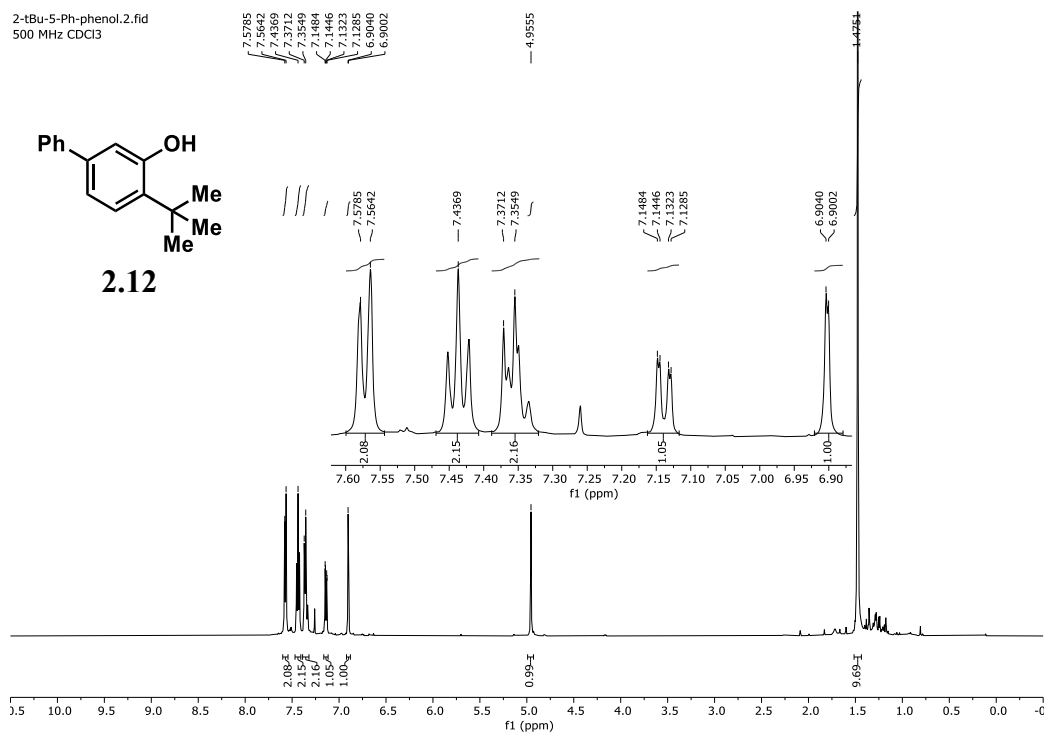


Figure 4.93. <sup>1</sup>H NMR spectrum of **2.11** (600 MHz, 298 K, CDCl<sub>3</sub>).



**Figure 4.94.** <sup>13</sup>C NMR spectrum of **2.11** (151 MHz, 298 K, CDCl<sub>3</sub>).



**Figure 4.95.** <sup>1</sup>H NMR spectrum of **2.12** (500 MHz, 298 K, CDCl<sub>3</sub>).

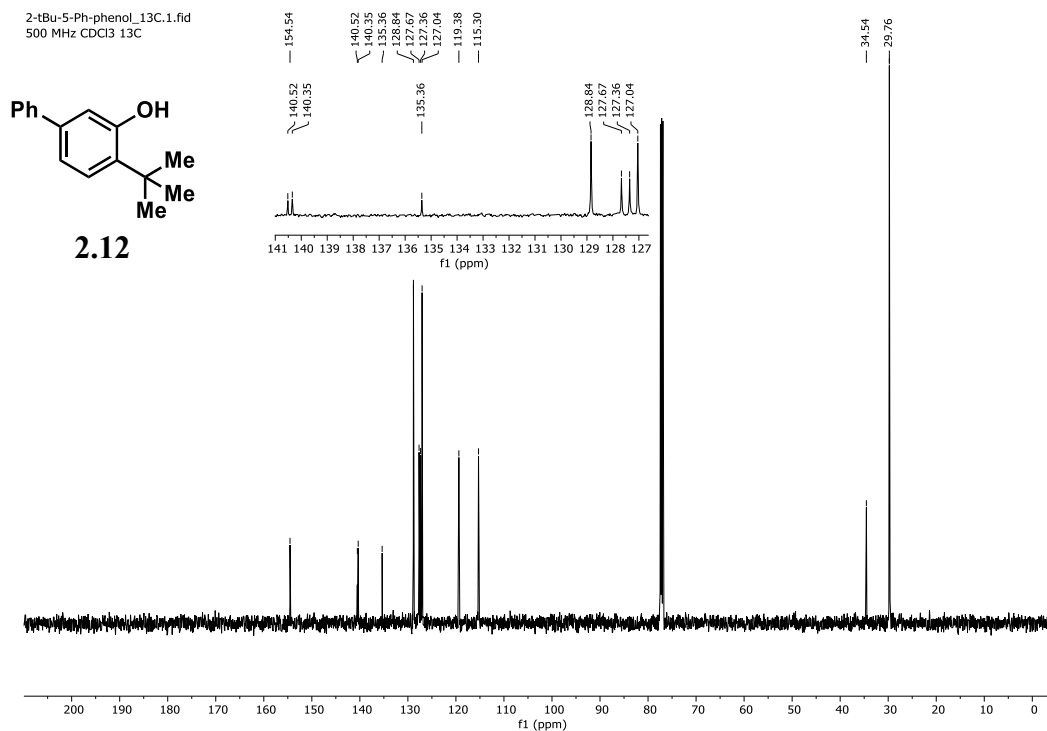


Figure 4.96. <sup>13</sup>C NMR spectrum of **2.12** (126 MHz, 298 K, CDCl<sub>3</sub>).

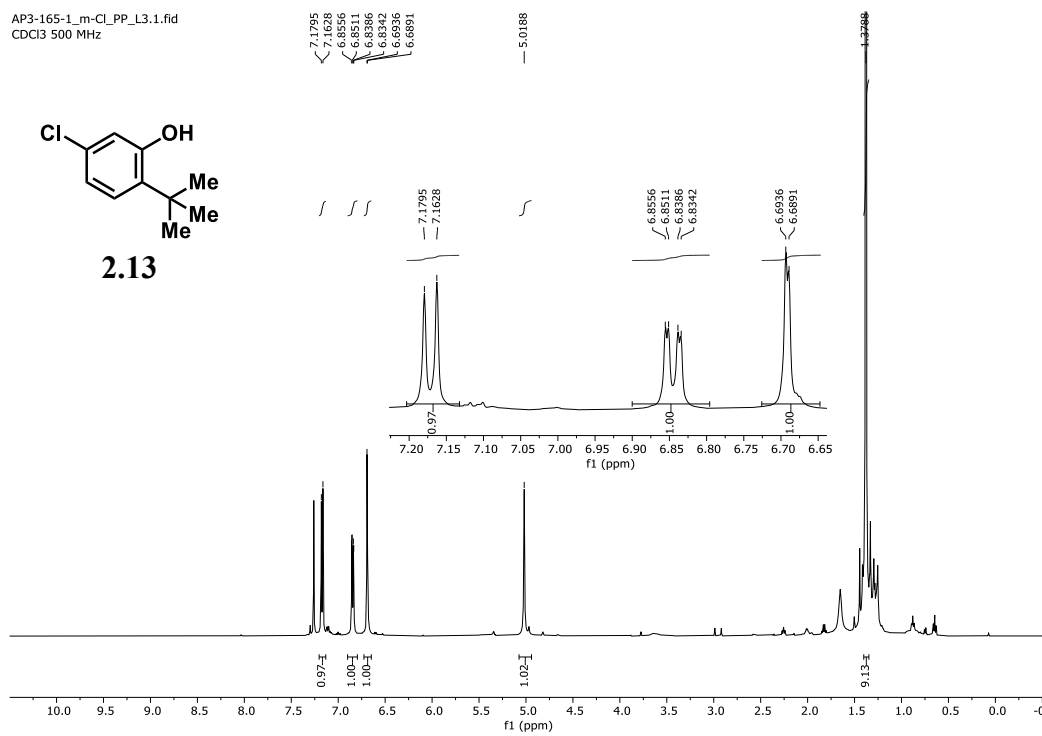


Figure 4.97. <sup>1</sup>H NMR spectrum of **2.13** (500 MHz, 298 K, CDCl<sub>3</sub>).



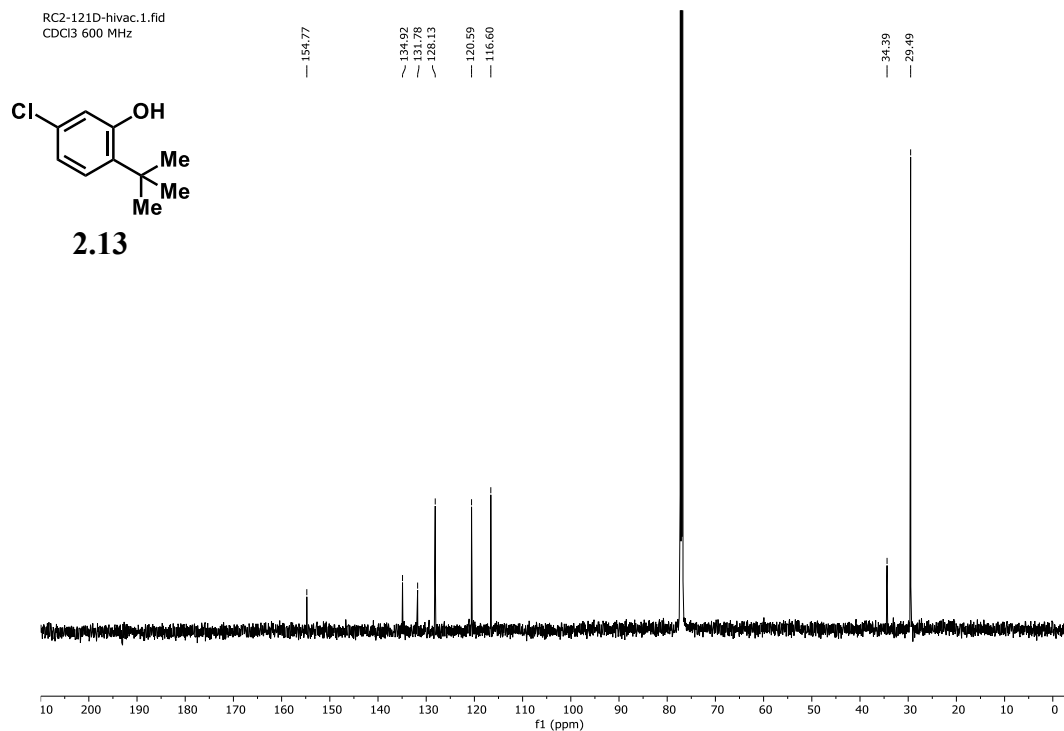


Figure 4.98. <sup>13</sup>C NMR spectrum of **2.13** (151 MHz, 298 K, CDCl<sub>3</sub>).

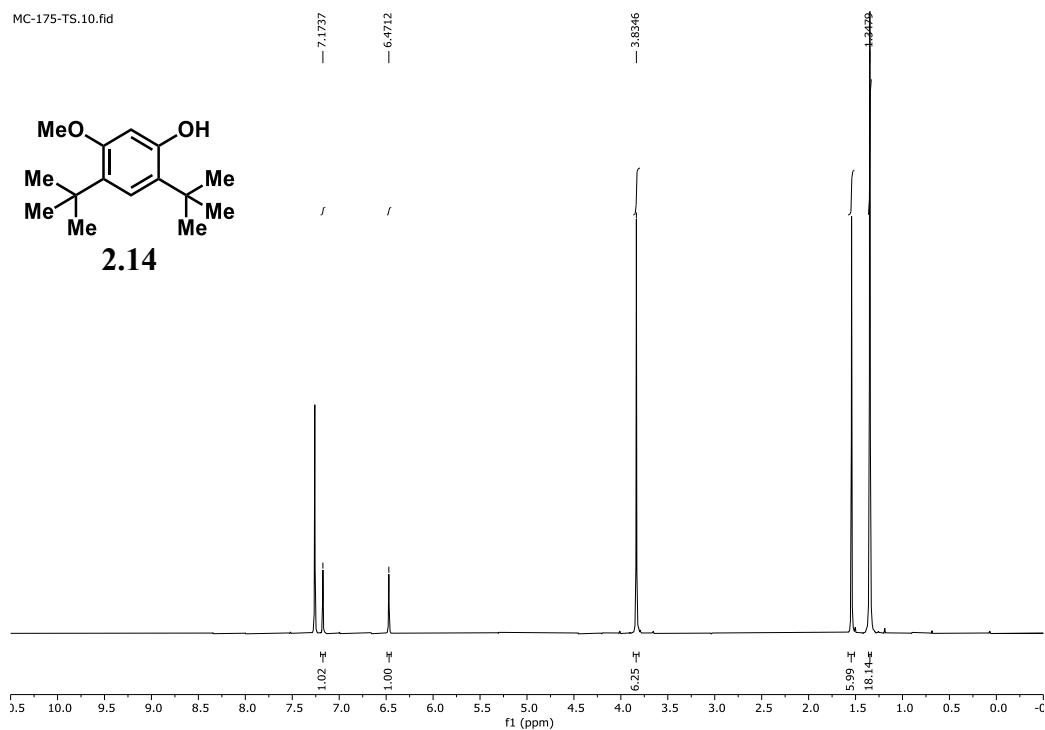


Figure 4.99. <sup>1</sup>H NMR spectrum of **2.14** (400 MHz, 295 K, CDCl<sub>3</sub>).

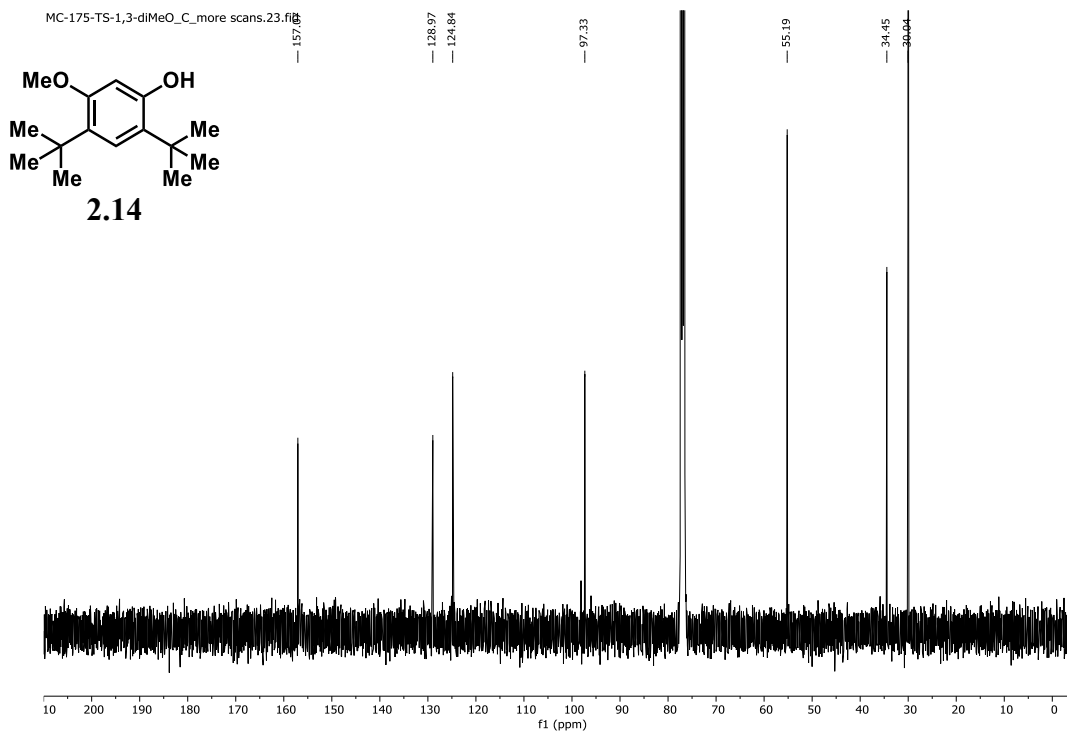


Figure 4.100.  $^{13}\text{C}$  NMR spectrum of **2.14** (101 MHz, 295 K,  $\text{CDCl}_3$ ).

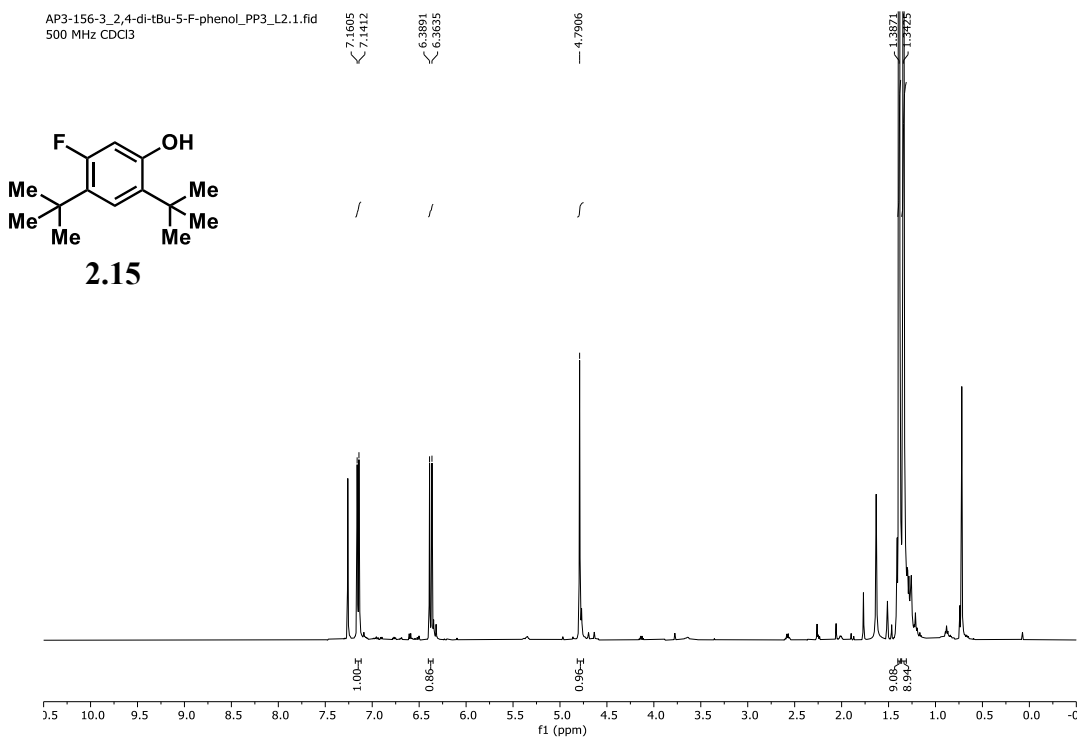


Figure 4.101.  $^1\text{H}$  NMR spectrum of **2.15** (500 MHz, 298 K,  $\text{CDCl}_3$ ).

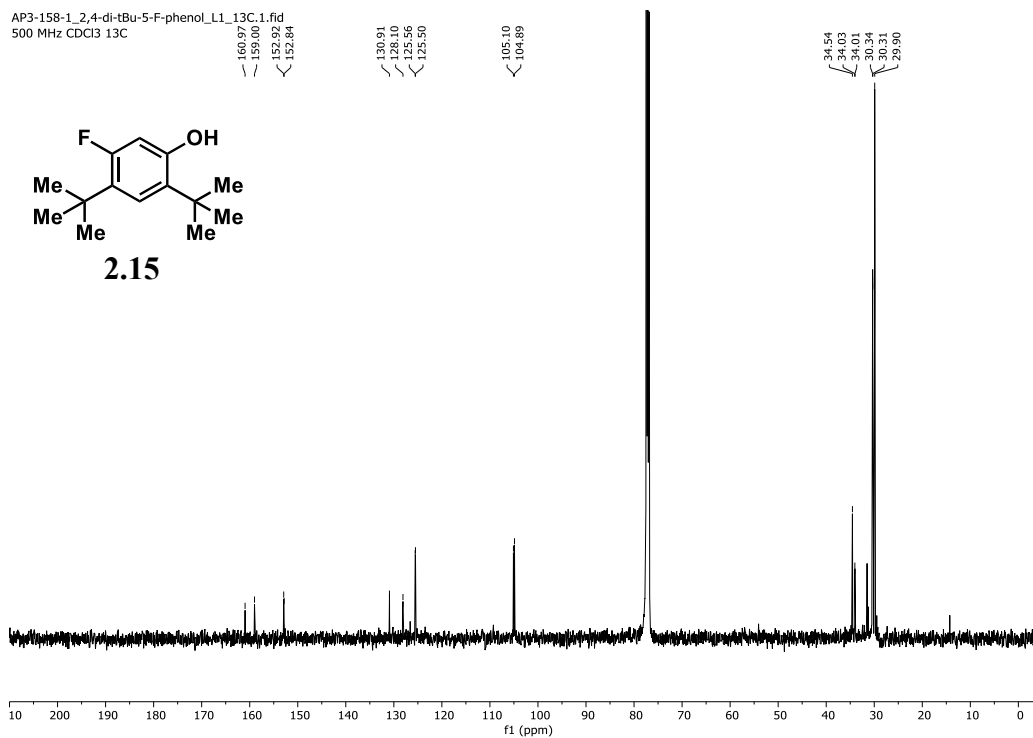


Figure 4.102. <sup>13</sup>C NMR spectrum of **2.15** (126 MHz, 298 K, CDCl<sub>3</sub>).

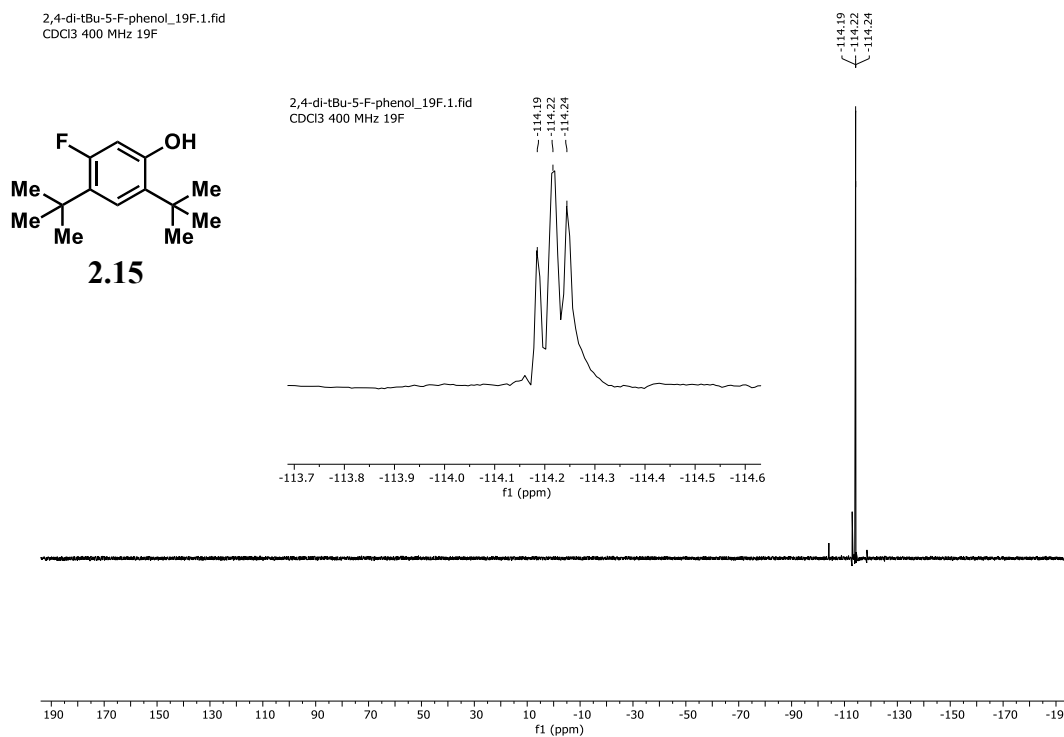


Figure 4.103. <sup>19</sup>F NMR spectrum of **2.15** (376 MHz, 295 K, CDCl<sub>3</sub>).

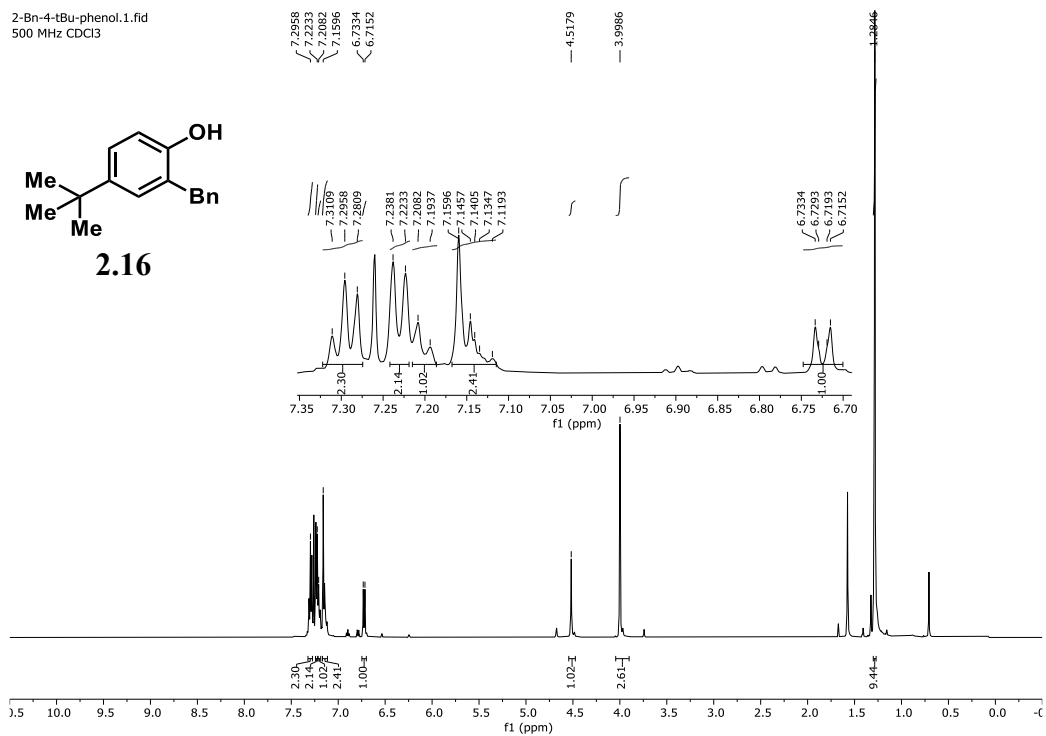


Figure 4.104. <sup>1</sup>H NMR spectrum of **2.16** (500 MHz, 298 K, CDCl<sub>3</sub>).

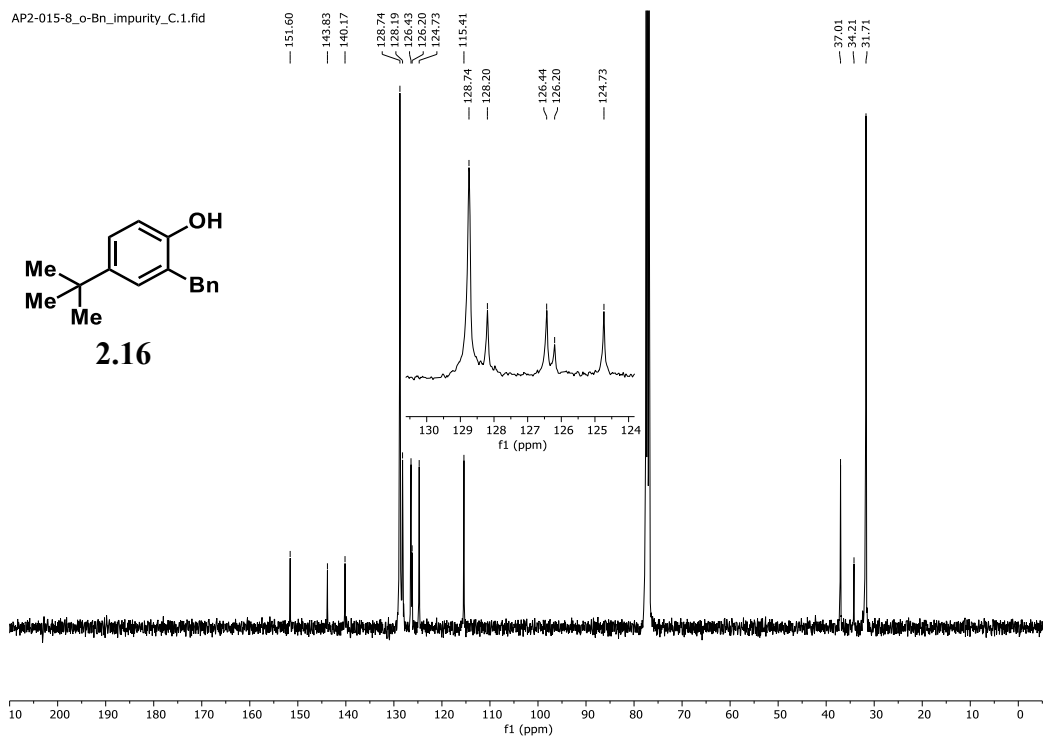
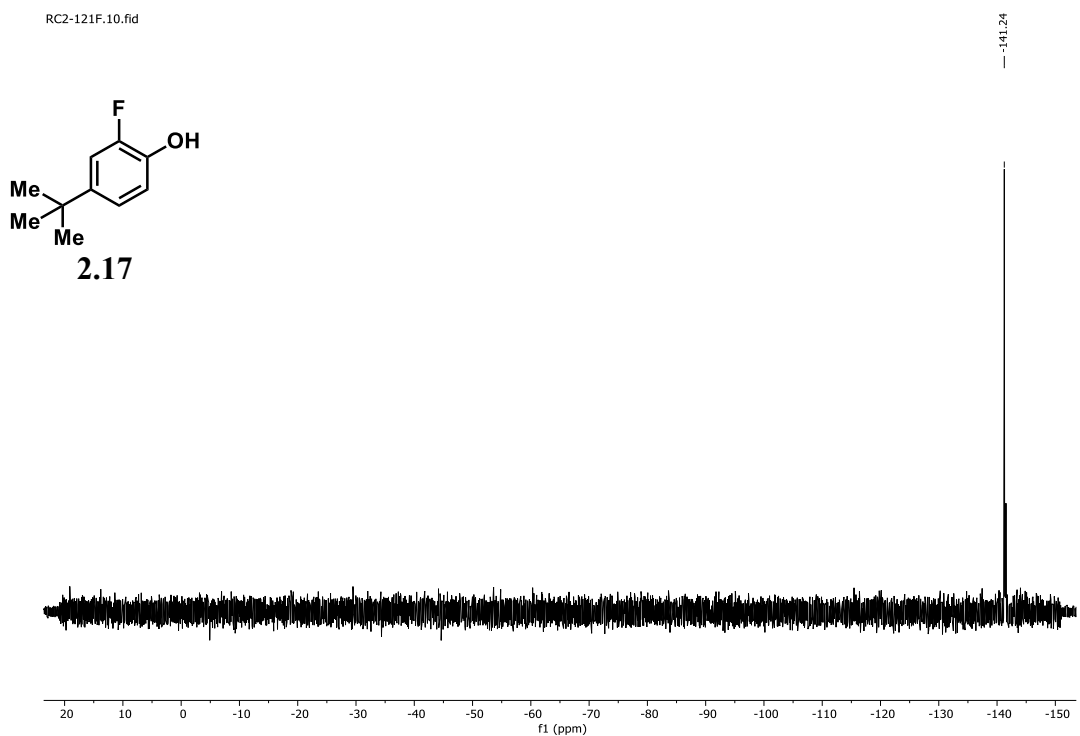
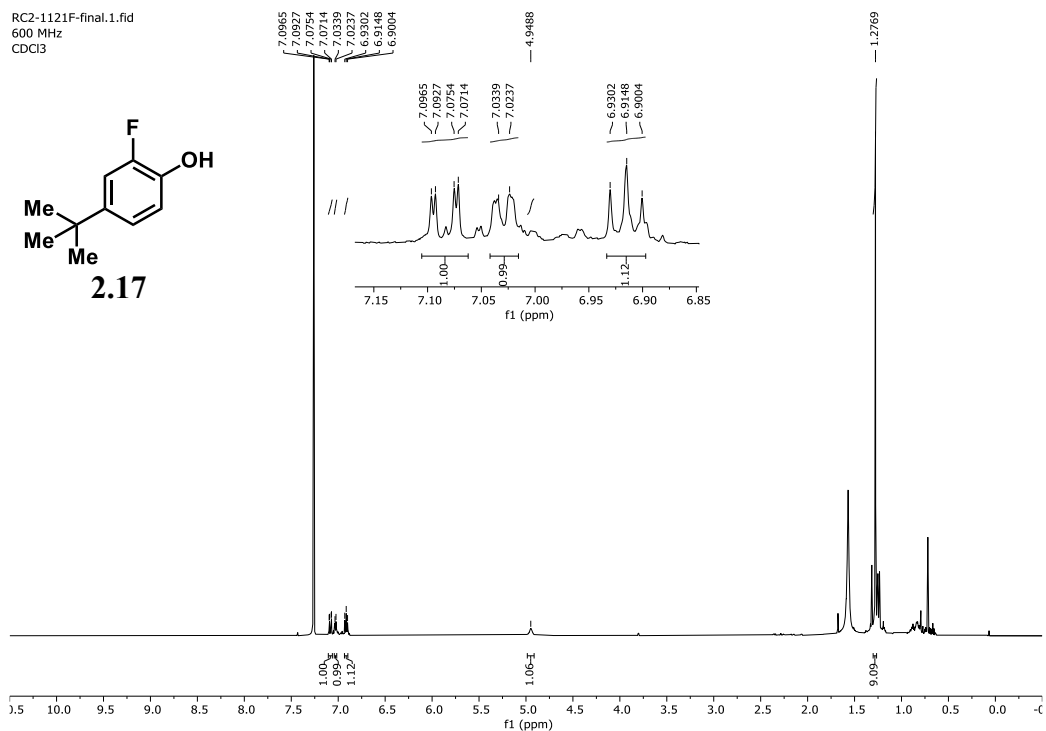


Figure 4.105. <sup>13</sup>C NMR spectrum of **2.16** (126 MHz, 298 K, CDCl<sub>3</sub>).



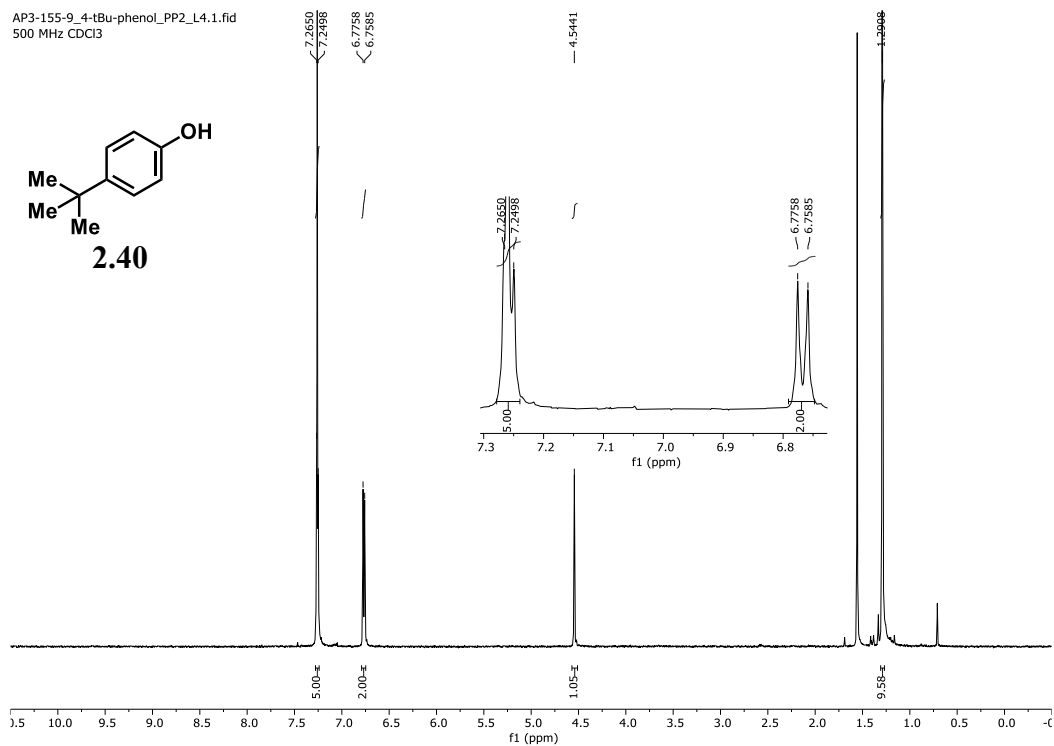


Figure 4.108. <sup>1</sup>H NMR spectrum of **2.40** (500 MHz, 298 K, CDCl<sub>3</sub>).

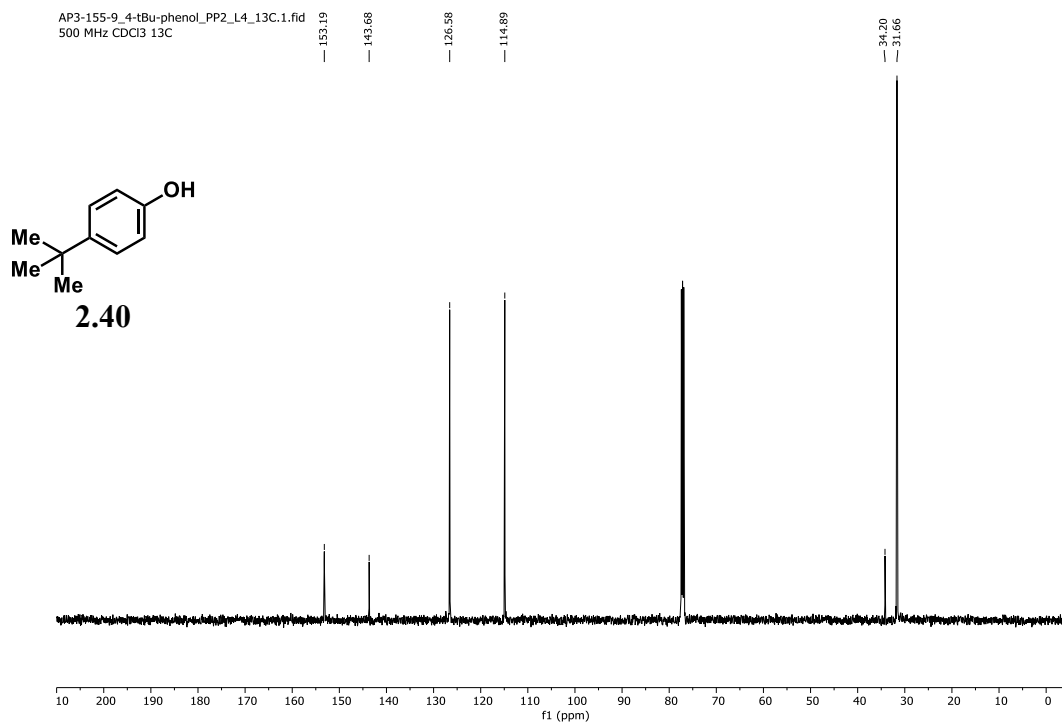


Figure 4.109. <sup>13</sup>C NMR spectrum of **2.40** (126 MHz, 298 K, CDCl<sub>3</sub>).

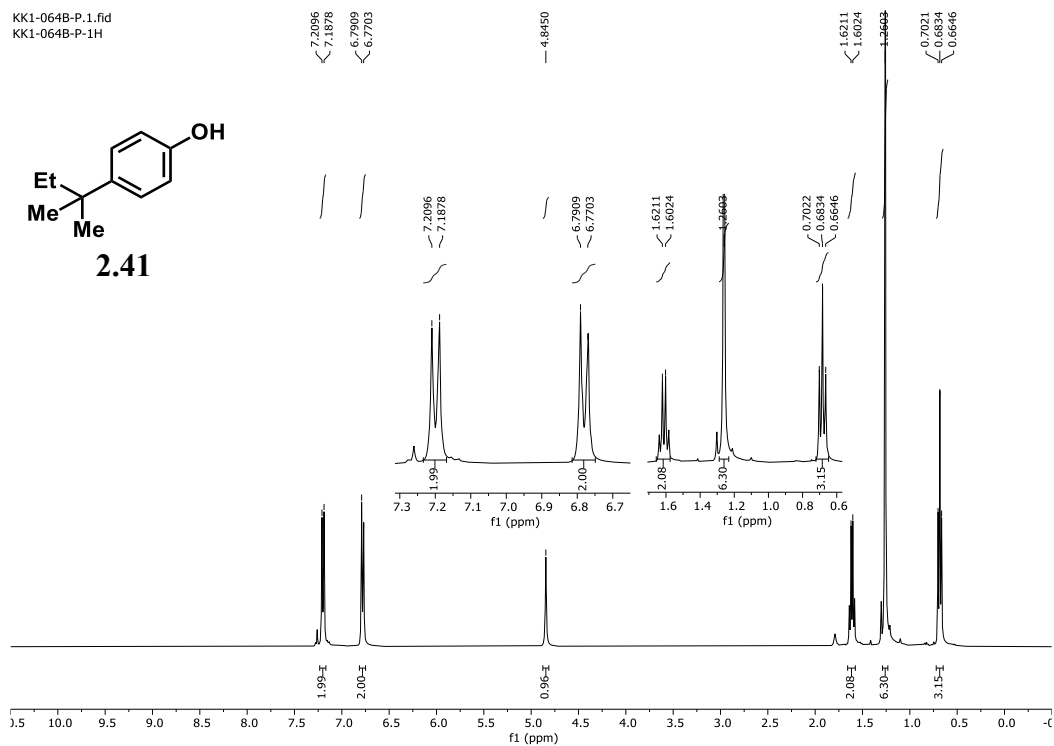


Figure 4.110.  $^1\text{H}$  NMR spectrum of **2.41** (400 MHz, 295 K,  $\text{CDCl}_3$ ).

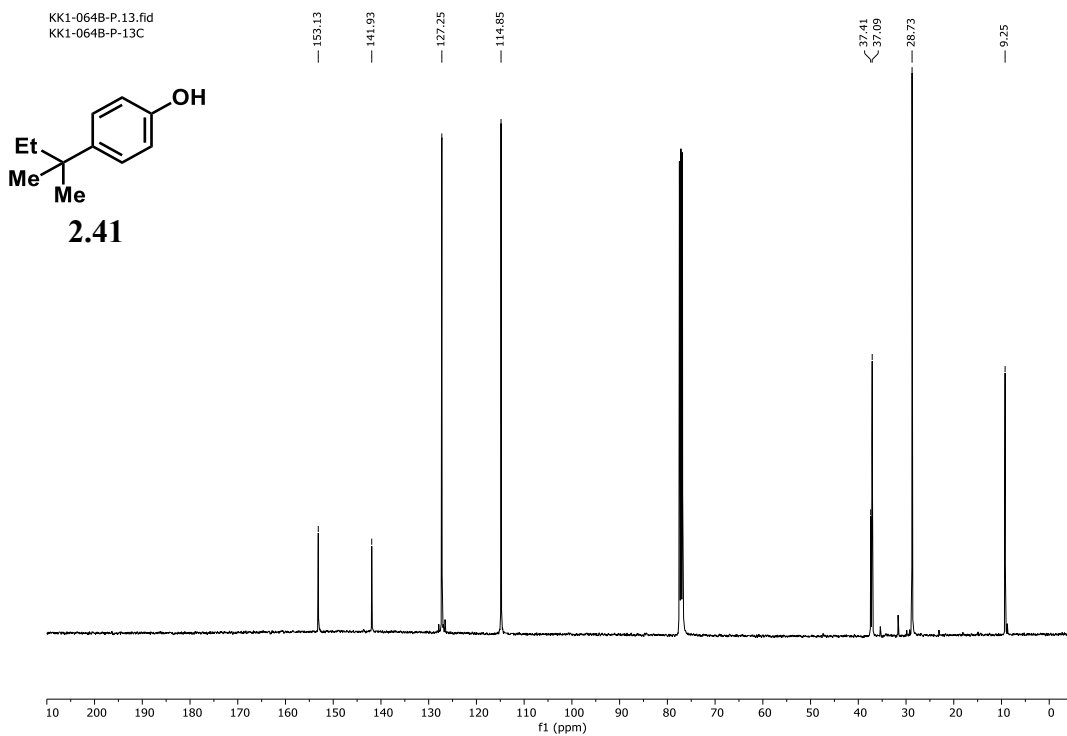


Figure 4.111.  $^{13}\text{C}$  NMR spectrum of **2.41** (101 MHz, 295 K,  $\text{CDCl}_3$ ).

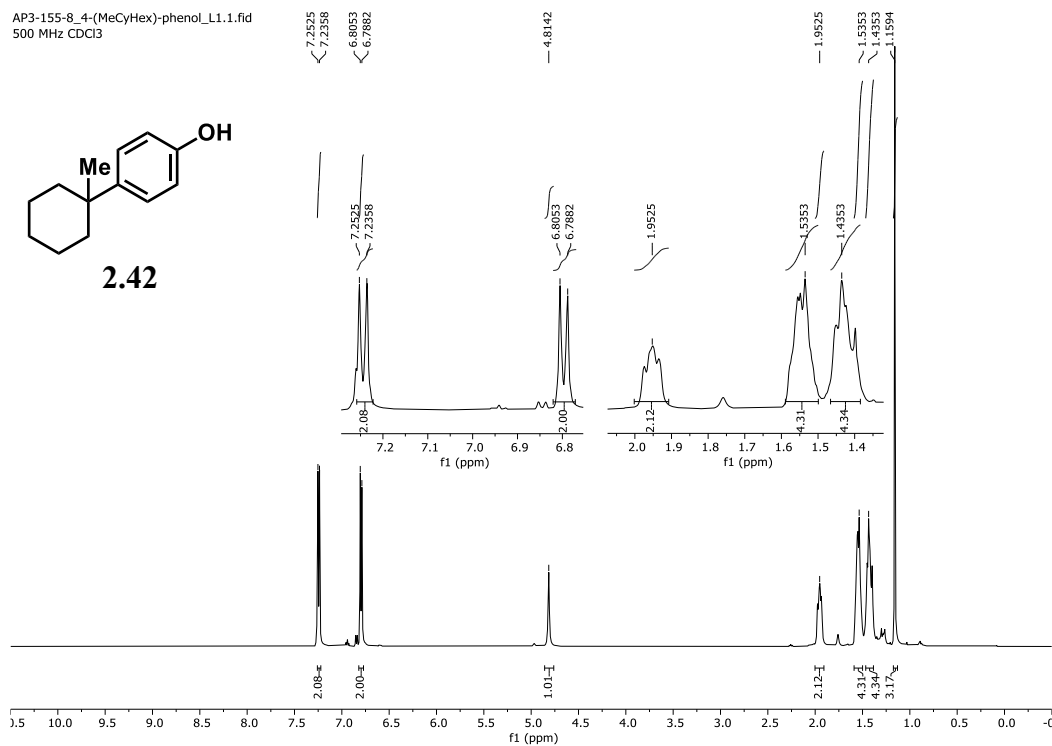


Figure 4.112. <sup>1</sup>H NMR spectrum of **2.42** (500 MHz, 298 K, CDCl<sub>3</sub>).

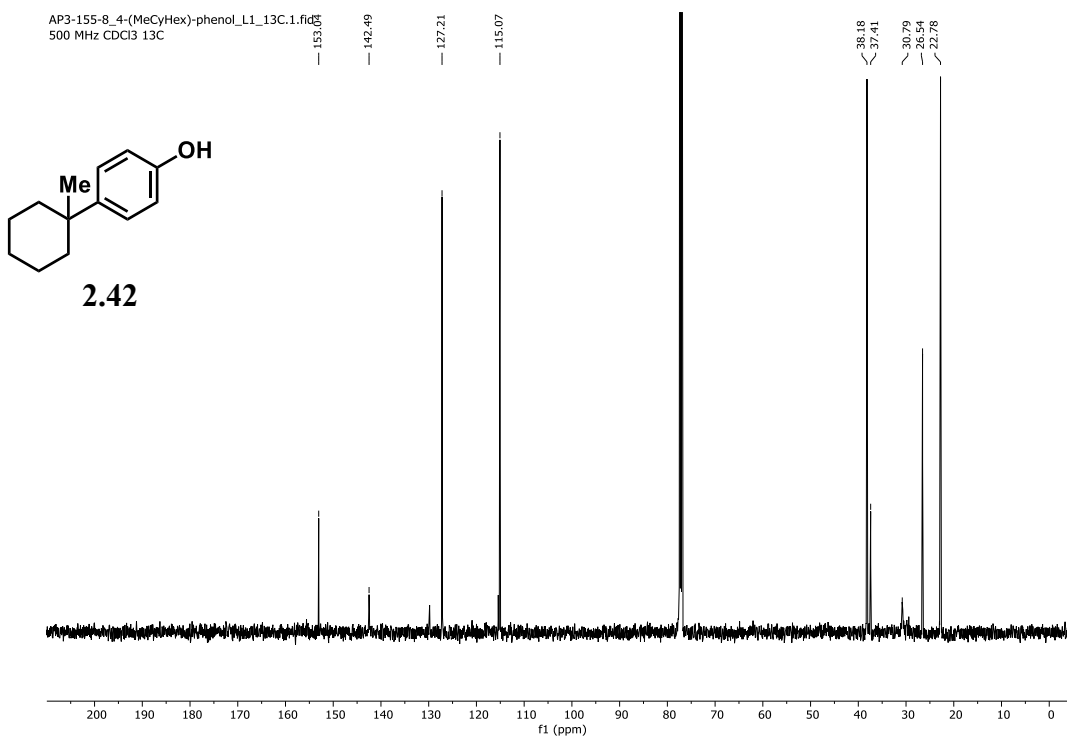


Figure 4.113. <sup>13</sup>C NMR spectrum of **2.42** (126 MHz, 298 K, CDCl<sub>3</sub>).



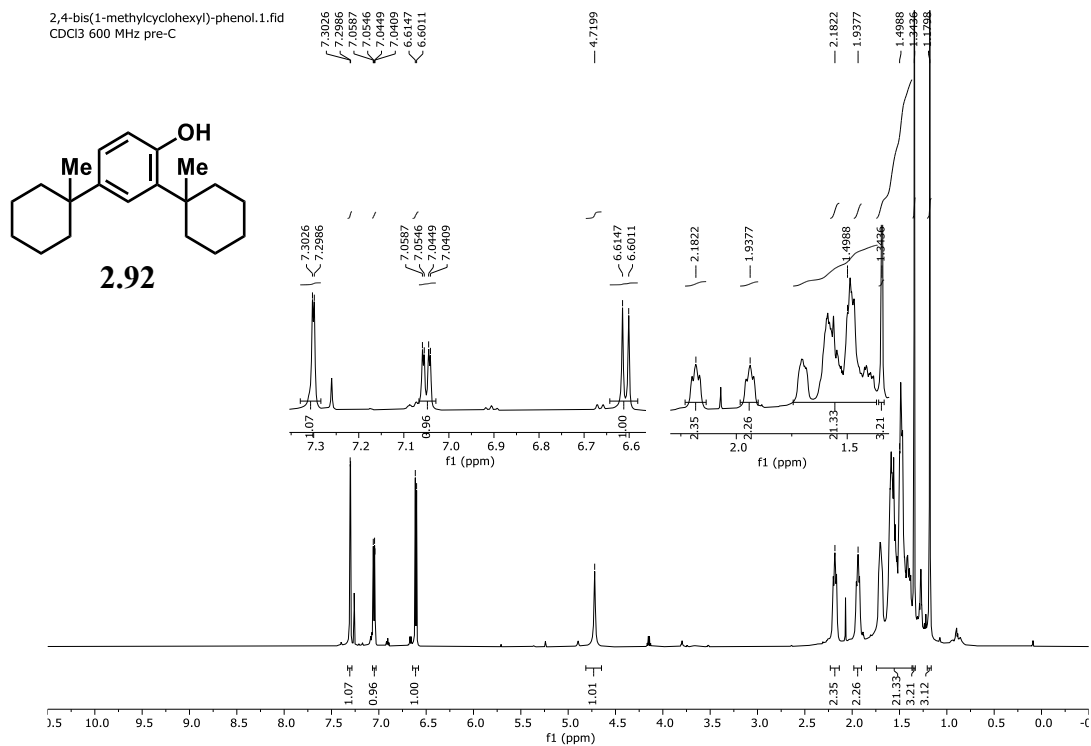


Figure 4.114. <sup>1</sup>H NMR spectrum of **2.92** (600 MHz, 298 K, CDCl<sub>3</sub>).

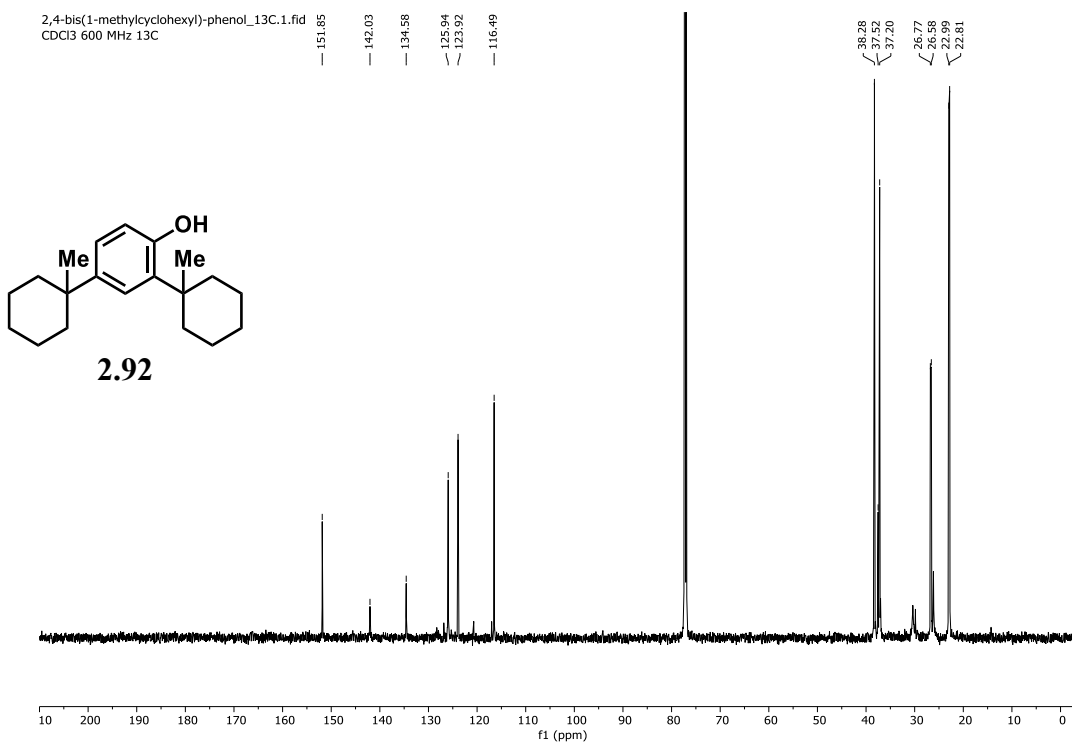


Figure 4.115. <sup>13</sup>C NMR spectrum of **2.92** (151 MHz, 298 K, CDCl<sub>3</sub>).

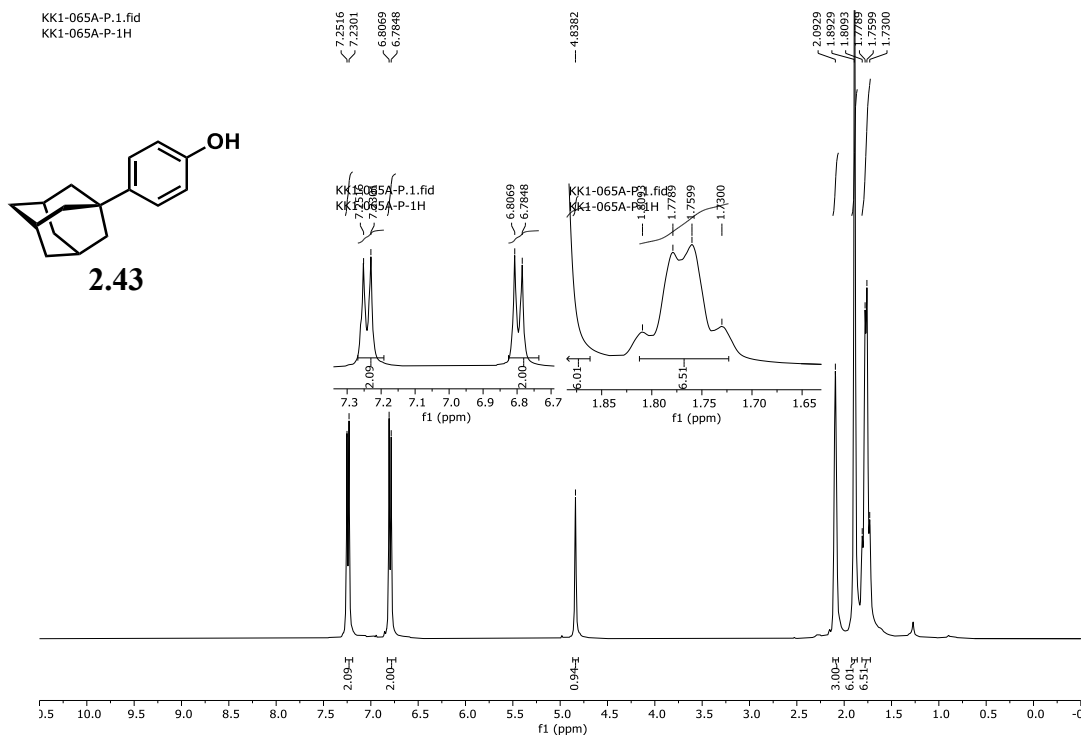


Figure 4.116.  $^1\text{H}$  NMR spectrum of **2.43** (400 MHz, 295 K,  $\text{CDCl}_3$ ).

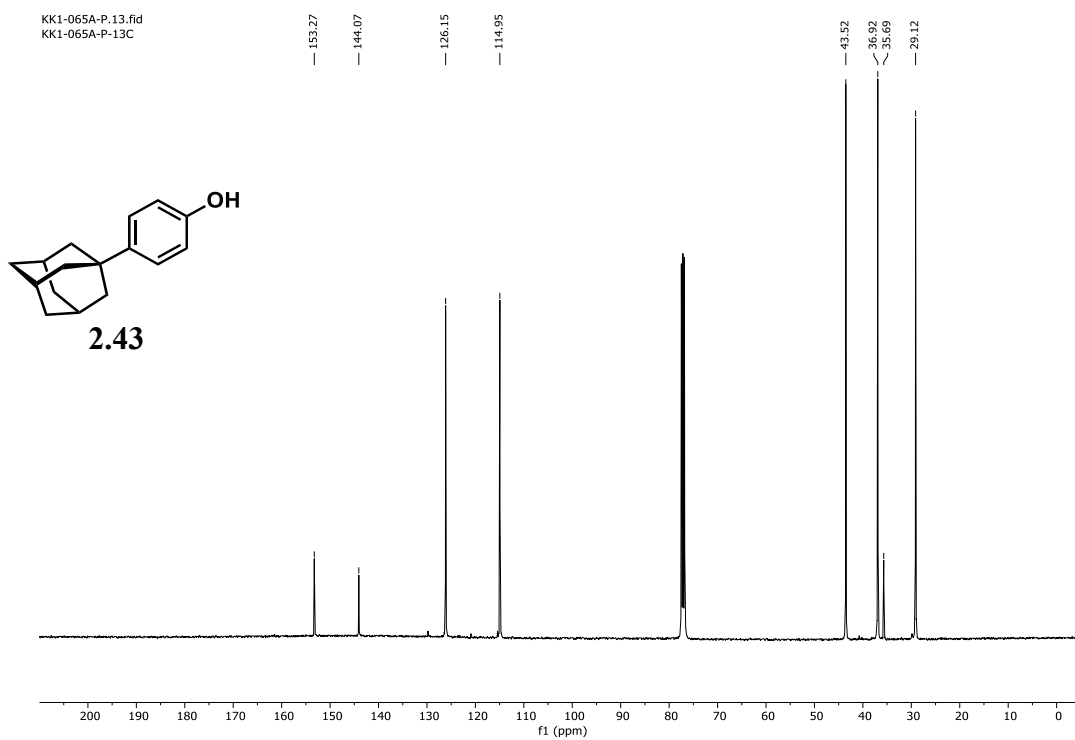


Figure 4.117.  $^{13}\text{C}$  NMR spectrum of **2.43** (101 MHz, 295 K,  $\text{CDCl}_3$ ).

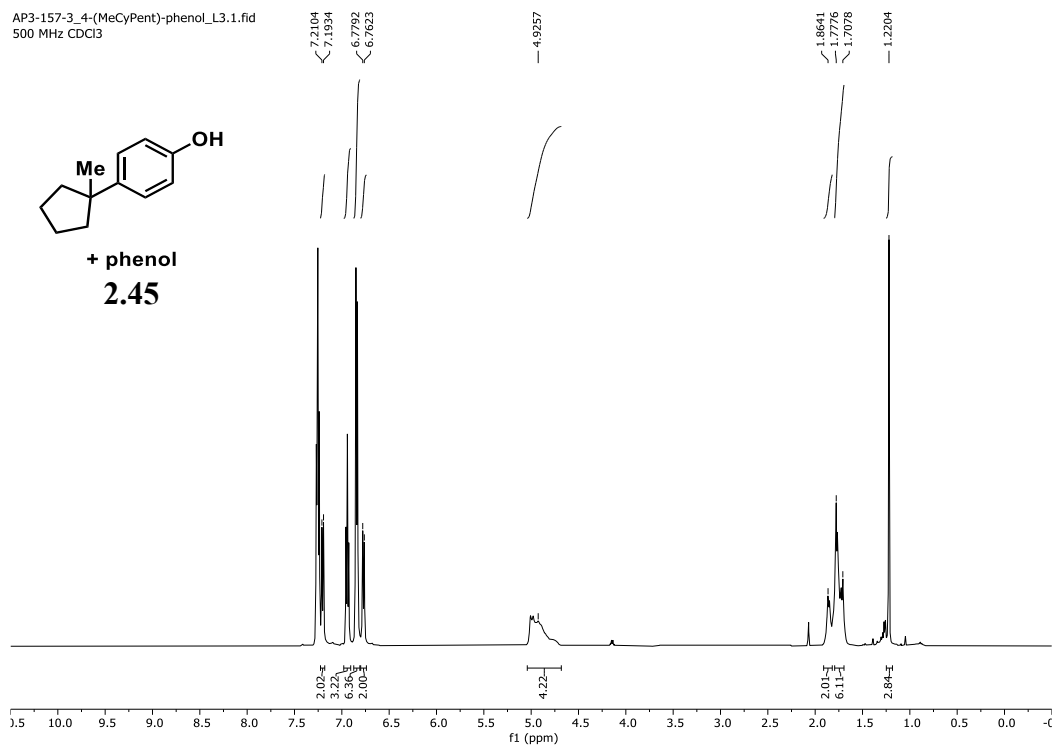


Figure 4.118. <sup>1</sup>H NMR spectrum of **2.45** (500 MHz, 298 K, CDCl<sub>3</sub>).

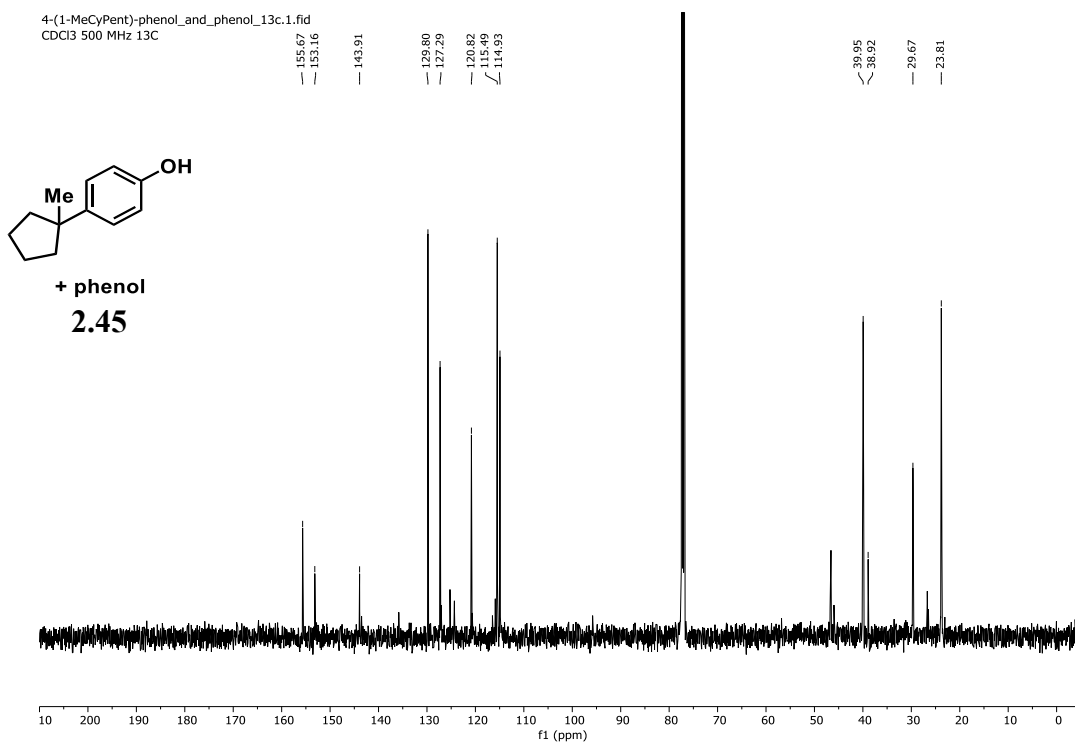


Figure 4.119. <sup>13</sup>C NMR spectrum of **2.45** (126 MHz, 298 K, CDCl<sub>3</sub>).

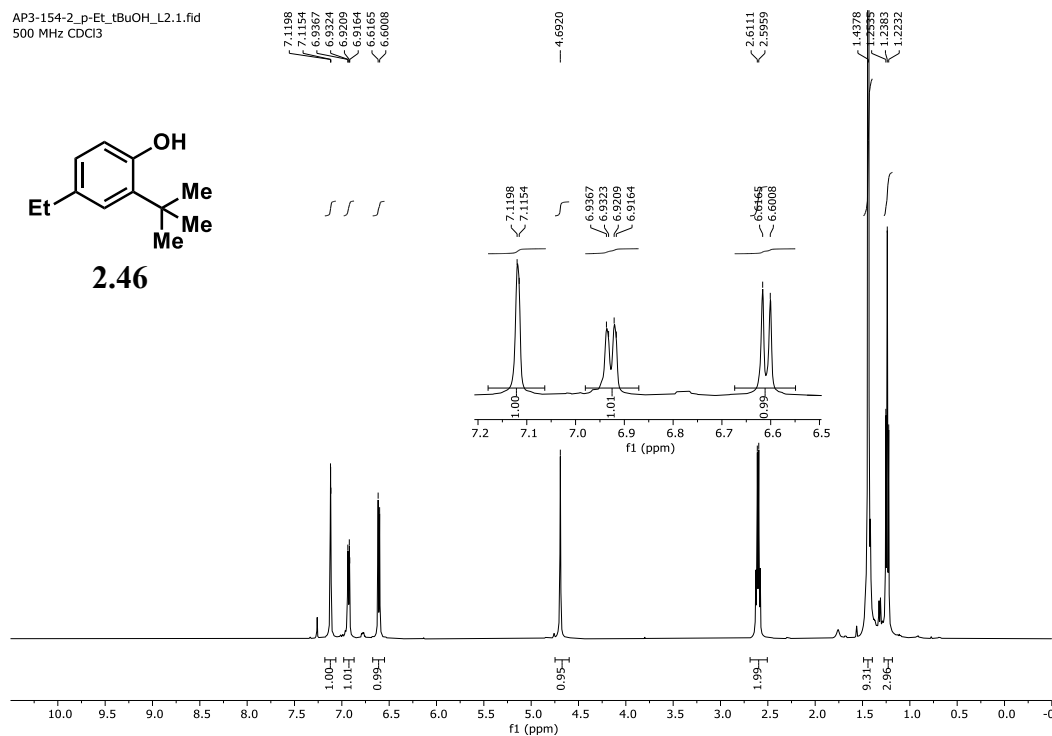


Figure 4.120. <sup>1</sup>H NMR spectrum of **2.46** (500 MHz, 298 K, CDCl<sub>3</sub>).

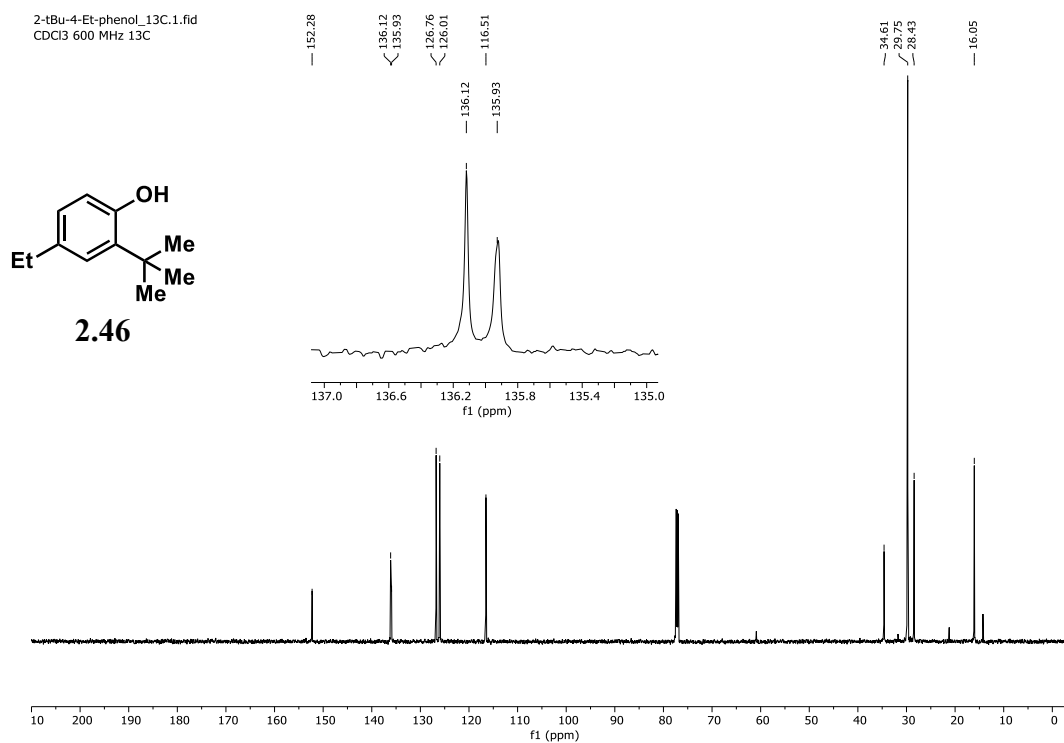


Figure 4.121. <sup>13</sup>C NMR spectrum of **2.46** (151 MHz, 298 K, CDCl<sub>3</sub>).

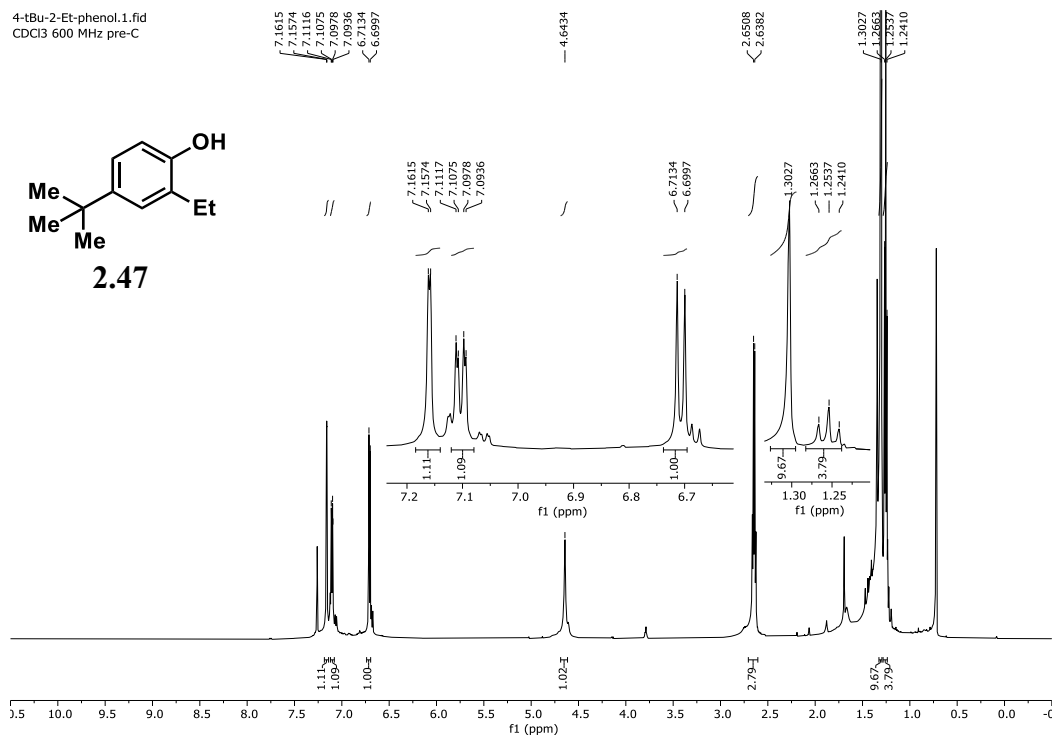


Figure 4.122. <sup>1</sup>H NMR spectrum of 2.47 (600 MHz, 298 K, CDCl<sub>3</sub>).

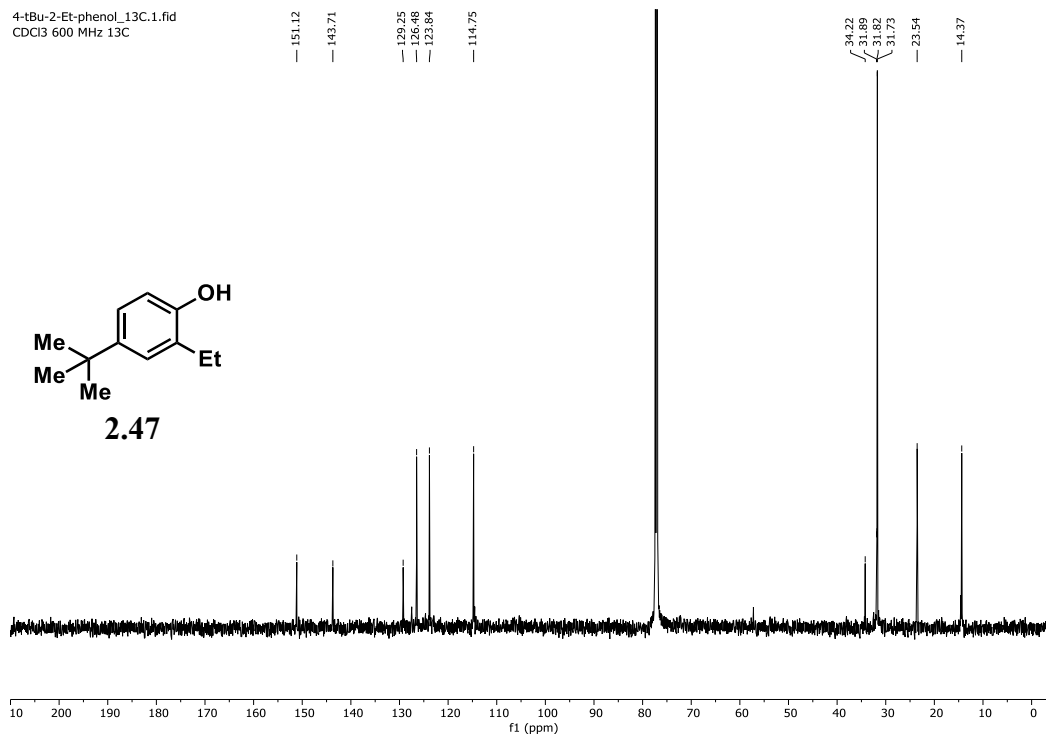
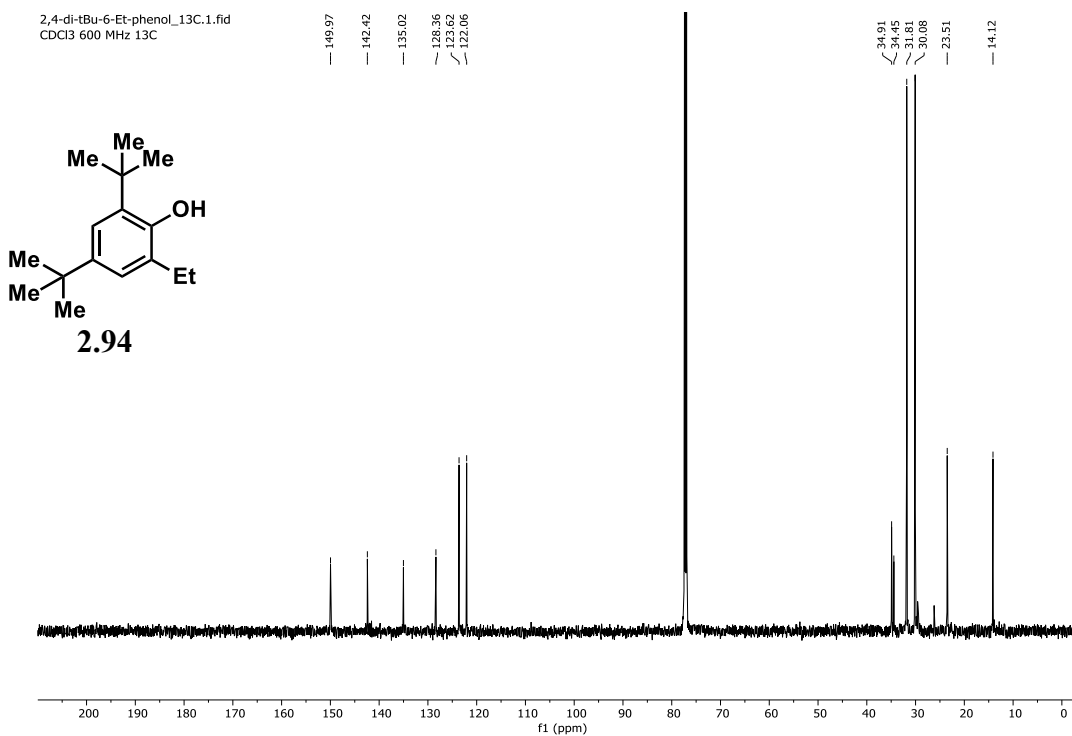
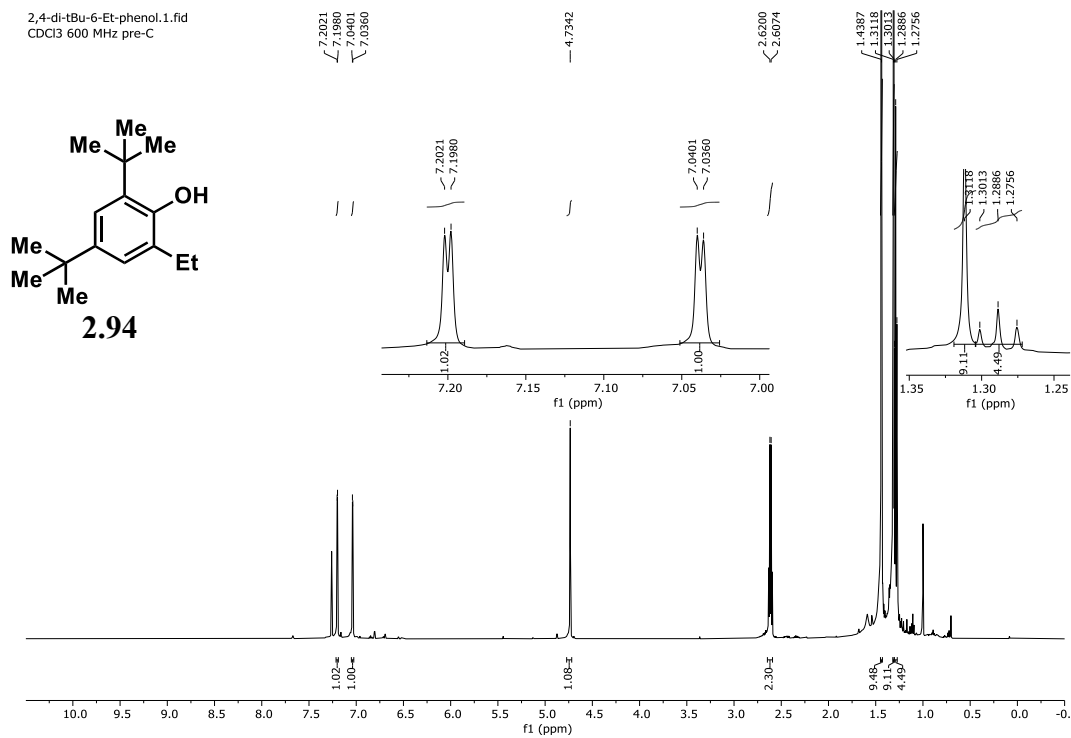


Figure 4.123. <sup>13</sup>C NMR spectrum of 2.47 (151 MHz, 298 K, CDCl<sub>3</sub>).





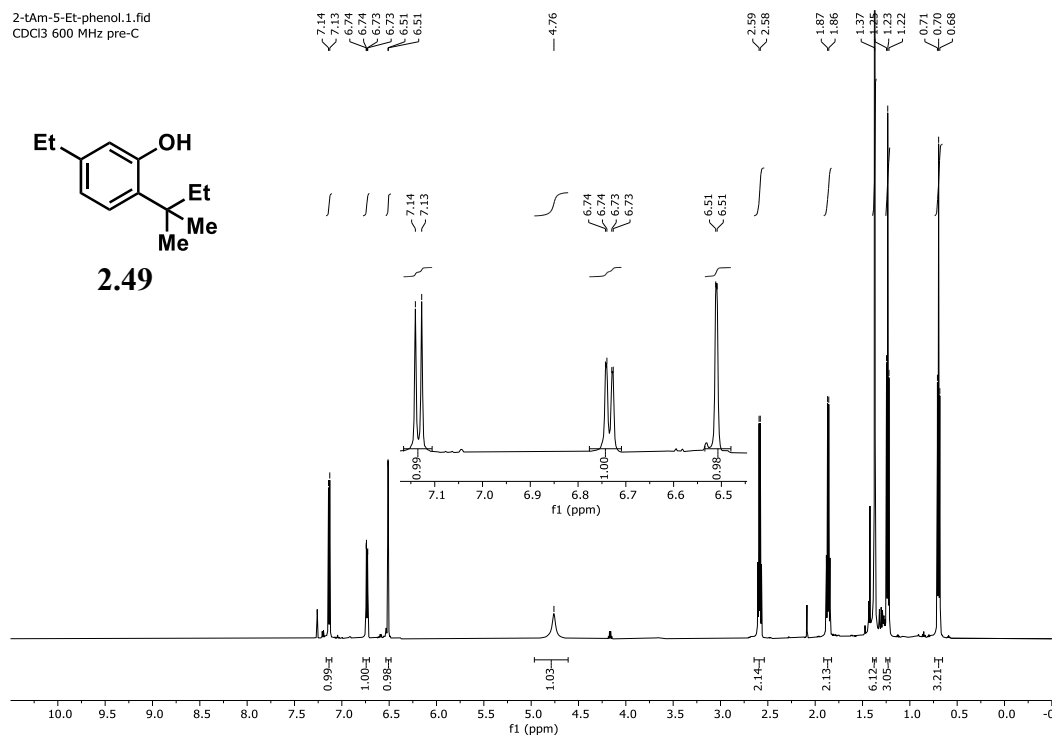


Figure 4.128. <sup>1</sup>H NMR spectrum of **2.49** (600 MHz, 298 K, CDCl<sub>3</sub>).

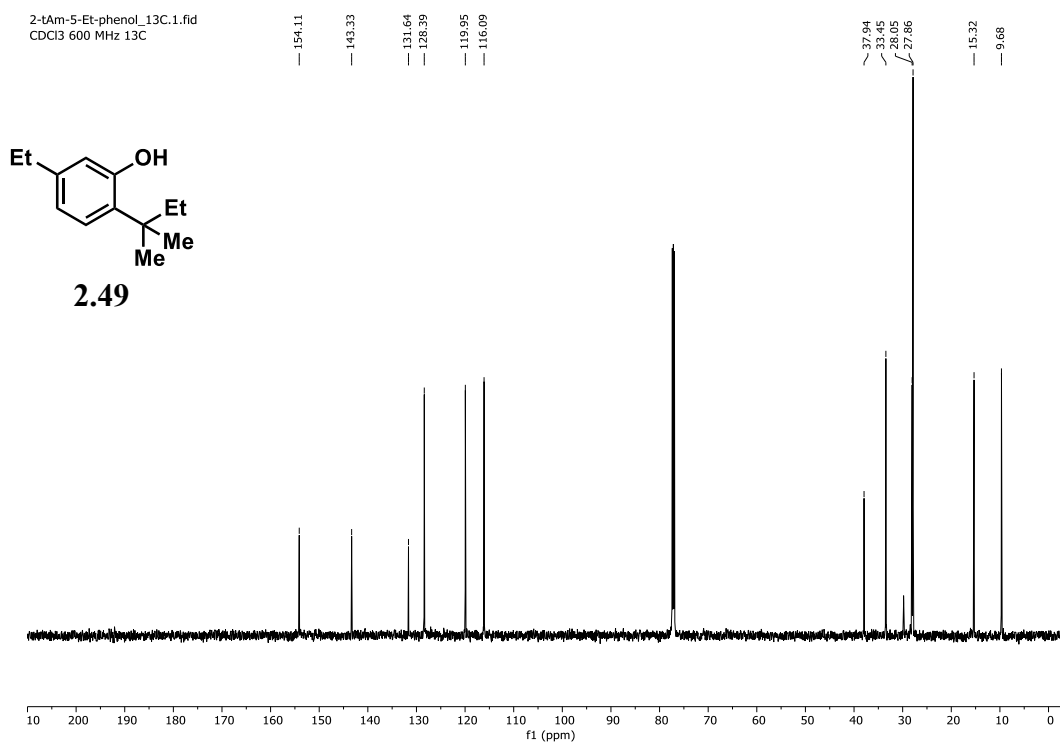


Figure 4.129. <sup>13</sup>C NMR spectrum of **2.49** (151 MHz, 298 K, CDCl<sub>3</sub>).



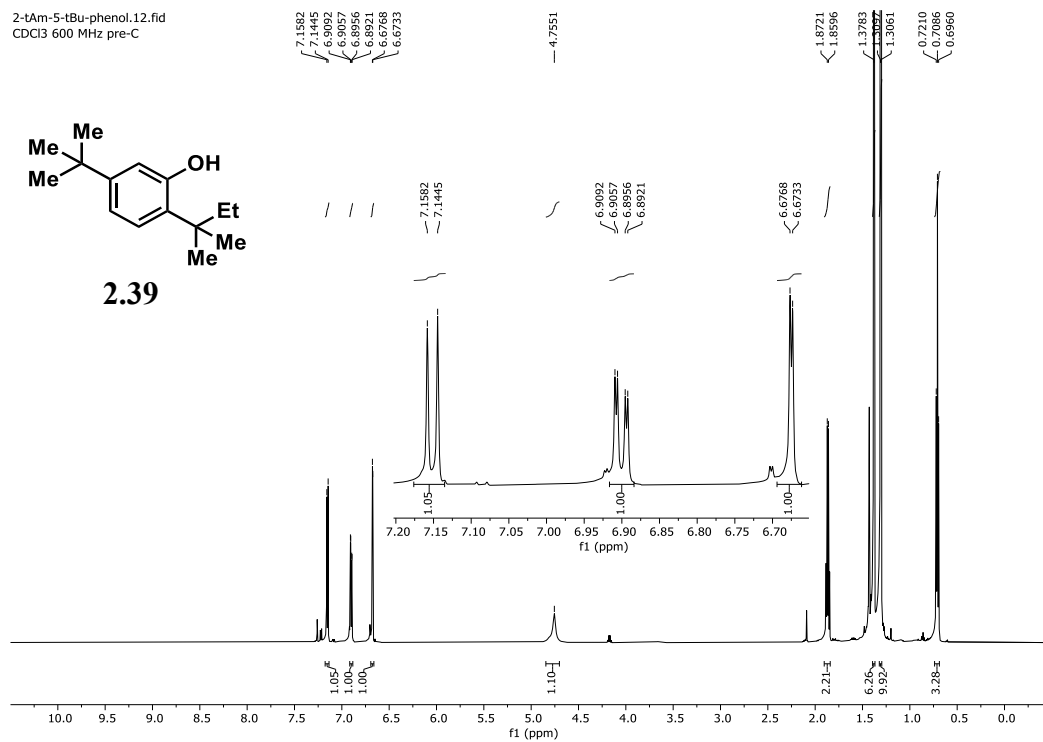


Figure 4.130. <sup>1</sup>H NMR spectrum of **2.39** (600 MHz, 298 K, CDCl<sub>3</sub>).

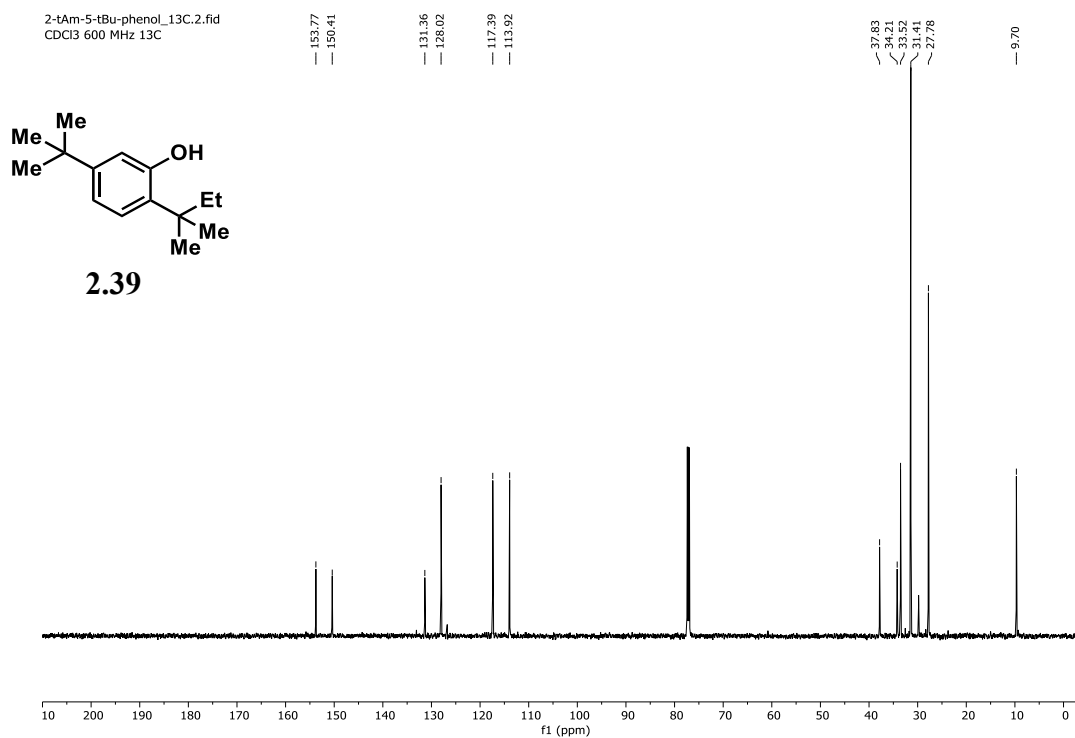


Figure 4.131. <sup>13</sup>C NMR spectrum of **2.39** (151 MHz, 298 K, CDCl<sub>3</sub>).

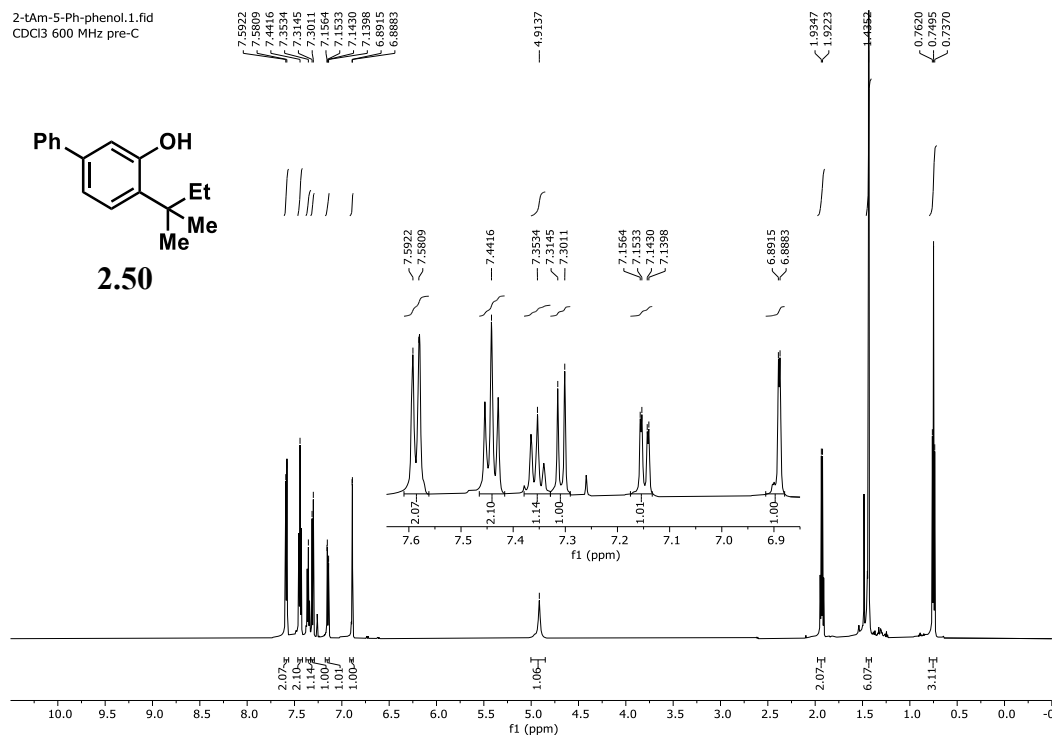


Figure 4.132. <sup>1</sup>H NMR spectrum of **2.50** (600 MHz, 298 K, CDCl<sub>3</sub>).

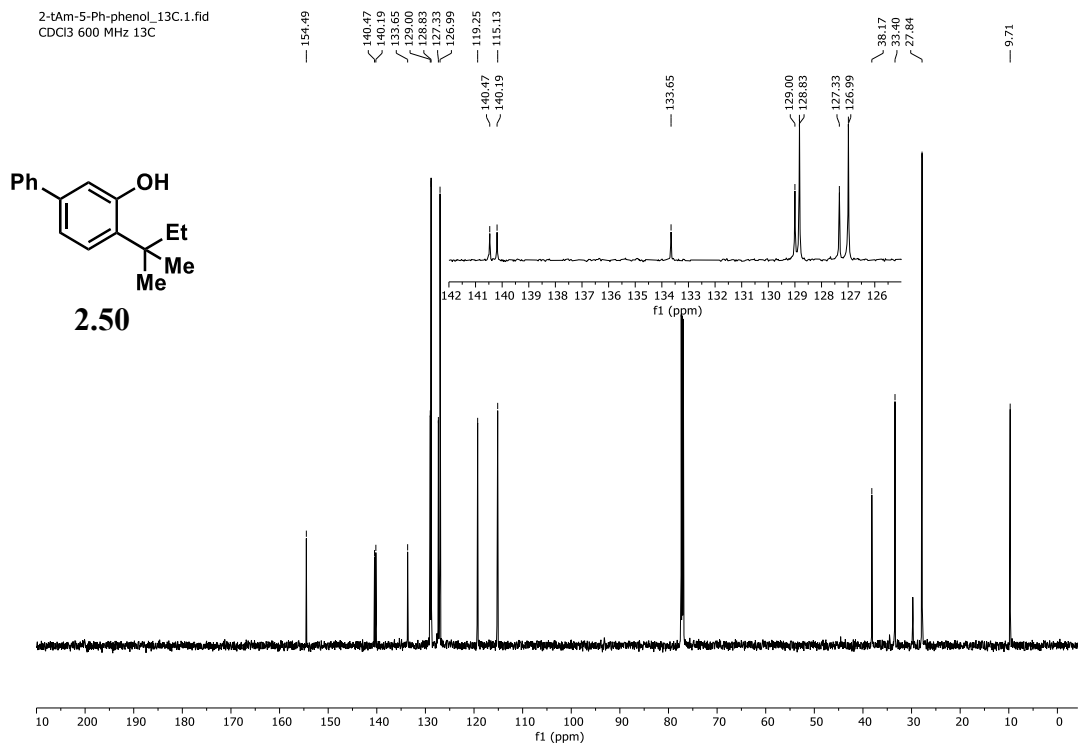


Figure 4.133. <sup>13</sup>C NMR spectrum of **2.50** (151 MHz, 298 K, CDCl<sub>3</sub>).

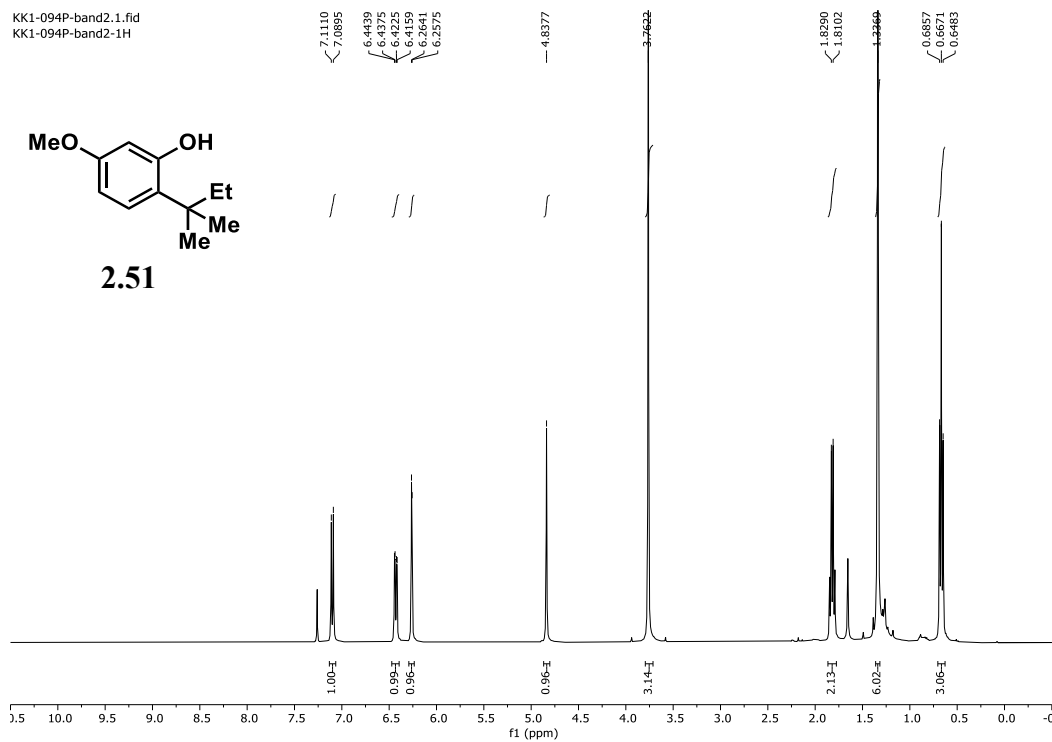


Figure 4.134.  $^1\text{H}$  NMR spectrum of **2.51** (400 MHz, 295 K,  $\text{CDCl}_3$ ).

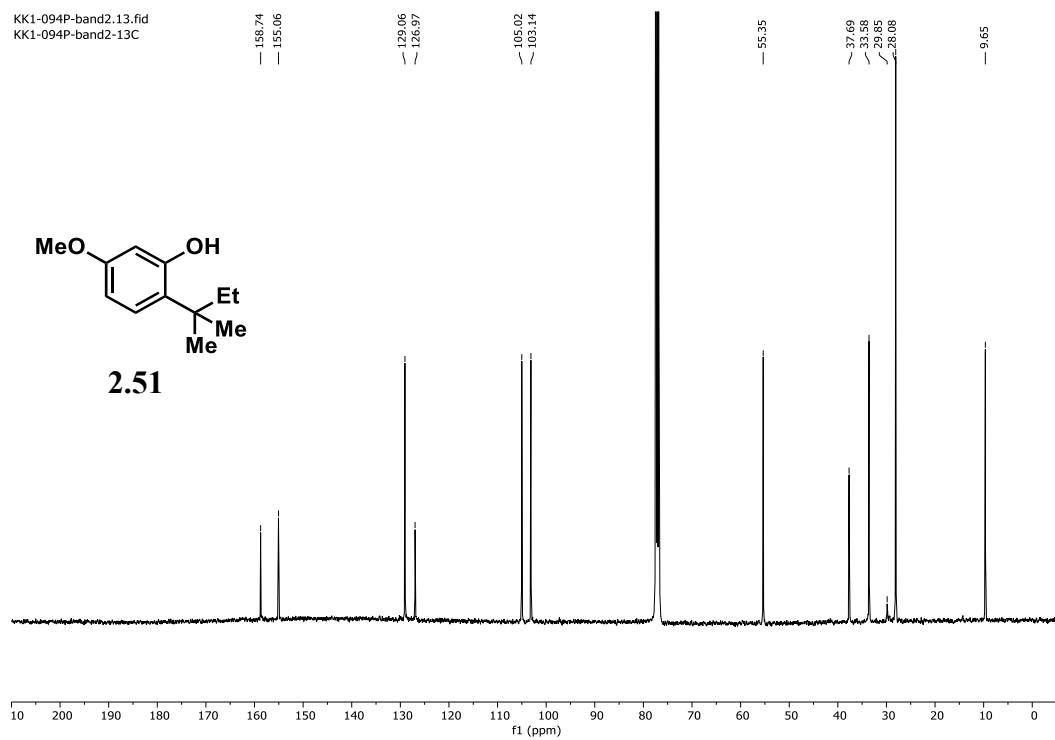
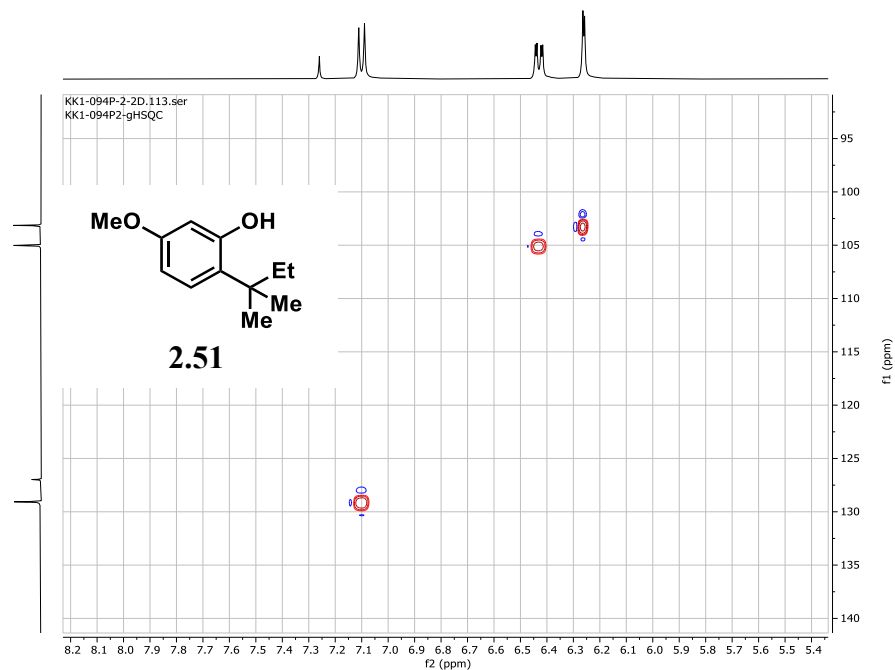
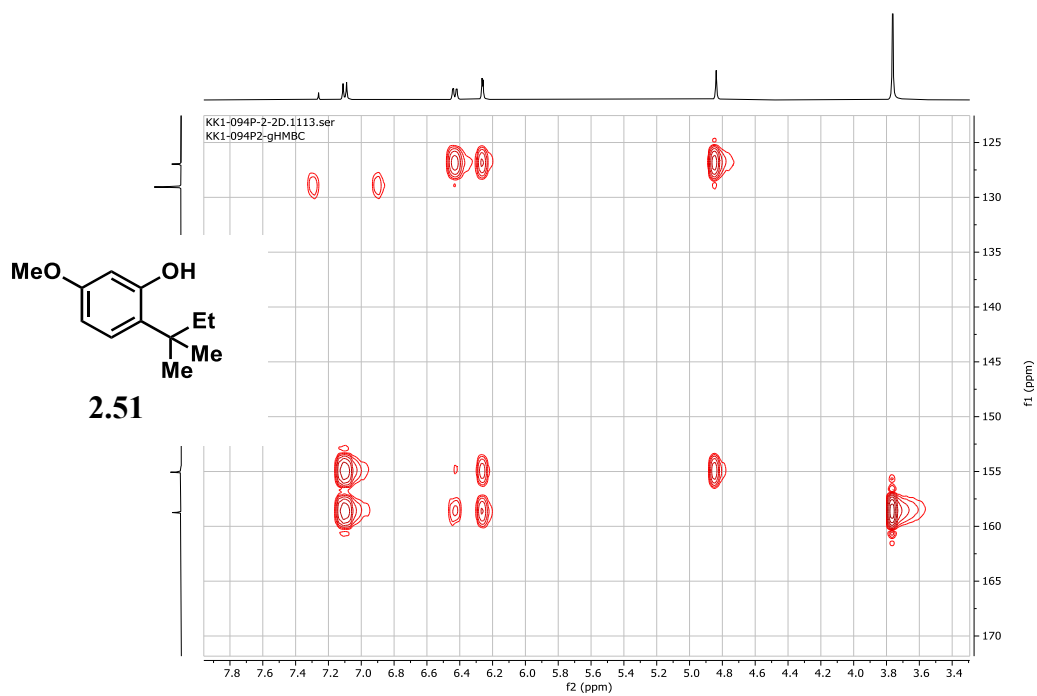


Figure 4.135.  $^{13}\text{C}$  NMR spectrum of **2.51** (101 MHz, 295 K,  $\text{CDCl}_3$ ).



**Figure 4.136.** HSQC NMR spectrum of **2.51** ( $^1\text{H}$  NMR 400 MHz,  $^{13}\text{C}$  NMR 101 MHz, 295 K,  $\text{CDCl}_3$ ).



**Figure 4.137.** HMBC NMR spectrum of **2.51** ( $^1\text{H}$  NMR 400 MHz,  $^{13}\text{C}$  NMR 101 MHz, 295 K,  $\text{CDCl}_3$ ).

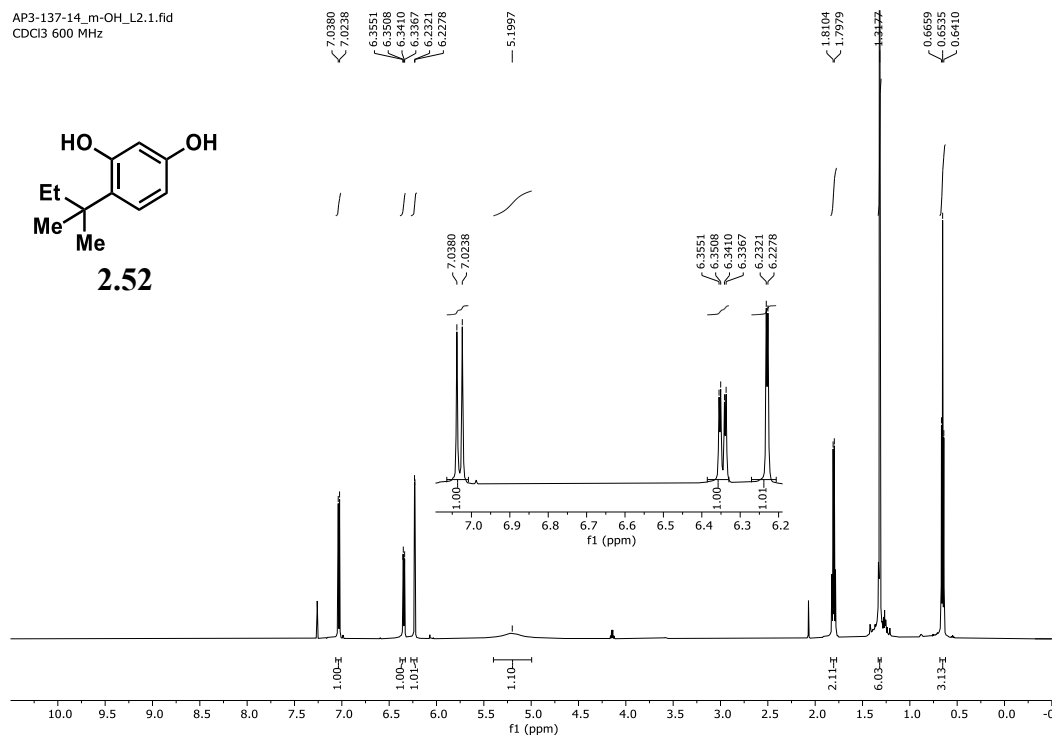


Figure 4.138. <sup>1</sup>H NMR spectrum of **2.52** (600 MHz, 298 K, CDCl<sub>3</sub>).

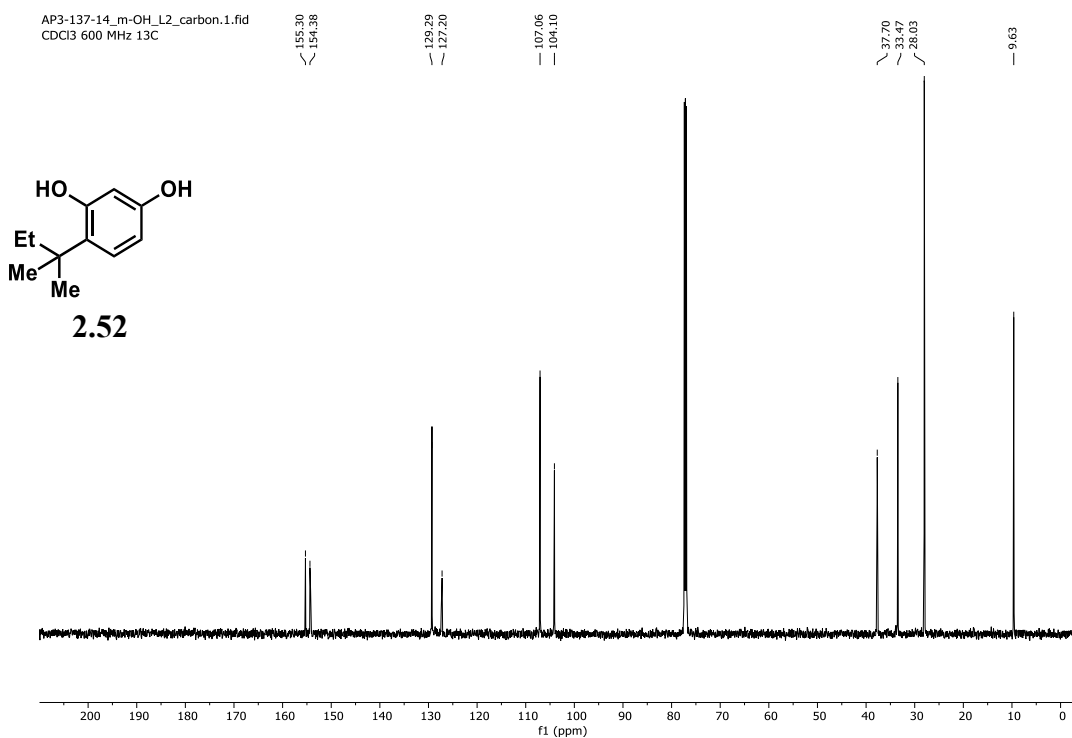
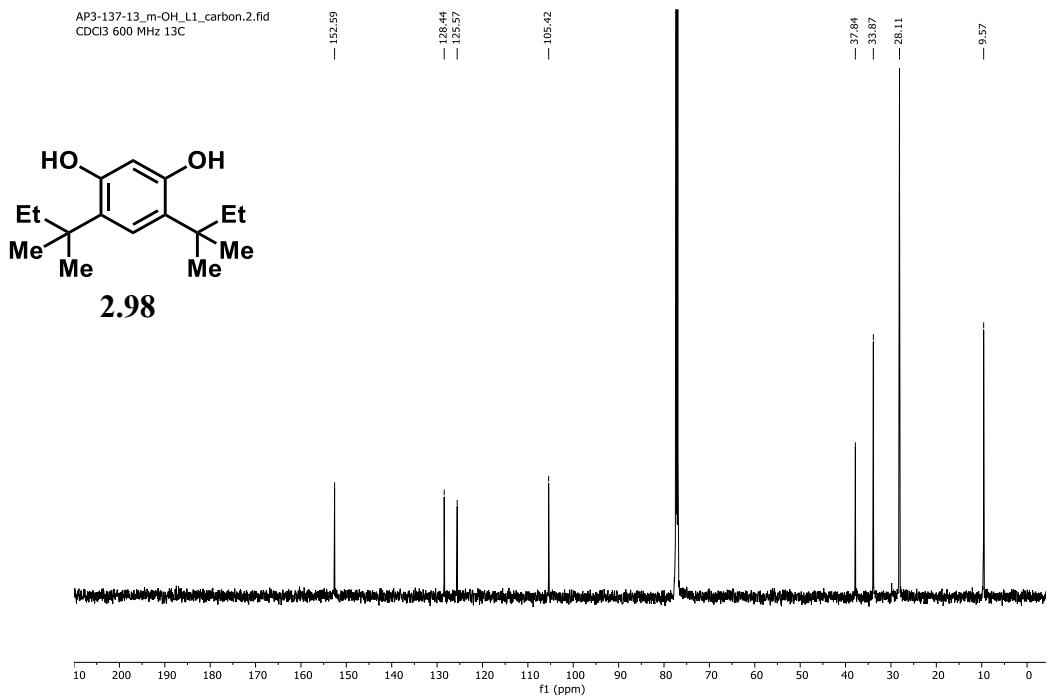
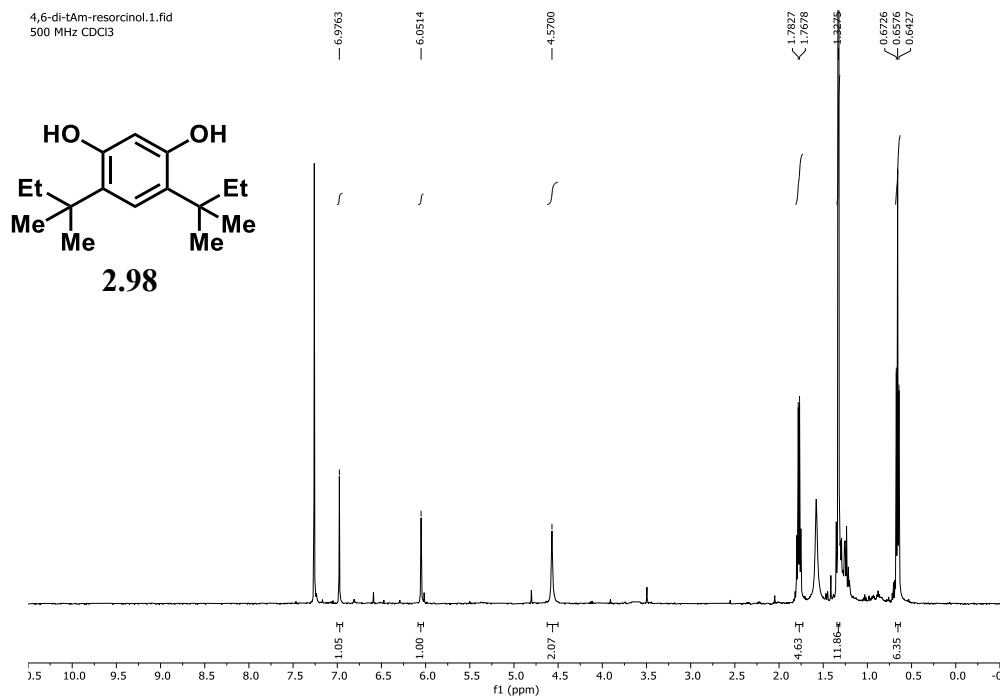


Figure 4.139. <sup>13</sup>C NMR spectrum of **2.52** (151 MHz, 298 K, CDCl<sub>3</sub>).



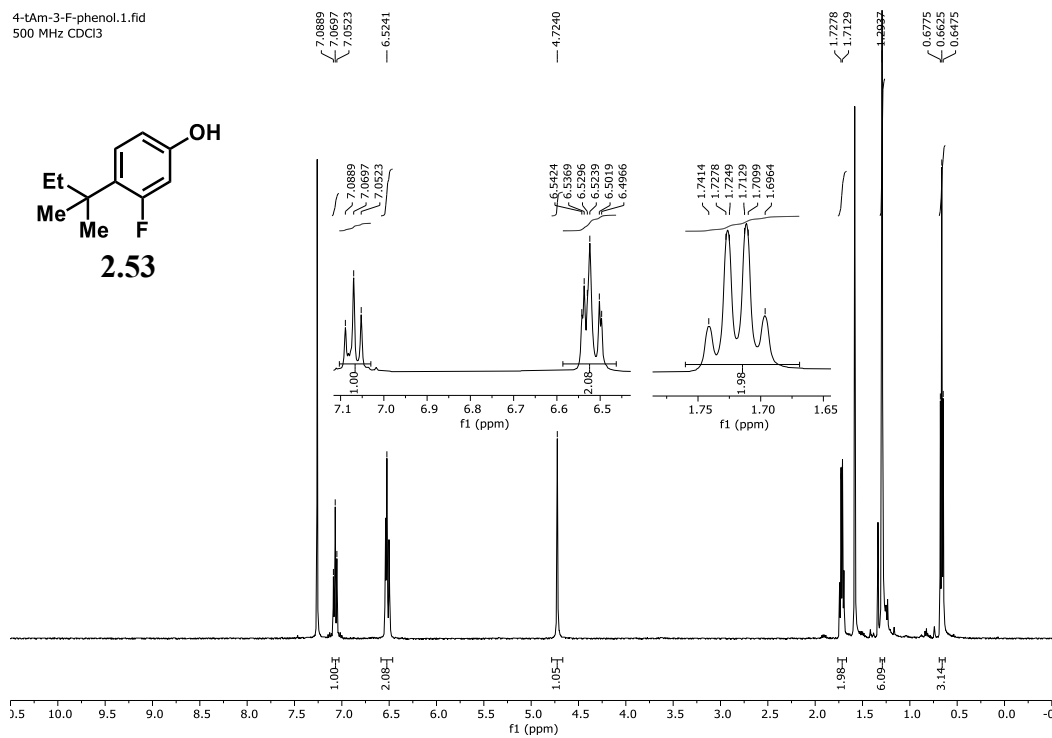


Figure 4.142. <sup>1</sup>H NMR spectrum of **2.53** (500 MHz, 298 K, CDCl<sub>3</sub>).

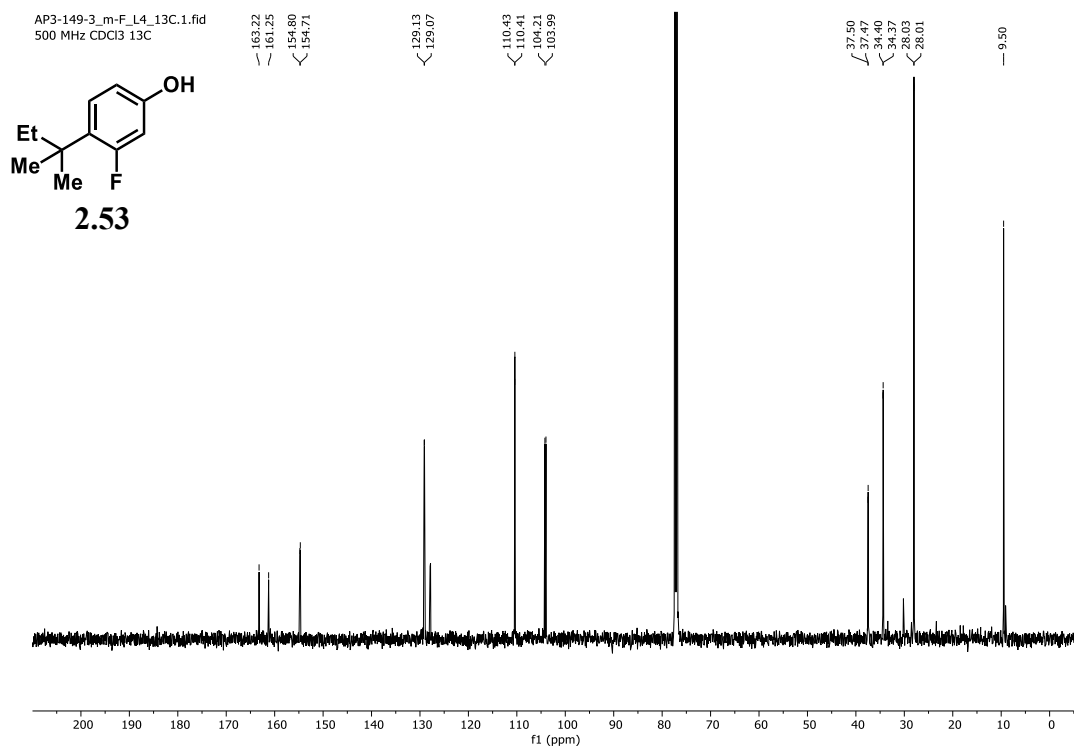


Figure 4.143. <sup>13</sup>C NMR spectrum of **2.53** (126 MHz, 298 K, CDCl<sub>3</sub>).

4-tAm-3-F-phenol\_19F.2.fid  
CDCl<sub>3</sub> 600MHz 19F

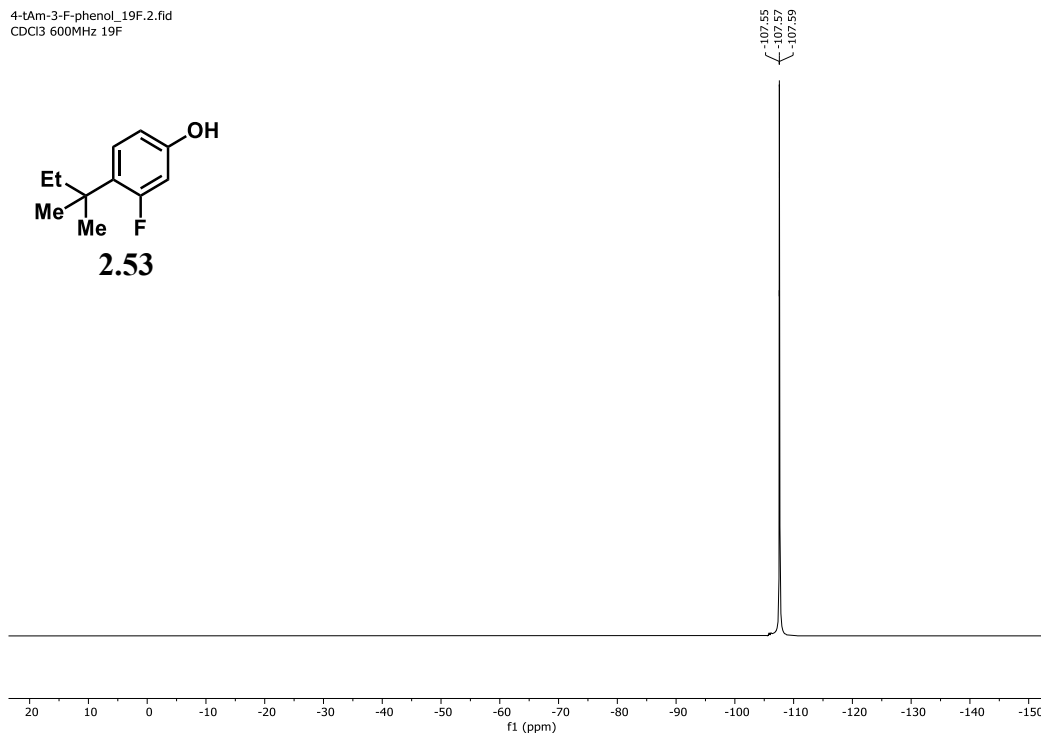


Figure 4.144. <sup>19</sup>F NMR spectrum of **2.53** (564 MHz, 298 K, CDCl<sub>3</sub>).

2,4-di-tAm-5-F-phenol.1.fid  
500 MHz CDCl<sub>3</sub>

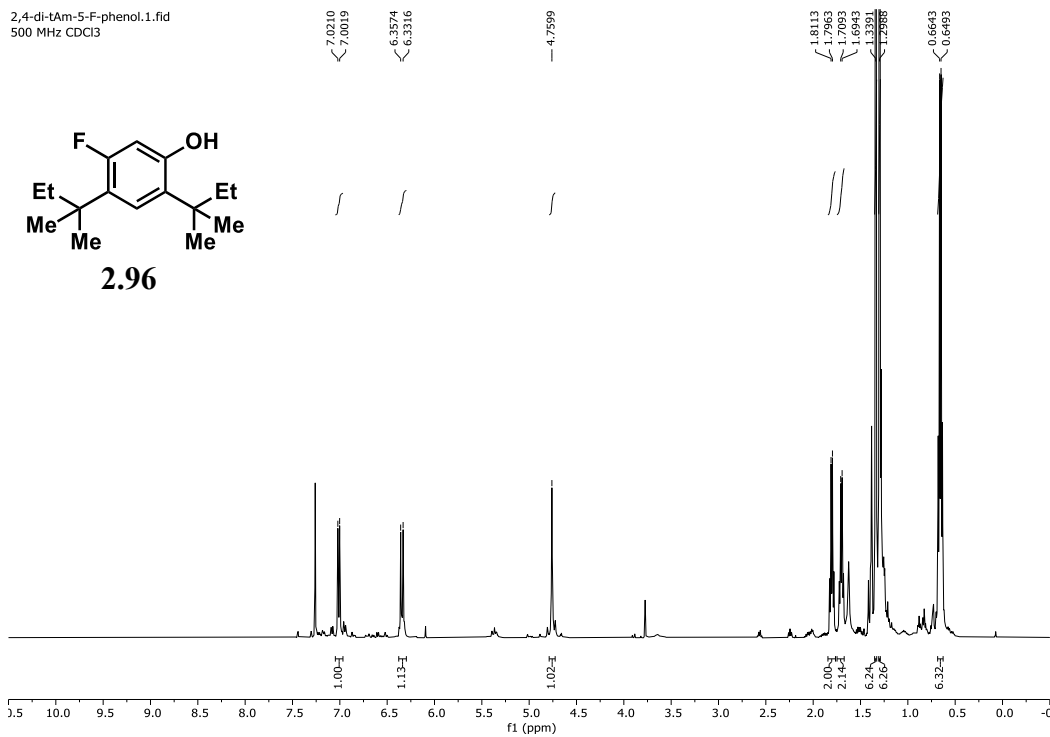


Figure 4.145. <sup>1</sup>H NMR spectrum of **2.96** (500 MHz, 298 K, CDCl<sub>3</sub>).



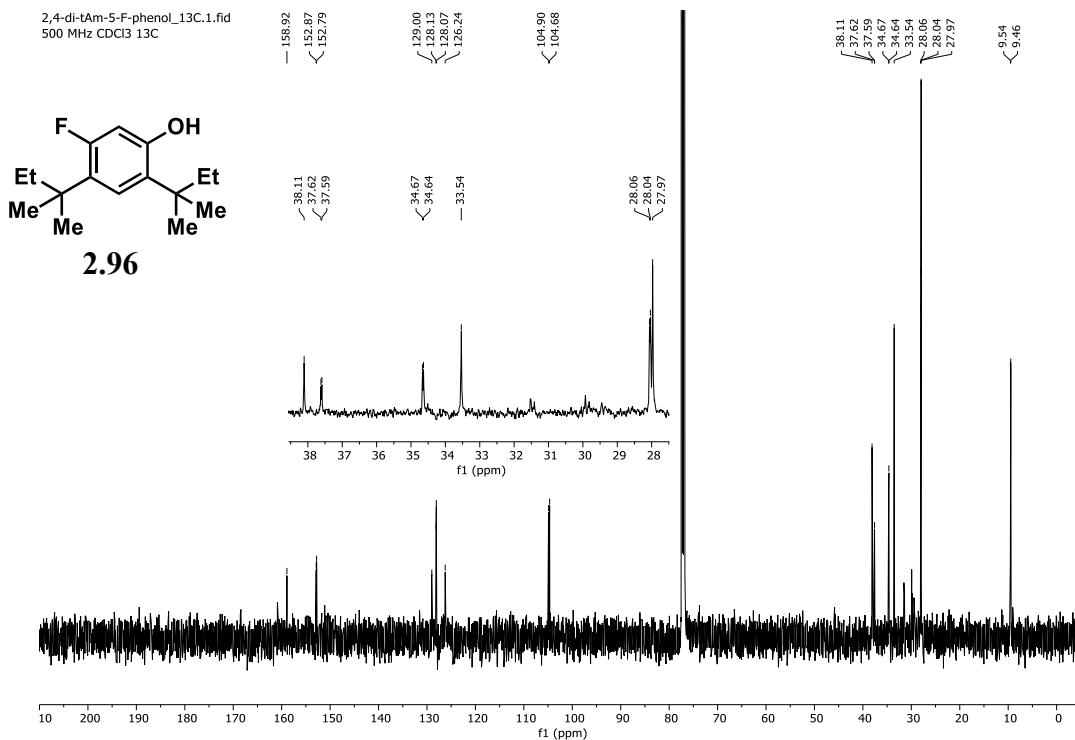


Figure 4.146. <sup>13</sup>C NMR spectrum of **2.96** (126 MHz, 298 K, CDCl<sub>3</sub>).

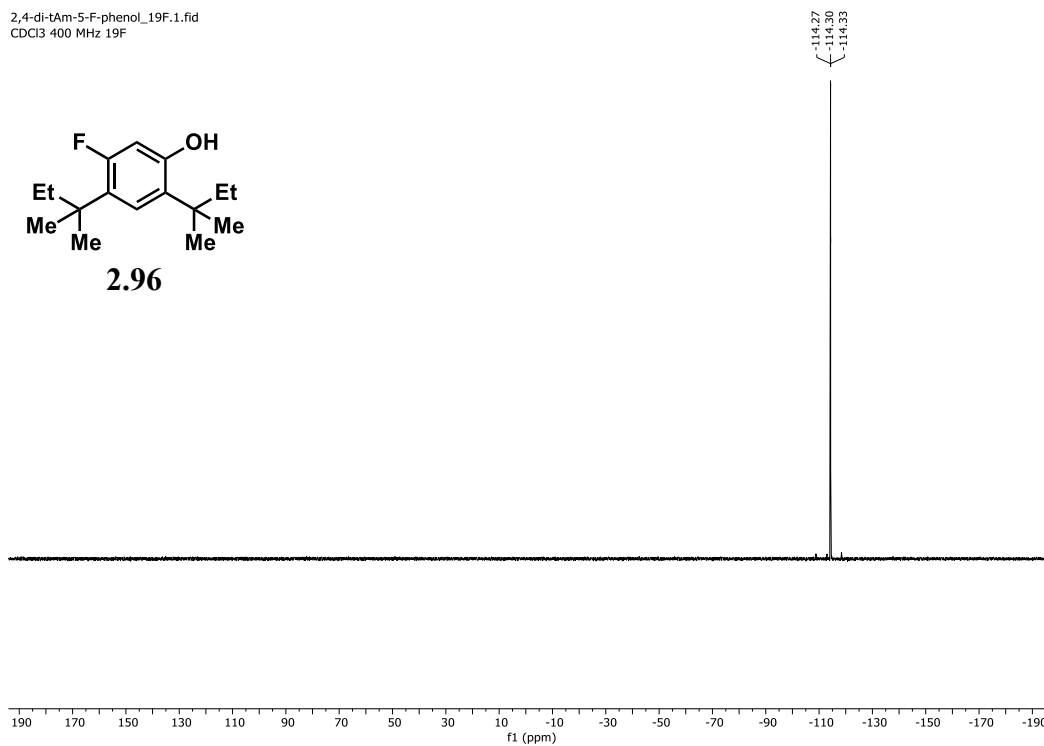


Figure 4.147. <sup>19</sup>F NMR spectrum of **2.96** (376 MHz, 295 K, CDCl<sub>3</sub>).

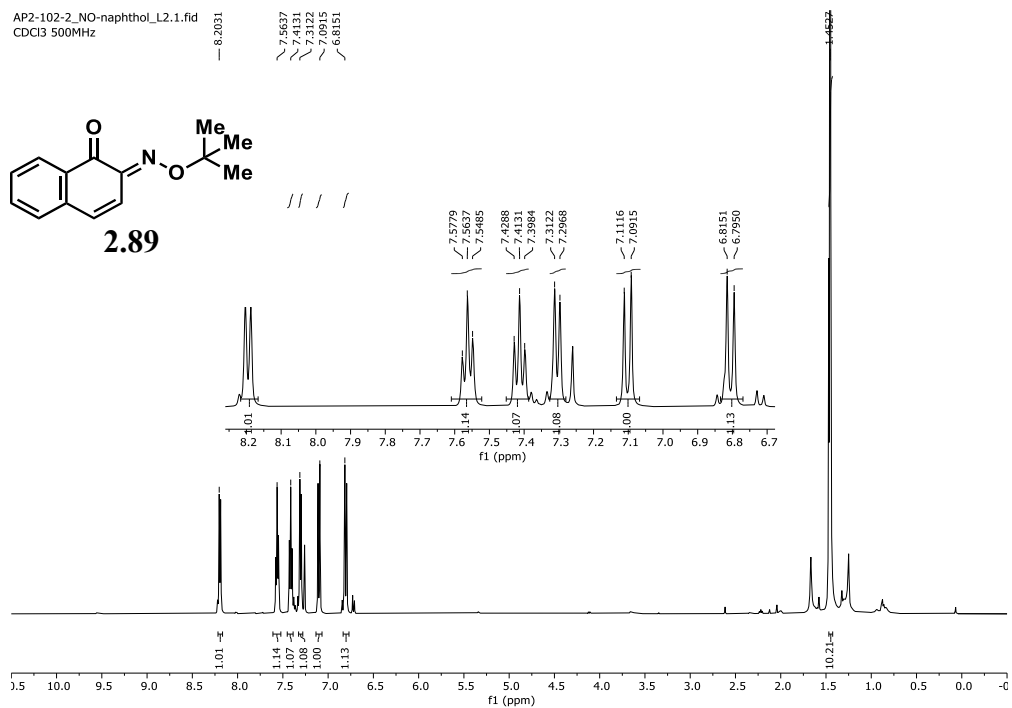


Figure 4.148. <sup>1</sup>H NMR spectrum of **2.89** (500 MHz, 298 K, CDCl<sub>3</sub>).

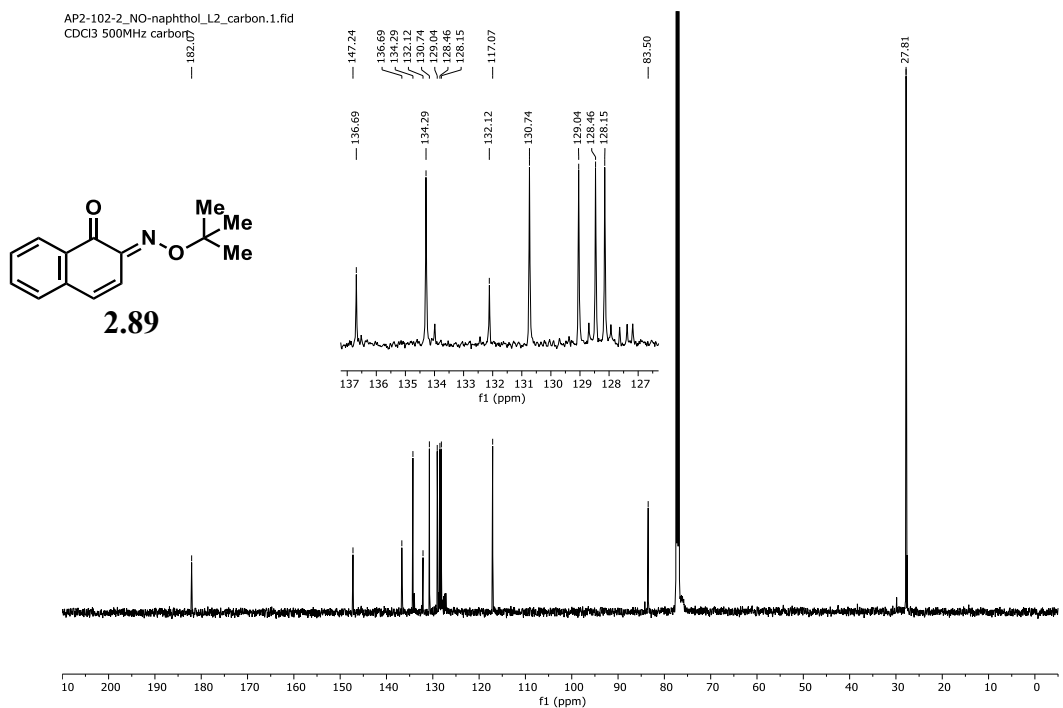


Figure 4.149. <sup>13</sup>C NMR spectrum of **2.89** (126 MHz, 298 K, CDCl<sub>3</sub>).

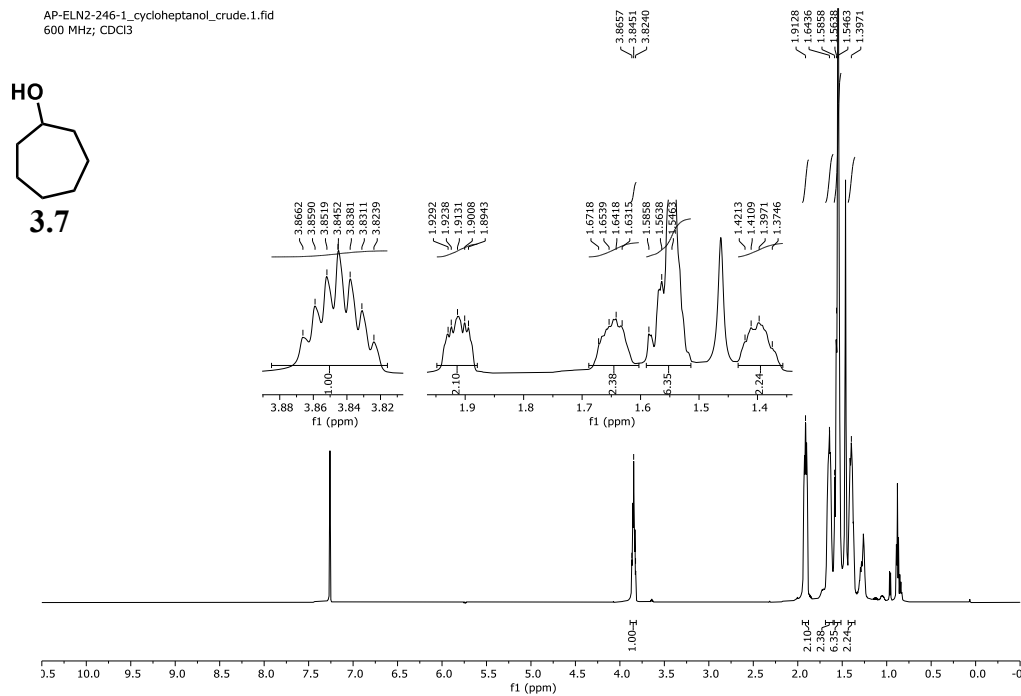


Figure 4.150. <sup>1</sup>H NMR spectrum of **3.7** (600 MHz, 298 K, CDCl<sub>3</sub>).

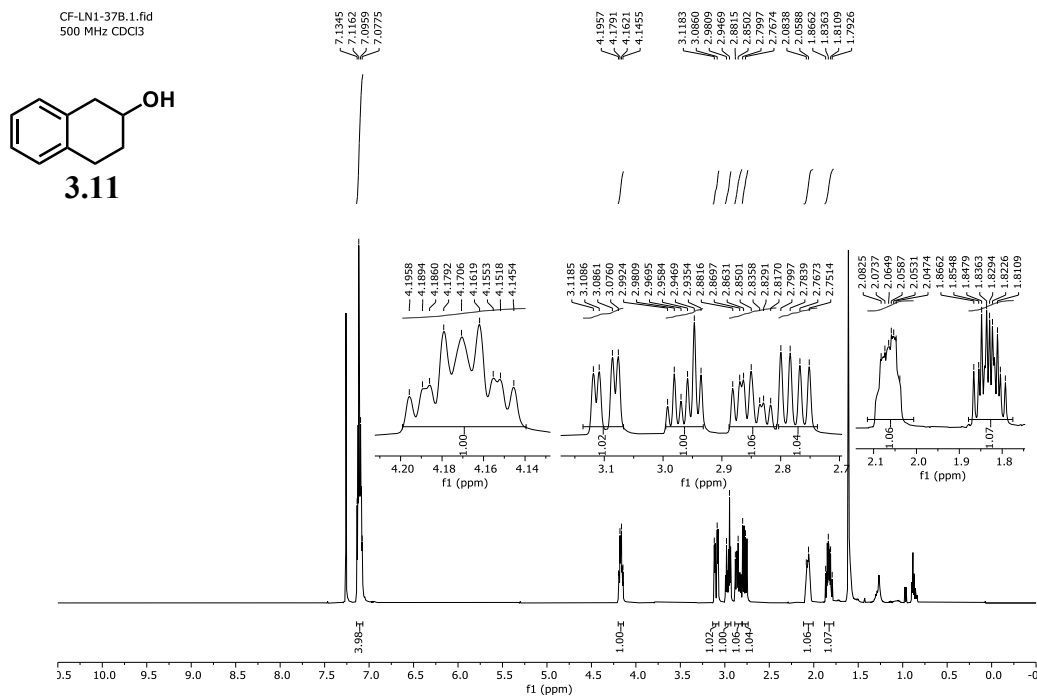


Figure 4.151. <sup>1</sup>H NMR spectrum of **3.11** (500 MHz, 298 K, CDCl<sub>3</sub>).

AP-ELN2-185-1\_1\_(1-Ad)-EtOH\_crude.1.fid  
500 MHz; CDCl<sub>3</sub>

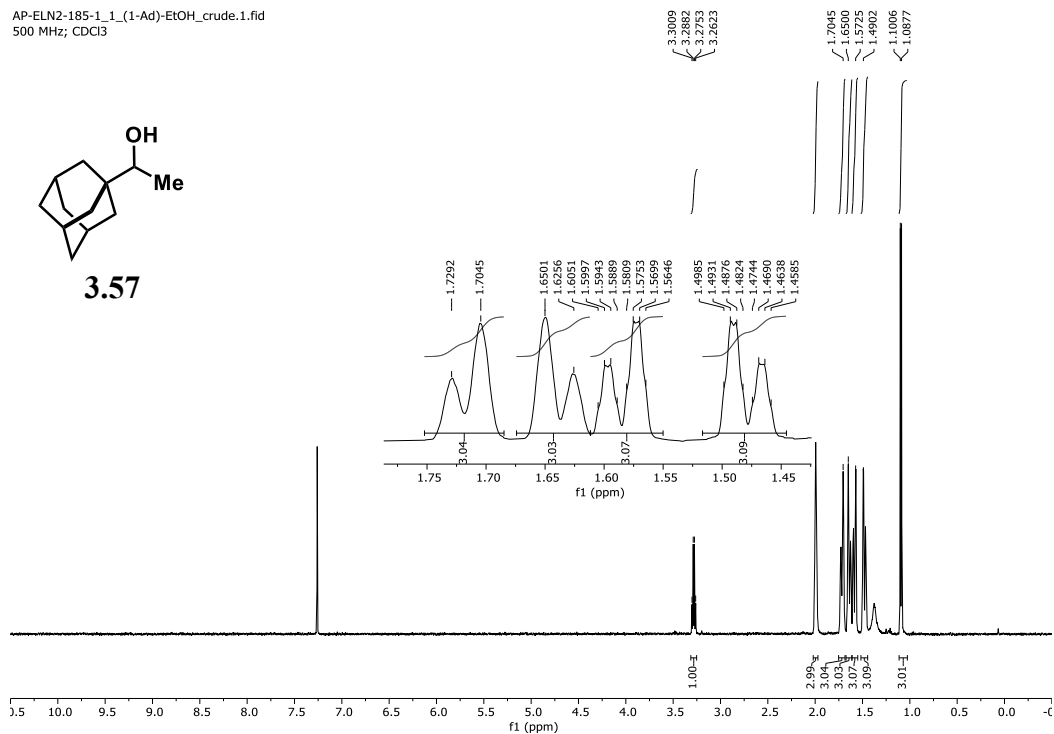


Figure 4.152. <sup>1</sup>H NMR spectrum of **2.57** (500 MHz, 298 K, CDCl<sub>3</sub>).

AP-ELN2-267-1\_TarB-NO2\_crude\_THF-d8.1.fid  
400 MHz d8-THF

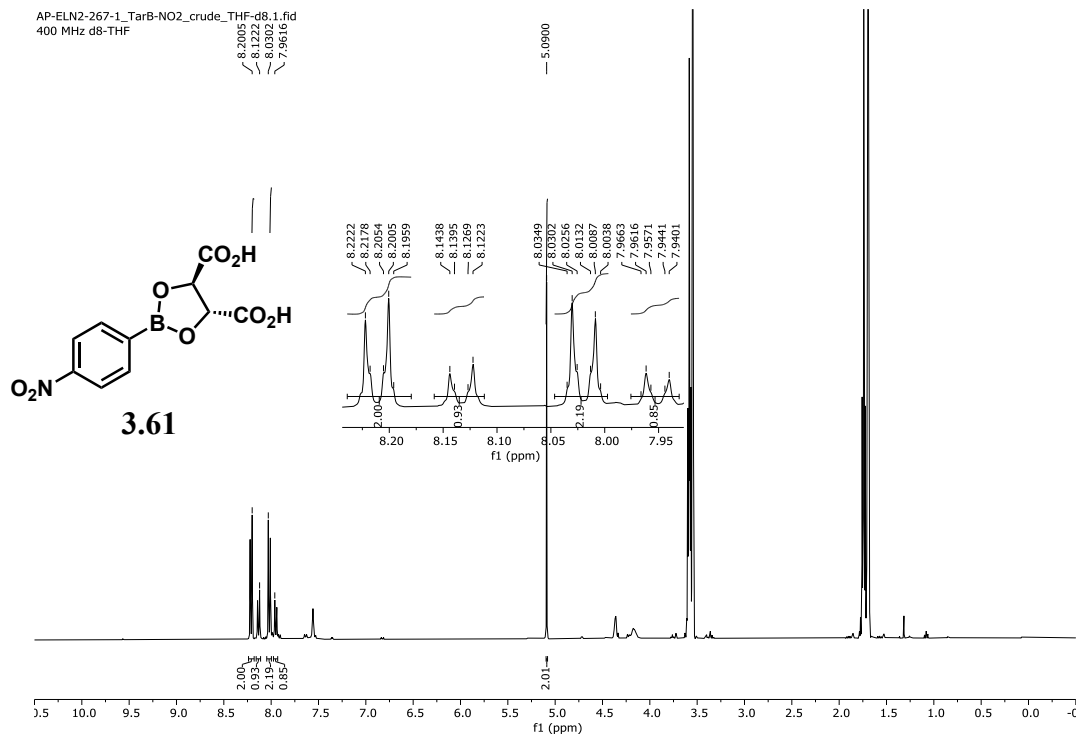


Figure 4.153. <sup>1</sup>H NMR spectrum of **3.61** (400 MHz, 295 K, d<sub>8</sub>-THF).

AP-ELN2-179-2\_norbormanol\_F7-9.1.fid

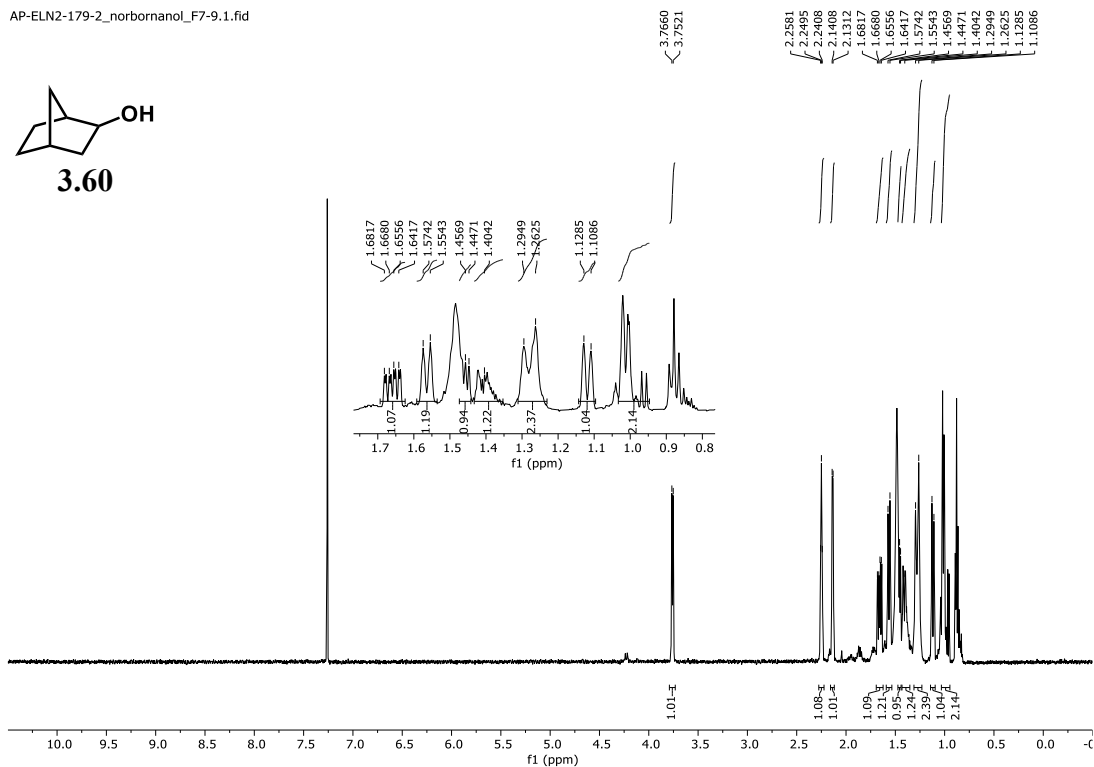


Figure 4.154. <sup>1</sup>H NMR spectrum of **3.60** (500 MHz, 298 K, CDCl<sub>3</sub>).

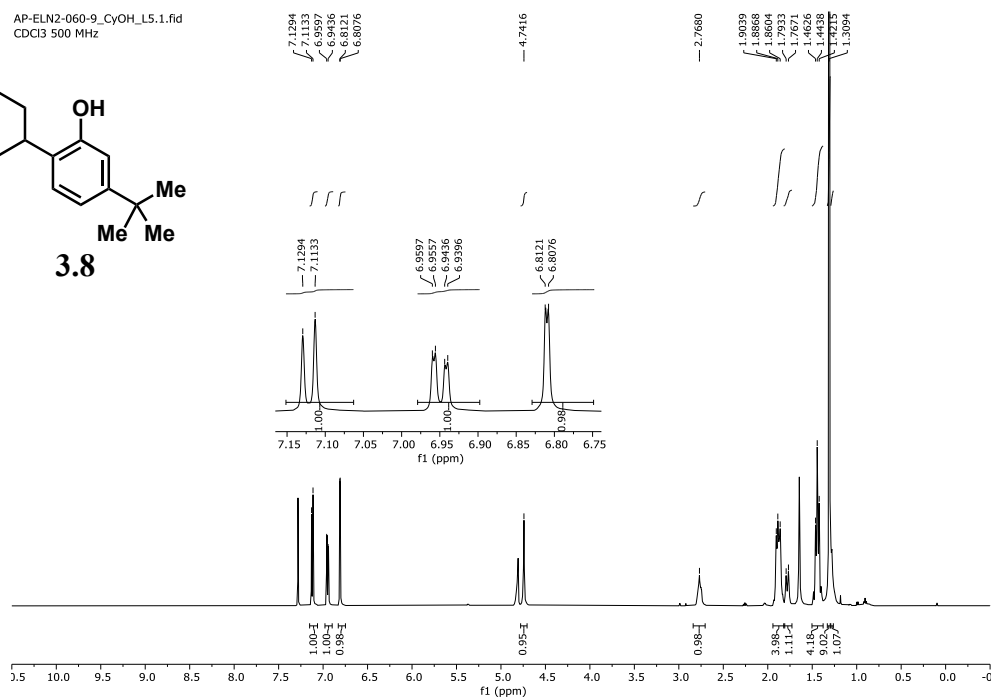


Figure 4.155. <sup>1</sup>H NMR spectrum of **3.8** (500 MHz, 298 K, CDCl<sub>3</sub>).

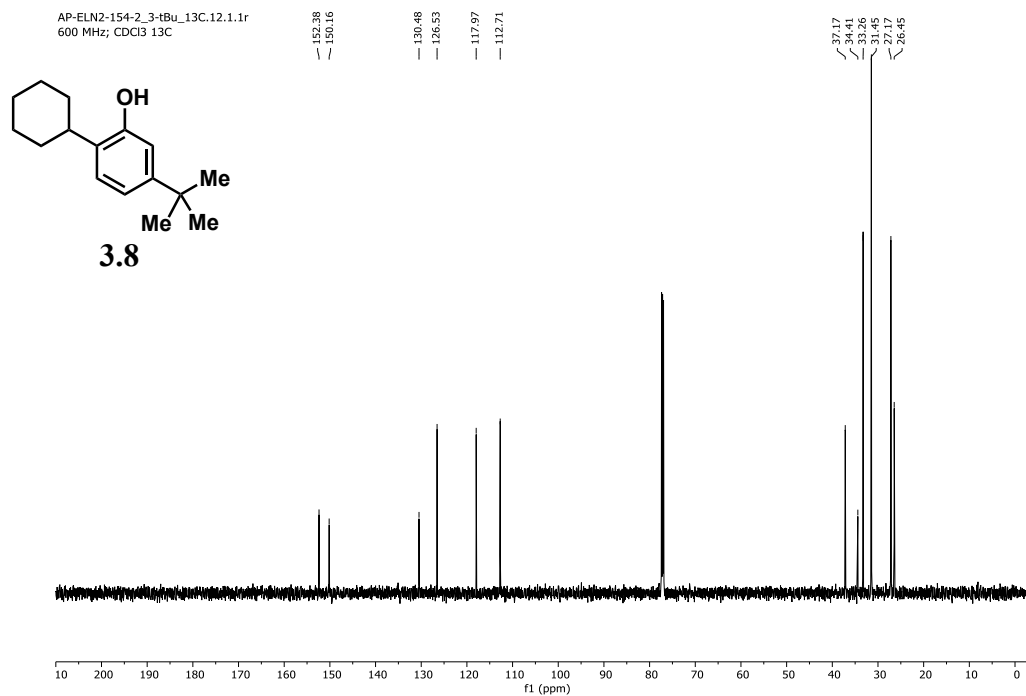


Figure 4.156. <sup>13</sup>C NMR spectrum of **3.8** (151 MHz, 298 K, CDCl<sub>3</sub>).

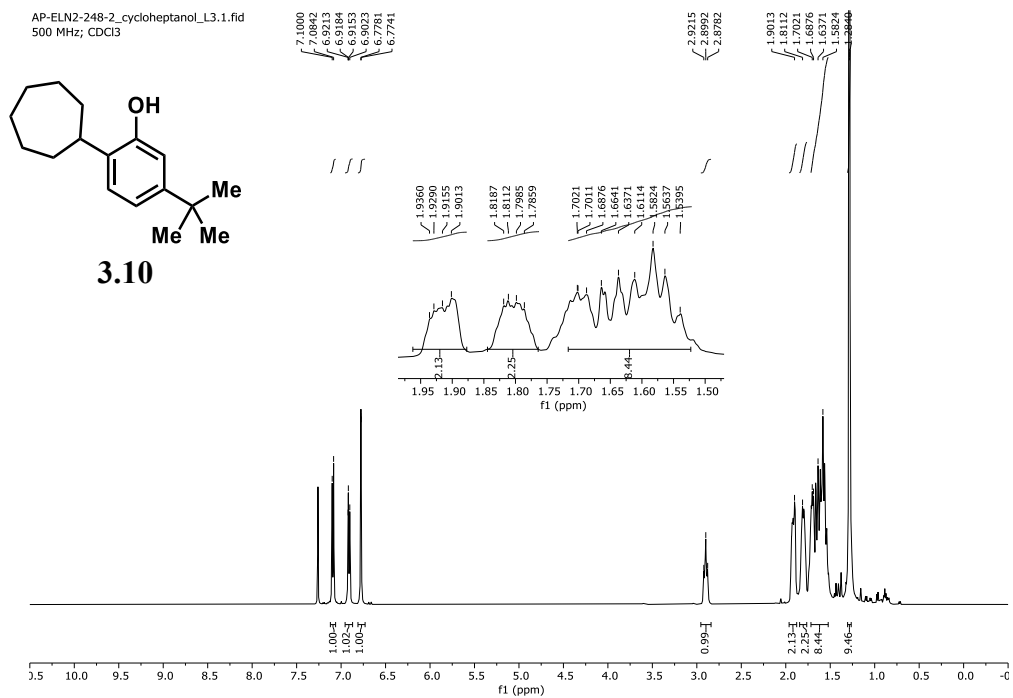


Figure 4.157. <sup>1</sup>H NMR spectrum of **3.10** (500 MHz, 298 K, CDCl<sub>3</sub>).

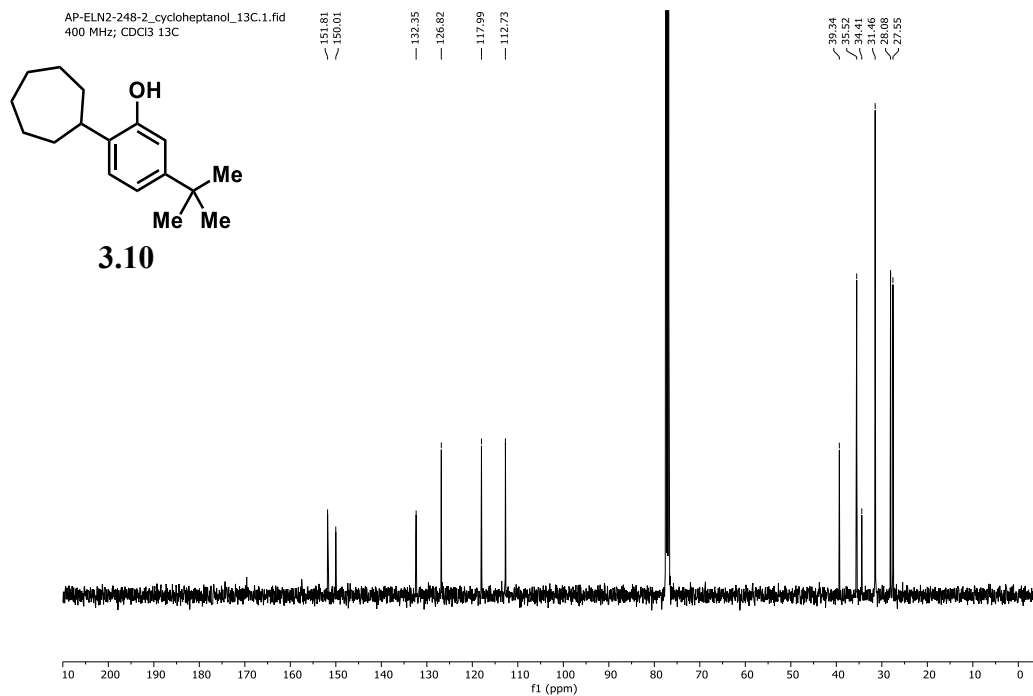


Figure 4.158. <sup>13</sup>C NMR spectrum of **3.10** (101 MHz, 295 K, CDCl<sub>3</sub>).

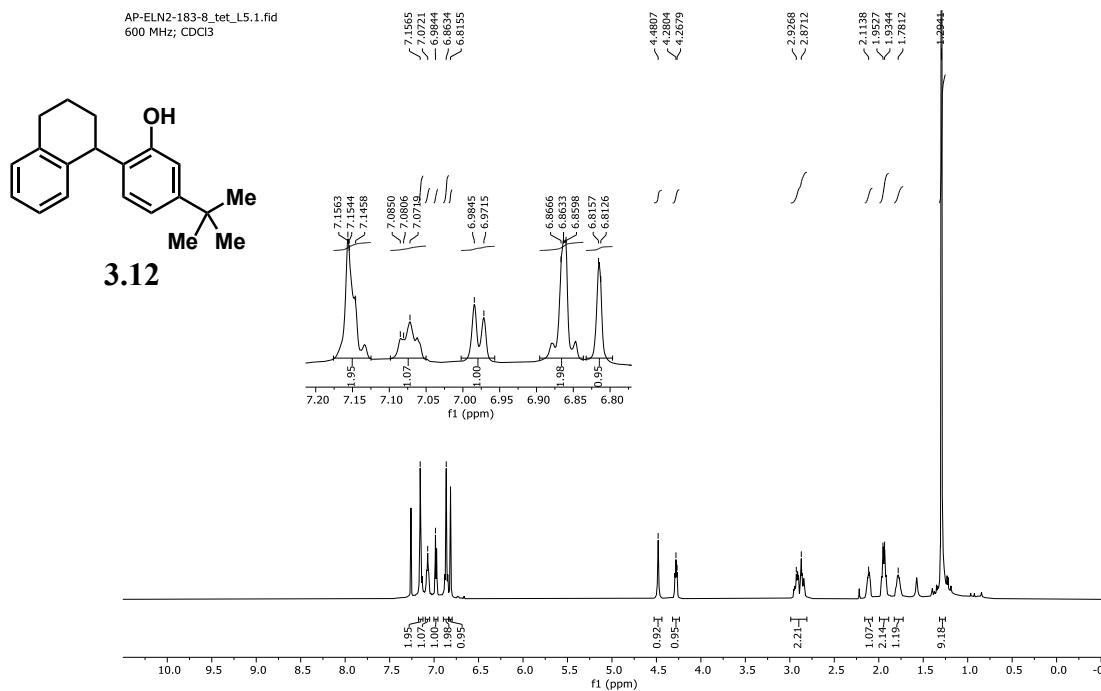


Figure 4.159. <sup>1</sup>H NMR spectrum of **3.12** (600 MHz, 298 K, CDCl<sub>3</sub>).





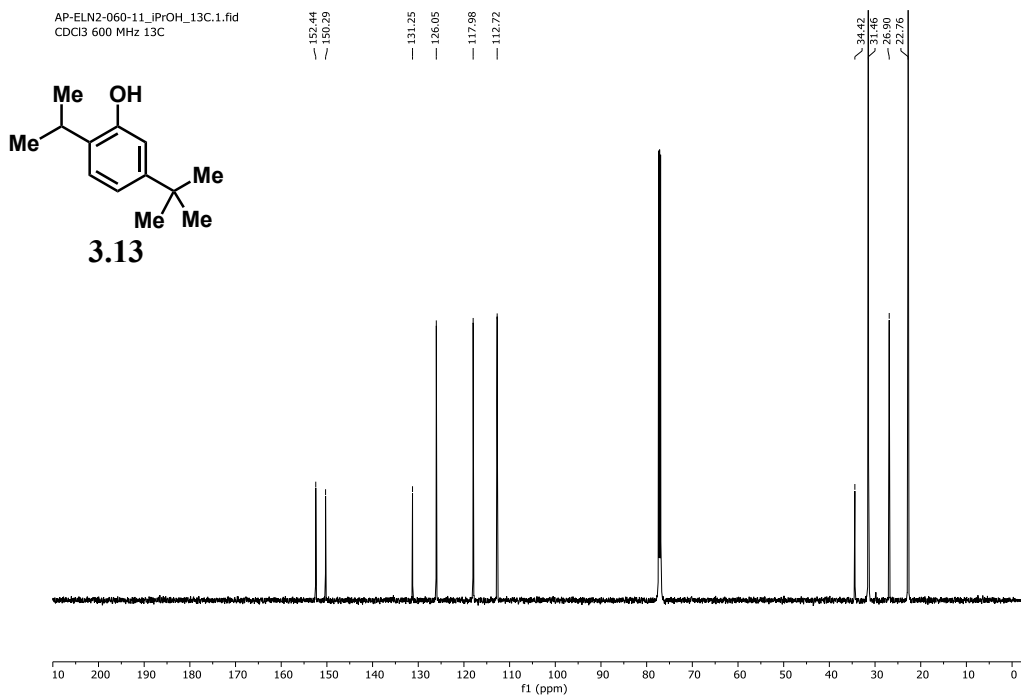


Figure 4.162. <sup>13</sup>C NMR spectrum of **3.13** (151 MHz, 298 K, CDCl<sub>3</sub>).

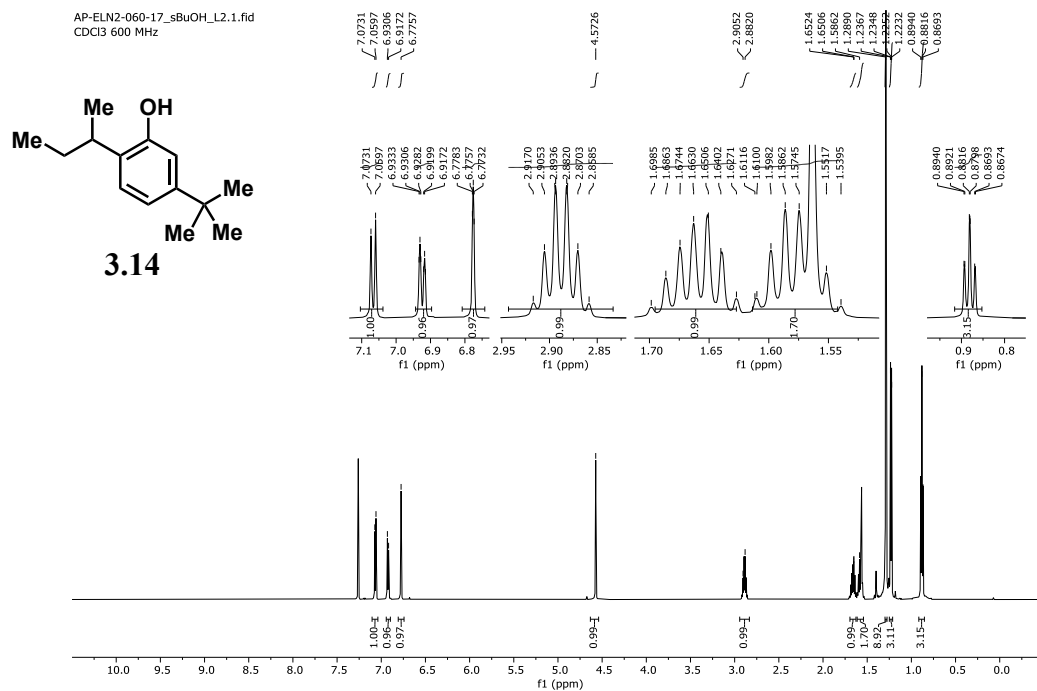


Figure 4.163. <sup>1</sup>H NMR spectrum of **3.14** (600 MHz, 298 K, CDCl<sub>3</sub>).

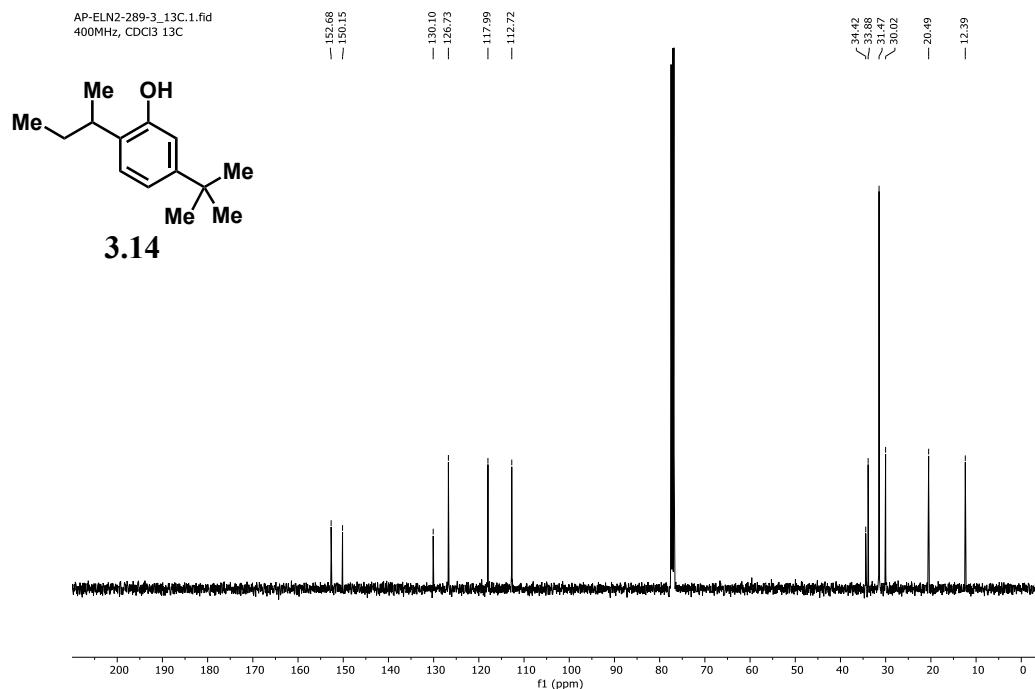


Figure 4.164. <sup>13</sup>C NMR spectrum of **3.14** (101 MHz, 295 K, CDCl<sub>3</sub>).

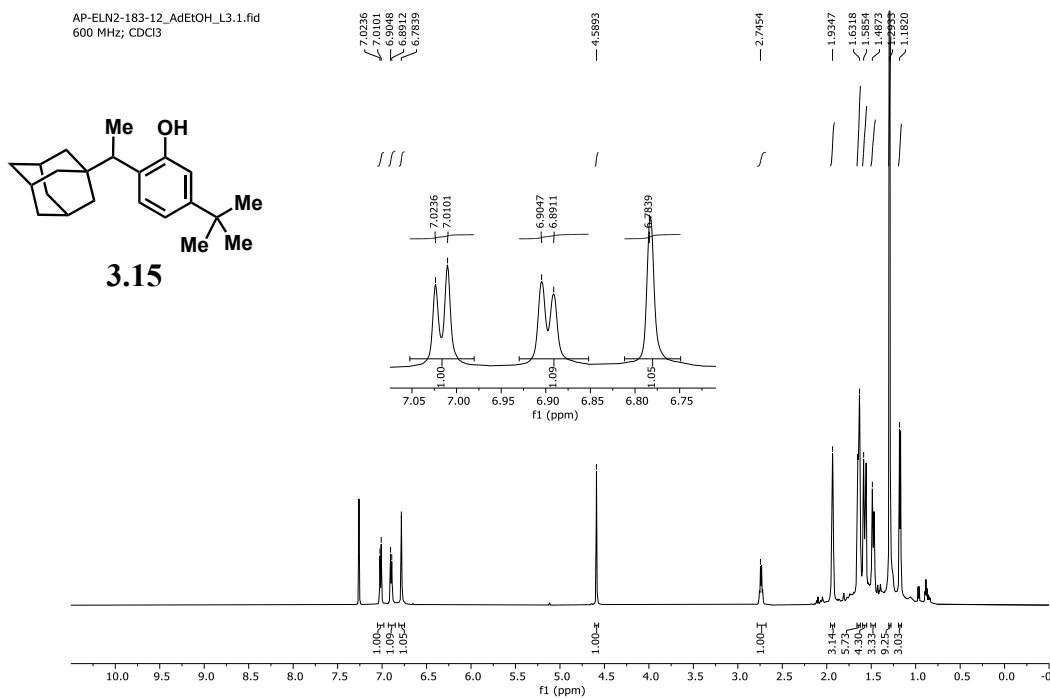


Figure 4.165. <sup>1</sup>H NMR spectrum of **3.15** (600 MHz, 298 K, CDCl<sub>3</sub>).

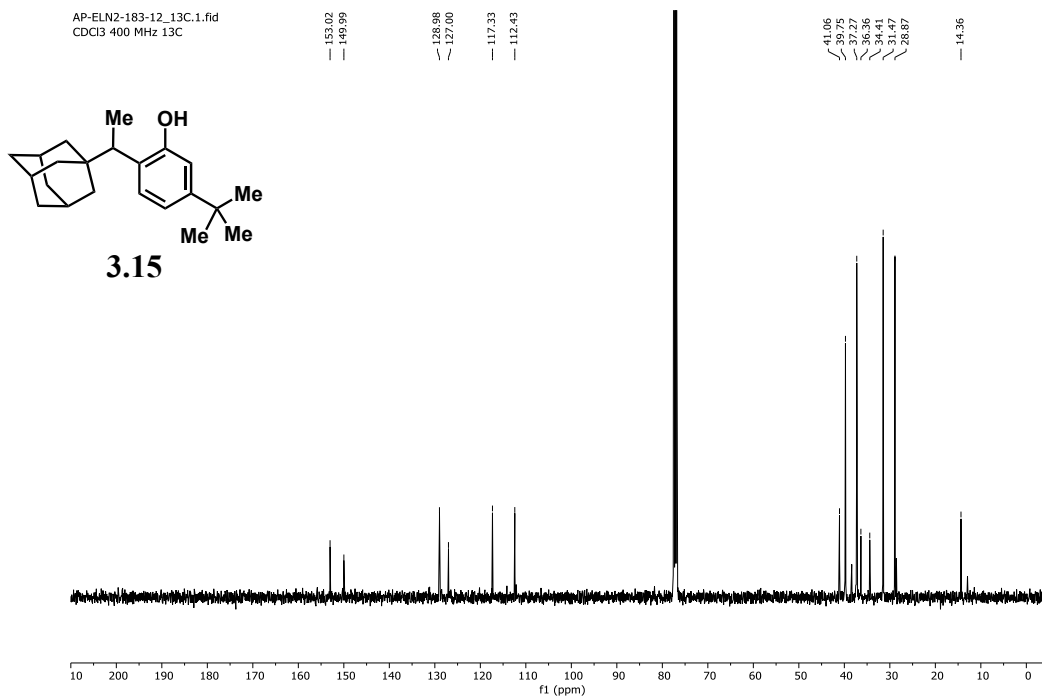


Figure 4.166. <sup>13</sup>C NMR spectrum of **3.15** (101 MHz, 295 K, CDCl<sub>3</sub>).

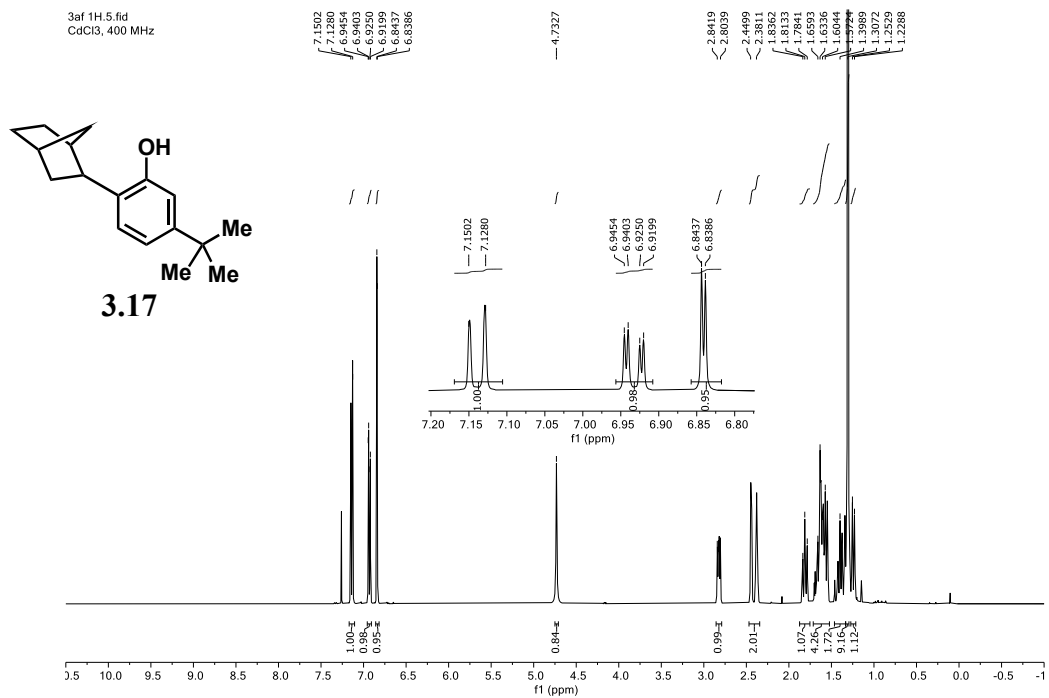


Figure 4.167. <sup>1</sup>H NMR spectrum of **3.17** (400 MHz, 295 K, CDCl<sub>3</sub>).

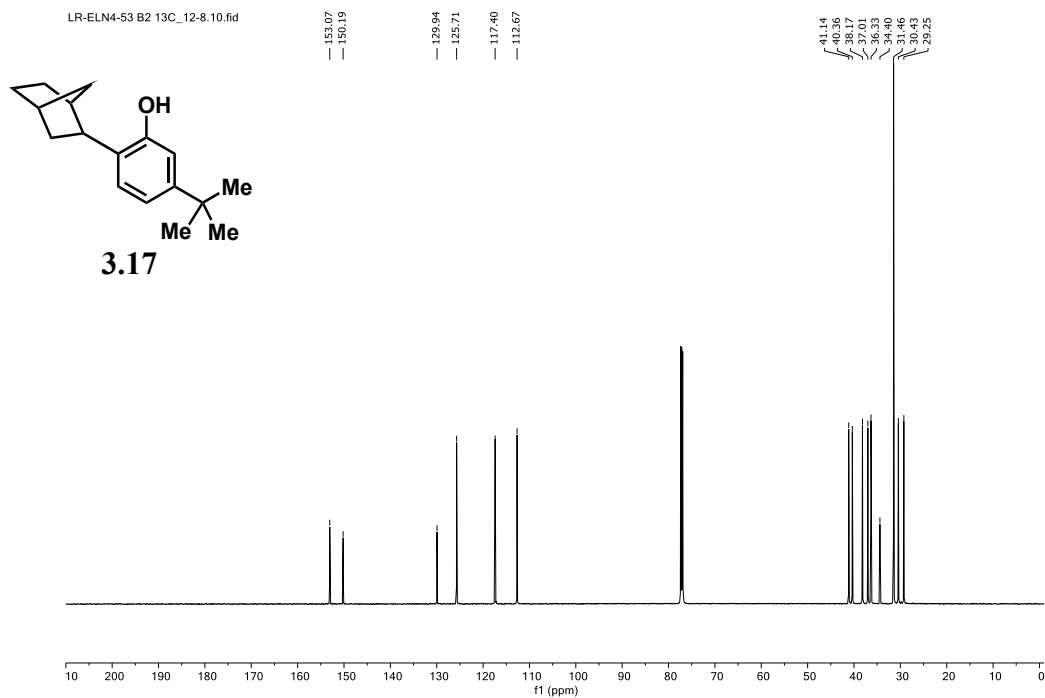


Figure 4.168.  $^{13}\text{C}$  NMR spectrum of **3.17** (151 MHz, 298 K,  $\text{CDCl}_3$ ).

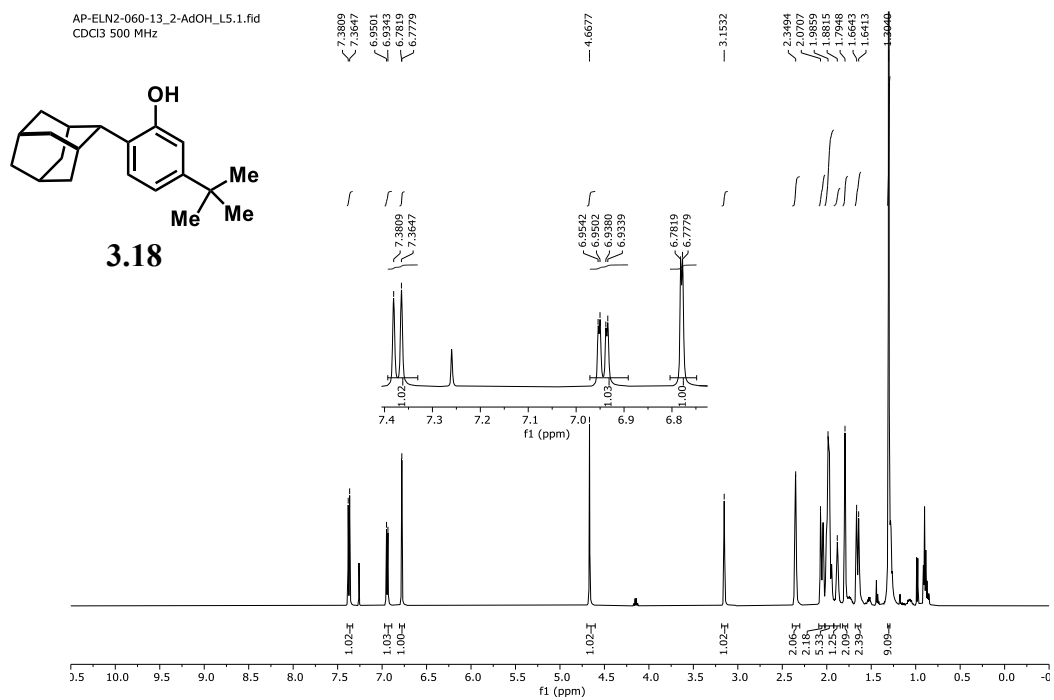


Figure 4.169.  $^1\text{H}$  NMR spectrum of **3.18** (500 MHz, 295 K,  $\text{CDCl}_3$ ).

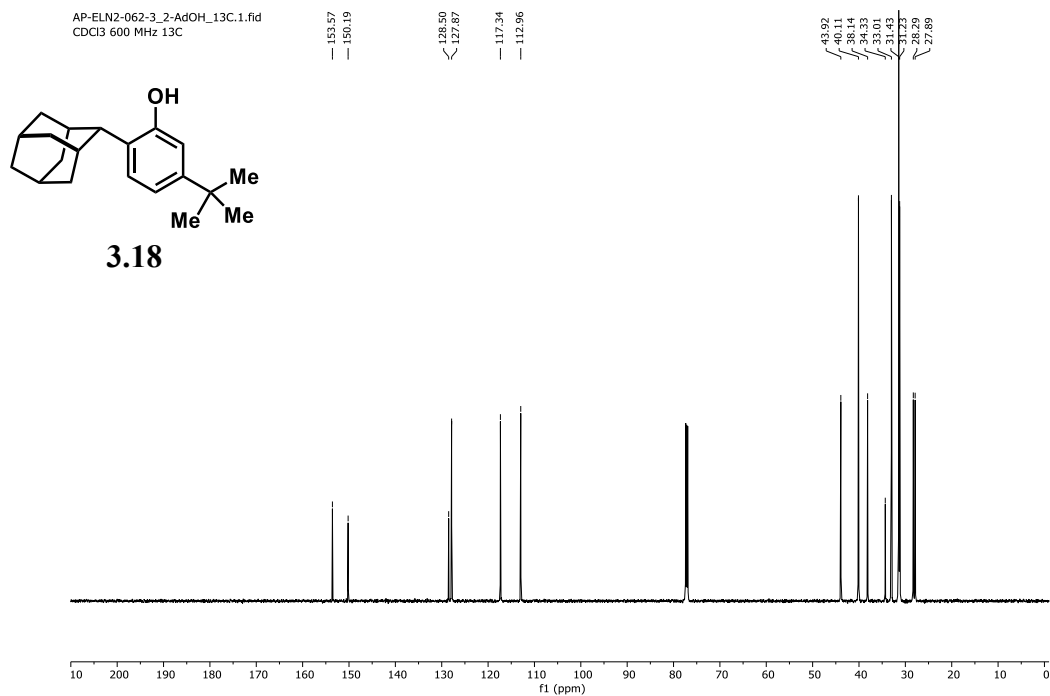


Figure 4.170. <sup>13</sup>C NMR spectrum of **3.18** (151 MHz, 298 K, CDCl<sub>3</sub>).

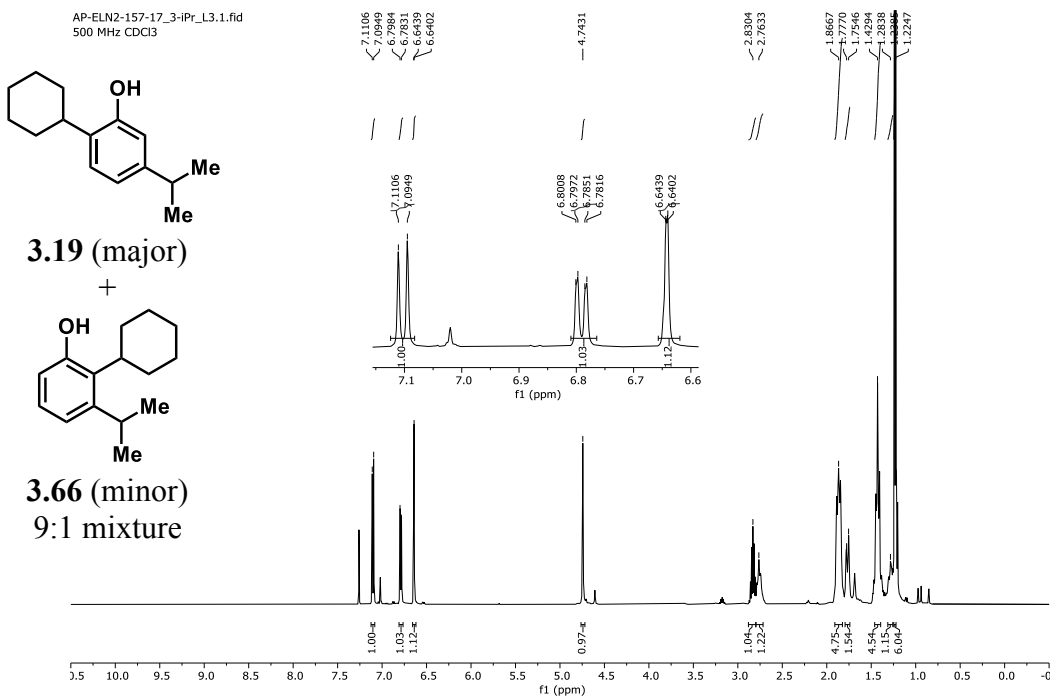


Figure 4.171. <sup>1</sup>H NMR spectrum of **3.19** + **3.66** (500 MHz, 295 K, CDCl<sub>3</sub>).

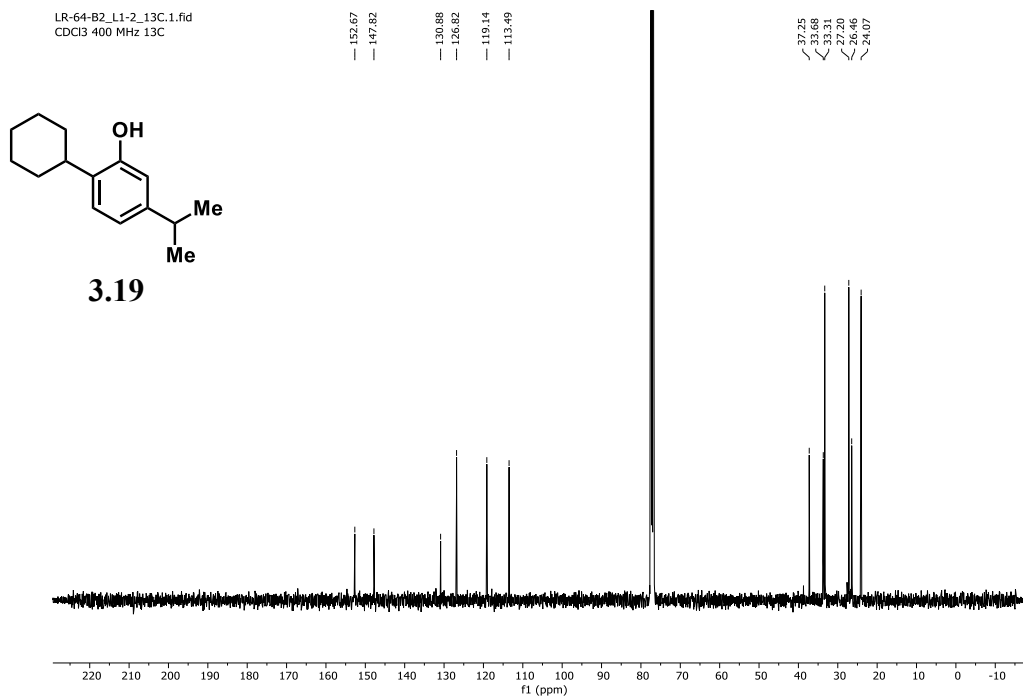


Figure 4.172. <sup>13</sup>C NMR spectrum of **3.19** (101 MHz, 295 K, CDCl<sub>3</sub>).

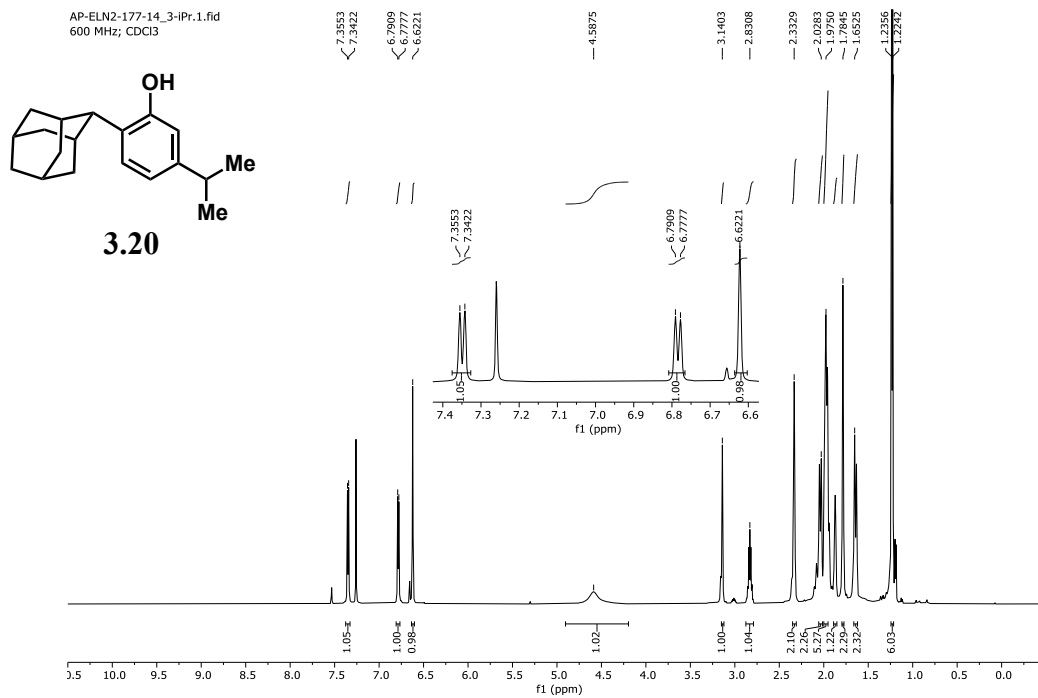


Figure 4.173. <sup>1</sup>H NMR spectrum of **3.20** (600 MHz, 295 K, CDCl<sub>3</sub>).

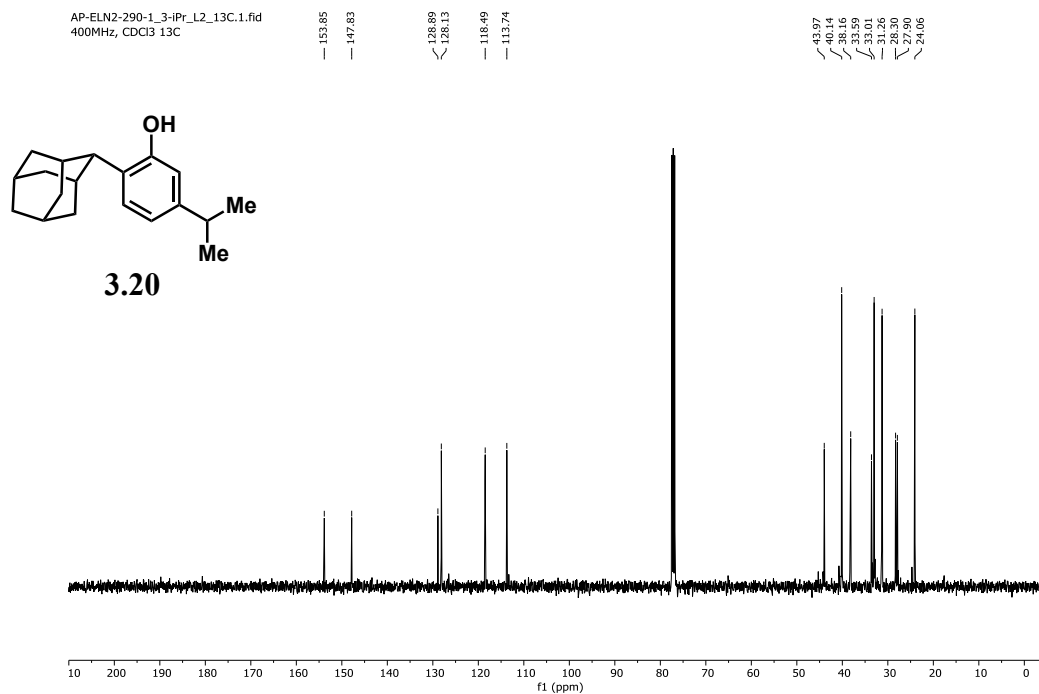


Figure 4.174. <sup>13</sup>C NMR spectrum of **3.20** (101 MHz, 295 K, CDCl<sub>3</sub>).

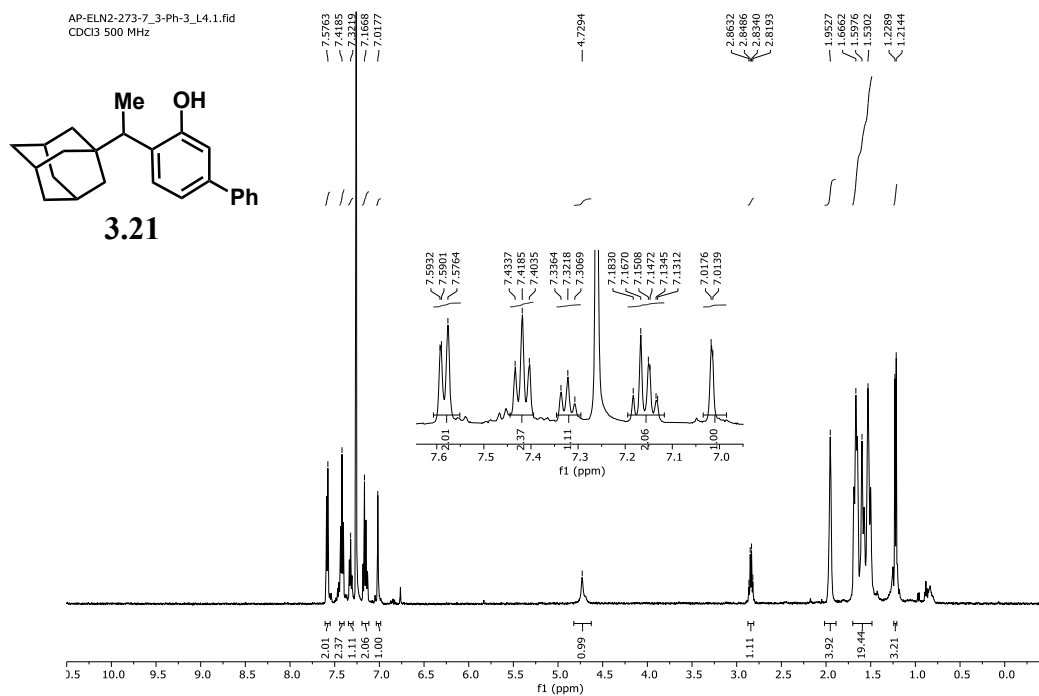


Figure 4.175. <sup>1</sup>H NMR spectrum of **3.21** (500 MHz, 298 K, CDCl<sub>3</sub>).

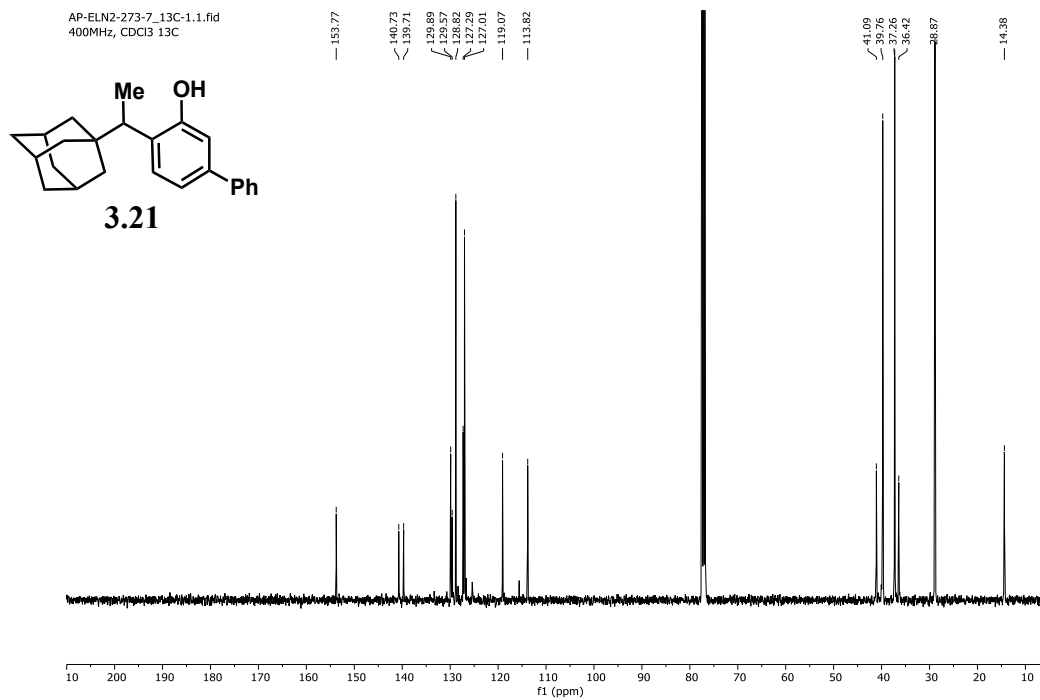


Figure 4.176. <sup>13</sup>C NMR spectrum of **3.21** (101 MHz, 295 K, CDCl<sub>3</sub>).

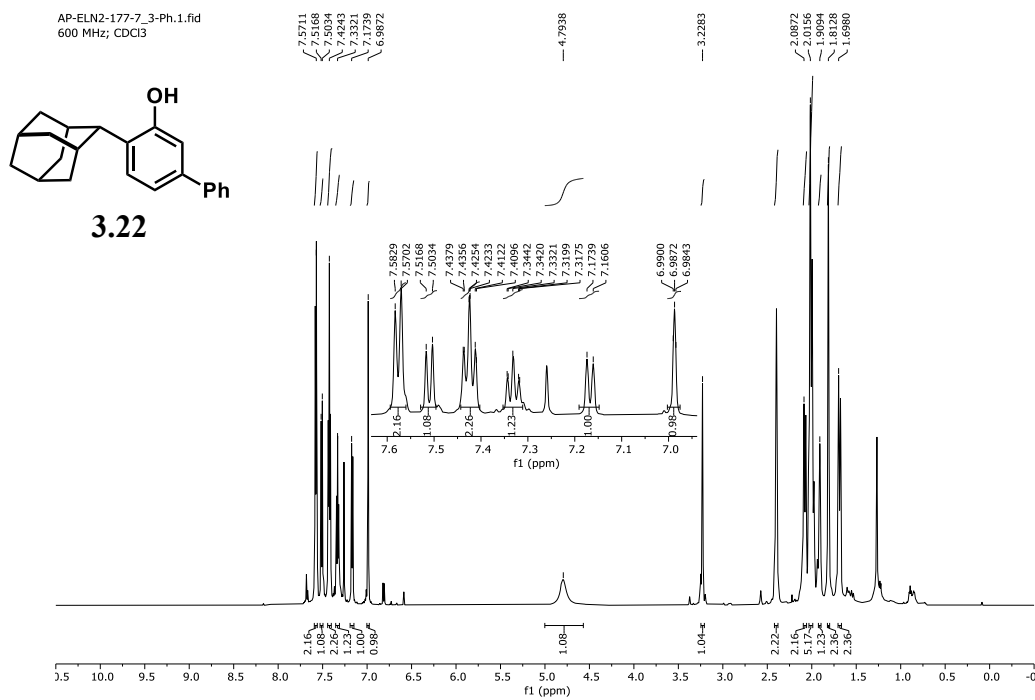


Figure 4.177. <sup>1</sup>H NMR spectrum of **3.22** (600 MHz, 298 K, CDCl<sub>3</sub>).



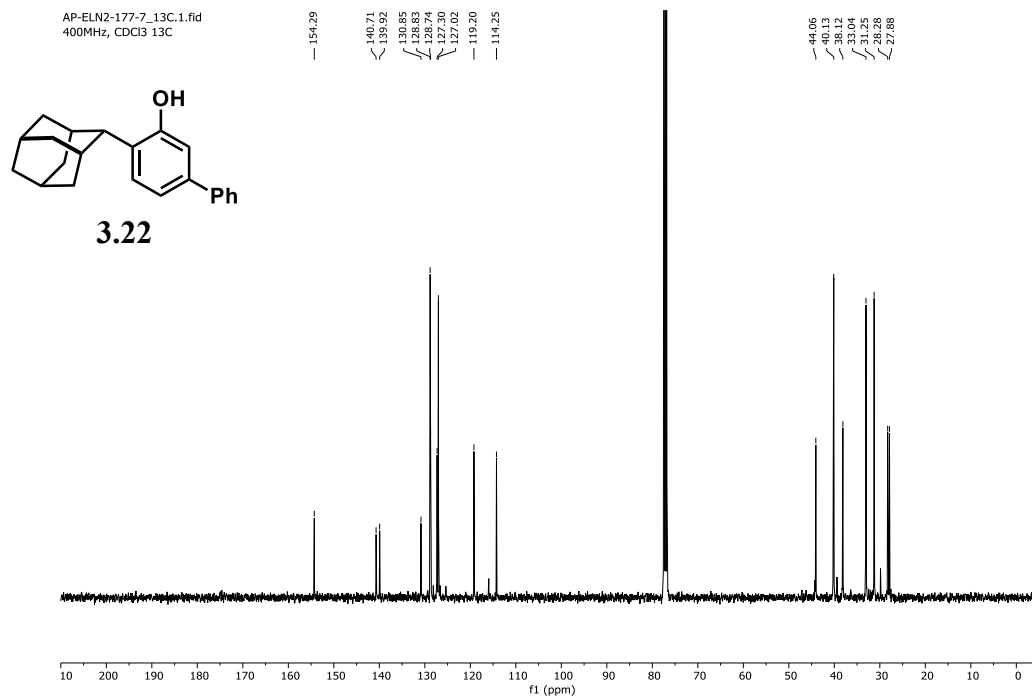


Figure 4.178. <sup>13</sup>C NMR spectrum of **3.22** (101 MHz, 295 K, CDCl<sub>3</sub>).

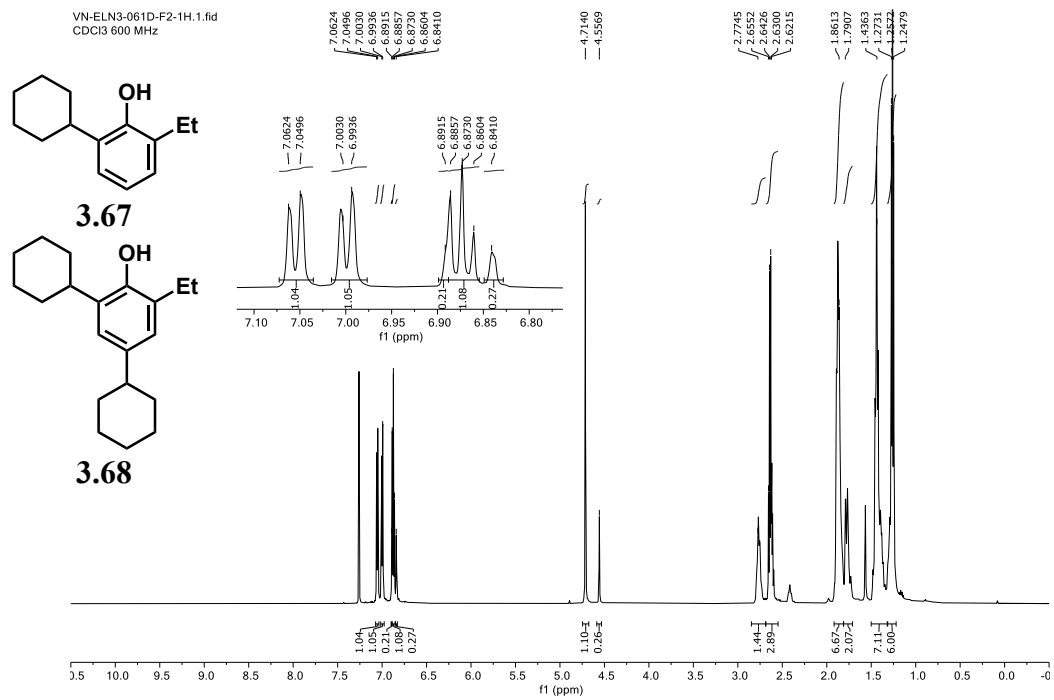


Figure 4.179. <sup>1</sup>H NMR spectrum of **3.67** + **3.68** (600 MHz, 298 K, CDCl<sub>3</sub>).

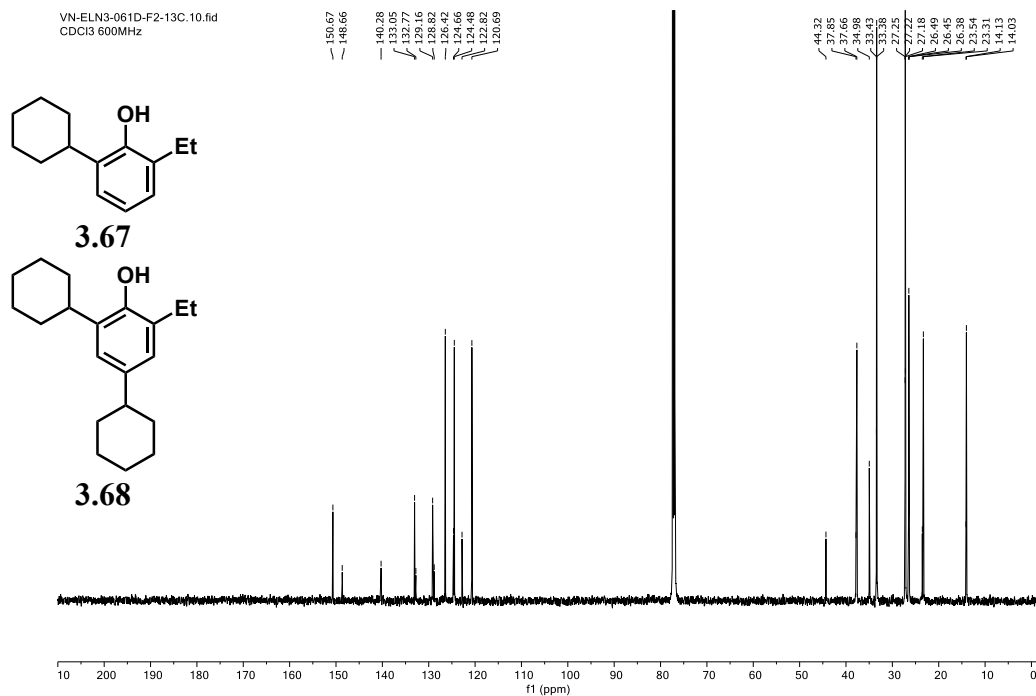


Figure 4.180. <sup>13</sup>C NMR spectrum of **3.67** + **3.68** (151 MHz, 298 K, CDCl<sub>3</sub>).

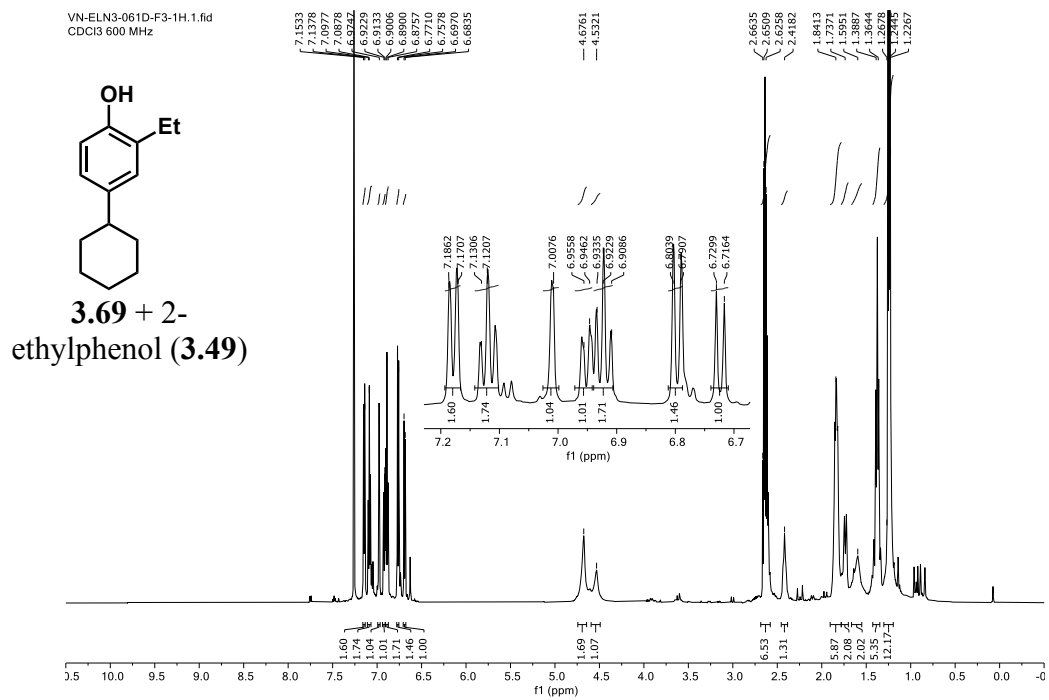
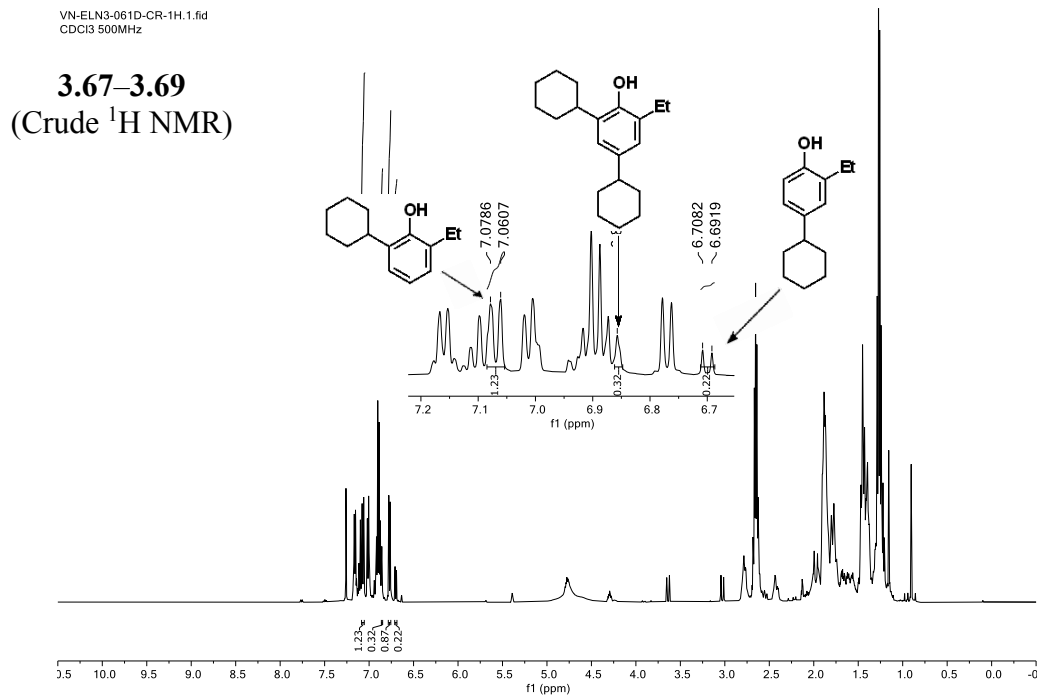
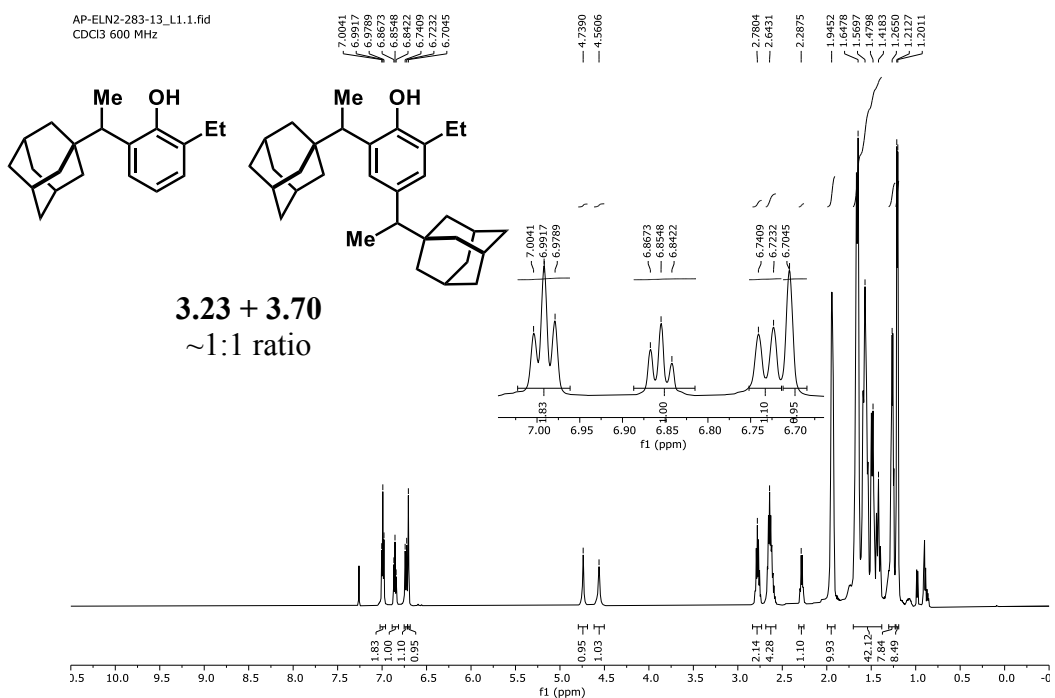


Figure 4.181. <sup>1</sup>H NMR spectrum of **3.69** + **3.49** (600 MHz, 298 K, CDCl<sub>3</sub>).



**Figure 4.182.** <sup>1</sup>H NMR spectrum of the crude mixture of **3.63–3.65** (500 MHz, 298 K, CDCl<sub>3</sub>). Assignments determined after purification.



**Figure 4.183.** <sup>1</sup>H NMR spectrum of **3.23 + 3.70** (600 MHz, 298 K, CDCl<sub>3</sub>).

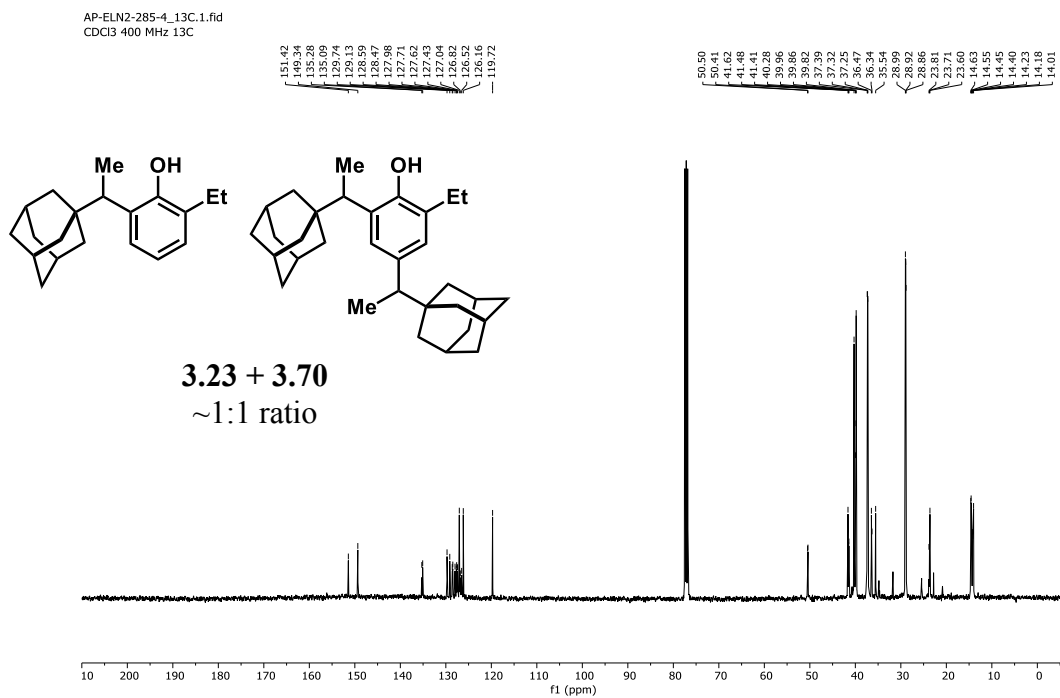


Figure 4.184. <sup>13</sup>C NMR spectrum of 3.23 + 3.70 (101 MHz, 295 K, CDCl<sub>3</sub>).

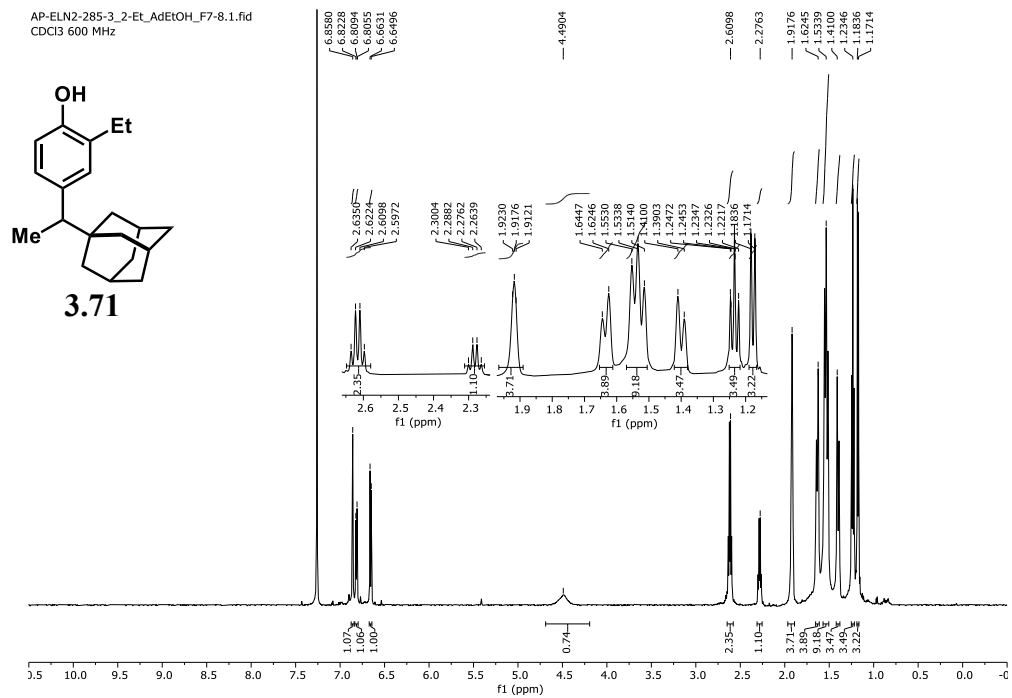
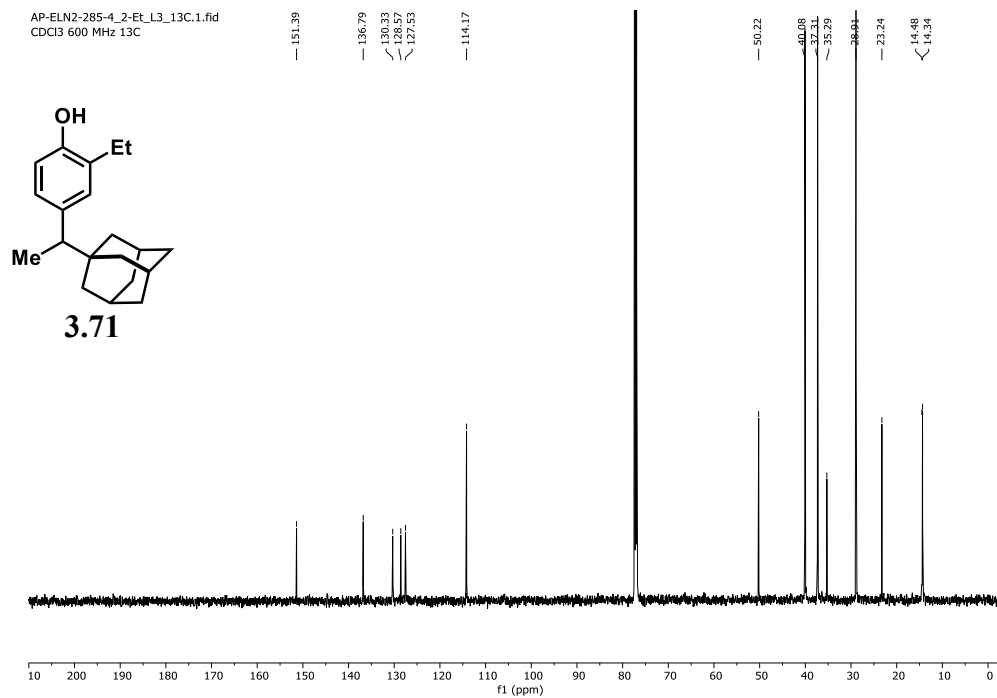
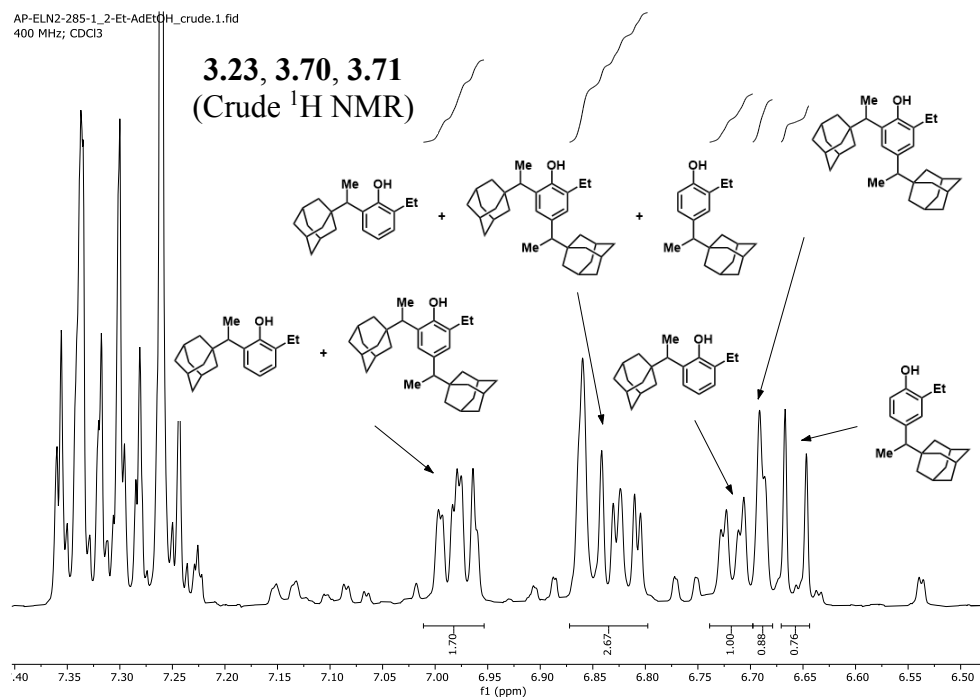


Figure 4.185. <sup>1</sup>H NMR spectrum of 3.71 (600 MHz, 298 K, CDCl<sub>3</sub>).



**Figure 4.186.** <sup>13</sup>C NMR spectrum of **3.71** (151 MHz, 298 K, CDCl<sub>3</sub>).



**Figure 4.187.** <sup>1</sup>H NMR spectrum of the crude mixture of **3.23, 3.70, 3.71** (400 MHz, 295 K, CDCl<sub>3</sub>). Assignments determined after purification.

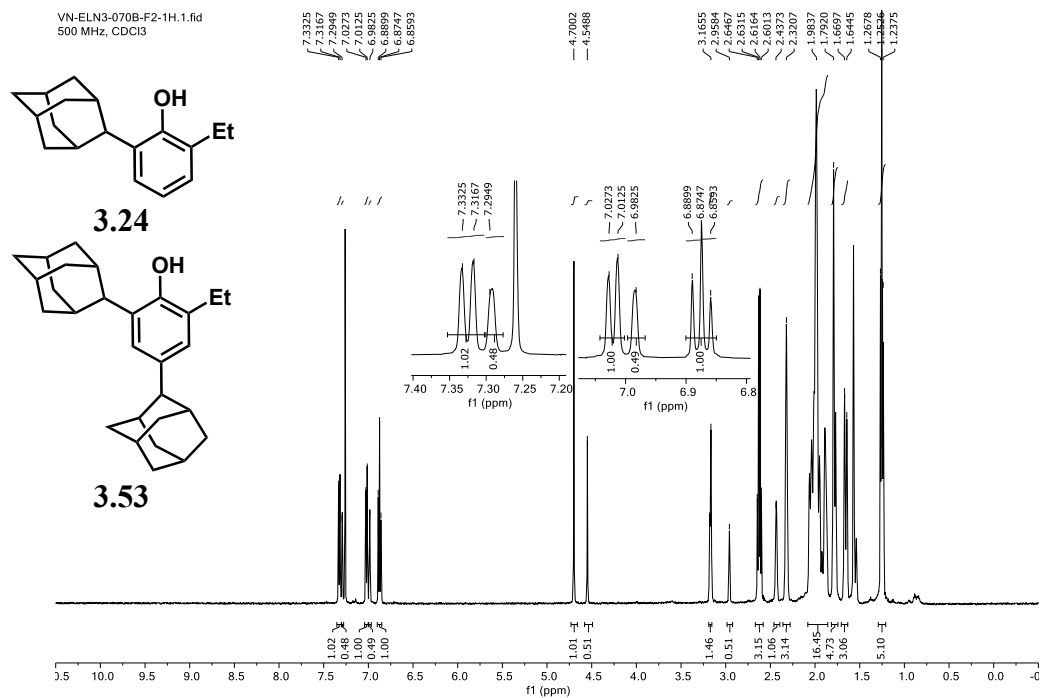


Figure 4.188. <sup>1</sup>H NMR spectrum of **3.24** + **3.53** (500 MHz, 298 K, CDCl<sub>3</sub>).

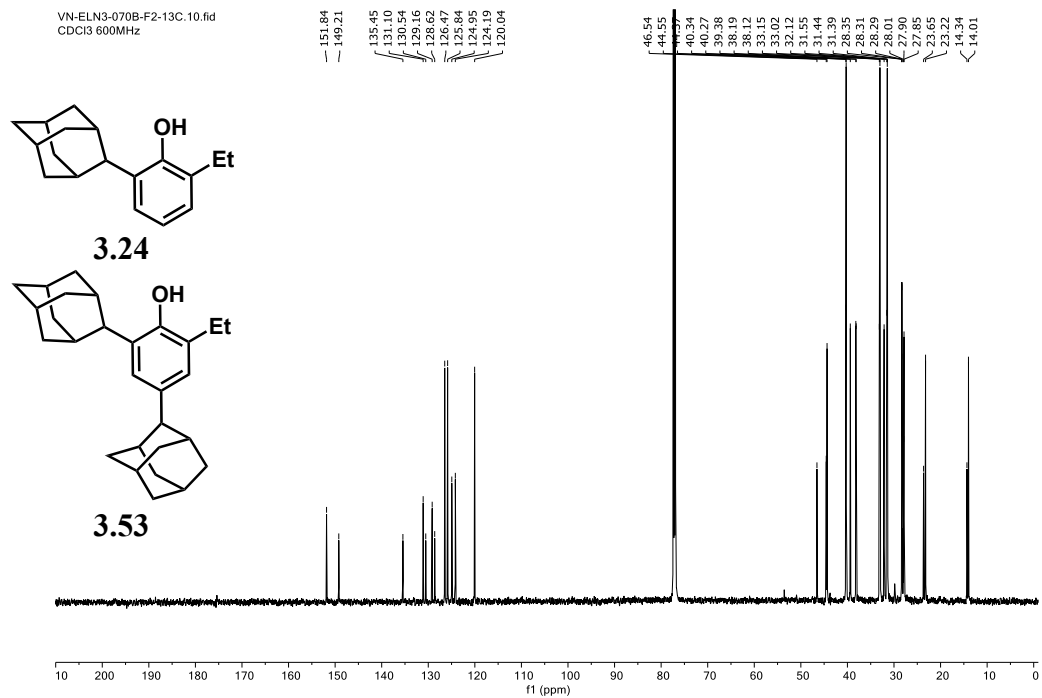
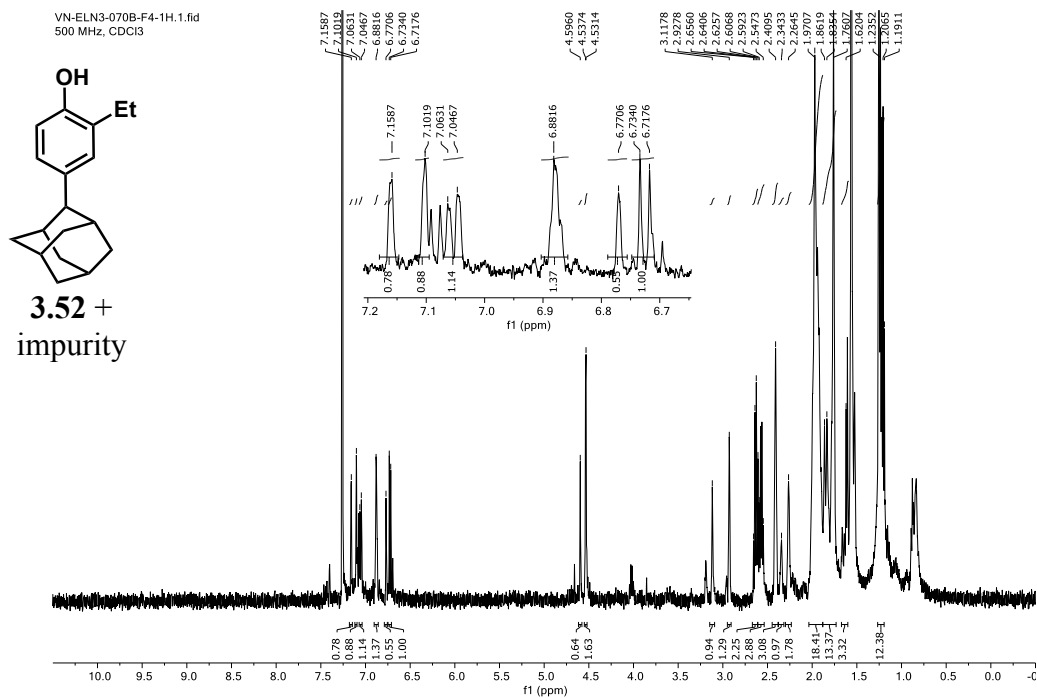
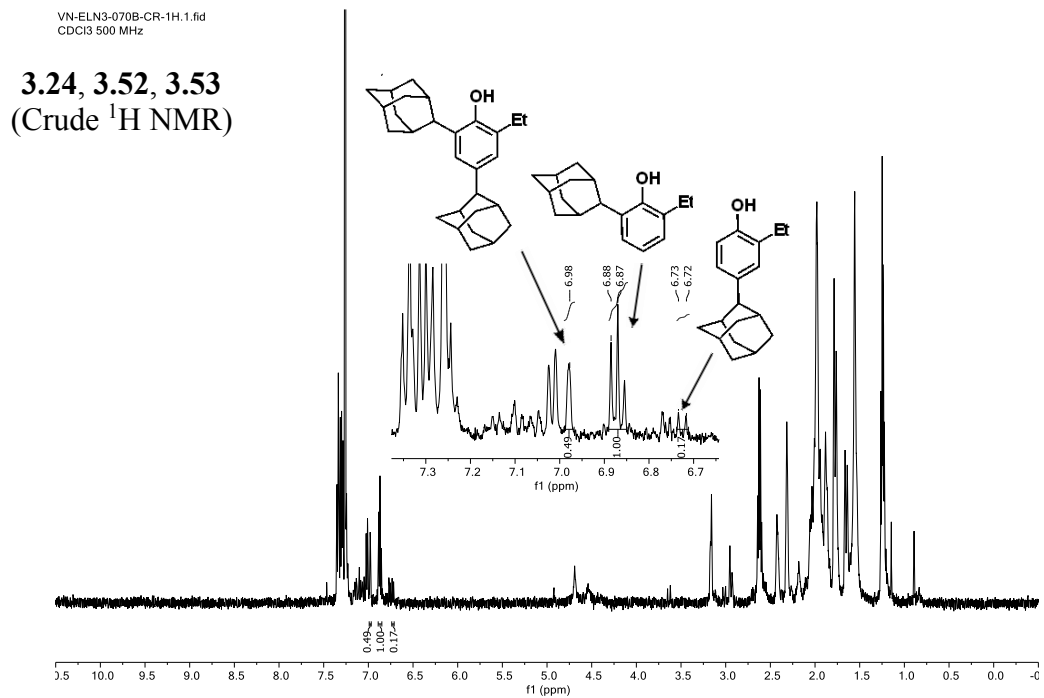


Figure 4.189. <sup>13</sup>C NMR spectrum of **3.24** + **3.53** (151 MHz, 298 K, CDCl<sub>3</sub>).



**Figure 4.190.** <sup>1</sup>H NMR spectrum of **3.52 + impurity** (500 MHz, 298 K, CDCl<sub>3</sub>).



**Figure 4.191.** <sup>1</sup>H NMR spectrum of crude mixture of **3.24, 3.52, 3.53** (500 MHz, 298 K, CDCl<sub>3</sub>). Assignments determined after purification.

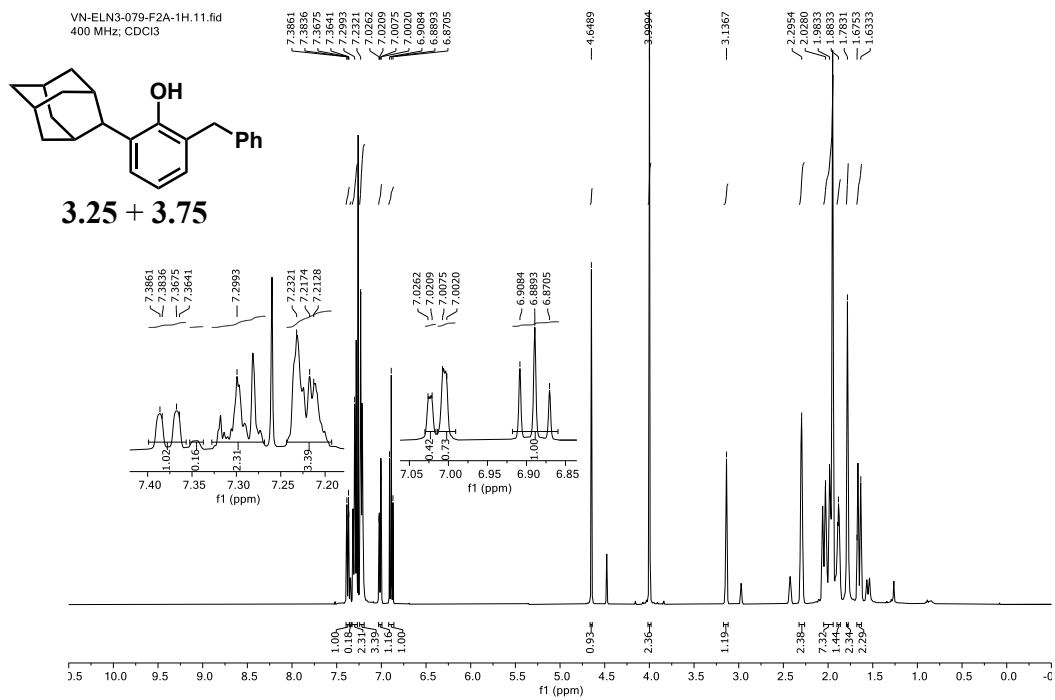


Figure 4.192. <sup>1</sup>H NMR spectrum of **3.25 + 3.75** (400 MHz, 295 K, CDCl<sub>3</sub>).

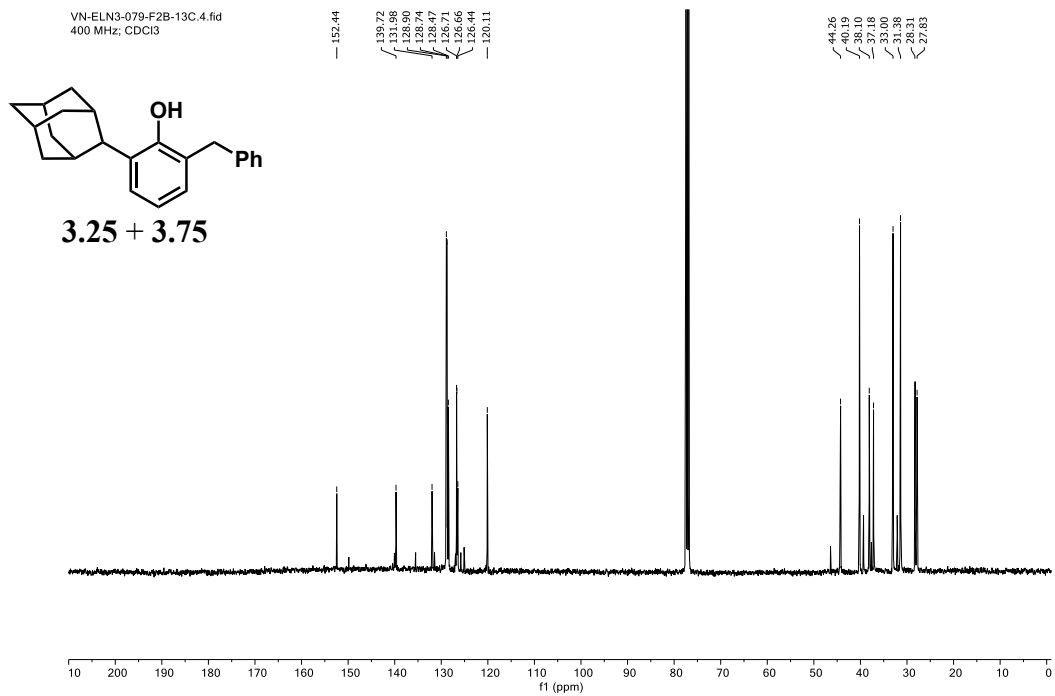


Figure 4.193. <sup>13</sup>C NMR spectrum of **3.25 + 3.75** (126 MHz, 295 K, CDCl<sub>3</sub>).





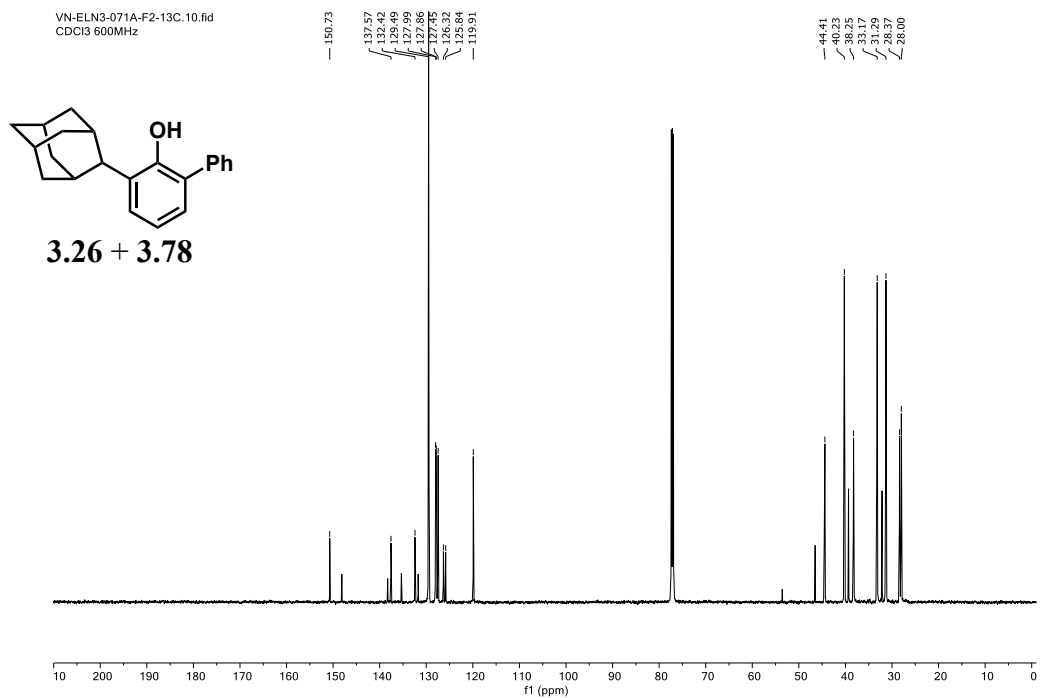


Figure 4.196. <sup>13</sup>C NMR spectrum of **3.26** + **3.78** (151 MHz, 298 K, CDCl<sub>3</sub>).

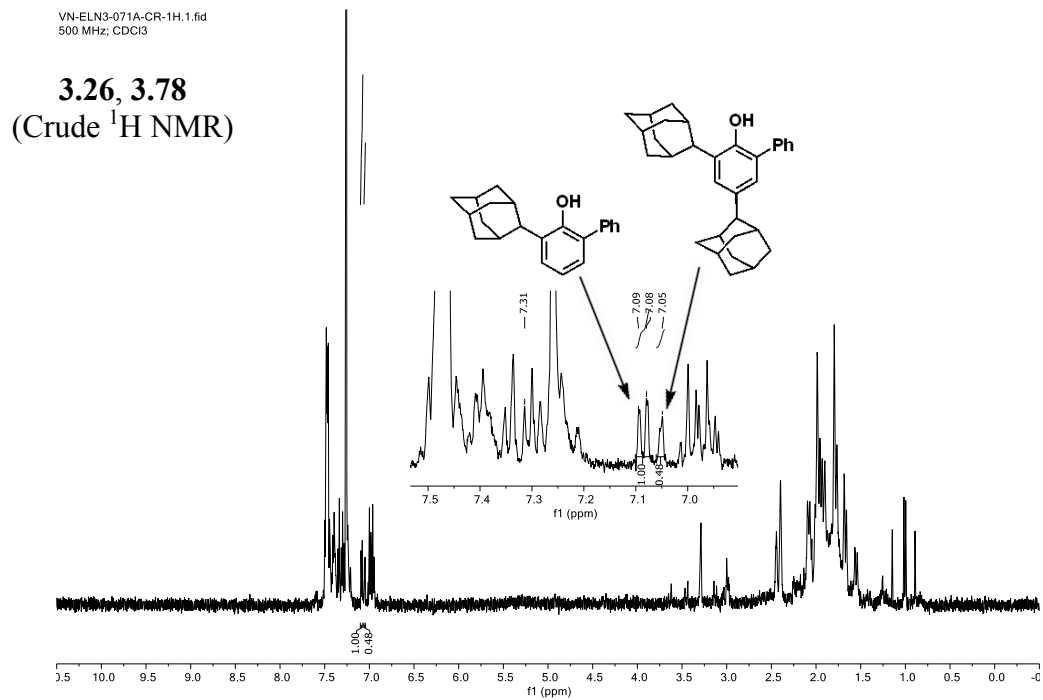
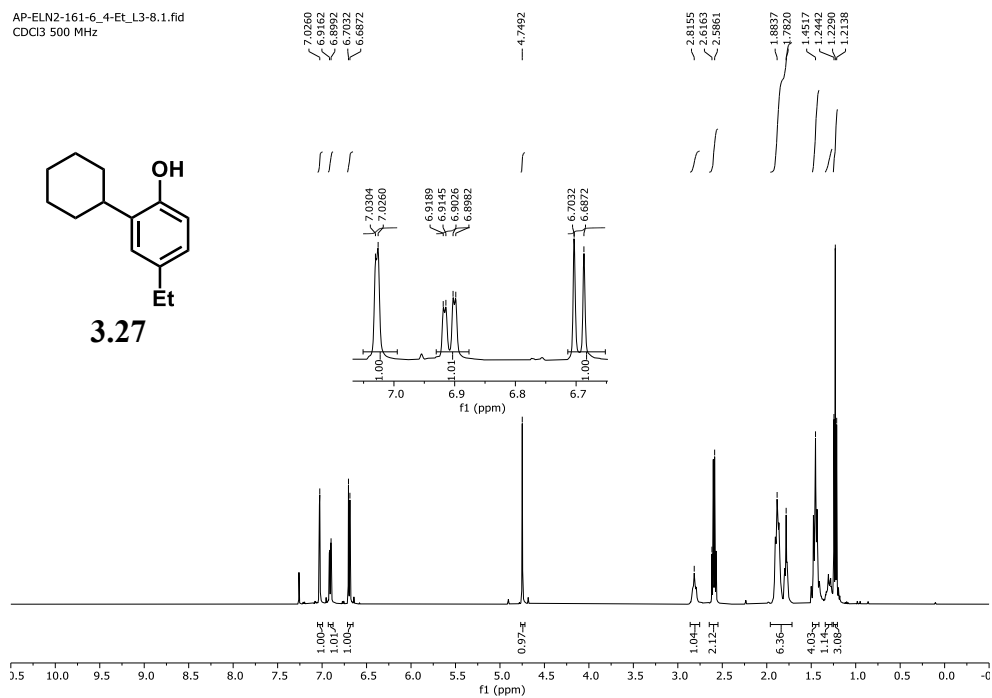
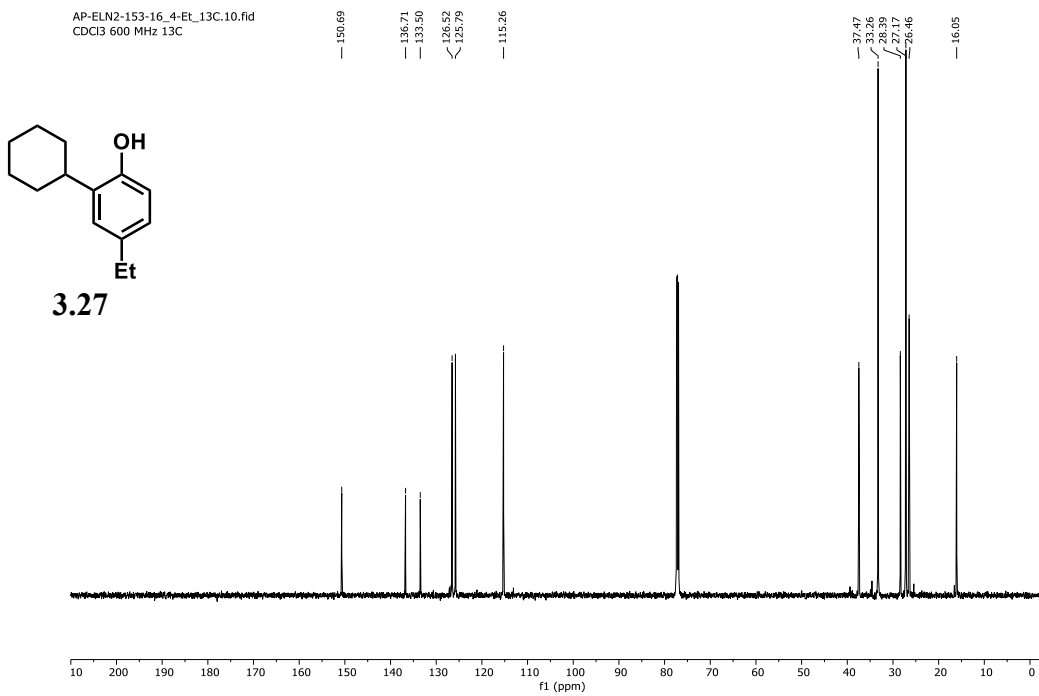


Figure 4.197. <sup>1</sup>H NMR spectrum of the crude mixture of **3.26**, **3.78** (500 MHz, 298 K, CDCl<sub>3</sub>). Assignments determined after purification.



**Figure 4.198.** <sup>1</sup>H NMR spectrum of **3.27** (500 MHz, 298 K, CDCl<sub>3</sub>).



**Figure 4.199.** <sup>13</sup>C NMR spectrum of **3.27** (151 MHz, 298 K, CDCl<sub>3</sub>).

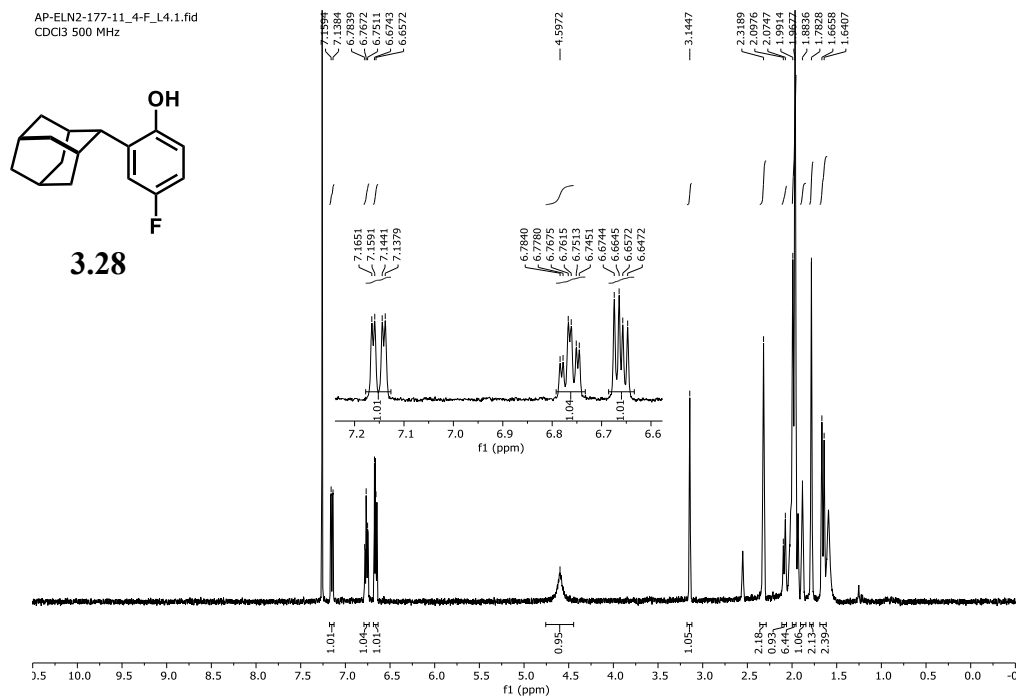


Figure 4.200. <sup>1</sup>H NMR spectrum of **3.28** (500 MHz, 298 K, CDCl<sub>3</sub>).

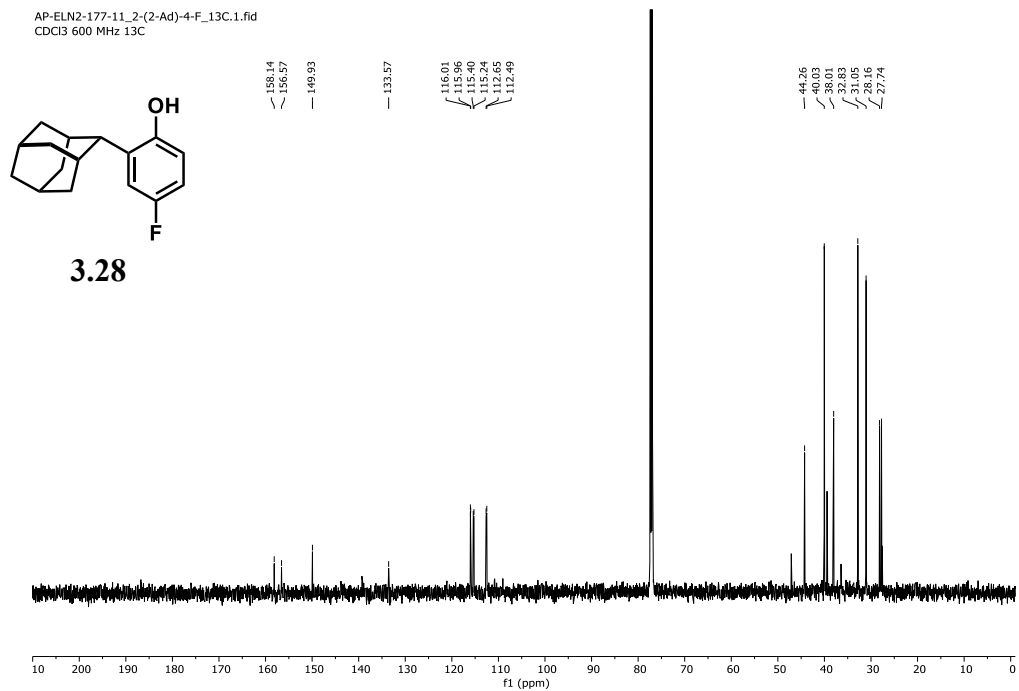
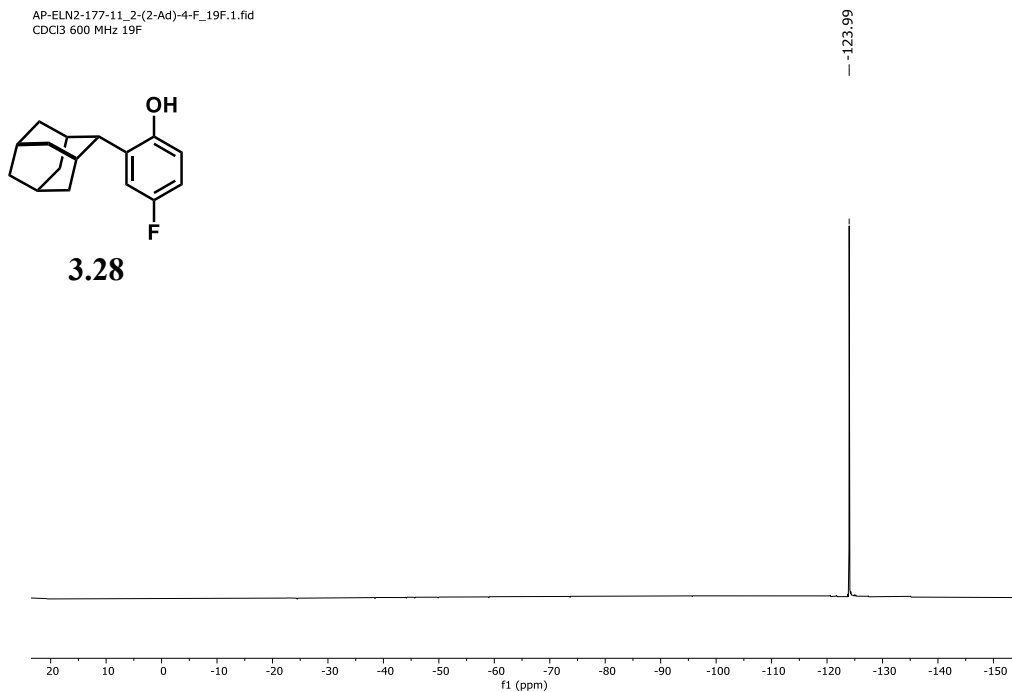
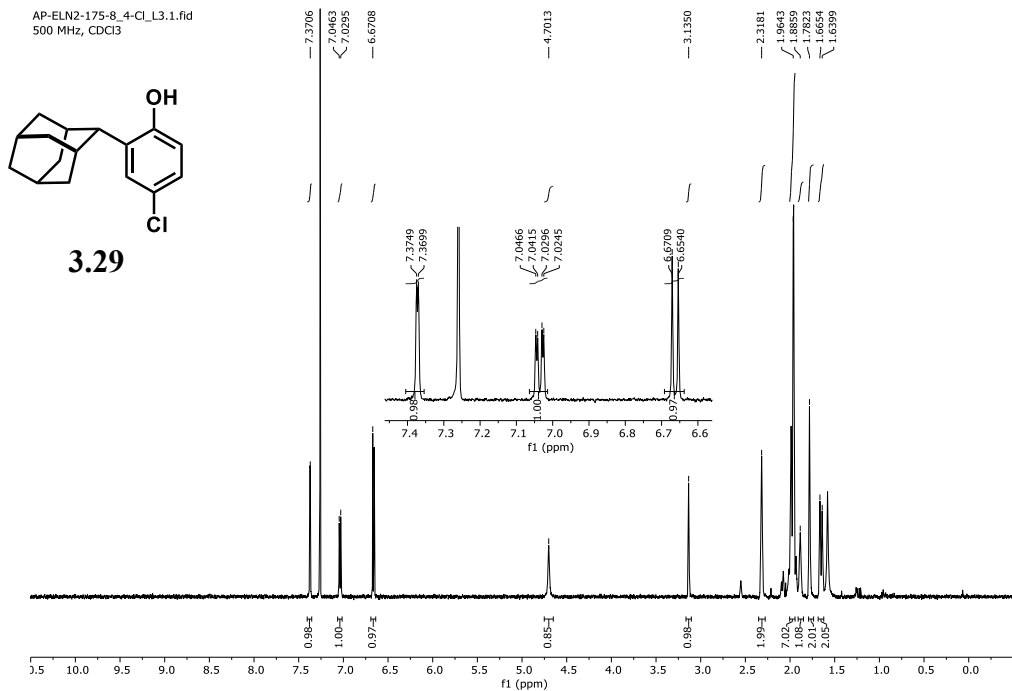


Figure 4.201. <sup>13</sup>C NMR spectrum of **3.28** (151 MHz, 298 K, CDCl<sub>3</sub>).



**Figure 4.202.** <sup>19</sup>F NMR spectrum of **3.28** (564 MHz, 298 K, CDCl<sub>3</sub>).



**Figure 4.203.** <sup>1</sup>H NMR spectrum of **3.29** (500 MHz, 298 K, CDCl<sub>3</sub>).

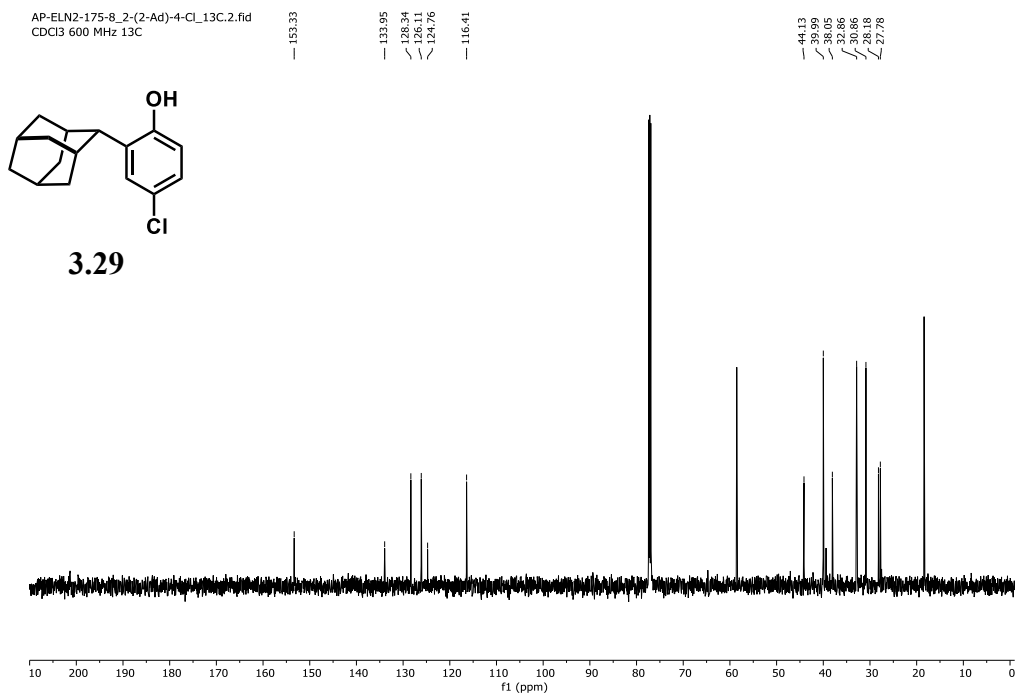


**Figure 4.204.** <sup>13</sup>C NMR spectrum of **3.29** (151 MHz, 298 K, CDCl<sub>3</sub>).

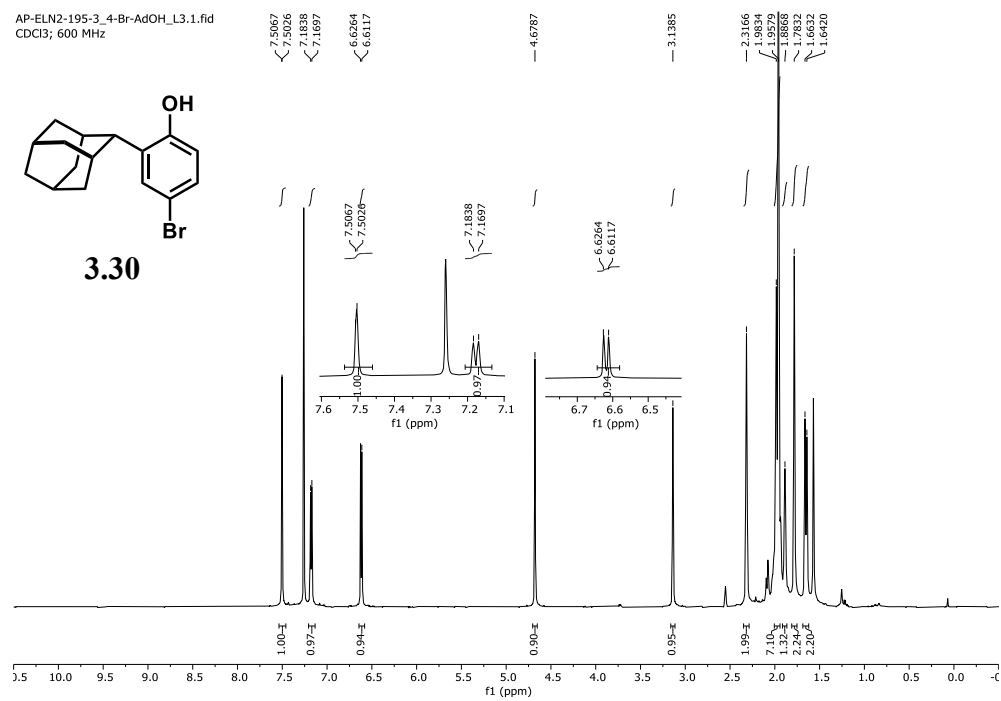


**Figure 4.205.** <sup>1</sup>H NMR spectrum of **3.30** (600 MHz, 298 K, CDCl<sub>3</sub>).

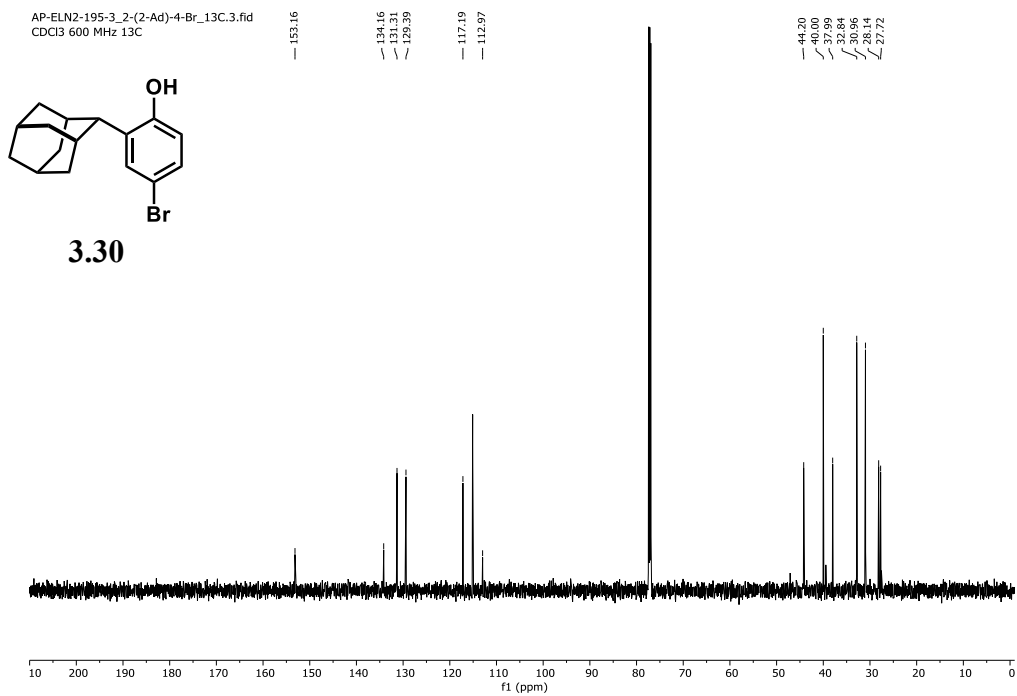


Figure 4.206. <sup>13</sup>C NMR spectrum of **3.30** (151 MHz, 298 K, CDCl<sub>3</sub>).

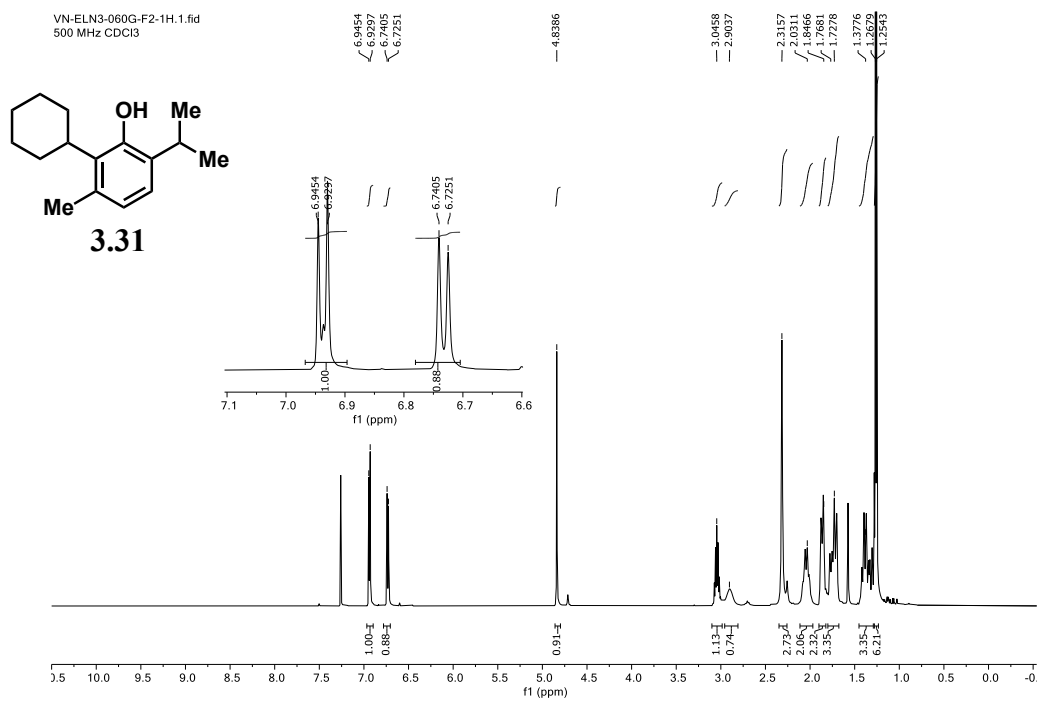


Figure 4.207. <sup>1</sup>H NMR spectrum of **3.31** (500 MHz, 298 K, CDCl<sub>3</sub>).

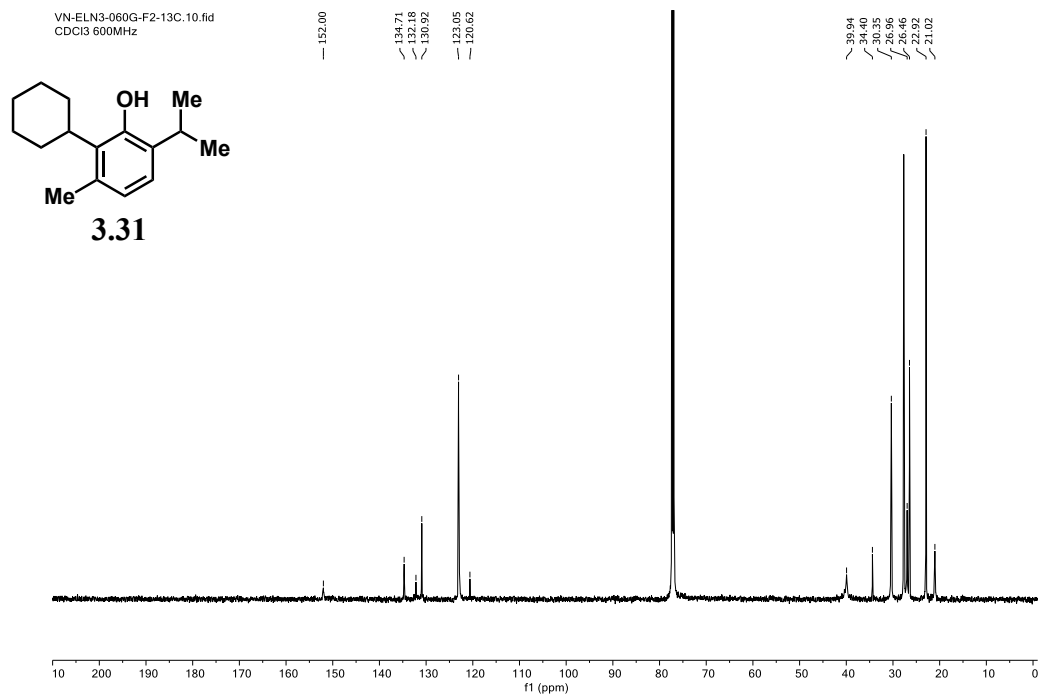


Figure 4.208. <sup>13</sup>C NMR spectrum of **3.31** (151 MHz, 298 K, CDCl<sub>3</sub>).

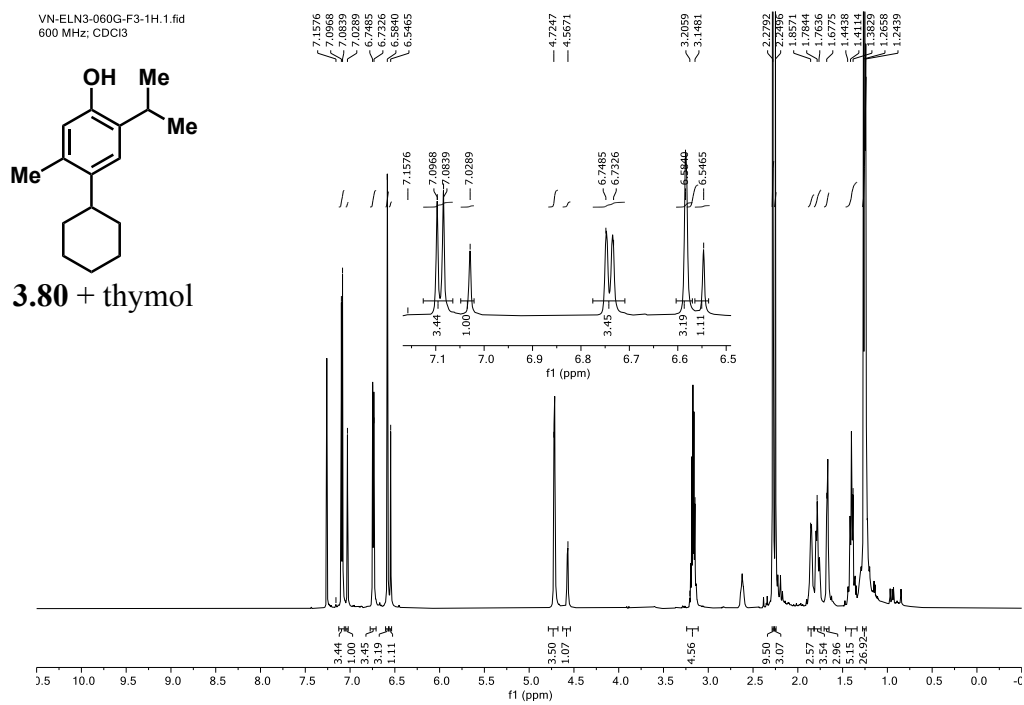


Figure 4.209. <sup>1</sup>H NMR spectrum of **3.80** + thymol (600 MHz, 298 K, CDCl<sub>3</sub>).



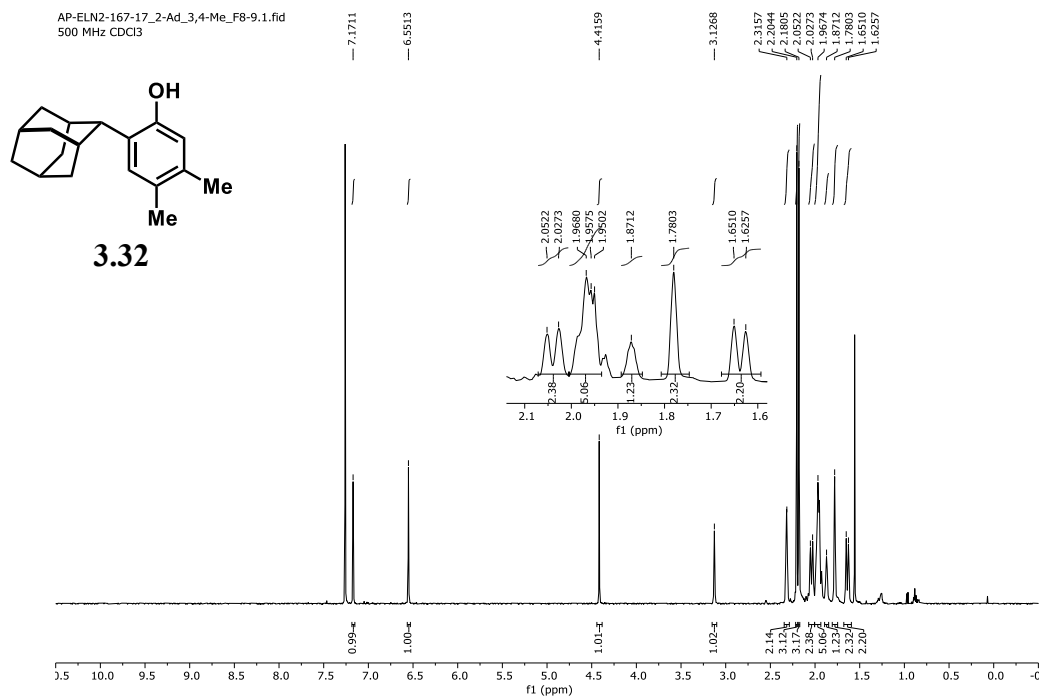


Figure 4.210. <sup>1</sup>H NMR spectrum of **3.32** (500 MHz, 298 K, CDCl<sub>3</sub>).

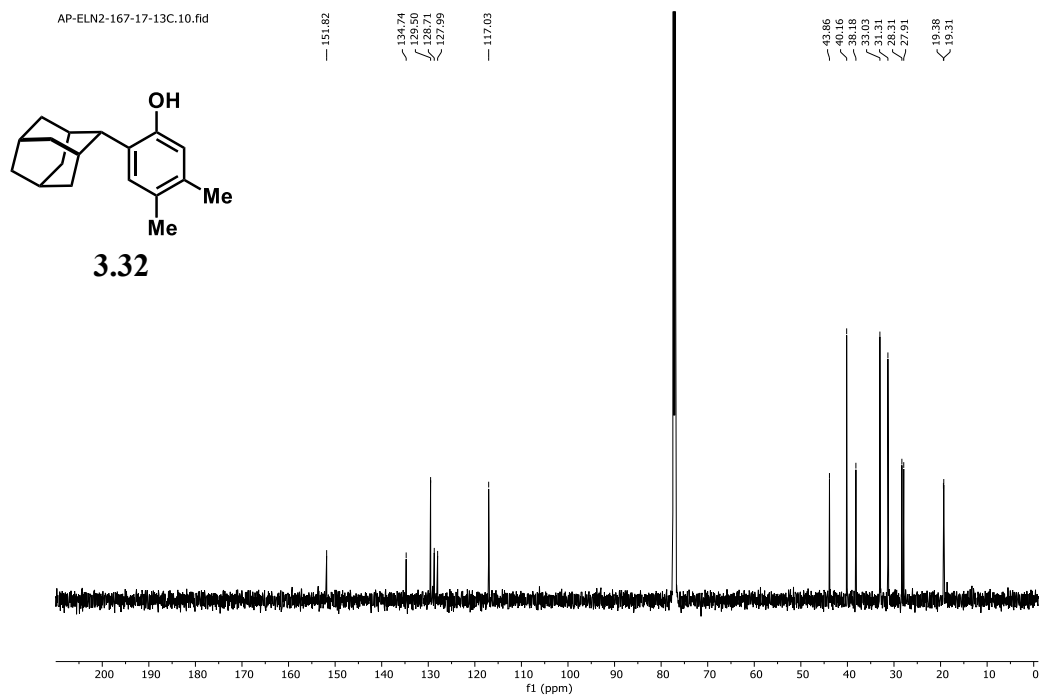


Figure 4.211. <sup>13</sup>C NMR spectrum of **3.32** (151 MHz, 298 K, CDCl<sub>3</sub>).

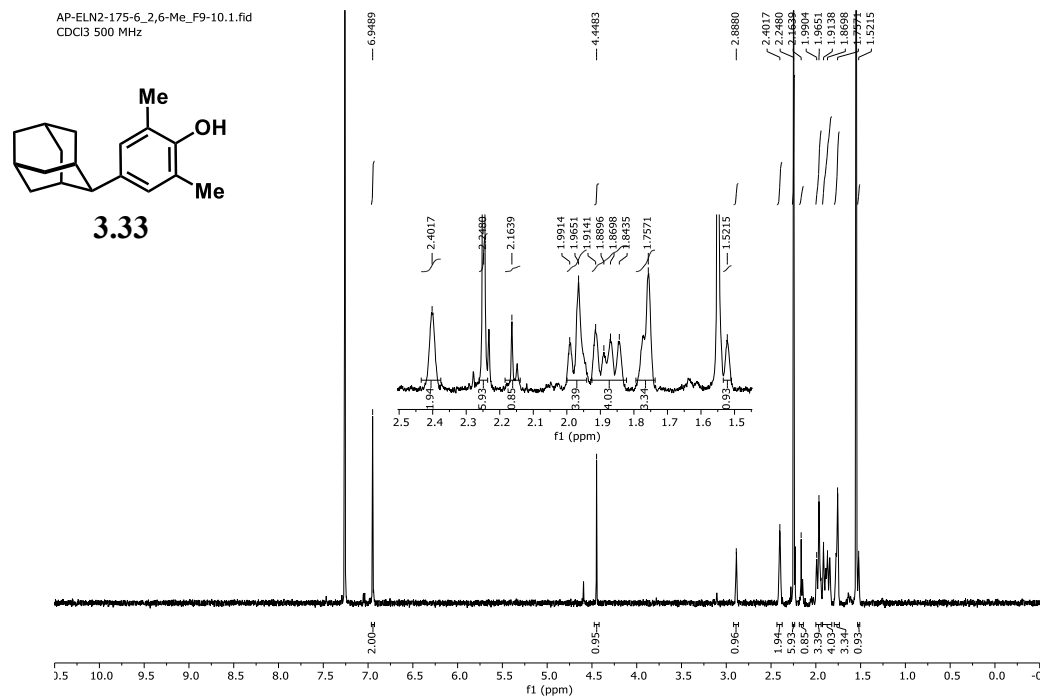


Figure 4.212. <sup>1</sup>H NMR spectrum of **3.33** (500 MHz, 298 K, CDCl<sub>3</sub>).

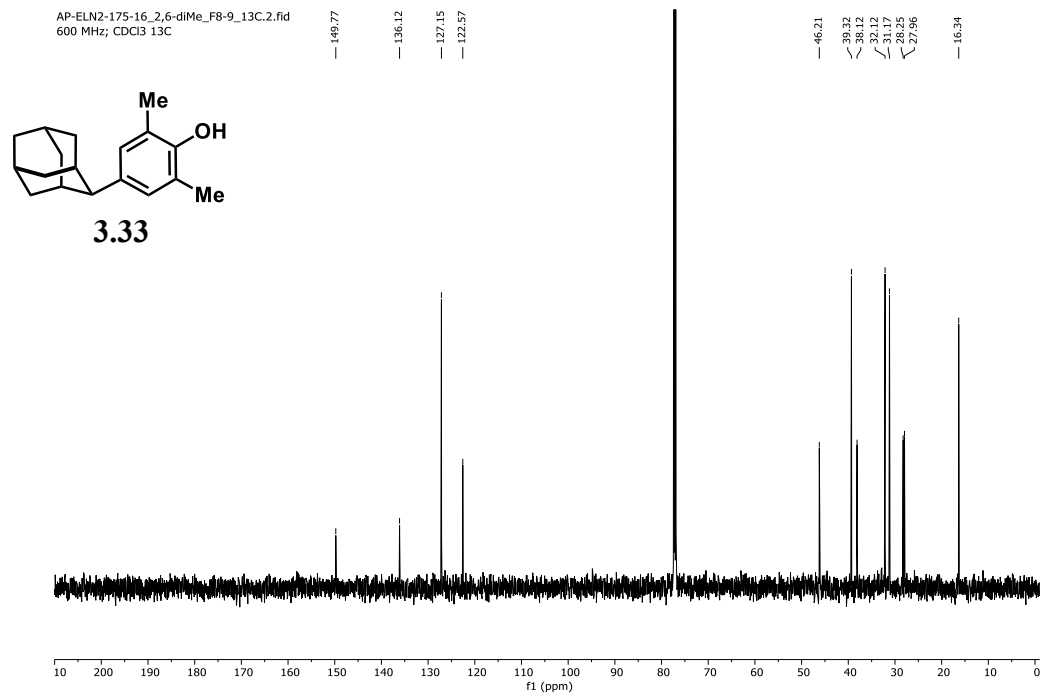


Figure 4.213. <sup>13</sup>C NMR spectrum of **3.33** (151 MHz, 298 K, CDCl<sub>3</sub>).

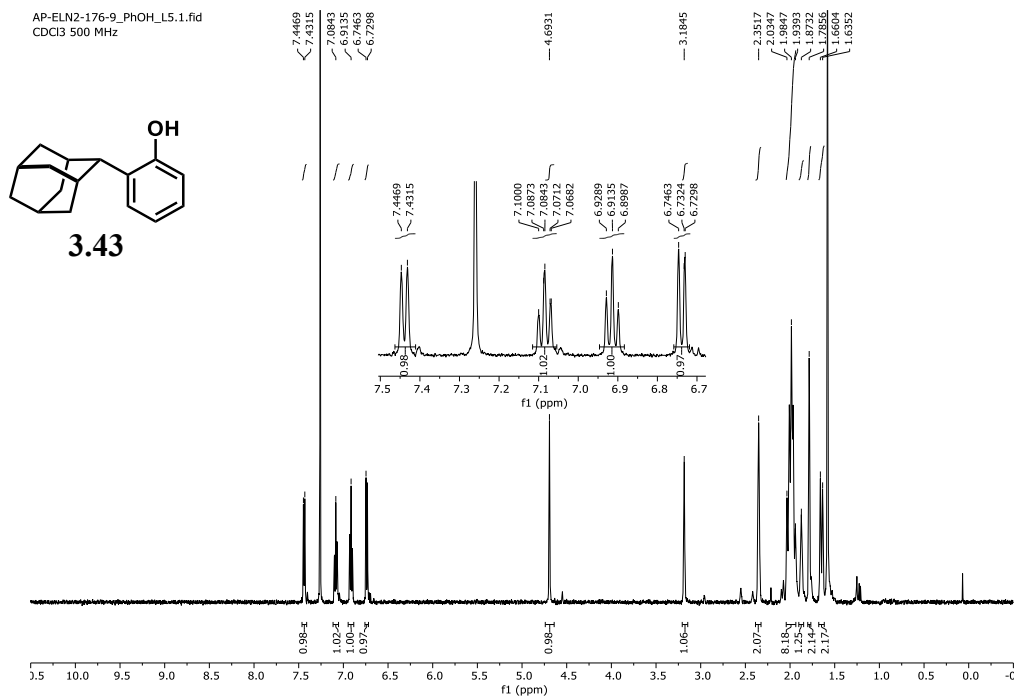


Figure 4.214. <sup>1</sup>H NMR spectrum of **3.43** (500 MHz, 298 K, CDCl<sub>3</sub>).

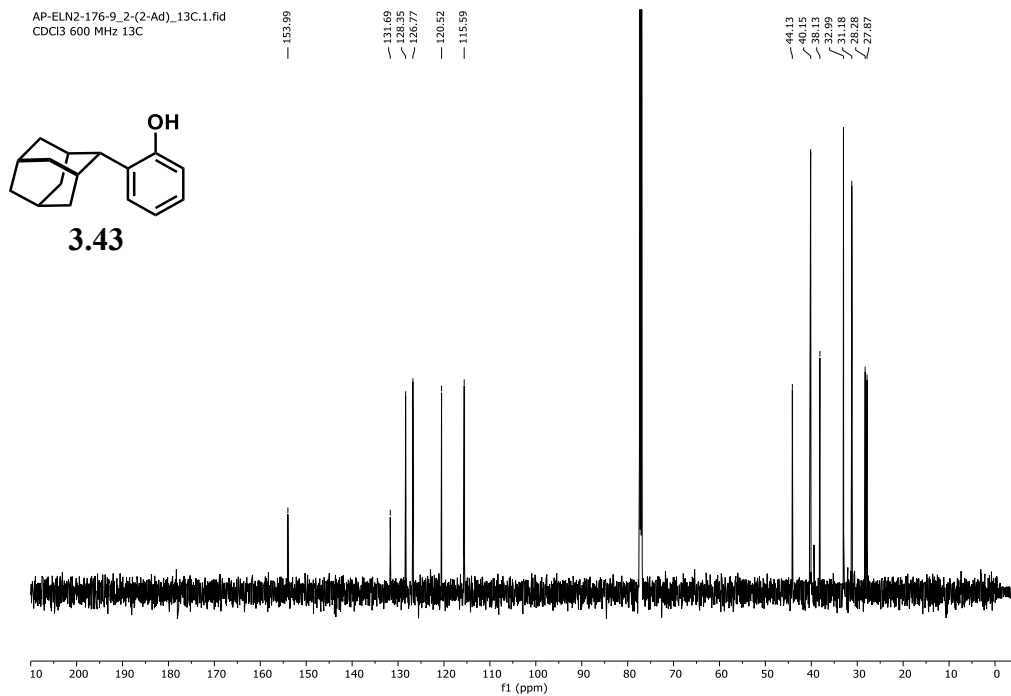


Figure 4.215. <sup>13</sup>C NMR spectrum of **3.43** (151 MHz, 298 K, CDCl<sub>3</sub>).



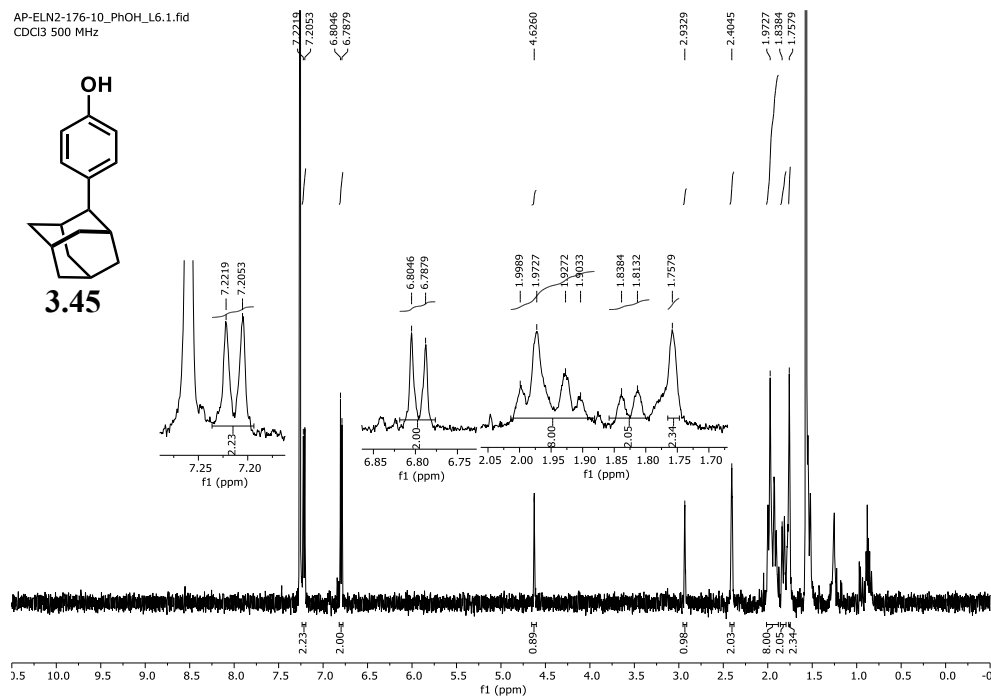


Figure 4.218. <sup>1</sup>H NMR spectrum of **3.45** (500 MHz, 298 K, CDCl<sub>3</sub>).

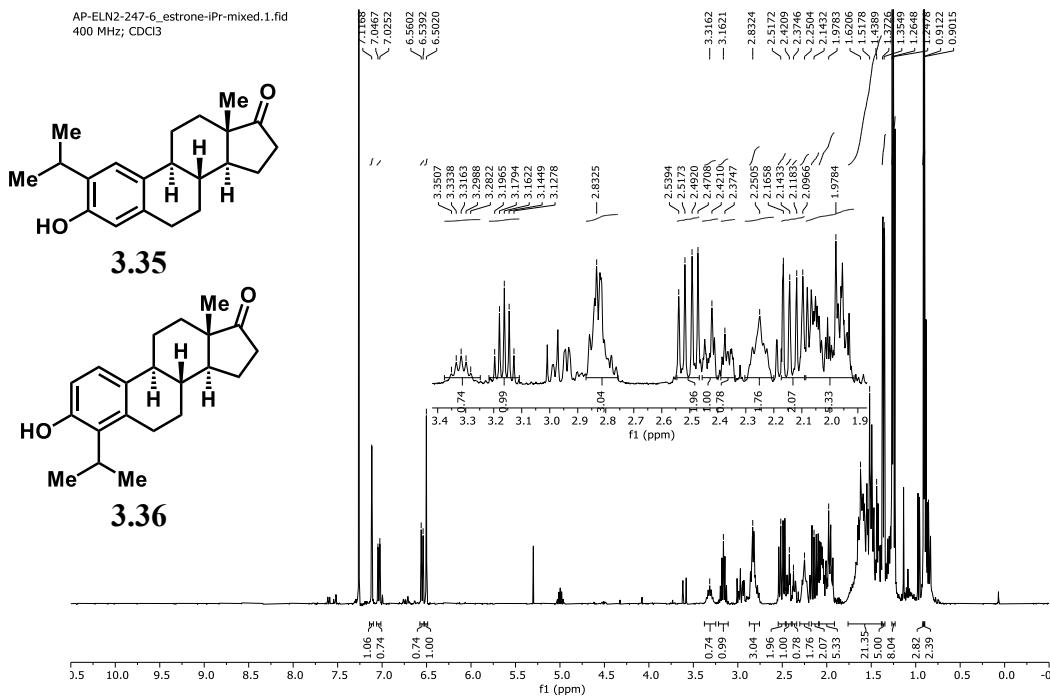


Figure 4.219. <sup>1</sup>H NMR spectrum of **3.35** + **3.36** (400 MHz, 295 K, CDCl<sub>3</sub>).



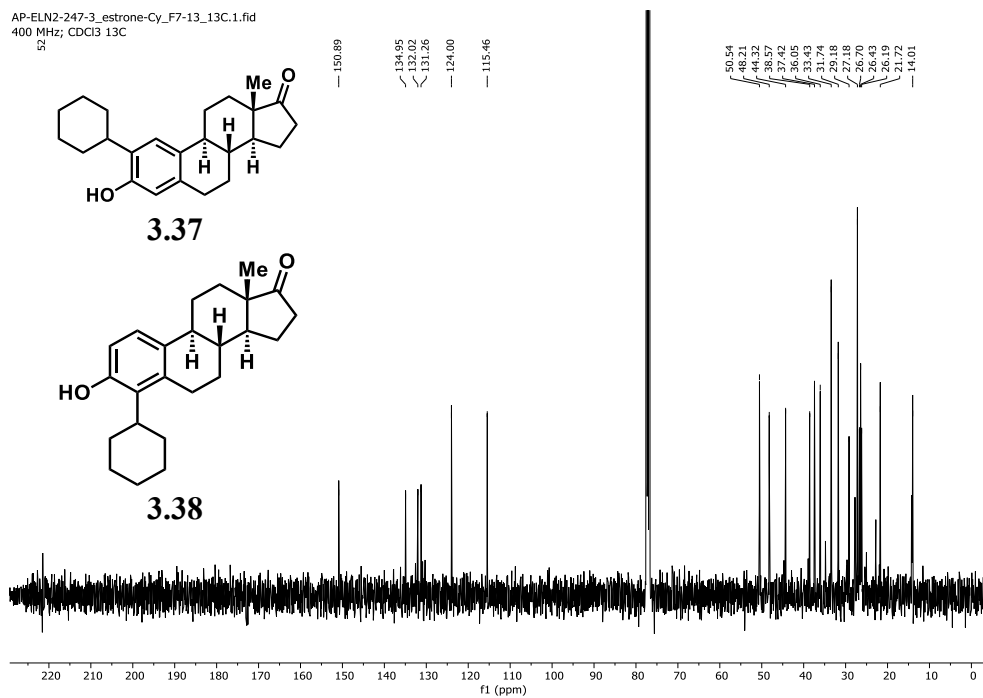


Figure 4.222. <sup>13</sup>C NMR spectrum of 3.37 + 3.38 (101 MHz, 295 K, CDCl<sub>3</sub>).

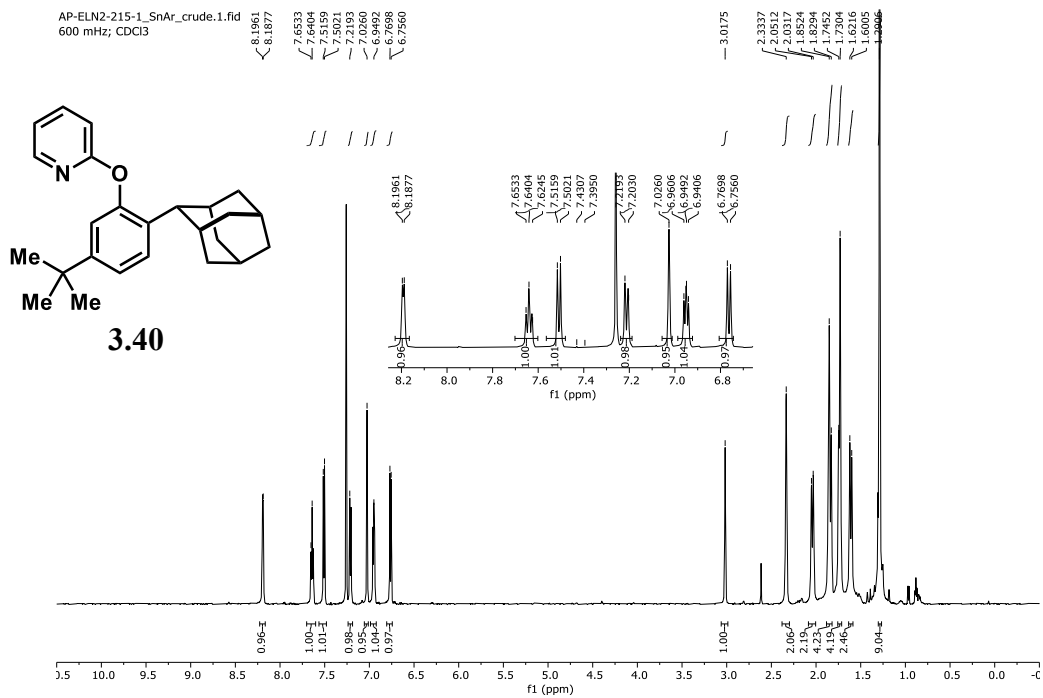


Figure 4.223. <sup>1</sup>H NMR spectrum of 3.40 (600 MHz, 298 K, CDCl<sub>3</sub>).

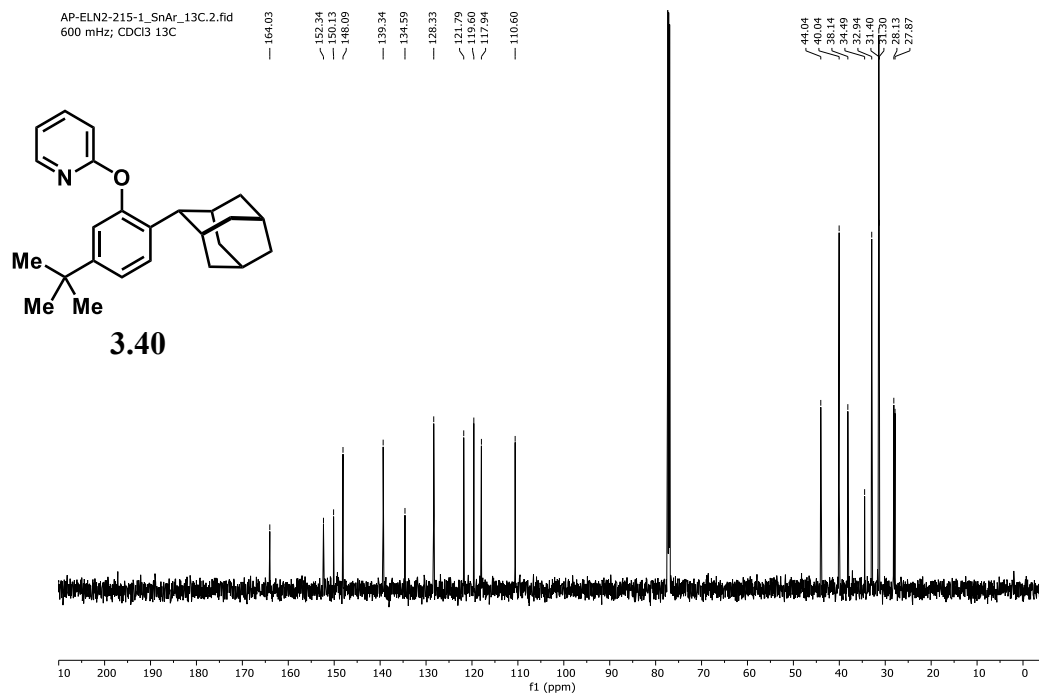


Figure 4.224. <sup>13</sup>C NMR spectrum of **3.40** (151 MHz, 298 K, CDCl<sub>3</sub>).

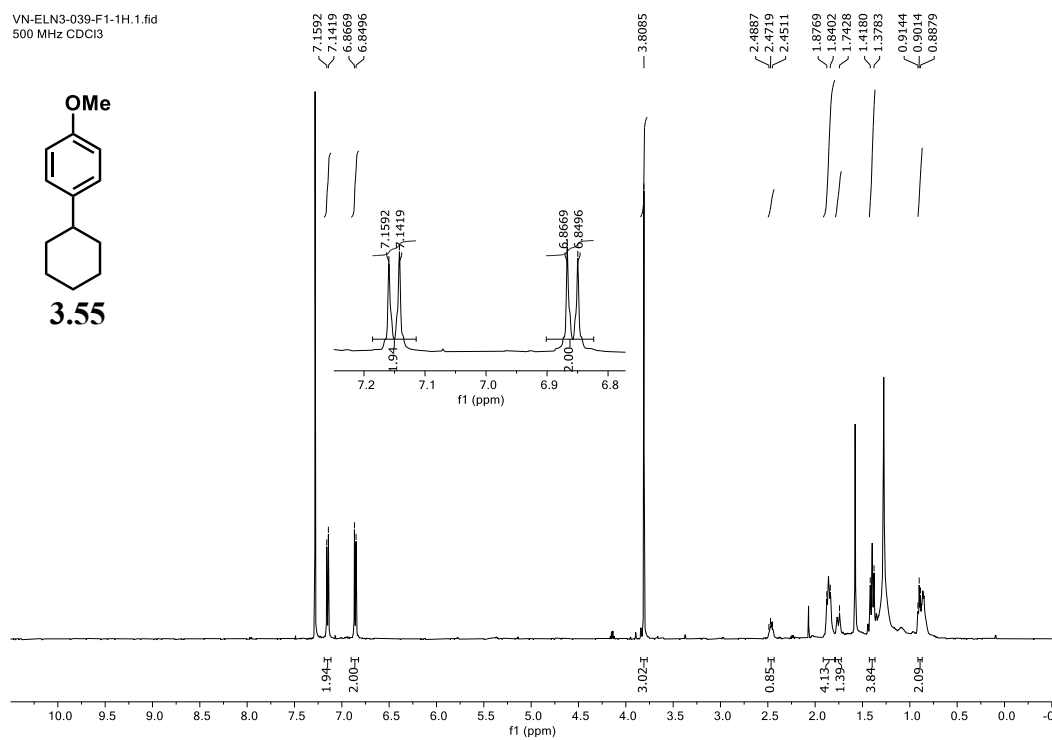


Figure 4.225. <sup>1</sup>H NMR spectrum of **3.55** (500 MHz, 298 K, CDCl<sub>3</sub>).



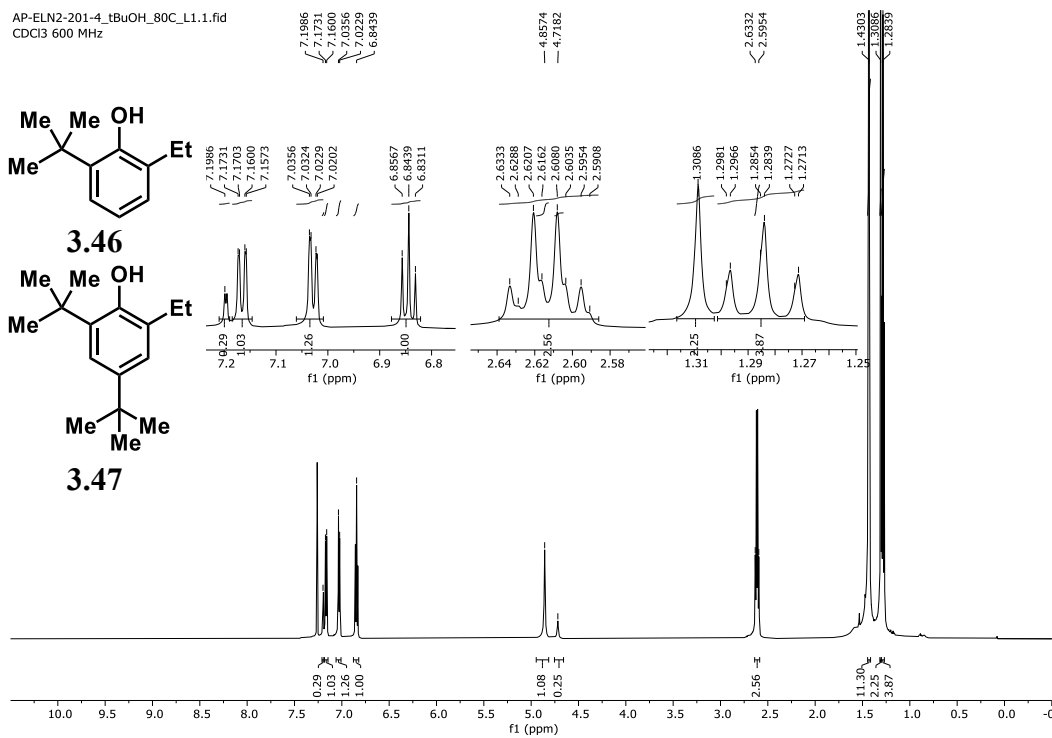


Figure 4.226. <sup>1</sup>H NMR spectrum of **3.46** + **3.47** (600 MHz, 298 K, CDCl<sub>3</sub>).

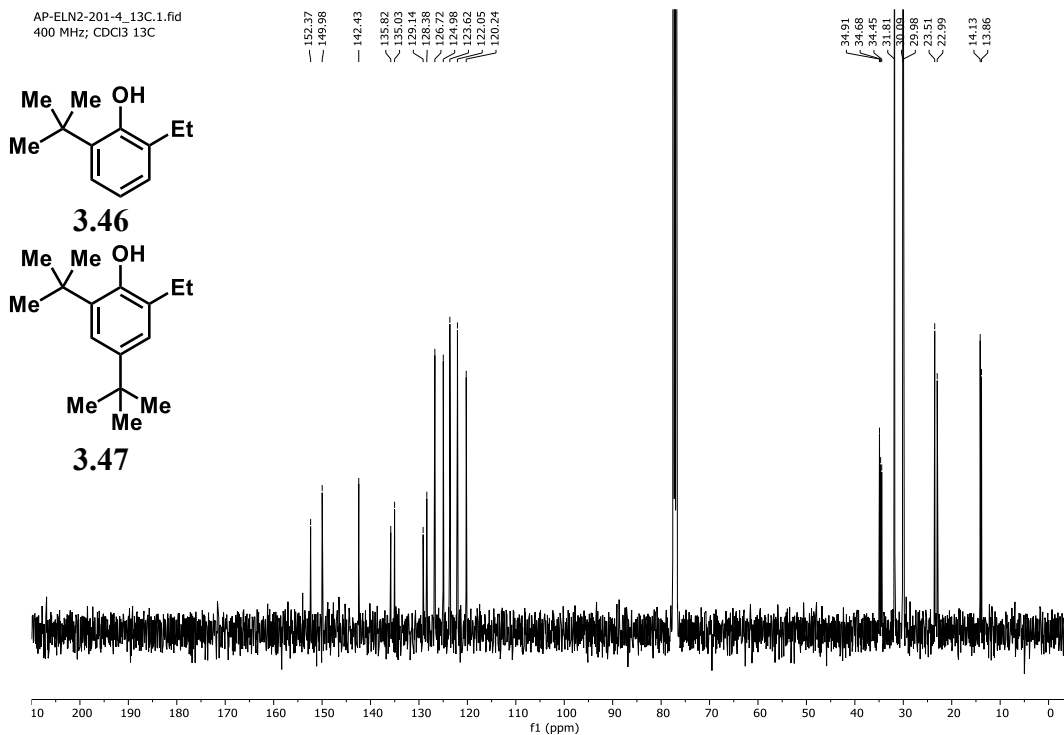


Figure 4.227. <sup>13</sup>C NMR spectrum of **3.46** + **3.47** (101 MHz, 295 K, CDCl<sub>3</sub>).

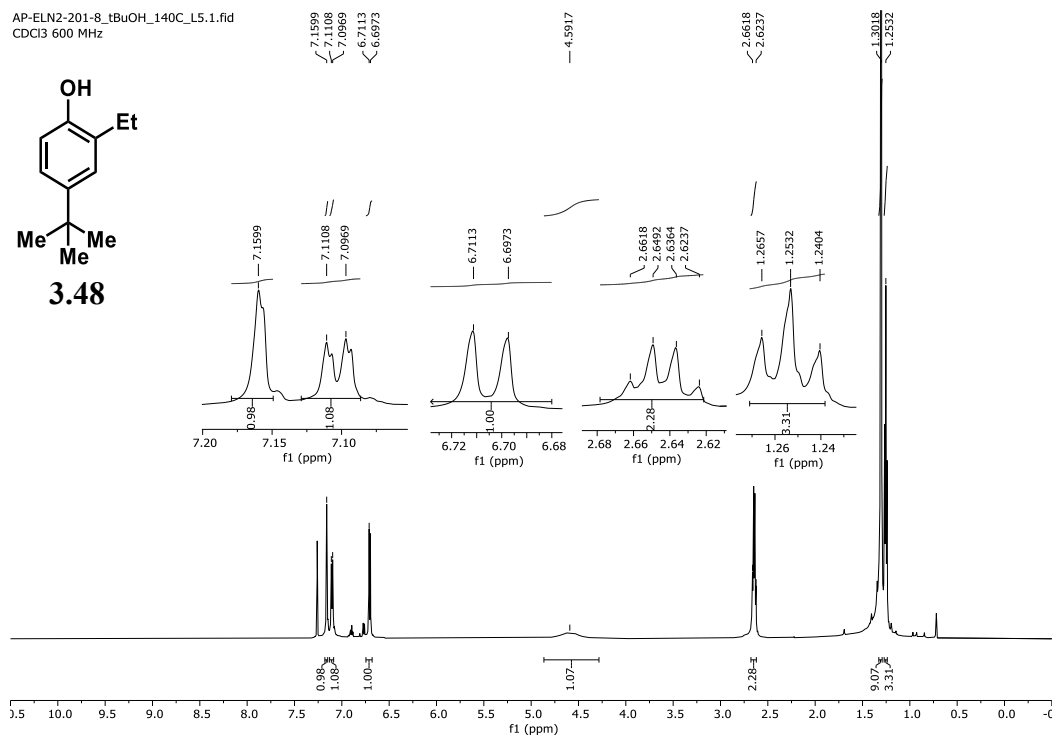


Figure 4.228. <sup>1</sup>H NMR spectrum of **3.48** (600 MHz, 298 K, CDCl<sub>3</sub>).